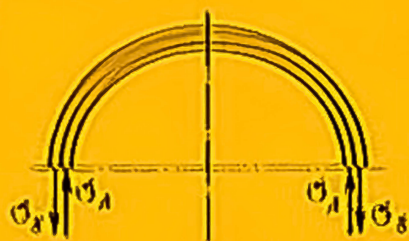


V. I. Feodosyev

Selected  
Problems and Questions  
in Strength of Materials



Mir Publishers Moscow

---

V. I. Feodosyev

---

Selected  
Problems and Questions  
in Strength of Materials

---

Selected Problems and Questions in Strength of Materials







---

**В. И. Феодосьев**

---

**Избранные задачи и вопросы  
по сопротивлению материалов**

---

**ИЗДАТЕЛЬСТВО «НАУКА»  
МОСКВА**

---

V. I. Feodosyev

---

Selected  
Problems and Questions  
in Strength of Materials

---

Translated from the Russian  
by  
M. Konyaeva

Mir Publishers Moscow

**First published 1977**

*На английском языке*

**© English translation, Mir Publishers, 1977**

# Contents

## PROBLEMS AND QUESTIONS 7

### I. Tension, Compression, and Torsion 7

### II. Geometrical Properties of Sections. Bending 23

### III. Combined Stresses and Strength Theories 41

### IV. Stability 48

### V. Miscellaneous Questions and Problems 71

## SOLUTION OF PROBLEMS AND ANSWERS TO QUESTIONS 86

### I. Tension, Compression, and Torsion 86

### II. Geometrical Properties of Sections. Bending 135

### III. Combined Stresses and Strength Theories 220

### IV. Stability 238

### V. Miscellaneous Questions and Problems 383

## LITERATURE 430



---

# Problems and Questions

---

## I. Tension, Compression, and Torsion

1. A system consisting of two bars is simultaneously loaded by forces  $P_1$  and  $P_2$  directed along the bars (Fig. 1a).

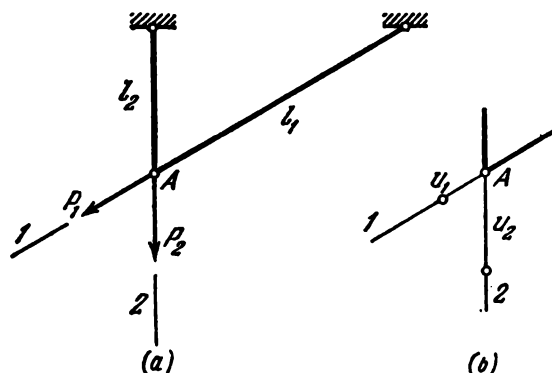


Fig. 1

The potential energy of strain is obviously equal to

$$U = \frac{P_1^2 l_1}{2E_1 A_1} + \frac{P_2^2 l_2}{2E_2 A_2}.$$

By taking the partial derivatives of the potential energy with respect to the forces  $P_1$  and  $P_2$ , we find the displacements of the point A in the 1 and 2 directions ( $u_1$  and  $u_2$ , Fig. 1b)

$$u_1 = \frac{P_1 l_1}{E_1 A_1}, \quad u_2 = \frac{P_2 l_2}{E_2 A_2}.$$

Show graphically what is the total displacement of the point A.

2. A plane truss (Fig. 2) consists of  $n > 2$  identical and equispaced bars connected into a common joint. A force  $P$  is applied in the plane of the truss. Show that the displacement of the joint  $O$  is always directed along the force  $P$  and the magnitude of this displacement is independent of the angle  $\alpha$ .

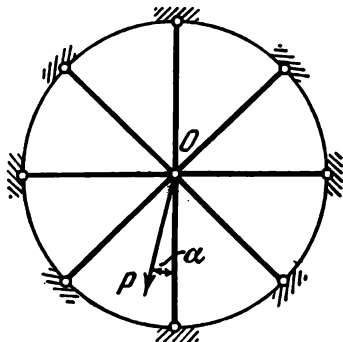


Fig. 2

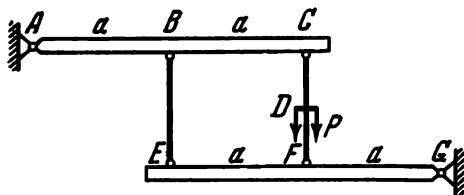


Fig. 3

3. A system consists of two rigid, hinged, weightless beams,  $AC$  and  $EG$ , and two bars,  $BE$  and  $CF$ . At a point  $D$  is applied a force  $P$  acting along the bar  $CF$  (Fig. 3).

(1) How many times is this system statically indeterminate?

(2) What are the forces induced in the bars?

4. There is a hole in an absolutely rigid plate. An elastic bolt is inserted into the hole and tightened with an initial force  $N_0$ . After tightening, a force  $P$  is applied to the lower nut (Fig. 4). How is the force exerted on the bolt altered?

5. The condition of the preceding problem is complicated by the fact that an elastic interlayer is mounted under the lower nut (Fig. 5). How is in this case the force on the bolt altered when the force  $P$  is applied to the lower nut if it is known that when the interlayer is compressed by the force  $P$  its thickness is reduced by the amount  $\Delta = P/k$ , where  $k$  is the stiffness of the interlayer?

6. Determine the braking moment and the displacement of the end of the lever of a belt brake (point  $A$ , Fig. 6) as a

function of the force  $P$ . The coefficient of friction on the surface of contact between the belt and the pulley is  $f$ .

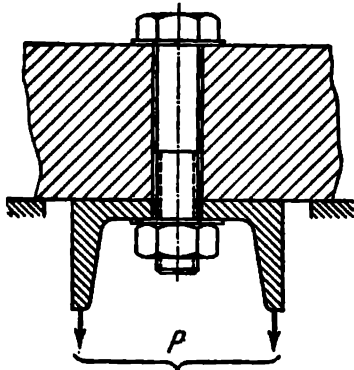


Fig. 4

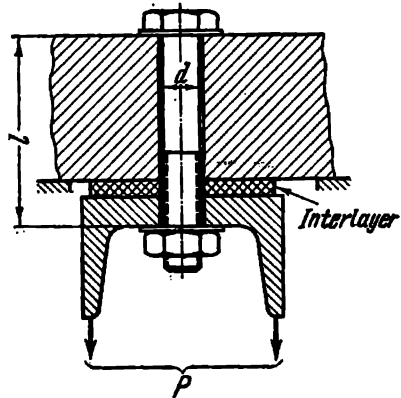


Fig. 5

The extensional stiffness of the belt is given. The lever and pulley may be regarded as absolutely rigid.

7. How is the solution of the preceding problem altered if the pulley rotates in the opposite sense?

8. In order to determine the magnitude of the modulus of elasticity of a metal in compression, the following experiment has been set up. A cylindrical specimen has been compressed between two heavy steel plates (Fig. 7).

To measure the deformation of the specimen two indicators have been mounted (Fig. 7) so as to eliminate errors due to the distortion of the plates. The measurements showed the modulus of elasticity of the test metal in compression to be

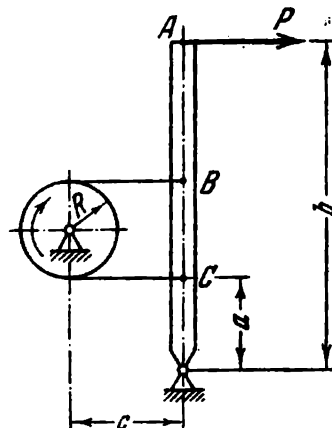


Fig. 6

$$E_c = 0.8 \times 10^6 \text{ kgf/cm}^2.$$

Can this result be trusted?

9. A straight homogeneous bar of uniform section is rigidly fixed at its ends (Fig. 8).

Show, without any calculations, that no axial displacements occur in the bar under uniform heating.

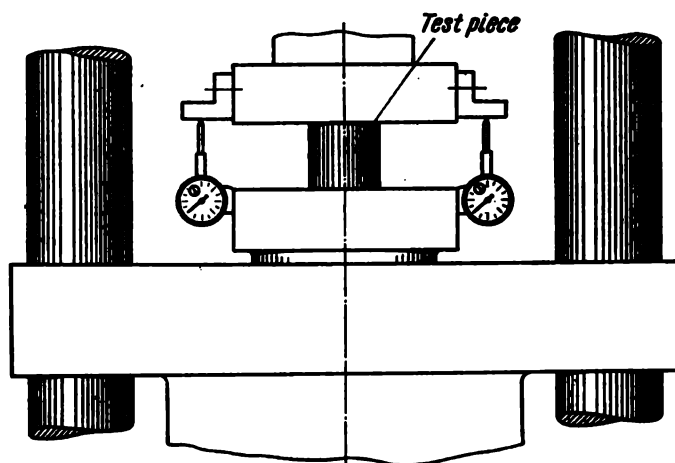


Fig. 7

10. A bar fixed at its upper end is loaded by a longitudinal force  $P$  (Fig. 9). There is a clearance  $\Delta$  between the

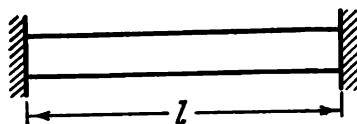


Fig. 8

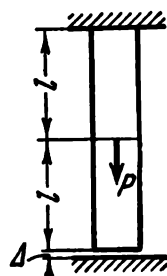


Fig. 9

lower end of the bar and the lower rigid support. When  $P \geq EA\Delta/l$ , the lower clearance is taken up. The reaction  $N$  of the lower support is determined from the condition

$$\frac{(P - N)l}{EA} - \frac{Nl}{EA} = \Delta;$$

consequently, the force in the lower part of the bar is

$$N = \frac{P}{2} - \frac{\Delta}{l} \frac{EA}{2}.$$

The upper part is extended by the force

$$P - N = \frac{P}{2} + \frac{\Delta}{l} \frac{EA}{2}.$$

The displacement of the point of application of the force  $P$  is

$$\delta = \frac{Pl}{2EA} + \frac{\Delta}{2}.$$

We determine the elastic energy stored in the bar. On the one hand, this energy may be determined as the sum of the energies contained in the upper and lower portions of the bar, i.e.,

$$U = \frac{(P - N)^2 l}{2EA} + \frac{N^2 l}{2EA}$$

or

$$U = \frac{P^2 l}{4EA} + \frac{EA \Delta^2}{4l}. \quad (1)$$

On the other hand, this energy is equal to the work done by the force  $P$  during the displacement  $\delta$ , i.e.,

$$U = \frac{P\delta}{2} = \frac{P^2 l}{4EA} + \frac{P\Delta}{4}. \quad (2)$$

As is seen, the expressions came out different. What is the matter? Which of these expressions is correct and which is not?

11. A straight homogeneous bar (Fig. 10a) is supported by a rigid base. We find the displacement of the centre of gravity of the bar under its own weight. This can be done in two ways.

(1) We find, by the usual procedure, the displacement of the point (centre of gravity) located at a distance  $l/2$  from the base (see the displacement diagram, Fig. 10b). As can easily be verified, this displacement is equal to

$$\Delta = \frac{3}{8} \frac{ql^2}{EA}, \quad (1)$$

where  $q$  is the weight of the bar per unit length,  $EA$  is the compression stiffness.

(2) We find the distance from the base to the centre of

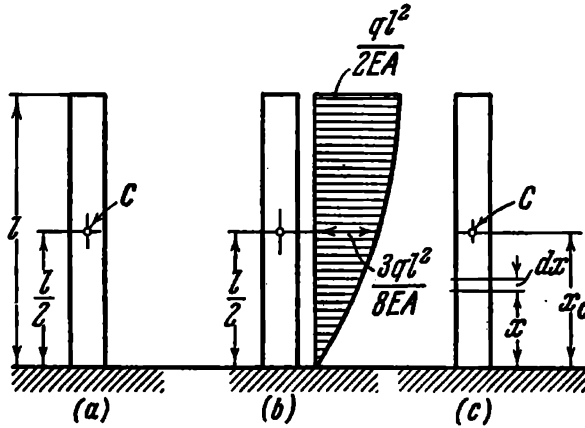


Fig. 10

gravity of the deformed bar (Fig. 10b). This distance is as follows:

$$x_c = \frac{\int_0^l (x-u) dm}{m}. \quad (2)$$

Here  $dm$  is the mass of an element of length  $dx$ ;

$$dm = \frac{q dx}{g}, \quad m = \frac{ql}{g},$$

$u$  is the current displacement determined from the diagram (Fig. 10b) by the formula

$$u = \frac{qx}{EA} \left( l - \frac{x}{2} \right).$$

Substituting for  $u$ ,  $m$ ,  $dm$  in expression (2) and integrating, we find

$$x_c = \frac{l}{2} - \frac{ql^2}{3EA}.$$

The required displacement is therefore

$$\Delta = \frac{l}{2} - x_c = \frac{ql^2}{3EA}, \quad (3)$$

which is at variance with the previously obtained expression (1).

What is the reason for the discrepancy?

12. A flexible string resting on a horizontal plane is tightened by a force  $T_0$  between two fixed supports (Fig. 11).

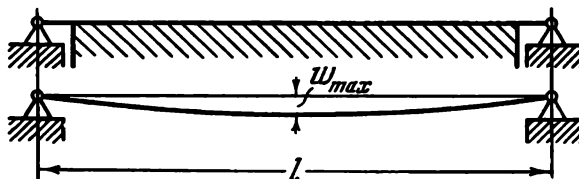


Fig. 11

After the intervening supporting plane is removed, the string sags.

Examine how the magnitude of the sag  $w_{\max}$  depends on the initial tension  $T_0$  and the weight  $q$  of the string per unit length assuming the extensional stiffness  $EA$  of the string and its length  $l$  to be given.

13. Figure 12 shows the suspension of an operating wire of a trolley-bus line.

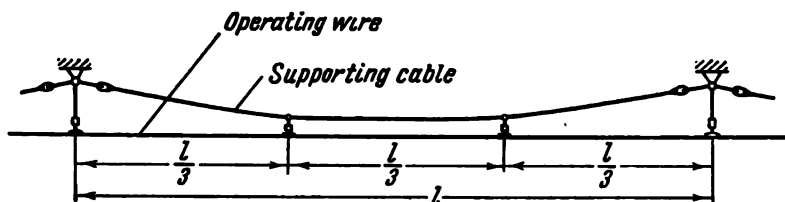


Fig. 12

Determine the tension and draw the sagging deflection curve of the supporting cable if it had an initial sag  $w_0 \max$  before the lower wire was suspended.

Carry out a numerical calculation with the following data given:  $l = 50$  m,  $w_0 \max = 0.5$  m, the cable is of steel, cross-sectional area  $A = 0.6$  cm<sup>2</sup>, reduced modulus of elasticity for cable\*  $E = 8 \times 10^5$  kgf/cm<sup>2</sup>, weight of wire  $q_w$  per unit length is 1.5 times larger than weight of cable  $q$ .

\* See Question 170.

14. How to find the distribution of forces between rivets *I*, *II*, *III*, *IV* of the longitudinal riveted joint shown in Fig. 13 if the results of the following preliminary experiment are known? Three sheets of thicknesses  $h_1$ ,  $h_2$ , and  $h_1$  and width  $b$

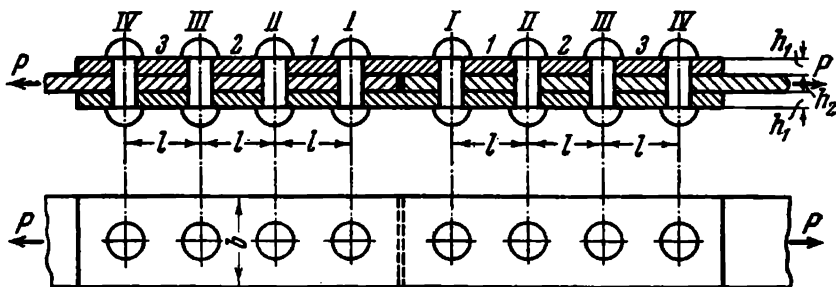


Fig. 13

joined together by a single rivet are tested in tension (Fig. 14). By precise measurements a relation is established for the change in distance between the points *A* (on the

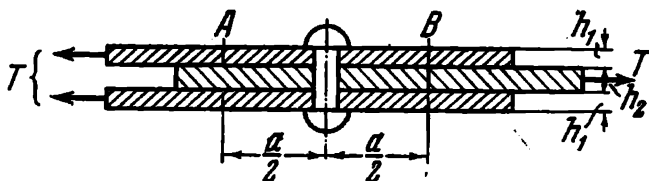


Fig. 14

top sheet) and *B* (on the middle sheet) (Fig. 14) and the force *T*. This relation is of the form

$$\Delta a = \frac{T}{k},$$

where  $k$  is a constant. The gauge length  $a$  is chosen sufficiently large for the stresses at the sections *A* and *B* to be considered uniformly distributed.

15. Generalize the solution of the preceding problem to the case of any number of rivets  $n$ .

16. A screw and a nut (Fig. 15) are extended by forces  $P$ . Find the law of distribution of normal forces along the length of the screw and nut (as a function of  $x$ ) if it is known that

the force per each turn of the thread is proportional to the relative displacement of the screw and nut:  $t = k(u_s - u_n)$ ;  $t$  is the force per unit length of the threaded surface,  $k$  is an experimentally found factor,  $u_s - u_n$  is

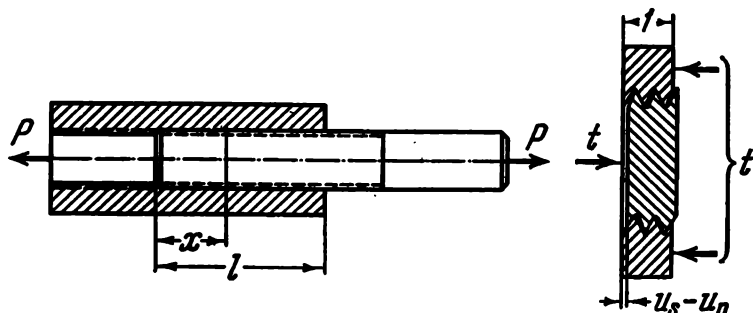


Fig. 15

the relative displacement along the axis of the screw and nut caused by the deformation of the thread (see Fig. 15).

17. A screw with a nut screwed on it (Fig. 16) is extended by forces  $P$ . With the condition of the preceding problem,

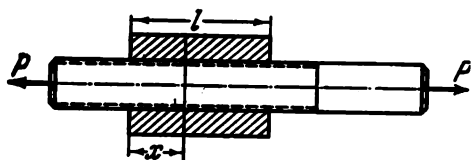


Fig. 16



Fig. 17

find the law of distribution of normal forces and forces on the thread along the length of the screw and nut.

18. On a screw (Fig. 17) is screwed a nut having a pitch of thread less than the screw pitch  $s$  by  $\Delta$ .

What is the law of distribution of the forces produced in the screw and nut and what are the forces on the thread if, as in the preceding two problems,

$$t = k(u_s - u_n)?$$

19. For what nut-design (of the first or second type, Fig. 18) are the operating conditions for the fillets of the screw more favourable?

20. Three identical rubber rods (Fig. 19) are loaded by a force  $P$ . Find the displacement of the joint  $A$  in relation

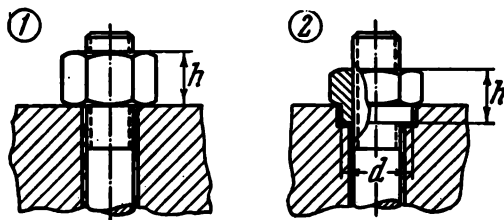


Fig. 18

to the force  $P$  if the tensile test diagram of each rod is given by the curve shown in Fig. 19.

21. A circular two-layer rubber-cord cylinder is subjected to an internal pressure  $p$  (Fig. 20). It has been observed

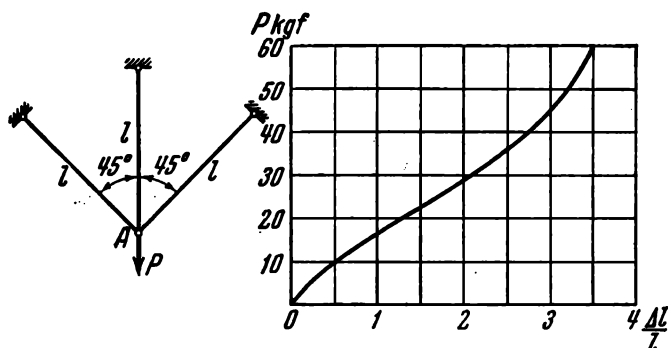


Fig. 19

that, depending on the position angle  $\alpha$  of the cords, the cylinder, deforming under internal pressure, may assume one of the shapes illustrated in Fig. 21. In Case 1 the curved generator of the cylinder is convex outward, and in Case 2 inward. In Case 3 no perceptible deformations are observed under the same pressure, and the cylinder maintains its shape as far as the cords may be assumed inextensible.

What are the values of the angle  $\alpha$  corresponding to each of the above types of deformation?

22. A thin-walled rubber sphere is reinforced with a large number of rigid cords placed along meridians (Fig. 22).

Experiment shows that if the sphere is pressurized through the air, it expands along the equator, shortens along the

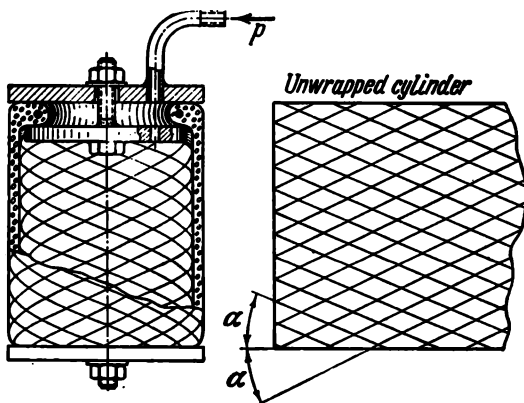


Fig. 20

axis of rotation and assumes a shape reminiscent of a pumpkin. Determine the degree of oblateness of this shape, neglecting the stiffness of the rubber shell.

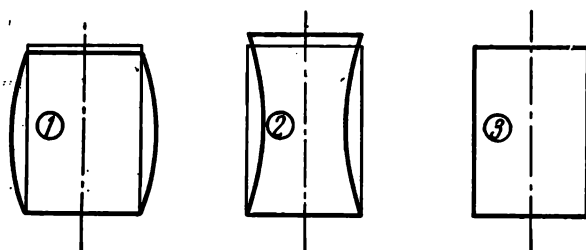


Fig. 21

23. A steel ring is fitted on an aluminium one with a given negative allowance (Fig. 23). Experiment shows that in some cases after the system is heated to a certain temperature and then cooled the inner ring falls out of the outer ring.

Examine the conditions under which this phenomenon is possible. What data are needed to obtain a numerical estimate of this phenomenon?

24. A thin ring is fitted loosely on a heavy rigid cone (Fig. 24). The cone and ring are simultaneously subjected to

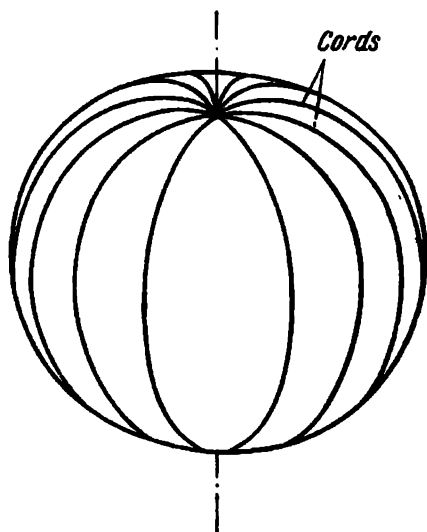


Fig. 22

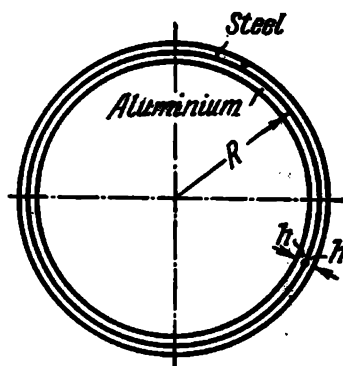


Fig. 23

periodically varying temperature. How may this affect the location of the ring along the axis of the cone? In other words, will the height  $h$  vary in time?

25. There is an absolutely rigid bar and a thin elastic tube whose inner diameter is less than the diameter of the bar by an amount  $2\Delta$ . The tube is heated and fitted on the bar (Fig. 25).

On cooling the tube develops circumferential stresses and, when friction is involved, axial stresses as well.

Determine the magnitude and the nature of the distribution of the stresses developed in the tube.

26. We complicate the condition of the preceding problem. Determine the force  $P$  that must be applied to the tube in order to remove it from the bar (Fig. 26). Consider two variants: (a) the force  $P$  is compressive, (b) the force  $P$  is tensile.

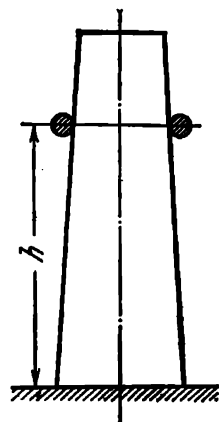


Fig. 24

27. Show that when a prismatic rod with a cross section in the form of a polygon is twisted the shearing stresses



Fig. 25

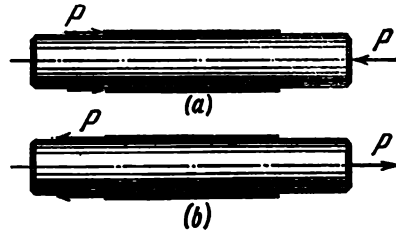


Fig. 26

at any of the exterior corners,  $A, B, C, \dots$  (Fig. 27), are zero.

28. When a circular straight rod is twisted, shearing stresses  $\tau$  occur on its cross sections whose magnitude is proportional to the distance  $r$  from the axis of the rod (Fig. 28). Since the shearing stresses always act in pairs, exactly the same shearing stresses  $\tau'$  occur on the plane  $xy$  of the axial section of the rod. The latter produce a resultant moment about the  $z$  axis.

The cut-off part of the rod must be in equilibrium. What balances the above-mentioned moment?

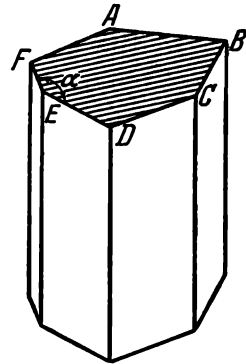


Fig. 27

29. How does the torsional rigidity of a thin strip depend on an axial tensile force  $P$  (Fig. 29) acting simultaneously with a torque?

30. A circular shaft (Fig. 30) inserted into a tube is held in it by frictional forces. The contact interference pressure which produces these frictional forces and the magnitude of the coefficient of friction may be assumed constant, with sufficient accuracy, for the entire zone of contact. To the shaft and the tube are applied equal and opposite moments  $M$ . When  $M > M_0$ , the shaft turns in the tube.

It is required to construct the twisting moment diagrams for the tube and shaft when  $M < M_0$ .

31. How to evaluate the strength of a glue joint of a rigid corner plate with a rigid base if the glue spot is of arbitrary shape (Fig. 31)?

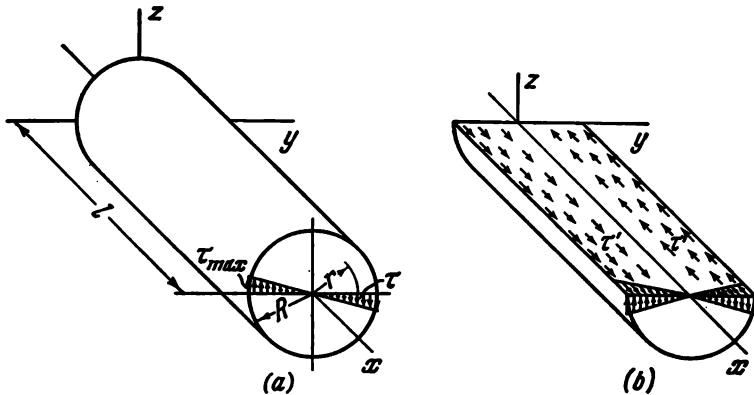


Fig. 28

The shape of the spot is known. The shearing stress occurring in the glue layer is proportional to the local relative

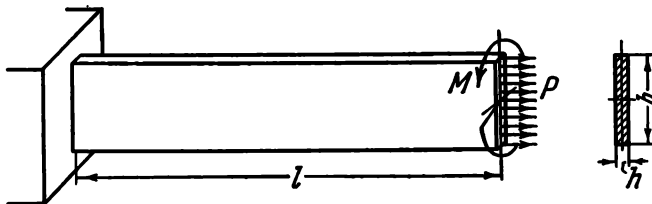


Fig. 29

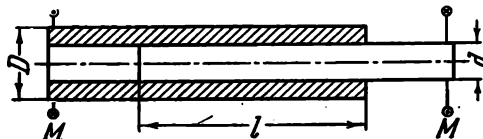


Fig. 30

displacement of the glued parts. The magnitude of the limiting failure stress for the glue is given.

32. An arbitrary closed curve is drawn on the cross section of a twisted rod (Fig. 32). The shearing stresses at each point of the curve are resolved into a normal ( $\tau_n$ ) and a tangential

( $\tau_n$ ) component to the drawn contour. No normal stresses occur on the section (unrestrained torsion).

Prove that, irrespective of the shape of the rod and the shape of the curve drawn on the section, the following formulas are valid:

$$(1) \quad \int \tau_n ds = 0,$$

$$(2) \quad \int \tau_s ds = 2GA_s\theta,$$

where  $ds$  is the differential of arc length of the contour,  $G$  is the shearing modulus,  $A_s$  is the area bounded by the curve,  $\theta$  is the angle of twist per unit length of the rod. (The integration is extended over the whole contour of the closed curve.)

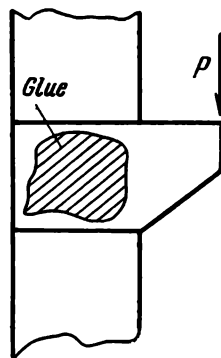


Fig. 31

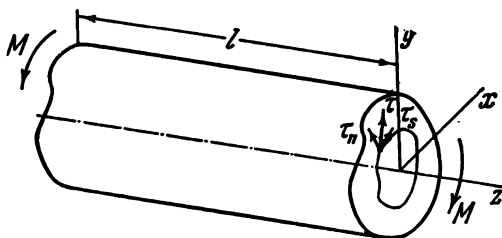


Fig. 32

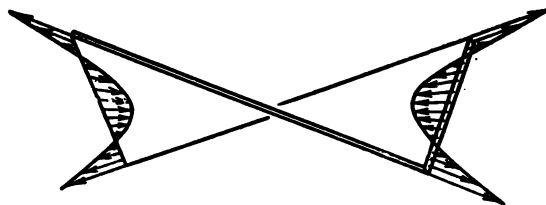


Fig. 33

33. As is known, when a narrow rectangular strip is twisted, secondary normal stresses are produced at cross sections. The stresses arising at the edges of the strip are tensile, and those at the middle are compressive (Fig. 33).

On what characteristics and how do these stresses depend in the case of an arbitrary shape of a thin-walled section?

34. A cylindrical bar is twisted by uniformly distributed surface moments  $m$  balanced by a moment  $M$  at the end

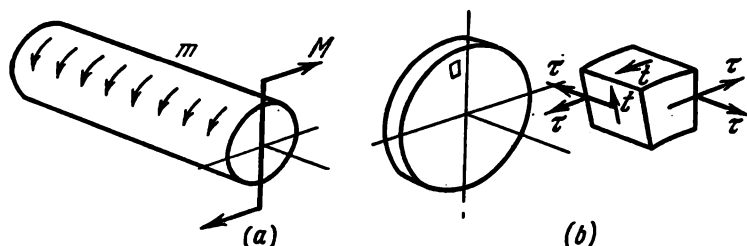


Fig. 34

(Fig. 34a). Under this loading, the bar develops, besides the usual stresses  $\tau$  acting at transverse sections, also shearing stresses  $t$  at cylindrical and axial sections (Fig. 34b).

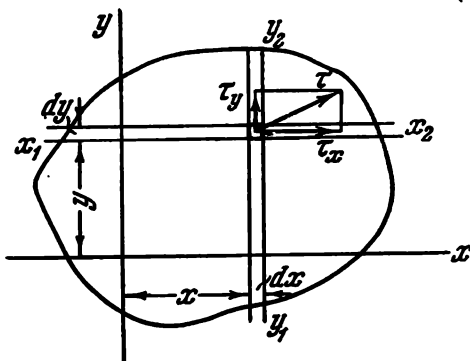


Fig. 35

Determine how these stresses are distributed over the volume of the bar. Give a comparative estimate of the magnitudes of  $\tau$  and  $t$ .

35. The shearing stresses  $\tau$  at a cross section of a rod in pure torsion can be resolved into two components,  $\tau_x$  and  $\tau_y$  (Fig. 35). The twisting moment at the section is obviously determined by the expression

$$M_t = \int_x \int_y \tau_x y \, dx \, dy - \int_x \int_y \tau_y x \, dx \, dy.$$

Show that, irrespective of the shape of the section, the following formulas are valid:

$$\int_x \int_y \tau_x y \, dx \, dy = \frac{M_t}{2}, \quad - \int_x \int_y \tau_y x \, dx \, dy = \frac{M_t}{2}.$$

## II. Geometrical Properties of Sections. Bending

36. Without recourse to integration, find the product of inertia  $I_{xy}$  of a right triangle with respect to centroidal axes parallel to the legs (Fig. 36).

37. Find the locus of constant polar moments of inertia of a plane figure.

38. Prove the following proposition:

If for a set of axes passing through some point it is possible to indicate more than one pair of non-coincident principal axes, then it can be stated that, in general, all axes passing through that point are principal.

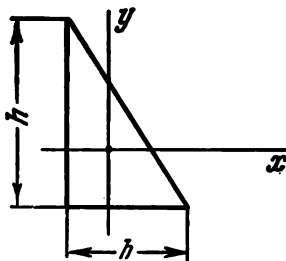


Fig. 36

39. In a plane section, find a point possessing the property that all axes through it are principal.

40. Consider a straight rod which is bent by two moments  $M$  (Fig. 37).

As is known, no stresses occur on the neutral plane  $OO$  in pure bending. Consequently, there is no force interaction

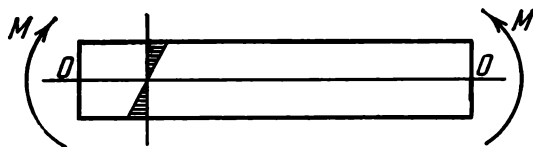


Fig. 37

between the upper and lower parts of the rod over this plane. The rod may then be divided by the section  $OO$  into two thinner rods, and this must not affect the operation of the system in any way.

On the other hand, a doubt arises regarding the legitimacy of this action. The two rods put together and loaded by the moments  $M$  bend so that longitudinal slipping occurs over

the surface of contact (Fig. 38), and the stress diagram at the normal section of both rods is entirely different from that of the solid rod.

Now how is it? Can the rod be divided into two parts without impairing its action, or not?



Fig. 38

41. How to trim a round log to provide a rod of rectangular cross section possessing maximum bending strength (Fig. 39)?

42. As is known, when a rod of large curvature is bent, the neutral axis does not pass through the centroid, but is somewhat shifted towards the centre of curvature.

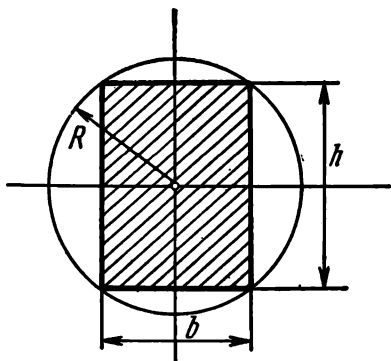


Fig. 39

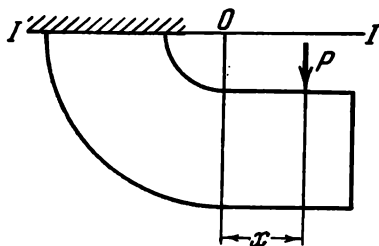


Fig. 40

If the rod is not only bent, but is simultaneously extended, the neutral axis of the total stress diagram can, in general, be displaced by any amount, depending on the magnitude of the tensile or compressive force.

At what distance  $x$  from the centre of curvature  $O$  of the curved rod must the force  $P$  be applied (Fig. 40) to make the neutral axis of the total stress diagram at the section  $I-I$  pass through the centroid of the section?

43. It is known that a straight rod of uniform rigidity subjected to an external moment  $M$  (Fig. 41) bends assuming the shape of a second-order parabola

$$y = \frac{M}{EI} \frac{x^2}{2}. \quad (1)$$

On the other hand, we know the following expression:

$$\frac{1}{\rho} = \frac{M_b}{EI}. \quad (2)$$

If  $M_b$  and  $EI$  are constants, which we assume to be the case here,  $1/\rho$  is also a constant. But the curvature is constant only for a circular arc and not for a parabola. So how is the beam bent? Into an arc of a parabola or a circle?



Fig. 41

44. What should be the initial deflection  $y$  (Fig. 42) of the skis in order that the weight of the skier be distributed uniformly over the length of the sliding surface when going on a smooth and hard road?

45. At what distance  $x$  from the end of the rod must the force  $P$  be applied to make the displacement of the point  $A$  zero (Fig. 43)?

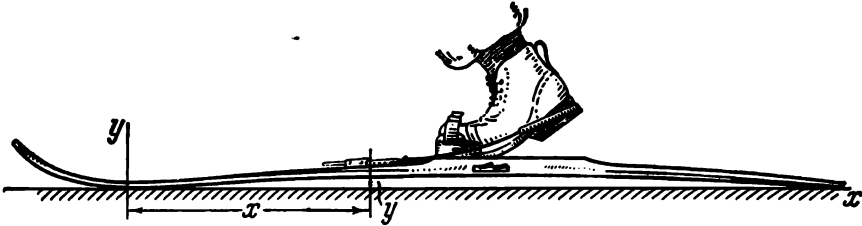


Fig. 42

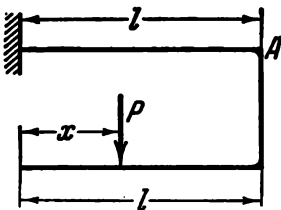


Fig. 43

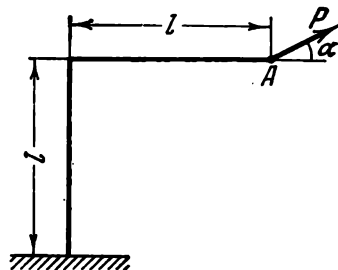


Fig. 44

46. A broken beam (Fig. 44) fixed at one end is loaded by a force  $P$  at the other. Select the angle of inclination  $\alpha$

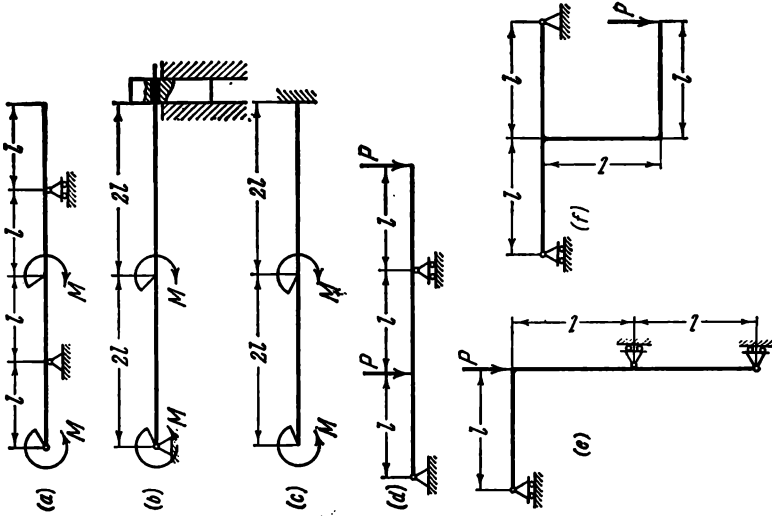


Fig. 46

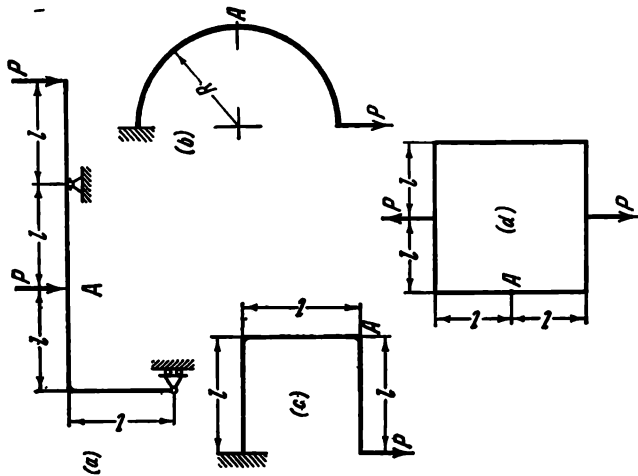


Fig. 45

of the line of action of the force so that the displacement of the point  $A$  will be in the direction of the force  $P$ .

47. Where is the point  $A$  displaced (Fig. 45)? Upward, downward, to the right, to the left?

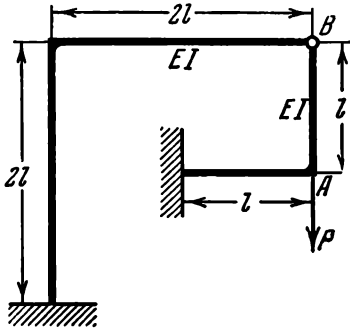


Fig. 47

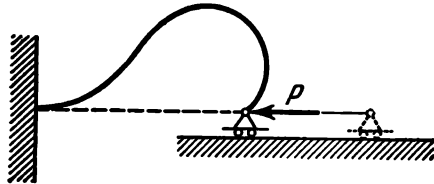


Fig. 48

48. Draw the shape of the elastic curve for the following systems (Fig. 46).

49. The frame shown in Fig. 47 is loaded by a force  $P$ . It is inquired whether the bar  $AB$  is in tension or compression.

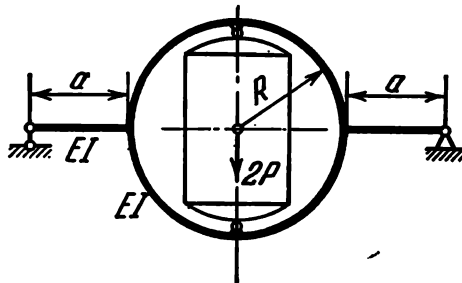


Fig. 49

50. The shape of the elastic curve of a severely bent slender bar and the magnitude of a force  $P$  have been determined by experiment (Fig. 48). How can the reactions at the supports be found most easily?

51. A heavy instrument of weight  $2P$  is mounted in a circular frame (Fig. 49). Select the dimension  $a$  so that

the stiffness of the suspension will be maximum. The stiffnesses of the ring and bars in bending are the same.

52. Which of the three frames shown in Fig. 50 is stiffest, i.e., gives the smallest displacement  $\delta$  under the action of a force  $P$ ? The cross-sectional dimensions are the same.

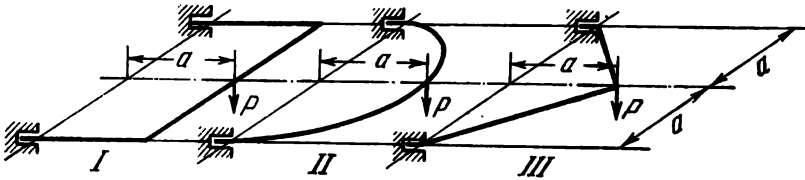


Fig. 50

53. Suppose you have a piston ring in your hand (Fig. 51a). You compress it along a diameter and notice that the flexibility of the ring varies depending on the particular diameter along which the compression is produced. We simplify

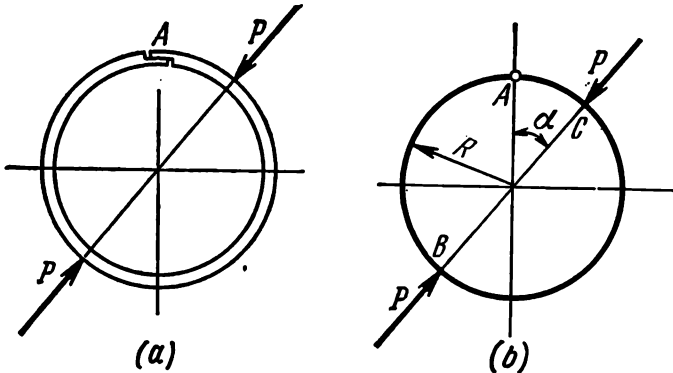


Fig. 51

the problem by representing the closing joint  $A$  as a hinge. Find the value of the angle  $\alpha$  (Fig. 51b) for which the relative displacement of the points  $B, C$  will be smallest under the same force.

54. A cylindrical coil spring fixed at one end is loaded by a transverse force  $P$  at the other (Fig. 52). Determine the vertical displacement of the point of application of the force. The lead angle of the coils may be assumed small.

55. The balance spring of a watch represents a flat spiral band (Fig. 53). The outside end of the band is fixed, and the inside end is rigidly connected to a reel seated on the balance

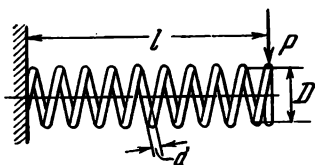


Fig. 52

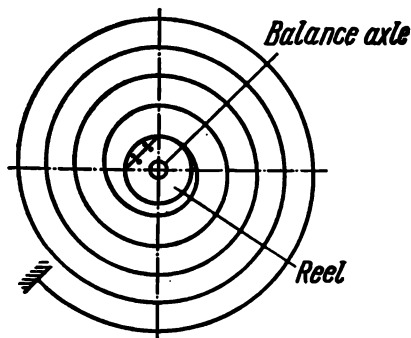


Fig. 53

axle. During vibration of the balance the reel rotates and the band of the spring bends. This bending is not, in general, pure bending, and both transverse and longitudinal forces may occur at the sections of the spring. The presence of these

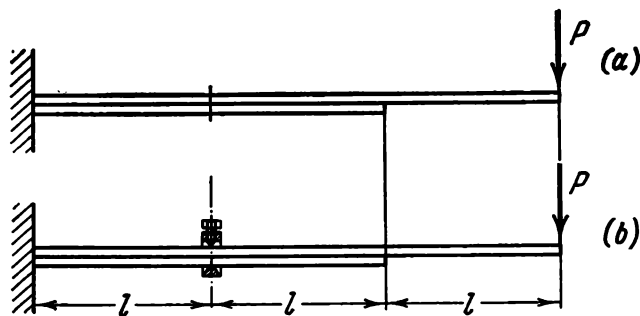


Fig. 54

forces is undesirable for the watch mechanism. If these forces are present, the balance axle distorts, the friction at the supports is increased, and the watch accuracy is reduced.

What are the geometrical conditions which must be satisfied by the spring in order that its bending due to a small rotation of the reel (Fig. 53) be pure bending?

56. A flat spring consisting of two leaves of length  $2l$  and  $3l$ , respectively, is loaded by a force  $P$  at its end (Fig. 54a).

Determine how the deflection and stresses in the spring are changed if its leaves are connected at a distance  $l$  from the fixed end (Fig. 54b). The connection is assumed to be tight while simultaneously permitting free longitudinal displacements of the leaves.

57. A spring consisting of three leaves of length  $6l$ ,  $4l$ , and  $2l$  (Fig. 55) is loaded by forces  $P$ . Determine the de-

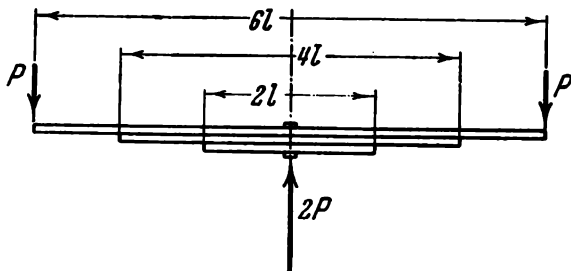


Fig. 55

flection of the spring and find the stresses induced in the leaves under the given load. Assume no friction.

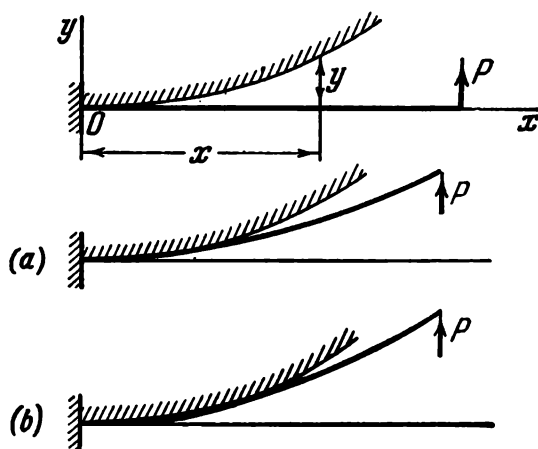


Fig. 56

58. A flat spring of uniform section (Fig. 56) subjected to bending is superposed on a rigid curve whose profile  $y = y(x)$  is given.

When considering the deflections of the spring, the question arises at the outset as to the nature of its attachment to the rigid curve. Two basic cases are possible here:

(1) The spring is closely attached to the rigid curve over a portion from the fixed end to some point (Fig. 56a).

(2) The spring makes contact with the rigid curve at one point only (Fig. 56b).

Assuming that the function  $y(x)$  is monotonic itself and monotonic in its nearest derivatives and, further, that  $y$  is small compared with  $x$ , examine in what case one or the other of the above-mentioned types of attachment will occur.

59. A homogeneous straight beam of length  $l$  and weight  $P$  rests on a rigid plane (Fig. 57). Determine the magnitude

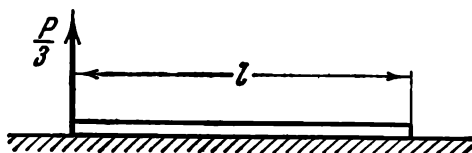


Fig. 57

of the stresses developed in the beam when a force  $P/3$  is applied to its end.

60. An elastic beam fits snugly, but without friction, in a hole drilled out in a rigid base (Fig. 58). Physical

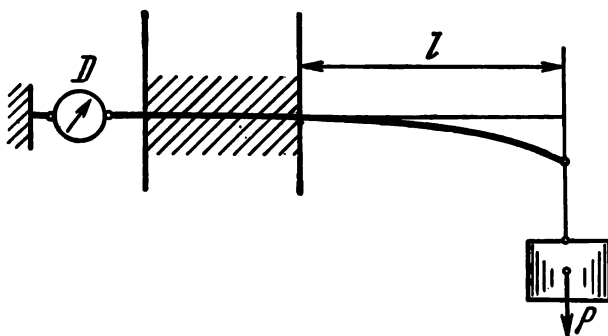


Fig. 58

intuition suggests that, on being loaded by a transverse force  $P$ , the beam will slip out from the hole. But... it is not clear

under the action of what forces. What will the dynamometer  $D$  show if the frictional forces are zero?

61. On a rigid shaft of diameter  $D$  (Fig. 59) is mounted a cut elastic ring whose inner diameter is  $D - \Delta$ , i.e., less than the diameter of the shaft by  $\Delta$ . When fitted, the ring obviously somewhat straightens out. Determine the law

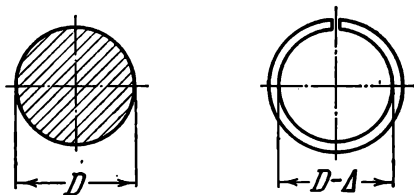


Fig. 59

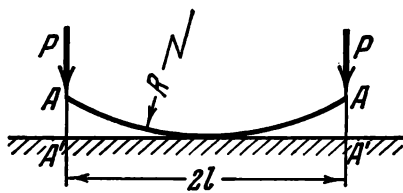


Fig. 60

of variation of the bending moment along the contour of the ring and examine the nature of the force interaction between the ring and shaft.

62. A cambered flexible spring bent into a circular arc of radius  $R$  is pressed against a rigid plane by two forces  $P$  (Fig. 60). At what values of the forces  $P$  will the points  $A$  be held against the plane?

63. Two beams of channel section are joined together by narrow transverse strips of great stiffness welded on the top

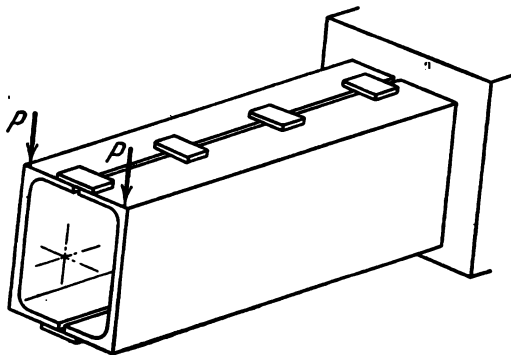


Fig. 61

and bottom flanges. The resultant composite beam is fastened at one end and loaded by forces  $P$  at the other (Fig. 61).

What are the forces sustained by the transverse strips?

64. Determine the distribution of shearing stresses in a thin-walled closed triangular section under transverse bending (Fig. 62).

65. Determine the law of distribution of shearing stresses at cross sections of a rod of variable thickness  $h$  (Fig. 63).

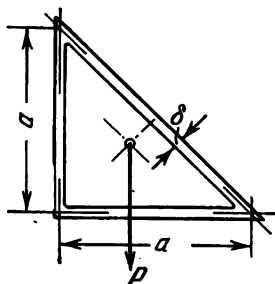


Fig. 62

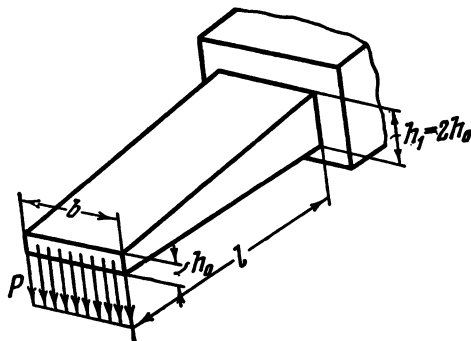


Fig. 63

66. Is it possible to select the law of distribution of a load  $q(x)$  which is not identically zero (Fig. 64) to keep the beam straight?

67. A very long continuous beam consisting of a large number of equal spans is loaded by a moment  $M$  at the left end (at the first support) (Fig. 65). Determine the bending moment and the slope of the beam at the  $i$ th support.

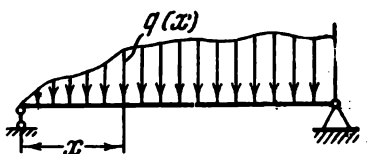


Fig. 64

68. Solve the preceding problem for the case of a finite number of supports  $n$  (Fig. 66).

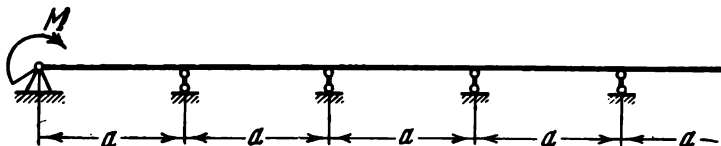


Fig. 65

69. By using the displacement equations open the statical indeterminacy of the following system (Fig. 67).

When the frame is loaded by a force  $P$ , the point  $A$  of the contour of the frame slides with friction along a rigid horizontal plane. The coefficient of friction is  $f$ . The rigidity of all segments of the frame is the same and equal to  $EI$ .

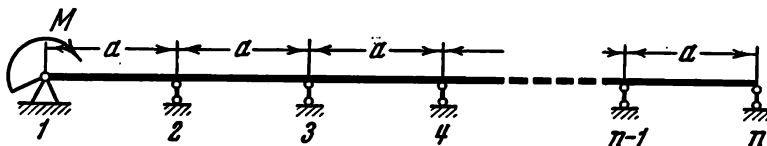


Fig. 66

70. A geometrically unchangeable system consisting of pin-connected bars is known as a truss. The bars of a truss act in tension or compression.

In actual structures the bars of a truss are not connected by pins but are rigidly connected by welding or riveting. Is it permissible in this case to design a truss on the assumption that the bars still act only in tension or compression and to disregard the bending of the bars in the design? If the bars are rigidly connected, a truss is no longer a truss but is transformed into a frame!

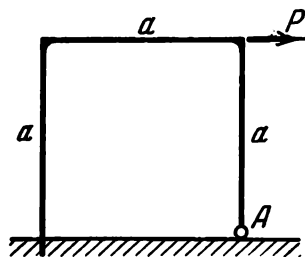


Fig. 67

71. Can the determinant of a system of canonical equations (displacement equations in the force method)

$$\begin{vmatrix} \delta_{11} & \delta_{12} & \delta_{13} & \dots & \delta_{1n} \\ \delta_{21} & \delta_{22} & \delta_{23} & \dots & \delta_{2n} \\ \dots & \dots & \dots & \dots & \dots \\ \delta_{n1} & \delta_{n2} & \delta_{n3} & \dots & \delta_{nn} \end{vmatrix}$$

be zero?

72. Determine the deflection of a slotted spring (Fig. 68) compressed by forces  $P$  assuming that the necks between the rings have sufficiently great stiffness compared with the other parts of the spring.

The dimensions of the spring are indicated in Fig. 68.

73. Show that the area under the moment diagram for any

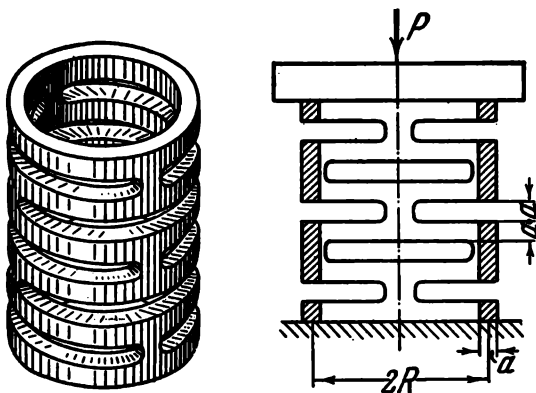


Fig. 68

closed contour of a plane frame of uniform rigidity is zero, i.e.,

$$\oint M_b ds = 0.$$

74. Show that, for any closed contour of a plane frame

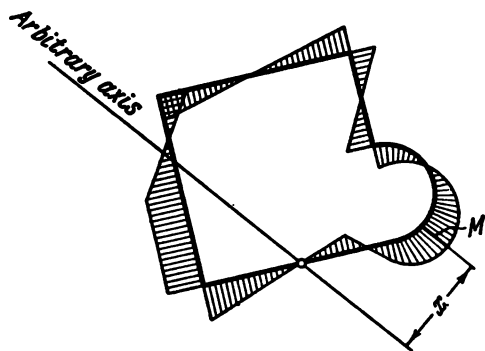


Fig. 69

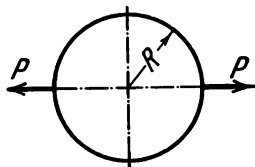


Fig. 70

having one hinge (on the assumption of uniform rigidity),

$$\oint M_b x ds = 0,$$

where  $M$  is the bending moment,  $x$  is the distance to any axis through the hinge (Fig. 69).

The integration is extended over the entire contour of the frame.

75. Show that the area bounded by the contour of a plane circular inextensible frame subjected to bending by a plane force system with small displacements remains unchanged, i.e., equal to  $\pi R^2$  (Fig. 70).

76. A straight wooden rod of rectangular cross section floats on the water surface (Fig. 71).

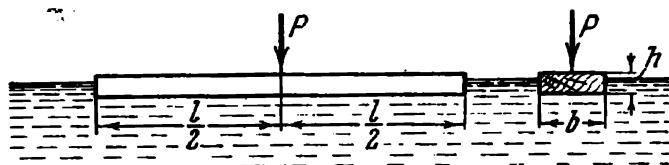


Fig. 71

Determine the stresses developed in the rod and the displacement of the point of application of the force  $P$  if  $P = 50$  kgf,  $l = 10$  m,  $b = 20$  cm,  $h = 10$  cm. The wood is pine with specific weight  $0.6$  gf/cm<sup>3</sup> and modulus of elasticity  $E \cong 10^6$  kgf/cm<sup>2</sup>.

77. Two sheets of equal thickness  $h$  and width  $b$  are bonded by a lap joint (Fig. 72). The sheets are bent in the plane of the drawing.

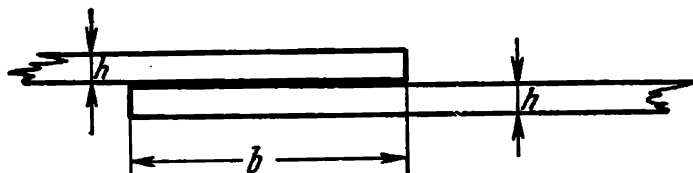


Fig. 72

Determine the law of force transmission from one sheet to the other on the assumption that the glue layer is elastic. The thickness of the glue layer is  $\delta$ , the moduli of elasticity are  $E_g$  and  $G_g$ .

78. Determine the forces acting in the spokes of a bicycle wheel and the stresses developed in the rim when a force  $P$  is applied to the wheel axle (Fig. 73). The ground on which the wheel bears may be assumed hard. The number of spokes

$n$  is large enough to allow the spokes to be treated not as separate bars but as a continuous medium.

Carry out a numerical calculation with the following data given:  $P = 40$  kgf, wheel radius  $R = 31$  cm, moment of inertia of rim section  $I = 0.3$  cm<sup>4</sup>, number of spokes  $n = 36$ , spoke diameter  $d = 2$  mm. The material of the rim and spokes is steel,  $E = 2 \times 10^6$  kgf/cm<sup>2</sup>.

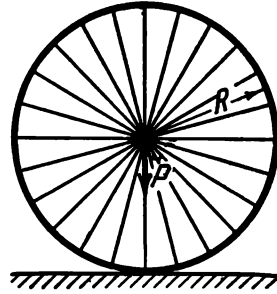


Fig. 73

79. Various temperature regulators very often incorporate so-called bimetallic elements. A bimetallic element represents two rigidly connected metallic plates with different coefficients of thermal expansion,  $\alpha_1$  and  $\alpha_2$  (Fig. 74). On being heated, the bimetallic plate is bent due to unequal extensions of its components. If one end of the plate is securely fastened, then the other, free, end will move by a certain amount. The resulting displacements are used as a source of motion and the necessary mechanical forces.

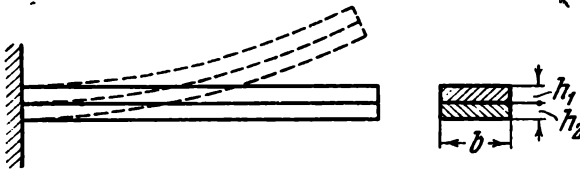


Fig. 74

Find how the curvature of the plate varies with its geometrical dimensions and the heating temperature.

80. A bimetallic ring having the dimensions indicated in Fig. 75 is heated  $t$  degrees centigrade. Determine the magnitude of the angle  $\varphi$  through which the section of the ring rotates, assuming the shape of this section to be unchanged.

The coefficients of thermal extension of the component parts of the ring are  $\alpha_1$  and  $\alpha_2$ .

81. A temperature regulator of a thermostat has been designed which employs as a sensitive element a bimetallic plate mounted as shown in Fig. 76. As the temperature rises, the

plate, in the designer's idea, begins to bend. When the temperature reaches a given value, the contact *A* closes and the

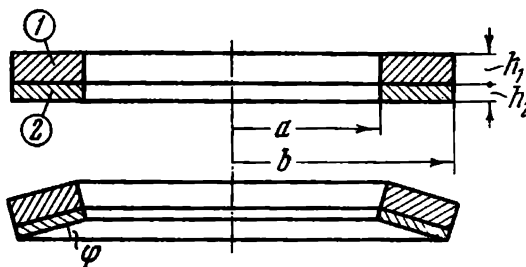


Fig. 75

command relay regulating the heating of the thermostat comes into action.

Will such a system function?

82. Show that a plane closed bimetallic frame of constant section, on being heated uniformly, does not change its curvature, irrespective of the shape of the contour (Fig. 77).

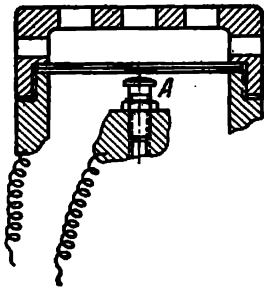


Fig. 76

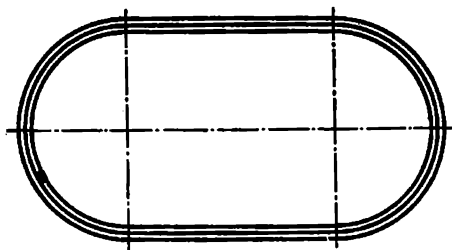


Fig. 77

83. Three rods having the same flexural rigidity but different shapes of cross section (Fig. 78) are bent in the vertical plane by moments  $M$ . Construct a graph showing the relation between the curvature and the moment  $M$  for each rod if the tensile stress-strain diagram of the material can be represented schematically by a broken line (Fig. 78)

$$\frac{\sigma_y}{E} = 0.002,$$

84. A rod of rectangular cross section (Fig. 79) is bent in the vertical plane so that plastic deformations are produced

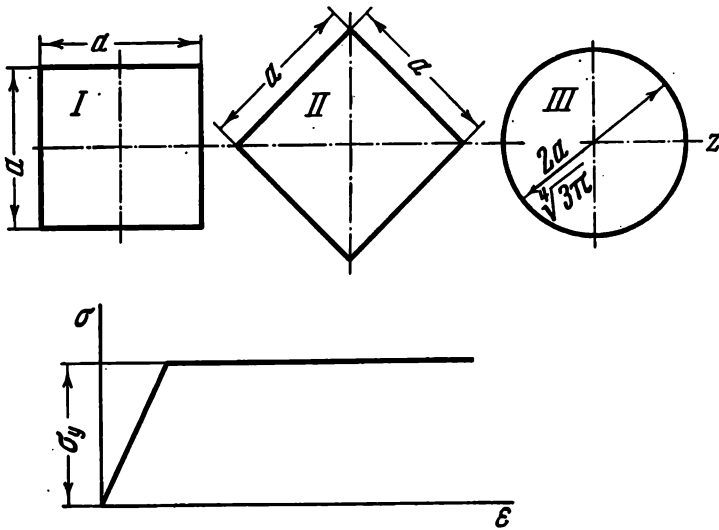


Fig. 78

in it. As in the preceding problem, the test diagram of the material corresponds to the properties of ideal plasticity.

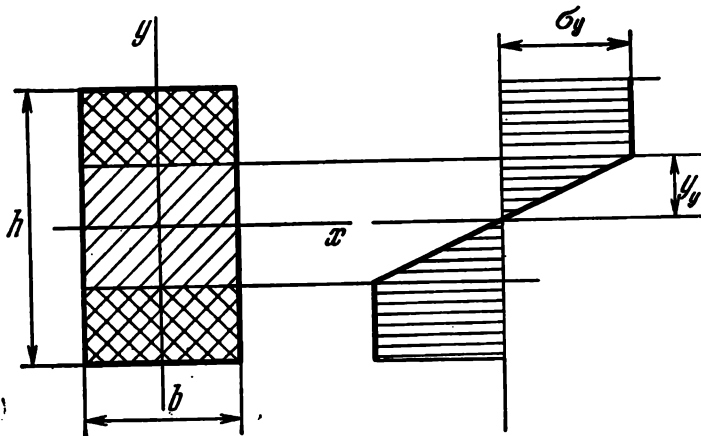


Fig. 79

Determine the flexural rigidity of the rod in the second principal plane if the moment  $M_y$  is applied while the moment  $M_x$  is held constant.

85. A set of thin circular disks (Fig. 80) are fitted on a bolt of the same material as the disks and tightened by a nut with a force  $P$ . The resulting rod is bent by two mo-



Fig. 80

ments  $M$ . Determine the change in curvature of the rod and the stresses developed in it on condition that the magnitude of the moment  $M$  is sufficient to open the contact surfaces on the bottom side of the rod. The material follows Hooke's law. The bolt diameter  $d$  may be taken equal to the inner diameter of the disks.

### III. Combined Stresses and Strength Theories

86. A cylinder of inner diameter  $d_1$  and outer diameter  $d_2$  is subjected to pressure uniformly distributed over (a) the ends, (b) the inside and outside surfaces, (c) the entire surface (Fig. 81).

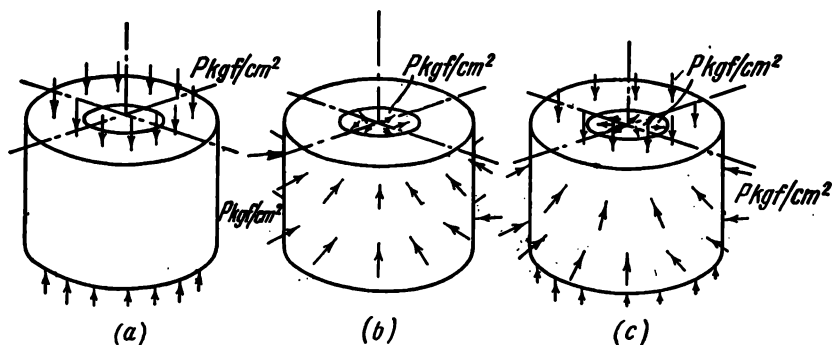


Fig. 81

Determine the change in inner diameter and the change in internal volume of the cylinder in each of the above cases of loading.

87. How many elastic constants must be introduced in order to characterize fully the elastic properties of wood?

88. Determine the principal stresses in the state of stress shown in Fig. 82.

89. For the general case of the state of stress (Fig. 83) show the following:

(1) If, for two mutually perpendicular planes (for example, for planes perpendicular to the  $x$  and  $y$  axes), the following condition is fulfilled

$$\tau_{yx} = k\sigma_x, \quad \tau_{yz} = k\tau_{xz}, \quad \sigma_y = k\tau_{xy}, \quad (1)$$

where  $k$  is some constant, then the state of stress cannot be triaxial (it is either biaxial or uniaxial).

(2) If, in addition to condition (1), the following condition is also fulfilled

$$\tau_{zx} = n\sigma_x, \quad \sigma_z = n\tau_{xz}, \quad \tau_{zy} = n\tau_{xy}, \quad (2)$$

then the state of stress is uniaxial.

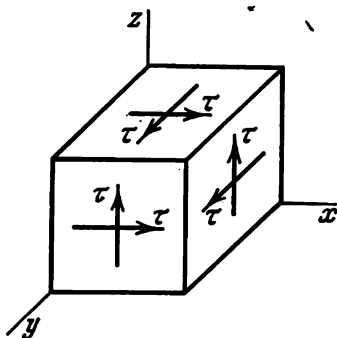


Fig. 82

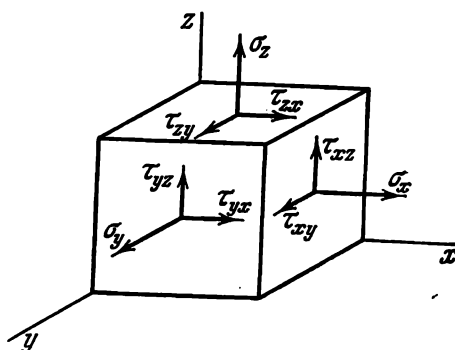


Fig. 83

90. Without determining the principal stresses and without calculating  $\sigma_{eq}$ , decide which of the two states of stress (Fig. 84) is more dangerous from the standpoint of the energy theory of strength.

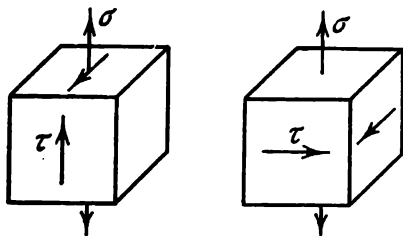


Fig. 84

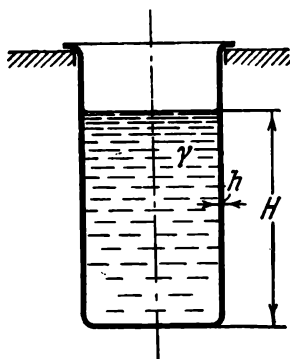


Fig. 85

91. According to the maximum shearing stress theory, construct the  $\sigma_{eq}$  diagram along a generator of a cylindrical vessel (Fig. 85) filled to a depth  $H$  with a liquid of specific weight  $\gamma$ . In solving the problem, assume that the cylinder is very thin-walled and the bending stresses developed in its walls are insignificant,

92. A thin-walled tube (Fig. 86) is subjected to internal pressure  $p$  and a bending moment  $M$ .

By using the maximum shearing stress theory, examine the relation between the design stress  $\sigma_{eq}$  and the magnitude of  $M$  for the given pressure  $p$ .

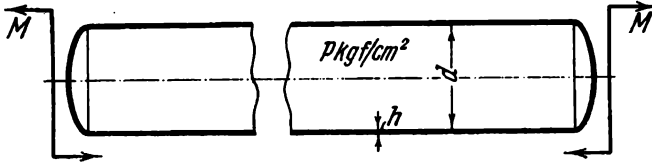


Fig. 86

93. A thin-walled spherical vessel of radius  $R = 0.5$  m and thickness  $h = 1$  cm is subjected to an internal pressure  $p_1 = 320$  at. and an external pressure  $p_2 = 300$  at. (Fig. 87).

It is required to determine the factor of safety  $n_y$  for the walls of the vessel if the yield stress of the material is known to be  $\sigma_y = 3000$   $\text{kgf/cm}^2$ .

Will the following solution be correct?

Consider an element isolated from the wall at the inner

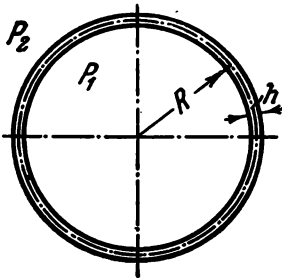


Fig. 87

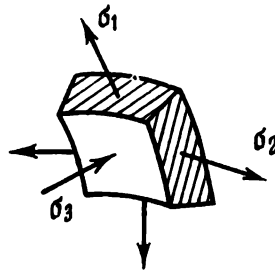


Fig. 88

surface of the vessel (Fig. 88). The principal stresses  $\sigma_1$  and  $\sigma_2$  are determined by the well-known stress formula for a spherical vessel

$$\sigma_1 = \sigma_2 = \frac{(p_1 - p_2)}{2h} R, \quad \sigma_3 = -p_1.$$

By the maximum shearing stress theory

$$\sigma_{eq} = \sigma_1 - \sigma_3 = \frac{(p_1 - p_2) R}{2h} + p_1.$$

$$\sigma_{eq} = \frac{20 \times 50}{2 \times 1} + 320 = 820 \text{ kgf/cm}^2, \quad n = \frac{\sigma_y}{\sigma_{eq}} = \frac{3000}{820} = 3.66.$$

94. A thin-walled tube of thickness  $h$  is mounted snugly, but without negative allowance, on a solid cylinder (Fig. 89).

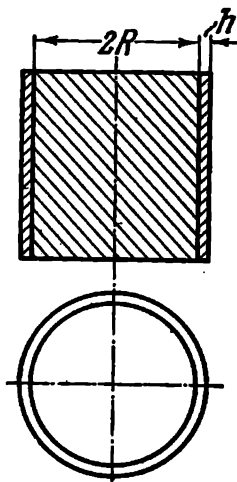


Fig. 89

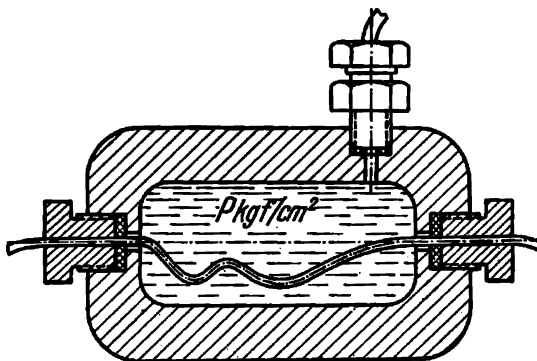


Fig. 90

The system is immersed in a liquid and subjected to a uniform pressure  $p$ . Based on the concepts of the maximum shearing stress theory, indicate the conditions under which there is a possible loss of elastic properties of the tube, if the elastic constants of the cylinder and tube are given.

95. In a vessel (Fig. 90) is placed a fine, perfectly flexible wire whose ends are brought out through holes in the bottoms of the vessel. The seals are made ideally and the wire passes in them without friction.

How will the wire behave if a pressure  $p$  is produced in the vessel? What is the state of stress in it?

96. In one of the books devoted to the problems in hydraulics we happened to see a description of the procedure for determining the compressibility factor of liquids.

"In determining the compressibility of a liquid it is necessary to eliminate the effect of the expansion of a vessel

under pressure. For this purpose a vessel *A* filled with a test liquid *C* and mercury *D* is placed in the Reck-nagel apparatus (Fig. 91) filled with water.

The pressure exerted on the piston, being transmitted by the Pascal law, acts on the mercury and, through it, on the test liquid in the vessel *A* compressing it. The vessel *A* is subjected to the same pressure inside and outside, and therefore it cannot change its capacity."

Does the procedure outlined above eliminate the effect of the change in volume of the vessel under pressure?

97. Two bars of mild steel are tested in tension (Fig. 92). The first bar is smooth. The diameter of the section is  $d$ .

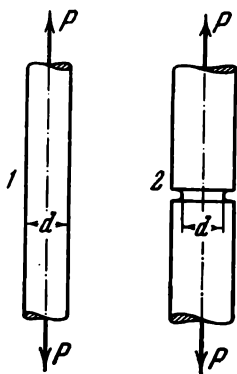


Fig. 92

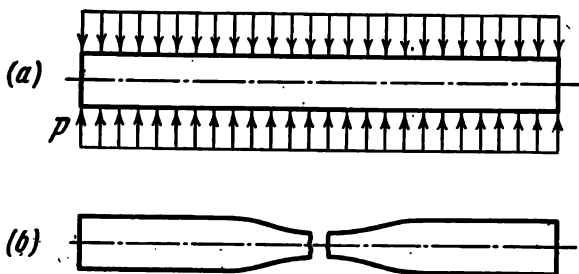


Fig. 93

The second bar has a narrow circular notch. The diameter of the weakened section is also  $d$ .

Which of the bars will sustain a larger static load under otherwise identical conditions?

98. What methods can you suggest for realizing pure shear?

99. How can a state of uniform all-round tension ( $\sigma_1 = \sigma_2 = \sigma_3 = \sigma > 0$ ) be achieved?

100. In studying the properties of materials under high pressure it has been found that at a sufficiently large pressure a straight cylindrical bar stressed by pressure over the cylindrical surface and free at the ends may rupture, as shown in Fig. 93, after necking. The bar appears to be "bitten" in two.

Explain the reasons for this type of fracture.

101. A notched specimen is made of a material whose tensile stress-strain diagram is shown in Fig. 94a. According

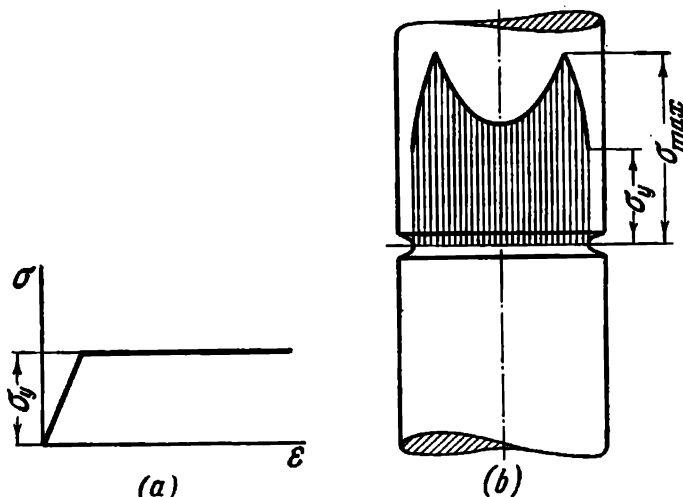


Fig. 94

to theoretical investigations by G. V. Uzhik,\* the normal stress diagram across the section of the bar in the zone of the notch is as shown in Fig. 94b. From the stress-strain diagram, however, it is seen that  $\sigma_{\max}$  cannot be greater than  $\sigma_y$ . The above stress diagram therefore gives rise to a doubt regarding its authenticity and the correctness of the analysis from which it was derived.

Is this doubt justified?

102. Can you indicate a point, in a long tensioned strip with a hole (Fig. 95), at which the state of stress is a uni-axial compression with the same stress  $\sigma$  as the tension applied to the strip?

\* Izv. Akad. Nauk SSSR. Otd. Tekh. Nauk, No. 10, 1547-1560 (1948).

103. A thin-walled circular cylinder having a small hole in its wall is simultaneously twisted by moments  $M$  and

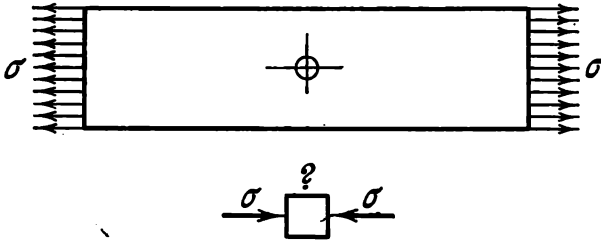


Fig. 95

extended by forces  $P$  (Fig. 96). If the cylinder were only twisted, the maximum stress  $\sigma_{\max}$  would occur at points  $A$  (Fig. 96a) and would be of amount  $2\tau$ . If the cylinder were

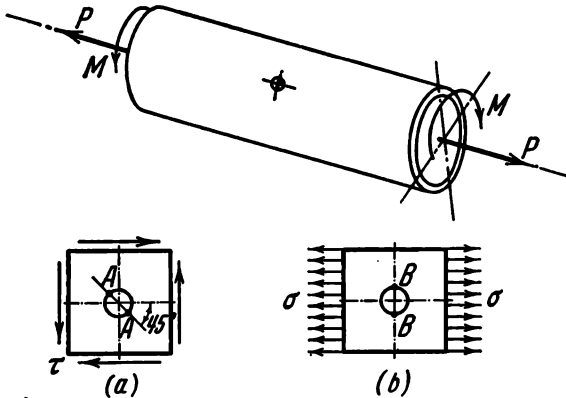


Fig. 96

only extended, the stress  $\sigma_{\max}$  would occur at points  $B$  (Fig. 96b) and would be of amount  $3\sigma$ .

What is  $\sigma_{\max}$  for the combination of the moments  $M$  and the forces  $P$ ? At what point does this stress occur? In solving the problem use only reference data on local stresses.

104. A straight rod of circular cross section is twisted by two moments  $M$ . The rod develops plastic strains. How can the relation between the torque  $M$  and the angle of twist  $\theta$  be determined if the tensile stress-strain diagram  $\sigma = f(\epsilon)$  of the material is given?

## IV. Stability

105. A slender elastic bar is mounted in vertical slides (Fig. 97). The bar is clamped at its lower end in a movable plug bearing on a coil spring of stiffness  $k$  ( $\lambda = \frac{P}{k}$ ).

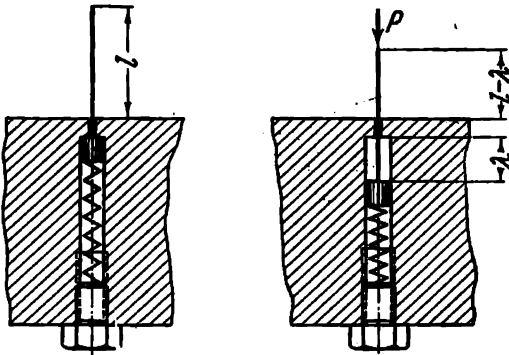


Fig. 97

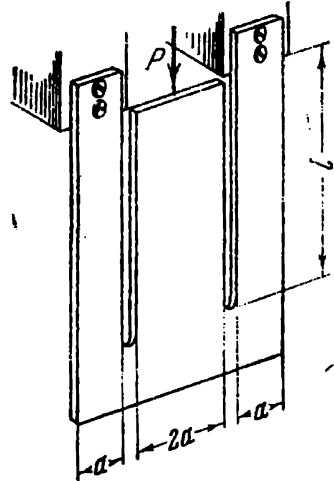


Fig. 98

As the compressive force  $P$  increases, the length  $l - \lambda$  of the outward-projecting part of the bar decreases, the length  $\lambda$  of the lower part increases. What should be the spring stiffness  $k$  in order that the bar, moving downward an amount  $l$ , does not lose stability in either the upper or the lower part?

106. A shaped plate is fixed and loaded as shown in Fig. 98. Determine the critical force for the plate in two cases:

- (1) the force acts downward;
- (2) the force acts upward.

The flexural rigidity of the middle part is equal to the sum of the rigidities of the outer parts.

107. Find the critical value of the force  $P$  for the bar shown in Fig. 99. The ends of the bar are hinged and undergo no horizontal or vertical displacements.

108. A long bolt fits loosely into a tube (Fig. 100). Determine the tightening force  $P$  on the bolt at which the system will lose stability. The dimensions of the tube are such

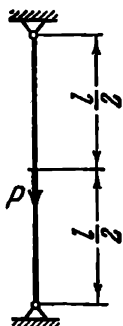


Fig. 99

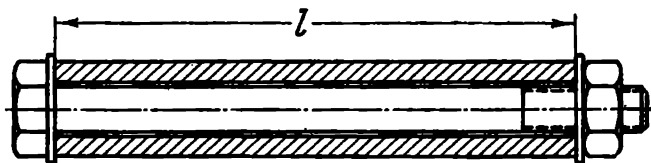


Fig. 100

that it is to be treated as a long bar and not as a shell. The flexural rigidity of the tube is  $E_1 I_1$ . The rigidity of the bolt is  $E_2 I_2$ .

109. A bar hinged at the ends (Fig. 101) is uniformly heated.

Assuming that the supports are absolutely stiff, we determine the normal compressive force induced in the bar. It obviously has the value  $N = \alpha t EA$ . When  $N = \pi^2 EI / l^2$ , the straight form of equilibrium of the bar must be unstable and, on further heating, the bar will buckle. From this we find the critical temperature

$$t_{cr} = \frac{\pi^2 I}{\alpha A l^2}.$$



However, the preceding discussion is open to doubt. When considering the problem of the stability of a column compressed by forces  $P$ , Fig. 101 it is assumed that the magnitude of the forces  $P$  remains unchanged during buckling and is independent of the curvature of the column. In the present case, however, the slightest curvature of the bar is accompa-

nied by a decrease in the force  $N$ , and hence there is no reason to extend formally the solution of the fundamental problem to this case. It is possible, therefore, that here the critical force  $N$  will differ from the adopted value  $\pi^2 EI/l^2$ .

How to clear up this doubt?

110. The principal approximate method of determining critical loads is the energy method. The required form of equilibrium is assigned approximately so as to satisfy the boundary conditions and to make the assumed function fit as closely as possible the true form of equilibrium, unknown to us but intuitively suggested by the physical nature of the problem.

Examine whether there is a danger here that, as the fitting function approximates indefinitely the exact shape of the elastic curve, we shall not obtain the exact value of the critical force.

111. Determine the critical force for the bracket shown in Fig. 102.

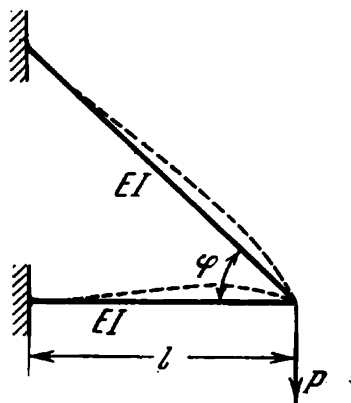


Fig. 102

The bars are fixed and rigidly connected to each other. The bending due to instability occurs in the plane of the bracket.

112. A plane hinged frame consisting of rigid bars is stiffened by two elastic diagonals connected together (Fig. 103), each of length  $2l$ . The cross section of the diagonals is rectangular with dimensions  $b$  and  $h$  ( $b \gg h$ ). If the frame is loaded by a force  $P\sqrt{2}$ , as shown in Fig. 103, one diagonal will be extended, and the other compressed by the forces  $P$ .

At what value of the force  $P$  will the bars buckle out of the frame plane?

113. It is known that a long straight bar twisted by two moments may lose stability under certain conditions. This kind of instability shows up most vividly when twisting threads and ropes. If a thread is twisted, it will very soon assume a curvilinear shape, such as is shown in Fig. 104. It is quite evident that if the thread is pulled while being

twisted, the torsional moment at which instability occurs markedly increases. During winding the rope must always be pulled in tension.

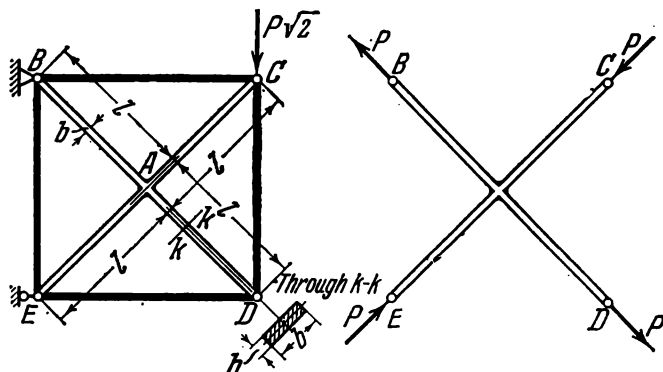


**Fig. 103**

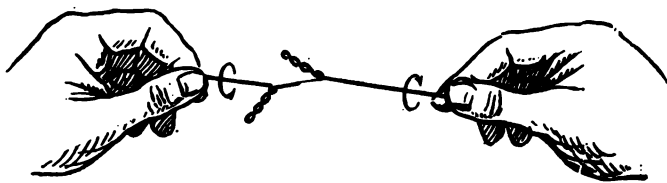


**Fig. 104**

Referring to a hinged bar (Fig. 105), determine the magnitude of the critical twisting moment and find how it depends on the tensile force.

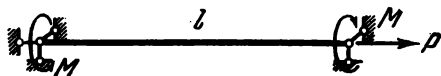


**Fig. 105**

114. A bar of constant section  $A$  is subjected to a uniform hydrostatic pressure  $p$  (Fig. 106). Under these conditions the bar is obviously acted on by a longitudinal compressive force  $P = pA$ .

Can this force cause an instability of the bar at a sufficiently large pressure?

115. A straight wooden bar of constant cross section is immersed in water at one end. The bar is clamped at water level (Fig. 107). Can this bar lose stability under the action of Archimedes buoyant forces if the length  $l$  is sufficiently great?

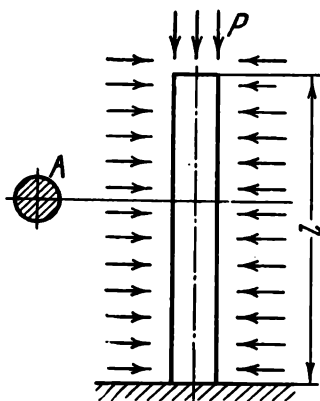


Fig. 106

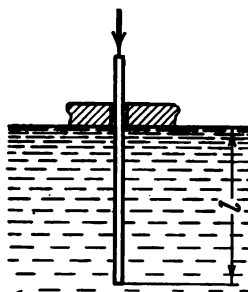


Fig. 107

116. A tube clamped at its lower end (Fig. 108) is being filled through the upper opening with a liquid of specific weight  $\gamma$ . Can this tube lose Euler stability while being filled?

117. A thick-walled straight tube (Fig. 109) is filled with an incompressible liquid. A plug is inserted without friction into the upper opening. The tube and plug are hinged as shown in Fig. 109. When a force  $P$  is applied to the plug, the liquid is compressed, but there is no longitudinal compressive force in the tube.

Can the tube lose Euler stability under these conditions?

118. A slender long tube is slipped without friction over a rigid stationary plug at its upper opening. The lower end of the tube is clamped in a rigid base (Fig. 110). A pressure  $p$  is delivered into the tube.

Can this tube lose stability at a sufficiently large pressure?

119. A fluid of specific weight  $\gamma$  is run through a tube simply supported at its ends (Fig. 111). Show that at a certain value of the velocity of the fluid  $v$  the tube loses stability, just as a bar loses Euler stability.

120. Consider the following problem. A bar (Fig. 112) having roundings at the ends of radius  $R$  is compressed

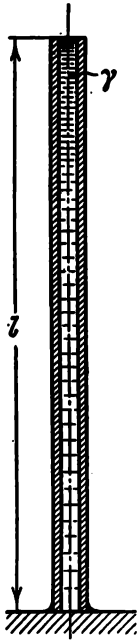


Fig. 108

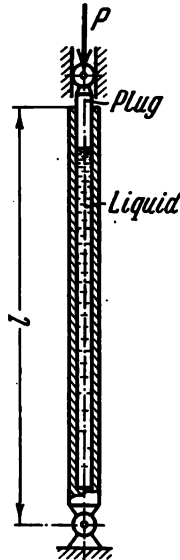


Fig. 109

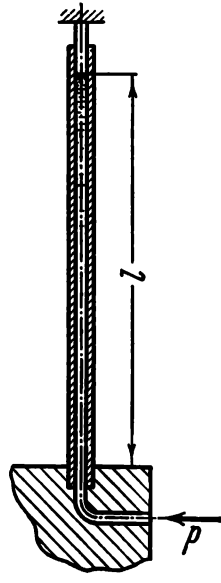


Fig. 110

without friction between two rigid plates. It is required to determine the critical force.

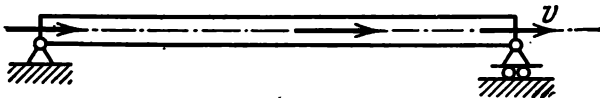


Fig. 111

Choosing the  $x$  axis along the line of action of the compressive forces, and denoting by  $y$  the transverse displacement of the axis of the rod, we obtain, as usual,

$$\begin{aligned} EIy'' + Py &= 0, \\ y'' + \alpha^2 y &= 0, \\ y &= A \sin \alpha x + B \cos \alpha x \\ (\alpha^2 &= \frac{P}{EI}). \end{aligned}$$

At the ends of the bar the displacement  $y$  is proportional to the slope  $y'$ , i.e.,

$$y = -Ry' \quad \text{when } x = 0;$$

since to a positive slope  $y'$  corresponds a negative displacement  $y$ , a minus sign is put before  $Ry'$ . We thus obtain

$$B = -\alpha RA,$$

$$y = A (\sin \alpha x - \alpha R \cos \alpha x).$$

Further,  $y = +Ry'$  when  $x = l$ ; here  $y$  is positive for a positive  $y'$ . Consequently,

$$\begin{aligned} A (\sin \alpha l - \alpha R \cos \alpha l) &= \\ &= A (\alpha R \cos \alpha l + \alpha^2 R^2 \times \\ &\times \sin \alpha l). \end{aligned}$$

Since  $A \neq 0$ , we find

$$\tan \alpha l = \frac{2\alpha l \frac{R}{l}}{1 - (\alpha l)^2 \frac{R^2}{l^2}}. \quad (1)$$

From this transcendental equation we determine the smallest non-zero value of  $\alpha l$  as a function of the ratio  $R/l$  and then find the critical force.

Since  $\alpha^2 = P/EI$ , the critical force is

$$P_{cr} = \frac{(\alpha l)^2 EI}{l^2}; \quad (2)$$

here for  $\alpha l$  we must substitute the first (smallest) root of Eq. (1).

We now determine the smallest root  $\alpha l$  of Eq. (1) as a function of  $R/l$ . This relation is most conveniently established by assigning several values of  $\alpha l$ , and then determining  $R/l$  from Eq. (1). The results of the calculations are represented as a curve in Fig. 113. From this we find that  $\alpha l = \pi$  when  $R/l = 0$ , and hence from (2)

$$P_{cr} = \frac{\pi^2 EI}{l^2}.$$

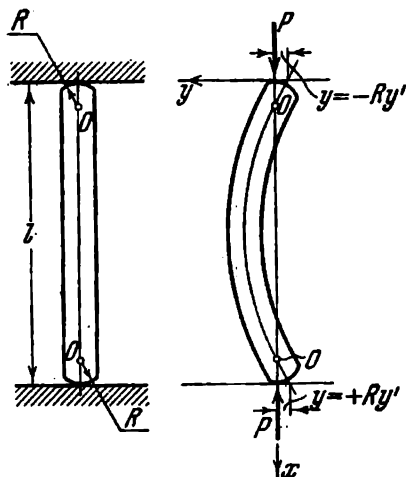


Fig. 112

The critical force is equal to the common Euler's force, which was to be expected.

As  $R/l$  increases, the quantity  $\alpha l$  rises, and so does the critical force. This is also quite evident. But, as follows

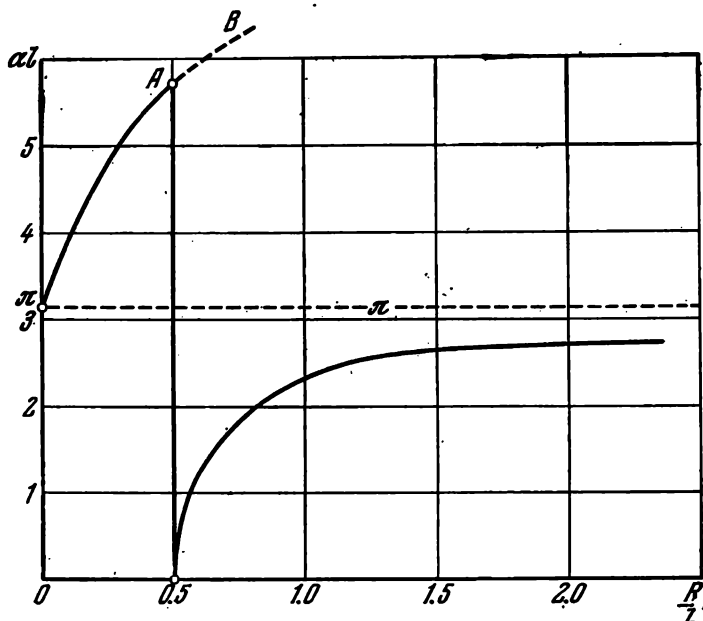


Fig. 113

from the curve, when  $R/l = 0.5$  the critical force suddenly drops to zero and then, as the radius  $R$  increases, begins again to rise regaining, in the limit when  $R/l = \infty$ , the value of Euler's force.

Interpret this result.

121. A long elastic bar with simply supported ends is inserted with a clearance  $\Delta$  into a rigid tube (Fig. 114).

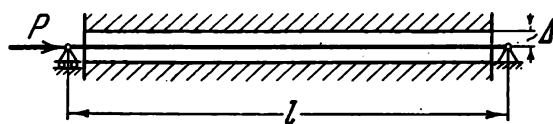


Fig. 114

What are the stresses occurring in the bar if it is compressed by a force greater than the first critical force, i.e.,

greater than  $\pi^2 EI/l^2$ ? The flexural rigidity of the bar is  $EI$ .

122. Determine the critical force for a bar fixed at both ends (Fig. 115).

The flexural rigidity of the bar is different ( $EI_1$  or  $EI_2$ ) depending on the sign of the bending moment. This is the property, for example, of a rod having slots on one side with tight-fitting strips (Fig. 115). The unequal flexural rigidity depending on the sign of the bending moment occurs

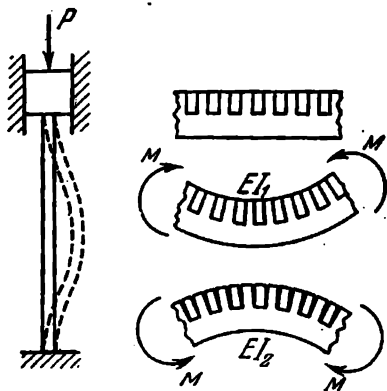


Fig. 115

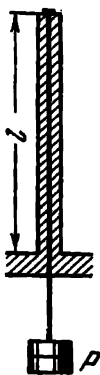


Fig. 116

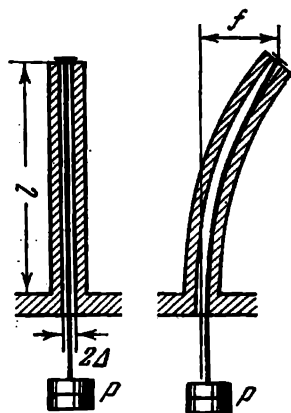


Fig. 117

also in the case of a compressed bar of unsymmetrical section if plastic deformations are involved (see Prob. 155).

123. A bar clamped at one end has an axial through hole into which is inserted without clearance and friction a flexible rope attached to the free end of the bar (Fig. 116). Can this bar lose stability if a sufficiently large weight  $P$  is suspended from the rope?

124. The scheme considered in the preceding problem is changed. The rope is inserted with a clearance equal to  $\Delta$  each way (Fig. 117). Determine the lateral displacement  $f$  of the end of the bar as a function of the force  $P$ .

125. A column fixed at its lower end is loaded at the free end by a vertical force transmitted through a rope (Fig. 118). Transmission of force through the rope is accomplished in two variants. In the first case the rope moves down freely. In the second case the rope passes without friction over two rigid pulleys. In which case is the critical force  $P_{cr}$  for the column larger?

126. Referring to the preceding question, we can pose the following problem. Determine the critical force for a

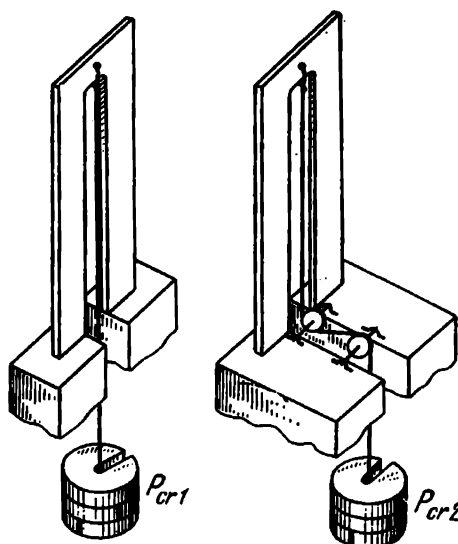


Fig. 118

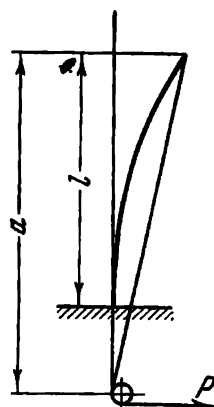


Fig. 119

column of length  $l$  as a function of the distance  $a$  from the end of the column to a pulley (Fig. 119).

127. Two bars of equal rigidity but different length (Fig. 120) are compressed by a longitudinal force  $P$ .

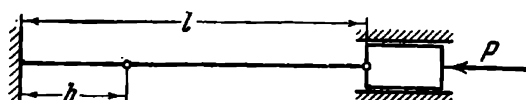


Fig. 120

At what distance from the fixed end should a hinge be placed in order to provide the same stability factor for both columns?

128. Over a frictionless bar there passes a cord at the end of which a force  $P/2$  is applied so that the bar is compressed by the force  $P$ . The left end of the cord is securely fastened (Fig. 121).

As the bar is deflected from the vertical, one-half of the cord comes into close contact with the lateral surface of the bar, giving rise to contact pressure. On the other side of the bar the cord freely assumes a vertical position.

Determine the critical force.

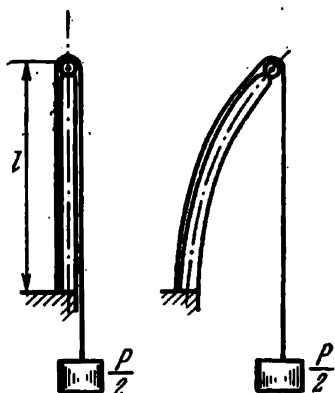


Fig. 121

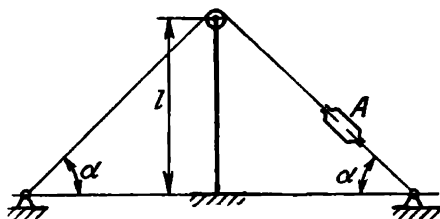


Fig. 122

129. A bar fixed at one end has a frictionless pulley at the other end over which passes a rope (Fig. 122). The rope is tightened by means of a screw joint  $A$ , and a compressive force  $P$  is produced in the bar.

Determine the value of the force  $P$  at which the straight-line form of equilibrium of the bar becomes unstable.

130. A ring is subjected to an external uniformly distributed load (Fig. 123). Will there be any difference in the values of the critical load if it is produced by a pressure which is always directed along the normal to an arc of the ring or if it is produced by radial forces always directed towards the centre?

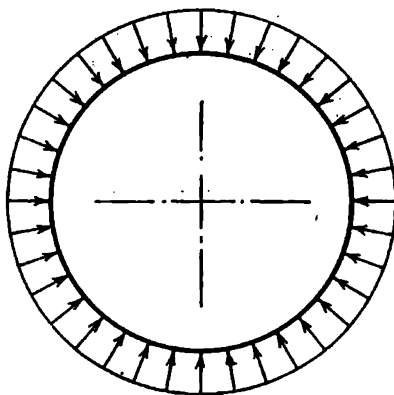


Fig. 123

The first type of loading may, for example, be realized by the pressure of the air delivered into a rubber ring-shaped

bag (Fig. 124a), and the second by a system of elastic cords passing through a centrally located stationary bush (Fig. 124b).

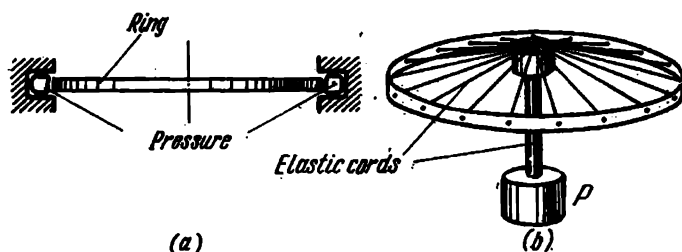


Fig. 124

131. There is a cylinder and two pistons with a pressure  $p$  delivered into the interspace between the pistons (Fig. 125).

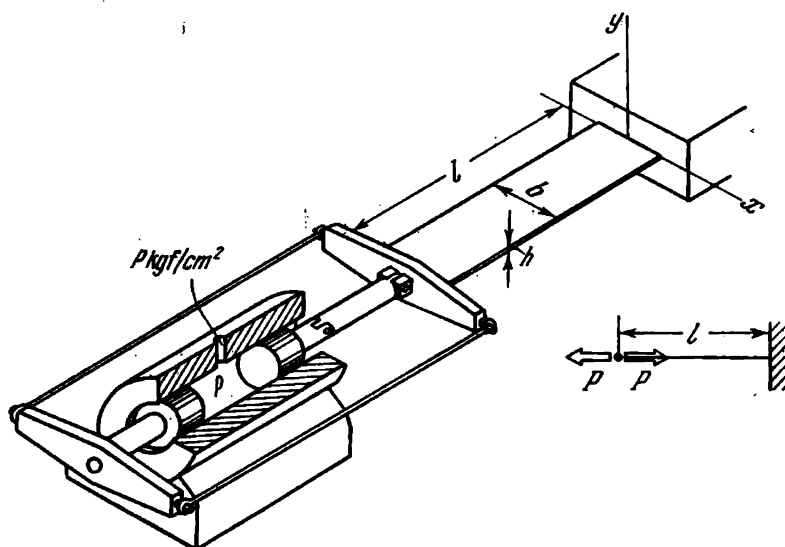


Fig. 125

The induced forces are transmitted through a piston rod and two tie rods to a bar of length  $l$ . Thus the bar is loaded by two equal and opposite forces  $P$  applied to its end.

Is this position of equilibrium stable?

132. A bar fixed at one end is loaded at the other by two equal and opposite moments produced by four weights  $P$  (Fig. 126). Examine the stability of the system.

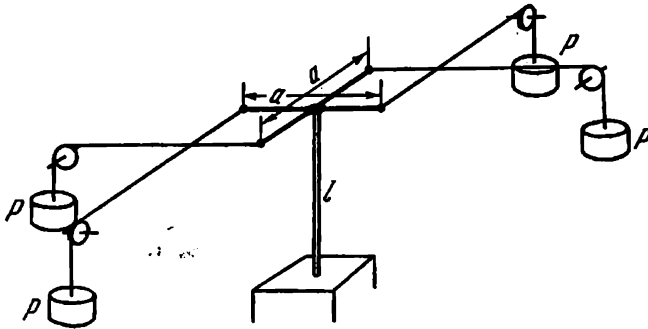


Fig. 126

133. With reference to the preceding problem the question arises as to whether the value of the critical moment depends on the manner in which the arms of the forces are oriented with respect to the principal axes of the section.

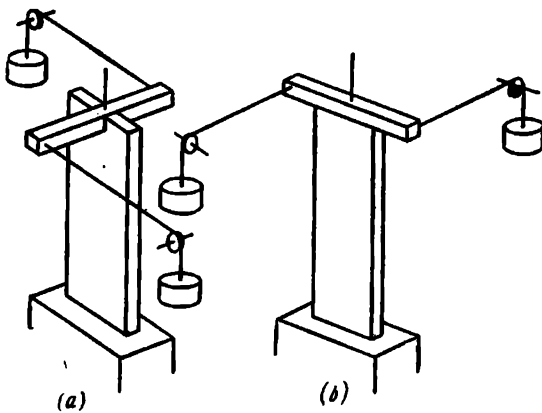


Fig. 127

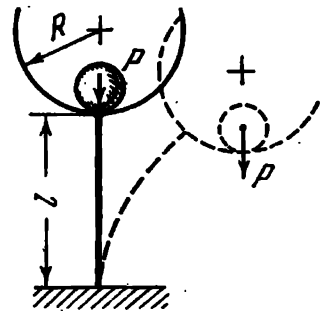


Fig. 128

In the case (a) (Fig. 127) the plane of the moment  $M$  rotates together with the end section during the bending about the axis of minimum rigidity, and in the case (b) during the bending about the axis of maximum rigidity.

134. How does the magnitude of the critical force  $P$  depend on the radius of a cup  $R$  (Fig. 128)?

135. When designing a water tower the question arose as to the stability of the structure shown in Fig. 129. At what level of the liquid in the tank will the supporting pole lose stability?

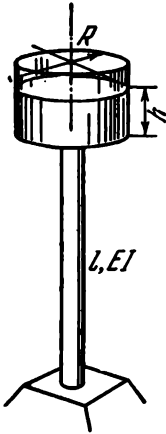


Fig. 129

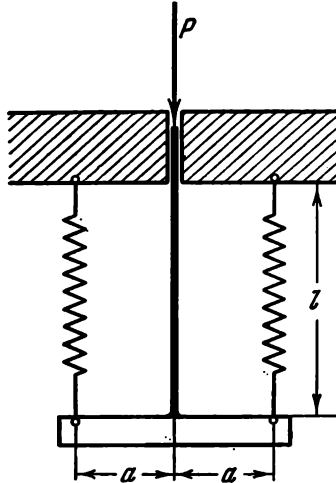


Fig. 130

136. Find the critical value of the force  $P$  for the system shown in Fig. 130 on the assumption that the bending of the bar takes place in the plane of the drawing.

The stiffness of the springs in tension is  $k$ . The strip of length  $2a$  is to be considered as absolutely rigid.

137. A bar having plane ends is compressed between two plates (Fig. 131a). After buckling there are two possible fundamental curvilinear forms of equilibrium: the first form, shown in Fig. 131b, at the critical force

$$P_{cr} = \frac{4\pi^2 EI}{(2l)^2}.$$

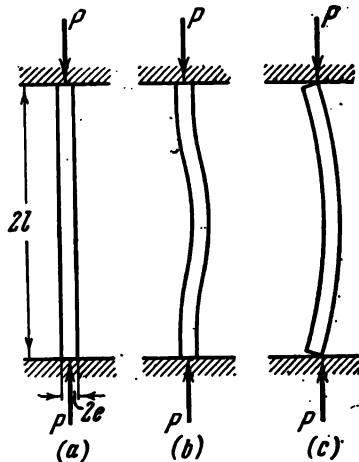


Fig. 131

and the second form, shown in Fig. 131c, when the bar bears against the planes only with its corners.

Obviously, if the ends are not very wide, the second mode of instability occurs at a force smaller than in the first case. In particular, if the width of the ends is zero, the critical force is

$$P_{cr} = \frac{\pi^2 EI}{(2l)^2}.$$

Determine the lowest critical force in the case when the width of each end is  $2e$ .

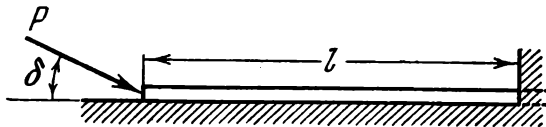


Fig. 132

138. A weightless beam (Fig. 132) fixed at one end rests on a rigid base. At the centre of the free end the beam is loaded by a force  $P$  directed at an angle  $\delta$  to the rigid base. At what value of  $P$  (for a given  $\delta$ ) will the beam lose stability?

139. An absolutely rigid  $\Gamma$ -shaped beam (Fig. 133) is stiffened by a thin elastic bar of length  $2l$ . Examine the stability of the system.

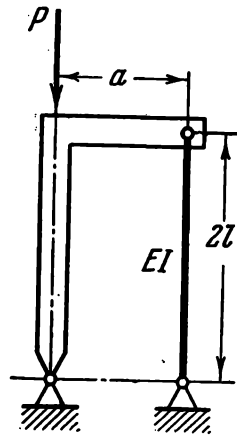


Fig. 133

140. On a thin-walled ring is thrown a thin inextensible absolutely flexible string which is subsequently tightened with a force  $P$  (Fig. 134). At what value of the force  $P$  will the ring lose stability? Friction between the surface of the ring and the string may be disregarded.

141. Into a rigid casing is inserted an elastic ring (Fig. 135) which is then heated. Contact forces are developed between the ring and the casing. Can the ring lose stability in these conditions?

142. A slender elastic bar hinged at both ends is compressed by a longitudinal force  $P$  equal to

$$10 \frac{\pi^2 EI}{l^2}.$$

Between hinged supports additional constraints are imposed on the bar which prevent it from buckling (Fig. 136).

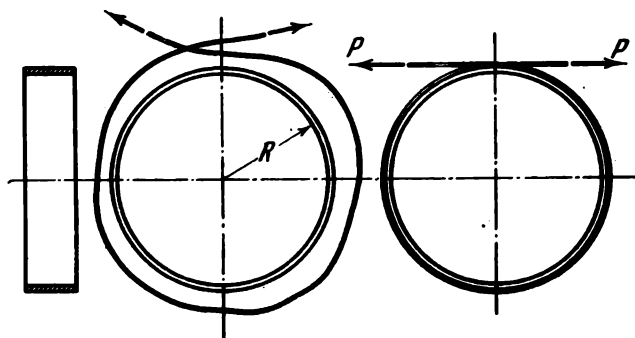


Fig. 134

If it were not for the presence of these constraints, the straight-line form of equilibrium would become unstable at

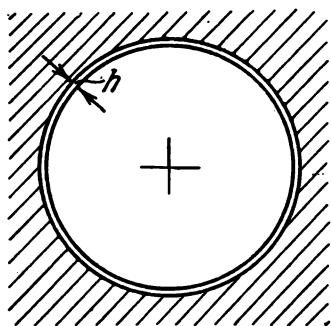


Fig. 135

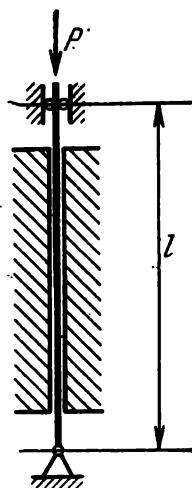


Fig. 136

a force as small as  $\frac{1}{10}P$ . In the range of the force between  $\pi^2 EI/l^2$  and  $10\pi^2 EI/l^2$  there are, as is known, two more critical values of the force, namely  $4\pi^2 EI/l^2$  and  $9\pi^2 EI/l^2$ , which correspond to the buckling of the bar in the form of two and three half-waves.

Suppose that the intermediate constraints supporting the bar are suddenly removed. Then the bar will undoubtedly buckle. But how? In one, two or three half-waves?

143. A bar (Fig. 137a) is fixed at one end. To the second end is applied a force  $P$  which possesses the property that during the bending of the bar it is always directed along the tangent to the elastic curve of the beam. Such a force may, for example, be realized by mounting a solid-propellant engine at the end of the bar (Fig. 137b).

It is required to examine the stability of the system.

144. A bar fixed at one end has, at the free end, a rigid disk to which is applied a force  $P$ . The point of application of the force is always located on the  $x$  axis (Fig. 138).

Examine the stability of the system in two cases: (a) the force  $P$  is induced by a stream of inelastic particles striking

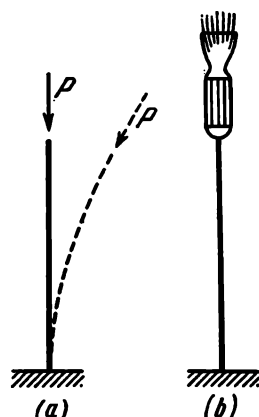


Fig. 137

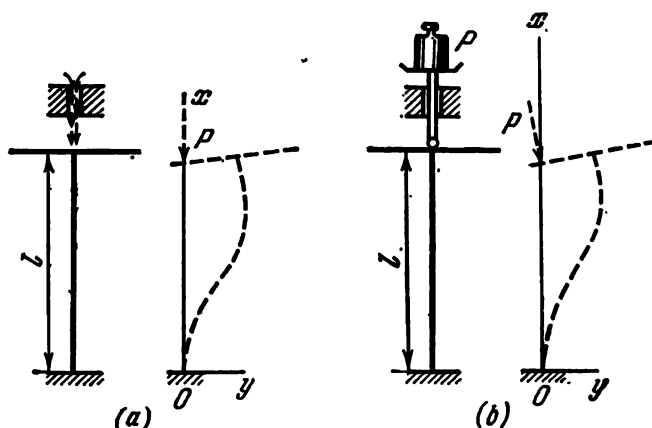


Fig. 138 ]

the disk (Fig. 138a); in this case, as the disk rotates the direction of the vector  $P$  remains unchanged; (b) the force  $P$  is induced by a weight transmitted through a rod (Fig. 138b); in this case the force  $P$  follows the normal to the disk.

145. A slender elastic homogeneous bar is in uniformly accelerated motion under the action of a follow-up force applied to one of the ends (Fig. 139). Examine the stability of the straight form of the bar.

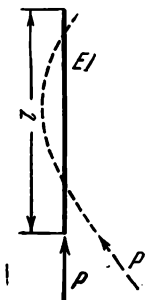


Fig. 139



Fig. 140

146. A homogeneous bar is compressed by two follow-up forces (Fig. 140). Examine the stability of the system.

147. Determine the moment  $M$  at which the cantilever (Fig. 141) bends out of its plane. The moment  $M$  is always in the vertical plane during the bending.

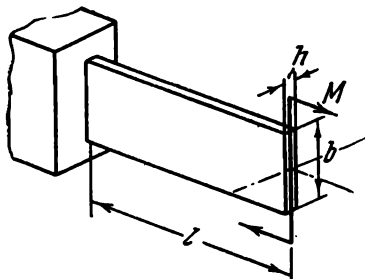


Fig. 141

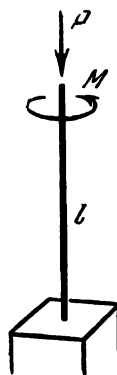


Fig. 142

148. Give an analysis of the stability of a fixed bar loaded at its end by a force  $P$  which maintains a vertical direction and by a moment  $M$  (Fig. 142).

149. Examine the stability of a pipeline, fixed at one end, in which a liquid flows (Fig. 143). The parameters of the pipeline and flow are given.

150. A thin long strip (Fig. 144) is heated uniformly along the length  $l$  and across the thickness  $h$  but non-uniformly across the width  $b$ .

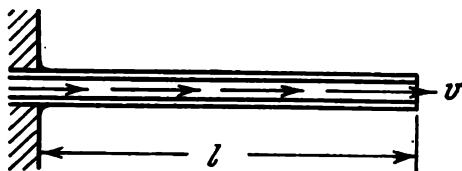


Fig. 143

Determine the conditions under which an instability of the strip occurs with twisting.

151. In all monographs and textbooks on the stability of elastic systems problems involving the stability of plane form

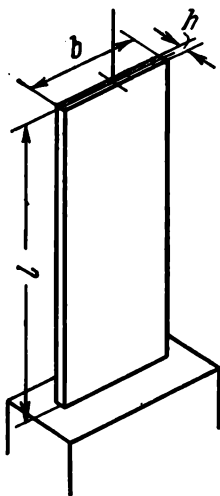


Fig. 144

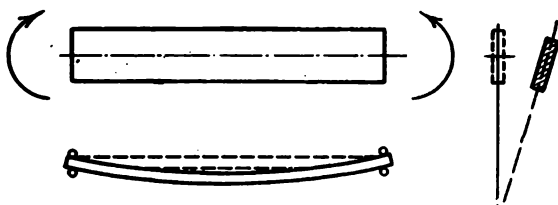


Fig. 145

of bending are formulated on the tacit assumption that the moment is applied in the plane of maximum rigidity (Fig. 145).

Can an instability of plane form of bending occur if the moment is applied, not in the plane of maximum rigidity, but in the plane of minimum rigidity?

152. A ring of radius  $R$  with a rectangular cross section (Fig. 146) is turned inside out so that the inner surface is outside and the outer surface becomes inner. For what

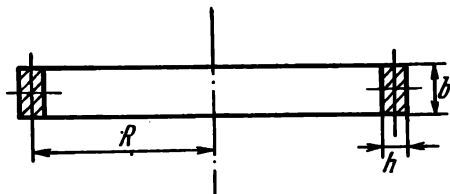


Fig. 146

relations between  $b$  and  $h$  will this form of equilibrium be stable? The deformations are assumed to be elastic.

153. A ring of rectangular cross section (Fig. 147) is heated on the inside or outside and the temperature is var-

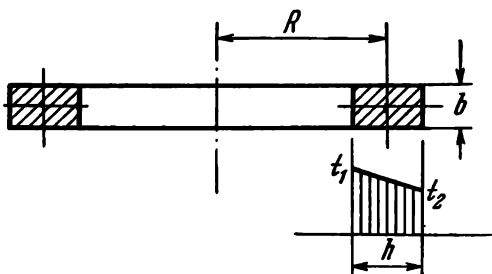


Fig. 147

iable across the thickness of the ring  $h$ . Find the conditions for stability of the original form of equilibrium assuming that  $h \ll R$ . The law of variation of the temperature may be taken as linear.

154. An elastic ring of radius  $R$  with a rectangular cross section is cut and unwrapped by two moments until its axis becomes straight (Fig. 148). The bar thus obtained is fixed at both ends.

In what cases will this form of equilibrium be stable?

155. A bar of channel section (Fig. 149) is compressed by a centrally applied force  $P$  producing plastic strains in the bar.

Which way is the bar most likely to bend during buckling?  
To the right or to the left?

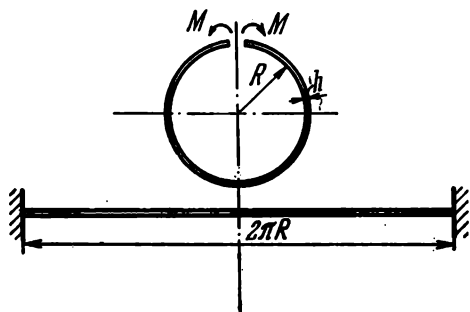


Fig. 148

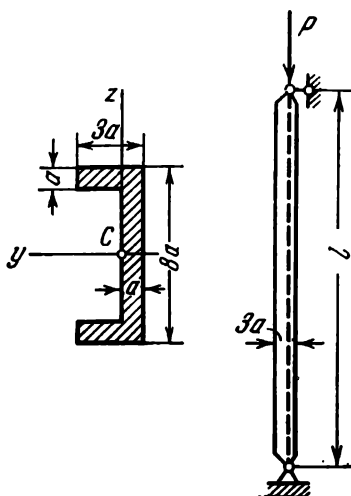


Fig. 149

156. Is it possible for a helical spring to lose stability in tension?

157. Two bars are loaded at a common joint by a force  $P$  (Fig. 150). Each bar is of telescopic construction, permitting large changes in length.

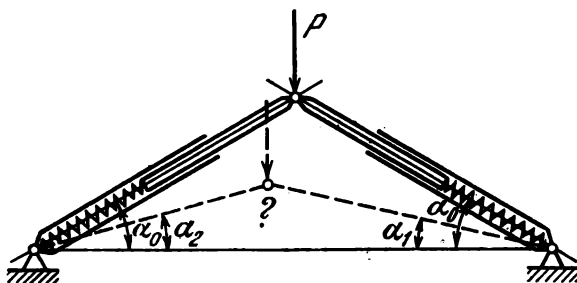


Fig. 150

Are there conditions under which the symmetrical form of equilibrium changes to an unsymmetrical one?

158. Four identical balls of mass  $m$  are fixed on bars as shown in Fig. 151.

The system rotates about an axis  $CC$  fitted in rigid bearings. If there were no bearings (if, for example, the system were hung by a cord), then, as is known from physics,

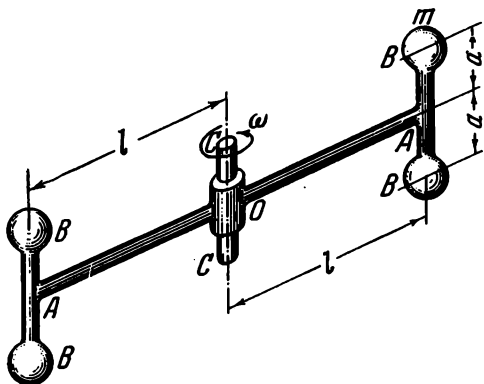


Fig. 151

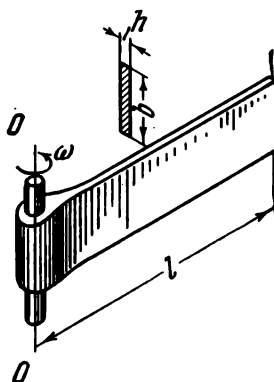


Fig. 152

the balls would turn about the axis  $AA$  into horizontal positions. In the present case such a rotation is prevented by the rigid bearings and the elastic bars  $AA$  having a

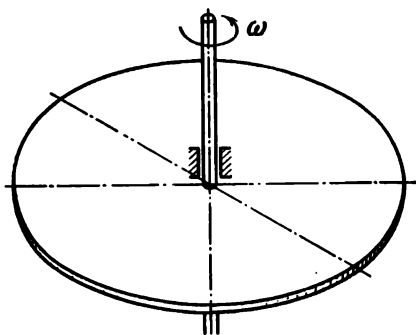


Fig. 153

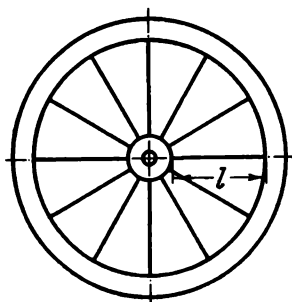


Fig. 154

circular cross section. Is it possible to select an angular velocity  $\omega$  to make the balls turn through a certain angle about the axis  $AA$ ?

159. A homogeneous bar with a narrow rectangular cross section rotates about an axis  $OO$  (Fig. 152) parallel to the longer side of the section. Determine the angular velocity

$\omega$  at which this bar will twist similarly to the bars  $AA$  of the system considered in the preceding problem.

160. A thin homogeneous disk (Fig. 153) rotates about a fixed axis perpendicular to its plane. Can this disk bend out of its plane?

161. Find the critical number of revolutions for a ring of mass  $m$  connected to a fixed axis by means of  $n$  equispaced spokes (Fig. 154). The stiffness of the spokes in tension is  $EA$ .

162. A thin-walled closed rubber spherical vessel is subjected to internal pressure.

Is the spherical form always stable?

163. Explain necking in a tensile test specimen in terms of stability of equilibrium.

## V. Miscellaneous Questions and Problems

164. What material has the highest ultimate strength?

165. What material can withstand a larger load in tension than in compression?

166. What material has the greatest modulus of elasticity?

167. What material has the least modulus of elasticity?

168. Does rubber obey Hooke's law?

169. In extending a wooden rod parallel to the grain measurements were made of the longitudinal extension and lateral contraction of the specimen. The ratio of the lateral strain to the longitudinal strain was found to be 0.6.

Is it possible to agree with this result?

170. Why is the reduced modulus of elasticity of a rope less than the modulus of elasticity of its constituent cords?

171. Why is a twisted thread stronger than an untwisted one?

172. A teacher, design supervisor, examining a design of a student, pointed out to him that the shaft of the designed machine was too long and would not have sufficient rigidity.

"This can easily be corrected without changing the construction", said the student. "I'll take a material of higher quality, make a shaft of alloy steel".

Was the student right?

173. For a certain beam (Fig. 155) loaded at a point  $A$  by a concentrated force  $P$  the need arose to make measurements of the elastic curve, i.e., to establish experimentally the law of variation of vertical displacements along the length  $x$ . The shape of the beam is so complex that the determination of the elastic curve by an analytical method would present considerable difficulties. At the experimenter's disposal there is only one indicator for measuring displacements, such as is shown in Fig. 155.

What is the easiest way to measure the elastic curve of the beam under these conditions if it is known beforehand that its deflections are proportional to the acting force  $P$ ?

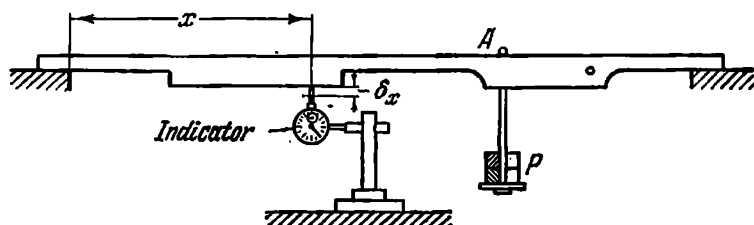


Fig. 155

174. A solid elastic cylinder of height  $H$  and radius  $R$  resting on a rigid plane (Fig. 156) is subjected to its own weight (the weight of the cylinder is  $P$ ). How will the volume of the cylinder be changed if it is placed on its side?

175. An elastic body of arbitrary shape is compressed by two equal and opposite forces  $P$  (Fig. 157).

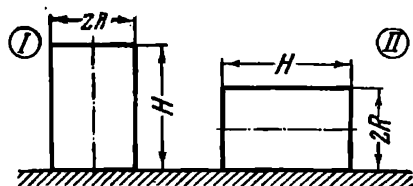


Fig. 156

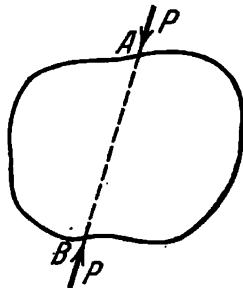


Fig. 157

Determine the change in volume of the elastic body.

176. A major part in pressure-measuring instruments is the so-called Bourdon spring which represents a hollow tube of oval or any other elongated section bent in the form of a circular arc (Fig. 158). Under the action of the internal pressure such a tube somewhat straightens out and the displacement of the end of the tube is transmitted to the pointer of a manometer through a multiplier (Fig. 159). The deflection of the pointer indicates the magnitude of the pressure being measured.

In one of the books devoted to measuring instruments we happened to see the following explanation of the principle of operation of the Bourdon tube:

"The action of the Bourdon spring is based on the fact that the pressure inside the tube on the outer surface of the spring is larger than the pressure on its inner surface. Indeed,

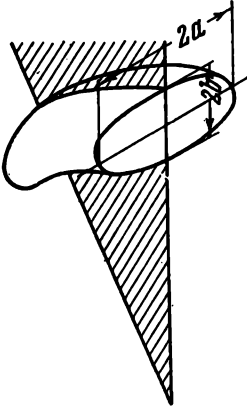


Fig. 158

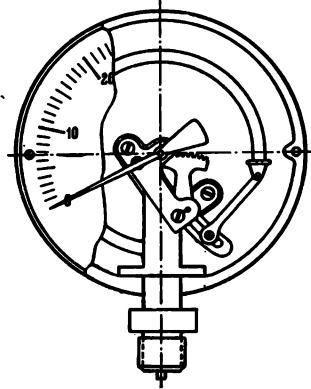
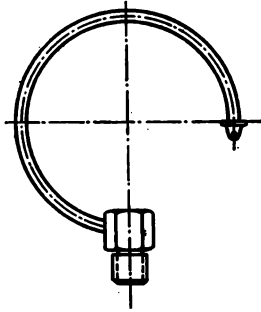


Fig. 159

if the tube is of rectangular section and if  $R_1$  and  $R_2$  denote the outside and inside radii of the tube, then the outer ( $S_1$ ) and inner ( $S_2$ ) surfaces of the tube are, respectively,

$$S_1 = \frac{2\pi\varphi}{360} R_1 a \quad \text{and} \quad S_2 = \frac{2\pi\varphi}{360} R_2 a,$$

where  $\varphi$  is the central angle of the spring,  $a$  is the dimension in a plane perpendicular to the plane of the drawing,  $R_1$  and  $R_2$  are the radii.

At a pressure  $p$  kgf/cm<sup>2</sup> the total pressure on the external surface is

$$P_1 = S_1 p \text{ kgf}$$

and on the internal surface

$$P_2 = S_2 p \text{ kgf},$$

the force  $P_1$  being greater than the force  $P_2$  and tending to straighten the spring."

Is this explanation correct?

177. A plywood sheet is an example of an anisotropic plate. If two differently oriented strips are cut out from it (Fig. 160) and tested in tension, they will show different extensions under the same force.

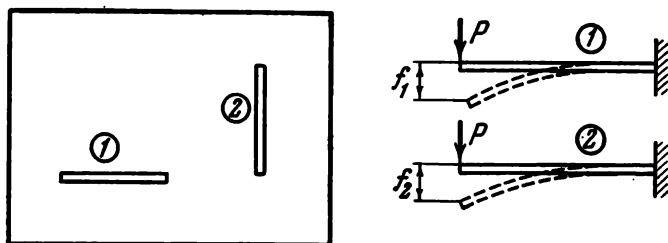


Fig. 160

Let the modulus of elasticity in tension for the first strip be  $E_{1t}$ , and for the second  $E_{2t}$ .

Can it be stated that the deflections of the strips  $f_1$  and  $f_2$  in a bending test will be in the same ratio as  $E_{2t}/E_{1t}$ ?

178. Consider a closed toroidal shell of the inner tube type (Fig. 161) under internal pressure  $p$  and determine

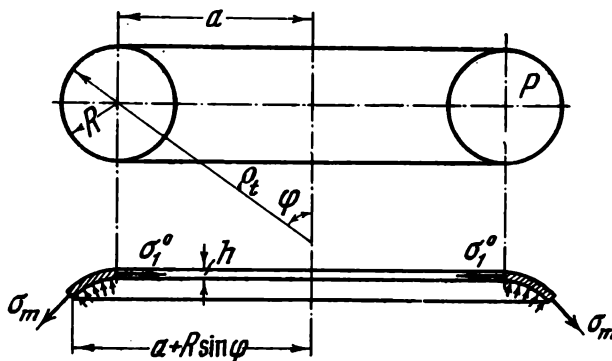


Fig. 161

the stresses occurring in this shell. From the condition of equilibrium for a part of the shell cut off by a conic section (Fig. 161) we obtain

$$p\pi [(a + R \sin \varphi)^2 - a^2] = \sigma_m 2\pi (\alpha + R \sin \varphi) h \sin \varphi,$$

$$\sigma_m = \frac{pR}{2h} \frac{2a + R \sin \varphi}{a + R \sin \varphi}. \quad (1)$$

The circumferential stress  $\sigma_t$  is found from the well-known equation

$$\frac{\sigma_m}{\rho_m} + \frac{\sigma_t}{\rho_t} = \frac{p}{h}.$$

In our case

$$\rho_m = R,$$

$$\rho_t = \frac{a}{\sin \varphi} + R.$$

On substituting for  $\rho_m$ ,  $\rho_t$ , and  $\sigma_m$ , we obtain

$$\sigma_t = \frac{pR}{2h}. \quad (2)$$

We now proceed to the determination of displacements. Denote by  $u$  the displacement of a point of the middle

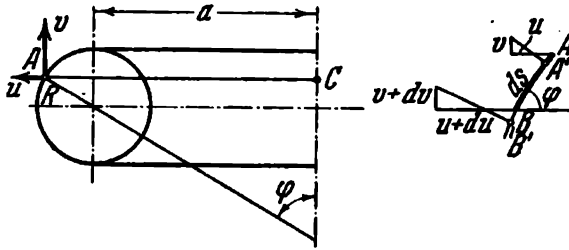


Fig. 162

surface in a direction perpendicular to the axis of rotation and by  $v$  the displacement along the axis of rotation (Fig. 162). The tensile strain in the circumferential direction is

$$\epsilon_t = \frac{u}{AC} = \frac{u}{a + R \sin \varphi}. \quad (3)$$

The meridional extension is

$$\epsilon_m = \frac{A'B' - AB}{AB} = \frac{BB' - AA'}{AB},$$

$$BB' = (u + du) \cos \varphi - (v + dv) \sin \varphi,$$

$$AA' = u \cos \varphi - v \sin \varphi, \quad AB = R d\varphi.$$

The extension along a meridian is therefore

$$\epsilon_m = \frac{1}{R} \left( \frac{du}{d\varphi} \cos \varphi - \frac{dv}{d\varphi} \sin \varphi \right). \quad (4)$$

On the other hand,

$$\varepsilon_t = \frac{1}{E} (\sigma_t - \mu \sigma_m), \quad \varepsilon_m = \frac{1}{E} (\sigma_m - \mu \sigma_t).$$

Taking into account expressions (1), (2), and (3), we find

$$u = \frac{pR}{2Eh} [a(1-2\mu) + R(1-\mu)\sin\varphi];$$

from (4) we obtain

$$\begin{aligned} \frac{dv}{d\varphi} &= \frac{pR^2}{2Eh} (1-\mu) \frac{\cos^2\varphi}{\sin\varphi} - \frac{\varepsilon_m R}{\sin\varphi} = \\ &= \frac{pR^2}{2Eh} \left[ -(1-\mu)\sin\varphi - \frac{a}{\sin\varphi(a+R\sin\varphi)} \right], \end{aligned}$$

whence

$$\begin{aligned} v = \frac{pR^2}{2Eh} \left[ (1-\mu)\cos\varphi - \ln \tan \frac{\varphi}{2} + \right. \\ \left. + \frac{2R}{\sqrt{a^2-R^2}} \arctan \left( \frac{a \tan \frac{\varphi}{2} + R}{\sqrt{a^2-R^2}} \right) \right] + C. \end{aligned}$$

The constant  $C$  determines the displacement of the torus as a rigid whole along the axis of symmetry and may be prescribed arbitrarily. When  $\varphi = 0$  and  $\varphi = \pi$ ,  $\ln \tan \frac{\varphi}{2}$  becomes infinite. Consequently, the displacement  $v$  at the same points also becomes infinite. Meanwhile, it is quite evident that this displacement cannot be infinitely large. Hence, the expression obtained for  $v$  fails to give the correct solution to the problem.

What is the matter? Where has a mistake been made?

179. Among other structural elements, in aircraft and rocket engineering use is made of high-pressure tanks. They are usually of cylindrical or spherical shape, and, as for other structural units, it is extremely important to fulfil the requirement of minimum weight for them.

A shaped cylinder construction is proposed such as is shown in Fig. 163. The walls of the vessel consist of several cylindrical sections connected by radial webs. Since the cy-

lindrical sections have a small radius, the stresses in them are reduced, and it is hoped that, in spite of the increase in weight due to the radial webs, the total weight of the struc-

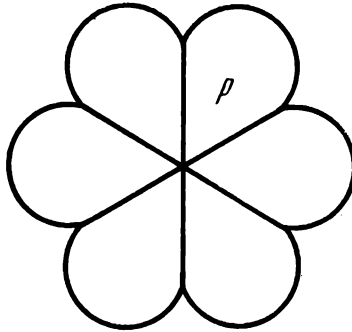


Fig. 163

ture will be smaller than for the usual cylinder having the same volume. How are these hopes justified?

180. A spring (Fig. 164) supports a weight  $P$ . If the spring has a stiffness  $k$ , the weight moves downward an

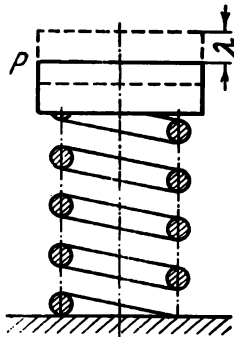


Fig. 164

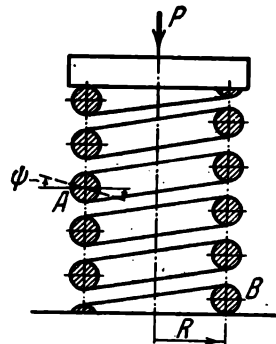


Fig. 165

amount  $\lambda = P/k$ . The potential energy of the weight (energy of position) is then reduced by

$$P\lambda = \frac{P^2}{k}. \quad (1)$$

The potential energy of the spring in the strained condition is

$$U_s = \frac{P\lambda}{2} = \frac{P^2}{2k}, \quad (2)$$

i.e., half the energy lost by the weight.

What is the matter? Where has part of the energy disappeared to?

181. Through what angle do the coils of a spring rotate in the axial plane (in the plane of Fig. 165) when the spring is compressed? (Angle  $\psi$  in Fig. 165.)

182. A helical spring with helix angle  $\alpha$  and radius of coils  $R$  is stretched by forces  $P$ . Determine the change in

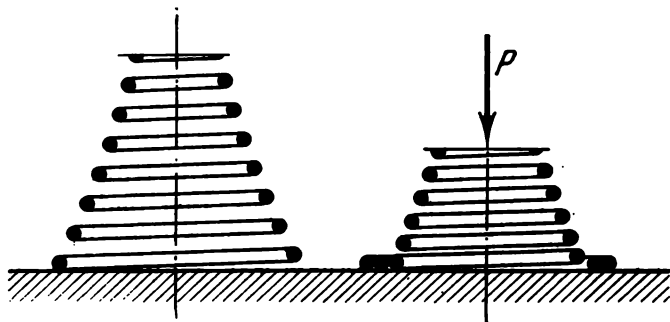


Fig. 166

height and diameter of the spring, and also the change in number of coils.

183. A shaped spring with settling-down coils (Fig. 166) is used in some instruments to obtain a non-linear relation between force and displacement. When such a spring is compressed, the lower (larger) coils deform more heavily, settle on the plane and become almost completely inoperative. Thus, as the compressive force increases, the number of operating coils of the spring decreases and the characteristic of the spring appears to be non-linear (Fig. 167a). The spring has a characteristic with increasing stiffness. The derivative of the force with respect to displacement  $dP/d\lambda$  increases.

Consider how, with the same spring, to obtain a characteristic of the type of Fig. 167b, i.e., with decreasing stiffness.

184. A  $\Pi$ -shaped frame (Fig. 168) is hinged at one end. At the other end of the frame there is a roller bearing on a rigid plane.

Determine the reaction at the lower support assuming that the force  $P$  and the stiffness of the frame are such that

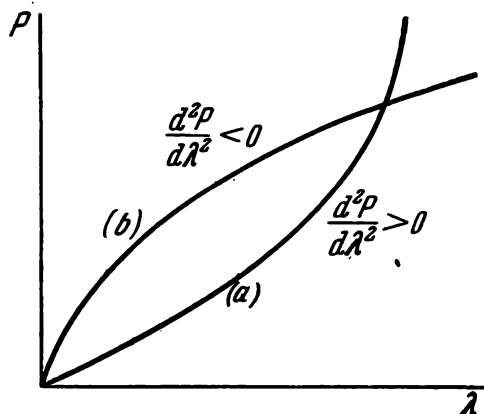


Fig. 167

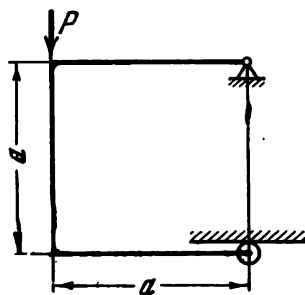


Fig. 168

the displacements produced in the frame are small compared with its original dimensions.

185. A slender flexible bar is loaded at its end by a vertical concentrated force (Fig. 169). The bar is constrained

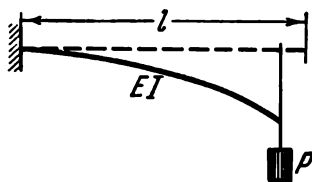


Fig. 169

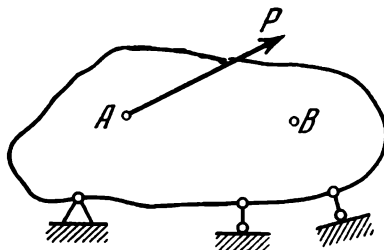


Fig. 170

to bend in the plane of action of the force (in the plane of the figure). What forms of equilibrium, besides the one shown, are possible for this bar?

186. A force  $P$  is applied at a point  $A$  of an elastic body (Fig. 170). What surface will be described by an arbitrarily

taken point  $B$  if the force  $P$  is made to rotate in space about the point  $A$ ?

187. A ring of circular cross section (Fig. 171) is loaded by uniformly distributed moments of intensity  $m$  kgf-cm/cm.

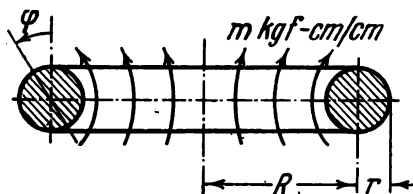


Fig. 171

Assuming  $r$  to be small compared with  $R$ , determine the angle of rotation  $\varphi$  of the sections of the ring in the axial plane as a function of  $m$  if the material of the ring follows Hooke's law.

188. How is the solution of the preceding problem altered if the ring under consideration preserves the stresses devel-

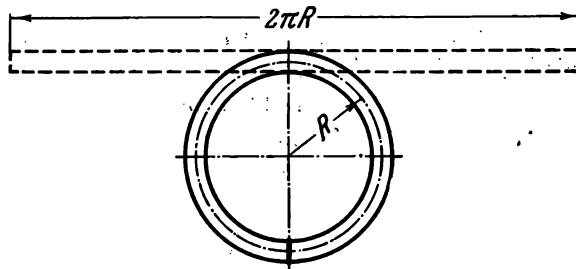


Fig. 172

oped during the bending of a straight rod into the ring (Fig. 172)? It is assumed that the bending stresses are entirely elastic.

189. In many instruments (for example, in a speedometer) a flexible shaft is used to transmit a torque, a shaft representing a thin cable which rotates freely in a stationary covering (Fig. 173). As one end of the cable rotates uniformly, so does the other end. In imperfect shafts, however, this uniformity of rotation is upset. The exit section first rotates with a deceleration and then with an acceleration so that on

the average the angular velocity at exit remains unchanged, but there is a varying component with the period of the

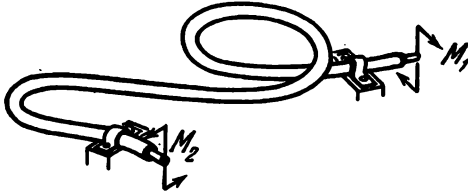


Fig. 173

rotation of the cable. This defect is due to the initial curvature present in the cable before it is placed into the covering.

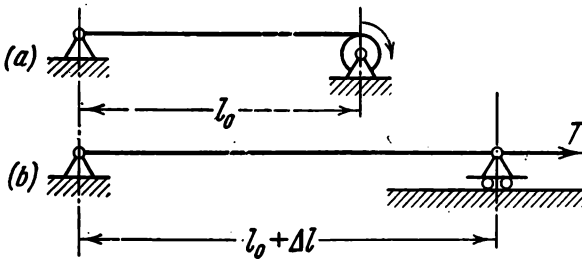


Fig. 174

Examine the above phenomenon and establish the conditions for eliminating the non-uniformity of motion. Friction between the cable and the covering may be disregarded.

190. It is well known that as a string is tightened, its frequency of vibration increases (the tone is raised).

Examine how the frequency of vibration of a rubber cord is changed as it is tightened in two cases of fixing shown in Fig. 174a

and b. The tensile test diagram of the cord is given (Fig. 175).

191. A long beam is fixed at one end. Under the action of forces of gravity  $q$  it drops on a rigid plane situated an amount  $h$  lower than the fixed end (Fig. 176). There remains

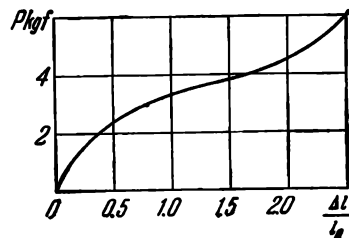


Fig. 175

a free portion of length  $l$ . At the right end of the free portion the beam is fixed, and the remaining free part of the

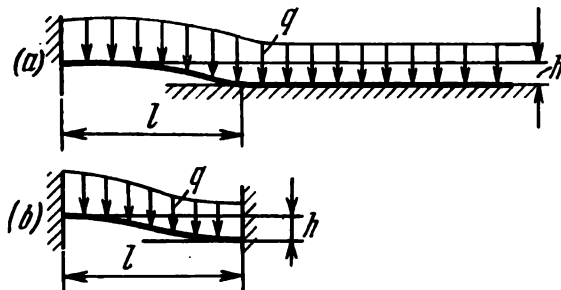


Fig. 176

supporting plane at the left is removed. Determine the fundamental frequency of the beam thus obtained (Fig. 176b)

192. An open-ended thin-walled rubber cylinder is turned inside out (Fig. 177). What shape will it assume after the

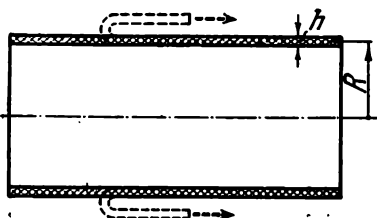


Fig. 177

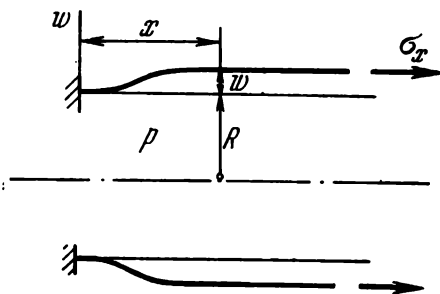


Fig. 178

above operation if it is known that the strains in the cylinder are purely elastic? The rubber may be taken to obey Hooke's law (see the answer to Question 168).

193. The solution of the problem of the axially symmetric deformation of a thin-walled cylinder under internal pressure (Fig. 178) is reduced, as is known, to the solution of the differential equation

$$w^{(IV)} + 4k^4 w = \frac{p}{D},$$

where  $w$  is the displacement normal to the surface of the shell,

$$D = \frac{Eh^3}{12(1-\mu^2)} \quad \text{and} \quad 4k^4 = \frac{Eh}{R^2D}.$$

If, in addition to the pressure  $p$ , the shell is acted on by an axial tensile force producing an axial stress  $\sigma_x$ , to the right-hand side of the equation is added a term  $-\mu h \sigma_x / RD$

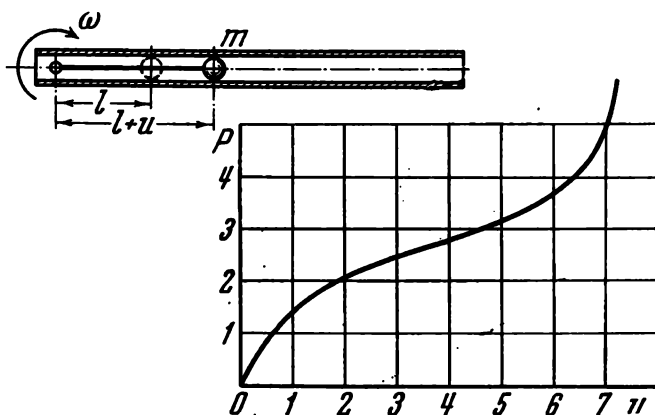


Fig. 179

which takes account of the presence of the lateral contraction of the cylinder due to Poisson's effect; and the matter usually rests here. Meanwhile, owing to the curvature of the meridian  $w''$ , the longitudinal stress  $\sigma_x$  gives a component force along a normal acting together with the pressure  $p$ , with the result that a term  $-\frac{h\sigma_x}{D} w''$  must be introduced into the left-hand side of the equation. The equation then becomes

$$w^{(IV)} - \frac{h\sigma_x}{D} w'' + 4k^4 w = \frac{p}{D} - \frac{\mu h \sigma_x}{RD}. \quad (1)$$

Within what limits may the conventional neglect of the second term on the left-hand side of the equation be considered legitimate?

194. A ball of mass  $m$  is placed in a tube rotating with a constant angular velocity  $\omega$ . The ball is attached to a rubber tie rod (Fig. 179).

The tensile test diagram of the tie rod is given by the curve shown in Fig. 179 (on the axes the relative units of force and displacement are laid off). Determine the relation between the displacement of the ball  $u$  and the angular velocity  $\omega$ .

195. A bar system (Fig. 180) consisting of three equal pin-connected bars is loaded at a common joint by a force  $P$ .

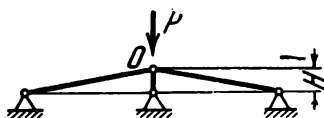
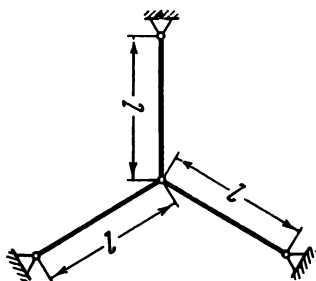


Fig. 180

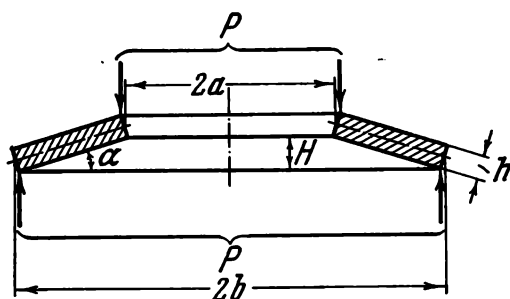


Fig. 181

Determine the displacement  $w$  of the point  $O$  as a function of the magnitude of the force  $P$ , assuming that  $H$  is small compared with  $l$ , and that the material of the bars obeys Hooke's law. Interpret the result obtained.

196. Determine the deflection of a disk spring (Fig. 181) as a function of the force  $P$ .

In solving the problem the spring is to be considered as a circular rod with a cross section in the form of a rectangle  $[h \times (b - a)]$ . The angle of elevation of the spring  $\alpha$  is small, the forces  $P$ , because of the smallness of the thickness  $h$  and the angle  $\alpha$ , may be assumed to be applied on circumferences of radii  $a$  and  $b$ .

197. Examine the question of stability and large displacements of the following system (Fig. 182).

A tube is hinged at its bottom and connected to a spiral spring producing a moment  $k\varphi$  when the tube is rotated through an angle  $\varphi$ . A spring and a piston are inserted into the tube, the piston being capable of moving in the tube without friction. The spring inserted into the tube has a stiffness  $k_1$ , i.e., it deflects an amount  $P/k_1$  under the force  $P$ .

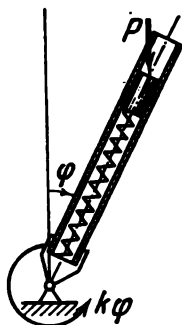
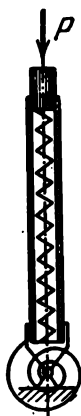


Fig. 182

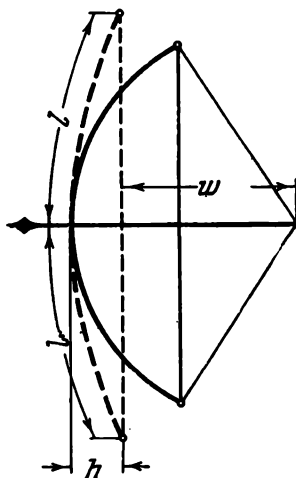


Fig. 183

198. Determine the relation between the velocity of an arrow propelled by a bow and the amount of drawing of the string  $w$  (Fig. 183). When the string is untied, the bow arch represents a straight beam of length  $2l$  and rigidity  $EI$ .

Carry out a numerical calculation of the initial velocity of the arrow for the case:

$$l = 60 \text{ cm}, \quad h = 0.3l, \quad E = 10^5 \text{ kgf/cm}^2 \text{ (wood),}$$

$$I = \frac{\pi d^4}{64} \quad (d = 2.0 \text{ cm}), \quad w = 1.6l, \quad \text{weight of arrow} = 40 \text{ gf.}$$

Assume that the energy of the drawn bow is completely transformed into the kinetic energy of the arrow; the string is to be considered inextensible.

# Solution of Problems and Answers to Questions

## I. Tension, Compression, and Torsion

1. The total displacement is naturally determined not by the diagonal of the parallelogram constructed on the segments  $u_1$  and  $u_2$ , as is often to be heard in answer to the question posed, but by the length of the segment measured from

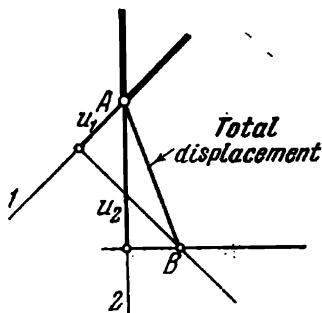


Fig. 184

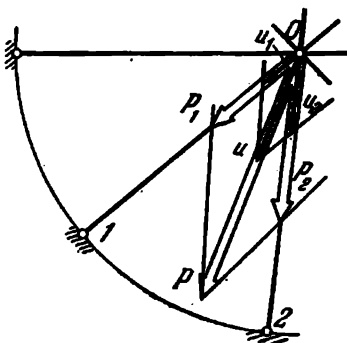


Fig. 185

the point  $A$  to the point of intersection of the perpendiculars drawn from the ends of the segments  $u_1$  and  $u_2$  (point  $B$  in Fig. 184).

The solution is based on the fact that the displacement in a given direction is the projection of the total displacement on this direction.

2. We resolve the force  $P$  into components  $P_1$  and  $P_2$  in the directions of two adjacent bars,  $1$  and  $2$  (Fig. 185). Since each of these bars is situated in the plane of symmetry, the total displacements  $u_1$  and  $u_2$  due to the forces  $P_1$  and  $P_2$  are directed along the lines of action of the corresponding forces, i.e., along the bars  $1$  and  $2$ .

The stiffness factor  $k$  for the directions 1 and 2 is the same; consequently,

$$u_1 = \frac{P_1}{k}, \quad u_2 = \frac{P_2}{k}.$$

Hence, the overall displacement  $u$  obtained by adding the displacements  $u_1$  and  $u_2$  according to the parallelogram rule passes along the line of action of the force  $P$  and has the value

$$u = \frac{P}{k}$$

independent of the angle  $\alpha$ .

Comparing the solution of this problem with the solution of the preceding problem, it is important to note that the displacements  $u_1$  and  $u_2$  in the present problem represent the *total* displacements due to the forces  $P_1$  and  $P_2$ , respectively. Hence, when the forces are acting simultaneously, the displacements  $u_1$  and  $u_2$  are added by the parallelogram rule. In the preceding problem, however,  $u_1$  and  $u_2$  represented the projections on the directions 1 and 2 of the total displacement caused by the simultaneous action of the forces  $P_1$  and  $P_2$ . This is why they were added in a different way.

3. The system is statically determinate.

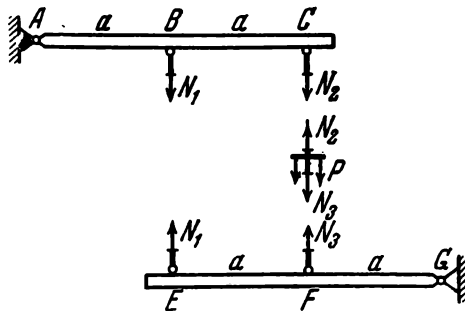


Fig. 186

The forces will be found from the conditions of equilibrium of elements of the system (Fig. 186). For the rigid beams we equate to zero the sums of the moments of the forces about the points A and G

$$2N_2 + N_1 = 0, \quad 2N_1 + N_3 = 0;$$

for the bar  $CF$  we obviously have

$$N_2 = P + N_3,$$

whence

$$N_1 = \frac{2}{3} P, \quad N_2 = -\frac{1}{3} P, \quad N_3 = -\frac{4}{3} P.$$

4. Since the plate is rigid, the length of the stretched bolt  $AB$  remains unchanged until the contacts open. Hence, the tension in the bolt also remains the same. If the force  $P$

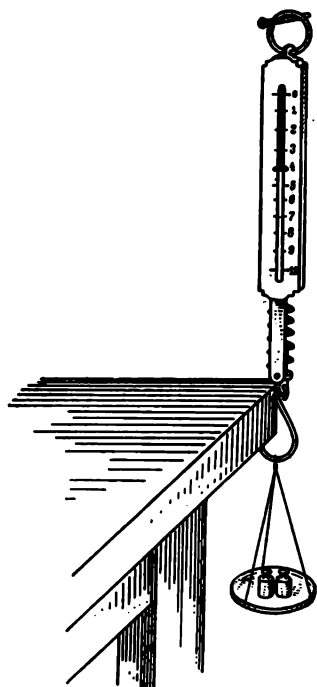


Fig. 187

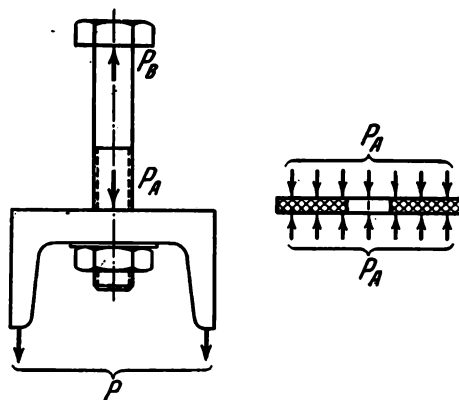


Fig. 188

is greater than the initial tightening force, the contact between the plane and the lower overlayer opens. The bolt tension is then equal to  $P$ .

Thus, when  $P \leq N_0$ , the bolt tension is  $N = N_0$ , and when  $P \geq N_0$ , it is  $N = P$ . The correctness of the result obtained is well illustrated by the following simple example.

Imagine spring scales (Fig. 187) the upper ring of which is put on a nail, and the lower hook, while being stretched,

is attached to some rigid projection, for example, to the edge of a table, as shown in Fig. 187. The scales then give some reading, for example 4 kgf. Let us liken these scales to the tensioned bolt. We now suspend small weights from the lower hook of the stretched scales. So long as the load remains smaller than the given force of tension, the indicator of the scales is invariably at four kilograms. Only when a load larger than four kilograms is hung from the hook, will the indicator move and show the corresponding weight.

5. To solve the problem we consider separately the bolt and the interlayer. The force compressing the interlayer is denoted by  $P_A$ , and the force exerted by the plate on the bolt head by  $P_B$  (Fig. 188).

Until the lower contact opens, the sum of the elongation of the bolt and the contraction of the interlayer

$$\frac{P_B l}{EA} + \frac{P_A}{k}$$

remains unchanged and equal to the sum of the same quantities during the tightening (i.e., when  $P = 0$ ); the latter is obviously equal to

$$\frac{N_0 l}{EA} + \frac{N_0}{k},$$

where  $A$  is the cross-sectional area of the bolt. Thus,

$$\frac{P_B l}{EA} + \frac{P_A}{k} = \frac{N_0 l}{EA} + \frac{N_0}{k}.$$

Moreover, we have the equality

$$P_B - P_A = P.$$

From these two equations we find

$$P_A = N_0 - \frac{P}{1 + \frac{EA}{kl}}, \quad P_B = N_0 + \frac{P \frac{EA}{kl}}{1 + \frac{EA}{kl}}.$$

The force  $N_0$  extending the bolt is equal to  $P_B$ ; when

$$P = N_0 \left( 1 + \frac{EA}{kl} \right)$$

we obtain  $P_A = 0$ , and the lower contact opens. Then  $N = P$ . For  $k = \infty$ , i.e., in the case of a rigid interlayer, we arrive at the solution of the preceding problem.

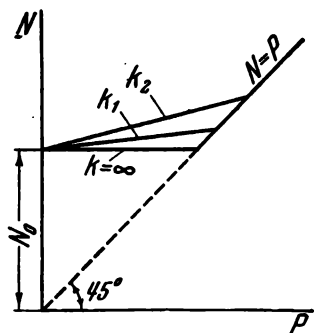


Fig. 189

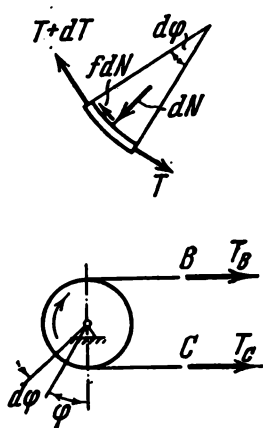


Fig. 190

Figure 189 shows the graph of the force  $N$  extending the bolt plotted against  $P$  for various  $k$

$$k_2 < k_1 < \infty.$$

6. Imagine sections  $B$  and  $C$  passed in the belt and consider the conditions for the equilibrium of the belt and lever (Fig. 190).

For the lever, we can obviously write the equality

$$T_C a + T_B (a + 2R) = P b. \quad (1)$$

We isolate a portion of length  $R d\varphi$  from the belt (Fig. 190). This element is acted on by the forces  $T$  and  $T + dT$ , the normal reaction of the pulley  $dN$ , and the frictional force  $f dN$ . From the conditions of equilibrium for the element of the belt we obtain

$$dT + f dN = 0,$$

$$dN = T d\varphi,$$

whence we find

$$\frac{dT}{T} = -f d\varphi.$$

Integrating gives

$$T = Ce^{-f\varphi}.$$

When  $\varphi = 0$ , we have  $T = T_C$ , hence  $C = T_C$  and  $T = T_C e^{-f\varphi}$ .

The force  $T_B$  is

$$T_B = T_{\varphi=\pi} = T_C e^{-f\pi}.$$

From condition (1) we determine  $T_C$

$$T_C = \frac{Pb}{a + e^{-f\pi}(a + 2R)}.$$

We now find the braking moment

$$\begin{aligned} M &= Rf \int_0^{\pi} dN = Rf \int_0^{\pi} T_C e^{-f\varphi} d\varphi = \\ &= T_C R (1 - e^{-f\pi}) = \frac{PbR (1 - e^{-f\pi})}{a + e^{-f\pi}(a + 2R)}. \end{aligned}$$

Before finding the displacement of the point  $A$ , we first determine the total elongation  $\Delta l$  of the belt

$$\Delta l = \frac{T_C c}{EA} + \frac{T_B c}{EA} + \int_0^{\pi} \frac{TR d\varphi}{EA} = \frac{T_C}{EA} \left[ c + ce^{-f\pi} + \frac{R}{f} (1 - e^{-f\pi}) \right].$$

But

$$\Delta l = u_B + u_C,$$

where  $u_B$  and  $u_C$  are the displacements of the points  $B$  and  $C$ . Moreover, from Fig. 190 it is seen that

$$u_A = u_C \frac{b}{a}, \quad u_A = u_B \frac{b}{a + 2R};$$

hence,

$$\Delta l = u_A \frac{a}{b} \left( 1 + \frac{a + 2R}{a} \right)$$

and

$$u_A = \frac{b}{2(a + R)} \frac{T_C}{EA} \left[ c + ce^{-f\pi} + \frac{R}{f} (1 - e^{-f\pi}) \right].$$

We have, finally,

$$u_A = \frac{P}{EA} \frac{b^2}{2(a+R)} \frac{c(1+e^{-f\pi}) + \frac{R}{f}(1-e^{-f\pi})}{a + (a+2R)e^{-f\pi}}.$$

7. If the pulley rotates in the opposite sense, the sign of the frictional forces is changed. The solution for this case is most easily obtained by reversing the sign of the coefficient of friction  $f$  in the final expressions. The braking moment  $M$  and the displacement  $u_A$  will accordingly assume new values different from those found above.

8. In the scheme described the indicators measure not the contraction of the specimen but the sum of this contraction

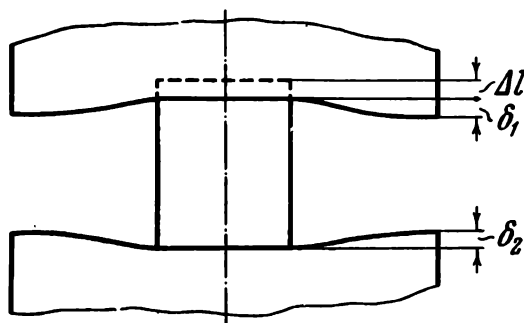


Fig. 191

and the relative displacement of the edges of the plates (Fig. 191), i.e., the quantity  $\Delta l + \delta_1 + \delta_2$ . In consequence, the resulting modulus of elasticity must be less than the true value. The relative error is larger the larger the modulus of elasticity of the test specimen.

The procedure outlined above is only suitable for the determination of elastic properties of rubber, plastic and wood, i.e., of the materials whose modulus of elasticity is appreciably lower than the modulus of elasticity of steel. Since the value of the modulus of elasticity of the test material given in the condition of the problem is comparable with the modulus of elasticity of steel, the result obtained cannot be trusted.

9. Because of symmetry, no axial displacements occur at the middle section of the bar. Consider now the right or the

left part of the bar. In this part of the bar, there are no displacements at the ends, the bar is homogeneous, and the heating is uniform. Consequently, by symmetry, the displacements at the middle of the part of the bar are also zero. By a similar reasoning, we can divide the bar into arbitrarily small portions at the ends of which the displacements are zero. From this it may be concluded that the axial displacements are absent for all sections of the bar.

10. The first expression for  $U$  is correct. The second one is erroneous. In the present case the work done by the force  $P$

$$U \neq \frac{P\delta}{2}$$

since the displacement  $\delta$  is not proportional to the force  $P$  over the entire portion. This can easily be [seen from the graph of Fig. 192 which shows the relation between  $\delta$  and  $P$ ] for the system under consideration. The work done by the force  $P$  is determined by the shaded area, i.e.,

$$U = \frac{\Delta^2 EA}{2l} + \left( \frac{Pl}{2EA} - \frac{\Delta}{2} \right) \frac{EA\Delta}{l} + \\ + \frac{1}{2} \left( P - \frac{EA\Delta}{l} \right) \left( \frac{Pl}{2EA} - \frac{\Delta}{2} \right) = \frac{P^2 l}{4EA} + \frac{EA\Delta^2}{4l};$$

this expression is identical with that obtained previously [see expression (4)].

11. In the first case we determined the displacement of the point at which the centre of gravity of the bar was before the deformation. In the second case we determined the distance from the point of the new position of the centre of gravity to the point of the old position, and this is not the same thing.

Thus, there is indeterminacy in the very statement of the question. It must be clearly specified what is to be understood by the term "displacement of the centre of gravity" since the latter is not rigidly fixed to any one of the points of the deformed body.

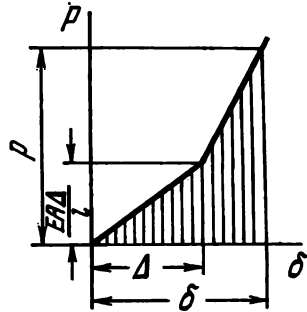


Fig. 192

12. Consider an element of the string, of length  $dx$  (Fig. 193). Denote by  $T$  the tension in the sagged string ( $T > T_0$ ) and by  $\vartheta$  the slope of the sagged string. Assuming

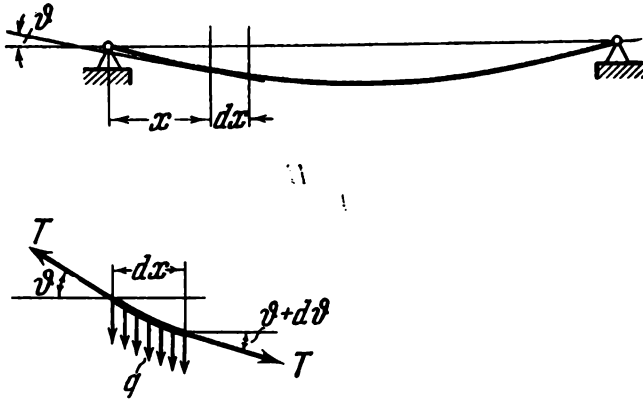


Fig. 193

this angle to be small, [we obtain from the conditions of equilibrium

$$T\vartheta - q dx - T(\vartheta + d\vartheta) = 0,$$

whence

$$\frac{q}{T} = -\frac{d\vartheta}{dx}.$$

Upon integration we find

$$\vartheta = \frac{q}{T}(C - x);$$

when  $x = l/2$ , we have  $\vartheta = 0$ , hence  $C = l/2$ ; consequently,

$$\vartheta = \frac{q}{T} \left( \frac{l}{2} - x \right) \quad (1)$$

and

$$w_{\max} = \int_0^{l/2} \vartheta dx = \frac{ql^2}{8T}. \quad (2)$$

We now find  $T$ . Since the forces  $T$  and  $T_0$  are unequal, the string lengthens by an amount equal to the difference

between the lengths of the curved and the straight string, i.e.,

$$\frac{(T-T_0)l}{EA} = \int_0^l \left( \frac{1}{\cos \theta} - 1 \right) dx = \int_0^l \frac{\theta^2}{2} dx,$$

whence

$$\frac{T-T_0}{EA} = \frac{q^2 l^2}{24T^2}.$$

Substituting for  $T$  from expression (2), we obtain

$$64 \left( \frac{w_{\max}}{l} \right)^3 + 24 \frac{w_{\max}}{l} \frac{T_0}{EA} = 3 \frac{ql}{EA}.$$

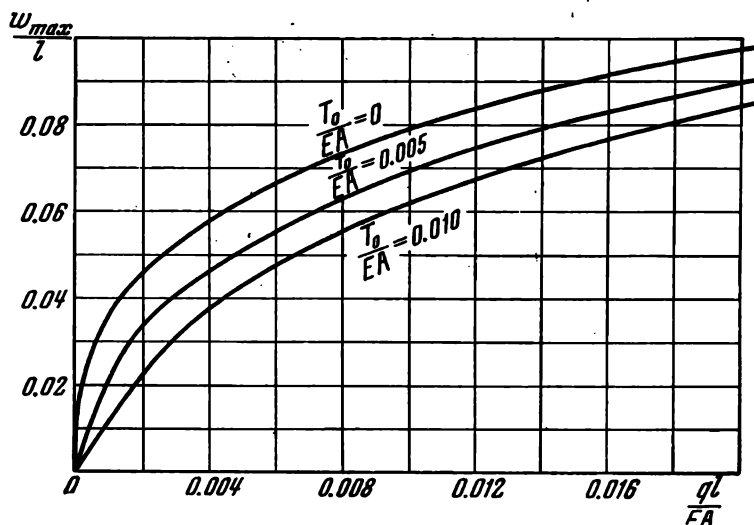


Fig. 194

This is the required relation among  $w_{\max}$ ,  $T_0$ , and  $q$ . The result obtained is represented in Fig. 194 in the form of curves

$$\frac{w_{\max}}{l} = f \left( \frac{T_0}{EA}; \frac{ql}{EA} \right).$$

13. The problem reduces to an analysis of a string loaded by two concentrated forces  $P = ql/3$  (Fig. 195).

By using expressions (1) and (2) of the preceding problem, we can write

$$\vartheta_0 = \frac{q}{T_0} \left( \frac{l}{2} - x \right), \quad T_0 = \frac{ql^2}{8w_0 \max},$$

where  $\vartheta_0$  and  $T_0$  are, respectively, the slope of the sagging deflection curve and the tension in the cable before the lower wire is suspended.

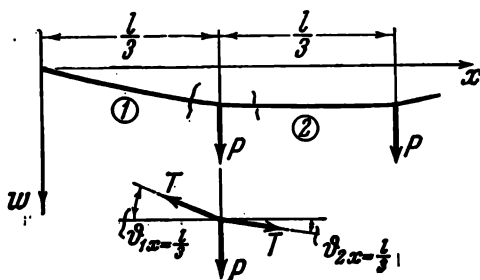


Fig. 195

Consider the left-hand portion (1) and one half of the middle portion (2) of the cable (Fig. 195). Corresponding to these portions we have

$$\left. \begin{aligned} \vartheta_1 &= \frac{q}{T} (C_1 - x), \\ w_1 &= \frac{q}{T} \left( A_1 + C_1 x - \frac{x^2}{2} \right) \end{aligned} \right\} \left( 0 \leq x \leq \frac{l}{3} \right);$$

$$\left. \begin{aligned} \vartheta_2 &= \frac{q}{T} (C_2 - x), \\ w_2 &= \frac{q}{T} \left( A_2 + C_2 x - \frac{x^2}{2} \right) \end{aligned} \right\} \left( \frac{l}{3} \leq x \leq \frac{l}{2} \right).$$

The constants  $A_1$ ,  $A_2$ ,  $C_1$ , and  $C_2$  are determined from the following conditions: when  $x = 0$ ,  $w_1 = 0$ ; when  $x = l/2$ ,  $\vartheta_2 = 0$ ; when  $x = l/3$ ,  $w_1 = w_2$  and  $T\vartheta_1 - T\vartheta_2 = P$ . In this case

$$A_1 = 0, \quad A_2 = \frac{Pl}{3q}, \quad C_1 = \frac{P}{q} + \frac{l}{2}, \quad C_2 = \frac{l}{2}.$$

The force  $T$  is determined by equating the difference between the lengths of the freely hanging and the tight cable

to the tensile elongation

$$\int_0^{1/3} \left(1 + \frac{\vartheta_1^2}{2}\right) dx + \int_{1/3}^{1/2} \left(1 + \frac{\vartheta_2^2}{2}\right) dx - \int_0^{1/2} \left(1 + \frac{\vartheta_0^2}{2}\right) dx = \frac{(T - T_0) l}{2EA}$$

or, after substitution of the values of  $\vartheta$ ,

$$\frac{q^2}{T^2} \int_0^{1/3} (C_1 - x)^2 dx + \frac{q^2}{T^2} \int_{1/3}^{1/2} (C_2 - x)^2 dx - \frac{q^2}{T_0^2} \int_0^{1/2} \left(\frac{l}{2} - x\right)^2 dx = \frac{(T - T_0) l}{EA},$$

whence, by integration, we find

$$\frac{q^2}{T^2} \left( \frac{P^2}{q^2} \frac{l}{3} + \frac{P}{q} \frac{2l^2}{9} + \frac{l^3}{24} \right) - \frac{q^2}{T_0^2} \frac{l^3}{24} = \frac{(T - T_0) l}{EA}.$$

Upon substitution for  $T_0$  we obtain

$$\left( \frac{Tw_0 \max}{ql^2} \right)^3 + \left( \frac{Tw_0 \max}{ql^2} \right)^2 \left[ \frac{8}{3} \frac{EA w_0^3 \max}{ql^4} - \frac{1}{8} \right] = \frac{1}{3} \frac{EA w_0^3 \max}{ql^4} \left( \frac{P^2}{q^2 l^2} + \frac{2}{3} \frac{P}{ql} + \frac{1}{8} \right).$$

Carry out a numerical calculation:

$$P = \frac{qw l}{3} = \frac{1.5ql}{3}, \quad \frac{P}{ql} = 0.5,$$

$$q = 0.6 \times 0.0078 = 0.00468 \text{ kgf/cm},$$

where 0.0078 kgf/cm<sup>3</sup> is the specific weight of steel; we thus obtain

$$\frac{EA w_0^3 \max}{ql^4} = 0.0205.$$

In this case the design equation is reduced to the following:

$$\left( \frac{Tw_0 \max}{ql^2} \right)^3 - 0.0704 \left( \frac{Tw_0 \max}{ql^2} \right)^2 - 0.00484 = 0,$$

whence

$$\frac{Tw_0 \max}{ql^2} = 0.196, \quad T = 460 \text{ kgf}.$$

The equations of the sagging deflection curve (the sag for the outer portion is  $w_1$ , and for the middle portion  $w_2$ ) become

$$w_1 = 254 \left( \frac{x}{l} - \frac{1}{2} \frac{x^2}{l^2} \right) \text{ cm},$$

$$w_2 = 254 \left( \frac{1}{6} + \frac{1}{2} \frac{x}{l} - \frac{1}{2} \frac{x^2}{l^2} \right) \text{ cm}.$$

The sagging deflection curve plotted by these equations is shown in Fig. 196.

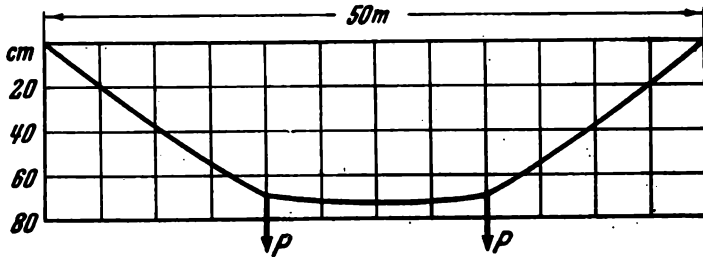


Fig. 196

14. If the sheets in the region of riveting were joined across the entire width  $b$  and the joint were perfectly rigid, we should have, by Hooke's law, for the sheets tested in tension

$$\Delta a_0 = \frac{T \frac{a}{2}}{E 2 b h_1} + \frac{T \frac{a}{2}}{E b h_2}, \quad (1)$$

where  $E$  is the modulus of elasticity of the sheets. The derived value  $\Delta a_0$  would be less than the measured value  $\Delta a$ . The difference between the measured value  $\Delta a$  and the calculated value (1) is due to the deformation of the rivet and the sheets at the junction. The resulting difference of the elongations is denoted by  $\Delta$

$$\Delta = T \left( \frac{1}{k} - \frac{a}{4 E b h_1} - \frac{a}{2 E b h_2} \right).$$

Denote further

$$\frac{1}{k} - \frac{a}{4 E b h_1} - \frac{a}{2 E b h_2} = \frac{1}{k_0}. \quad (2)$$

The difference of the elongations is then  $\Delta = \frac{T}{k_0}$ .

Consider now the deformation of the sheets (Fig. 197). Denote by  $N_i$  the normal tensile force in the  $i$ th span of the inner sheet. In the two outer sheets the overall force is obviously equal to the difference  $P - N_i$  (see Fig. 197).

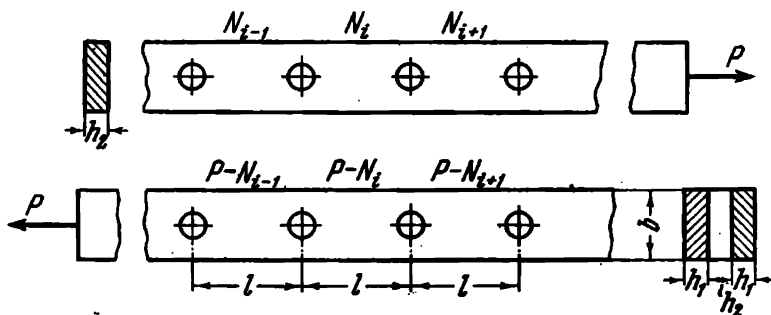


Fig. 197

The difference in the elongations of the inner and outer sheets in the  $i$ th span

$$\frac{N_i l}{E b h_2} - \frac{(P - N_i) l}{2 E b h_1}$$

is equal to the difference in the displacements of the ends of the span due to the deformation of the rivets, i.e.,

$$\frac{N_{i+1} - N_i}{k_0} - \frac{N_i - N_{i-1}}{k_0},$$

where  $N_i - N_{i-1}$  and  $N_{i+1} - N_i$  are the forces exerted, respectively, on the left- and right-hand rivets of the  $i$ th span.

By equating the above differences of the displacements, we obtain

$$N_{i-1} \alpha - N_i \beta + N_{i+1} \alpha = -P, \quad (3)$$

where

$$\alpha = \frac{2 E b h_1}{l k_0}, \quad \beta = 2\alpha + 1 + \frac{2 h_1}{h_2}. \quad (4)$$

The resulting equation (3) which is analogous to the well-known equation of three moments is written successively for

the first, second, and third spans (Fig. 13)

$$0 \cdot \alpha - N_1 \beta + N_2 \alpha = -P,$$

$$N_1 \alpha - N_2 \beta + N_3 \alpha = -P,$$

$$N_2 \alpha - N_3 \beta + P \alpha = -P.$$

From this we obtain formulas for the normal forces

$$N_1 = P \frac{\beta^2 + \alpha^3 + \alpha \beta}{\beta (\beta^2 - 2\alpha^2)},$$

$$N_2 = P \frac{\beta (\beta + 2\alpha + \alpha^2)}{\beta (\beta^2 - 2\alpha^2)},$$

$$N_3 = P \frac{\beta^2 (1 + \alpha) - \alpha^3 + \alpha \beta}{\beta (\beta^2 - 2\alpha^2)}.$$

The forces exerted on the rivets are the following:

$$P_I = N_1 = P \frac{\beta^2 + \alpha^3 + \alpha \beta}{\beta (\beta^2 - 2\alpha^2)},$$

$$P_{II} = N_2 - N_1 = P \frac{\alpha (\beta + \alpha \beta - \alpha^2)}{\beta (\beta^2 - 2\alpha^2)},$$

$$P_{III} = N_3 - N_2 = P \frac{\alpha (\beta^2 - \beta \alpha - \alpha^2 - \beta)}{\beta (\beta^2 - 2\alpha^2)},$$

$$P_{IV} = P - N_3 = P \left[ 1 - \frac{\beta^2 (1 + \alpha) - \alpha^3 + \alpha \beta}{\beta (\beta^2 - 2\alpha^2)} \right].$$

If  $h_2 = 2h_1$ , we have

$$\beta = 2(\alpha + 1)$$

and the forces are then

$$P_I = P_{IV} = \frac{P}{4} \frac{\alpha^3 + 6\alpha^2 + 10\alpha + 4}{(\alpha + 1)(\alpha^2 + 4\alpha + 2)},$$

$$P_{II} = P_{III} = \frac{P}{4} \frac{\alpha}{\alpha + 1}.$$

If the joint is perfectly rigid ( $k_0 = \infty$ ), then the factor  $\alpha = 0$  and we obtain

$$P_I = P_{IV} = \frac{P}{2}, \quad P_{II} = P_{III} = 0.$$

Consequently, in this case only the extreme rivets of the joint work.

For very flexible rivets  $k_0$  is small and  $\alpha$  is large. In the limit as  $\alpha \rightarrow \infty$  we have

$$P_I = P_{II} = P_{III} = P_{IV} = \frac{P}{4}.$$

It was indicated in the condition of the problem that the factor  $k$  was determined by testing the riveted sheets with a gauge length  $a$  sufficiently large for the stresses at the sections  $A$  and  $B$  to be considered uniformly distributed (Fig. 14). In this sense the solution obtained will be sufficiently accurate if the distance between the rivets is not less than  $a$ . But even for a smaller distance between rivets when the stresses across the thickness of the sheet from rivet to rivet do not level off, the solution holds true. There is only a change in expression (2) for  $k_0$  in which the width  $b$  of the sheet must be replaced by some equivalent reduced value.

15. Let there be  $n$  rivets in the longitudinal joint. From expression (3) (p. 99) we obtain the following  $n - 1$  equations according to the number of spans:

$$\begin{aligned} -N_1\beta + N_2\alpha &= -P, \\ N_1\alpha - N_2\beta + N_3\alpha &= -P, \\ N_2\alpha - N_3\beta + N_4\alpha &= -P, \\ &\dots\dots\dots \\ N_{i-1}\alpha - N_i\beta + N_{i+1}\alpha &= -P, \\ &\dots\dots\dots \\ N_{n-2}\alpha - N_{n-1}\beta &= -P(1 + \alpha). \end{aligned}$$

From these equations we must determine the unknowns

$$N_1, N_2, N_3, \dots, N_{n-1}.$$

Note that if we put

$$N_1 = N_2 = N_3 = \dots = N_{n-1} = -\frac{P}{2\alpha - \beta}$$

all equations, except the first and the last, will be satisfied.

Assume further

$$\begin{aligned} N_1 &= Ax - \frac{P}{2\alpha - \beta}, & N_2 &= Ax^2 - \frac{P}{2\alpha - \beta}, \\ N_i &= Ax^i - \frac{P}{2\alpha - \beta}, & \dots, \end{aligned}$$

where  $A$  and  $x$  are some arbitrary constants.

Let  $x$  be selected so as to satisfy again all equations except the first and the last. Substituting for  $N_{i-1}$ ,  $N_i$ , and  $N_{i+1}$  in the equation

$$N_{i-1}\alpha - N_i\beta + N_{i+1}\alpha = -P,$$

we obtain

$$Ax^{i-1}\alpha - \frac{P\alpha}{2\alpha-\beta} - \beta Ax^i + \frac{P\beta}{2\alpha-\beta} + Ax^{i+1}\alpha - \frac{P\alpha}{2\alpha-\beta} = -P$$

or

$$\alpha - \beta x + \alpha x^2 = 0,$$

whence we find

$$x_1 = \frac{\beta + \sqrt{\beta^2 - 4\alpha^2}}{2\alpha}, \quad x_2 = \frac{\beta - \sqrt{\beta^2 - 4\alpha^2}}{2\alpha}.$$

Evidently, all equations, except the first and the last, are now satisfied by the following expressions:

$$N_1 = Ax_1 + Bx_2 - \frac{P}{2\alpha-\beta},$$

$$N_2 = Ax_1^2 + Bx_2^2 - \frac{P}{2\alpha-\beta},$$

$$\dots\dots\dots$$

$$N_i = Ax_1^i + Bx_2^i - \frac{P}{2\alpha-\beta}$$

for any values of the arbitrary constants  $A$  and  $B$ . The latter will be selected so as to satisfy the first and last equations of the system

$$\begin{aligned} -\beta \left( Ax_1 + Bx_2 - \frac{P}{2\alpha-\beta} \right) + \alpha \left( Ax_1^2 + Bx_2^2 - \frac{P}{2\alpha-\beta} \right) &= -P, \\ \alpha \left( Ax_1^{n-2} + Bx_2^{n-2} - \frac{P}{2\alpha-\beta} \right) - \beta \left( Ax_1^{n-1} + Bx_2^{n-1} - \frac{P}{2\alpha-\beta} \right) &= \\ &= -P(\alpha + 1). \end{aligned}$$

From this we determine  $A$  and  $B$  and, noting that  $x_1x_2 = 1$  and  $x_1 + x_2 = \frac{\beta}{\alpha}$ , after simple transformation we obtain

$$N_i = \frac{P}{2\alpha-\beta} \left[ \frac{(\beta-1-2\alpha)(x_1^i - x_2^i) + x_2^{n-i} - x_1^{n-i}}{x_2^n - x_1^n} - 1 \right].$$

The forces in the rivets are

$$\begin{aligned} P_{\text{I}} &= N_1, \\ P_{\text{II}} &= N_2 - N_1, \\ P_{\text{III}} &= N_3 - N_2, \\ &\dots\dots\dots \\ P_n &= P - N_{n-1}. \end{aligned}$$

16. Consider the conditions of equilibrium for an element of the screw (Fig. 198). Obviously,

$$\frac{dN_s}{dx} = t. \quad (1)$$

Further, according to the condition of the problem,

$$t = k(u_s - u_n); \quad (2)$$

but

$$\frac{du_s}{dx} = \epsilon_s, \quad \frac{du_n}{dx} = \epsilon_n$$

and

$$\epsilon_s = \frac{N_s}{E_s A_s}, \quad \epsilon_n = \frac{N_n}{E_n A_n}.$$

Consequently, on differentiating expression (2) we obtain

$$\frac{dt}{dx} = k \left( \frac{N_s}{E_s A_s} - \frac{N_n}{E_n A_n} \right).$$

Substituting for  $t$  from the equation of equilibrium (1), we have

$$\frac{d^2 N_s}{dx^2} = k \left( \frac{N_s}{E_s A_s} - \frac{N_n}{E_n A_n} \right).$$

By using the condition

$$N_n = P - N_s,$$

we find

$$\frac{d^2 N_s}{dx^2} - \alpha^2 N_s = -\frac{kP}{E_n A_n}, \quad (3)$$

where

$$\alpha^2 = k \left( \frac{1}{E_s A_s} + \frac{1}{E_n A_n} \right).$$

The solution of the homogeneous equation

$$\frac{d^2 N_s}{dx^2} - \alpha^2 N_s = 0$$

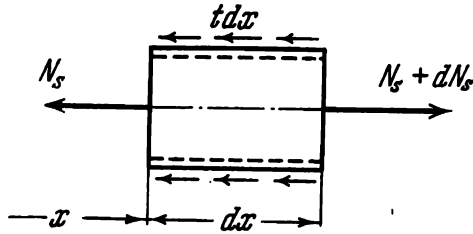


Fig. 198

is

$$N_s = A \sinh \alpha x + B \cosh \alpha x.$$

By adding a particular solution of Eq. (3), we obtain

$$N_s = A \sinh \alpha x + B \cosh \alpha x + \frac{kP}{\alpha^2 E_n A_n}. \quad (4)$$

The constants  $A$  and  $B$  are found from the boundary conditions:

$$\begin{aligned} \text{when } x = 0, \quad N_s &= 0; \\ \text{when } x = l, \quad N_s &= P. \end{aligned}$$

Upon solution we obtain

$$A = -\frac{kP}{\alpha^2 E_n A_n} \frac{1 - \cosh \alpha l}{\sinh \alpha l} + \frac{P}{\sinh \alpha l}, \quad B = -\frac{kP}{\alpha^2 E_n A_n}.$$

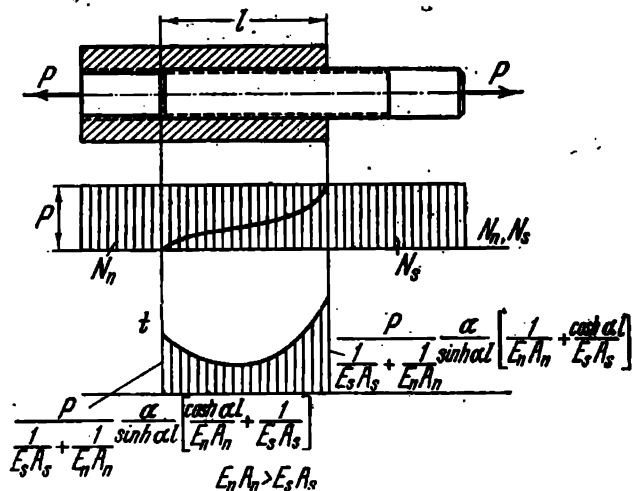


Fig. 199

The normal force in the screw is

$$N_s = \frac{P}{\frac{1}{E_s A_s} + \frac{1}{E_n A_n}} \frac{1}{\sinh \alpha l} \left[ \frac{\sinh \alpha l - \sinh \alpha (l-x)}{E_n A_n} + \frac{\sinh \alpha x}{E_s A_s} \right].$$

The normal force in the nut is

$$N_n = P - N_s.$$

The force on the fillets of the screw is

$$t = \frac{dN_s}{dx} = \frac{P}{\frac{1}{E_s A_s} + \frac{1}{E_n A_n}} \frac{\alpha}{\sinh \alpha l} \left[ \frac{\cosh \alpha (l-x)}{E_n A_n} + \frac{\cosh \alpha x}{E_s A_s} \right].$$

Figure 19 shows the nature of the variation of these quantities along the axis of the screw and nut.

17. The problem is solved in exactly the same way as the preceding one. The difference is introduced only by the boundary conditions which are now as follows:

$$\text{when } x=0, \quad N_s = P,$$

$$\text{when } x=l, \quad N_s = P.$$

These conditions are satisfied for the following values of the constants  $A$  and  $B$ :

$$A = \frac{1 - \cosh \alpha l}{\sinh \alpha l} \times$$

$$\times \left( P - \frac{kP}{\alpha^2 E_n A_n} \right),$$

$$B = P - \frac{kP}{\alpha^2 E_n A_n}.$$

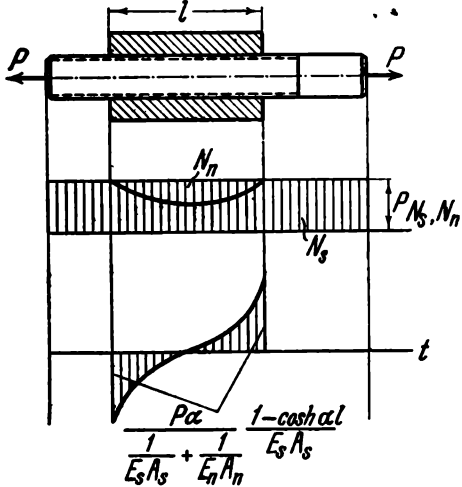


Fig. 200

The normal force in the screw is

$$N_s = \frac{P}{\frac{1}{E_s A_s} + \frac{1}{E_n A_n}} \frac{1}{\sinh \alpha l} \left[ \frac{\sinh \alpha x + \sinh \alpha (l-x)}{E_s A_s} + \frac{\sinh \alpha l}{E_n A_n} \right].$$

The normal force in the nut is

$$N_n = P - N_s.$$

The force on the fillets of the screw is

$$t = \frac{dN_s}{dx} = \frac{P\alpha}{\frac{1}{E_s A_s} + \frac{1}{E_n A_n}} \frac{\cosh \alpha x - \cosh \alpha (l-x)}{E_s A_s \sinh \alpha l}.$$

The nature of the variation of the quantities  $N_s$ ,  $N_n$ , and  $t$  along the length of the screw is shown in Fig. 200.

18. If a compressive force  $P$  is applied to the screw so as to reduce its pitch by  $\Delta$ , and then the nut is screwed on, there will be no forces in the thread. If the bolt is now unloaded, the forces arising in the system will be the same as in the system considered in the preceding problem. The previously obtained solution is therefore suitable for the present case if only the force  $P$  gives an elongation  $\Delta$  per pitch in the freely stretched screw.

By Hooke's law,

$$\Delta = \frac{Ps}{E_s A_s},$$

where  $s$  is the pitch. Thus, in order to obtain the desired solution it is sufficient to replace  $P$  by  $\frac{\Delta}{s} E_s A_s$  in the expressions of the last problem.

19. The most favourable conditions are those in which the forces on the fillets are distributed more uniformly. In the first case the top fillet is severely overloaded.

In the second case the tightening force is applied to the nut above the first fillet. The diameter of the nut in its lower part is reduced. The forces on the first fillet will therefore be smaller in this case. The remaining fillets are thereby additionally loaded (with the same tightening force). The operating conditions for the fillets in the second case are more favourable.

It should not be concluded from the above, however, that one must apply type 2 nuts in all cases (Fig. 18). It is clear that the complication of any construction, and particularly of the construction of such a common standard part as a nut, can be justified only in the case when this complication yields really perceptible results. Since the overloading of a few fillets of the screw in comparison with the other fillets limits the strength of a threaded joint only in exceptional cases, the application of nuts of the type described can accordingly be recommended as an exception.

20. We consider the bar system in the deformed state (Fig. 201) and, assigning a displacement of the point  $A$ , seek the force  $P$ . We measure the angle  $\alpha$ ,  $\Delta l_1/l$ , and  $u_A/l$  on the drawing. From the curve of Fig. 19 we find the forces  $P_1$  and  $P_2$  corresponding to the elongations  $\Delta l_1/l$  and  $u_A/l$ .

The force  $P$  is determined from the condition of equilibrium

$$P = 2P_1 \cos \alpha + P_2.$$

By assigning several values of  $u_A$ , we can plot the relation between  $u_A$  and  $P$ . The resulting curve  $u_A = f(P)$  for the given tensile test diagram of the rods is shown in Fig. 201.

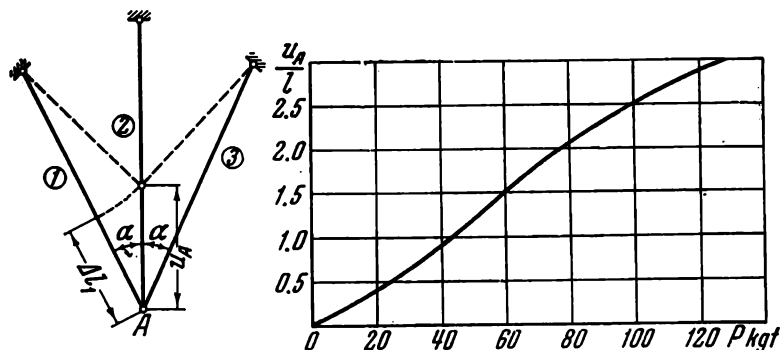


Fig. 201

21. Case 1 occurs for large angles  $\alpha$ , and Case 2 for small angles  $\alpha$ . Case 3 is intermediate between the first two. The value of the corresponding angle  $\alpha$  can be found approximately on the assumption that the stiffness of the cord considerably exceeds the stiffness of the rubber, and hence almost all the load is carried by the cords.

Isolate an element of the rubber-cord cylinder (Fig. 202) with dimensions  $a$  and  $a \tan \alpha$ . With this choice of dimensions, the same number of cords falls within both sections of the element,  $AB$  and  $BC$ . Denote the force in the cord by  $P$ ; the resultant of the forces at the section  $AB$  is then

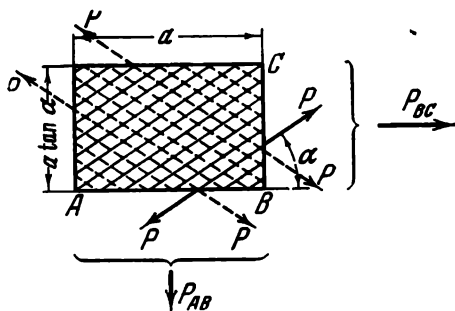


Fig. 202

$$P_{AB} = Pn \sin \alpha,$$

where  $n$  is the number of cords which fall within the section  $AB$ . The corresponding resultant at the section  $BC$  is

$$P_{BC} = Pn \cos \alpha.$$

But we know that when the cylinder is loaded by internal pressure the circumferential average stress is twice the axial stress. Consequently,

$$\frac{P_{BC}}{a \tan \alpha} = 2 \frac{P_{AB}}{a}.$$

Substituting for  $P_{AB}$  and  $P_{BC}$ , we find

$$\tan^2 \alpha = \frac{1}{2}, \quad \alpha = 35^\circ 16'.$$

For this value of the angle  $\alpha$ , the cylindrical shape of the shell is maintained. For  $\alpha > 35^\circ 16'$  the cylinder deforms as shown in Fig. 21,1, and for  $\alpha < 35^\circ 16'$  as in Fig. 21,2.

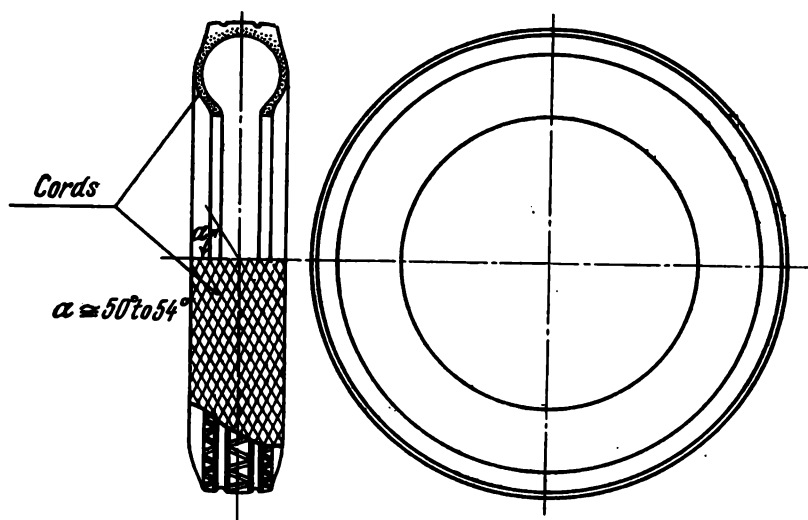


Fig. 203

In passing, we note that problems involving such rubber-cord structures arise in the design of auto-tyre casings. The choice of the position angle of cords (Fig. 203) is of great importance for the durability of a tyre casing. The change of the angle either way from the optimum value for a given type

of casing entails a reduction of the service life of the tyre. It should be noted, however, that this angle for a casing is determined not by the conditions of equilibrium, as in the example considered, but by the optimum conditions of fatigue strength of cords under varying stresses occurring in the wheel during rolling.

22. Consider the equilibrium of an isolated cord (Fig. 204). It is acted on by a distributed load  $q$  kgf/cm exerted by the rubber shell. This load is variable since the distance between the cords is different at different points. It is greatest at the equator, where

$$q_e = p \frac{2\pi r_e}{n},$$

$p$  is the pressure, and  $n$  is the number of cords.

At a point distant  $r$  from the axis

$$q = q_e \frac{r}{r_e}.$$

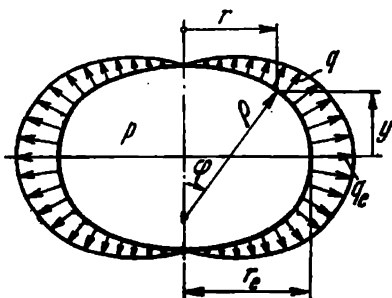


Fig. 204

The tension  $T$  in the cord is constant along an arc of a meridian. It is equal to  $T = q\rho$ , where  $\rho$  is the local radius of curvature of the meridian.

Eliminating  $q$  and then  $q_e$ , we find

$$T = \frac{2\pi}{n} p\rho r.$$

On the other hand, from the condition of equilibrium of the hemisphere it follows that

$$T = \frac{p\pi r_e^3}{n}.$$

Eliminating  $T$ , we obtain

$$\rho = \frac{r_e^3}{2r}.$$

Let  $\varphi$  be the angle between the normal to the deformed surface and the axis of rotation. Then  $dr = \rho \cos \varphi d\varphi$  or

$$dr = \frac{r_e^3}{2r} \cos \varphi d\varphi.$$

Integrating gives

$$r^3 = r_e^3 \sin \varphi + C_1.$$

Since  $\varphi$  becomes zero when  $r = 0$ , then  $C_1 = 0$  and

$$\sin \varphi = \frac{r^3}{r_e^3}.$$

Denote by  $y$  the distance of some point from the plane of the equator. Obviously,

$$\frac{dy}{dr} = -\tan \varphi$$

or

$$dy = -\frac{\frac{r^2}{r_e^3} dr}{\sqrt{1 - \frac{r^4}{r_e^4}}}.$$

To integrate this expression we apply the substitution

$$r = r_e \cos \psi.$$

Then

$$dy = r_e \frac{\cos^2 \psi d\psi}{\sqrt{1 + \cos^2 \psi}}$$

or

$$y = r_e \frac{\sqrt{2}}{2} \left[ 2 \int_0^\psi \sqrt{1 - \frac{1}{2} \sin^2 \psi} d\psi - \int_0^\psi \frac{d\psi}{\sqrt{1 - \frac{1}{2} \sin^2 \psi}} \right] + C_2.$$

The quantity  $C_2$  is zero since  $\psi = 0$  at the equator and  $y$  vanishes.

The relative oblateness of the equilibrium figure is determined by the ratio  $y_0/r_e$ , where  $y_0$  is the vertical semi-axis of the body of revolution

$$\begin{aligned} \frac{y_0}{r_e} &= \frac{\sqrt{2}}{2} \times \\ &\times \left[ 2 \int_0^{\pi/2} \sqrt{1 - k^2 \sin^2 \psi} d\psi - \int_0^{\pi/2} \frac{d\psi}{\sqrt{1 - k^2 \sin^2 \psi}} \right] = \\ &= \frac{\sqrt{2}}{2} (2E - F). \end{aligned}$$

Here  $F$  and  $E$  are the complete elliptic integrals of the first and second kinds having the modulus  $k = \sqrt{1/2}$ . These integrals are tabulated; from tables we find

$$F = 1.85407 \quad \text{and} \quad E = 1.35064.$$

Finally,

$$\frac{y_0}{r_e} = 0.599.$$

A curious detail: the derived shape of the shell has the largest volume among other bodies of revolution having the same given arc length of the meridian. This follows naturally from the fact that the cords are assumed to be inextensible and the energy of the system is expressed only by the pressure force potential. The pressure does an amount of work  $pV$ . This work is maximum when the volume  $V$  is largest, and the external force potential ( $-pV$ ) correspondingly has a minimum in comparison with all neighbouring shapes.

23. The phenomenon in question can occur if sufficiently large plastic deformations arise in the aluminium ring on heating. Denote by  $\Delta$  the difference between the external radius of the inner ring and the internal radius of the outer ring before fitting. Obviously,

$$\varepsilon_A + \varepsilon_S = \frac{\Delta}{R}, \quad (1)$$

where  $\varepsilon_A$  is the contraction per unit arc length of the aluminium ring and  $\varepsilon_S$  is the elongation per unit arc length of the steel ring.

On further heating within the elastic range of strains

$$\varepsilon_A = \frac{\sigma_A}{E_A} - \alpha_A t, \quad \varepsilon_S = \frac{\sigma_S}{E_S} + \alpha_S t,$$

where  $\sigma_A$  and  $\sigma_S$  are the stresses in the aluminium and steel rings,  $\alpha_A$  and  $\alpha_S$  are the corresponding coefficients of linear expansion. On the other hand, if the thicknesses of the rings are equal,  $\sigma_S = \sigma_A = \sigma$ , as follows from the conditions of equilibrium (Fig. 205). Equation (1) gives

$$\sigma = \frac{\frac{\Delta}{R} + t(\alpha_A - \alpha_S)}{\frac{1}{E_A} + \frac{1}{E_S}}. \quad (2)$$

Suppose that the tensile or compression test diagram of aluminium can be schematized as shown in Fig. 206. The yield stress of aluminium is lower than the yield stress of steel. Since the stresses in both rings are the same, the steel ring will act elastically in all cases.

The stress of the initial negative allowance for the rings, which is denoted by  $\sigma_0$ , is

$$\sigma_0 = \frac{\frac{\Delta}{R}}{\frac{1}{E_A} + \frac{1}{E_S}}.$$

Expression (2) then becomes

$$\sigma = \sigma_0 + \frac{t(\alpha_A - \alpha_S)}{\frac{1}{E_A} + \frac{1}{E_S}}. \quad (3)$$

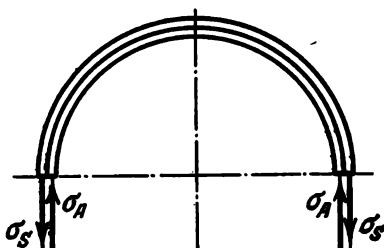


Fig. 205

Note that  $\sigma$  cannot be greater than  $\sigma_{yA}$ . If the heating temperature

$$t > (\sigma_{yA} - \sigma_0) \left( \frac{1}{E_A} + \frac{1}{E_S} \right) \frac{1}{\alpha_A - \alpha_S},$$

then plastic deformations occur in the aluminium ring and  $\sigma = \sigma_{yA}$ .

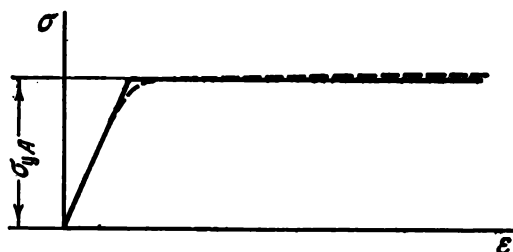


Fig. 206

On cooling the rings will deform elastically. The residual stresses can then be found as the algebraic sum of  $\sigma_{yA}$  and the "cooling stress" obtained from expression (3) by reversing the sign of  $t$ , i.e.,

$$\sigma_{\text{res}} = \sigma_{yA} - \frac{t(\alpha_A - \alpha_S)}{\frac{1}{E_A} + \frac{1}{E_S}} \quad (4)$$

When  $\sigma_{\text{res}} < 0$ , the aluminium ring falls out of the steel ring. Consequently, the condition for falling-out is

$$t(\alpha_A - \alpha_S) > \sigma_{yA} \left( \frac{1}{E_A} + \frac{1}{E_S} \right). \quad (5)$$

A situation is possible when plastic deformations occur in the aluminium ring during fitting before heating. Expression (4) as well as (5) hold good irrespective of the manner in which the yield stress  $\sigma_{yA}$  has been reached.

24. If the temperature elongations of the ring and cone are the same, the height  $h$  remains obviously unchanged.

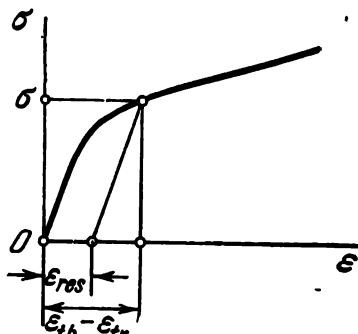


Fig. 207

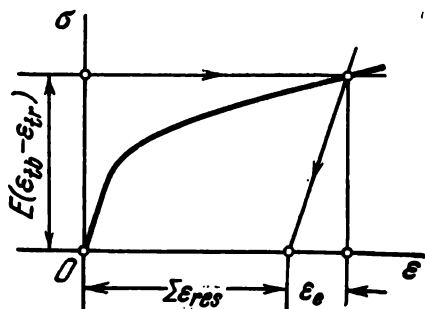


Fig. 208

Suppose that the temperature elongation of the conical bar is larger than the temperature elongation of the ring

$$\epsilon_{tb} > \epsilon_{tr}.$$

In this case the ring, on heating, develops a tensile stress  $\sigma$  whose magnitude depends on the difference of the temperature strains  $\epsilon_{tb} - \epsilon_{tr}$  (Fig. 207). If the stress  $\sigma$  remains below the elastic limit, the ring recovers its dimensions on cooling and the height  $h$  is unchanged. If, however, the difference  $\epsilon_{tb} - \epsilon_{tr}$  is sufficiently large, the ring undergoes a permanent deformation and moves down on cooling. On reheating it is again extended and subsequently again moves down. This downward motion will continue until the elastic strain  $\epsilon_e$  equals the difference  $\epsilon_{tb} - \epsilon_{tr}$  (Fig. 208). From the value of the overall residual strain  $\sum \epsilon_{\text{res}}$  it is easy to determine the new height of the ring.

A similar situation occurs when  $\epsilon_{tb} < \epsilon_{tr}$ . In this case the downward motion of the ring takes place during heating and its extension during cooling.

25. The strain in the tube in the circumferential direction is given as

$$\epsilon_t = \frac{\Delta}{R} = \frac{1}{E} (\sigma_t - \mu \sigma_x).$$

Denote the contact pressure by  $p$  and the axial force induced in the tube by  $N$ . Then

$$\sigma_t = \frac{pR}{h}, \quad \sigma_x = \frac{N}{2\pi R h},$$

where  $h$  is the thickness of the tube. Thus,

$$\frac{\Delta}{R} = \frac{1}{Eh} \left( pR - \mu \frac{N}{2\pi R} \right). \quad (1)$$

But the axial force at the section  $x$  is determined by the integral of the frictional forces in the interval  $(0 - x)$ , i.e.,

$$N = \int_0^x f p 2\pi R dx, \quad (2)$$

where  $f$  is the coefficient of friction. Expression (1) now becomes

$$\frac{\Delta}{R} = \frac{1}{Eh} \left( pR - \mu f \int_0^x p dx \right).$$

On differentiating this expression with respect to  $x$ , we obtain

$$\frac{dp}{dx} - \frac{\mu f}{R} p = 0,$$

whence

$$p = p_0 e^{\frac{\mu f}{R} x}.$$

The constant  $p_0$  represents the contact pressure at the end of the tube. It is found from expression (1) by setting  $N = 0$ ; we have

$$p_0 = \frac{Eh}{R^2} \Delta.$$

Consequently,

$$p = \frac{Eh\Delta}{R^2} e^{\frac{\mu f}{R} x}.$$

From expression (2) we find the axial force

$$N = \frac{2\pi Eh\Delta}{\mu} (e^{\frac{\mu f}{R} x} - 1).$$

Thus, the contact pressure and the axial force increase with the distance from the end of the tube. This increase obviously ceases where the axial extension due to the forces  $N$  and  $p$  becomes equal to the initial axial extension of the tube. But for the heated tube uniformly expanding in all directions, the axial extension at the moment of fitting was equal to the circumferential extension, i.e.,  $\Delta/R$ . We express the axial extension in terms of  $p$  and  $N$

$$\begin{aligned} \varepsilon_x &= \frac{1}{E} (\sigma_x - \mu \sigma_t), \\ \varepsilon_x &= \frac{\Delta}{\mu R} [(1 - \mu^2) e^{\frac{\mu f}{R} x} - 1]. \end{aligned}$$

Denote by  $a$  the distance from the end of the tube at which slipping still occurs and there are frictional forces. From the last expression, setting  $\varepsilon_x = \Delta/R$  and  $x = a$ , we find

$$a = \frac{R}{\mu f} \ln \frac{1}{1 - \mu}.$$

When  $x > a$ ,  $\varepsilon_x = \varepsilon_t = \frac{\Delta}{R} = \text{constant}$  and we have

$$N = \frac{2\pi Eh\Delta}{1 - \mu}, \quad p = \frac{Eh\Delta}{R^2} \frac{1}{1 - \mu}.$$

At the other end of the tube the distribution of the forces is similar.

Figure 209 shows the laws of variation of the normal force  $N$ , the frictional forces  $dN/dx$ , and the contact pressure  $p$  along the axis of the tube. For comparison, the same graphs are shown alongside for the case of a shorter tube ( $l < 2a$ ).

26. Consider the case (a). The normal force at the section of the tube (Fig. 210) is

$$N = \int_0^x fp2\pi R dx - P. \quad (1)$$

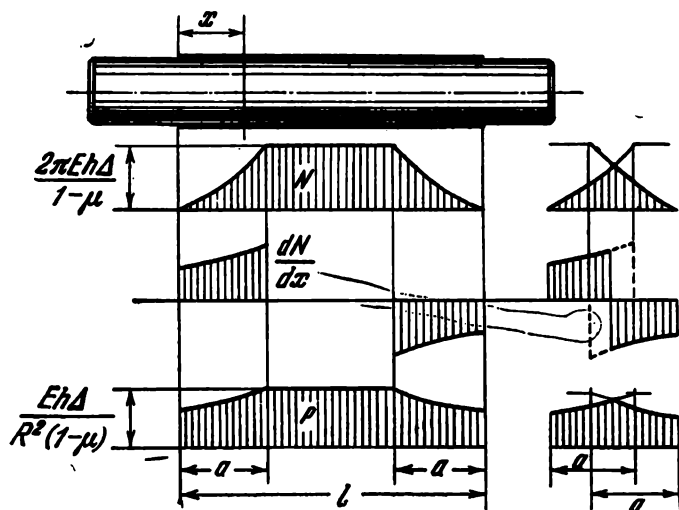


Fig. 209

Instead of expression (1) obtained in the solution of the

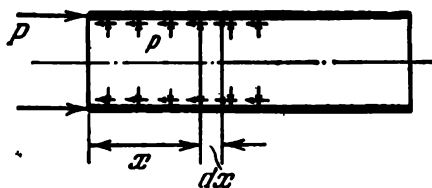


Fig. 210

preceding problem, we have

$$\frac{\Delta}{R} = \frac{1}{Eh} \left[ pR - \frac{\mu}{2\pi R} \left( -P + 2\pi Rf \int_0^x p dx \right) \right]. \quad (2)$$

As before,

$$p = p_0 e^{\frac{\mu f}{R} x}.$$

The magnitude of  $p_0$  is determined from Eq. (2) by setting  $x = 0$  in it

$$\frac{\Delta}{R} = \frac{1}{Eh} \left( p_0 R + \frac{\mu}{2\pi R} P \right),$$

whence

$$p_0 = \frac{Eh}{R^2} \Delta - \frac{\mu P}{2\pi R^2}.$$

We thus obtain

$$p = \left( \frac{Eh\Delta}{R^2} - \frac{\mu P}{2\pi R^2} \right) e^{\frac{\mu f}{R} x}$$

and from Eq. (1)

$$N = -\frac{2\pi Eh\Delta}{\mu} + \left( \frac{2\pi Eh\Delta}{\mu} - P \right) e^{\frac{\mu f}{R} x}.$$

Figure 211 shows the graphs of the variation of the force  $N$ , the frictional forces  $dN/dx$ , and the contact pressure  $p$

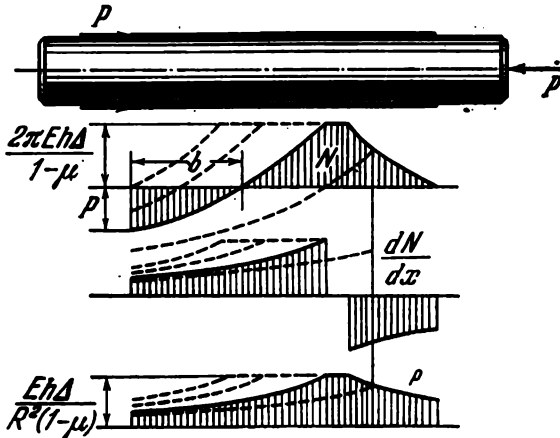


Fig. 211

along the length of the tube. Dashed lines indicate the course of the curves for  $P = 0$  and for some other values of  $P$ .

The tube will be removed from the bar at a force  $P'$  at which the segment  $b$  (Fig. 211) becomes equal to the length of the tube  $l$ .

Setting  $N = 0$  and  $x = l$  in the last expression, we find

$$P' = \frac{2\pi Eh\Delta}{\mu} \left( 1 - e^{-\frac{\mu f}{R} l} \right).$$

Consider now the case (b). Here both the force  $P$  and the frictional forces near the left end of the tube reverse their sense. Hence,

$$N = P - \int_0^x fp2\pi R \, dx$$

and, instead of Eq. (2), we obtain

$$\frac{\Delta}{R} = \frac{1}{Eh} \left[ pR - \frac{\mu}{2\pi R} \left( P - 2\pi Rf \int_0^x p \, dx \right) \right].$$

Then

$$p = p_0 e^{-\frac{\mu f}{R} x},$$

where

$$p_0 = \frac{Eh}{R^2} \Delta + \frac{\mu P}{2\pi R^2}.$$

Further,

$$N = -\frac{2\pi Eh\Delta}{\mu} + \left( \frac{2\pi Eh\Delta}{\mu} + P \right) e^{-\frac{\mu f}{R} x}.$$

The corresponding laws of variation of  $N$ ,  $dN/dx$ , and

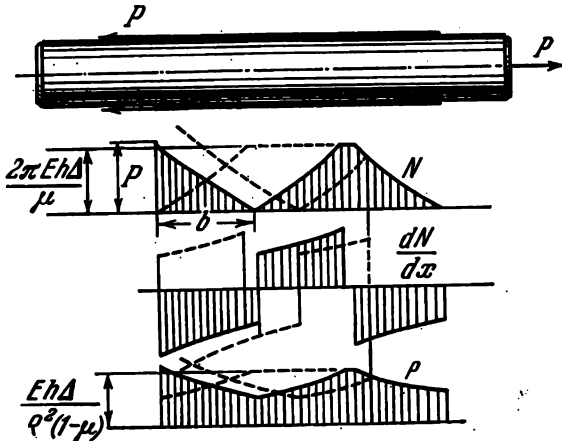


Fig. 212

$p$  are shown in Fig. 212. When  $x = b$ , the frictional forces reverse abruptly their direction.

Setting  $N = 0$  and  $x = l$  in the last expression, we find the required value of the force  $P'$  at which the tube is removed from the bar

$$P' = \frac{2\pi E h \Delta}{\mu} \left( e^{\frac{\mu f}{R} l} - 1 \right).$$

The magnitude of this force is found to be larger than in the case (a), which is quite obvious since the tensile force produces a contraction of the tube and an increase of the frictional forces.

27. Suppose that a shearing stress  $\tau$  occurs at an angular point of the cross section of the rod (Fig. 213).

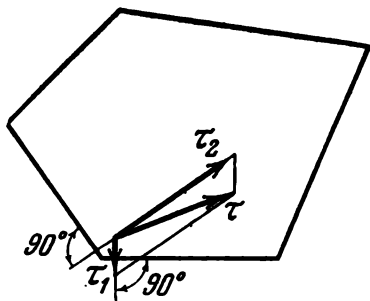


Fig. 213

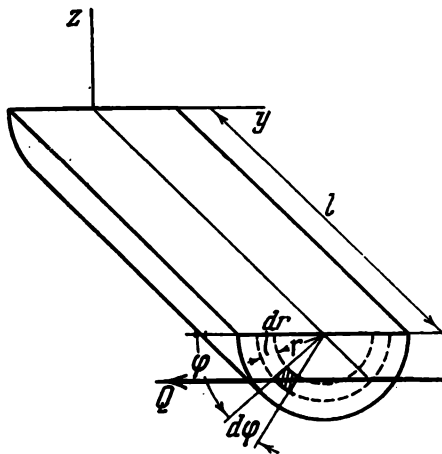


Fig. 214

Resolve it into two components,  $\tau_1$  and  $\tau_2$ , perpendicular to the sides of the polygon. Since the shearing stresses always occur in pairs, there must be equal shearing stresses  $\tau_1$  and  $\tau_2$  on the lateral faces of the rod. But the lateral surface is free from stress. Consequently,  $\tau_1 = \tau_2 = 0$ . It follows that  $\tau = 0$ .

It is clear that the proposition proved above remains true for any value of the angle less than 180 degrees.

28. The resultant moment of the stresses  $\tau'$  is balanced by the moment of the resultant force  $Q$  produced in the plane of the normal section (Fig. 214). The magnitude of

this force is evidently given by

$$Q = \int_0^R \int_0^\pi \tau r \sin \varphi \, dr \, d\varphi.$$

But we have

$$\tau = \tau_{\max} \frac{r}{R};$$

hence,

$$Q = \int_0^R \int_0^\pi \tau_{\max} \frac{r^2}{R} \sin \varphi \, dr \, d\varphi = \frac{2}{3} \tau_{\max} R^2.$$

The moment of the force  $Q$  about the  $z$  axis is

$$M = \frac{2}{3} \tau_{\max} R^2 l.$$

Exactly the same moment is produced by the stresses  $\tau'$

$$M = 2l \int_0^R \tau' r \, dr = \frac{2\tau_{\max} l}{R} \int_0^R r^2 \, dr = \frac{2}{3} \tau_{\max} R^2 l.$$

29. If the rod were twisted without extension, there would be the following relation between the angle of twist per unit length  $\theta$  and the moment  $M$  in the range of small displacements:

$$\theta = \frac{3M}{Gbh^3},$$

i.e., the torsional rigidity would be equal to

$$C_0 = \frac{1}{3} Gbh^3.$$

Consider now the case of twisting the rod in the presence of the tensile force  $P$ . When the end section rotates, the normal stresses  $P/bh$  retain the direction of the longitudinal fibres of the twisted strip (Fig. 215). The projections of these stresses on a plane perpendicular to the axis of the strip are

$$\frac{P}{bh} \frac{d\varphi}{dx} y = \frac{P}{bh} \theta y$$

(Fig. 215). These stresses give an additional twisting moment

$$M_P = \int_{-b/2}^{+b/2} \frac{P}{bh} \theta y^2 h dy = P\theta \frac{b^2}{12}.$$

By adding this moment to the moment produced by the shearing stresses, we find

$$M = C_0\theta + P\theta \frac{b^2}{12} = \theta \left( C_0 + \frac{Pb^2}{12} \right).$$

Thus, the torsional rigidity of the stretched strip is

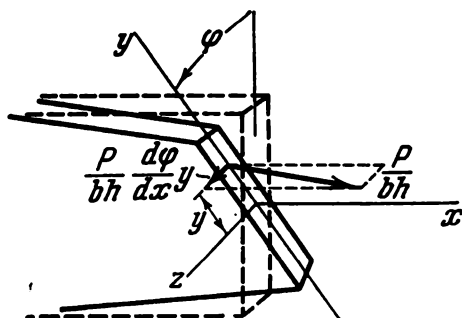


Fig. 215

equal to the torsional rigidity of the unstretched strip plus the quantity

$$\frac{Pb^2}{12}.$$

30. Since the tube and the shaft are not rigid, local slipping on the contact surface begins before the magnitude of the moment reaches the value  $M_0$ . At first slipping occurs in the end zones of the contact region. When  $M = M_0$ , slipping occurs over the entire surface of contact. The moment of the frictional forces attains its limiting value  $M_0$  and the shaft begins to turn in the tube throughout the length of contact.

We divide the segment of contact  $l$  into three zones,  $a$ ,  $b$ , and  $c$  (Fig. 216). In the portion  $a$ , the twisting moment in the tube is larger than in the shaft, and accordingly the angle of twist is larger. As we pass from section  $A$  to section  $B$ , the twisting moment is transmitted from the tube to the shaft, and at the section  $B$  the angles of twist of the tube and shaft become equal.

In the portion  $b$  no slipping occurs. In the portion  $c$  there is again slipping. Here the twisting moment in the shaft is larger than in the tube. The angle of twist is accord-

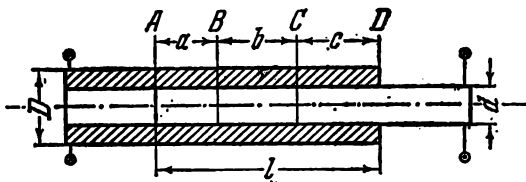


Fig. 216

ingly larger. As we pass from section  $C$  to section  $D$ , the moment in the tube drops to zero and increases to  $M$  in the shaft.

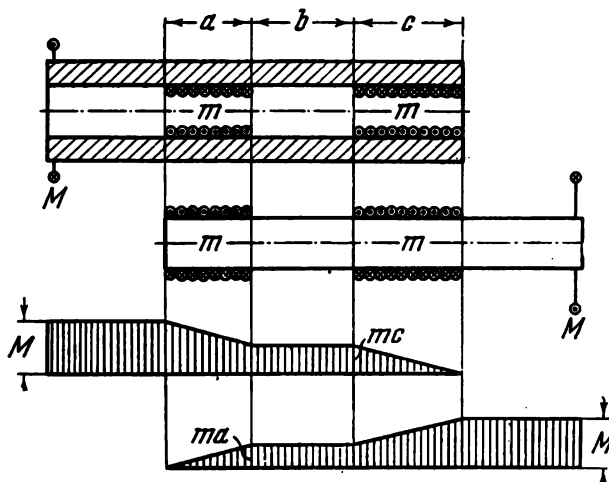


Fig. 217

The intensity of moments of the frictional forces is

$$m = \frac{M_0}{l}. \quad (1)$$

The magnitude of  $m$  is independent of the moment  $M$  and is determined only by the coefficient of friction and the amount of negative allowance.

Determine now the lengths of the portions  $a$ ,  $b$ ,  $c$ . To do this we consider the tube and shaft separately (Fig. 217).

Obviously, from the condition of equilibrium we have

$$m(a + c) = M \quad (2)$$

and from the condition of equal angles of twist in the portion  $b$  we obtain

$$\frac{mc}{(GI_p)_t} = \frac{ma}{(GI_p)_s}. \quad (3)$$

From Eqs. (2) and (3) we find

$$a = \frac{\frac{Ml}{M_0}}{1 + \frac{(GI_p)_t}{(GI_p)_s}}, \quad c = \frac{\frac{Ml}{M_0}}{1 + \frac{(GI_p)_s}{(GI_p)_t}}. \quad (4)$$

If the rigidities of the tube and shaft are the same, then from (4) we obtain

$$a = c = \frac{Ml}{2M_0}.$$

With the known  $a$  and  $c$  we construct the moment diagrams (Fig. 217).

As the moment  $M$  increases, the portions  $a$  and  $c$  become longer and the portion  $b$  contracts. When  $M = M_0$ , the sum  $a + c$  is equal to  $l$  and  $b = 0$ . After this the moment of the frictional forces which increases due to an increase in the portions  $a$  and  $c$  can no longer rise, and a general slipping begins over the contact surface.

31. We place the origin of co-ordinates  $x, y$  (Fig. 218) at the centroid of the glue spot. Suppose that the glued plate, on being loaded, shifts to the left by  $\Delta_x$  and down by  $\Delta_y$  and, besides, rotates clockwise through a small angle  $\varphi$ .

We determine the stresses  $\tau_x$  and  $\tau_y$  acting on the corner plate. They are proportional to the local displacement, i.e., to the displacement of a point with co-ordinates  $x, y$

$$\tau_x = k(\Delta_x - \varphi y), \quad \tau_y = k(\Delta_y + \varphi x),$$

where  $k$  is some factor of proportionality between stress and displacement.

We write the equations of equilibrium

$$\begin{aligned} \int_A \tau_x dA &= 0, & \int_A \tau_y dA &= P, \\ \int_A (\tau_y x - \tau_x y) dA &= M, \end{aligned}$$

where  $M$  is the moment of the force  $P$  about the origin. The integration is extended over the entire area of the spot or over the total area of spots if they are several.

Noting that the  $x$  and  $y$  axes are centroidal, we obtain

$$\Delta_x = 0, \quad k\Delta_y A = P, \quad k\varphi I_p = M,$$

where  $I_p$  is the polar moment of inertia of the glue spot with respect to the centroid. Inserting  $\Delta_x$ ,  $\Delta_y$ , and  $\varphi$  in

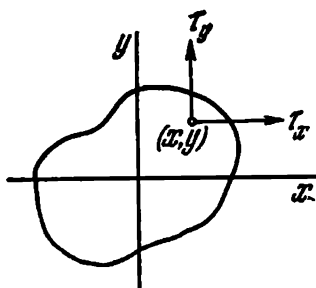


Fig. 218

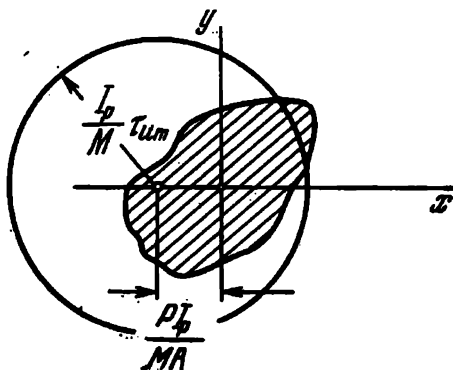


Fig. 219

the expressions for the stresses  $\tau_x$  and  $\tau_y$ , we obtain

$$\tau_x = -\frac{M}{I_p} y, \quad \tau_y = \frac{P}{A} + \frac{M}{I_p} x.$$

The total stress is

$$\tau = \sqrt{\tau_x^2 + \tau_y^2}.$$

Substituting the expressions for  $\tau_x$  and  $\tau_y$ , we determine the locus of points where the total stress attains its limiting value  $\tau_{lim}$

$$\left(x + \frac{P}{M} \frac{I_p}{A}\right)^2 + y^2 = \left(\frac{I_p \tau_{lim}}{M}\right)^2.$$

As seen, this is a circle of radius  $I_p \tau_{lim} / M$ . The centre of the circle is on the  $x$  axis and is shifted to the left by the amount

$$\frac{P}{M} \frac{I_p}{A}$$

(Fig. 219). If the circle intersects the contour of the glue spot, the stress in the outside region of the spot exceeds the

limiting value. If the glue spot lies entirely within the circle, the strength condition is fulfilled.

32. (1) By a cylindrical surface passing along the given contour we isolate the interior of the rod (Fig. 220). Shearing stresses equal to  $\tau_n$  are produced on the drawn cylindrical

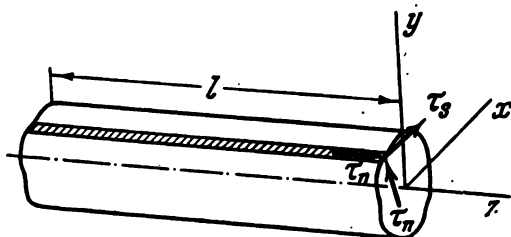


Fig. 220

surface. By projecting on the  $z$  axis all forces acting on the isolated part of the rod, we obtain

$$\int_z \tau_n l ds = 0$$

or

$$\int_z \tau_n ds = 0.$$

(2) Consider an element  $ds dz$  of the cylindrical surface passed through the drawn contour (Fig. 221). After loading

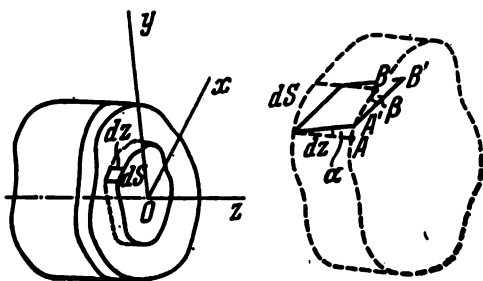


Fig. 221

the rod, this element distorts and assumes the shape of the parallelogram as shown in Fig. 221. The angle of shear  $\gamma$

is determined by the sum of the angles  $\alpha$  and  $\beta$ , i.e.,

$$\gamma = \alpha + \beta.$$

We now find an expression for each of these components. The angle  $\alpha$  is determined by the angle of twist  $\theta$  and the distance from the centre of twist; indeed, from Fig. 221 we have

$$\alpha = \frac{AA'}{dz};$$

but  $AA' = n d\phi$ , where  $d\phi$  is the relative angle of rotation of sections a distance  $dz$  apart,  $n$  is the distance from the centre of twist  $O$  (Fig. 222) to the tangent to the contour at the point  $A$ . Since  $d\phi/dz = \theta$ ,  $\alpha = \theta n$ .

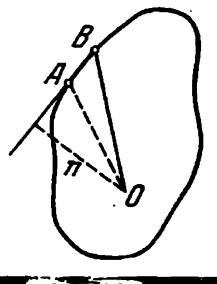


Fig. 222

The cross section of the rod does not remain plane during twisting but undergoes a certain displacement  $w(x, y)$  in the  $z$  direction. Obviously (Fig. 221),

$$\beta = \frac{dw}{ds}.$$

Since  $\gamma = \tau_s/G$ ,

$$\frac{\tau_s}{G} = \theta n + \frac{dw}{ds},$$

whence

$$dw = \left( \frac{\tau_s}{G} - \theta n \right) ds.$$

The integral of  $dw$  round the closed contour is zero. Hence,

$$\frac{1}{G} \int \tau_s ds - \theta \int n ds = 0.$$

But  $n ds$  is equal to twice the area of the triangle  $OAB$  (Fig. 222); consequently,

$$\int n ds = 2A_s, \quad \int \tau_s ds = 2GA_s\theta.$$

33. Figure 223 shows a thin-walled section whose principal centroidal axes are  $x, y$ . Suppose that during twisting the

section rotates through an angle  $\varphi$  about some point  $C$  having co-ordinates  $x_c, y_c$ . The generator  $AB$  (Fig. 223)

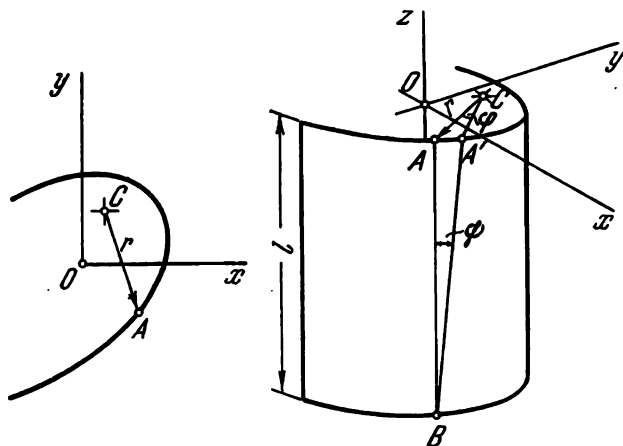


Fig. 223

then rotates through an angle  $\psi = r\varphi/l = r\theta$ . This gives rise to the longitudinal extension

$$\varepsilon = \frac{A'B - AB}{AB} = \frac{1}{\cos \psi} - 1, \quad \varepsilon \cong \frac{1}{2} \psi^2$$

or

$$\varepsilon = \frac{1}{2} r^2 \theta^2.$$

Simultaneously with the rotation about the longitudinal axis, there may be a relative rotation of sections about the  $x$  and  $y$  axes and a relative axial displacement. As a result, the expression for  $\varepsilon$  will involve an additional component linearly dependent on  $x$  and  $y$ , i.e., we have

$$\varepsilon = \frac{1}{2} r^2 \theta^2 + a + bx + cy$$

and, accordingly,

$$\sigma = E \left( \frac{1}{2} r^2 \theta^2 + a + bx + cy \right). \quad (1)$$

The warping of the section does not affect the extension  $\varepsilon$  since we consider unrestrained torsion ( $\theta$  does not change along the length of the bar).

The constants  $a$ ,  $b$ , and  $c$  must be chosen so as to make the normal force at the section and the bending moments about the  $x$  and  $y$  axes vanish

$$N = \int_A \sigma dA = 0, \quad M_x = \int_A \sigma y dA = 0, \quad M_y = \int_A \sigma x dA = 0,$$

whence

$$a = -\frac{\theta^2 I_p}{2A}, \quad b = -\frac{\theta^2 H_y}{2I_y}, \quad c = -\frac{\theta^2 H_x}{2I_x},$$

where  $I_x$ ,  $I_y$ , and  $I_p$  are the axial and polar moments of inertia of the section,  $H_x$  and  $H_y$  are new geometrical characteristics

$$H_x = \int_A r^2 y dA, \quad H_y = \int_A r^2 x dA.$$

Expression (1) becomes

$$\sigma = \frac{E\theta^2}{2} \left( r^2 - \frac{I_p}{A} - \frac{H_y}{I_y} x - \frac{H_x}{I_x} y \right). \quad (2)$$

The stresses  $\sigma$  give an additional twisting moment at the section

$$M_z = \int_A \sigma \psi r dA$$

or

$$M_z = \frac{E\theta^3}{2} \int_A \left( r^2 - \frac{I_p}{A} - \frac{H_y}{I_y} x - \frac{H_x}{I_x} y \right) r^2 dA,$$

$$M_z = \frac{E\theta^3}{2} K,$$

where  $K$  stands for a new geometrical characteristic

$$K = \int_A r^4 dA - \frac{I_p^2}{A} - \frac{H_y^2}{I_y} - \frac{H_x^2}{I_x}. \quad (3)$$

The twisting moment at the section consists of the "ordinary" moment produced by the shearing stresses and of the additional moment

$$M_t = \frac{1}{3} s \delta^3 G \theta + \frac{E\theta^3}{2} K = \frac{1}{3} s \delta^3 G \theta \left( 1 + \frac{E}{G} \frac{3}{2\delta^3 s} \theta^2 K \right), \quad (4)$$

where  $s$  is the arc length of the contour of the section.

By making the substitution of  $(x - x_c)^2 + (y - y_c)^2$  for  $r^2$  in expressions (2) and (3), we note that the coordinates  $x_c$  and  $y_c$  are eliminated in the expressions for  $\sigma$  and  $K$ . This means that the pole  $C$  may be chosen arbitrarily and

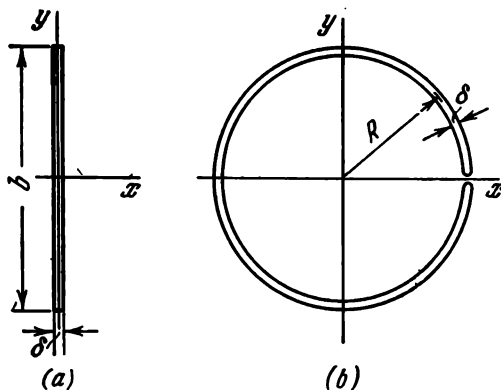


Fig. 224

here one should be guided exclusively by considerations of convenience.

Consider special cases.

(a) A strip of rectangular cross section with sides  $b$  and  $\delta$  (Fig. 224a). In this case we have

$$A = b\delta, \quad I_p = \frac{b^3\delta}{12}, \quad H_x = H_y = 0,$$

$$K = \delta \int_{-b/2}^{+b/2} y^4 dy - \frac{b^5\delta}{144} = \frac{b^5\delta}{180}.$$

Then

$$\sigma = \frac{E\theta^2}{2} \left( y^2 - \frac{b^2}{12} \right), \quad M_t = \frac{1}{3} b\delta^3 G\theta \left( 1 + \frac{E}{G} \frac{b^4}{120\delta^2} \theta^2 \right).$$

The last term in the expression for  $M_t$  gives a quantitative estimate of the non-linear effect.

(b) A circular unclosed section (Fig. 224b)

$A = 2\pi R\delta$ ,  $I_p = 2\pi R^3\delta$ ,  $H_x = H_y = 0$ ,  $K = 0$ ;  
consequently,  $\sigma = 0$ ,

$$M_t = \frac{1}{3} 2\pi R\delta^3 G\theta.$$

The non-linear effect is absent in this case.

34. We isolate an elementary ring of thickness  $dz$  from the bar by two cylindrical surfaces of radii  $r$  and  $r + dr$  and two transverse sections (Fig. 225).

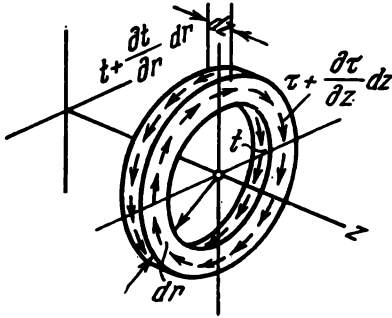


Fig. 225

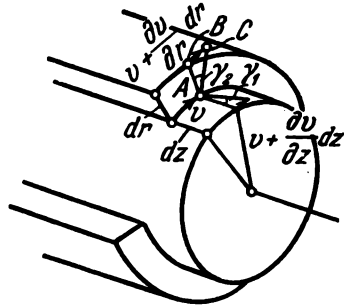


Fig. 226

By equating to zero the sum of the moments about the  $z$  axis, we obtain

$$\begin{aligned} & \left( \tau + \frac{\partial \tau}{\partial z} dz \right) 2\pi r^2 dr - \tau 2\pi r^2 dr = \\ & = \left( t + \frac{\partial t}{\partial r} dr \right) 2\pi (r + dr)^2 dz - t 2\pi r^2 dz, \end{aligned}$$

whence

$$r^2 \frac{\partial \tau}{\partial z} = \frac{\partial}{\partial r} (tr^2). \quad (1)$$

Denote by  $v$  the displacement in the direction of the tangent to a circular arc (Fig. 226). The angle of shear in the cylindrical surface is, as usual,

$$\gamma_1 = \frac{\partial v}{\partial z}$$

and the stress is given by

$$\tau = G \frac{\partial v}{\partial z}. \quad (2)$$

The angle of shear  $\gamma_2$  in the plane of the cross section is equal to the ratio of the segments  $BC/AB$  (Fig. 226). But

$$BC = v + \frac{\partial v}{\partial r} dr - v \frac{r + dr}{r}, \quad AB = dr;$$

consequently,

$$\gamma_2 = \frac{\partial v}{\partial r} - \frac{v}{r}$$

and the corresponding stress is

$$t = -G \left( \frac{\partial v}{\partial r} - \frac{v}{r} \right). \quad (3)$$

Substituting for  $\tau$  and  $t$  in the equation of equilibrium (1), we obtain

$$\frac{\partial^2 v}{\partial z^2} + \frac{\partial}{\partial r} \left[ \frac{1}{r} \frac{\partial}{\partial r} (vr) \right] = 0. \quad (4)$$

It is natural to assume that the displacement  $v$  varies as a function of  $z$  according to a quadratic law, as in the usual torsion, i.e.,

$$v = v_0 + v_1 z + v_2 z^2,$$

where  $v_0, v_1, v_2$  depend only on  $r$ . After substituting for  $v$ , Eq. (4) falls into the following three equations:

$$\left[ \frac{1}{r} (v_0 r)' \right]' = -2v_2, \quad \left[ \frac{1}{r} (v_1 r)' \right]' = 0, \quad \left[ \frac{1}{r} (v_2 r)' \right]' = 0, \quad (5)$$

whence

$$v_1 = A_1 r + \frac{B_1}{r}, \quad v_2 = A_2 r + \frac{B_2}{r}.$$

Finally, on substituting for  $v_2$  in the right side of the first of Eqs. (5), we obtain

$$v_0 = A_0 r + \frac{B_0}{r} - \frac{A_2}{4} r^3 - B_2 r \ln r.$$

Since the displacements on the axis of the bar are zero, we must set  $B_0 = B_1 = B_2 = 0$ . Then

$$v = A_0 r - \frac{A_2}{4} r^3 + A_1 r z + A_2 r z^2$$

and, according to expressions (2) and (3),

$$\tau = G(A_1 + 2A_2 z)r, \quad t = G \frac{1}{2} A_2 r^2.$$

The shearing stresses at the left end ( $z = 0$ ) are zero. Consequently,  $A_1 = 0$ . On the surface of the cylinder ( $r =$

$= d/2$ )  $t = m/\pi d$ , hence  $A_2 = 8m/\pi l^3 G$  and we obtain, finally,

$$\tau = \frac{16m}{\pi d^3} rz, \quad t = \frac{4m}{\pi d^3} r^2.$$

Thus, the stresses  $\tau$  are linearly distributed along  $r$  and  $z$ , which follows also from the conventional theory of torsion. The stresses  $t$  are distributed along the radius according to a quadratic law. The ratio of the maximum values of  $\tau$  and  $t$  is

$$\frac{\tau_{\max}}{t_{\max}} = \frac{16m}{\pi d^3} \frac{d}{2} l : \frac{4m}{\pi d^3} \frac{d^2}{4} = 8 \frac{l}{d}.$$

Consequently, for a long cylinder the stress  $t_{\max}$  is very much less than  $\tau_{\max}$ .

35. Consider the conditions of equilibrium of an element  $dx dy dz$  (Fig. 227a).

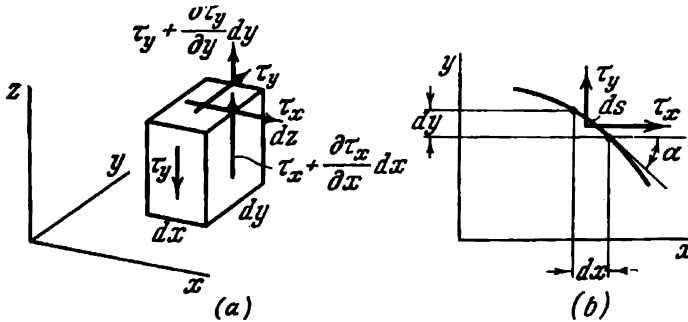


Fig. 227

Equating to zero the sum of the projections of all forces on the  $z$  axis gives

$$\frac{\partial \tau_x}{\partial x} + \frac{\partial \tau_y}{\partial y} = 0. \quad (1)$$

On the contour (Fig. 227b) we have the boundary condition

$$\tau_y \cos \alpha + \tau_x \sin \alpha = 0$$

or

$$\tau_y \frac{dx}{ds} + \tau_x \frac{dy}{ds} = 0, \quad \tau_y dx = -\tau_x dy. \quad (2)$$

We now consider the integrals indicated in the condition of the problem

$$\int \int \tau_{xy} dx dy, \quad \int \int \tau_{yx} dx dy.$$

Integration by parts of the first expression with respect to  $dx$  and of the second expression with respect to  $dy$  leads to

$$\int \int \tau_{xy} dx dy = \int \left[ \tau_{xx} \Big|_{x_1}^{x_2} - \int \frac{\partial \tau_{xx}}{\partial x} x dx \right] y dy,$$

$$\int \int \tau_{yx} dy dx = \int \left[ \tau_{yy} \Big|_{y_1}^{y_2} - \int \frac{\partial \tau_{yy}}{\partial y} y dy \right] x dx,$$

giving the expressions

$$\int \int \tau_{xy} dx dy = \int \tau_{xx} \Big|_{x_1}^{x_2} y dy - \int \int \frac{\partial \tau_{xx}}{\partial x} xy dx dy,$$

$$\int \int \tau_{yx} dx dy = \int \tau_{yy} \Big|_{y_1}^{y_2} x dx - \int \int \frac{\partial \tau_{yy}}{\partial y} xy dx dy.$$

According to the boundary condition (2), we obtain

$$\int \tau_{xx} \Big|_{x_1}^{x_2} y dy = - \int \tau_{yy} \Big|_{y_1}^{y_2} x dx$$

and from the condition of equilibrium (1) we have

$$\int \int \frac{\partial \tau_{xx}}{\partial x} xy dx dy = - \int \int \frac{\partial \tau_{yy}}{\partial y} xy dx dy.$$

Consequently, we arrive at the equality

$$\int \int \tau_{xy} dx dy = - \int \int \tau_{yx} dx dy.$$

But since

$$\int \int \tau_{xy} dx dy - \int \int \tau_{yx} dx dy = M_t,$$

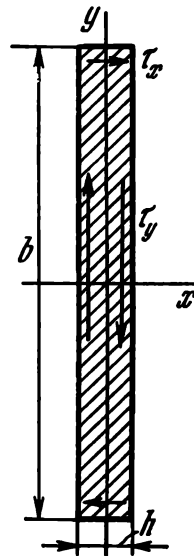


Fig. 228

we obtain, finally,

$$\int_x \int_y \tau_x y \, dx \, dy = \frac{M_t}{2}, \quad - \int_x \int_y \tau_y x \, dx \, dy = \frac{M_t}{2}.$$

There is an element of instructiveness in the relations obtained. For example, in the torsion of a narrow rectangular strip (Fig. 228) we always neglect the stresses  $\tau_x$  in comparison with  $\tau_y$ . This is correct. But if we neglected the moment of small stresses  $\tau_x$  in determining the twisting moment, that would halve the moment. For small stresses  $\tau_x$  on a large arm  $y$  give exactly the same moment as large stresses  $\tau_y$  on a small arm  $x$ .

## II. Geometrical Properties of Sections. Bending

36. The product of inertia of a right triangle with respect to axes parallel to the legs and passing through their middles is zero (Fig. 229).

By the parallel-axis formula we obtain

$$I_{xy} = I_{x_0y_0} - \frac{b}{6} \frac{h}{6} \frac{bh}{2},$$

where

$$I_{x_0y_0} = 0,$$

consequently,

$$I_{xy} = -\frac{b^2h^2}{72}.$$

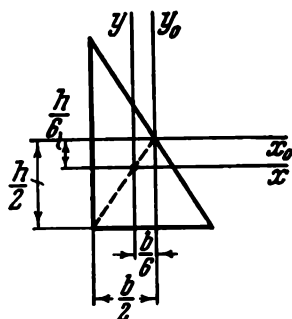


Fig. 229

37. Denote by  $I_{p_0}$  the polar moment of inertia of a figure with respect to its centroid and by  $I_p$  the moment with respect to some arbitrary point with co-ordinates  $a, b$  (Fig. 230).

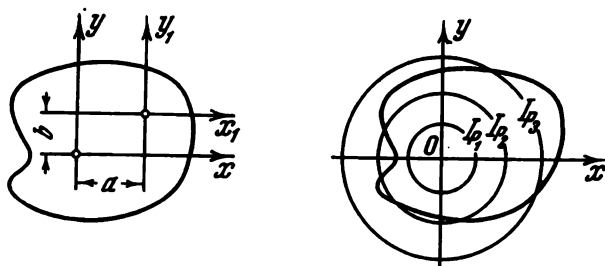


Fig. 230

Obviously,

$$I_p = I_{x_1} + I_{y_1} = I_x + I_y + (a^2 + b^2) A,$$

whence

$$a^2 + b^2 = \frac{I_p - I_{p_0}}{A}.$$

Consequently, the locus of constant polar moments of inertia of a plane figure is a family of concentric circles centred at the point  $O$  (see Fig. 230).

The radius of each circle is given by  $I_p$

$$R = \sqrt{\frac{I_p - I_{p0}}{A}}.$$

38. Consider a plane section (Fig. 231). Let the  $x$  and  $y$  axes be principal. Suppose that there exist one more pair of principal axes  $u, v$  not coinciding with  $x, y$  (angle  $\alpha$  is not an integer multiple of  $\pi/2$ ). If the  $u, v$  axes are principal, then  $I_{uv} = 0$ . But it is known that

$$I_{uv} = I_{xy} \cos 2\alpha + \frac{I_x - I_y}{2} \sin 2\alpha$$

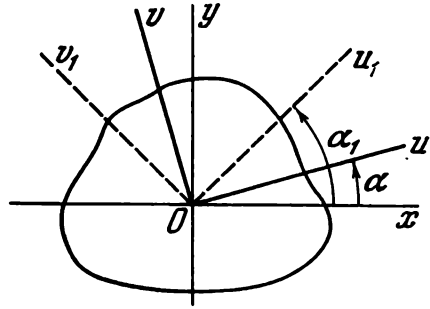


Fig. 231

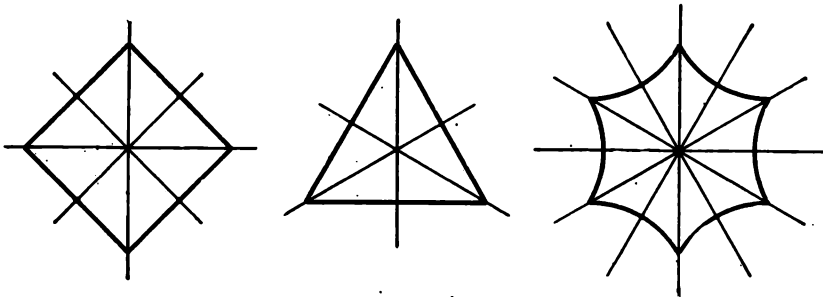


Fig. 232

and since the  $x, y$  axes are also principal,  $I_{xy} = 0$ . Consequently,

$$\frac{I_x - I_y}{2} \sin 2\alpha = 0,$$

but  $\sin 2\alpha \neq 0$ , hence

$$I_x = I_y. \quad (1)$$

We now consider an arbitrarily taken pair of axes  $u_1, v_1$  for which

$$I_{u_1 v_1} = I_{xy} \cos 2\alpha_1 + \frac{I_x - I_y}{2} \sin 2\alpha_1.$$

Obviously, irrespective of the angle  $\alpha_1$  we have  $I_{u_1v_1} = 0$ , i.e., every pair of axes  $u_1, v_1$  are principal.

It follows from the above that for every section having three or more axes of symmetry all centroidal axes are principal and the axial moment of inertia with respect to any centroidal axis is the same [this follows from expression (1)].

This property is found, for example in sections such as shown in Fig. 232 (square, equilateral triangle, curvilinear hexagon, etc.).

39. Consider a plane section with principal centroidal axes  $x, y$  (Fig. 233). Let the point  $A$  that we are seeking have

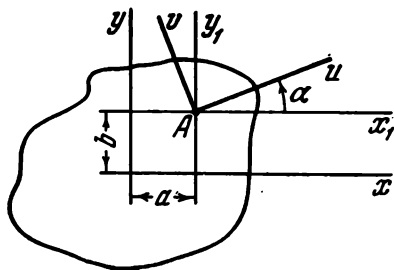


Fig. 233

co-ordinates  $a, b$ . We now choose  $a$  and  $b$  so as to make  $I_{uv}$  zero for all  $\alpha$ . We first determine, by the parallel-axis formulas,

$$I_{x_1} = I_x + b^2 A, \quad I_{y_1} = I_y + a^2 A, \quad I_{x_1 y_1} = abA.$$

Further, by the formula for rotated axes we have

$$I_{uv} = I_{x_1 y_1} \cos 2\alpha + \frac{I_{x_1} - I_{y_1}}{2} \sin 2\alpha.$$

For  $I_{uv}$  to be zero for any angle  $\alpha$ , it is obviously necessary that

$$I_{x_1 y_1} = 0, \quad I_{x_1} - I_{y_1} = 0$$

or

$$abA = 0, \quad I_x - I_y = (a^2 - b^2) A.$$

From the first equation it follows that either  $b$  or  $a$  or a combination of  $a$  and  $b$  is zero, i.e., the required point is, in any case, on one of the principal centroidal axes.

Suppose that  $I_y \geq I_x$  and set  $b = 0$  to begin with. Then

$$a = \pm \sqrt{\frac{I_x - I_y}{A}}.$$

In the case of  $I_y > I_x$   $a$  is an imaginary number. When  $I_y = I_x$ ,  $a = 0$ .

We now set  $a = 0$ . Then

$$b = \pm \sqrt{\frac{I_y - I_x}{A}}.$$

When  $I_y > I_x$ ,  $b$  is real. When  $I_y = I_x$ ,  $b = 0$ .

We thus obtain four required points with co-ordinates

$$(1) \quad a = + \sqrt{\frac{I_x - I_y}{A}}, \quad b = 0;$$

$$(2) \quad a = - \sqrt{\frac{I_x - I_y}{A}}, \quad b = 0;$$

$$(3) \quad a = 0, \quad b = + \sqrt{\frac{I_y - I_x}{A}};$$

$$(4) \quad a = 0, \quad b = - \sqrt{\frac{I_y - I_x}{A}}.$$

The points lying on the axis of minimum moment of inertia are imaginary. The points lying on the axis of maximum moment of inertia are real. If the principal moments of inertia are equal to ( $I_x = I_y$ ), all four points are real and are at the centroid. Then all axes through the centroid are principal (circle, square, equilateral triangle, etc.).

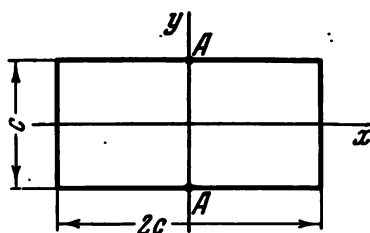


Fig. 234

As an example let us consider a rectangle of sides  $c$  and  $2c$  (Fig. 234)

$$I_x = \frac{2c \cdot c^3}{12}, \quad I_y = \frac{c \cdot (2c)^3}{12}, \quad A = 2c^2.$$

The co-ordinates of the required real points are

$$a = 0,$$

$$b = \pm \sqrt{\frac{\frac{c \cdot (2c)^3}{12} - \frac{2c \cdot c^3}{12}}{2c^2}} = \pm \frac{c}{2}.$$

These points (*A*) are marked in Fig. 234. All axes passing through these points are principal.

40. If there are no stresses on the neutral plane *OO*, the rod can, of course, be divided into two parts and the strains

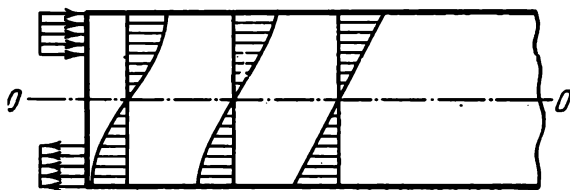


Fig. 235

and stresses in it will not be affected, but for this it is necessary to preserve the same loading conditions at the ends of the rod. When we draw a moment at the ends of a rod (as, for example, is done in Fig. 37), this merely means that the resultant moment of the stresses at the end of the rod is *M*. We usually say nothing about the law of distribution of the stresses, which reduce to *M*, over the end itself. But this is unimportant. No matter how we apply the forces, the stresses level off very rapidly with the distance from the end of the rod and their law of distribution assumes the form of the well-known linear relation.

Figure 235 shows a gradual modification of the normal stress diagram from the end of the rod towards its middle. By way of example we take an arbitrary law of stepwise stress distribution for the end. The stresses level off over a very short portion of the rod, but in this portion rather large shearing stresses act in the neutral plane *OO*.

In the formulation the problem is given it is no longer immaterial how the stresses are distributed over the end of the rod in the two cases. In the first variant of the rod (Fig. 37) the stresses are assumed to be distributed at the

end according to one law (Fig. 236*a* and *c*), and in the second case (Fig. 38) according to another law (Fig. 236*b* and *d*).

If we are able to ensure the same linear law of stress distribution over the end of the cut rod as for the solid rod

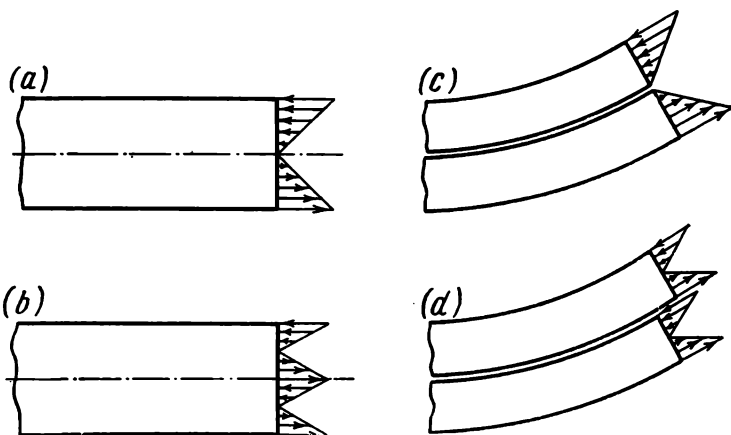


Fig. 236

(Fig. 236*c*), the rod can be divided into two parts without disturbing its operation. From the standpoint of design this is not difficult to accomplish. For that it is sufficient, for



Fig. 237

example, to provide a rigid bracing member for both cut parts at the ends of the rod (Fig. 237).

41. This is the so-called Parent problem.\* Since

$$b^2 + h^2 = 4R^2,$$

the section modulus for the rectangular cross section with respect to the  $x$  axis (Fig. 238) is

$$Z_x = \frac{bh^2}{6} = \frac{b}{6} (4R^2 - b^2).$$

\* The French scientist (1666-1716).

This quantity is a maximum when  $b = 2R/\sqrt{3}$  and accordingly when  $h = b\sqrt{2}$ .

Parent gave the answer in a form convenient for a craftsman working with an axe. It is necessary to divide the diameter of the circle (Fig. 239) into three parts and to draw

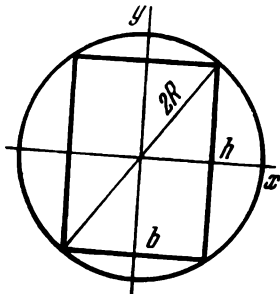


Fig. 238

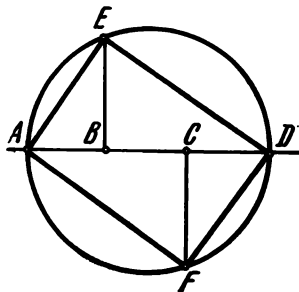


Fig. 239

perpendiculars from the points  $B$  and  $C$  until they intersect the circle. The rectangle  $AEDF$  is the required section of the rod.

42. For the neutral axis of the total stress ( $\sigma$ ) diagram to pass through the centroid of the section  $I-I$ , the force must pass through the centre of curvature, i.e.,  $x = 0$ .

The bending stresses in a rod of large curvature are determined by the formula

$$\sigma_b = -\frac{My}{Ae(r+y)},$$

where  $r$  is the distance from the centre of curvature to the neutral axis,  $e$  is the distance from the neutral axis to the centroid. In our case  $M = P(r+e+x)$ . At the centroid, i.e., when  $y = e$ ,

$$\sigma_b = -\frac{P(r+e+x)e}{Ae(r+e)}.$$

According to the condition of the problem, the algebraic sum of this stress and the direct tensile stress must be zero

$$-\frac{P(r+e+x)}{A(r+e)} + \frac{P}{A} = 0,$$

from which we obtain

$$x = 0.$$

43. Expression (1) follows from the differential equation

$$y'' = \frac{M_b}{EI}$$

obtained from expression (2) on the assumption that the displacements of the rod are small

$$\frac{1}{\rho} = \frac{y''}{(1 + y'^2)^{3/2}} \cong y''.$$

Consequently, strictly speaking, in pure bending the beam bends into a circular arc which can be represented by a second-order parabola to a very high degree of accuracy in the range of small displacements.

44. The shape of the initially bent ski must be the same as a straight ski assumes under a uniformly distributed load

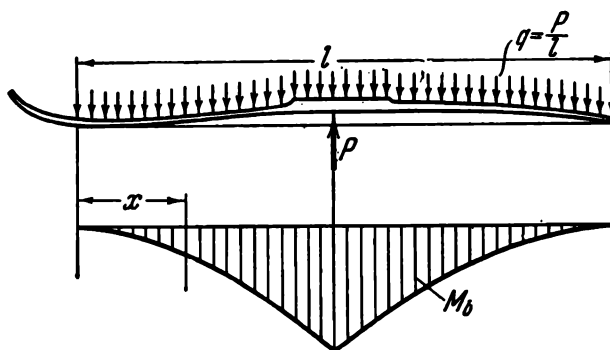


Fig. 240

(Fig. 240). In this case the required function  $y$  is determined from the equation

$$EIy'' = M_b \quad (1)$$

with the boundary conditions

$$y_{x=0} = 0, \quad y_{x=l} = 0.$$

The rigidity  $EI$  depends on  $x$  in a rather complicated way. Hence, Eq. (1) will be integrated graphically.

Consider an example. Mountain skis have a lengthwise varying section as shown in Fig. 241. We construct a graph showing the variation of the moment of inertia  $I$  along the length of the ski (Fig. 241a). Further, taking for wood  $E =$

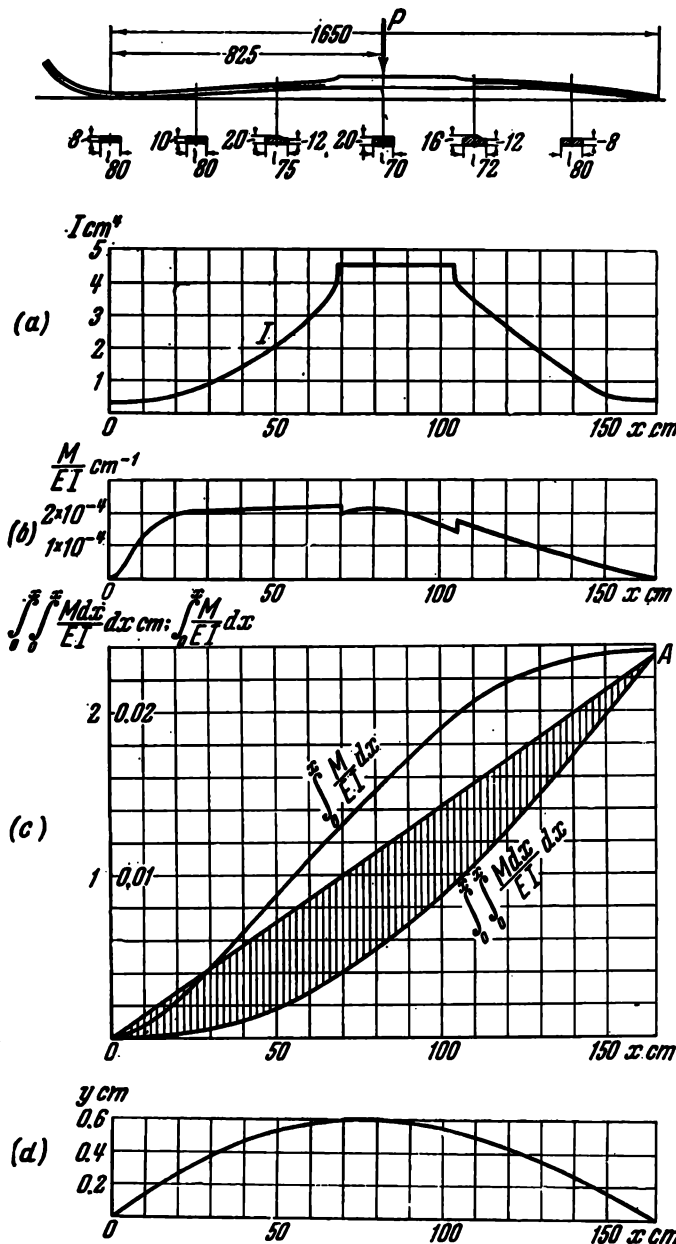


Fig. 241

$= 10^5$  kgf/cm<sup>2</sup> and assuming the load on the ski to be  $P = 60$  kgf, we plot, according to Figs. 240 and 241, a curve showing the variation of the curvature  $M/EI$  (Fig. 241b).

Integrating the  $M/EI$  curve twice, we obtain the curve

$$\int_0^x \int_0^x \frac{M dx}{EI}$$

shown in Fig. 241c. The ordinates included between this curve and the straight line  $OA$  give the required function  $y$  satisfying the boundary conditions.

In Fig. 241d the  $y$  curve is carried down to the horizontal axis giving,

$$y_{\max} = 6 \text{ mm.}$$

If the initial deflection is larger, which is usually the case in practice, the pressure on the snow at the ends of the ski is greater than in the middle. When sliding on the hard snow, this ensures better controllability and stability of motion. If, however,  $y_{\max}$  is too large, this will make the sliding conditions worse.

45. We apply a unit force at the point  $A$  and multiply the unit diagram by the diagram of the given force (Fig. 242).

For  $\delta_A$  to be zero, it is necessary that the centroid of the unit diagram ( $C$ ) coincide with the zero point of the given diagram (Fig. 242). Obviously,

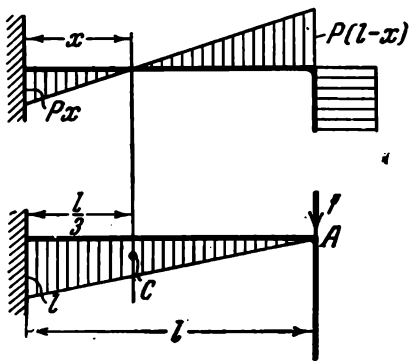
$$x = \frac{1}{3} l.$$


Fig. 242

46. Under the specified condition the displacement of the point  $A$  in a direction perpendicular to the line of action of the force is zero. This is the condition from which the angle  $\alpha$  is determined.

At the point  $A$  we apply a unit force perpendicular to  $P$  and then construct bending moment diagrams (Fig. 243).

Multiplying these diagrams and equating the resulting displacement to zero, we obtain

$$\tan 2\alpha = 1, \quad \alpha = \frac{\pi n}{2} + \frac{\pi}{8},$$

where  $n$  is any integer.

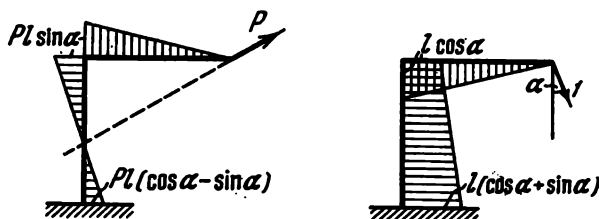


Fig. 243

47. (a) The point A (Fig. 45a) is displaced upward by  $Pl^3/6EI$ .

(b) The point A (Fig. 45b) is displaced to the right by  $PR^3/2EI$  and upward by  $\frac{PR^3}{EI} \left(1 - \frac{\pi}{4}\right)$ .

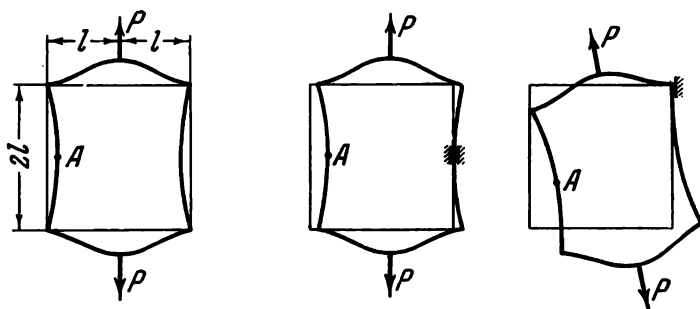


Fig. 244

(c) The point A (Fig. 45c) is displaced upward by  $Pl^3/6EI$  and to the right by  $Pl^3/EI$ .

(d) For Fig. 45d no answer can be given to the question posed until constraints are prescribed which prevent displacement of the frame as a rigid whole. The displacement of the point A will be different depending on the nature of these constraints (Fig. 244).

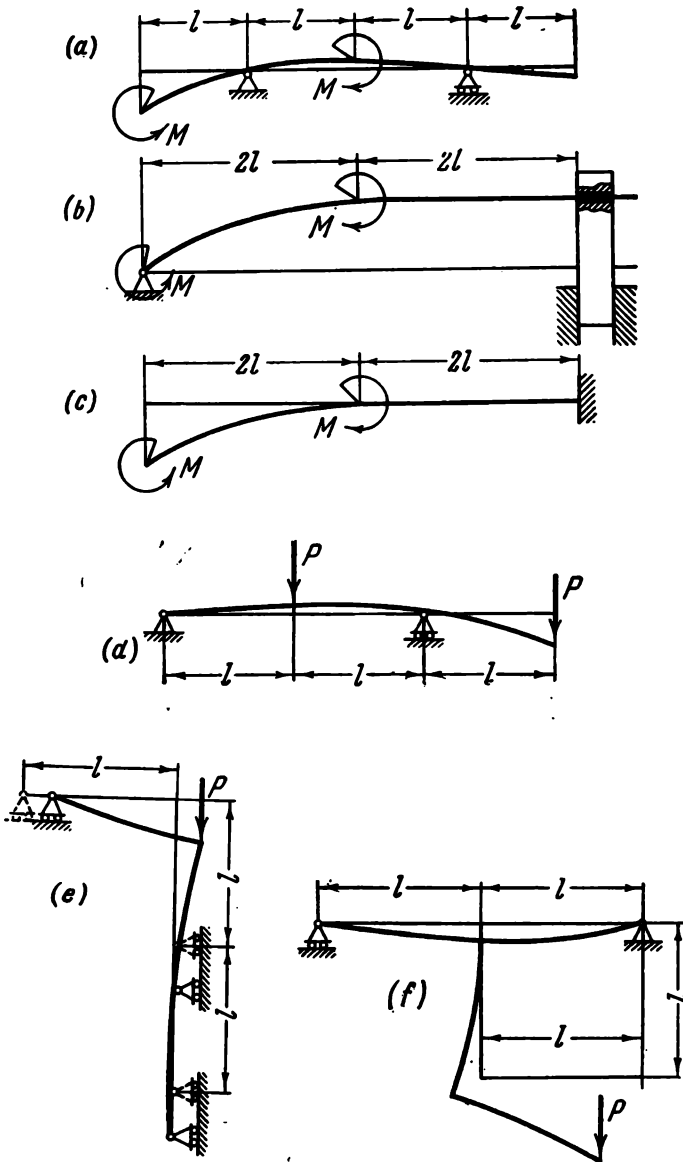


Fig. 245

According to the given constraints we obtain, for example:  
 in the first case—to the right by  $\frac{Pl^3}{16EI}$ ,

in the second case—to the right by  $\frac{Pl^3}{8EI}$ ,

in the third case—to the right by  $\frac{3Pl^3}{16EI}$  and downward by  $\frac{Pl^3}{4EI}$ .

48. See Fig. 245.

49. The bar  $AB$  is in compression. In order to verify this, it is necessary to open the static indeterminacy of the

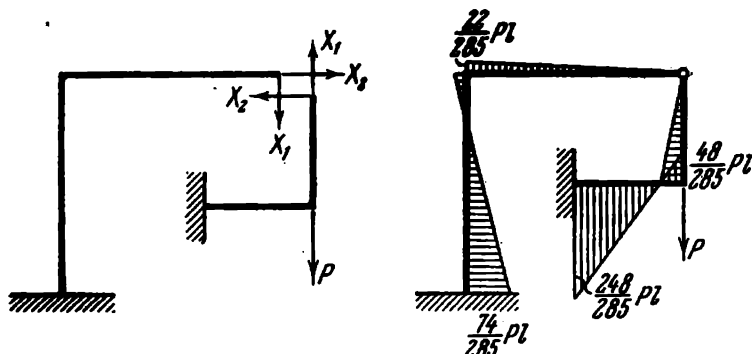


Fig. 246

frame. The forces in the hinge (Fig. 246) are

$$X_1 = -\frac{11}{285}P, \quad X_2 = \frac{48}{285}P.$$

50. The resultant of the force  $P$  and of the reaction at the right support passes through the inflection point of the

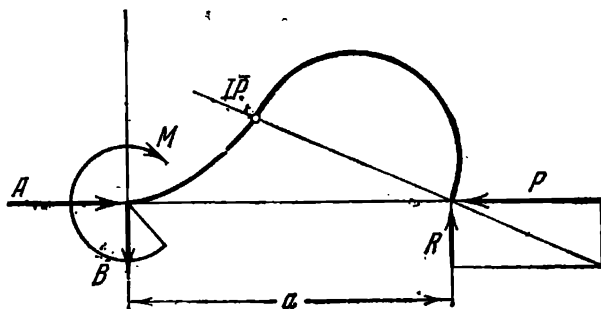


Fig. 247

elastic curve of the bar (Fig. 247). The reaction  $R$  is determined from this condition. The other reactions are deter-

mined from the equilibrium equations

$$A = P, \quad B = R, \quad M = Ra.$$

51. The displacement at the point of application of each of the forces  $P$  (Fig. 248) is determined by the usual method and has the magnitude

$$\delta = \frac{PR^3}{\pi EI} \left[ \left( \frac{3\pi^2}{8} - \pi - \frac{1}{2} \right) + \alpha \left( \frac{\pi^2}{2} - \pi - 2 \right) + \alpha^2 \left( \frac{\pi^2}{4} - 2 \right) + \alpha^3 \frac{\pi}{3} \right],$$

where  $\alpha = a/R$ .

The displacement  $\delta$  assumes the smallest value when  $\alpha = 0.148$ .

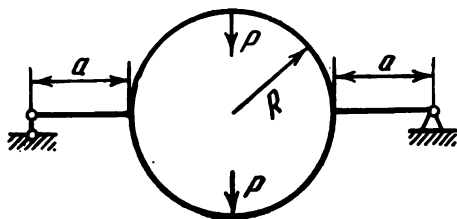


Fig. 248

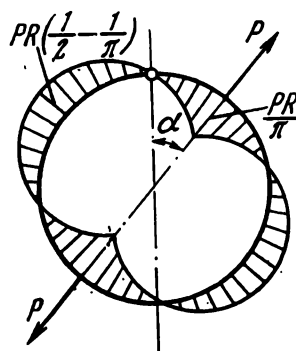


Fig. 249

52. The displacements at the point  $A$  for the three frames are the following:

$$\delta_I = \frac{Pa^3}{3EI}, \quad \delta_{II} = \frac{Pa^3}{2} \left( \frac{\pi - 3}{GI_p} + \frac{\frac{\pi}{2} - 1}{EI} \right),$$

$$\delta_{III} = \frac{Pa^3 \sqrt{2}}{4} \left( \frac{1}{GI_p} + \frac{1}{3EI} \right).$$

For a circular cross section of the beam, i.e., when  $EI/GI_p = 1.3$ , we have

$$\delta_{II} = 1.13 \delta_I, \quad \delta_{III} = 1.72 \delta_I.$$

Thus, frame I is stiffest.

53. If a hinge is fitted in a closed ring, the stiffness of the ring can only be reduced. In the extreme case it remains equal to the stiffness of the closed ring. The latter occurs only if the hinge is at the point where the bending moment for the closed ring is zero (Fig. 249).

The required angle is  $\arcsin \frac{2}{\pi}$ .

54. The problem posed may be solved in two ways.

The first method, suitable for springs of large lead angle as well, consists in treating the spring as a space rod. The

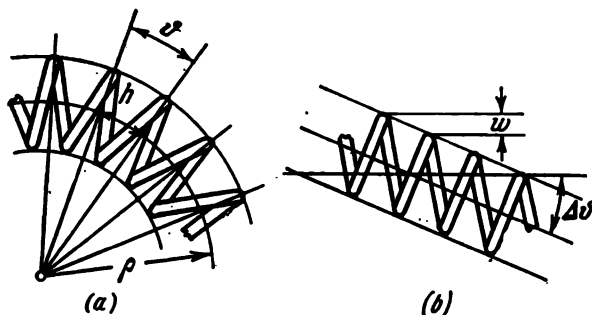


Fig. 250

displacements are determined by Mohr's method. The main difficulty lies in the complexity of geometrical relations.

The second (simplified) method, which will be used here, is to replace the spring by some equivalent straight rod. The flexural rigidity of this rod is calculated according to the relative rotation of coils (Fig. 250a). In addition to bending displacements the rod has appreciable shearing displacements in the vertical plane (Fig. 250b).

In order to determine the bending and shear stiffnesses of the equivalent rod, we consider a coil of the spring assuming the lead angle to be zero. The coil is isolated by sections located in the vertical plane (Fig. 251a). At the end sections of the coil moments  $M$  and forces  $Q$  are induced. Their magnitudes are easily determined from the conditions of equilibrium of the removed part of the spring. The moment  $M$  produces a relative rotation of the sections through an angle

$\vartheta$  (Fig. 251b) whose magnitude is determined by means of Mohr's integral

$$\vartheta = \int_0^{2\pi} \frac{M_t M_{t1} R d\varphi}{GI_p} + \int_0^{2\pi} \frac{M_b M_{b1} R d\varphi}{EI},$$

where the twisting and bending moments are, as seen from Fig. 251c,

$$M_t = M \cos \varphi, \quad M_b = M \sin \varphi,$$

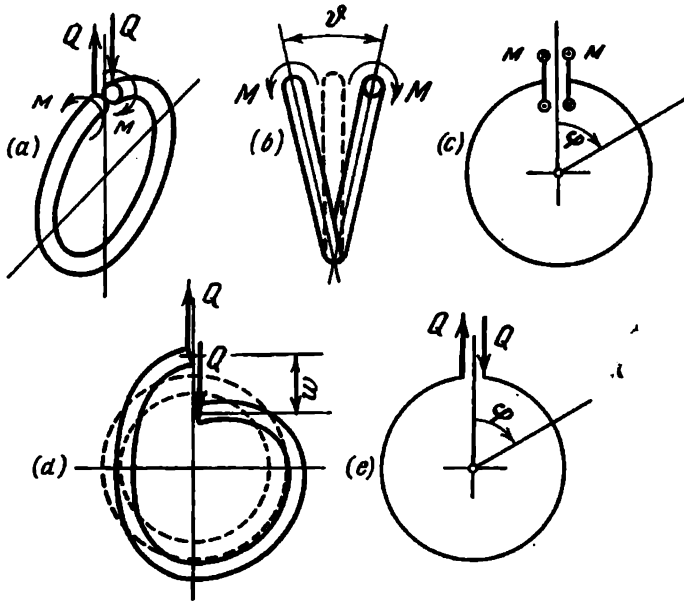


Fig. 251

The moments due to the unit factors have the corresponding values

$$M_{t1} = \cos \varphi, \quad M_{b1} = \sin \varphi.$$

On integrating we obtain

$$\vartheta = \frac{M\pi D}{2} \left( \frac{1}{GI_p} + \frac{1}{EI} \right)$$

or

$$\vartheta = \frac{32MD}{E\sigma^4} (2 + \mu).$$

As follows from Fig. 250a,  $1/\rho = \vartheta/h$ , where  $h$  is the pitch of the spring. If the number of coils is  $n$ , we have  $h = l/n$ . Then

$$\frac{1}{\rho} = \frac{\vartheta n}{l}$$

or

$$\frac{1}{\rho} = \frac{M}{\frac{Ed^4l}{32Dn(2+\mu)}}.$$

The quantity

$$\frac{Ed^4l}{32Dn(2+\mu)}$$

may be regarded as the flexural rigidity of the equivalent rod. Denote it by  $C_b$

$$\frac{Ed^4l}{32Dn(2+\mu)} = C_b, \quad (1)$$

$$\frac{1}{\rho} = \frac{M}{C_b}. \quad (2)$$

The shearing displacements are caused by the bending of the coil in its plane (Fig. 251d). Obviously,

$$w = \int_0^{2\pi} \frac{M_b M_{b1} R d\varphi}{EI},$$

where

$$M_b = QR \sin \varphi, \quad M_{b1} = R \sin \varphi.$$

Integrating gives

$$w = \frac{QD^3\pi}{8EI}.$$

The additional angular displacement is

$$\Delta\vartheta = \frac{w}{h} = \frac{Q}{\frac{Ed^4l}{8D^3n}}.$$

This expression may be written as

$$\Delta\vartheta = \frac{Q}{C_{sh}}, \quad (3)$$

where

$$C_{sh} = \frac{Ed^4l}{8D^3n}. \quad (4)$$

The deflection of the spring loaded by transverse forces is

$$f = f_b + f_{sh}.$$

In the specific case being considered, the case of the rod fixed at one end, the bending displacement is

$$f_b = \frac{Pl^3}{3EI},$$

where the quantity  $EI$  must be replaced by  $C_b$ .

The shearing displacement is

$$f_{sh} = \Delta\theta l = \frac{Pl}{C_{sh}}.$$

Thus,

$$f = \frac{Pl^3}{3C_b} + \frac{Pl}{C_{sh}}.$$

The quantities  $C_b$  and  $C_{sh}$  are determined by expressions (1) and (4). The problem is solved for other types of loading in a similar way.

55. The centre of gravity of the spring must coincide with the balance axis

By separating the reel, we consider the inner part of the spring (Fig. 252). At the section made,  $A$ , we apply a bend-

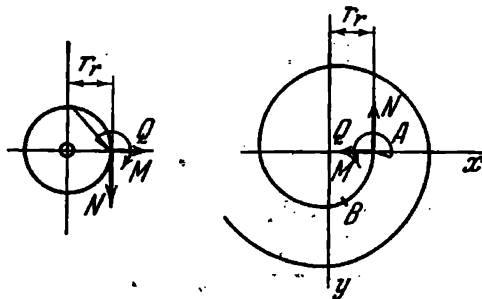


Fig. 252

ing moment  $M$ , a normal force  $N$ , and a transverse force  $Q$ . The same forces act on the reel.

At a point  $B$  with co-ordinates  $x, y$  the bending moment due to these forces is, obviously,  $M_b = M + Qy + N(r_r - x)$ , where  $r_r$  is the radius of the reel.

As the reel rotates counterclockwise through a small angle  $\varphi$ , so does the section  $A$ . Besides, it is displaced along the  $y$  axis by the amount  $r_r\varphi$ . The shift along the  $x$  axis for small displacements is a small quantity of higher order. We express the displacements through integrals in terms of the bending moments

$$\begin{aligned}\frac{1}{EI} \int_s M_b M_{1M} ds &= \varphi, & \frac{1}{EI} \int_s M_b M_{1N} ds &= r_r \varphi, \\ \frac{1}{EI} \int_s M_b M_{1Q} ds &= 0,\end{aligned}$$

where  $M_{1M}$ ,  $M_{1N}$ , and  $M_{1Q}$  are the bending moments due to the unit force factors corresponding to the moment  $M$  and the forces  $N$  and  $Q$ , i.e.,  $M_{1M} = 1$ ,  $M_{1N} = r_r - x$ ,  $M_{1Q} = y$ .

The integration is extended over the whole length of the spring. Consequently, we have

$$\begin{aligned}\int_s [M + Qy + N(r_r - x)] ds &= EI\varphi, \\ \int_s [M + Qy + N(r_r - x)](r_r - x) ds &= EI r_r \varphi, \\ \int_s [M + Qy + N(r_r - x)] y ds &= 0\end{aligned}$$

or upon integration

$$\begin{aligned}Ml + QS_x + N(r_r l - S_y) &= EI\varphi, \\ M(r_r l - S_y) + Q(r_r S_x - I_{xy}) + N(r_r^2 l - 2r_r S_y + I_y) &= EI r_r \varphi, \\ MS_x + QI_x + N(r_r S_x - I_{xy}) &= 0,\end{aligned}$$

where

$$\begin{aligned}S_x &= \int_s y ds, & S_y &= \int_s x ds, \\ I_x &= \int_s y^2 ds, & I_{xy} &= \int_s xy ds, & I_y &= \int_s x^2 ds,\end{aligned}$$

$l$  is the length of the band. Assume  $Q = N = 0$ . We then obtain  $Ml = EI\varphi$  and  $S_x = S_y = 0$ . The last condition means that the  $x$  and  $y$  axes must pass through the centre of gravity of the spring.

Since the centre of gravity of the Archimedean spiral, which is the contour of the spring, does not coincide with the centre of rotation of the reel, it is common practice in watch

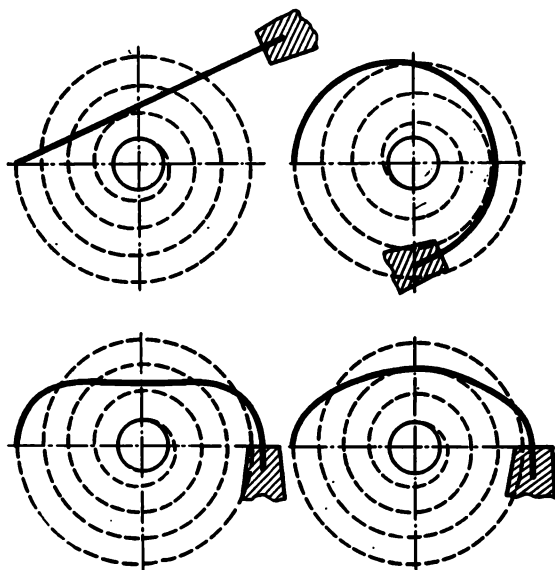


Fig. 253

manufacture to mount a balance spring with its outside end unbent to fulfil the above condition. Typical examples of such springs are shown in Fig. 253.

56. The main question which arises in solving this problem is to examine the nature of contact between the leaves of the spring.

Suppose that the connected leaves make point contact at the end of the shorter leaf and, besides, at the point of connection, where the vertical displacement and the angle of rotation are the same for both leaves. The corresponding force scheme is shown in Fig. 254a. For the unconnected leaves  $X_2 = 0$ ,  $X_3 = 0$ .

By multiplying the unit moment diagrams (Fig. 254b), we obtain

$$\begin{aligned} EI\delta_{11} &= \frac{16}{3} l^3, & EI\delta_{12} &= \frac{5}{3} l^3, & EI\delta_{13} &= 3l^2; \\ EI\delta_{22} &= \frac{2}{3} l^3, & EI\delta_{23} &= l^2, & EI\delta_{33} &= 2l; \\ EI\delta_{1P} &= -\frac{14}{3} Pl^3, & EI\delta_{2P} &= -\frac{4}{3} Pl^3, & EI\delta_{3P} &= -\frac{5}{2} Pl^2. \end{aligned}$$

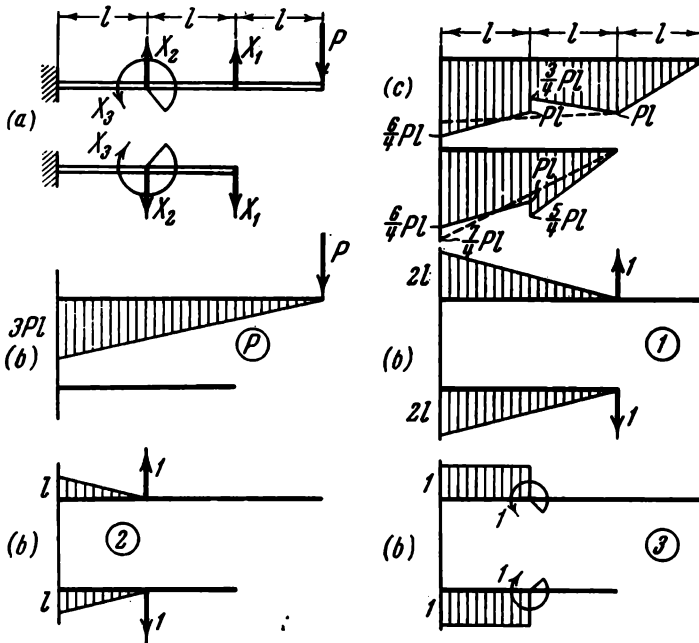


Fig. 254

By solving the equations of the force method

$$\frac{16}{3} X_1 l + \frac{5}{3} X_2 l + 3X_3 = \frac{14}{3} Pl,$$

$$\frac{5}{3} X_1 l + \frac{2}{3} X_2 l + X_3 = \frac{4}{3} Pl,$$

$$3X_1 l + X_2 l + 2X_3 = \frac{5}{2} Pl,$$

we find

$$X_1 = \frac{5}{4} P, \quad X_2 = -\frac{3}{4} P, \quad X_3 = -\frac{1}{4} Pl.$$

For the unconnected leaves

$$X_1 = \frac{7}{8} P, \quad X_2 = 0, \quad X_3 = 0.$$

In Fig. 254c the solid lines show the overall diagrams for the connected leaves, and the dashed lines for the free leaves.

It is now necessary to verify the correctness of the assumption made regarding the nature of contact between the leaves. Consider first the dashed diagrams (Fig. 254c). The bending moment, and hence the curvature of the lower leaf in the zone of fixing, is larger than that for the upper leaf. This means that the elastic curve of the lower leaf is below the elastic curve of the upper leaf, which corresponds to the assumption made.

For the connected leaves, the diagrams in the first portion are exactly the same. Consequently, here complete contact occurs without any force interaction, which is also consistent with the assumption made. In the second portion the elastic curve of the lower leaf passes below the elastic curve of the upper leaf.

Thus, the assumption made regarding the nature of contact between the leaves is supported by the solution obtained.

The displacement of the point of application of the force  $P$  is determined by multiplying the overall diagram of the upper leaf by the unit diagram, giving  $118 \frac{Pl^3}{24 EI}$  for the unconnected leaves and  $115 \frac{Pl^3}{24 EI}$  for the connected leaves.

The connection of the leaves reduced the maximum bending moment from  $\frac{7}{4} Pl$  to  $\frac{6}{4} Pl$ .

57. Consider the right-hand half of the spring, assuming that contact between the leaves occurs at points  $A$  and  $B$  (Fig. 255a).

The forces  $X_1$  and  $X_2$  are determined from the equations of the force method

$$\delta_{11}X_1 + \delta_{12}X_2 = -\delta_{1P}, \quad \delta_{21}X_1 + \delta_{22}X_2 = -\delta_{2P}. \quad (1)$$

The coefficients  $\delta_{11}$ ,  $\delta_{12}$ ,  $\delta_{22}$ ,  $\delta_{1P}$ , and  $\delta_{2P}$  are determined by multiplying the diagrams (Fig. 255b)

$$EI\delta_{11} = \frac{16}{3} l^3, \quad EI\delta_{12} = -\frac{5}{6} l^3, \quad EI\delta_{22} = \frac{2}{3} l^3, \\ EI\delta_{1P} = -\frac{14}{3} Pl^3, \quad \delta_{2P} = 0.$$

From Eqs. (1) we now find  $X_1$  and  $X_2$ ,

$$X_1 = \frac{112}{103} P, \quad X_2 = \frac{140}{103} P.$$

The overall bending moment diagrams are constructed in Fig. 256.

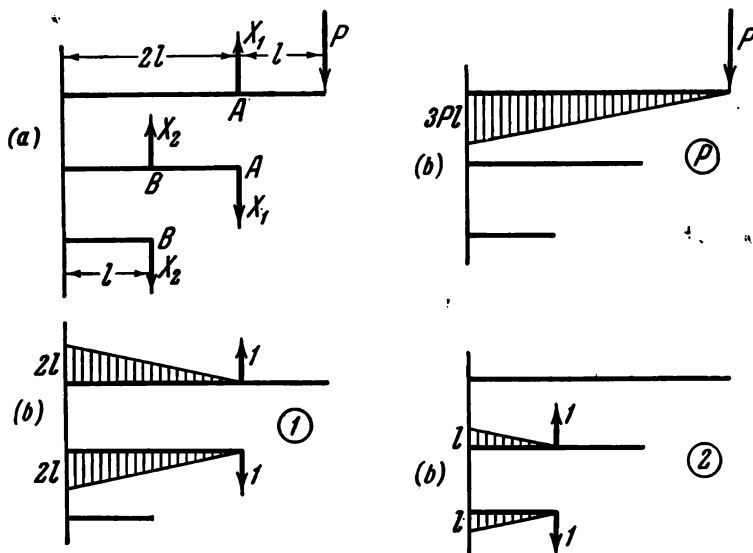


Fig. 255

From an inspection of these diagrams it follows that in the zone of fixing the bending moment, and hence the curvature of the first leaf, is larger than that of the second leaf. This means that the elastic curve of the second leaf must be above the elastic curve of the first leaf under these conditions. This is not possible, however. Consequently, the above assumption regarding the nature of contact between the leaves is wrong, and the design scheme must be modified.

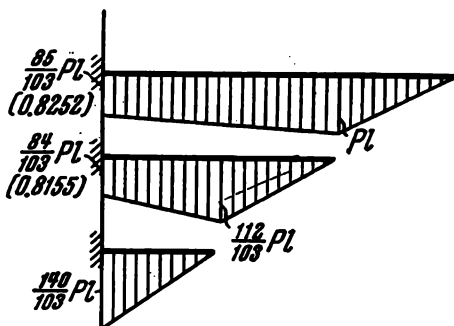


Fig. 256

Assume now that the first and second leaves make contact at two points, namely at the point  $A$ , as before, and at a point  $C$  situated at some undetermined distance  $a$  from the fixed end (Fig. 257).

By adding to the diagrams of Fig. 255*b* the unit diagram corresponding to the forces  $X_3$  (Fig. 258), we determine the coefficients in the equations of the force method

$$EI\delta_{11} = \frac{16}{3} l^3, \quad EI\delta_{12} = -\frac{5}{6} l^3, \quad EI\delta_{13} = a^2 \left( 2l - \frac{a}{3} \right),$$

$$EI\delta_{22} = \frac{2}{3} l^3, \quad EI\delta_{23} = -\frac{a^2}{2} \left( l - \frac{a}{3} \right), \quad EI\delta_{33} = \frac{2}{3} a^3,$$

$$EI\delta_{1p} = -\frac{14}{3} Pl^3, \quad \delta_{2p} = 0, \quad EI\delta_{3p} = -\frac{a^2}{2} \left( 3l - \frac{a}{3} \right) P$$

(it is assumed that  $a \leq l$ ). In this case the system of equations becomes

$$32X_1 - 5X_2 + 2\alpha^2 (6 - \alpha)X_3 = 28P,$$

$$-5X_1 + 4X_2 - \alpha^2 (3 - \alpha)X_3 = 0,$$

$2(6 - \alpha)X_1 - (3 - \alpha)X_2 + 4\alpha X_3 = (9 - \alpha)P$ ,  
where  $\alpha = a/l$ . By solving these equations for  $X_1$ ,  $X_2$ , and  $X_3$ , we find

$$X_1 = \frac{P}{\Delta} (448 - 549\alpha + 228\alpha^2 - 31\alpha^3),$$

$$X_2 = \frac{P}{\Delta} (560 - 684\alpha + 270\alpha^2 - 34\alpha^3),$$

$$X_3 = \frac{P}{\Delta} \frac{1}{\alpha} (3 - 19\alpha), \quad \Delta = 412 - 504\alpha + 204\alpha^2 - 28\alpha^3.$$

The quantity  $a$  (and hence  $\alpha$ ) is determined from the condition of equal angles of rotation for the first and second leaves at the point  $C$ .

By applying a unit moment at this point (Fig. 259) and multiplying the corresponding diagrams, we obtain

$$\begin{aligned} a \left( 3l - \frac{a}{2} \right) P - a \left( 2l - \frac{a}{2} \right) X_1 - \frac{a^2}{2} X_3 &= \\ &= a \left( 2l - \frac{a}{2} \right) X_1 - a \left( l - \frac{a}{2} \right) X_2 + \frac{a^2}{2} X_3, \\ 2(4 - \alpha)X_1 - (2 - \alpha)X_2 + 2\alpha X_3 &= (6 - \alpha)P. \end{aligned}$$

Substituting the values found for  $X_1$ ,  $X_2$ , and  $X_3$  gives

$$3\alpha^3 - 15\alpha^2 + 19\alpha - 1 = 0,$$

whence  $\alpha = 0.054993 < 1$ . If  $\alpha$  turned out to be greater than 1, the solution should be repeated on the assumption  $a > l$ .

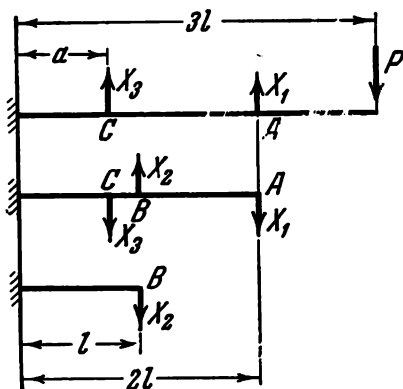


Fig. 257

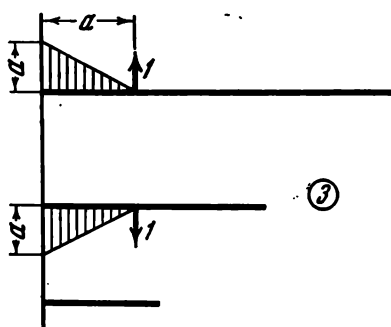


Fig. 258

For the derived value of  $\alpha$  we determine  $X_1$ ,  $X_2$ , and  $X_3$

$$X_1 = 1.0873P, \quad X_2 = 1.3593P, \quad X_3 = 0.09237P.$$

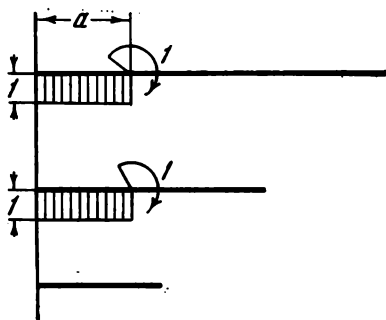


Fig. 259

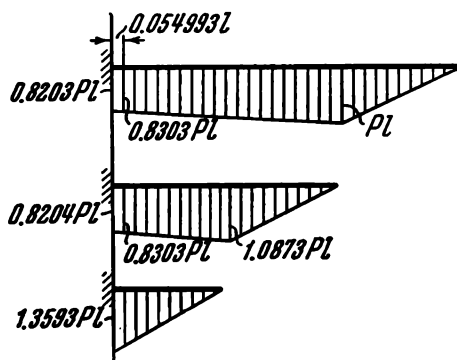


Fig. 260

Note that for the given relation of the lengths of the leaves the forces  $X_1$  and  $X_2$  differ only slightly from those previously obtained.

We again construct bending moment diagrams (Fig. 260).

From an inspection of these diagrams it follows that the curvature of the second leaf in the zone of fixing is larger than the curvature of the first leaf and the curvature of the third leaf is larger than the curvature of the second. Accordingly, the elastic curve of each succeeding leaf is below the elastic curve of the preceding one. Thus, the assumption made regarding the nature of contact between the leaves receives confirmation.

The design bending moment is  $M_b^{\max} = 1.36 Pl$ ; it occurs in the zone of fixing of the lower leaf.

The deflection of the spring determined by the displacement of the end of the first leaf is

$$EI\delta = 9Pl^3 - \frac{14}{3}X_1l^3 - \frac{1}{6}X_3a^2(9l-a),$$

whence

$$\delta = 3.926 \frac{Pl^3}{EI}.$$

58. Suppose that the spring is forced to assume the shape of the rigid curve over a certain portion. For this it is evidently necessary to apply some forces and moments to the ends of the portion and a distributed load of intensity  $q$  at the intermediate points.

From the properties of the elastic curve it is known that

$$q(x) = EIy^{(IV)}.$$

If the distributed load acts upward, it is taken that  $q(x) > 0$ .

It is now quite obvious that when  $y^{IV} > 0$  the spring will separate off from the rigid curve, and when  $y^{IV} < 0$  it will adhere to it. If  $y^{IV} = 0$  (the contour of the rigid curve represents a power-law curve of degree not higher than 3), the spring will be closely attached to the rigid curve over a certain portion without pressing against it. At the end of the portion a concentrated force  $P_1$  will be induced (Fig. 261).

59. After applying the force  $P_1$ , the left-hand part of the beam rises a little over a certain length  $a$  (Fig. 262). The right-hand part continues to lie on the plane and remains straight. Consequently, at all sections of the right-hand portion the bending moment is zero. In particular, the moment is zero at the section  $x = a$  as well.

This condition determines the length of the segment  $a$ , i.e. (see Fig. 262),

$$P_1 a = \frac{P}{l} \frac{a^2}{2}, \quad a = \frac{2P_1}{P} l.$$

From the condition that the sum of the projections of all forces on a vertical axis is zero it follows that the rigid plane produces a reaction  $P_1$  at the point  $x = a$  (Fig. 262).

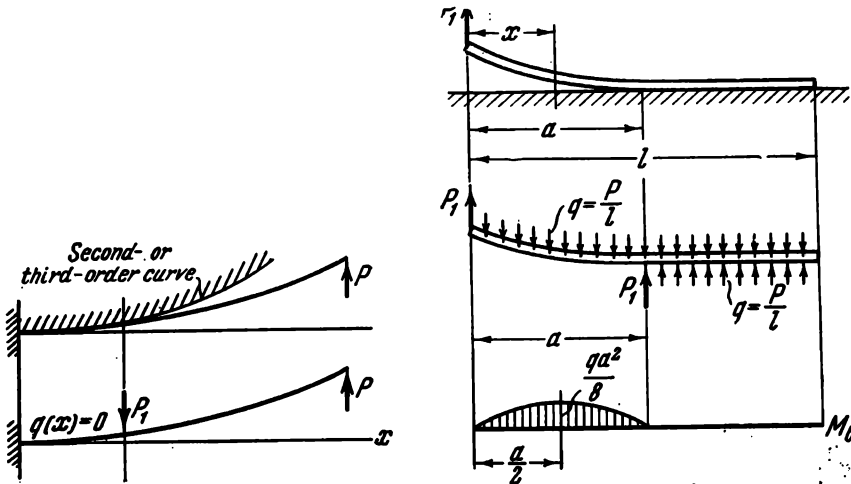


Fig. 261

[Fig. 262

With this system of forces, the left-hand overhanging part of the beam may be regarded as a simply supported beam of length  $a$  subjected to a uniformly distributed load of intensity  $P/l$ . The maximum bending moment occurs at the middle of the overhanging portion and is equal to

$$\frac{qa^2}{8} = \frac{P_1 l}{2P}.$$

When  $P_1 = P/3$ , we obtain

$$M_{\max} = \frac{Pl}{18}, \quad \sigma_{\max} = \frac{Pl}{18Z}, \quad a = \frac{2}{3} l.$$

The most interesting and instructive thing in the problem considered, as generally in all problems involving contact between an elastic beam and a rigid surface, is the occurrence

of the concentrated force  $P_1$  at the boundary of the segment of attachment.

The appearance of this force is at first glance somewhat unexpected, though, formally, its existence is in full accord with the equilibrium and deformation equations. The occurrence of this force is due to the choice of the design scheme. In solving the problem, we considered only the flexural rigidity of the beam and assumed no shearing strains at the cross sections. The consideration of these strains is sufficient to reveal that the scheme of contact forces as a uniformly distributed load and a concentrated force  $P_1$  is approximate. There is no need then to elaborate upon the fact that due to the compression of the beam in the transverse direction (as in usual contact problems) the force  $P_1$  is distributed over some small area.

Consider shearing strains in the beam.

The curvature of the beam related to the bending moment is determined by

$$\frac{1}{\rho} = y''_M = \frac{M}{EI}.$$

If the deflections caused by shear are denoted by  $y_Q$ , the angle of additional slope of the elastic curve for any section is obtained as

$$y'_Q = -\frac{kQ}{GA},$$

where  $k$  is a numerical factor depending on the shape of the cross section of the beam. For a rectangle, for example,  $k = 6/5$ , for a circle  $k = 10/9$ , etc. We thus obtain

$$y'' = \frac{M}{EI} - \frac{kQ'}{GA}.$$

The minus sign on  $kQ'/GA$  is put for the simple reason that when  $M$  and  $Q$  are positive both these factors give a change in curvature of opposite sign (Fig. 263).

Since  $Q = dM/dx$ , the above differential equation becomes

$$y'' = \frac{M}{EI} - \frac{kM''}{GA}. \quad (1)$$

In the problem under consideration, when  $x < a$ ,

$$M = P_1 x - \frac{Px^2}{2l}, \quad M'' = -\frac{P}{l}. \quad (2)$$

According to expression (1) we obtain

$$y'' = \frac{1}{EI} \left[ P_1 x - \frac{Px^2}{2l} \right] + \frac{kP}{lGA},$$

whence

$$y = \frac{1}{EI} \left[ P_1 \frac{x^3}{6} - \frac{Px^4}{24l} \right] + \frac{kP}{lGA} \frac{x^2}{2} + C_1 x + C_2. \quad (3)$$

The constant  $C_2$  is of no interest. It can easily be selected so as to make the displacement  $y$  zero at  $x = a$ . As regards

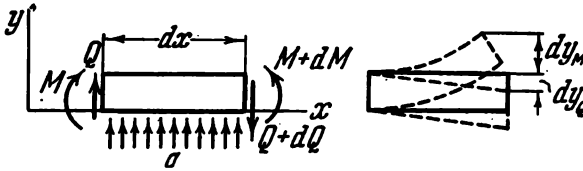


Fig. 263

the constant  $C_1$ , its determination requires the fulfilment of a special condition for linking up with the second portion in which the curvature is zero. Consequently, according to (1)

$$M'' - \alpha^2 M = 0, \quad \text{where} \quad \alpha^2 = \frac{GA}{EI k}, \quad (4)$$

whence

$$M = C_3 \sinh \alpha x + C_4 \cosh \alpha x. \quad (5)$$

When  $x = a$ ,  $M = P_1 a - Pa^2/2l$ ; when  $x = l$ ,  $M = 0$ . From these conditions we determine the arbitrary constants  $C_3$  and  $C_4$  and obtain the bending moment as

$$M = \left( P_1 a - \frac{Pa^2}{2l} \right) \frac{\sinh \alpha (l-x)}{\sinh \alpha (l-a)}. \quad (6)$$

It must further be required that in linking up the portions the angle of rotation for the section of contact be the same. But this angle,  $\theta$ , differs from the slope of the tangent to the elastic curve by the amount  $kQ/GA$ , i.e.,

$$\theta = y' + \frac{kQ}{GA}.$$

We determine the angle  $\theta$  at  $x = a$  for the left-hand part of the beam. For this purpose expression (3) is used, giving

$$\theta = \frac{1}{EI} \left( P_1 \frac{a^2}{2} - \frac{Pa^3}{6l} \right) + \frac{kP}{lGA} a + C_1 + \frac{k}{GA} \left( P_1 - \frac{Pa}{l} \right).$$

For the right-hand part of the beam  $y' \equiv 0$ . Hence, the angle  $\theta$  contains only the shearing component. From expression (6) we obtain

$$\theta = \frac{k}{GA} \alpha \left( P_1 a - \frac{Pa^2}{2l} \right) \coth \alpha (l - a)$$

By equating the angles  $\theta$ , we find

$$C_1 = -\frac{1}{EI} \left( P_1 \frac{a^2}{2} - \frac{Pa^3}{6l} \right) - \frac{kP_1}{GA} - \frac{k\alpha}{GA} \left( P_1 a - \frac{Pa^2}{2l} \right) \coth \alpha (l - a).$$

It now remains to verify that the elastic curve of the left-hand portion satisfies the condition for non-intersection of the plane of support. The point is that in the presence of shear the elastic curve of the beam undergoes a bend at the point of application of concentrated forces. But we do not, as yet, know whether or not a concentrated force arises in the zone of contact. If such a force arises and if it is directed upward (but it can only be directed upward), the point of the bend is also directed upward and the elastic curve for the left-hand portion of the beam intersects the plane of support. The question is decided by the sign of  $y'$  in the neighbourhood of the point of linking up. Thus, it is necessary to fulfil the condition that  $y' \leq 0$  when  $x = a$ .

From expression (3), taking into account the value found for  $C_1$ , we obtain

$$y'_{x=a} = \frac{k}{GA} \left[ P \frac{a}{l} - P_1 - \alpha l \frac{a}{l} \left( P_1 - \frac{1}{2} P \frac{a}{l} \right) \coth \alpha l \left( 1 - \frac{a}{l} \right) \right].$$

It is revealed that for  $P_1 = P/3$  and for the value  $a = \frac{2}{3}l$  found previously the derivative of  $y$  is positive and the elastic curve intersects the plane of support. By reducing the magnitude of  $a$ , it is possible to obtain a negative value for  $y'$ . At the point of linking up the elastic curve will then

have a bend with its point directed downward. But this means that when  $x = a$  the reaction forces contain a concentrated component directed downward, which is not possible with one-sided constraints. The only alternative is to take  $y'$  equal to zero when  $x = a$  and to determine  $a$  from this condition. Consequently,

$$\frac{P_1}{P} - \frac{a}{l} = -\alpha l \frac{a}{l} \frac{\frac{P_1}{P} - \frac{1}{2} \frac{a}{l}}{\tanh \alpha l \left(1 - \frac{a}{l}\right)}.$$

According to the condition of the problem  $\frac{P_1}{P} = \frac{1}{3}$ , hence

$$\frac{1}{3} - \frac{a}{l} = -\alpha l \frac{a}{l} \frac{\frac{1}{3} - \frac{1}{2} \frac{a}{l}}{\tanh \alpha l \left(1 - \frac{a}{l}\right)}. \quad (7)$$

From this transcendental equation we determine  $a/l$  for given

$$\alpha l = \sqrt{\frac{GAl^2}{EI k}}.$$

If  $\alpha l = \infty$ , i.e., if the beam has no shearing strains, from (7) we find  $a/l = 2/3$ , which was obtained previously. When  $\alpha l = 50$ , we obtain  $a/l = 0.646$ , and when  $\alpha l = 10$ , we have  $a/l = 0.58$ .

We now determine the distributed load  $q$  along the second portion of the beam ( $q$  is the difference between the distributed reaction of the plane and the dead-weight of the beam  $P/l$ ). From (5) we obtain

$$q = M'' = \frac{P}{l} \frac{a}{l} \alpha^2 l^2 \left( \frac{P_1}{P} - \frac{1}{2} \frac{a}{l} \right) \frac{\sinh \alpha (l-x)}{\sinh \alpha (l-a)}.$$

When  $x = l$ ,  $q = 0$ , i.e., the reaction of the plane of support is equal to the weight of the beam per unit length. When  $x = a$ , we have

$$q_a = \frac{P}{l} \frac{a}{l} \alpha^2 l^2 \left( \frac{P_1}{P} - \frac{1}{2} \frac{a}{l} \right).$$

As  $\alpha l$  increases, i.e., as the shear stiffness increases,  $q_a$  tends to infinity, and in the limit when  $\alpha l = \infty$  we obtain a concentrated force at the point  $x = a$ .

The variation of the law of distribution of the reaction of the plane with increasing  $\alpha l$  is shown in Fig. 264.

It is interesting to note that the shearing displacements in the beam have changed the distribution of the contact forces not only in the transition zone but also beyond it.

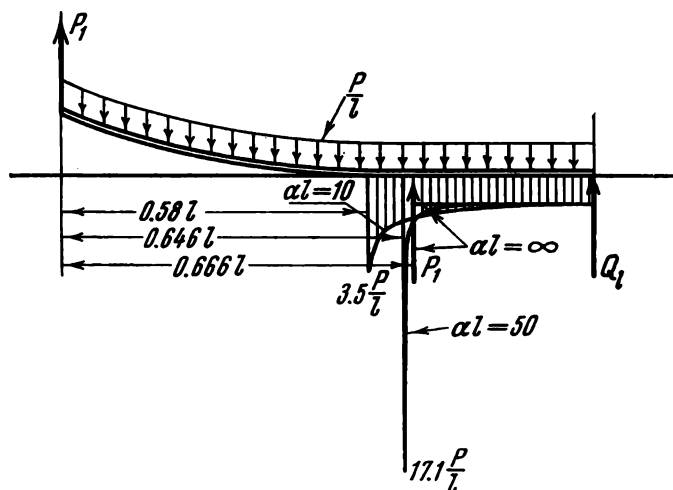


Fig. 264

There is now a concentrated reaction force induced at the right end of the beam. Differentiating expression (6) and setting  $x = l$ , we find the transverse force

$$Q_l = -\frac{a}{l} \left( P_l - \frac{1}{2} P \frac{a}{l} \right) \frac{\alpha l}{\sinh \alpha l \left( 1 - \frac{a}{l} \right)}.$$

In this expression one can easily see the role of the shearing displacements as a means of spreading the deformation along the length of the straight beam. As the shear stiffness increases the force  $Q_l$  rapidly decreases.

60. Consider first the conditions of contact between the beam and the rigid base in the presence of a small clearance (Fig. 265).

Let the amount of the clearance be  $\Delta$ . In the left-hand part the beam remains straight and closely attached to the upper surface of the hole. At the point of separation of the beam from this surface a reaction  $A = P \frac{l}{a}$  arises. The magnitude of the arm  $a$  is as yet undetermined.

At the point of exit of the rod from the hole a reaction  $B$  arises which is directed, in the absence of frictional forces, along the normal to the surface of the beam. Since the angle of deflection of this force from the vertical is small, we have

$$B = P + A = P \left( 1 + \frac{l}{a} \right).$$

We take the point  $O$  as the origin of displacements. When  $x = a$ , the vertical displacement of the beam is  $\Delta$

$$\Delta = \frac{Aa^3}{6EI} = \frac{Pla^2}{6EI},$$

whence

$$a = \sqrt{\frac{6EI\Delta}{Pl}}.$$

We find the angle of rotation  $\theta$

$$\theta = \frac{Aa^2}{2EI} = \frac{1}{2} \sqrt{\frac{Pl}{EI}} 6\Delta,$$

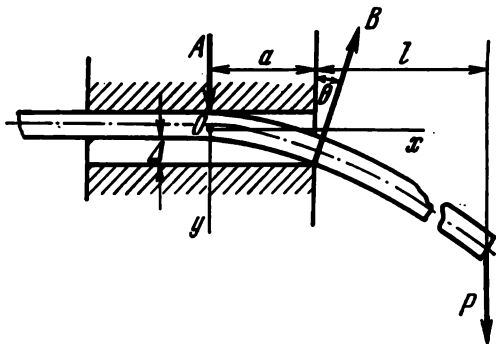


Fig. 265

As the clearance  $\Delta$  decreases, the angle  $\theta$  and the quantity  $a$  tend to zero, while the forces  $A$  and  $B$  increase indefinitely. Let us see how the horizontal component of the force  $B$  then varies

$$B\theta = P \left( 1 + \frac{l}{a} \right) \frac{1}{2} \sqrt{\frac{Pl}{EI}} 6\Delta$$

or

$$B\theta = \frac{P}{2} \left( \frac{Pl^2}{EI} + \sqrt{\frac{Pl}{EI}} 6\Delta \right).$$

As is seen, when  $\Delta \rightarrow 0$ , the horizontal component of the force  $B$  tends to a definite limit

$$B\theta = \frac{P^2 l^2}{2EI}.$$

The dynamometer will show this value of the force.\*

\* The development of the ideas relating to this problem may be found in the paper by L. I. Balabukh, M. N. Vul'fson, B. V. Mukoseev, and Ya. G. Panovko, *On the Work of Reaction Forces at Movable Supports*, in "Issledovaniya po Teorii Sooruzhenii", Vyp. 18, Stroiizdat, Moscow, 1970, pp. 190-200.

61. When fitted on the shaft, the ring will not make contact with the shaft along the entire contour. In the portions  $AB$  the ring separates off from the shaft and close contact occurs only in the portion  $BB$  (Fig. 266).

The ends  $A$  are acted on by forces  $Q_1$  exerted by the shaft. At the points  $B$  there act forces  $Q_2$ . The nature of these forces is exactly the same as in Prob. 59.

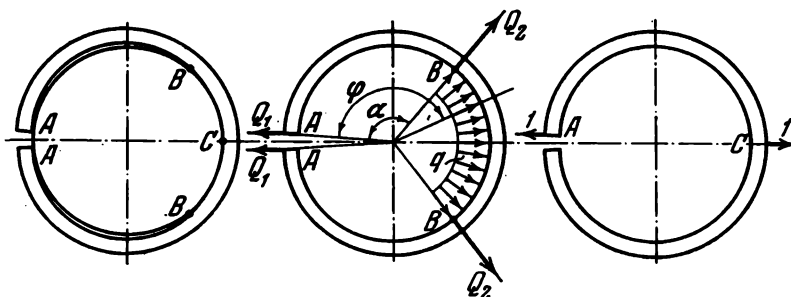


Fig. 266

In the zone of close attachment we may imagine a uniformly distributed load of intensity  $q$ . If, by selecting the forces  $Q_1$ ,  $Q_2$ ,  $q$  and the angle  $\alpha$ , we are able to satisfy all deformation conditions for the ring, the correctness of the chosen force scheme will thereby be proved.

Since, by hypothesis, the portion  $BB$  is closely attached to the shaft, the curvature of the ring in this portion is obviously equal to the constant value  $2/D$ . The change in curvature

$$\frac{2}{D-\Delta} - \frac{2}{D} \cong \frac{2\Delta}{D^2}$$

is also a constant. The bending moment in the portion  $BB$  is

$$M_{BB} = EI \frac{2\Delta}{D^2},$$

where  $EI$  is the flexural rigidity of the ring. Consequently, the forces  $Q_1$ ,  $Q_2$ , and  $q$  must be chosen so that the moment in the portion  $BB$  will be constant, and moreover will have a preassigned value,

At an arbitrary section of the ring in the portion  $BB$  (Fig. 266)

$$M_{BB} = Q_1 \frac{D}{2} \sin \varphi + Q_2 \frac{D}{2} \sin (\varphi - \alpha) + \\ + \frac{1}{2} q \frac{D^2}{4} \sin^2 (\varphi - \alpha) + \frac{1}{2} q \frac{D^2}{4} [1 - \cos (\varphi - \alpha)]^2$$

or

$$M_{BB} = \sin \varphi \left[ Q_1 \frac{D}{2} + Q_2 \frac{D}{2} \cos \alpha - q \frac{D^2}{4} \sin \alpha \right] - \\ - \cos \varphi \left[ Q_2 \frac{D}{2} \sin \alpha + q \frac{D^2}{4} \cos \alpha \right] + q \frac{D^2}{4}.$$

The moment remains constant if we require that each of the bracketed expressions vanish

$$\left. \begin{aligned} Q_1 + Q_2 \cos \alpha - q \frac{D}{2} \sin \alpha &= 0, \\ Q_2 \sin \alpha + q \frac{D}{2} \cos \alpha &= 0; \end{aligned} \right\} \quad (1)$$

we then obtain

$$q = EI \frac{8\Delta}{D^4}.$$

Thus,  $q$  is found. Two equations (1) are not sufficient to determine  $Q_1$ ,  $Q_2$ , and  $\alpha$ .

We now require that the distance between the points  $A$  and  $C$  of the ring be increased by  $\Delta$ . This condition is written as

$$\Delta = \int_0^\alpha \frac{M_{AB} M_1 D d\varphi}{2EI} + \int_\alpha^\pi \frac{M_{BB} M_1 D d\varphi}{2EI},$$

where  $M_{AB}$  and  $M_{BB}$  are the bending moments in the portions  $AB$  and  $BB$ ,  $M_1$  is the bending moment due to the unit forces applied in the direction  $AC$ ; they are equal, respectively, to

$$M_{AB} = Q_1 \frac{D}{2} \sin \varphi, \quad M_{BB} = EI \frac{2\Delta}{D^2}, \quad M_1 = \frac{D}{2} \sin \varphi.$$

After substitution and integration we obtain

$$\Delta = Q_1 \frac{D^3}{16EI} \left( \alpha - \frac{1}{2} \sin 2\alpha \right) + \frac{\Delta}{2} (1 + \cos \alpha).$$

We solve this equation simultaneously with Eqs. (1) and determine  $Q_1$  and  $Q_2$

$$Q_1 = \frac{4EI\Delta}{D^3 \sin \alpha}, \quad Q_2 = -\frac{4EI\Delta}{D^3} \cot \alpha.$$

The value of  $\alpha$  is determined from the transcendental equation

$$2 = \frac{\alpha}{\sin \alpha} + \cos \alpha$$

giving  $\alpha = 122^\circ 35'$ . We have then

$$Q_1 = 4.75 \frac{EI\Delta}{D^3}, \quad Q_2 = 2.56 \frac{EI\Delta}{D^3}.$$

By satisfying, thus, all geometrical conditions, we have confirmed the correctness of the chosen force scheme.

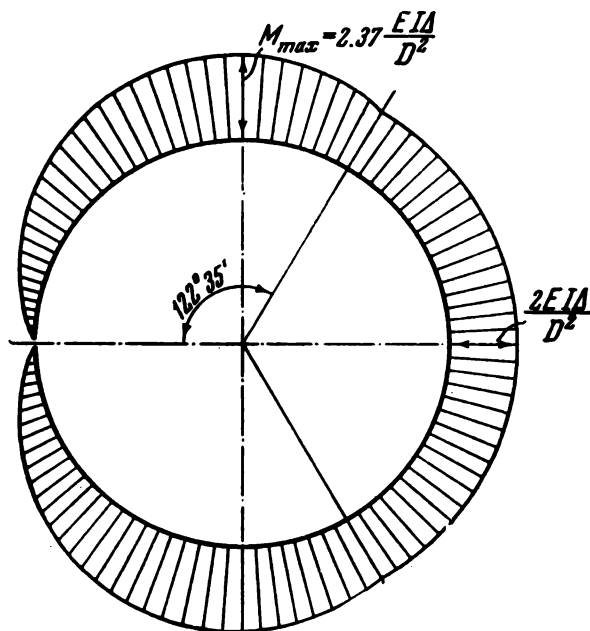


Fig. 267

The bending moment diagram is shown in Fig. 267.

62. When solving the problem of the deformation of the flexible spring (Fig. 60), it is necessary to take into account

the effect of shear on the shape of the elastic curve of the spring.

If we proceed from the usual relation between the bending moment and the change of curvature

$$\frac{1}{R} = \frac{M}{EI},$$

we shall inevitably come to the conclusion that the points  $A$  will touch the plane only when  $P = \infty$ . Indeed, the bending moment at the ends of the spring is zero for any finite value of the forces  $P$ ; to straighten out the spring completely, however, it is necessary that the moment be  $M = EI/R$  at all its points. In actual conditions the required force is naturally finite.

This contradiction is due to the fact that, when bending is produced by the forces  $P$ , the change in curvature at the ends of the spring, where the bending moment is small, is caused mainly by the shearing deformations which must be taken into account in the solution of the problem.

We now turn to expression (1) (p. 162). The change in curvature of the spring pressed against the rigid plane is  $y'' = -1/R$ . In this case we obtain

$$M'' - \alpha^2 M = \frac{1}{R} \frac{GA}{k}, \quad \alpha^2 = \frac{GA}{EI k}.$$

By solving this equation, we find

$$M = A \sinh \alpha x + B \cosh \alpha x - \frac{EI}{R}.$$

The constants are determined from the following conditions:

$$\text{when } x=0, \quad Q = M' = 0;$$

$$\text{when } x=l, \quad M = 0,$$

whence

$$A = 0, \quad B = \frac{EI}{R} \frac{1}{\cosh \alpha l}, \quad M = \frac{EI}{R} \left( \frac{\cosh \alpha x}{\cosh \alpha l} - 1 \right).$$

The required force is

$$P = Q_{x=l} = M'_{x=l} = \frac{EI}{R} \alpha \tanh \alpha l.$$

When  $GA = \infty$  (no shears),  $\alpha$  also becomes infinite. In this case  $\tanh \alpha l = 1$  and, as might be expected,  $P = \infty$ .

The contact pressure over the surface of contact between the spring and the rigid plane is determined as

$$q = M''_1 = \frac{EI}{R} \alpha^2 \frac{\cosh \alpha x}{\cosh \alpha l} = \frac{GA}{Rk} \frac{\cosh \alpha x}{\cosh \alpha l}.$$

The law of distribution of  $q$  along the length of the spring is shown as a curve in Fig. 268.

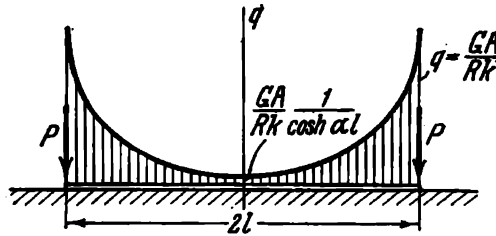


Fig. 268

63. Consider separately one of the component beams (Figs. 61 and 269).

Since the force  $P$  is not applied at the shear centre, the beam represented in Fig. 269 will be simultaneously twisted

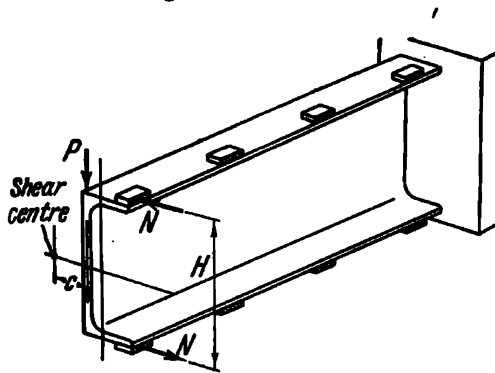


Fig. 269

during bending. By applying forces  $N$  at sections through the first strips so that the moment of the two forces is equal to the moment  $Pc$ , we eliminate this twisting for all sections of the beam. Then  $N = Pc/H$ .

Thus, the first upper strip is compressed and the first lower strip is extended by the forces  $N$ . The remaining strips

are not subjected to any forces during bending. This conclusion is true, naturally, only so long as the strips may be considered rigid. If they deformed markedly, the forces induced in them could be determined in the same way as the forces in the rivets of Prob. 14.

64. We resolve the force  $P$  along the principal  $x$  and  $y$  axes (Fig. 270) and cut the section at the angular point  $A$ . At the same time we introduce an undetermined shear flow  $\tau_0$ . The shearing stress at an arbitrary point  $B$  is

$$\tau = \frac{P\sqrt{2}}{2\delta} \left( \frac{S_x^*}{I_x} + \frac{S_y^*}{I_y} \right) + \tau_0.$$

After simple computation we find

$$b = a \frac{\sqrt{2}}{2} \frac{1}{2 + \sqrt{2}},$$

$$I_x = \frac{a^3\delta}{6} (2 + \sqrt{2}),$$

$$I_y = \frac{a^3\delta}{6} \frac{1 + 2\sqrt{2}}{2 + \sqrt{2}}.$$

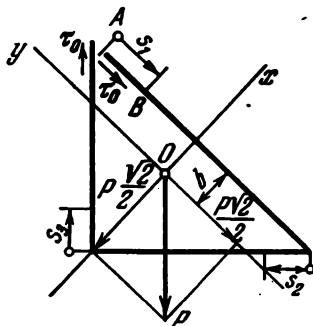


Fig. 270

For each of the three segments of the section we obtain

$$\tau_1 = \frac{3\sqrt{2}}{2} \frac{P}{a^3\delta} \left[ \frac{s_1 a \sqrt{2} - s_1^2}{2 + \sqrt{2}} + \frac{a \sqrt{2} s_1}{1 + 2\sqrt{2}} \right] + \tau_0,$$

$$\tau_2 = \frac{3\sqrt{2}}{2} \frac{P}{a^3\delta} \left[ \frac{\frac{\sqrt{2}}{2} s_2^2 - a \sqrt{2} s_2}{2 + \sqrt{2}} + \frac{2a^2 + a \sqrt{2} s_2 - (1 + \sqrt{2}) s_2^2}{1 + 2\sqrt{2}} \right] + \tau_0, \quad (1)$$

$$\tau_3 = \frac{3\sqrt{2}}{2} \frac{P}{a^3\delta} \left[ \frac{\frac{\sqrt{2}}{2} s_3^2 - a^2}{2 + \sqrt{2}} + \frac{a^2 - a(2 + \sqrt{2}) s_3 + (1 + \sqrt{2}) s_3^2}{1 + 2\sqrt{2}} \right] + \tau_0,$$

where  $s_1$ ,  $s_2$ , and  $s_3$  are the co-ordinates measured from the angular points along the contour.

In order that no relative displacements occur at the section  $A$ , it is necessary to fulfil the condition

$$\int_s \gamma ds = 0$$

or

$$\int_0^{a\sqrt{2}} \tau_1 ds_1 + \int_0^a \tau_2 ds_2 + \int_0^a \tau_3 ds_3 = 0;$$

from this the value of  $\tau_0$  is determined as

$$\tau_0 = \frac{3\sqrt{2}}{2} \frac{P}{a\delta} \left( \frac{\sqrt{2}}{3(2+\sqrt{2})^2} - \frac{1}{1+2\sqrt{2}} \right).$$

Substituting for  $\tau_0$  in expressions (1) and carrying out the necessary computations, we obtain

$$\tau_1 = \frac{P}{a\delta} (-0.47 + 1.66\zeta_1 - 0.62\zeta_1^2),$$

$$\tau_2 = \frac{P}{a\delta} (0.64 - 0.095\zeta_2 - 0.90\zeta_2^2),$$

$$\tau_3 = \frac{P}{a\delta} (-0.35 - 1.89\zeta_3 + 1.78\zeta_3^2),$$

where

$$\zeta_i = \frac{s_i}{a} \quad (i = 1, 2, 3).$$

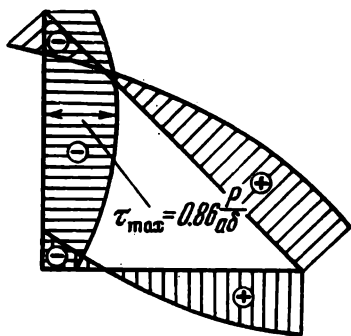


Fig. 271

Figure 271 shows the shearing stress diagram; it is found that

$$\tau_{\max} = 0.86 \frac{P}{a\delta}.$$

65. We isolate an elementary portion of length  $dx$  from the rod by two sections distant  $x$  and  $x + dx$  from the end (Fig. 272).

The separated element in turn is divided into two parts by a horizontal plane passing at a distance  $y$  from the middle line; we consider the condition of equilibrium for the

upper part  $ABCD$ . Obviously, it reduces to

$$\int_y^{(h+dh)/2} (\sigma + d\sigma) b dy - \int_y^{h/2} \sigma b dy = \tau b dx.$$

Since

$$\sigma = \frac{12My}{bh^3},$$

$$\sigma + d\sigma = \frac{12y}{b} \left[ \frac{M}{h^3} + d \left( \frac{M}{h^3} \right) \right].$$

The condition of equilibrium is now rewritten as follows:

$$\frac{12}{b} \left[ \frac{M}{h^3} + d \left( \frac{M}{h^3} \right) \right] \int_y^{(h+dh)/2} y dy - \frac{12M}{bh^3} \int_y^{h/2} y dy = \tau dx,$$

whence

$$\tau = 3 \frac{M}{bh^2} \frac{dh}{dx} + \frac{6}{b} \left( \frac{h^2}{4} - y^2 \right) \frac{d}{dx} \left( \frac{M}{h^3} \right).$$

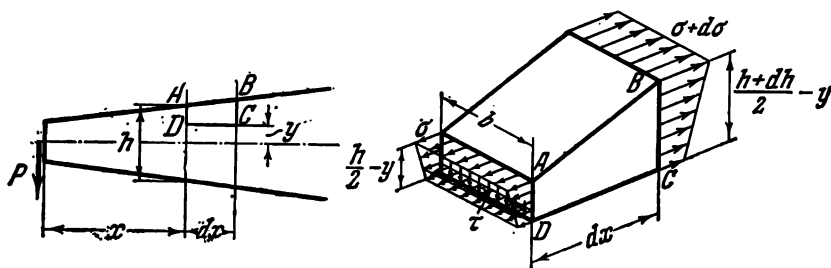


Fig. 272

If the law of variation of  $h$  and  $M$  is linear, then, given that  $h_1 = 2h_0$ , we obtain

$$h = h_0 \left( 1 + \frac{x}{l} \right), \quad M = Px,$$

$$\tau = \frac{6P}{\left( 1 + \frac{x}{l} \right)^2 bh_0} \left[ \frac{1}{2} \frac{x}{l} + \frac{1}{h_0^3} \left( \frac{h^2}{4} - y^2 \right) \frac{1 - 2 \frac{x}{l}}{\left( 1 + \frac{x}{l} \right)^2} \right].$$

The  $\tau$  diagrams for several sections of the beam are shown in Fig. 273. Here, in contrast to a rod of uniform thickness,

the shearing stresses do not vanish at the upper and the lower point of the section since the cutting plane is not perpendicular to the upper ( $A'B'$ ) and lower ( $C'D'$ ) bounding surfaces. For the end section the diagram is shown dashed since here the law of distribution of the stresses depends entirely on the mode of applying the external force  $P$ .

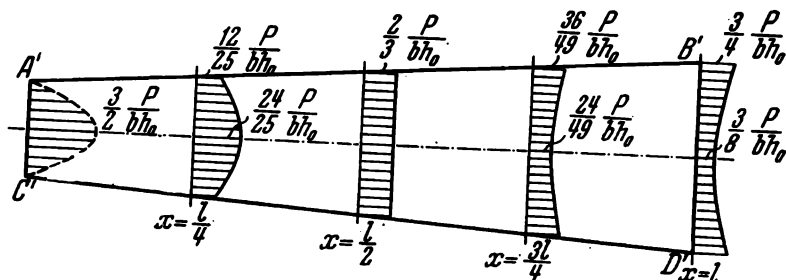


Fig. 273

If the thickness  $h$  of the beam does not vary too rapidly as a function of  $x$ , i.e., if the taper angle of the beam is small, the solution derived above is identical with that obtained by the methods of the theory of elasticity for a wedge.

66. It is possible to select a distributed load under which the beam remains straight. This load, however, produces transverse forces so large that it is necessary to determine the elastic curve of the beam with consideration of shearing deformations.

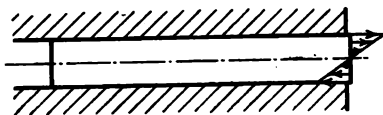


Fig. 274

That the selection of the proper law for  $q(x)$  is possible can be seen from the following simple example. Imagine a beam fitted tightly in rigid guides (Fig. 274) and bent by a moment applied at one of the ends. This beam remains straight under bending and we can state that the loads exerted on it by the guides are of the required type. This is also demonstrated by the solution of Prob. 59. There the right-hand part of the beam remains straight although the distributed load acting on it is not zero.

Take Eq. (1) (p. 162)

$$y'' = \frac{M}{EI} - \frac{kM''}{GA}.$$

We require that  $y'' = 0$ . We then obtain

$$M'' - \alpha^2 M = 0,$$

where  $\alpha^2 = GA/kEI$ . By solving the differential equation, we have, successively,

$$M = C_1 \sinh \alpha x + C_2 \cosh \alpha x, \quad (1)$$

$$Q = C_1 \alpha \cosh \alpha x + C_2 \alpha \sinh \alpha x, \quad (2)$$

$$q = Q' = C_1 \alpha^2 \sinh \alpha x + C_2 \alpha^2 \cosh \alpha x, \quad (3)$$

where the quantities  $C_1$  and  $C_2$  must be assigned according to the nature of the boundary conditions. If the beam is simply supported at the ends, i.e., if when  $x = 0$  and  $x = l$

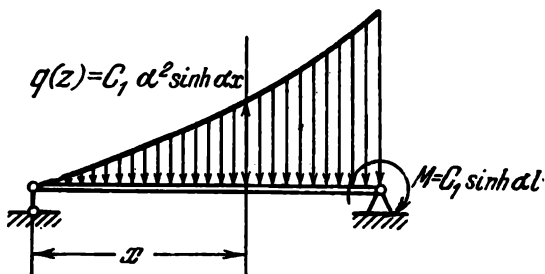


Fig. 275

$M = 0$ , then  $C_1 = C_2 = 0$  and  $q = 0$ . This means that the beam maintains its straight-line form only under a load equal to zero.

The possibility exists, however, of applying not only distributed loads, but also concentrated force factors at the ends of the rod. Suppose, for example, that the moment at the left support is zero, as before, and for the right support we reserve the possibility of applying any concentrated moment. Assuming that when  $x = 0$   $M = 0$ , we obtain

$$C_2 = 0, \quad M = C_1 \sinh \alpha x,$$

where  $C_1$  is any constant; further, by Eq. (2),

$$Q = C_1 \alpha \cosh \alpha x$$

and the required load is, from Eq. (3),

$$q(x) = C_1 \alpha^2 \sinh \alpha x.$$

The reaction at the left support is

$$Q_{x=0} = C_1 \alpha$$

and at the right support

$$Q_{x=l} = C_1 \alpha \cosh \alpha l,$$

$$M_{x=l} = C_1 \sinh \alpha l.$$

The required force system is presented in Fig. 275.

67. Since the beam is very long, by cutting it at the  $i$ th support, we can again consider its right-hand part as a very long beam similar to the given one though loaded not by the moment  $M$ , but by the moment  $M_i$ . This is also true for the  $(i+1)$ th,  $(i+2)$ th, ... supports. Consequently, if the bending moment at the  $(i+1)$ th support is a certain fraction of the  $i$ th moment, the  $(i+2)$ th moment is exactly the same fraction of the  $(i+1)$ th moment, i.e.,

$$M_{i+1} = x M_i,$$

$$M_{i+2} = x M_{i+1} = x^2 M_i,$$

etc.

We write the expression of the theorem of three moments for the  $i$ th and  $(i+1)$ th spans. In the absence of external loading on the spans we obtain

$$M_i a + 2M_{i+1} (a + a) + M_{i+2} a = 0$$

or, taking into account the expressions for  $M_{i+1}$  and  $M_{i+2}$ ,

$$1 + 4x + x^2 = 0,$$

from which we find

$$x = -2 \pm \sqrt{3}.$$

Since  $x$  must be less than unity in absolute value, we take the plus sign.\* Then

$$x = -(2 - \sqrt{3}).$$

The bending moment at the  $i$ th support is

$$M_i = M x^{i-1} = M (\sqrt{3} - 2)^{i-1}.$$

---

\* The minus sign corresponds to the case when the external moment is applied not at the extreme left-hand support, but at the extreme right-hand support.

The angle of rotation at the  $i$ th support is determined by multiplying the moment diagram for the  $i$ th span by the diagram due to the unit moment (Fig. 276)

$$EI\theta_i = \frac{Ma}{6} \sqrt{3} (\sqrt{3} - 2)^{i-1}.$$

68. We write a system of  $n - 2$  equations required to determine the support moments

$$M + 4M_2 + M_3 = 0,$$

$$M_2 + 4M_3 + M_4 = 0,$$

$$\dots \dots \dots$$

$$M_{n-2} + 4M_{n-1} = 0.$$

Assume that  $M_i = Ax^{i-1}$ . Substituting this value for  $M_i$

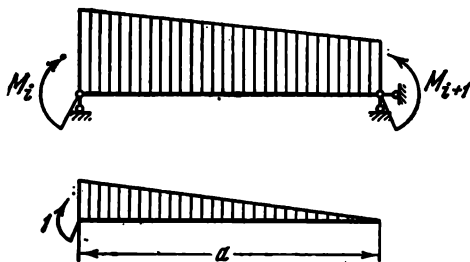


Fig. 276

in all equations except the first and the last, we obtain

$$1 + 4x + x^2 = 0,$$

$$x = -2 \pm \sqrt{3}.$$

It is now easy to ascertain that all equations, except the first and the last, are satisfied if we assume

$$M_2 = Ax_1 + Bx_2,$$

$$M_3 = Ax_1^2 + Bx_2^2,$$

$$\dots \dots \dots$$

$$M_i = Ax_1^{i-1} + Bx_2^{i-1},$$

where

$$x_1 = -2 + \sqrt{3},$$

$$x_2 = -2 - \sqrt{3},$$

$A$  and  $B$  are any constants which are selected so as to satisfy the first and last equations of the system

$$\begin{aligned} M + 4(Ax_1 + Bx_2) + Ax_1^2 + Bx_2^2 &= 0, \\ Ax_1^{n-3} + Bx_2^{n-3} + 4Ax_1^{n-2} + 4Bx_2^{n-2} &= 0, \end{aligned}$$

from which we have

$$\begin{aligned} A &= M \frac{x_2^{n-2}}{x_1(x_2^{n-1} - x_1^{n-1})}, \\ B &= -M \frac{x_1^{n-2}}{x_2(x_2^{n-1} - x_1^{n-1})}. \end{aligned}$$

We obtain, finally,

$$M_i = M \frac{(-2 - \sqrt{3})^{n-i} - (-2 + \sqrt{3})^{n-i}}{(-2 - \sqrt{3})^{n-1} - (-2 + \sqrt{3})^{n-1}}.$$

The determination of the angle of rotation at the  $i$ th support when  $M_i$  is known presents no difficulty. By multiplying the diagrams (Fig. 276), we obtain

$$EI\theta_i = M_i \frac{a}{3} + M_{i+1} \frac{a}{6}.$$

69. Denote the normal reaction at the right support by  $X_1$ . The frictional force is  $fX_1$  (Fig. 277). The equation of the force method is of the form

$$\delta_{11}X_1 + \delta_{1p} = 0.$$

Since  $\delta_{11}X_1$  is the displacement in the direction 1 produced by the forces  $X_1$  and  $fX_1$ , and  $\delta_{1p}$  is the displacement in

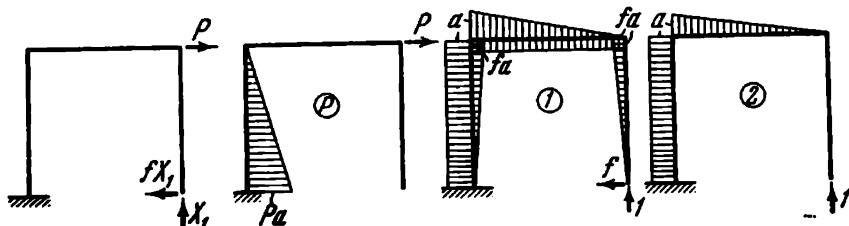


Fig. 277

the same direction caused by the force  $P$ ,  $\delta_{11}$  is determined by multiplying the diagrams (1) and (2), and  $\delta_{1p}$  by multi-

plying the diagrams (P) and (2)

$$\delta_{11} = \frac{a^3}{EI} \left( \frac{4}{3} - f \right),$$

$$\delta_{1P} = -\frac{Pa^3}{2EI}.$$

The reaction is then found to be

$$X_1 = \frac{P}{2\left(\frac{4}{3} - f\right)}.$$

The overall bending moment diagram is shown in Fig. 278.

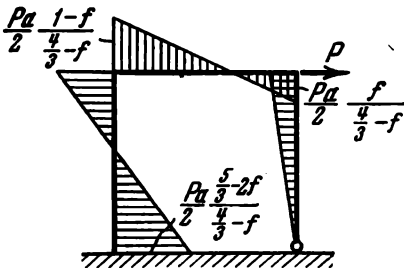


**Fig. 278**

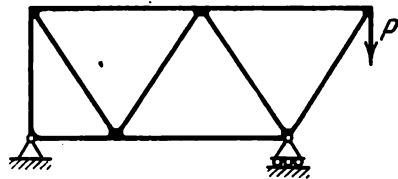


**Fig. 279**

70. It is permissible to design a truss with rigid joints on the assumption that the bars act only in tension or compression if the forces are applied at the joints. Indeed, consider a frame made up of a number of closed contours (Fig. 279) such that when the bars are connected by pins, the system will remain geometrically unchangeable.

Suppose that the frame is loaded by forces applied only at the joints (force  $P$  and support reactions). With the use of the force method we open the static indeterminacy of the frame by fitting hinges in its joints and introducing moments  $X_1, X_2, X_3, \dots$  at the joints as elastic constraints (Fig. 280). Thus, for the given system we obtain twelve equations of the ordinary type

[illegible]



any hinged rod is bent by a moment  $M$ , the displacements are of the order

$$\frac{Ml^2}{EI}$$

and in tension  $\frac{Pl}{EA}$ .

In the present case the order of these quantities is the same, i.e.,

$$\frac{Ml^2}{EI} \sim \frac{Pl}{EA}.$$

But

$$M = \sigma_b Z, \quad P = \sigma_t A,$$

hence we have

$$\sigma_b \sim \sigma_t \frac{I}{Zl},$$

i.e.,  $\sigma_b$  is of the order of  $\sigma_t \frac{I}{Zl}$ . But  $I/Z$  is equal to the maximum distance of a point of the section from the neutral axis passing through the centroid; consequently,  $I/Zl$  is a very small quantity (the ratio of a part of the cross-sectional dimension of the bar to its length).

Accordingly,  $\sigma_b$  is of the same order of magnitude in comparison with  $\sigma_t$ .

71. The determinant cannot be zero. If it becomes zero, this indicates that the system of equations is set up incorrectly.

Each of the equations of the canonical system represents the condition that the displacements caused by the external load are equal to the sum of the displacements due to the unknown internal forces

$$\delta_{1p} = -\delta_{11}X_1 - \delta_{12}X_2 - \delta_{13}X_3 - \dots,$$

$$\delta_{2p} = -\delta_{21}X_1 - \delta_{22}X_2 - \delta_{23}X_3 - \dots,$$

$$\dots \dots \dots$$

$$\delta_{np} = -\delta_{n1}X_1 - \delta_{n2}X_2 - \delta_{n3}X_3 - \dots$$

In setting up the equations, only independent displacements are considered. None of the displacements can be expressed in terms of the others. Consequently, none of the equations can be a combination of the remaining equations. All equations are thus independent, and in particular linear-

ly independent. As is known, the determinant of a system of linearly independent equations cannot be zero. If a system is set up incorrectly, i.e., dependent displacements are

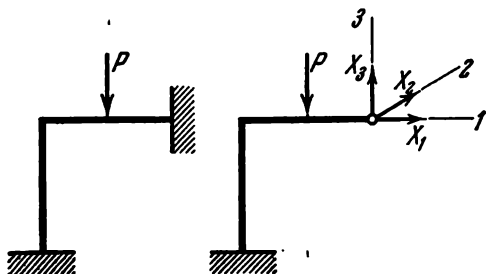


Fig. 281

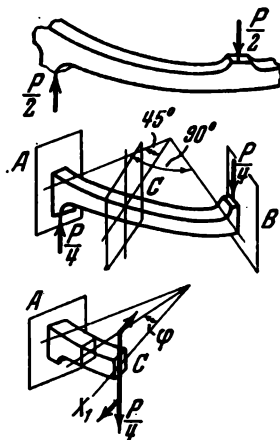


Fig. 282

considered (for example, the displacements along the axes 1, 2, 3 in the plane frame shown in Fig. 281), the determinant

$$\begin{vmatrix} \delta_{11} & \delta_{12} & \delta_{13} \\ \delta_{21} & \delta_{22} & \delta_{23} \\ \delta_{31} & \delta_{32} & \delta_{33} \end{vmatrix} = 0.$$

72. Consider a quarter ring of the spring (Fig. 282). The section A does not rotate with respect to the section B, but is displaced in the axial direction.

At the section C a transverse force  $P/4$  and a twisting moment  $X_1$  are produced (Fig. 282).

Let us determine this quantity following the general method of opening the statical indeterminacy of frames

$$\begin{aligned} \delta_{11}X_1 + \delta_{1P} &= 0, \\ \delta_{11} &= \frac{1}{EI} \int_0^{\pi/4} M_{1b}^2 R d\varphi + \frac{1}{C} \int_0^{\pi/4} M_{1t}^2 R d\varphi, \\ \delta_{1P} &= \frac{1}{EI} \int_0^{\pi/4} M_{1b} M_{Pb} R d\varphi + \frac{1}{C} \int_0^{\pi/4} M_{1t} M_{Pt} R d\varphi, \end{aligned}$$

where

$$\begin{aligned} M_{1b} &= \sin \varphi, & M_{1t} &= \cos \varphi, \\ M_{pb} &= -\frac{PR}{4} \sin \varphi, & M_{pt} &= \frac{PR}{4} (1 - \cos \varphi), \end{aligned}$$

$C$  is the torsional rigidity. For a square section

$$C = 0.141Ga^4.$$

Integrating gives

$$\begin{aligned} \delta_{11} &= \frac{R}{4EI} \left( \frac{\pi}{2} - 1 \right) + \frac{R}{4C} \left( \frac{\pi}{2} + 1 \right), \\ \delta_{1p} &= -\frac{PR^2}{16EI} \left( \frac{\pi}{2} - 1 \right) + \frac{PR^2}{16C} \left( 2\sqrt{2} - \frac{\pi}{2} - 1 \right), \\ X_1 &= \frac{PR}{4} \frac{\frac{\pi}{2} - 1 - \frac{EI}{C} \left( 2\sqrt{2} - \frac{\pi}{2} - 1 \right)}{\frac{\pi}{2} - 1 + \frac{EI}{C} \left( \frac{\pi}{2} + 1 \right)}. \end{aligned}$$

For a square section with  $\mu = 0.3$  we have

$$\frac{EI}{C} = \frac{E \frac{a^4}{12}}{0.141 \frac{E}{2(1+\mu)} a^4} = \frac{1+\mu}{0.846} \cong 1.54;$$

the twisting moment is then

$$X_1 = 0.0375 \frac{PR}{4}.$$

The total bending moment is

$$M_b = -\frac{PR}{4} 0.962 \sin \varphi.$$

The total twisting moment is

$$M_t = \frac{PR}{4} (1 - 0.962 \cos \varphi).$$

The vertical displacement of the section  $C$  relative to  $A$  is

$$\lambda_C = \frac{R}{EI} \int_0^{\pi/4} M_b M'_b d\varphi + \frac{R}{C} \int_0^{\pi/4} M_t M'_t d\varphi,$$

where  $M_b$  and  $M_t$  are the total bending and twisting moments,  $M'_b$  and  $M'_t$  are the corresponding moments due to

a unit vertical force applied at the section  $C$ , i.e.,

$$M'_b = -R \sin \varphi, \quad M'_t = R(1 - \cos \varphi).$$

We thus find

$$\begin{aligned} \lambda_c &= \frac{PR^3}{4EI} 0.962 \int_0^{\pi/4} \sin^2 \varphi \, d\varphi + \\ &+ \frac{PR^3}{4C} \int_0^{\pi/4} (1 - 0.962 \cos \varphi)(1 - \cos \varphi) \, d\varphi = \\ &= \frac{PR^3}{16EI} 0.962 \left( \frac{\pi}{2} - 1 \right) + \frac{PR^3}{16C} \left[ \pi - 2\sqrt{2} - \right. \\ &\quad \left. - 0.962 \cdot 2\sqrt{2} + 0.962 \left( \frac{\pi}{2} + 1 \right) \right]; \end{aligned}$$

or finally

$$\lambda_c = \frac{PR^3}{EI} 0.0405.$$

In order to obtain the total deflection of the spring, we must multiply the quantity  $\lambda_c$  by double the number of operating rings  $2n$

$$\lambda = 2n \frac{PR^3}{EI} 0.0405 \quad \text{or} \quad \lambda = 0.972 \frac{PR^3}{Ea^4} n.$$

On comparing this with the deflection of a coiled spring of square section with the same number of operating coils  $n$ , i.e.

$$\lambda = \frac{PR^3 2\pi n}{G 0.141a^4} \cong 116 \frac{PR^3 n}{Ea^4},$$

we come to the conclusion that the slotted spring is about 120 times stiffer than the coiled spring.

73. Consider some plane closed frame of uniform rigidity  $EI$  and assume that the bending moment diagram is constructed for it (Fig. 283). We cut the contour of this frame at an arbitrary point and determine the relative angle of rotation of the sections at the place where the frame is cut. From the continuity condition this angle is zero. To

determine the relative angle of rotation we take the integral

$$\int \frac{MM_1 ds}{EI},$$

where  $M_1$  is the bending moment due to unit moments applied at the place of the cut (Fig. 283), i.e.,  $M_1 = 1$ . For  $EI = \text{constant}$ , we obtain therefore

$$\int M ds = 0.$$

The proposition developed above applies not only to closed frames, but, in general, to all framed systems where the

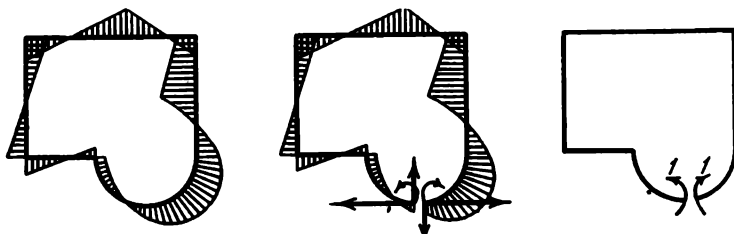


Fig. 283

conditions of fixing prevent any rotation of one end section with respect to the other. For example, in each of the systems represented in Fig. 284 the area under the bending diagram is zero for any loading if  $EI = \text{constant}$ .

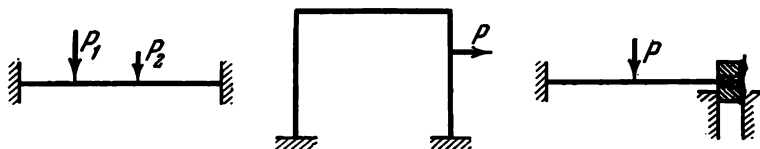


Fig. 284

**74.** We cut the frame through the hinge and determine the relative displacement of the sections at the place where the frame is cut. For this we apply two opposite unit forces to the cut frame at the hinge (Fig. 285). The choice of the line of action of the forces may be made arbitrarily.

The required displacement  $\delta$  is equal to

$$\delta = \int \frac{M M_1 ds}{EI}.$$

But  $M_1 = x$  and, since  $\delta = 0$ , we have  $\int M x ds = 0$ .

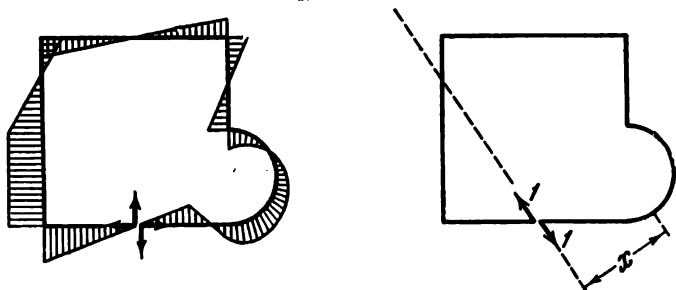


Fig. 285

75. We remark first that the area  $\Delta A$  swept out by any beam during bending is determined by the following integral:

$$\Delta A = \int \frac{M M_{1q} ds}{EI},$$

where  $M$  is the bending moment due to external forces,  $M_{1q}$  is the bending moment due to a distributed load of intensity "unity" ( $q = 1$  kgf/cm).

This expression is most easily derived in the same way as the usual expressions for linear and angular displacements.

In order to determine the change in the area bounded by the closed frame, we must first find the expression for  $M_{1q}$  by applying a unit distributed load  $q = 1$  to the frame (Fig. 286).

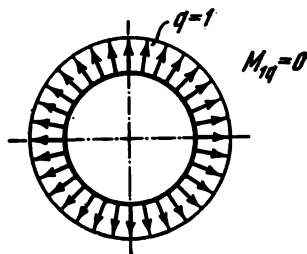


Fig. 286

But for a circular closed frame  $M_{1q} = 0$ , consequently,  $\Delta A = 0$ . The above statement is thereby proved. It is quite evident that this statement is true, on the one hand, only so long as the extension of the contour of the ring is negli-

ble and, on the other hand, provided that the system acts in the range of small displacements. For a very flexible ring, the area bounded by its contour does not remain invariant when the change of shape is appreciable.

76. Denote by  $y$  the vertical displacement of the rod when loaded by the force  $P$ . The differential equation of the elastic curve of the beam

$$EIy'' = M_b$$

is rewritten as

$$EIy^{(IV)} = M_b'' = q,$$

where  $q$  kgf/cm is the load intensity, i.e., the force per unit length of the rod. In the case considered, this force is obviously equal to the weight of water displaced by a unit length of the rod during the displacement  $y$ , i.e.,

$$q = -1 \cdot b\gamma y,$$

where  $\gamma$  is the specific weight of water. Since the intensity  $q$  is directed oppositely to the displacement  $y$ , the minus sign is put before  $b\gamma y$ . We now have

$$y^{(IV)} + \frac{b\gamma}{EI} y = 0.$$

Denote

$$\frac{b\gamma}{EI} = 4k^4, \quad (1)$$

where  $k$  is a constant. The equation becomes

$$y^{(IV)} + 4k^4 y = 0. \quad (2)$$

This equation is called the equation of a beam on an elastic foundation. A typical example of such a beam is a floating beam of rectangular section. For it, the reaction of the foundation (water) at each point is proportional to the displacement  $y$ .

Equation (2) is satisfied by the functions  $\sinh kx \sin kx$ ,  $\cosh kx \cos kx$ ,  $\sinh kx \cos kx$ ,  $\cosh kx \sin kx$  and by any linear combinations of them. In using these functions it is most convenient to take the combinations proposed by A. N. Krylov, which are called the Krylov functions. They are convenient because the derivative of each of these functions gives one of the same functions. Below is a table of the

$n$	$Y_n(kx)$	$Y'_n(kx)$	$Y''_n(kx)$	$Y'''_n(kx)$	$Y^{IV}_n(kx)$
1	$\cosh kx \cos kx$	$-4kY_4$	$-4k^2Y_3$	$-4k^3Y_2$	$-4k^4Y_1$
2	$\frac{1}{2} (\cosh kx \sin kx +$ $\quad + \sinh kx \cos kx)$	$kY_1$	$-4k^2Y_4$	$-4k^3Y_3$	$-4k^4Y_2$
3	$\frac{1}{2} \sinh kx \sin kx$	$kY_2$	$k^2Y_1$	$-4k^3Y_4$	$-4k^4Y_3$
4	$\frac{1}{4} (\cosh kx \sin kx -$ $\quad - \sinh kx \cos kx)$	$kY_3$	$k^2Y_2$	$k^3Y_1$	$-4k^4Y_4$

Krylov functions. The expression for  $y$  may be written as follows:

$$y = y_0 Y_1(kx) + y'_0 \frac{1}{k} Y_2(kx) + \frac{M_0}{EI} \frac{1}{k^2} Y_3(kx) + \frac{Q_0}{EI} \frac{1}{k^3} Y_4(kx),$$

where  $y_0$ ,  $y'_0$ ,  $M_0$ , and  $Q_0$  are, respectively, the displacement, angle of rotation, bending moment, and shearing force for  $x = 0$ . If the origin of  $x$  is chosen at the left end of the rod (Fig. 71), we obviously have

$$Q_0 = 0, \quad M_0 = 0.$$

The quantities  $y_0$  and  $y'_0$  are determined from the following conditions:

$$\text{when } x = \frac{l}{2}, \quad y' = 0, \quad Q = \frac{P}{2}.$$

According to the table we have

$$\frac{1}{k} y' = -4y_0 Y_4(kx) + y'_0 \frac{1}{k} Y_1(kx),$$

$$\frac{1}{k^2} y'' = -4y_0 Y_3(kx) - y'_0 \frac{4}{k} Y_4(kx),$$

$$\frac{1}{k^3} y''' = -4y_0 Y_2(kx) - y'_0 \frac{4}{k} Y_3(kx),$$

and the boundary conditions are then written as

$$-4y_0 Y_4\left(\frac{kl}{2}\right) + y'_0 \frac{1}{k} Y_1\left(\frac{kl}{2}\right) = 0,$$

$$-4y_0 Y_2\left(\frac{kl}{2}\right) - y'_0 \frac{4}{k} Y_3\left(\frac{kl}{2}\right) = \frac{P}{2EI k^3},$$

from which we find the displacement and the angle of rotation for  $x = 0$

$$y_0 = \frac{P}{8EI k^3} \frac{-Y_1\left(\frac{kl}{2}\right)}{Y_2\left(\frac{kl}{2}\right) Y_1\left(\frac{kl}{2}\right) + 4Y_3\left(\frac{kl}{2}\right) Y_4\left(\frac{kl}{2}\right)},$$

$$\frac{y'_0}{k} = \frac{P}{8EI k^3} \frac{-4Y_4\left(\frac{kl}{2}\right)}{Y_2\left(\frac{kl}{2}\right) Y_1\left(\frac{kl}{2}\right) + 4Y_3\left(\frac{kl}{2}\right) Y_4\left(\frac{kl}{2}\right)}.$$

Now  $y$  and  $y''$  become

$$y = -P_0 \left[ Y_1\left(\frac{kl}{2}\right) Y_1(kx) + 4Y_4\left(\frac{kl}{2}\right) Y_2(kx) \right],$$

$$y'' = 4P_0 k^2 \left[ Y_1\left(\frac{kl}{2}\right) Y_3(kx) + 4Y_4\left(\frac{kl}{2}\right) Y_4(kx) \right],$$

where

$$P_0 = \frac{P}{8EI k^3} \frac{1}{Y_1\left(\frac{kl}{2}\right) Y_2\left(\frac{kl}{2}\right) + 4Y_3\left(\frac{kl}{2}\right) Y_4\left(\frac{kl}{2}\right)}.$$

Carry out a numerical calculation:

$$k^4 = \frac{3\gamma}{Eh^3} = \frac{3 \times 10^{-3}}{10^5 \times 10^3}, \quad k = 2.34 \times 10^{-3} \text{ cm}^{-1}, \quad \frac{kl}{2} = 1.17.$$

Further, using tables of trigonometric and hyperbolic functions, we find, according to the expressions for  $Y_n(kx)$  (p. 190),

$$Y_1\left(\frac{kl}{2}\right) = 0.689, \quad Y_2\left(\frac{kl}{2}\right) = 1.097,$$

$$Y_3\left(\frac{kl}{2}\right) = 0.670, \quad Y_4\left(\frac{kl}{2}\right) = 0.265,$$

whereupon we obtain

$$P_0 = 0.0401P,$$

$$y = -0.0401P [0.689Y_1(kx) + 1.058Y_2(kx)] \text{ cm}, \quad (3)$$

$$M = EI y'' = 146.2P [0.689Y_3(kx) + 1.058Y_4(kx)] \text{ kgf-cm}. \quad (4)$$

The solution obtained is true only if the upper plane of the beam comes out above the water surface throughout its length. Only in this case can the water reaction be considered

proportional to the vertical displacement. Thus, the applicability of the foregoing solution depends on the maximum displacement  $y_{\max}$ .

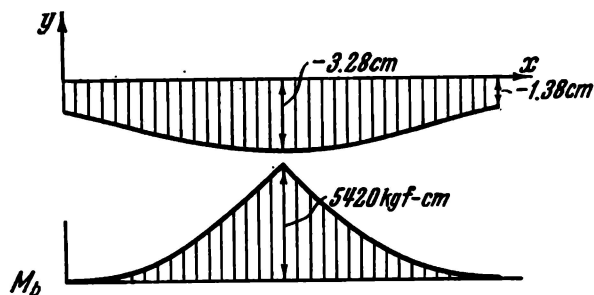


Fig. 287

Under no load, the beam is immersed in water by an amount equal to  $0.6 h$  (since its specific weight is 0.6 of the spe-

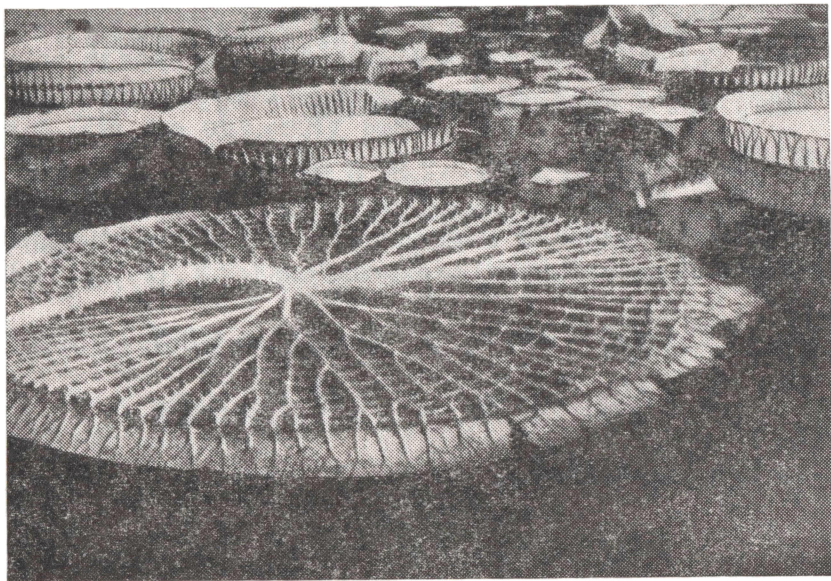


Fig. 288

cific weight of water). The upper plane of the beam rises above the water level by  $0.4h = 4$  cm. Consequently, the con-

dition for applicability of the derived solution is  $|y_{\max}| \leq 4$  cm.

By formula (3) we find:  $|y_{\max}| = 3.28$  cm  $< 4$  cm.

In Fig. 287 are shown the shape of the elastic curve of the deflected beam and the moment diagram constructed on the basis of expression (4).

The maximum bending moment occurring at the middle section is 5420 kgf-cm and the stress is given by

$$\sigma_{\max} = \frac{M}{Z} \cong 16.3 \text{ kgf/cm}^2.$$

The problem of the bending of a floating plate is solved in a similar (but, naturally, more complicated) way. The solution of this problem is not presented here. But we wish to call the reader's attention to an interesting construction that nature creates to ensure the strength of a large floating leaf.

In Fig. 288 is given the photograph of a turned-over leaf of *Victoria regia*. Were it not for the radial and circular reinforcing the huge leaf (more than one metre in diameter) would inevitably break in the very first rough water.

77.\* The external load is reduced to the ends of the joint as shearing forces and moments (Fig. 289).

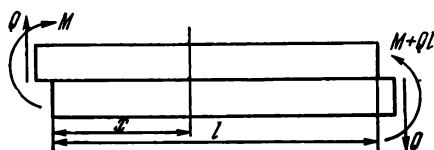


Fig. 289

The internal forces and moments relating to the upper sheet are denoted by the subscript 1, and those relating to the lower sheet by the subscript 2. For a part of the joint of length  $x$  (Fig. 290), the conditions of equilibrium give

$$\begin{aligned} N_1 &= -N_2 = N, \\ Q_1 + Q_2 &= Q, \\ M_1 + M_2 &= M + Qx + Nh. \end{aligned} \quad (1)$$

\* See also S. E. Korotkova, *The Investigation of the Operation of a Lap Glue Joint Under Bending*, in "Soprotivlenie Materialov i Teoriya Sooruzhenii", Vyp. 7, Budivel'nik, Kiev, 1968, pp. 120-128.

There occurs a relative displacement  $\Delta$  along the  $x$  axis between the lower surface of the upper sheet and the upper

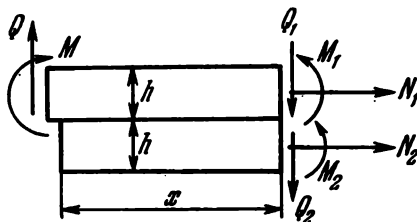


Fig. 290

surface of the lower sheet. It can be determined as the integral of the difference in the strains

$$\Delta = \int (\epsilon_1 - \epsilon_2) dx + C,$$

but

$$\epsilon_1 = \frac{N}{Ebh} + \frac{6M_1}{Ebh^2}, \quad \epsilon_2 = -\frac{N}{Ebh} - \frac{6M_2}{Ebh^2},$$

hence

$$\Delta = \frac{1}{Ebh} \int \left[ 2N + \frac{6}{h} (M_1 + M_2) \right] dx + C. \quad (2)$$

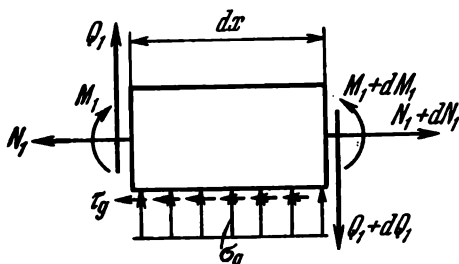


Fig. 291

The quantity  $\Delta$  is related to the shearing stresses  $\tau_g$  in the glue layer by the obvious equality

$$G_g \frac{\Delta}{\delta} = \tau_g,$$

where  $\delta$  is the thickness of the glue layer.

From the condition for equilibrium of an element of length  $dx$  (Fig. 291) it follows that

$$b\tau_g = N', \quad (3)$$

hence

$$G_g \frac{\Delta}{\delta} = \frac{N'}{b}.$$

Differentiating both sides of this equality with respect to  $x$  and eliminating  $M_1 + M_2$  from expression (2) by means of expression (1), we obtain the following equation for the determination of  $N$ :

$$N'' - \frac{8G_g}{Eh\delta} N = \frac{6G_g}{Eh^2\delta} (M + Qx).$$

Denote

$$\frac{8G_g}{Eh\delta} = \alpha^2, \quad (4)$$

we then obtain

$$N = A \sinh \alpha x + B \cosh \alpha x - \frac{3}{4h} (M + Qx).$$

The constants  $A$  and  $B$  are determined from the condition that the normal force  $N$  is zero at the ends of the glue joint

$$N_{x=0} = N_{x=l} = 0.$$

Finally,

$$N = \frac{3 \sinh \alpha x}{4h \sinh \alpha l} [M (1 - \cosh \alpha l) + Ql] + \frac{3M}{4h} \cosh \alpha x - \frac{3}{4h} (M + Qx) \quad (5)$$

and the shearing stress  $\tau_g$  in the glue joint is, according to expression (3),

$$\tau_g = \frac{3\alpha \cosh \alpha x}{4bh \sinh \alpha l} [M (1 - \cosh \alpha l) + Ql] + \frac{3\alpha M}{4bh} \sinh \alpha x - \frac{3}{4bh} Q. \quad (6)$$

The glue layer acts not only in shear, but also in tension and compression in a direction perpendicular to the plane of glueing.

The normal stress in the glue layer is

$$\sigma_g = \frac{y_2 - y_1}{\delta} E_g,$$

where  $y_1$  and  $y_2$  are the vertical displacements of the upper and lower sheets, respectively.

We add two more equations of equilibrium set up for the element  $dx$  (Fig. 291)

$$\sigma_g b = Q'_1, \quad (7)$$

$$Q_1 = M'_1 - \frac{h}{2} N'. \quad (8)$$

Eliminating  $\sigma_g$  and  $Q_1$  from these three equations gives

$$(y_2 - y_1) \frac{bE_g}{\delta} = M''_1 - \frac{h}{2} N''.$$

But since  $EIy''_1 = M_1$  and  $EIy''_2 = M_2$ , we have

$$\frac{M_2 - M_1}{EI} \frac{bE_g}{\delta} = \left( M_1 - \frac{h}{2} N \right)^{(IV)}.$$

Finally, on eliminating  $M_2$  between this and Eq. (1), there results

$$\left( M_1 - \frac{h}{2} N \right)^{(IV)} + \frac{2bE_g}{\delta EI} \left( M_1 - \frac{h}{2} N \right) = \frac{bE_g}{\delta EI} (M + Qx).$$

Denote

$$M_1 - \frac{h}{2} N = Y, \quad \frac{2bE_g}{\delta EI} = 4k^4;$$

then

$$Y^{(IV)} + 4k^4 Y = 2k^4 (M + Qx).$$

To solve this equation we may use the Krylov functions (see Prob. 76). Then

$$Y = C_1 Y_1(kx) + C_2 Y_2(kx) + C_3 Y_3(kx) + C_4 Y_4(kx) + \frac{1}{2} (M + Qx), \quad (9)$$

where the constants  $C_1$ ,  $C_2$ ,  $C_3$ , and  $C_4$  are determined from four conditions

$$\begin{aligned} Y_{x=0} &= M_{1x=0} = M, & Q_{1x=0} &= Y'_{x=0} = Q, \\ M_{1x=l} &= 0, & Y'_{x=l} &= 0. \end{aligned}$$

After transformation and replacing the Krylov functions by their expressions, we obtain, finally,

$$\begin{aligned}
 C_1 &= \frac{M}{2}, & C_2 &= \frac{Q}{2k}, \\
 C_3 &= -M \frac{\sinh(kl) + \sin(kl)}{\sinh(kl) - \sin(kl)} - \frac{Q}{k} \frac{\cosh(kl) + \cos(kl)}{\sinh(kl) + \sin(kl)} - \\
 &\quad - 2Ql \frac{\sinh(kl) \sin(kl)}{\sinh^2(kl) - \sin^2(kl)}, \\
 C_4 &= 2M \frac{\cosh(kl) + \cos(kl)}{\sinh(kl) - \sin(kl)} + \frac{Q}{k} \frac{\sinh(kl) + \sin(kl)}{\sinh(kl) + \sin(kl)} + \\
 &\quad + 2Ql \frac{\cosh(kl) \sin(kl) + \sinh(kl) \cos(kl)}{\sinh^2(kl) - \sin^2(kl)}.
 \end{aligned}$$

The bending moment  $M_1$  is now determined from the expression  $M_1 = Y + \frac{h}{2} N$ , where  $N$  is given by function (5).

The normal stress in the glue layer is, according to Eqs. (7) and (8),

$$\begin{aligned}
 \sigma_g &= \frac{1}{b} Y'', \\
 \sigma_g &= \frac{k^2}{b} [-4C_1 Y_3(kx) - 4C_2 Y_4(kx) + C_3 Y_1(kx) + C_4 Y_2(kx)].
 \end{aligned} \tag{10}$$

The positive value of  $\sigma_g$  corresponds to compression of the glue layer. By formulas (6) and (10) it is possible to plot the graphs of the variation of shearing and normal stresses in the glue layer, and by formulas (5) and (9) to construct the normal force and bending moment diagrams in the upper plate.

For the case of a very long glue joint the problem is appreciably simplified by the fact that the stresses in the glue layer are of a local nature. In this case, in determining  $N$  and  $Y$  we can separate the damped part of the solution and take

$$\begin{aligned}
 N &= Ae^{-\alpha x} - \frac{3}{4h} (M + Qx), \\
 Y &= e^{-\alpha x} (C_1 \sin kx + C_2 \cos kx) + \frac{1}{2} (M + Qx).
 \end{aligned}$$

The constants  $A$ ,  $C_1$ , and  $C_2$  are determined from the boundary conditions at the left edge, i.e., at  $x = 0$ , where  $N = 0$ ,  $Y = M$ , and  $Y' = Q$ .

78. If the spokes are treated as a continuous elastic medium, then for every point of the rim the force exerted by the spokes is proportional to the radial displacement  $w$  of the corresponding point of the rim. Thus, we are confronted here with the problem of designing a ring with an elastic foundation. In a unit length of the rim there are  $n/2\pi R$

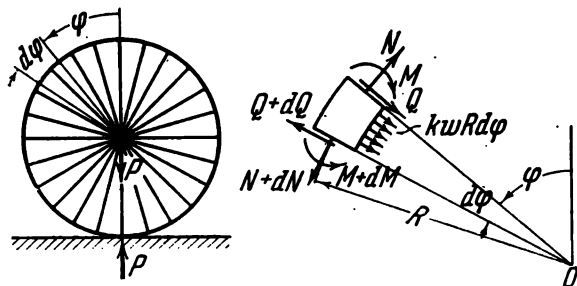


Fig. 292

spokes. Each spoke exerts a force  $\frac{EA}{l} w$  on the rim, where  $l$  is the length of the spoke ( $l \cong R$ ),  $A$  is the cross-sectional area of the spoke.

A unit length of the rim is thus acted on by the force

$$\frac{EAn}{2\pi R^2} w = kw,$$

whence

$$k = \frac{EAn}{2\pi R^2}. \quad (1)$$

Let us now set up the differential equation of the elastic curve of the ring. For the independent variable we choose the angle  $\varphi$  measured from the top of the ring (Fig. 292).

We isolate an element of length  $R d\varphi$  from the ring and apply internal forces  $N$ ,  $Q$ , and  $M$  at the sections made. The force exerted by the spokes on this element is  $kwR d\varphi$ . We set up the equations of equilibrium for this elementary portion. By projecting all forces on the radial axis, we obtain

$$\frac{dQ}{d\varphi} = N + kRw.$$

The condition that the sum of the projections of all forces on the axis tangential to a circular arc is zero gives

$$\frac{dN}{d\varphi} + Q = 0.$$

By equating to zero the sum of the moments of the forces about the point  $O$

$$R \frac{dN}{d\varphi} + \frac{dM}{d\varphi} = 0$$

and eliminating  $Q$  and  $N$  from these equations, we have

$$kR^2 \frac{dw}{d\varphi} = \frac{dM}{d\varphi} + \frac{d^3M}{d\varphi^3}.$$

The change in curvature  $\Delta (1/\rho)$  is related to the bending moment  $M$  by the following equation:

$$M = EI \Delta \left( \frac{1}{\rho} \right);$$

but, as is known,

$$\Delta \left( \frac{1}{\rho} \right) = - \left( \frac{w}{R^2} + \frac{1}{R^2} \frac{d^2w}{d\varphi^2} \right).$$

Since for the positive displacement  $w$  directed away from the centre of the circle the curvature of the ring decreases, the minus sign is introduced on the right-hand side of this expression. The change in curvature in this expression consists of two components. The first term  $w/R^2$  corresponds to the change in curvature due to a simple expansion of the ring.

The second term  $\frac{1}{R^2} \frac{d^2w}{d\varphi^2}$  equal to  $d^2w/ds^2$  represents the usual change in curvature which we have in a straight rod.

After substitution for  $M$ , the differential equation takes the following final form:

$$\frac{d^5w}{d\varphi^5} + 2 \frac{d^3w}{d\varphi^3} + a^2 \frac{dw}{d\varphi} = 0,$$

where

$$a^2 = \frac{R^4 k}{EI} + 1. \quad (2)$$

The solution of this equation is

$$w = C_0 + C_1 \cosh \alpha \varphi \cos \beta \varphi + C_2 \sinh \alpha \varphi \sin \beta \varphi + \\ + C_3 \cosh \alpha \varphi \sin \beta \varphi + C_4 \sinh \alpha \varphi \cos \beta \varphi,$$

where

$$\alpha = \sqrt{\frac{a-1}{2}}, \quad \beta = \sqrt{\frac{a+1}{2}}. \quad (3)$$

Since the ring deforms symmetrically with respect to the vertical axis, the function  $w$  must be an even function, i.e., it must remain invariant when the sign of  $\varphi$  is changed from plus to minus. The arbitrary constants  $C_3$  and  $C_4$  appearing in the odd functions are therefore set equal to zero. The remaining constants are determined from the following conditions:

$$(a) \text{ when } \varphi = \pi, \quad \frac{dw}{d\varphi} = 0,$$

$$(b) \text{ when } \varphi = \pi, \quad Q = -\frac{P}{2},$$

$$(c) \int_0^\pi w d\varphi = 0.$$

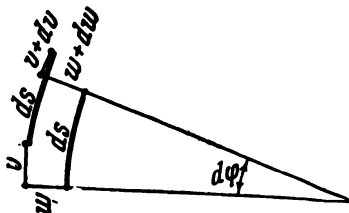


Fig. 293

The last condition expresses the fact that when the wheel is loaded the upper and lower points remain on the same vertical. Indeed, if an element of the rim of the wheel is considered before and after deformation (Fig. 293), it can easily be ascertained that the condition for its inextensibility is written as

$$dv + w d\varphi = 0,$$

where  $v$  is the displacement along the tangent to an arc of the contour or

$$v = - \int w d\varphi.$$

The displacement along the tangent at the points  $\varphi = 0$  and  $\varphi = \pi$  is zero; hence the condition (c).

With  $C_3 = C_4 = 0$ , the expressions for the bending moment

$$M = -\frac{EI}{R^2} \left( w + \frac{d^2 w}{d\varphi^2} \right)$$

and the shearing force

$$Q = \frac{1}{R} \frac{dM}{d\varphi}$$

become

$$M = -\frac{EI}{R^2} (C_0 - 2\alpha\beta C_1 \sinh \alpha\varphi \sin \beta\varphi + \\ + 2\alpha\beta C_2 \cosh \alpha\varphi \cos \beta\varphi),$$

$$Q = 2\alpha\beta \frac{EI}{R^3} [(\alpha C_1 + \beta C_2) \cosh \alpha\varphi \sin \beta\varphi + \\ + (\beta C_1 - \alpha C_2) \sinh \alpha\varphi \cos \beta\varphi].$$

By expanding the boundary conditions (a), (b), and (c), we now obtain

$$(a) \ C_1 [\alpha \sinh \alpha\pi \cos \beta\pi - \beta \cosh \alpha\pi \sin \beta\pi] + \\ + C_2 [\beta \sinh \alpha\pi \cos \beta\pi + \alpha \cosh \alpha\pi \sin \beta\pi] = 0,$$

$$(b) \ C_1 (\alpha \cosh \alpha\pi \sin \beta\pi + \beta \sinh \alpha\pi \cos \beta\pi) - \\ - C_2 (\alpha \sinh \alpha\pi \cos \beta\pi - \beta \cosh \alpha\pi \sin \beta\pi) = -\frac{P}{4EI} \frac{R^3}{\alpha\beta},$$

$$(c) \ C_0\pi + \frac{C_1}{\alpha^2 + \beta^2} (\alpha \sinh \alpha\pi \cos \beta\pi + \beta \cosh \alpha\pi \sin \beta\pi) + \\ + \frac{C_2}{\alpha^2 + \beta^2} (\alpha \cosh \alpha\pi \sin \beta\pi - \beta \sinh \alpha\pi \cos \beta\pi) = 0.$$

We solve these equations

$$C_0 = \frac{PR^3}{2\pi\alpha^2 EI},$$

$$C_1 = -\frac{P}{4EI} \frac{R^3}{\beta\alpha} \frac{\alpha \cosh \alpha\pi \sin \beta\pi + \beta \sinh \alpha\pi \cos \beta\pi}{a (\sinh^2 \alpha\pi + \sin^2 \beta\pi)},$$

$$C_2 = \frac{P}{4EI} \frac{R^3}{\alpha\beta} \frac{\alpha \sinh \alpha\pi \cos \beta\pi - \beta \cosh \alpha\pi \sin \beta\pi}{a (\sinh^2 \alpha\pi + \sin^2 \beta\pi)}.$$

The expressions for  $w$  and  $M$  become, finally,

$$w = \frac{PR^3}{4\alpha\beta EI} \left( \frac{2\alpha\beta}{\pi a^2} - A \cosh \alpha\psi \cos \beta\varphi + B \sinh \alpha\varphi \sin \beta\varphi \right), \quad (4)$$

$$M = -\frac{PR}{2} \left( \frac{1}{\pi a^2} + A \sinh \alpha\varphi \sin \beta\varphi + B \cosh \alpha\varphi \cos \beta\varphi \right), \quad (5)$$

where, for shortness, we write

$$\left. \begin{aligned} A &= \frac{\alpha \cosh \alpha \pi \sin \beta \pi + \beta \sinh \alpha \pi \cos \beta \pi}{a (\sinh^2 \alpha \pi + \sin^2 \beta \pi)}, \\ B &= \frac{\alpha \sinh \alpha \pi \cos \beta \pi - \beta \cosh \alpha \pi \sin \beta \pi}{a (\sinh^2 \alpha \pi + \sin^2 \beta \pi)}. \end{aligned} \right\} \quad (6)$$

The force per one spoke is obviously equal to

$$P_s = \frac{EA}{R} w. \quad (7)$$

Carry out a numerical calculation. From expressions (1) and (2), assuming the moduli of elasticity of the spokes and rim to be the same, we obtain

$$a^2 = \frac{R^2 A n}{2\pi I} + 1 = \frac{\frac{\pi \times 0.2^2}{4} \times 36 \times 31^2}{2\pi \times 0.3} + 1 = 577.7, \\ a = 24.04.$$

Further, according to (3) we calculate

$$\alpha = \sqrt{\frac{24.04 - 1}{2}} = 3.395, \quad \beta = \sqrt{\frac{24.04 + 1}{2}} = 3.539.$$

We now find

$$\sinh \alpha \pi \cong \cosh \alpha \pi \cong \frac{1}{2} e^{10.66}, \\ \sin \beta \pi = -0.992, \quad \cos \beta \pi = +0.1223.$$

From (6) we have

$$A = -0.245e^{-10.66}, \quad B = +0.326e^{-10.66}.$$

Expressions (5) and (7) can be rewritten as

$$M = P (-0.00855 + 3.80e^{-10.66} \sinh \alpha \varphi \sin \beta \varphi - \\ - 5.05e^{-10.66} \cosh \alpha \varphi \cos \beta \varphi) \text{ kgf-cm}, \\ P_s = P (0.0278 + 0.514e^{-10.66} \cosh \alpha \varphi \cos \beta \varphi + \\ + 0.683e^{-10.66} \sinh \alpha \varphi \sin \beta \varphi) \text{ kgf}.$$

From this it is seen that for small values of  $\varphi$  the second and third terms in the parentheses are very small, and  $M$  and  $P_s$

remain practically constant. On the basis of these expressions we construct diagrams for the bending moment  $M$  and the forces  $P_s$  in the spokes (Fig. 294).

When the force  $P = 40$  kgf, we obtain:  $M_{\max} = 88$  kgf-cm; the maximum force per spoke  $P_{s, \max} = 11.2$  kgf. It is

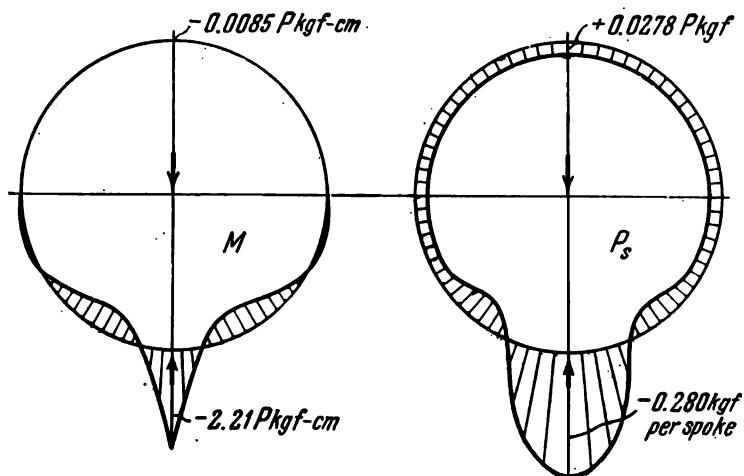


Fig. 294

clear that the result obtained does not include the pre-tension in the spokes which is applied to them during assembling. Naturally, this pre-tension must exceed  $P_{s, \max}$  in absolute value.

The problem considered was first solved by N. E. Zhukovskii.

79. We isolate from the bimetallic strip an elementary portion of length  $ds$  and initial curvature of the junction surface  $1/\rho_0$  (bimetallic elements are often made curved) (Fig. 295).

The extension of a fibre distant  $y$  from the junction surface is made up of two parts, namely the extension in the junction  $\varepsilon_0$  and the extension due to the bending of the strip

$$y \left( \frac{1}{\rho} - \frac{1}{\rho_0} \right).$$

where  $\frac{1}{\rho}$  is the new curvature. Thus,

$$\varepsilon = \varepsilon_0 + y \left( \frac{1}{\rho} - \frac{1}{\rho_0} \right).$$

By subtracting the thermal extension and multiplying the resulting difference by the modulus of elasticity  $E$ , we find

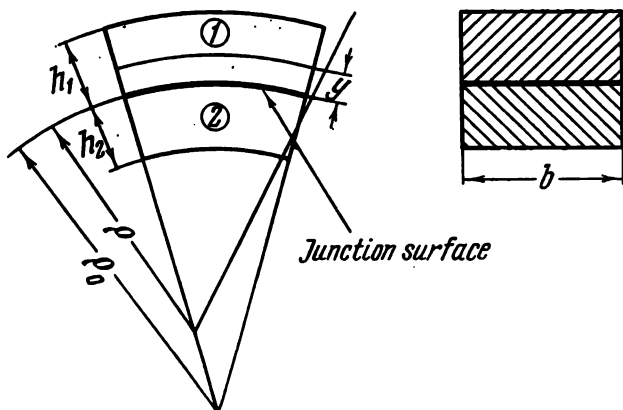


Fig. 295

the stress acting in a fibre distant  $y$  from the junction surface. For the first plate we have

$$\sigma_1 = E_1 \left[ \varepsilon_0 + y \left( \frac{1}{\rho} - \frac{1}{\rho_0} \right) - \alpha_1 t \right] \quad (0 \leq y \leq h_1),$$

for the second

$$\sigma_2 = E_2 \left[ \varepsilon_0 + y \left( \frac{1}{\rho} - \frac{1}{\rho_0} \right) - \alpha_2 t \right] \quad (-h_2 \leq y \leq 0);$$

$E_1$  and  $E_2$  are the moduli of elasticity for the first and second plates.

The normal force and bending moment at the section of the bimetallic element are zero. Hence,

$$\int_0^{h_1} \sigma_1 b dy + \int_{-h_2}^0 \sigma_2 b dy = 0, \quad \int_0^{h_1} \sigma_1 b y dy + \int_{-h_2}^0 \sigma_2 b y dy = 0.$$

Substituting for  $\sigma_1$  and  $\sigma_2$  and integrating, we obtain

$$\begin{aligned} \epsilon_0 (E_1 h_1 + E_2 h_2) - (\alpha_1 E_1 h_1 + \alpha_2 E_2 h_2) t + \\ + \frac{1}{2} \left( \frac{1}{\rho} - \frac{1}{\rho_0} \right) (E_1 h_1^3 - E_2 h_2^3) = 0, \\ \frac{1}{2} \epsilon_0 (E_1 h_1^3 - E_2 h_2^3) - \frac{1}{2} (E_1 \alpha_1 h_1^3 - E_2 \alpha_2 h_2^3) t + \\ + \frac{1}{3} \left( \frac{1}{\rho} - \frac{1}{\rho_0} \right) (E_1 h_1^3 + E_2 h_2^3) = 0. \end{aligned}$$

Eliminating  $\epsilon_0$ , we find the change in curvature

$$\frac{1}{\rho} - \frac{1}{\rho_0} = \frac{6t(\alpha_1 - \alpha_2)}{\frac{(E_1 h_1^3 - E_2 h_2^3)^2}{E_1 E_2 h_1 h_2 (h_1 + h_2)} + 4(h_1 + h_2)}.$$

The change in curvature is proportional to the change in temperature and to the difference in the coefficients of thermal expansion. As is seen from the above expression, the maximum change in curvature occurs when the thicknesses of the component plates are selected so that

$$E_1 h_1^3 = E_2 h_2^3.$$

Then

$$\frac{1}{\rho} - \frac{1}{\rho_0} = \frac{3}{2} t \frac{\alpha_1 - \alpha_2}{h_1 + h_2}.$$

80. By hypothesis, the section of the ring may be considered non-deformable. As is known, the displacement of every figure in a plane may be represented as two linear displacements of any one point of the figure and a subsequent rotation of the entire figure about this point as a whole.

Take some point at the section of the ring, say  $O$  (Fig. 296), situated at the inner radius  $a$  at the junction of the rings. The total displacement of the section of the ring can now be represented as successive displacements of the point  $O$  along the axis of symmetry, perpendicular to it, and a rotation about the point  $O$  through an angle  $\varphi$ .

So far as the first displacement is concerned, it corresponds to the displacement of the ring as a rigid whole and produces no strains in it. We shall therefore not consider this

displacement. The second component of linear displacement is denoted by  $\Delta$ . The radial displacement of the point  $A$  is thus made up of the displacement  $\Delta$  and the displacement due

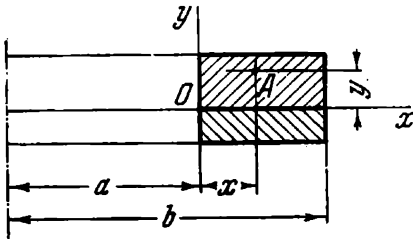


Fig. 296

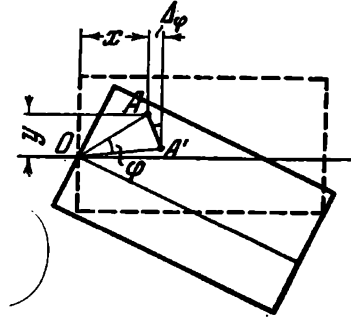


Fig. 297

to the rotation of the section about the point  $O$ . This latter component  $\Delta_\varphi$  is, as seen from Fig. 297,

$$\Delta_\varphi = y\varphi$$

(the angle  $\varphi$  is assumed to be small).

The radial displacement of the point  $A$  is

$$\Delta + y\varphi$$

and the circumferential extension is

$$\varepsilon = \frac{\Delta + y\varphi}{a + x}.$$

The circumferential stress for the first ring is

$$\sigma_1 = E_1 \left( \frac{\Delta + y\varphi}{a + x} - \alpha_1 t \right) \\ (0 \leq y \leq h_1)$$

and for the second ring

$$\sigma_2 = E_2 \left( \frac{\Delta + y\varphi}{a + x} - \alpha_2 t \right) \\ (-h_2 \leq y \leq 0).$$

If the ring is cut by an axial diametral plane and the equilibrium of one half of the ring is considered, it can easily be verified that the bending moment  $M$  and the normal force  $N$  are zero at the sections of this ring (Fig. 298).

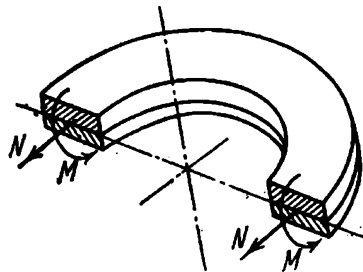


Fig. 298

Consequently,

$$N = \int_0^{b-a} \int_0^{h_1} \sigma_1 dx dy + \int_0^{b-a} \int_{-h_2}^0 \sigma_2 dx dy = 0,$$

$$M = \int_0^{b-a} \int_0^{h_1} \sigma_1 y dx dy + \int_0^{b-a} \int_{-h_2}^0 \sigma_2 y dx dy = 0.$$

Substituting for  $\sigma_1$  and  $\sigma_2$ , we find

$$E_1 \left[ \left( h_1 \Delta + \frac{h_1^3 \varphi}{2} \right) \ln \frac{b}{a} - \alpha_1 t (b-a) h_1 \right] +$$

$$+ E_2 \left[ \left( h_2 \Delta - \frac{h_2^3 \varphi}{2} \right) \ln \frac{b}{a} - \alpha_2 t (b-a) h_2 \right] = 0,$$

$$E_1 \left[ \left( \frac{h_1^3}{2} \Delta + \frac{h_1^3}{3} \varphi \right) \ln \frac{b}{a} - \alpha_1 t (b-a) \frac{h_1^2}{2} \right] +$$

$$+ E_2 \left[ \left( -\Delta \frac{h_2^3}{2} + \frac{h_2^3}{3} \varphi \right) \ln \frac{b}{a} + \alpha_2 t (b-a) \frac{h_2^2}{2} \right] = 0.$$

Eliminating  $\Delta$  from this, we have

$$\varphi = \frac{b-a}{\ln \frac{b}{a}} \frac{6t(\alpha_1 - \alpha_2)}{\frac{(E_1 h_1^3 - E_2 h_2^3)^2}{E_1 E_2 h_1 h_2 (h_1 + h_2)} + 4(h_1 + h_2)}.$$

As in the previously considered case,  $\varphi$  is maximum if

$$E_1 h_1^3 = E_2 h_2^3.$$

The required angle is then

$$\varphi = \frac{b-a}{\ln \frac{b}{a}} \frac{3t(\alpha_1 - \alpha_2)}{2(h_1 + h_2)}.$$

81. The temperature-control sensor will not function since the bimetallic plate clamped at the ends does not change its curvature under uniform heating.

Indeed, if the plate were simply supported, it would bend into a circular arc under uniform heating. In the present case the plate is acted on by the moments exerted by the fixed supports. Under their action the plate also bends into a circular arc but in the opposite sense (Fig. 299).

By imposing the requirement that the angles of rotation  $\varphi_1$  and  $\varphi_2$  at the ends of the plate be equal, we must neces-

sarily require the equality of the curvatures of both circles, and this means that the total angles of rotation and displacements at all points of the plate (if the condition  $\varphi_1 = \varphi_2$  is fulfilled) are zero. Thus, the bimetallic plate clamped at its ends will not bend under uniform heating.

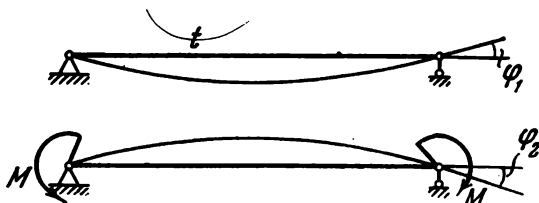


Fig. 299

Consequently, in order that the system in question (Fig. 76) serve its purpose, it is sufficient, for example, to replace the clamped plate by a simply supported one.

82. Imagine the frame cut and apply internal force factors  $M_0$ ,  $N$ , and  $Q$  at the section made (Fig. 300).

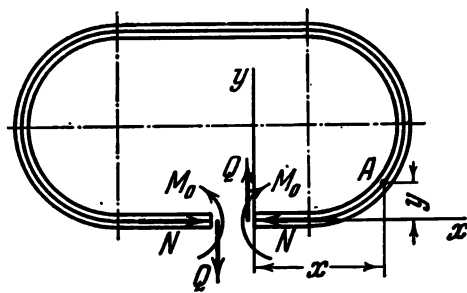


Fig. 300

The bending moment at a section  $A$  produced by these forces is

$$M_b = M_0 + Qx + Ny.$$

The cut frame, on being heated, changes its curvature. This change in curvature remains constant for all points of the frame contour since the temperature and the shape of the cross section remain constant. But if this is so, the effect of temperature can be replaced by the action of some equivalent moment  $M_t$  applied at the section made.

We now require that the relative linear and angular displacements of the sections due to the moment  $M_0$  and the forces  $Q$  and  $N$  be equal to the same relative displacements due to the action of equivalent temperature moments  $M_t$ .

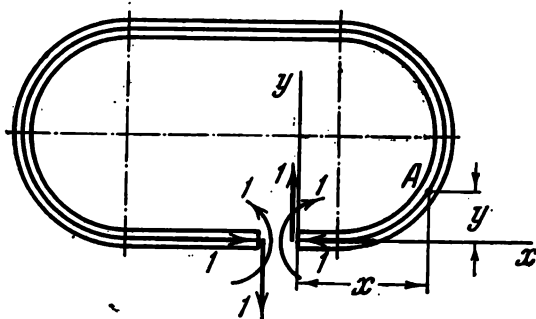


Fig. 301

The bending moments due to unit force factors (Fig. 301) corresponding to the forces  $M_0$ ,  $Q$ , and  $N$  are as follows:

1,  $x$ ,  $y$ .

We then obtain

$$\begin{aligned} \int_s (M_0 + Qx + Ny) \times 1 \times ds &= \int_s M_t \times 1 \times ds, \\ \int_s (M_0 + Qx + Ny) x ds &= \int_s M_t x ds, \\ \int_s (M_0 + Qx + Ny) y ds &= \int_s M_t y ds \end{aligned}$$

or

$$\begin{aligned} (M_0 - M_t) \int_s ds + Q \int_s x ds + N \int_s y ds &= 0, \\ (M_0 - M_t) \int_s x ds + Q \int_s x^2 ds + N \int_s yx ds &= 0, \\ (M_0 - M_t) \int_s y ds + Q \int_s xy ds + N \int_s y^2 ds &= 0, \end{aligned}$$

whence we find the forces:  $Q = N = 0$ ,  $M_0 = M_t$ .

Consequently, the moment  $M_0$  is equal to the equivalent temperature moment  $M_t$ . Hence, the change in curvature produced by the moments  $M_0$  is equal to the temperature change in curvature. Thus, the curvature of the uniformly heated closed bimetallic frame remains unchanged.

83. So long as the beams act elastically, we have

$$\frac{1}{\rho} = \frac{12M}{Ea^4} \quad \text{or} \quad \frac{a}{\rho} = 12 \frac{M}{Ea^3}$$

and a linear relation exists between curvature and moment

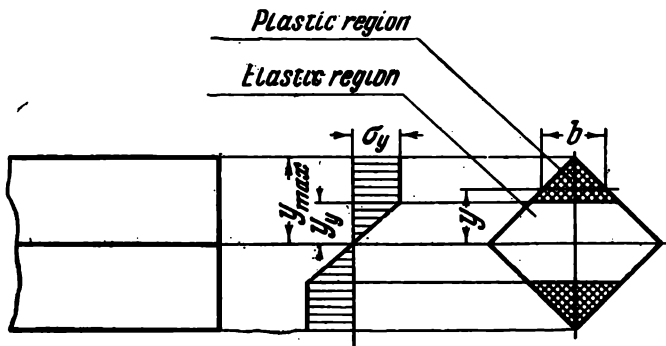


Fig. 302

which is maintained until the maximum stress reaches the yield point  $\sigma_y$ . This occurs when

$$\sigma_y = \frac{12M}{a^4} y_{\max} \quad \text{or} \quad \frac{M}{Ea^3} = \frac{1}{12} \frac{\sigma_y}{E} \frac{a}{y_{\max}}$$

For each of the sections we obtain

$$(I) \quad \frac{M}{Ea^3} = 3.33 \times 10^{-4},$$

$$(II) \quad \frac{M}{Ea^3} = 2.36 \times 10^{-4},$$

$$(III) \quad \frac{M}{Ea^3} = 2.92 \times 10^{-4}.$$

When the bending moment is larger than the above value, there are two regions to be considered at the cross section of the rod, namely the elastic region ( $0 \leq y \leq y_y$ ) and the plastic region ( $y_y \leq y \leq y_{\max}$ ) (Fig. 302).

The bending moment at the section is determined by the following expression:

$$M = 2 \int_0^{y_y} \sigma_y b dy + 2 \int_{y_y}^{y_{\max}} \sigma_y b dy.$$

The extension is  $\varepsilon = y/\rho$ . In the elastic region we have

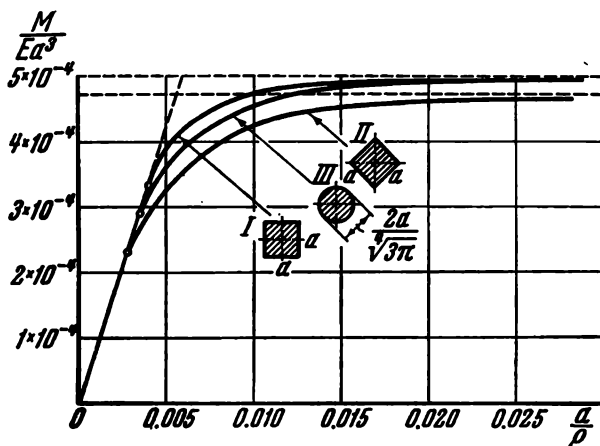


Fig. 303

$\sigma = Ey/\rho$ , and at the boundary between the regions  $y_y = \sigma_y \rho/E$ . Thus,

$$\frac{M}{Ea^3} = \frac{a}{\rho} \frac{2}{a^4} \int_0^{\sigma_y \rho/E} b y^2 dy + \frac{2}{a^3} \frac{\sigma_y}{E} \int_{\sigma_y \rho/E}^{y_{\max}} b y dy.$$

For each of the sections we obtain, after integration,

$$(I) \quad \frac{M}{Ea^3} = \frac{1}{4} \frac{\sigma_y}{E} - \frac{1}{3} \frac{\sigma_y^3}{E^3} \frac{\rho^2}{a^2},$$

$$(II) \quad \frac{M}{Ea^3} = \frac{\sqrt{2}}{6} \frac{\sigma_y}{E} - \frac{\sqrt{2}}{3} \frac{\sigma_y^3}{E^3} \frac{\rho^2}{a^2} + \frac{1}{3} \frac{\sigma_y^4}{E^4} \frac{\rho^3}{a^3},$$

$$(III) \quad \frac{M}{Ea^3} = \frac{1}{6\pi} \frac{a}{\rho} \arcsin \alpha + \frac{1}{6} \frac{\sigma_y}{E} (3\pi)^{-\frac{3}{4}} (5 - 2\alpha^2) \sqrt{1 - \alpha^2} \\ \left( \alpha = \frac{\sigma_y}{E} \frac{\rho}{a} \sqrt[4]{3\pi} \right).$$

The  $M/Ea^3 = f(a/\rho)$  curves are shown in Fig. 303. In each case, as  $a/\rho \rightarrow \infty$  the moment  $M$  has a limiting value (the

so-called plastic hinge moment). It determines the limiting load for the beam. For each of the sections we obtain, with  $\sigma_y/E = 0.002$ ,

$$(I) \frac{M_{lim}}{Ea^3} = 0.0005, \quad (II) \frac{M_{lim}}{Ea^3} = 0.000471,$$

$$(III) \frac{M_{lim}}{Ea^3} = 0.000497.$$

If the sections were not symmetrical about the horizontal axis, the solution would be much more complicated. In this case it would be necessary first to determine the position of the neutral axis from the condition

$$\int_A \sigma dA = 0.$$

84. The flexural rigidity depends on the magnitude of the initially applied moment  $M_x$  or, which is the same thing, on how deep the plastic region extends at the section, i.e., on the value of  $y_y$ .

After the moment  $M_y$  is applied, the rod changes its curvature in both planes, and an additional elongation occurring at an arbitrarily taken point with co-ordinates  $x$  and  $y$  is given by

$$\Delta \varepsilon = \kappa_x y + \kappa_y x,$$

where  $\kappa_x$  and  $\kappa_y$  are the changes in curvature of the rod, respectively, in the planes  $yz$  and  $xz$ .

We transform to non-dimensional co-ordinates  $\eta$  and  $\zeta$

$$y = \frac{h}{2} \eta, \quad x = \frac{b}{2} \zeta.$$

Then  $y_y = \frac{h}{2} \eta_y$ .

The rectangle  $b \times h$  is changed into a square  $2 \times 2$  (Fig. 304)

$$\Delta \varepsilon = \kappa_y \frac{b}{2} (k\eta + \zeta),$$

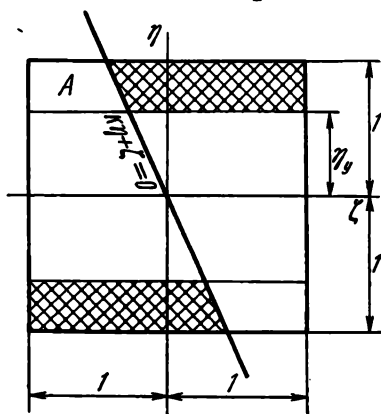


Fig. 304

where  $k = \frac{\kappa_x}{\kappa_y} \frac{h}{b}$  determines the ratio of the changes in curvature in the two planes. It must be found from the condition that the moment  $M_x$  is invariant. The straight line  $\Delta\varepsilon = 0$ , or  $k\eta + \zeta = 0$  (Fig. 304), separates the regions of additional loading and unloading. In the cross-hatched regions the stress remains equal to  $\pm\sigma_y$  and no additional stresses occur. In the unshaded region the additional stress is

$$\Delta\sigma = E \Delta\varepsilon = E\kappa_y \frac{b}{2} (k\eta + \zeta). \quad (1)$$

The additional moment about the  $\zeta$  axis is determined by integrating the elementary moments within the trapezoid  $A$  and the upper rectangle  $2 \times \eta_y$

$$\begin{aligned} \Delta M_x = \int_{\eta_y}^1 \int_{-1}^{-k\eta} \Delta\sigma \frac{h}{2} \eta \frac{b}{2} d\zeta \frac{h}{2} d\eta + \\ + \int_0^{\eta_y} \int_{-1}^{-1} \Delta\sigma \frac{h}{2} \eta \frac{b}{2} d\zeta \frac{h}{2} d\eta. \end{aligned} \quad (2)$$

According to the condition of the problem, this moment is zero. Upon integration we obtain

$$3k^2(1 - \eta_y^4) - 8k(1 - \eta_y^3) + 6(1 - \eta_y^2) = 0. \quad (3)$$

From this  $k$  is determined as a function of  $\eta_y$ . Relation (3) is true so long as the region  $A$  is a trapezoid. But when  $k \geq 1$ , it is transformed into a triangle, and the straight line  $k\eta + \zeta = 0$  intersects not the upper but the left side of the square. In this case, the upper limit of the first of the integrals involved in expression (2) is changed, and instead of  $\int_{\eta_y}^1$  one must write  $\int_{\eta_y}^{1/k}$ . Expression (3) then becomes

$$3k^2 \left( \frac{1}{k^4} - \eta_y^4 \right) - 8k \left( \frac{1}{k^3} + \eta_y^3 \right) + 6 \left( \frac{1}{k^2} - \eta_y^2 \right) = 0,$$

whence  $1 - 3k^4\eta_y^4 - 8k^3\eta_y^3 - 6k^2\eta_y^2 = 0$ . This equation is satisfied for  $k\eta_y = 1/3$ . Consequently,

$$k = \frac{1}{3\eta_y}. \quad (4)$$

Hence, when  $\eta_v \leq 1/3$  the quantity  $k$  is determined from expression (4), and when  $\eta_v \geq 1/3$  from expression (3).

We now determine the moment  $M_v$  for  $k \leq 1$

$$M_v = 2 \int_{\eta_v}^1 \int_{-1}^{-k\eta} \Delta\sigma \frac{b}{2} \zeta \frac{b}{2} d\zeta \frac{h}{2} d\eta + 2 \int_0^{\eta_v+1} \int_{-1}^{\eta_v+1} \Delta\sigma \frac{b}{2} \zeta \frac{b}{2} d\zeta \frac{h}{2} d\eta. \quad (5)$$

On integrating we obtain

$$M_v = \kappa_v EI_v \left[ \frac{k^3}{16} (1 - \eta_v^4) - \frac{3}{8} k (1 - \eta_v^2) + \frac{1}{2} (1 + \eta_v) \right], \quad (6)$$

where  $I_v = b^3 h / 12$ .

The bracketed expression is always less than unity and may be termed the rigidity reduction factor. Denote it by  $\beta$ . For an elastically bent bar  $\eta_v = 1$ ,  $k = 0$ , and  $\beta = 1$ . As the initial plastic strains increase, the factor  $\beta$  decreases.

When  $k \geq 1$ , the upper limit of the first integral in expression (5) is again replaced by  $1/k$ , giving

$$\beta = \frac{k^3}{16} \left( \frac{1}{k^4} - \eta_v^4 \right) - \frac{3}{8} k \left( \frac{1}{k^2} - \eta_v^2 \right) + \frac{1}{2} \left( \frac{1}{k} + \eta_v \right).$$

On substituting  $k = 1/3\eta_v$  from (4), we obtain

$$\beta = \frac{32}{27} \eta_v;$$

this expression is valid for  $\eta_v \leq 1/3$ .

When  $1 \geq \eta_v \geq 1/3$ , it is necessary first to determine the quantity  $k$  from expression (3) and then make use of expression (6). Figure 305 shows the graph of the variation of  $\beta$  as a function of  $\eta_v$ .

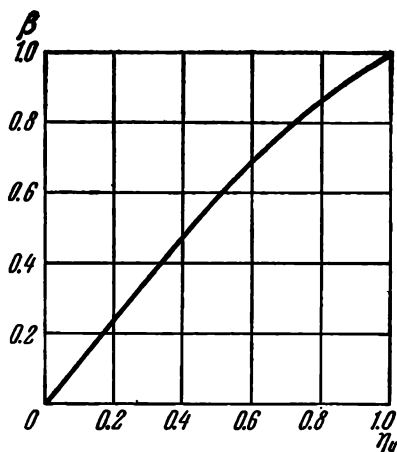


Fig. 305

85. So long as the moment  $M$  is small, the contact surfaces of the disks do not open up. In this case the curvature of the rod is determined by the usual formula

$$\frac{1}{\rho} = \frac{M}{EI} = \frac{64M}{E\pi D^4}.$$

The maximum compressive stress in the disks is

$$\sigma = \frac{4P}{\pi(D^2 - d^2)} + \frac{32MD}{\pi D^4}.$$

The maximum tensile stress in the bolt is

$$\sigma = \frac{4P}{\pi d^2} + \frac{32MD}{\pi D^4}.$$

The contact surfaces in the lower part of the rod begin to open when  $M$  reaches the value  $M_1$ . Then

$$\frac{4P}{\pi(D^2 - d^2)} = \frac{32M_1 D}{\pi D^4}, \quad M_1 = P \frac{D^3}{8(D^2 - d^2)}.$$

When  $M > M_1$ , the contact planes are partially opened, and the problem requires a new solution.

Denote by  $\rho$  the radius of curvature of the bolt axis (Fig. 306). The extension of any layer distant  $y$  from the axis is made up of three parts.

The *first* part represents the extension caused by the pre-tension of the system. For the bolt, this is

$$\epsilon'_b = \frac{4P}{E\pi d^2}. \quad (1)$$

For the disk

$$\epsilon'_d = -\frac{4P}{E\pi(D^2 - d^2)}. \quad (2)$$

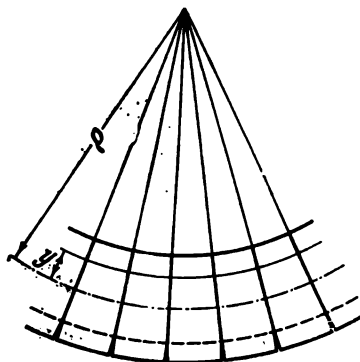


Fig. 306

The *second* part,  $\epsilon_0$ , represents an extension of the axis, as yet unknown, resulting from the bending of the rod (this quantity is the same for the bolt and disks).

The *third* part,  $y/\rho$  (the same for the bolt and disks), represents an extension which the fibre would undergo as

a result of the bending of the rod if its axis were not elongated. We thus obtain

$$\varepsilon_b = \varepsilon'_b + \varepsilon_0 - \frac{y}{\rho}, \quad \varepsilon_d = \varepsilon'_d + \varepsilon_0 - \frac{y}{\rho}.$$

The corresponding stresses are

$$\sigma_b = E \left( \varepsilon'_b + \varepsilon_0 - \frac{y}{\rho} \right), \quad \sigma_d = E \left( \varepsilon'_d + \varepsilon_0 - \frac{y}{\rho} \right).$$

The quantity  $\sigma_d$  can only be negative (compression), and hence in the expression for  $\sigma_d$

$$y \geq y_1 = \rho (\varepsilon'_d + \varepsilon_0). \quad (3)$$

We now write the equations of equilibrium

$$\begin{aligned} \int_{y_1}^{D/2} \sigma_d dA_d + \int_{-d/2}^{+d/2} \sigma_b dA_b &= 0, \\ \int_{y_1}^{D/2} \sigma_d y dA_d + \int_{-d/2}^{+d/2} \sigma_b y dA_b &= -M. \end{aligned}$$

After substituting for  $\sigma_b$  and  $\sigma_d$  and integrating, we obtain

$$(\varepsilon'_d + \varepsilon_0) A_d^* - \frac{1}{\rho} S_d^* + (\varepsilon'_b + \varepsilon_0) A_b = 0, \quad (4)$$

$$-E (\varepsilon'_d + \varepsilon_0) S_d^* + \frac{E}{\rho} I_d^* + \frac{E}{\rho} I_b = M, \quad (5)$$

where  $A_b$  and  $I_b$  are the area and the moment of inertia of the section of the bolt with respect to its diameter,  $A_d^*$ ,  $S_d^*$ , and  $I_d^*$  are the area, the static moment and the moment of inertia of the effective section of the disk, i.e.,

$$A_d^* = \int_{y_1}^{D/2} dA_d, \quad S_d^* = \int_{y_1}^{D/2} y dA_d, \quad I_d^* = \int_{y_1}^{D/2} y^2 dA_d.$$

Taking into account expressions (1), (2), and (3), we reduce Eq. (4) to

$$\varepsilon_0 = \varepsilon'_d \frac{S_d^* + y_1 (A_d - A_d^*)}{y_1 (A_d^* + A_b) - S_d^*}. \quad (6)$$

From Eq. (5) we obtain

$$\frac{M}{E} = \frac{\varepsilon'_d + \varepsilon_0}{y_1} (I_b + I_d^* - y_1 S_d^*).$$

Substituting for  $\varepsilon_0$  from (6), we find

$$\frac{M}{E} = \varepsilon'_d (I_b + I_d^* - y_1 S_d^*) \frac{A_d + A_b}{y_1 (A_d^* + A_b) - S_d^*}. \quad (7)$$

Substituting for  $\varepsilon_0$  from (6) in expression (3), we have

$$\frac{1}{\rho} = \varepsilon'_d \frac{A_d + A_b}{y_1 (A_d^* + A_b) - S_d^*}. \quad (8)$$

Since  $\varepsilon'_d$  is given and  $A_d^*$ ,  $S_d^*$ ,  $I_d^*$  depend only on  $y_1$ , expressions (7) and (8) may be regarded as a parametric relation between the curvature  $1/\rho$  and the moment  $M$  with the parameter  $y_1$ . The maximum compressive stress in the disks and the maximum tensile stress in the bolt are easily expressed in terms of the same parameter  $y_1$

$$\left. \begin{aligned} \sigma_{c,d} &= E\varepsilon'_d \frac{(A_d + A_b) \left( y_1 - \frac{D}{2} \right)}{y_1 (A_d^* + A_b) - S_d^*}, \\ \sigma_{t,b} &= E\varepsilon'_d \frac{(A_d + A_b) \left( \frac{S_d^* - y_1 A_d^*}{A_b} + \frac{d}{2} \right)}{y_1 (A_d^* + A_b) - S_d^*}. \end{aligned} \right\} \quad (9)$$

The problem can thus be considered solved.

The procedure for computation must be as follows. By assigning several values of  $y_1$ , we determine the values of the moment  $M$  by formula (7). When the calculated  $M$  coincides with the given one, from formulas (8) and (9) we find  $\frac{1}{\rho}$ ,  $\sigma_d$ , and  $\sigma_b$  for the corresponding  $y_1$ .

It remains to write out the expressions for  $A_d^*$ ,  $S_d^*$ , and  $I_d^*$ . These quantities are determined by integrating the expressions for

$$dA, \quad ydA, \quad y^2dA$$

over the effective area of the disks (Fig. 307).

In Case I  $\left(-\frac{d}{2} \geq y_1 \geq -\frac{D}{2}\right)$  we have

$$A_d^* = \frac{D^2}{4} \left[ \frac{\pi}{2} - \arcsin \frac{2y_1}{D} - \frac{2y_1}{D} \sqrt{1 - 4 \frac{y_1^2}{D^2}} \right] - \frac{\pi d^2}{4},$$

$$S_d^* = \frac{D^3}{12} \left( 1 - 4 \frac{y_1^2}{D^2} \right)^{3/2},$$

$$I_d^* = \frac{D^4}{64} \left[ \frac{\pi}{2} - \arcsin \frac{2y_1}{D} + \frac{2y_1}{D} \left( 1 - \frac{y_1^2}{D^2} \right) \sqrt{1 - 4 \frac{y_1^2}{D^2}} \right] - \frac{\pi d^4}{64}.$$

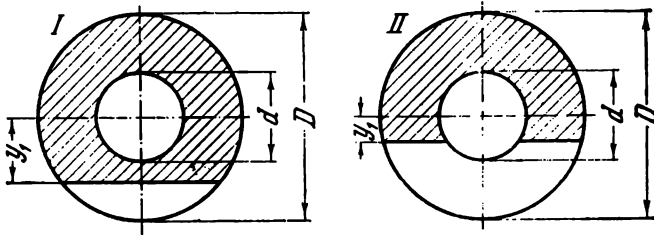


Fig. 307

In Case II  $\left(+\frac{d}{2} \geq y_1 \geq -\frac{d}{2}\right)$  we obtain

$$A_d^* = \frac{D^2}{4} \left[ \frac{\pi}{2} - \arcsin \frac{2y_1}{D} - \frac{2y_1}{D} \sqrt{1 - 4 \frac{y_1^2}{D^2}} \right] - \frac{d^2}{4} \left[ \frac{\pi}{2} - \arcsin \frac{2y_1}{d} - \frac{2y_1}{d} \sqrt{1 - 4 \frac{y_1^2}{d^2}} \right],$$

$$S_d^* = \frac{D^3}{12} \left( 1 - 4 \frac{y_1^2}{D^2} \right)^{3/2} - \frac{d^3}{12} \left( 1 - 4 \frac{y_1^2}{d^2} \right)^{3/2},$$

$$I_d^* = \frac{D^4}{64} \left[ \frac{\pi}{2} - \arcsin \frac{2y_1}{D} + \frac{2y_1}{D} \left( 1 - 8 \frac{y_1^2}{D^2} \right) \sqrt{1 - 4 \frac{y_1^2}{D^2}} \right] - \frac{d^4}{64} \left[ \frac{\pi}{2} - \arcsin \frac{2y_1}{d} + \frac{2y_1}{d} \left( 1 - 8 \frac{y_1^2}{d^2} \right) \sqrt{1 - 4 \frac{y_1^2}{d^2}} \right].$$

These quantities can also be determined numerically by summing the elementary areas of the section multiplied by the first and second powers of  $y$ , i.e.,  $A_d^* = \sum \Delta A_n$ ,  $S_d^* = \sum y_n \Delta A_n$ ,  $I_d^* = \sum y_n^2 \Delta A_n$  (Fig. 308).

In expressions (7), (8), and (9) the pre-tension of the system is determined by the factor  $\varepsilon'_d$  from (2). If  $P = 0$ , then  $\varepsilon'_d = 0$  and we obviously have [see, for example, ex-

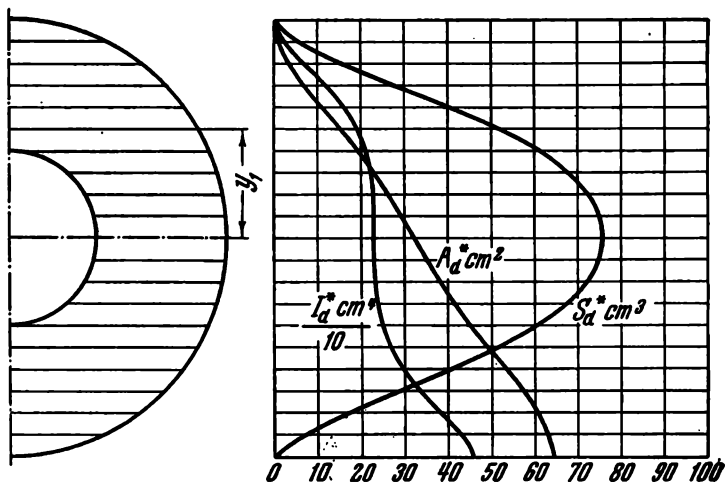


Fig. 308

pression (7)]  $y_1 (A_d^* + A_b) - S_d^* = 0$  (since  $M$  is not, in general, zero).

From this the constant  $y_1$  can be found. Thus, in the absence of pre-tension the position of the boundary of disk opening ( $y_1$ ) is independent of the bending moment and is determined by the foregoing relation. When  $\varepsilon'_d < 0$ , the quantity  $y_1 (A_d^* + A_b) - S_d^*$  must remain negative. The value of  $y_1$  is, therefore, always less than it would be in the absence of pre-tension.

### III. Combined Stresses and Strength Theories

86. (a) In the case represented in Fig. 81a the diameter increases by  $\frac{\mu}{E} E p d_1$ , the volume decreases by  $p \frac{1-2\mu}{E} V$ .

(b) In the case represented in Fig. 81b the diameter decreases by  $\frac{1-\mu}{E} p d_1$ , the volume decreases by  $2p \frac{1-2\mu}{E} V$ .

(c) In the case represented in Fig. 81c the diameter decreases by  $\frac{1-2\mu}{E} p d_1$ , the volume decreases by  $3p \frac{1-2\mu}{E} V$ , where  $V$  is the initial internal volume.

87. Consider a wooden block (Fig. 309). Let the  $z$  axis be chosen parallel to the grain, the  $x$  axis along the normal to the annual rings, and the  $y$  axis along the tangent to them. The co-ordinate planes coincide with the planes of elastic symmetry. The extension in the  $x$  direction depends linearly on the stresses  $\sigma_x$ ,  $\sigma_y$ , and  $\sigma_z$ , i.e.,

$$\varepsilon_x = C_{11}\sigma_x + C_{12}\sigma_y + C_{13}\sigma_z,$$

where  $C_{11}$ ,  $C_{12}$ ,  $C_{13}$  are the elastic constants. In a similar way we can write

$$\varepsilon_y = C_{21}\sigma_x + C_{22}\sigma_y + C_{23}\sigma_z,$$

$$\varepsilon_z = C_{31}\sigma_x + C_{32}\sigma_y + C_{33}\sigma_z.$$

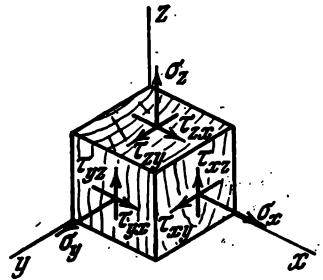


Fig. 309

The angles of shear are proportional to the corresponding shearing stresses

$$\gamma_{yz} = C_{44}\tau_{yz}, \quad \gamma_{zx} = C_{55}\tau_{zx}, \quad \gamma_{xy} = C_{66}\tau_{xy}.$$

It can easily be established that according to the reciprocity principle for displacements  $C_{12} = C_{21}$ ,  $C_{13} = C_{31}$ ,  $C_{23} = C_{32}$ . We thus obtain nine elastic constants:  $C_{11}$ ,  $C_{12}$ ,  $C_{13}$ ,  $C_{22}$ ,  $C_{23}$ ,  $C_{33}$ ,  $C_{44}$ ,  $C_{55}$ , and  $C_{66}$ .

It may be shown that these elastic constants are independent. The anisotropy considered is termed rhombic.

88. Each plane passing through the  $x$ ,  $y$  or  $z$  axis and equally inclined to the other two axes is principal.

Let us isolate from the element (Fig. 82) a new elementary parallelepiped as shown in Fig. 310. The  $x'$  axis is princi-

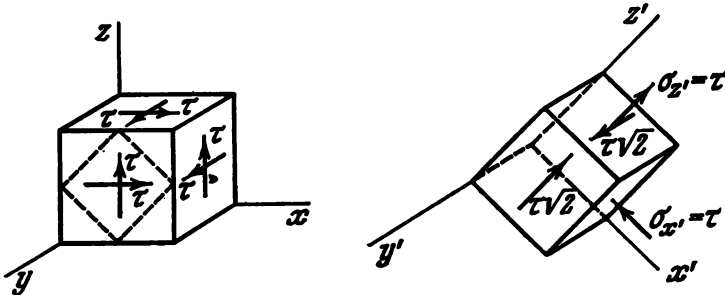


Fig. 310

pal ( $\sigma_{x'} = -\tau$ ). The remaining principal stresses are found by the formula

$$\sigma_{pr} = \frac{\sigma_{z'}}{2} \pm \sqrt{\frac{\sigma_{z'}^2}{4} + \tau_{yz}^2}$$

or

$$\sigma_{pr} = \frac{\tau}{2} \pm \sqrt{\frac{\tau^2}{4} + (\tau\sqrt{2})^2}, \quad \sigma' = -\tau, \quad \sigma'' = +2\tau.$$

We thus obtain

$$\sigma_1 = 2\tau, \quad \sigma_2 = -\tau, \quad \sigma_3 = -\tau.$$

This problem can also be solved by resorting to the general method of determining the principal stresses, known from the theory of combined stresses. We write out the following determinant:

$$\begin{vmatrix} \sigma_x - \sigma & \tau_{xy} & \tau_{xz} \\ \tau_{yx} & \sigma_y - \sigma & \tau_{yz} \\ \tau_{zx} & \tau_{zy} & \sigma_z - \sigma \end{vmatrix} = 0. \quad (A)$$

In the present case

$$\begin{aligned} \sigma_x &= \sigma_y = \sigma_z = 0, \\ \tau_{xy} &= \tau_{xz} = \tau_{yz} = \tau. \end{aligned}$$

Hence,

$$\begin{vmatrix} -\sigma & \tau & \tau \\ \tau & -\sigma & \tau \\ \tau & \tau & -\sigma \end{vmatrix} = 0$$

or

$$\sigma^3 - 3\tau^2\sigma - 2\tau^3 = 0$$

from which we find three roots of the equation

$$\sigma_1 = 2\tau, \quad \sigma_2 = -\tau, \quad \sigma_3 = -\tau.$$

89. It must be shown that in the first case at least one and in the second case two principal stresses are zero.

For this purpose, the equation (A) (p. 221) is rewritten as

$$\sigma^3 - I_1\sigma^2 + I_2\sigma - I_3 = 0,$$

where

$$\begin{aligned} I_1 &= \sigma_x + \sigma_y + \sigma_z, \\ I_2 &= \sigma_x\sigma_y + \sigma_y\sigma_z + \sigma_x\sigma_z - \tau_{xy}^2 - \tau_{xz}^2 - \tau_{yz}^2, \\ I_3 &= \begin{vmatrix} \sigma_x & \tau_{xy} & \tau_{xz} \\ \tau_{yx} & \sigma_y & \tau_{yz} \\ \tau_{zx} & \tau_{zy} & \sigma_z \end{vmatrix} \end{aligned}$$

are the invariants of the state of stress.

In the first case, according to the properties of the determinant

$$I_3 = \begin{vmatrix} \sigma_x & \tau_{xy} & \tau_{xz} \\ k\sigma_x & k\tau_{xy} & k\tau_{xz} \\ \tau_{zx} & \tau_{zy} & \sigma_z \end{vmatrix} = 0$$

and one of the roots of the cubic equation vanishes.

In the second case  $I_3 = 0$  and  $I_2 = 0$ , and hence two roots of the cubic equation vanish.

From the proof given above it may, for example, be said at once that the state of stress

$$\begin{pmatrix} 800 & 200 & 400 \\ 200 & 50 & 100 \\ 400 & 100 & 200 \end{pmatrix}$$

is uniaxial.

90. The states of stress are equally dangerous. Indeed, the work done by the normal forces in the first case is equal to the work done by the same forces in the second case. This is also true for the tangential forces. Consequently, the internal energy in the two cases is also the same. This is the condition of equally dangerous (equivalent) states of stress for the energy theory irrespective of which strength theory is concerned (the distortion energy theory or the total energy theory).

91. Consider the state of stress in an element (Fig. 311) isolated from the cylinder a distance  $x$  below the liquid level.

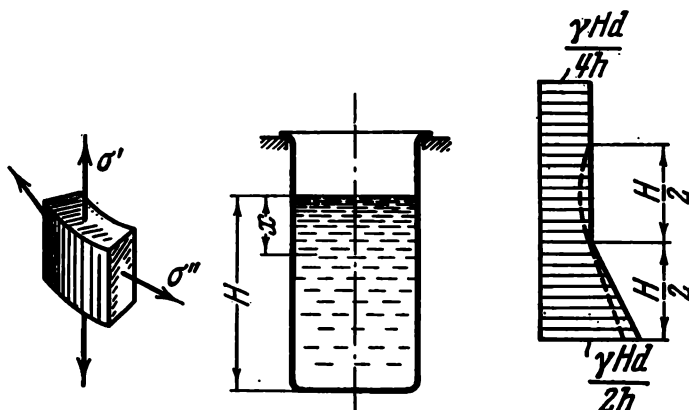


Fig. 311

The stress  $\sigma'$  is constant along the length of the generator and is equal to the weight of liquid  $\gamma \frac{\pi d^2}{4} H$  divided by the cross-sectional area of the cylinder

$$\sigma' = \gamma = \frac{Hd}{4h}.$$

Above the liquid level  $\sigma'' = 0$ , and below

$$\sigma'' = \frac{pd}{2h} = \frac{\gamma xd}{2h}.$$

The equivalent stress  $\sigma_{eq} = \sigma_1 - \sigma_3$ . Consequently, when  $\sigma' \geq \sigma''$ , we have  $\sigma_{eq} = \sigma - 0 = \sigma'$

When  $\sigma' \leq \sigma''$ , we obtain

$$\sigma_{eq} = \sigma'' - 0 = \sigma''.$$

Thus, when  $x \leq \frac{H}{2}$ ,

$$\sigma_{eq} = \sigma' = \frac{\gamma H d}{4h};$$

when  $x \geq \frac{H}{2}$ ,

$$\sigma_{eq} = \sigma'' = \frac{\gamma x d}{2h}.$$

The  $\sigma_{eq}$  diagram is shown in Fig. 311. This diagram has a bend at  $x = H/2$  which is a consequence of the fact that at this point the planes corresponding to the stresses  $\sigma_1$  and  $\sigma_2$  are interchanged. The dashed curve in Fig. 311 represents the  $\sigma_{eq}$  diagram obtained by the energy theory of strength.

92. Consider the state of stress at points of the cylinder at the top (A) and bottom (B) generators (Fig. 312), where

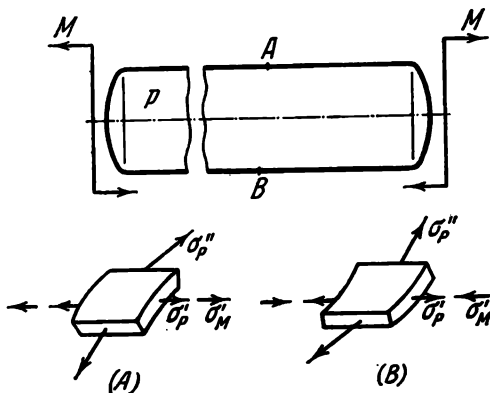


Fig. 312

$\sigma_p'$  and  $\sigma_p''$  are the stresses produced by the pressure  $p$ ,  $\sigma_M'$  is the bending stress.

It can easily be established that

$$\sigma_p' = \frac{pd}{4h}, \quad \sigma_p'' = \frac{pd}{2h}, \quad \sigma_M' = \frac{4M}{\pi d^2 h} \quad (1)$$

and, since  $2\sigma_p' = \sigma_p''$ , when

$$|\sigma_M'| \leq \sigma_p'$$

we have the following condition both at the point  $A$  and at the point  $B$ :

$$\sigma_{eq} = \sigma_1 - \sigma_3 = \sigma_p'' - 0 = \sigma_p''.$$

If, however,  $|\sigma_M'| > \sigma_p'$ , then at the point  $A$

$$\sigma_{eq} = \sigma_1 - \sigma_3 = (\sigma_p' + \sigma_M') - 0 = \sigma_p' + \sigma_M'$$

and at the point  $B$

$$\sigma_{eq} = \sigma_1 - \sigma_3 = \sigma_p'' + (\sigma_M' - \sigma_p') = \sigma_p' + \sigma_M'.$$

Consequently, in all cases the points  $A$  and  $B$  are equally dangerous. The graph of  $\sigma_{eq}$  plotted against  $\sigma_M'$  is shown in Fig. 313.

The quantities  $\sigma_p'$ ,  $\sigma_p''$ , and  $\sigma_M'$  are determined by (1). When  $|\sigma_M'| < \sigma_p'$ , the reserve of strength of the system is

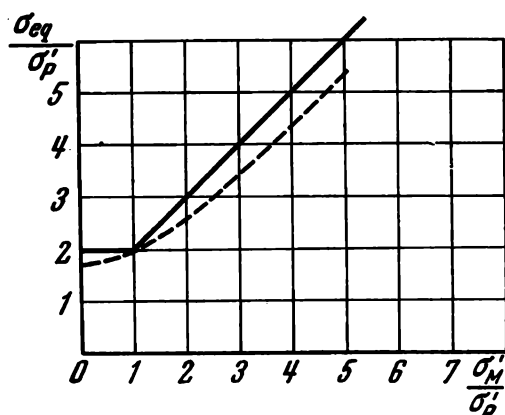


Fig. 313

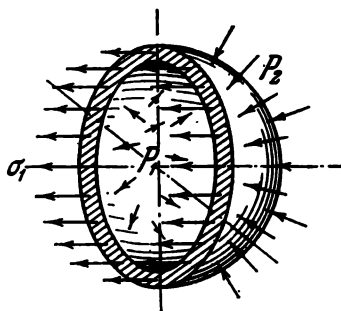


Fig. 314

independent of the magnitude of the applied moment  $M$ . This conclusion is a consequence of the maximum shearing stress theory of strength which excludes the role of  $\sigma_3$ , i.e., the role of the intermediate principal stress. By the energy theory of strength,  $\sigma_{eq}$  depends continuously on the moment  $M$ . In the graph of Fig. 313 this relation is shown by the dashed curve.

93. The solution presented on p. 43 is wrong since the stresses  $\sigma_1$  and  $\sigma_2$  are calculated incorrectly in it. Consider

the condition for the equilibrium of a part of the sphere (Fig. 314)

$$p_1\pi \left(R - \frac{h}{2}\right)^2 - p_2\pi \left(R + \frac{h}{2}\right)^2 = \sigma_1 2\pi R h.$$

In the usual conditions the term  $h/2$  in the parentheses can be neglected in comparison with  $R$ . Here this cannot be done since  $p_1$  and  $p_2$  are great and the difference between them is small. Hence,

$$(p_1 - p_2) R^2 - (p_1 + p_2) R h + (p_1 - p_2) \frac{h^2}{4} = \sigma_1 2 R h.$$

The third term on the left-hand side of this equation can be neglected.

If  $p_1$  and  $p_2$  differed greatly, we would neglect the second term as well, but now this cannot be done. Thus,

$$\sigma_1 = \sigma_2 = \frac{(p_1 - p_2) R}{2h} - \frac{p_1 + p_2}{2}, \quad \sigma_3 = -p_1,$$

$$\sigma_{eq} = \frac{p_1 - p_2}{2h} R - \frac{p_1 + p_2}{2} + p_1 = 510 \text{ kgf/cm}^2,$$

$$n_y = \frac{\sigma_y}{\sigma_{eq}} = \frac{3000}{510} = 5.88.$$

94. Denote by  $p_1$  the contact pressure acting on the surface of contact between the cylinder and tube, and determine the principal stresses for both members.

For the tube (Fig. 315), from the conditions of equilibrium we obtain

$$\sigma = p_1 \frac{R}{h} - p \frac{R+h}{h}.$$

At the inner surface the other two principal stresses are  $-p$  and  $-p_1$ ; hence, the circumferential extension of the tube is

$$\epsilon_t = \frac{1}{E_t} [\sigma - \mu_t (-p - p_1)],$$

where  $E_t$  and  $\mu_t$  are, respectively, the modulus of elasticity and Poisson's ratio of the tube material. Substituting for  $\sigma$ , we obtain

$$\epsilon_t = \frac{1}{E_t} \left[ \frac{p_1 R}{h} - \frac{p(R+h)}{h} + \mu_t (p + p_1) \right].$$

For the cylinder we have

$$\varepsilon_c = \frac{1}{E_c} [-p_1 - \mu_c (-p - p_1)].$$

But  $\varepsilon_t = \varepsilon_c$ ; from this condition we find  $p_1$

$$p_1 = p \frac{\frac{1}{E_t} \left( \frac{R}{h} + 1 - \mu_t \right) + \frac{\mu_c}{E_c}}{\frac{1}{E_t} \left( \frac{R}{h} + \mu_t \right) + \frac{1 - \mu_c}{E_c}}.$$

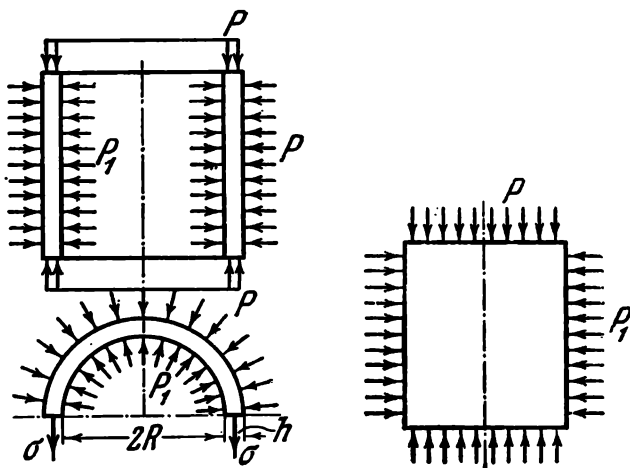


Fig. 315

Eliminating  $p_1$  from the expression for  $\sigma$ , we obtain

$$\sigma = p \frac{R}{h} \frac{\frac{1 - 2\mu_t}{E_t} - \frac{1 - 2\mu_c}{E_c}}{\frac{1}{E_t} \left( \frac{R}{h} + \mu_t \right) + \frac{1 - \mu_c}{E_c}} - p.$$

Assume that

$$\frac{1 - 2\mu_t}{E_t} > \frac{1 - 2\mu_c}{E_c}.$$

Then, it can easily be shown that  $p_1 > p$  and  $\sigma > -p$ . Consequently,

$$\begin{aligned} \sigma_1 &= \sigma, \\ \sigma_2 &= -p, \\ \sigma_3 &= -p_1, \end{aligned} \quad \sigma_{eq} = \sigma_1 - \sigma_3 = \sigma + p_1,$$

whence

$$\sigma_{eq} = p \left( \frac{R}{h} + 1 \right) \frac{\frac{1-2\mu_t}{E_t} - \frac{1-2\mu_c}{E_c}}{\frac{1}{E_t} \left( \frac{R}{h} + \mu_t \right) + \frac{1-\mu_c}{E_c}}.$$

Since  $R/h$  is very much greater than unity,

$$\sigma_{eq} = pE_t \left( \frac{1-2\mu_t}{E_t} - \frac{1-2\mu_c}{E_c} \right)$$

and the condition for the occurrence of plastic deformations in the tube can then be written as

$$pE_t \left( \frac{1-2\mu_t}{E_t} - \frac{1-2\mu_c}{E_c} \right) = \sigma_y.$$

If  $\frac{1-2\mu_t}{E_t} < \frac{1-2\mu_c}{E_c}$ , we have  $p_t < p$ . In this case the contact between tube and cylinder opens up and the two bodies deform independently.

In order to estimate the order of magnitude of the pressure  $p$ , let us solve a numerical example. The cylinder is of steel

$$E_c = 2 \times 10^6 \text{ kgf/cm}^2, \quad \mu_c = 0.3.$$

For the tube of organic glass, the following data are given:  $E_t = 3 \times 10^4 \text{ kgf/cm}^2$ ,  $\mu_t = 0.35$ ,  $\sigma_y = 750 \text{ kgf/cm}^2$ . The calculation gives

$$p = \frac{\sigma_y}{1-2\mu_t - \frac{E_t}{E_c}(1-2\mu_c)} = 2550 \text{ kgf/cm}^2.$$

This figure is approximate since in the above solution no account is taken of the change in properties of organic glass under pressure and the given value of  $\mu_t$  is not sufficiently accurate.

95. The ends of the bent wire will be pushed out by the pressure forces and the wire will be straightening out. If the wire is maintained in the bent position, the pushing-out forces are equal to the product of the pressure  $p$  and the uncompensated area  $A^*$  (Fig. 316;  $A-A$  is the section most

deflected from the axis). The area  $A^*$  obviously cannot be larger than the cross-sectional area of the wire.

If the wire is perfectly flexible, it straightens out completely and undergoes no extension ( $A^* = 0$ ). The state of stress for this case is shown in Fig. 317.

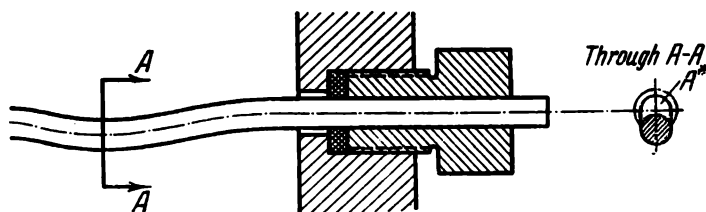


Fig. 316

If the wire has a flexural rigidity, it does not straighten out completely and a tension  $pA^*$  occurs in it. Moreover, it develops bending stresses.

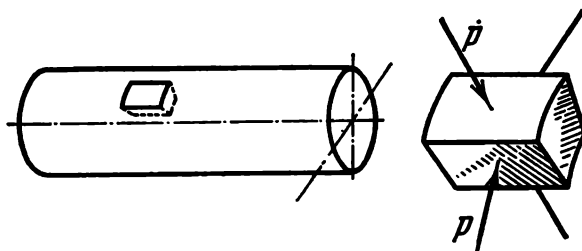


Fig. 317

96. The experimental procedure outlined in the problem does not eliminate the effect of volume change. The fractional change in internal volume of the vessel is equal to the fractional change in volume of vessel material. In order to determine the true value of the compressibility factor, it is therefore necessary to add the compressibility factor for the vessel material to that found by the procedure which has been outlined.

The change in volume measured by the meniscus of the mercury  $D$  is

$$\Delta V = \Delta V_C - \Delta V_A,$$

where  $\Delta V_C$  is the change in volume of liquid  $C$ ,  $\Delta V_A$  is the change in internal volume of the vessel. Thus,

$$\begin{aligned}\Delta V_C &= \beta_C V p, & \Delta V_A &= \beta_A V p, \\ \Delta V &= pV (\beta_C - \beta_A), & \beta_C &= \frac{\Delta V}{pV} + \beta_A,\end{aligned}$$

$\beta_C$  is the required compressibility factor of the liquid,  $\beta_A$  is the compressibility factor for the vessel material,  $V$  is the internal volume of the vessel.

Consequently, the change in volume of the vessel can be neglected only if  $\beta_A \ll \beta_C$ .

For glass, for example,

$$\beta_A = 0.25 \times 10^{-5} \text{ at}^{-1}.$$

The compressibility factor for liquids varies over a very wide range and has the following values:

mercury	$0.38 \times 10^{-5} \text{ at}^{-1}$ ,
water	$5.0 \times 10^{-5} \text{ at}^{-1}$ ,
alcohol	$7.6 \times 10^{-5} \text{ at}^{-1}$ ,
ether	$14.5 \times 10^{-5} \text{ at}^{-1}$ .

Consequently, for low-compressible liquids the correction  $\beta_A$  is of considerable importance.

97. The second bar will sustain a larger load.

Indeed, in the first case the fracture of the bar is preceded by necking and rupture occurs when the cross-sectional area in the zone of fracture is appreciably reduced. In the second case the neck does not form or hardly forms since here the heavier parts prevent shear over planes inclined to the axis of the bar. The fracture occurs without reduction in cross-sectional area.

If the material of the test pieces were brittle and not ductile, the first specimen would not be weaker than the second one, and for some materials most sensitive to local stresses it would even be stronger.

98. To produce a uniform pure shear, i.e., such in which the stresses remain invariant at all points of a body, the following procedures may be suggested:

(1) Twisting of a straight thin tube (not necessarily circular) of constant wall thickness (Fig. 318a).

(2) Loading of a thin cylinder by internal pressure  $p$  while applying an axial compressive force  $P = 0.75 \pi p d^2$ . At a sufficient distance from the bottoms the axial compressive stresses are then equal to the circumferential tensile stresses (Fig. 318b).

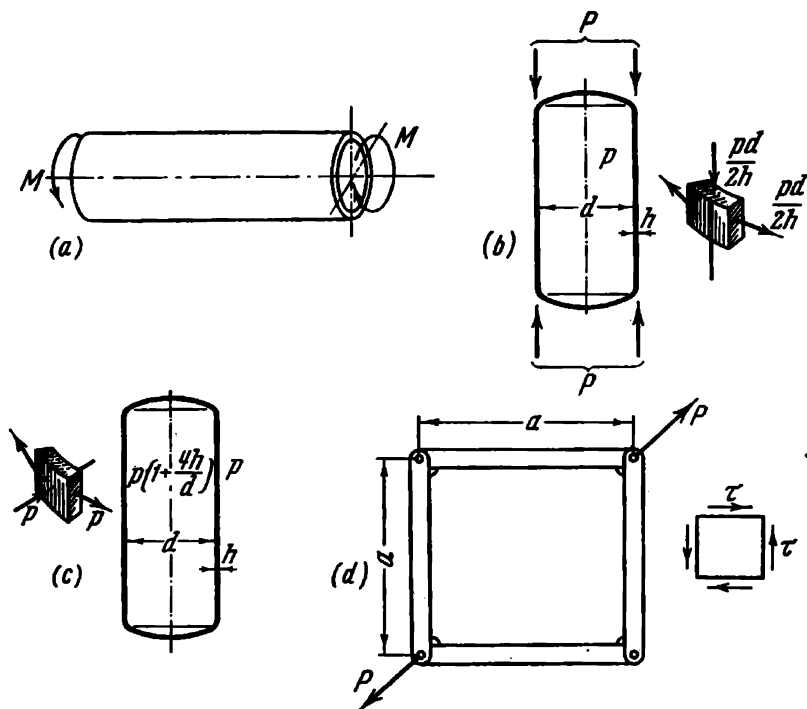


Fig. 318

(3) Loading of a thin-walled cylinder by external pressure  $p$  and internal pressure  $p(1 + 4h/d)$  (Fig. 318c). The walls of this cylinder are compressed along the normal to the middle surface with a stress  $p$  and extended in the circumferential direction with the same stress. The cylinder undergoes no extension in the axial direction.

(4) Extension of a hinged parallelogram with a plate fixed in it by diagonal forces  $P$ . If the links of the parallelogram are comparatively stiff,

$$\tau = \frac{P}{ah\sqrt{2}},$$

where  $h$  is the thickness of the plate (Fig. 318d).

Under actual conditions the state of stress in the end zones is somewhat different from pure shear in all these cases.

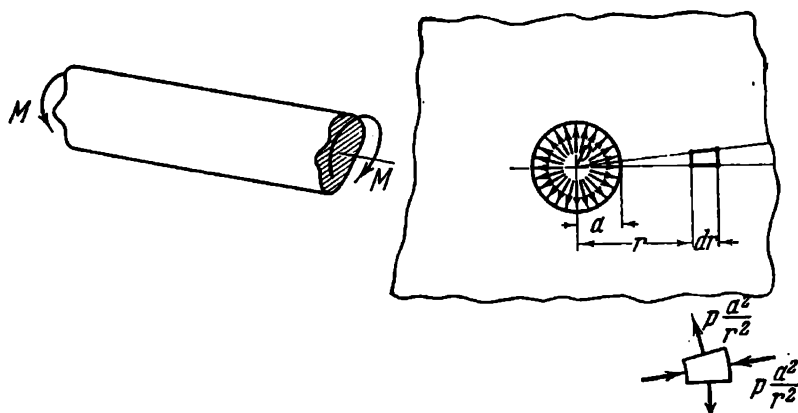


Fig. 319

A non-uniform pure shear, i.e., such in which the magnitude of the stresses is not the same for different points of a body is realized, for example, in twisting a prismatic rod with any shape of cross section or in loading a very thick tube by internal pressure  $p$  (Fig. 319).

99. The only method of producing uniform all-round tension known at present is the following.

A pre-cooled solid homogeneous sphere is heated rapidly. The state of stress indicated above is then realized at the centre of the sphere. Unfortunately, this method is unsuitable for the investigation of the properties of materials in this state of stress (for example, for the determination of the so-called separation characteristic).

An all-round (but not uniform) tension occurs in the central part of a specimen, viz. in the zone of a groove in a cylindrical specimen under tension (Fig. 320).\*

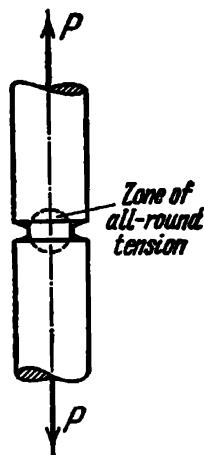


Fig. 320

\*It is assumed that the radius of the groove is comparable with the diameter of the specimen,

100. The phenomenon is most easily explained from the standpoint of the strength theory.

By adding and subtracting axial forces  $pA$  ( $A$  is the cross-sectional area of the specimen), we supplement the external load acting on the bar to give uniform compression (Fig. 321). By the maximum shearing stress theory and the energy theory, the hydrostatic stress has no effect on the occurrence of plastic deformations. The axial tension, however, gives rupture preceded by necking.

The phenomenon may also be explained from the standpoint of the stability of equilibrium forms. If some disturb-

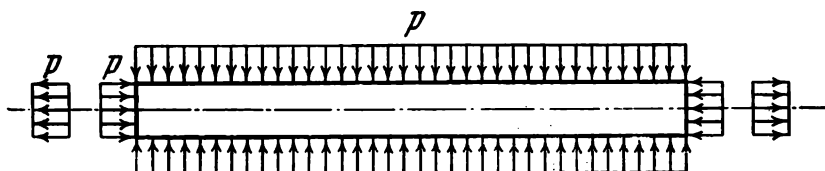


Fig. 321

ance initiates necking in the bar, an axial tensile force is developed which is equal to the product of the pressure and the difference of the areas  $A_1 - A_2$ , where  $A_1$  is the cross-sectional area of the bar in the part well away from the neck,  $A_2$  is the cross-sectional area in the neck. The appearance of the tensile force leads to further development of the neck, an increase in the tensile force and subsequent rupture.

101. The above-mentioned consideration does not provide the justification for a doubt regarding the correctness of the solution.

The stress-strain diagram (Fig. 94a) has been obtained for a uniaxial state of stress. In the zone of the notch, however, the state of stress is triaxial, with the exception of points at the surface. The circumferential and radial stresses are here tensile. The axial stress, therefore, here reaches values greater than  $\sigma_y$ .

102. Points  $A$  and  $B$  (Fig. 322) at the contour of the hole.

103. In solving the problem, a combination of the above-mentioned data on local stresses for the forces and the

moments does not lead to the positive result, and here one must proceed as follows.

Consider first the state of stress at points of the cylinder remote from the hole (rectangle  $abdc$ , Fig. 323a). Obviously,

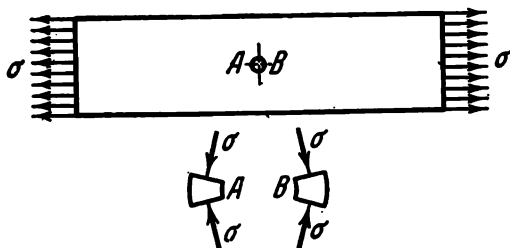


Fig. 322

$\tau = \frac{2M}{\pi d^2 h}$ ,  $\sigma = \frac{P}{\pi d h}$ . The principal stresses  $\sigma_1$  and  $\sigma_3$  are found by the formula

$$\sigma_{1,3} = \frac{\sigma}{2} \pm \frac{1}{2} \sqrt{\sigma^2 + 4\tau^2}.$$

The area on which the maximum stress  $\sigma_1$  acts is inclined to an arc of the normal circle at an angle  $\alpha$ . By the properties

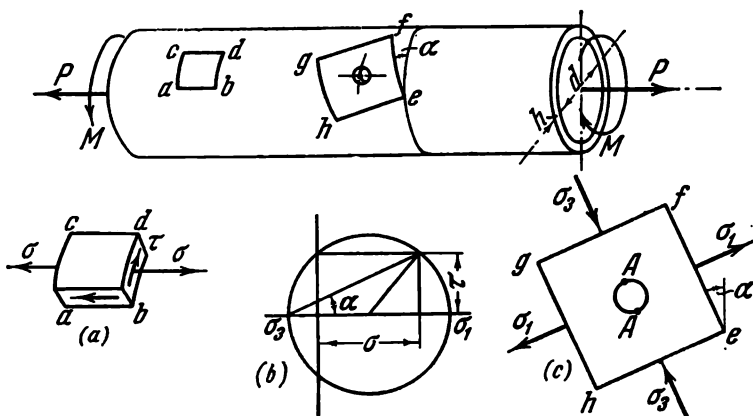


Fig. 323

of the state of plane stress (see Fig. 323b), this angle is determined from the relation  $\tan 2\alpha = \frac{2\tau}{\sigma} = \frac{4M}{Pd}$ .

We now isolate from the tube by principal planes a portion  $efgh$  enclosing the hole under consideration and the adjacent zone of local stresses (Fig. 323c). By the reference data, for this type of loading of the plate\* with the hole we have  $\sigma_{\max} = 3\sigma' - \sigma''$ , where  $\sigma'$  is the larger and  $\sigma''$  the smaller of the stresses being considered. In the present case

$$\sigma' = \sigma_1, \quad \sigma'' = \sigma_3, \quad \sigma_{\max} = \sigma + 2\sqrt{\sigma^2 + 4\tau^2}.$$

This stress occurs at the edge of the hole at the ends of a diameter parallel to the axis 3 (points  $A$ , Fig. 323c).

104. The problem belongs to the simplest problems of the theory of small plastic deformations. To solve it we must first convert the  $\sigma = f(\varepsilon)$  diagram to a  $\tau = \varphi(\gamma)$  diagram.

According to the theory of plasticity, a definite functional relation exists between the stress intensity

$$\sigma_i = \frac{1}{\sqrt{2}} \sqrt{(\sigma_2 - \sigma_3)^2 + (\sigma_3 - \sigma_1)^2 + (\sigma_1 - \sigma_2)^2}$$

and the strain intensity

$$\varepsilon_i = \frac{\sqrt{2}}{3} \sqrt{(\varepsilon_2 - \varepsilon_3)^2 + (\varepsilon_3 - \varepsilon_1)^2 + (\varepsilon_1 - \varepsilon_2)^2}$$

for a given material, namely a relation

$$\sigma_i = \Phi(\varepsilon_i) \quad (1)$$

which is invariant under all stress conditions, and in particular in tension when

$$\begin{aligned} \sigma_1 &= \sigma, & \sigma_2 &= \sigma_3 = 0, & \sigma_i &= \sigma, \\ \varepsilon_1 &= \varepsilon, & \varepsilon_2 &= \varepsilon_3 = \mu\varepsilon, & \varepsilon_i &= \frac{2}{3}(1 + \mu)\varepsilon. \end{aligned}$$

---

\*A cylindrical shell in the zone of a hole may be considered as a plate if  $\rho^2/\sqrt{Rh} < 0.1$ , where  $\rho$  is the radius of the hole,  $R$  is the radius of the cylinder, and  $h$  is its thickness. See A. I. Lur'e, "The Statics of Thin-walled Elastic Shells", Gostekhizdat, Moscow-Leningrad, 1947.

If we take  $\mu = 0.5$ , then  $\varepsilon_i = \varepsilon$ . In torsion

$$\begin{aligned}\sigma_1 &= \tau, & \sigma_2 &= 0, & \sigma_3 &= -\tau, & \sigma_i &= \sqrt{3}\tau, \\ \varepsilon_1 &= \frac{\gamma}{2}, & \varepsilon_2 &= 0, & \varepsilon_3 &= -\frac{\gamma}{2}, & \varepsilon_i &= \frac{\gamma}{\sqrt{3}}.\end{aligned}$$

But according to expression (1),

$$\sigma = \Phi(\varepsilon), \quad \tau \sqrt{3} = \Phi\left(\frac{\delta}{\sqrt{3}}\right).$$

The first of these equations is the equation of the tensile stress-strain diagram of the material. The conversion of the

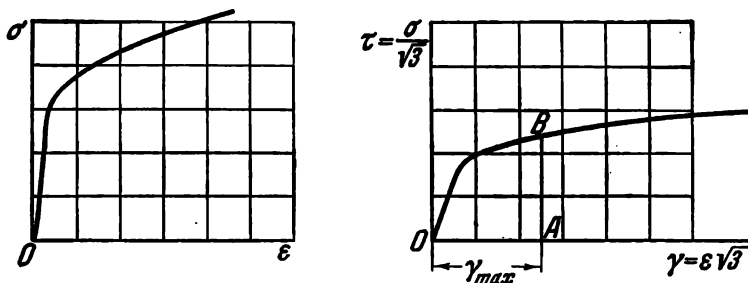


Fig. 324

diagram is consequently made by a simple change of  $\sigma$  to  $\tau\sqrt{3}$  and of  $\varepsilon$  to  $\gamma/\sqrt{3}$ .

Figure 324 shows an example of such a conversion of the diagram. The angle of twist  $\theta$  as a function of the moment  $M$  is determined similarly to the change of curvature in Prob. 83. The angle of shear  $\gamma$  at a distance  $\rho$  from the axis of the rod is

$$\gamma = \rho\theta, \quad \gamma_{\max} = \frac{d}{2}\theta, \quad (2)$$

where  $d$  is the diameter of the section. The twisting moment is equal to

$$M = 2\pi \int_0^{d/2} \tau \rho^2 d\rho;$$

but since the distance  $\rho = \frac{d}{2} \frac{\gamma}{\gamma_{\max}}$ , we have

$$M = \frac{\pi d^3}{4\gamma_{\max}^3} \int_0^{\gamma_{\max}} \tau \gamma^2 d\gamma. \quad (3)$$

The integral appearing in this expression is the moment of inertia of the curvilinear triangle  $OAB$  with respect to the axis of ordinates (Fig. 324). Thus, the determination of the required relation is performed as follows. By assigning a value of  $\gamma_{\max}$ , we determine the moment of inertia of the triangle  $OAB$ . Further, by formulas (2) and (3) we determine  $\theta$  and  $M$ . Carrying out this operation for several values of  $\gamma_{\max}$ , we can plot the required relation.

## IV. Stability

105. The length of the upper free part of the bar is equal to

$$l - \lambda = l - \frac{P}{k}.$$

The existence of the form of equilibrium with a deflected axis for this portion is possible when

$$P > \frac{\pi^2 EI}{4 \left( l - \frac{P}{k} \right)^2},$$

and for the lower portion having the length  $\lambda = P/k$  when

$$P > \frac{4\pi^2 EI}{\left( \frac{P}{k} \right)^2}.$$

Denote

$$\frac{\lambda}{l} = \frac{P}{kl} = p, \quad \frac{\pi^2 EI}{l^3 k} = p_0.$$

The foregoing conditions for the existence of curvilinear forms of equilibrium then become

$$p(1-p)^2 > \frac{1}{4} p_0,$$

$$p^3 > 4p_0. \quad (1)$$

Since  $\lambda \leq l$ , then  $0 \leq p \leq 1$ .

In this range of  $p$  we plot the graph of the functions  $p(1-p)^2$  and  $p^3$  (Fig. 325). From this graph and relations (1) it is seen that in order for the bar not to lose stability, the following conditions must be fulfilled:

$$\frac{1}{4} p_0 > \frac{4}{27} \quad \text{and} \quad 4p_0 > 1,$$

whence

$$p_0 > \frac{16}{27};$$

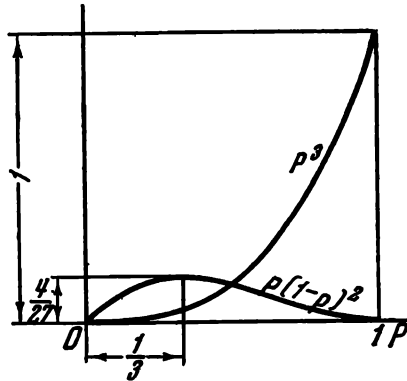


Fig. 325

but from the foregoing

$$P_0 = \frac{\pi^2 EI}{l^3 k};$$

consequently, the spring stiffness  $k$  must be less than

$$\frac{27}{16} \frac{\pi^2 EI}{l^3}.$$

106. Consider the contour of the deflected plate (Fig. 326).

The differential equations of the elastic curve for the first and second parts of the plate with the force  $P$  acting downward are

$$EI y_1'' + P y_1 = 0,$$

$$EI y_2'' - P y_2 = 0.$$

Denoting  $\frac{P}{EI} = \alpha^2$ , we obtain

$$y_1'' + \alpha^2 y_1 = 0,$$

$$y_2'' - \alpha^2 y_2 = 0,$$

whence

$$y_1 = A_1 \sin \alpha x + B_1 \cos \alpha x,$$

$$y_2 = A_2 \sinh \alpha x + B_2 \cosh \alpha x.$$

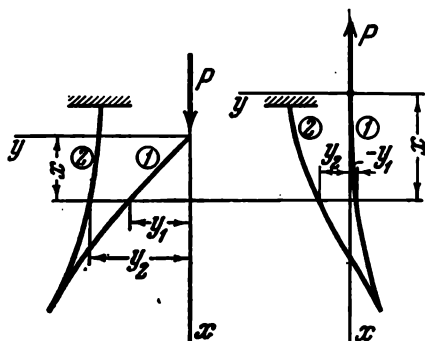


Fig. 326

The constants are determined from the following conditions:

- (1) when  $x = 0$ ,  $y_1 = 0$ ;
- (2) when  $x = l$ ,  $y_1 = y_2$ ;
- (3) when  $x = l$ ,  $y_1' = y_2'$ ;
- (4) when  $x = 0$ ,  $y_2' = 0$ .

From the first and last conditions we obtain

$$B_1 = A_2 = 0,$$

from the second and third

$$A_1 \sin \alpha l = B_2 \cosh \alpha l,$$

$$A_1 \cos \alpha l = B_2 \sinh \alpha l,$$

whence

$$\tan \alpha l \tanh \alpha l = 1 \quad (1)$$

or

$$\alpha l = 0.938, \quad P_{cr} = \frac{0.88 EI}{l^2}.$$

If the force  $P$  acts upward, the sign of  $\alpha^2$  is reversed and the transcendental equation (1) becomes

$$\tan ial \tanh ial = 1.$$

But  $\tan ial = -\frac{\tanh^* \alpha l}{i}$  and  $\tanh ial = i \tan \alpha l$ . We have, therefore,

$$\tan \alpha l \tanh \alpha l = -1,$$

from which

$$\alpha l = 2.35, \quad P_{cr} = \frac{5.53EI}{l^2}.$$

107. Consider the bar in the deflected condition with the upper support removed (Fig. 327). The vertical reaction of this support is denoted by  $P_1$ , and the horizontal reaction by  $Q$ .

The first question to arise here is that of the magnitude of these reactions. The force  $Q$  is determined from the condition that the sum of the moments about the point  $A$  is zero, giving

$$Q = P \frac{f}{l}.$$

Before buckling occurs, the force  $P_1 = P/2$ . Since the departure from the straight-line form may be assumed arbitrarily small, during buckling the force  $P_1$  may also be taken equal to  $P/2$  (see the solution of Prob. 109). We now set up the differential equations of the deflected axis of the bar for each portion

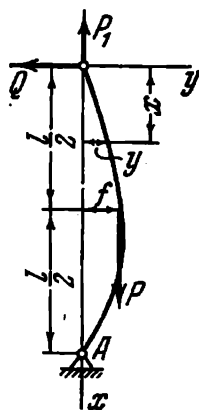


Fig. 327

$$EIy_1' = P_1 y_1 - Qx \quad \left(0 \leq x \leq \frac{l}{2}\right),$$

$$EIy_2' = P_1 y_2 - Qx - P(y_2 - f) \quad \left(\frac{l}{2} \leq x \leq l\right),$$

or alternatively

$$y_1'' - \alpha^2 y_1 = -2\alpha^2 \frac{f}{l} x,$$

$$y_2'' + \alpha^2 y_2 = -2\alpha^2 \frac{f}{l} x + 2\alpha^2 f,$$

where

$$\alpha^2 = \frac{P}{2EI}.$$

By solving the equations, we obtain

$$y_1 = A \sinh \alpha x + B \cosh \alpha x + \frac{2f}{l} x,$$

$$y_2 = C \sin \alpha x + D \cos \alpha x - \frac{2f}{l} x + 2f.$$

When  $x=0$ ,  $y_1=0$ ; when  $x=l/2$ ,  $y_1=y_2=f$  and  $y'_1=y'_2$ ;  
when  $x=l$ ,  $y_2=0$ .

Consequently,

$$(1) B=0,$$

$$(2) A \sinh \frac{\alpha l}{2} + B \cosh \frac{\alpha l}{2} + f = f,$$

$$(3) C \sin \frac{\alpha l}{2} + D \cos \frac{\alpha l}{2} + f = f,$$

$$(4) A\alpha \cosh \frac{\alpha l}{2} + B\alpha \sinh \frac{\alpha l}{2} + \frac{2f}{l} = C\alpha \cos \frac{\alpha l}{2} - D\alpha \sin \frac{\alpha l}{2} \times \frac{\alpha l}{2} - \frac{2f}{l},$$

$$(5) C \sin \alpha l + D \cos \alpha l = 0.$$

From the second equation it follows that  $A=0$  (i.e., the upper part of the bar does not buckle). The last three equations become

$$C \sin \frac{\alpha l}{2} + D \cos \frac{\alpha l}{2} = 0,$$

$$C\alpha \cos \frac{\alpha l}{2} - D\alpha \sin \frac{\alpha l}{2} - \frac{4f}{l} = 0,$$

$$C \sin \alpha l + D \cos \alpha l = 0.$$

When the determinant of the system is not zero, all the constants  $[C, D, f]$  vanish. Then  $y_1 = y_2 = 0$  and the bar remains straight. The solution can be different from zero only if the determinant is equal to zero. This enables one to

find the critical load  $P_{cr}$

$$\begin{vmatrix} \sin \frac{\alpha l}{2} & \cos \frac{\alpha l}{2} & 0 \\ \alpha \cos \frac{\alpha l}{2} & -\alpha \sin \frac{\alpha l}{2} & -\frac{4}{l} \\ \sin \alpha l & \cos \alpha l & 0 \end{vmatrix} = 0,$$

whence

$$\sin \frac{\alpha l}{2} = 0, \quad \frac{\alpha l}{2} = \pi, \quad P_{cr} = \frac{8\pi^2 EI}{l^2}.$$

If the upper end of the bar were able to move vertically, the critical force would be reduced by more than a factor of four, giving  $18.7 EI/l^2$ .

108. Imagine that the nut is removed from the bolt and consider the forces acting on the bolt and tube. Figure 328 shows the axes of the bolt and tube after instability occurs and the internal force factors  $P$ ,  $Q$ , and  $M_0$ . Obviously, for the tube

$$M_b = Py_1 - Qx - M_0,$$

for the bolt

$$M_b = -Py_2 + Qx + M_0.$$

The differential equations of the elastic curves of the tube and bolt are the following:

$$\begin{aligned} E_1 I_1 y_1'' + Py_1 &= Qx + M_0, \\ E_2 I_2 y_2'' - Py_2 &= -Qx - M_0. \end{aligned}$$

Denote

$$\frac{P}{E_1 I_1} = \alpha_1^2, \quad \frac{P}{E_2 I_2} = \alpha_2^2;$$

we then have

$$\begin{aligned} y_1'' + \alpha_1^2 y_1 &= \frac{Q}{P} \alpha_1^2 x + \frac{M_0}{P} \alpha_1^2, \\ y_2'' - \alpha_2^2 y_2 &= -\frac{Q}{P} \alpha_2^2 x - \frac{M_0}{P} \alpha_2^2. \end{aligned}$$

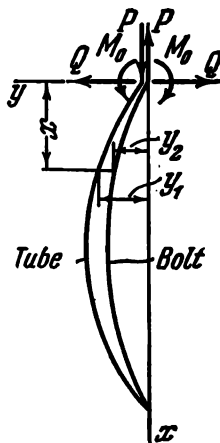


Fig. 328

By solving these equations, we obtain

$$y_1 = A_1 \sin \alpha_1 x + B_1 \cos \alpha_1 x + \frac{Q}{P} x + \frac{M_0}{P},$$

$$y_2 = A_2 \sinh \alpha_2 x + B_2 \cosh \alpha_2 x + \frac{Q}{P} x + \frac{M_0}{P}.$$

The last two terms in both expressions represent particular solutions of the equations. The constants  $A_1$ ,  $B_1$ ,  $A_2$ ,  $B_2$ ,  $Q$ , and  $M_0$  are determined from the following conditions: when  $x = 0$ ,

$$y_1 = 0, \quad y_2 = 0, \quad y'_1 = y'_2;$$

when  $x = l$ ,

$$y_1 = 0, \quad y_2 = 0, \quad y'_1 = y'_2.$$

From the first three conditions we find

$$B_1 = B_2 = -\frac{M_0}{P}, \quad A_2 = A_1 \frac{\alpha_1}{\alpha_2}. \quad [(1)]$$

The last three conditions give

$$A_1 \sin \alpha_1 l + B_1 \cos \alpha_1 l + \frac{Q}{P} l + \frac{M_0}{P} = 0,$$

$$A_2 \sinh \alpha_2 l + B_2 \cosh \alpha_2 l + \frac{Q}{P} l + \frac{M_0}{P} = 0,$$

$$A_1 \alpha_1 \cos \alpha_1 l - B_1 \alpha_1 \sin \alpha_1 l = A_2 \alpha_2 \cosh \alpha_2 l + B_2 \alpha_2 \sinh \alpha_2 l.$$

If we substitute for  $B_1$ ,  $B_2$ , and  $A_2$  from (1) in these equations, they become

$$A_1 \sin \alpha_1 l + \frac{Q}{P} l + \frac{M_0}{P} (1 - \cos \alpha_1 l) = 0,$$

$$A_1 \frac{\alpha_1}{\alpha_2} \sinh \alpha_2 l + \frac{Q}{P} l + \frac{M_0}{P} (1 - \cosh \alpha_2 l) = 0,$$

$$A_1 \alpha_1 (\cos \alpha_1 l - \cosh \alpha_2 l) + \frac{M_0}{P} (\alpha_1 \sin \alpha_1 l + \alpha_2 \sinh \alpha_2 l) = 0.$$

By equating the determinant of the system to zero, we obtain

$$\begin{vmatrix} \sin \alpha_1 l & [l] & 1 - \cos \alpha_1 l \\ \frac{\alpha_1}{\alpha_2} \sinh \alpha_2 l & l & 1 - \cosh \alpha_2 l \\ \alpha_1 (\cos \alpha_1 l - \cosh \alpha_2 l) & 0 & \alpha_1 \sin \alpha_1 l + \alpha_2 \sinh \alpha_2 l \end{vmatrix} = 0,$$

whence

$$2z_1z_2(\cosh z_2 \cos z_1 - 1) = (z_2^2 - z_1^2) \sinh z_2 \sin z_1, \quad (2)$$

where  $z_1 = \alpha_1 l$ ,  $z_2 = \alpha_2 l$ . If the ratio of the rigidities is given, we can express  $z_2$  in terms of  $z_1$  and then, on solving the transcendental equation (2), determine the critical tightening force  $P$ .

In particular, when  $E_1 I_1 = E_2 I_2 = EI$ , we have  $z_1 = z_2 = z$ , and then  $\cosh z \cos z = 1$ , whence

$$z = 4.73, \quad P_{cr} = \frac{z^2 EI}{l^2} = \frac{22.4 EI}{l^2}.$$

109. It may be stated that the shape of the elastic curve of the deflected bar for a given compressive force is the same irrespective of the manner in which this compressive force is produced.

For a given departure of the bar from the straight position, the force compressing the bar must be the same in all circumstances. By reducing indefinitely the curvature of the bar, we inevitably come to the conclusion that the critical force for the bar under consideration is the same both in the usual case of loading the bar by a dead load and in the case of temperature effect considered above.

We may also reason as follows. The bending moment in the bar is proportional to the first power of the deflection  $y$ , and the change in the compressive force takes place in a vertical displacement proportional to the second power of  $y'$ . Consequently,  $y$  may always be chosen sufficiently small for the change in the force to be disregarded.

110. With a formal approach to the choice of the approximating function, the result obtained may be very far from reality.

Assume, for example, that the shape of the elastic curve for a hinged compressed bar (Fig. 329) is expressed by the function

$$y = A \left( \sin \frac{\pi x}{l} + \frac{l}{m} \sin \frac{\pi m x}{l} \right). \quad (1)$$

As  $m \rightarrow \infty$ , the assumed function indefinitely approaches the exact value of the function expressing the shape of the elastic curve, i.e.,

$$y_{m \rightarrow \infty} = A \sin \frac{\pi x}{l}.$$

The critical force  $P$  found on the basis of this function by the energy method is equal to

$$P_{cr} = \frac{EI \int_0^l y'^2 dx}{\int_0^l y'^2 dx} = \frac{1+m^2}{2} \frac{\pi^2 EI}{l^2}$$

and, as seen, when  $m \rightarrow \infty$ , it departs indefinitely from the exact value.

A feature of function (1) is that it reflects well the form of the primitive  $y$  but differs greatly from it in the second derivative, i.e., in the expression of the curvature.

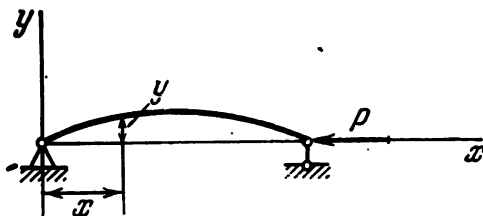


Fig. 329

The example is instructive because it underlines, in a particularly vivid way, the general rule. In choosing an approximating function, care must also be given to the degree of approximation to derivatives, including the highest-order derivative which occurs in the expression of the energy.

111. We first solve an auxiliary problem.

Take a hinged bar of length  $l$  loaded by a compressive force  $N$  and moments  $M_0$  and  $M_1$  (Fig. 330a). The differential equation of the elastic curve of the bar is

$$EIy'' = M_0 - Rx - Ny,$$

where  $R$  is the reaction at the supports. Further we have

$$y = A \sin \alpha x + B \cos \alpha x + \frac{1}{EI\alpha^2} (M_0 - Rx), \quad (1)$$

where  $\alpha^2 = N/EI$ .

Obviously, when  $x = 0$  and  $x = l$ , the displacement  $y = 0$ . Assume further that when  $x = 0$ ,  $y' = 0$ . By using

these conditions, and noting that

$$R = \frac{M_0 - M_1}{l},$$

we eliminate  $A$ ,  $B$ ,  $M_0$  and  $R$  from expression (1). We then obtain

$$y = \frac{M_1}{EI\alpha^2} \frac{(1 - \cos \alpha l)(\alpha l - \sin \alpha l)}{\alpha l \cos \alpha l - \sin \alpha l} \left[ \frac{1 - \cos \alpha x}{1 - \cos \alpha l} - \frac{\alpha x - \sin \alpha x}{\alpha l - \sin \alpha l} \right].$$

The magnitude of the moment  $M_1$  remains undetermined.

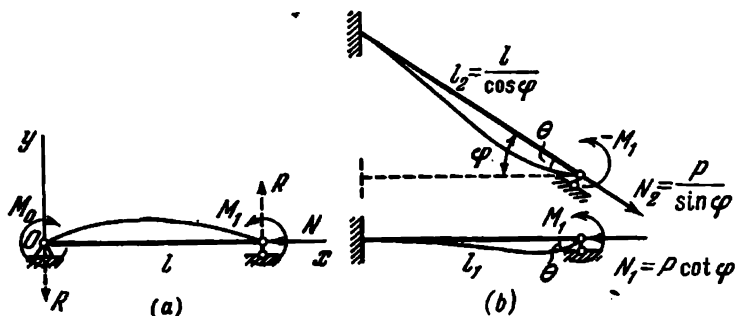


Fig. 330

The angle of rotation of the bar at the right support is

$$\theta = y'_{x=l} = \frac{M_1}{EI\alpha} \frac{-2 + 2 \cos \alpha l + \alpha l \sin \alpha l}{\alpha l \cos \alpha l - \sin \alpha l}. \quad (2)$$

If the force  $N$  is not compressive, but tensile, then  $\alpha$  must be replaced by  $i\alpha$ ,  $\cos \alpha l$  by  $\cosh \alpha l$ , and  $\sin \alpha l$  by  $i \sinh \alpha l$ . Expression (2) then becomes

$$\theta = -\frac{M_1}{EI\alpha} \frac{-2 + 2 \cosh \alpha l - \alpha l \sinh \alpha l}{\alpha l \cosh \alpha l - \sinh \alpha l}. \quad (3)$$

We now turn to the given bar system (Fig. 330b). The lower horizontal bar is compressed by the force  $N_1 = P \cot \varphi$  and the upper bar is extended by the force  $N_2 = P / \sin \varphi$ .

At the point of application of the force  $P$  the displacements for either bar are zero, apart from a small quantity of higher order. The left ends of the bars are fixed. Consequently, the scheme of a bar fixed at one end and hinged at the other (Fig. 330a) corresponds to the conditions of fixing and load-

ing of the bars making up the given frame. It only remains to fulfil the matching conditions. These conditions reduce to the equality of angles  $\theta$  and the equality of moments at the common point.

We now turn to expressions (2) and (3). In the first of these we replace  $\alpha l$  by  $\alpha_1 l_1$ , and in the second by  $\alpha_2 l_2$ . Obviously,

$$\alpha_1 l_1 = l \sqrt{\frac{P \cot \varphi}{EI}}, \quad \alpha_2 l_2 = \frac{l}{\cos \varphi} \sqrt{\frac{P}{EI \sin \varphi}}. \quad (4)$$

Since the moments at the junction are directed towards each other, the sign of  $M_1$  is reversed in either expression (2) or expression (3). By equating the angles  $\theta$ , we obtain the following transcendental equation:

$$\frac{1}{\alpha_1 l_1} \frac{-2 + 2 \cos \alpha_1 l_1 + \alpha_1 l_1 \sin \alpha_1 l_1}{\alpha_1 l_1 \cos \alpha_1 l_1 - \sin \alpha_1 l_1} = \frac{1}{\alpha_2 l_2 \cos \varphi} \frac{-2 + 2 \cosh \alpha_2 l_2 - \alpha_2 l_2 \sinh \alpha_2 l_2}{\alpha_2 l_2 \cosh \alpha_2 l_2 - \sinh \alpha_2 l_2}.$$

To this equation is added the relation

$$\alpha_1 l_1 = \alpha_2 l_2 \cos^{3/2} \varphi.$$

On determining the quantity  $\alpha_1 l_1 = \sqrt{\frac{Pl^2}{EI} \cot \varphi}$  for several values of  $\varphi$ , we obtain the following table:

$\varphi^\circ$	0	10	20	30	40	50	60	70	80	90
$\frac{P_{cr} l^2}{EI}$	0	5.55	11.46	18.21	26.57	38.08	56.18	91.37	196.9	$\infty$

112. Suppose that the point  $A$  has moved out of the plane  $BCDE$ . We apply forces  $P_1$  to the beams  $BD$  and  $CE$  at the point  $A$  (Fig. 331), whereupon we consider the beams separately. The differential equation of bending for the beam  $BD$  is

$$EIy'' - Py = -\frac{1}{2} P_1 x.$$

For the beam  $CE$  we have

$$EIy'' + Py = +\frac{1}{2} P_1 x.$$

The solutions of these equations are, in succession,

$$y_1 = C_1 \sinh \alpha x + C_2 \cosh \alpha x + \frac{1}{2} \frac{P_1}{P} x,$$

$$y_2 = C_3 \sin \alpha x + C_4 \cos \alpha x + \frac{1}{2} \frac{P_1}{P} x,$$

where

$$\alpha^2 = \frac{P}{EI}.$$

At the point  $x = 0$  the deflection  $y$  vanishes in both cases. Hence,

$$C_2 = C_4 = 0.$$

For symmetrical forms of instability, the slope  $y' = 0$  when  $x = l$ , from which

$$C_1 = -\frac{P_1}{2P\alpha} \frac{1}{\cosh \alpha l}, \quad C_3 = -\frac{P_1}{2P\alpha} \frac{1}{\cos \alpha l}.$$

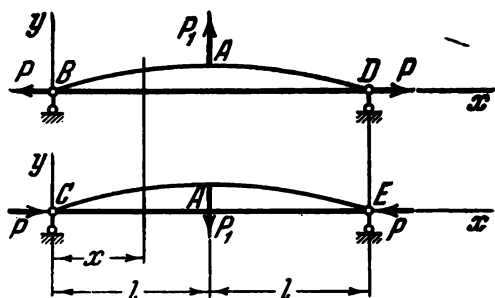


Fig. 331

Finally, from the condition of equality of beam deflections at the point  $A$  we obtain

$$C_1 \sinh \alpha l = C_3 \sin \alpha l$$

or, according to the foregoing,

$$\tanh \alpha l = \tan \alpha l,$$

whence

$$\alpha l = 3.926, \quad P_{cr} = \frac{15.4EI}{l^2}. \quad (1)$$

Moreover, there is a second possibility of instability for the compressed bar  $CE$ . This bar may bend into two half-

waves with the point  $A$  remaining fixed. The bar is then twisted. Consider the two bars separately (Fig. 332). The differential equation of the deflected axis of the bar  $CE$  is

$$EIy'' + Py = \frac{M}{2l}x,$$

whence

$$y = C_1 \sin \alpha x + C_2 \cos \alpha x + \frac{M}{2Pl}x;$$

$$\text{when } x=0, \quad y=0;$$

$$\text{when } x=l, \quad y=0;$$

$$\text{when } x=l, \quad y' = -\varphi. \quad \left. \begin{array}{l} \\ \\ \end{array} \right\} \quad (2)$$

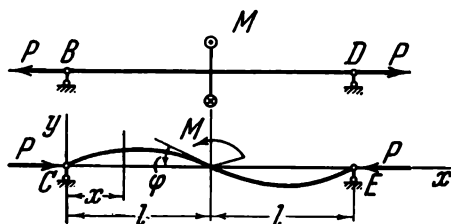


Fig. 332

Here  $\varphi$  is the angle of rotation of the middle section of the bar  $BD$  which is equal to

$$\varphi = \frac{M}{2} \frac{l}{k},$$

where  $k$  is the torsional rigidity of the stretched thin bar; according to the solution of Prob. 29 we have

$$k = \frac{1}{3} Gbh^3 + \frac{Pb^2}{12}.$$

The boundary conditions (2) give

$$C_2 = 0, \quad C_1 \sin \alpha l + \frac{M}{2P} = 0,$$

$$C_1 \alpha \cos \alpha l + \frac{M}{2Pl} = -\frac{M}{2} \frac{1}{\frac{1}{3} Gbh^3 + \frac{Pb^2}{12}}$$

from which, by equating the determinant of the system to zero, we obtain

$$\frac{1}{\alpha} \tan \alpha l = \frac{\frac{1}{P}}{\frac{1}{Pl} + \frac{l}{\frac{1}{3} Gbh^3 + \frac{Pb^2}{12}}}.$$

Since

$$P = \alpha^2 EI, \quad G = \frac{E}{2(1+\mu)},$$

$$I = \frac{bh^3}{12},$$

$$\tan \alpha l = \alpha l \frac{\frac{2}{1+\mu} + \frac{b^2}{12l^2} \alpha^2 l^2}{\frac{2}{1+\mu} + \alpha^2 l^2 \left( \frac{b^2}{12l^2} + 1 \right)}.$$

Since  $b$  is very much less than  $l$ , and  $\alpha l$  must be of the order of 3 to 4 units, the terms containing  $b^2$  may obviously be neglected on the right-hand side of the equation; we then obtain

$$\tan \alpha l = \frac{2\alpha l}{2 + (1+\mu) \alpha^2 l^2}.$$

When  $\mu = 0.3$ ,

$$\alpha l = 3.51, \quad P_{cr} = \frac{12.3EI}{l^2}. \quad (3)$$

This value of  $P_{cr}$  is less than the previously calculated value (1). Consequently, the instability of the bar  $CE$  occurs in the form of two half-waves.

With a further increase in  $P$ , the force in the compressed bar remains almost unchanged, and most of the load is carried by the stretched diagonal  $BC$ .

The system considered in the problem is the analogue of a thin-walled panel  $BCDE$  (Fig. 333) operating under conditions of shear. Elements of this kind are typical of aircraft and rocket structures. Instability involves diagonal wave formation, but the panel, having lost the ability to carry an additional compressive load along the diagonal  $CE$ , can successfully resist tensile forces acting in a perpendicular direction.

113. We set up the differential equation of the deflected axis of the rod, assuming the displacements to be small.

We introduce a system of co-ordinates  $x, y, z$  (Fig. 334). At the section  $x$  the bending moments due to the force  $P$

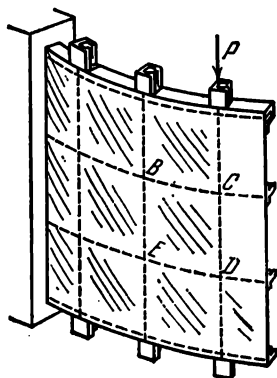


Fig. 333

and the torque  $M$  are  $Py$  and  $Mz'$  in the  $xy$  plane, and  $Pz$  and  $-My'$  in the  $xz$  plane. The plus or minus sign before the moment is taken according to whether the sense of the moment is in the direction in which the positive curvature increases or decreases in the corresponding plane of bending.

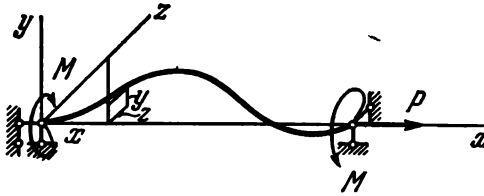


Fig. 334

If the flexural rigidities in the  $xy$  and  $xz$  planes are assumed to be the same, the equations of the elastic curve can be written as

$$\left. \begin{aligned} EIy'' &= Py + Mz', \\ EIz'' &= Pz - My'. \end{aligned} \right\} \quad (1)$$

The solution of this system is taken in the form

$$y = A \cos \alpha_1 x + B \sin \alpha_1 x + C \cos \alpha_2 x + D \sin \alpha_2 x,$$

$$z = A \sin \alpha_1 x - B \cos \alpha_1 x + C \sin \alpha_2 x - D \cos \alpha_2 x,$$

where  $\alpha_1$  and  $\alpha_2$  are the roots of the quadratic equation

$$\alpha^2 + \frac{M}{EI} \alpha + \frac{P}{EI} = 0. \quad (2)$$

In the case of a hinged bar we have the following boundary conditions:

$$\text{when } x = 0, \quad y = z = 0;$$

$$\text{when } x = l, \quad y = z = 0.$$

From these we obtain four equations

$$A + C = 0, \quad B + D = 0,$$

$$A \cos \alpha_1 l + B \sin \alpha_1 l + C \cos \alpha_2 l + D \sin \alpha_2 l = 0,$$

$$A \sin \alpha_1 l - B \cos \alpha_1 l + C \sin \alpha_2 l - D \cos \alpha_2 l = 0.$$

By equating the determinant of this system to zero, we find

$$\cos(\alpha_2 - \alpha_1)l = 1,$$

or

$$(\alpha_2 - \alpha_1)l = 0, 2\pi, 4\pi, \dots$$

But, according to Eq. (2),

$$\alpha_2 - \alpha_1 = \pm 2 \sqrt{\left(\frac{M}{2EI}\right)^2 - \frac{P}{EI}};$$

consequently,

$$M_{cr} = \pm 2 \sqrt{EI} \sqrt{P_e + P},$$

where  $P_e$  is Euler's force

$$P_e = \frac{\pi^2 EI}{l^2}.$$

Thus, as the tensile force  $P$  increases, so does the critical moment. If the force  $P$  is compressive, the moment  $M$  decreases. When the compressive force  $P = P_e$ , the magnitude of  $M_{cr}$ , as might be expected, is zero.

114. The bar cannot lose stability. Indeed, suppose that for some reason the bar is slightly bent (Fig. 335). In the usual case, i.e., when the bar is loaded only by longitudinal forces, this deflection gives rise to a bending moment  $M = Py$  which tends to increase the curvature of the bar.

When the force  $P$  is sufficiently large, the bar (after the cause of the deflection is removed) does not regain its original straight-line form of equilibrium. We then say that the straight-line form of equilibrium of the bar is unstable.

In the problem under consideration it is quite different. No external moments act on the bar in the bent position. The pressure exerted on the surface of the bar located above the section  $AA$  gives no bending moment and reduces only to a normal force at the section equal to  $pA$ . If, therefore, the cause of the deflection is removed, the bar is free to return to its original straight position,

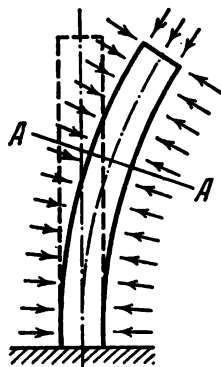


Fig. 335

no matter how large the pressure  $p$  may be. The straight-line form of equilibrium is thus always stable.

In confirmation of the above we may refer to our everyday observations. The atmospheric pressure does not prevent a thin straw from maintaining its straight form whatever its length and stiffness!

115. The bar will lose stability at the same length as a vertically standing bar (Fig. 336) having a specific weight equal to the difference in the weights of liquid and wood.

116. The tube filled with liquid will behave in exactly the same way as a freely standing bar under its own weight. If, therefore, the total weight of the tube and the filling liquid is larger than the critical weight for a bar of the same length and stiffness, the tube will lose stability.

117. The system loses stability just as though the force were applied directly to the tube itself. In the present case  $P_{cr} = \pi^2 EI / l^2$ .

It is sometimes to be heard that in the case under consideration the tube can lose stability under no conditions whatsoever. This opinion is based on the false concept that the presence of an internal compressive force plays a leading role in Euler stability. Actually, this is not so.

In order to solve the stated problem correctly, it is sufficient to consider the tube in the deflected condition (Fig. 337). As for a compressed column, the differential equation of the curved axis for the tube is the following:

$$y'' + \frac{P}{EI} y = 0.$$

From this we obtain the above value of the critical force for hinged end conditions.

118. After investigation of the preceding problem it can at once be said that the tube loses stability when

$$pA = \frac{4\pi^2 EI}{l^2},$$

where  $A$  is the clear cross-sectional area of the tube.



Fig. 336

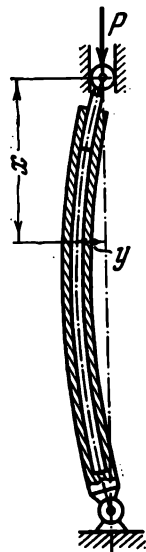


Fig. 337

The existence of the critical pressure for the given system is easily revealed from energy considerations as well. In the bent position the internal volume of the tube increases by

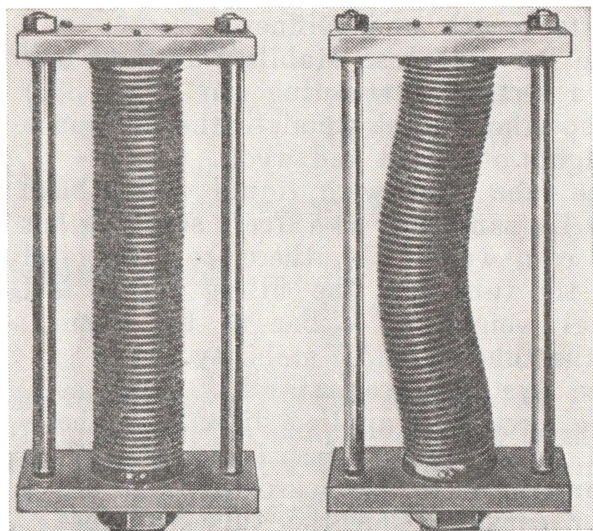


Fig. 338

$A\lambda$  due to the fact that during bending the tube comes off the upper plug by the amount  $\lambda$ , where

$$\lambda = \frac{1}{2} \int_0^l y'^2 dx.$$

The critical force is determined from the condition

$$p_{cr} A \lambda = U_b.$$

Under the usual loading of the bar by a compressive force

$$P_{cr} \lambda = U_b,$$

whence we again obtain

$$p_{cr} A = P_{cr} = \frac{4\pi^2 EI}{l^2}.$$

The case of instability considered above occurs in a particularly vivid way when thin-walled bellows (Fig. 338) are

stressed by internal pressure. The magnitude of the critical pressure is determined here in the same way as for a bar. The only difference is that the flexural rigidity  $EI$  must be replaced by a certain equivalent stiffness of the bellows in bending, and  $A$  by the cross-sectional area based on the mean diameter.

119. Suppose, that for some reason the tube is slightly deflected. Figure 339 shows this deflection, the curvature being taken positive. The fluid mass in a length  $dx$  of the tube at a given instant is

$$dm = \frac{\gamma}{g} A dx, \quad (1)$$

where  $A$  is the clear cross-sectional area of the tube. With the curvature of the channel  $1/\rho = d^2y/dx^2$ , the running fluid over the length  $dx$  gives an inertia force

$$dm \frac{v^2}{\rho} = \frac{\gamma}{g} A dx v^2 \frac{d^2y}{dx^2},$$

directed away from the centre of curvature. The intensity of inertia force, i.e., the force per unit of arc length is

$$q = -\frac{\gamma}{g} A v^2 \frac{d^2y}{dx^2}.$$

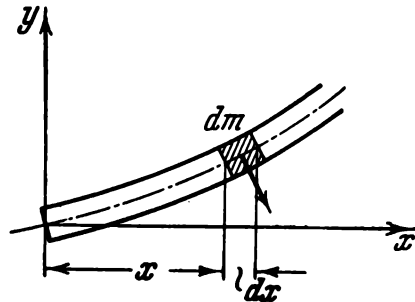


Fig. 339

The minus sign is taken because when the curvature is positive the force  $q$  is directed oppositely to the displacement  $y$ . But it is known that

$$EI \frac{d^4y}{dx^4} = q.$$

Consequently,

$$EI \frac{d^4y}{dx^4} + \frac{\gamma}{g} A v^2 \frac{d^2y}{dx^2} = 0.$$

Denote

$$\frac{\gamma}{g} \frac{A v^2}{EI} = \alpha^2.$$

We then obtain

$$\frac{d^4 y}{dx^4} + \alpha^2 \frac{d^2 y}{dx^2} = 0,$$

whence

$$y = A \sin \alpha x + B \cos \alpha x + Cx + D.$$

When  $x = 0$  and  $x = l$ , we have  $d^2 y/dx^2 = 0$  and  $y = 0$ . From these conditions we obtain

$$B = 0, \quad C = 0, \quad D = 0, \quad A \sin \alpha l = 0, \\ \alpha l = \pi, \quad v_{cr} = \frac{\pi}{l} \sqrt{\frac{g}{\gamma} \frac{EI}{A}}. \quad (2)$$

It is of interest that the instability occurs in the form of a sine curve, i.e., in the same way as under axial compression. Moreover, the instability occurs at the velocity at which the jet efficiency is exactly equal to Euler's critical force. Indeed, the jet efficiency, i.e., the reactive thrust of the jet is known to be

$$P = \frac{dm}{dt} v,$$

where  $dm/dt$  is the mass rate of flow and  $v$  is the jet velocity. (Incidentally, the rocket propulsion is determined by this formula.) According to (1)

$$P = \frac{\gamma}{g} A v^2.$$

Substituting in this the value of  $v$  from (2), we find that the jet thrust is equal to Euler's critical force  $P = \pi^2 EI/l^2$ . It should not be thought, however, that the tube is compressed by the thrust. The tube loses stability without any compressive force acting on it, in much the same way as in the case considered in Prob. 117.

120. Let us consider the well-known formula: "we take the smallest non-zero root of the equation..."

Because of its evidence, this expression has assumed, figuratively speaking, a coded character, and no thought is usually taken for its content.

Indeed, "smallest" because we are interested in the first, smallest value of the critical force. "Non-zero" because for the zero value of the root we obtain the original *zero* form of equilibrium. This solution is of no interest.

In the system under consideration, when  $R/l \leq 0.5$  it is the zero value of  $\alpha l$  that must be taken. In the absence of frictional forces the system represents a mechanism. The bar loses stability as a rigid whole under an arbitrarily small force  $P$ . When  $R/l = 0.5$ , both ends are described by arcs of a circle whose centre is at the middle of the bar (Fig. 340a). This is the limiting value of the parameter  $R/l$ , a further increase of which involves bending forms of instability.

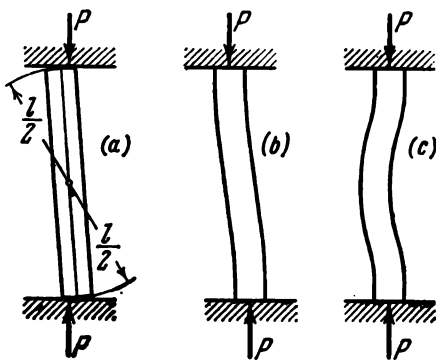


Fig. 340

Thus, in the absence of frictional forces the critical states are characterized in the diagram (Fig. 341) by the curve  $OAB$ .

As the radius  $R$  increases, the instability occurs with a progressively larger deflection of the bar in the presence of

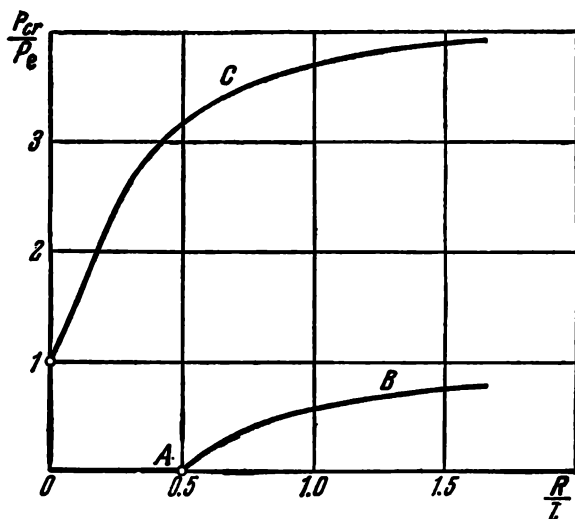


Fig. 341

the transverse sliding of the ends or the free transverse displacement of the plates. In the limit when  $R = \infty$  the in-

stability occurs in the form shown in Fig. 340b, i.e., when  $\alpha l = \pi$  and hence  $P_{cr} = \pi^2 EI/l^2$ .

If the plates are not allowed to move freely in the transverse direction and the frictional forces are sufficient to prevent slipping, the critical state of the bar as a function of  $R/l$  is characterized by the curve  $C$  (Fig. 341). When  $R/l = \infty$ , the instability occurs in the form of Fig. 340c; then  $P_{cr}/P_e = 4$ , and hence

$$P_{cr} = \frac{4\pi^2 EI}{l^2}.$$

121. When the force  $P = \pi^2 EI/l^2$ , the bar loses stability and then touches the tube walls with its middle part.

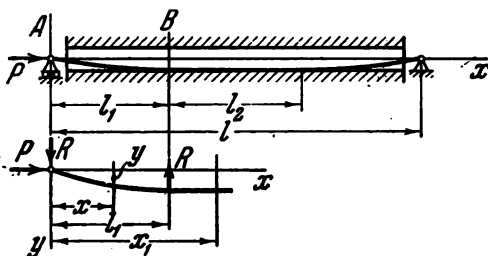


Fig. 342

Suppose that when  $P > \pi^2 EI/l^2$  there is a zone  $l_2$  of close attachment of the bar to the walls of the tube (Fig. 342). We set up the equation of the elastic curve of the bar in the portion  $0 \leq x \leq l_1$

$$EIy'' + Py = Rx,$$

$$y = A \sin \alpha x + B \cos \alpha x + \frac{R}{P} x \quad \left( \alpha^2 = \frac{P}{EI} \right);$$

$$\text{when } x=0, \quad y=0;$$

$$\text{when } x=l_1, \quad y=\Delta;$$

$$\text{when } x=l_1, \quad y'=0,$$

whence  $B=0$ ,

$$\left. \begin{aligned} A \sin \alpha l_1 + \frac{R}{P} l_1 &= \Delta, \\ A \alpha \cos \alpha l_1 + \frac{R}{P} &= 0. \end{aligned} \right\} \quad (1)$$

In the portion  $l_2$  the bar remains straight. Consequently, in this portion  $M_b = 0$ . Hence, according to Fig. 342

$$P\Delta - Rx_1 + R(x_1 - l_1) = 0,$$

whence

$$R = P \frac{\Delta}{l_1}.$$

From Eqs. (1) we find

$$A = \frac{\Delta}{\pi},$$

$$l_1 = \frac{\pi}{\alpha}, \quad P = \frac{\pi^2 EI}{l_1^3}, \quad (2)$$

$$y = \frac{\Delta}{\pi} (\sin \alpha x + \alpha x); \quad (3)$$

from expression (2) it follows that when  $l_1 = l/2$

$$P = \frac{4\pi^2 EI}{l^2}. \quad (4)$$

This means that in the case

$$\frac{\pi^2 EI}{l^2} < P < \frac{4\pi^2 EI}{l^2}$$

the bar makes contact with the wall at a single point, and it is only when

$$P > \frac{4\pi^2 EI}{l^2}$$

that attachment takes place over a certain portion.

If the middle straight portion becomes sufficiently long, there may also be an instability in it. We determine the length  $l_1$  at which this occurs. The critical force for the middle portion is

$$P = \frac{4\pi^2 EI}{l_2^3} \quad (l_2 = l - 2l_1).$$

But, on the other hand,  $P = \frac{\pi^2 EI}{l_1^3}$ . By equating these forces, we find

$$l_1 = \frac{l}{4}, \quad P = \frac{16\pi^2 EI}{l^2}.$$

After the middle portion has bent,  $l_1$  abruptly changes its value and becomes equal to  $l/6$ . Considering, now, each one-third of the bar as a new independent bar, we may retain the above equations by replacing  $l$  by  $l/3$  in them. Expression (4) then gives

$$l_1 = \frac{l}{6}, \quad P = \frac{36\pi^2 EI}{l^2}.$$

This means that when

$$P > \frac{36\pi^2 EI}{l^2}$$

the bar becomes again attached to the walls over some portions. When

$$\frac{16\pi^2 EI}{l^2} < P < \frac{36\pi^2 EI}{l^2}$$

the bar makes contact with the walls at three points.

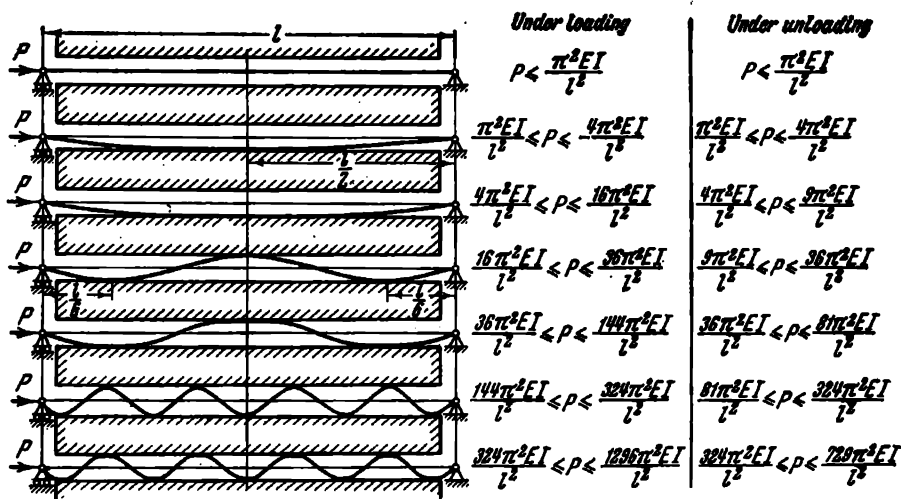


Fig. 343

During unloading, the bar separates off from the upper wall, not at the force  $P = 16\pi^2 EI/l^2$ , but obviously at  $P = 9\pi^2 EI/l^2$ .

Figure 343 shows the basic forms of equilibrium of the bar and gives the ranges of forces under loading and unloading.

For all values of the force  $P$ , the curved portions of the bar from the inflection point to the adjacent point of attachment to the wall are of length  $l_1$  and are described by expression (3) set up for the extreme left portion. The bending moment

$$EIy'' = -EI \frac{\Delta\pi}{l_1^3} \sin \alpha x$$

has a maximum value  $M_{\max} = EI \frac{\Delta\pi}{l_1^3}$ .

The maximum stress is

$$\sigma_{\max} = \frac{P}{A} + \frac{EI\Delta\pi}{l_1^3 Z},$$

where  $Z$  is the section modulus.

If the bar has a circular cross section, then

$$\sigma_{\max} = \frac{P4}{\pi d^2} + \Delta \frac{\pi}{2} \frac{Ed}{l_1^3}. \quad (5)$$

Consider two examples.

(1) Suppose that the force  $P$  compressing the bar is equal to

$$\frac{30\pi^2 EI}{l^2}.$$

From the drawings (Fig. 343) we see that in the range

$$\frac{16\pi^2 EI}{l^2} \leq P \leq \frac{36\pi^2 EI}{l^2}$$

$$l_1 = \text{constant} = \frac{l}{6}.$$

Expression (5) gives

$$\sigma_{\max} = \frac{3\pi dE}{8l^2} (5\pi d + 48\Delta).$$

(2) Suppose that the force  $P = 49\pi^2 EI/l^2$ . In the range

$$\frac{36\pi^2 EI}{l^2} \leq P \leq \frac{144\pi^2 EI}{l^2}$$

$l_1$  depends on  $P$ . Consequently, according to expression (2)

$$l_1 = \frac{\pi}{\sqrt{\frac{P}{EI}}} = \frac{l}{7}.$$

Then from formula (5)

$$\sigma_{\max} = \frac{49\pi dE}{16l^2} (\pi d + 8\Delta).$$

**122.** On the elastic curve of the deflected bar (Fig. 344) the points of inflection separate the portions of the bar having, respectively, the rigidities  $EI_1$  and  $EI_2$ . The length of the

segment  $l_1$  is determined from the condition of equal critical forces for the portions. Obviously,

$$P_{cr} = \frac{\pi^2 EI_1}{4l_1^2} = \frac{\pi^2 EI_2}{(l - 2l_1)^2}, \quad (1)$$

whence

$$l_1 = \frac{l}{2} \frac{\sqrt{k}}{\sqrt{k} + 1},$$

where

$$k = \frac{EI_1}{EI_2}.$$

If  $k = 1$ , then, as might be expected,  $l_1 = l/4$ . When  $k = 0$ , we have  $l_1 = 0$ , and when  $k = \infty$ , we obtain  $l_1 = l/2$ . The shape of the elastic curve of the deflected bar for

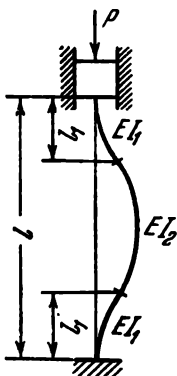


Fig. 344

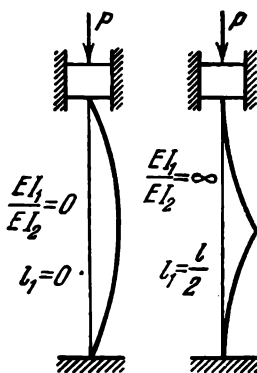


Fig. 345

these special cases is shown in Fig. 345. The critical force is determined from expression (1) by eliminating  $l_1$

$$P_{cr} = \frac{\pi^2 EI_1}{l^2} \frac{(1 + \sqrt{k})^2}{k}. \quad (2)$$

If when instability occurs the bar buckles in the opposite direction, i.e., not to the right, but to the left, the rigidities  $EI_1$  and  $EI_2$  must be interchanged in the expressions obtained. The length  $l_1$  then changes, but the critical force, re-

mains the same. Indeed, if the bar buckles to the left, replacing  $EI_1$  by  $EI_2$  gives

$$P_{cr} = \frac{\pi^2 EI_2}{l^2} \frac{\left(1 + \sqrt{\frac{1}{k}}\right)^2}{\frac{1}{k}},$$

which leads to expression (2).

123. If the bar is deflected from the vertical (Fig. 346), we see that the position of the weight does not change. The force  $P$  does no work. The stability of the straight-line form of equilibrium is maintained for any  $P$ .

124. Naturally, in contrast to the preceding case, here the bar loses stability when  $P = \pi^2 EI/4l^2$ .

So long as the rope has not lain down on the tube wall, i.e., so long as the deflection  $f$  has not exceeded  $\Delta$ , the relation between  $P$  and  $f$  is expressed by a segment of the straight line

$$P = \frac{\pi^2 EI}{4l^2} = \text{constant}$$

(Fig. 348). The deflection is undetermined. The departures from this straight line can be revealed only by using the theory of large displacements. A curious feature of the problem is that subsequently, with increasing deflections, the displacement  $f$  is again determined on the basis of the ordinary linear theory.

After a part of the rope has lain down on the curved wall of the tube, we have two portions,  $OA$  and  $AB$  (Fig. 347).

In the portion  $OA$  the bending moment is equal to  $P\Delta$ , and the tube is bent into a second-order curve

$$y = \frac{P\Delta}{2EI} x^2.$$

The deflection at the point  $A$  is

$$f_1 = \frac{P\Delta}{2EI} (l-a)^2.$$

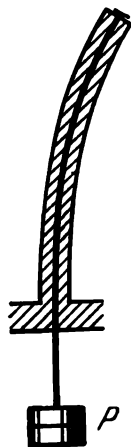


Fig. 346

If the bar were not bent in the portion  $AB$ , the displacement at the point  $B$  would be as follows:

$$\frac{P\Delta}{2EI} (l-a)^2 + y'_{x=l-a} a = \frac{P\Delta}{2EI} (l-a)^2 + \frac{P\Delta}{EI} (l-a) a.$$

But the second portion curves just far enough for the point  $B$

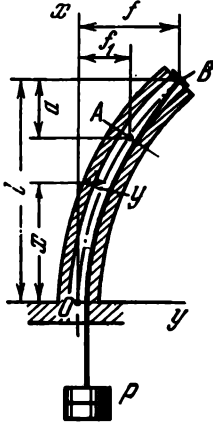


Fig. 347

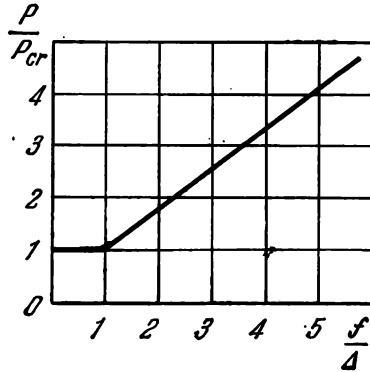


Fig. 348

to depart from the tangent  $AB$  by  $\Delta$ . Consequently,

$$f = \frac{P\Delta}{2EI} (l-a)^2 + \frac{P\Delta}{EI} (l-a) a + \Delta$$

or

$$f = \frac{P\Delta}{2EI} (l^2 - a^2) + \Delta.$$

The quantity  $a$  represents the length of a bar fixed at one end which loses stability under the force  $P$ , i.e.,

$$P = \frac{\pi^2 EI}{4a^2}.$$

Consequently,  $a^2 = \pi^2 EI/4P$  and then

$$f = \Delta \left( \frac{Pl^2}{2EI} - \frac{\pi^2}{8} + 1 \right)$$

or

$$\frac{f}{\Delta} = \frac{\pi^2}{8} \left( \frac{P}{P_e} - 1 \right) + 1,$$

where  $P_e = \pi^2 EI / 4l^2$ . The relation between  $f$  and  $P$  is shown in Fig. 348.

125. In the second case the critical force is four times greater than in the first case. To verify this, it is sufficient to consider the column in both cases in the deflected condition (Fig. 349).

In the first case

$$P_{cr} = \frac{\pi^2 EI}{4l^2}.$$

In the second case, as the rod bends, the force follows up its lower end, and in consequence the bending moment at the

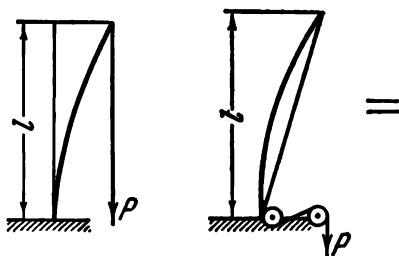


Fig. 349

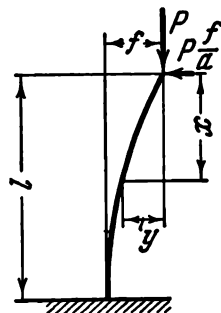


Fig. 350

fixed end is zero at all times. Hence, the second case of loading the column differs in no way from the case of a hinged-ended column (Fig. 349). Here, therefore,  $P_{cr} = \pi^2 EI / l^2$ .

126. We resolve the force  $P$  into a vertical and a horizontal component (Fig. 350)

$$P_v \cong P, \quad P_h \cong P \frac{f}{a}$$

and write the equation of the elastic curve of the beam

$$EIy'' = -Py + P \frac{f}{a} x.$$

Denote  $\frac{P}{EI} = \alpha^2$ . The equation and its solution are then

$$y'' + \alpha^2 y = \alpha^2 \frac{f}{a} x,$$

$$y = A \sin \alpha x + B \cos \alpha x + \frac{f}{a} x.$$

To determine  $A$ ,  $B$ , and  $f$  we have the following boundary conditions:

$$\begin{aligned} \text{when } x = 0, \quad y &= 0; \\ \text{when } x = l, \quad y &= f \text{ and } y' = 0, \end{aligned}$$

whence

$$B = 0, \quad A \sin \alpha l + \frac{f}{a} l = f, \quad A \alpha \cos \alpha l + \frac{f}{a} = 0.$$

The critical value of the force  $P$  is found from the following transcendental equation:

$$\tan \alpha l = \alpha l \left( 1 - \frac{a}{l} \right). \quad (1)$$

If  $a = \infty$  (the first case of the preceding problem),

$$\alpha l = \frac{\pi}{2}, \quad P_{\text{cr}} = \frac{\pi^2 EI}{4l^2}.$$

If  $a = l$  (the second case of the preceding problem),

$$\alpha l = \pi, \quad P_{\text{cr}} = \frac{\pi^2 EI}{l^2}.$$

When  $a = 0$ , the line of action of the force always intersects the initial vertical at the point  $x = 0$ . This is possible

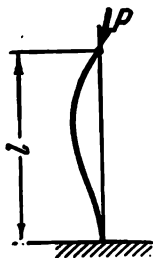


Fig. 351

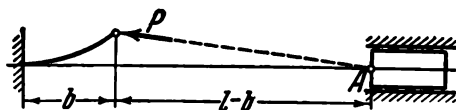


Fig. 352

only if the end of the bar does not move (Fig. 351). Then

$$\tan \alpha l = \alpha l, \quad \alpha l = 4.49, \quad P_{\text{cr}} = 20.19 \frac{EI}{l^2}.$$

127. After investigation of the preceding two problems the correct solution of this problem presents no difficulty.

The left-hand bar of length  $b$  is subjected to a turning compressive force (Fig. 352) whose line of action always passes through the point  $A$ . Hence, the critical force for the

left-hand bar is not  $\pi^2 EI/4b^2$ , as may seem at first glance, but is given by the transcendental equation (1) of the preceding problem if  $b$  is written for  $l$  in it and  $a$  is replaced by  $a = -(l - b)$ , i.e.,  $\tan \alpha b = \alpha l$ , where  $\alpha = \sqrt{P/EI}$ .

The critical force for the right-hand bar is

$$P_{cr} = \frac{\pi^2 EI}{(l-b)^2}.$$

The stability factor for the bars will be the same if the critical forces are equal. Hence,

$$\alpha = \sqrt{\frac{P_{cr}}{EI}} = \frac{\pi}{l-b}, \quad \tan \frac{\pi b}{l-b} = \frac{\pi l}{l-b}.$$

From this we find the required ratio  $b/l$

$$\tan \frac{\pi \frac{b}{l}}{1 - \frac{b}{l}} = \frac{\pi}{1 - \frac{b}{l}}, \quad \frac{b}{l} = 0.301.$$

128. To determine the critical force there is no need to consider the contact pressure between the bar and the rope.

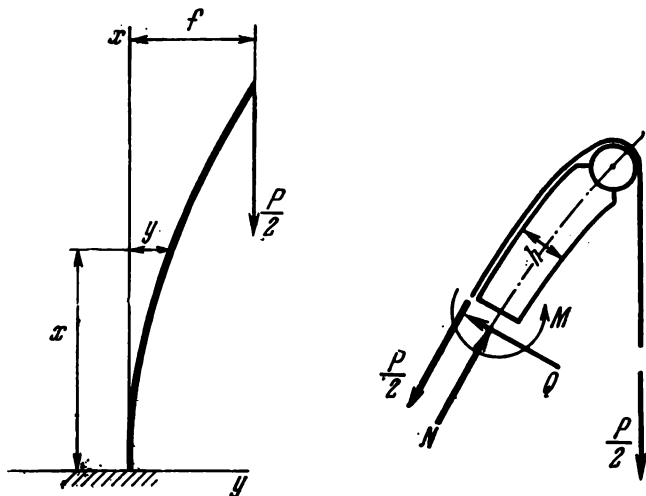


Fig. 353

We cut off a part of the bar (Fig. 353) and determine the bending moment

$$M = \frac{P}{2} \left( f - y + \frac{h}{2} \right) - \frac{P}{2} \frac{h}{2},$$

where  $h/2$  is half the thickness of the bar. Hence,

$$EIy'' = \frac{P}{2} (f - y).$$

Thus, we have the usual case of a fixed bar loaded by the force  $P/2$

$$\left(\frac{P}{2}\right)_{\text{cr}} = \frac{\pi^2 EI}{4l^2}.$$

129. Suppose that the upper end of the bar undergoes a horizontal displacement  $f$  (Fig. 354a). The angle of inclination of the left half of the rope is then reduced by  $\Delta\alpha$  and the angle of inclination of the right half is increased by the same amount. As a result, a horizontal force is developed, equal to

$$P_1 = N \cos(\alpha - \Delta\alpha) - N \cos(\alpha + \Delta\alpha),$$

where  $N$  is the tension in the rope.

Since  $\Delta\alpha$  is small, we have

$$P_1 = 2N \sin \alpha \cdot \Delta\alpha.$$

But  $2N \sin \alpha = P$ , hence  $P_1 = P \Delta\alpha$ . Further, from the triangle  $ABC$  it follows that

$$OA \cdot \Delta\alpha = f \sin \alpha$$

and since  $OA = \frac{l}{\sin \alpha}$  we have

$$\Delta\alpha = \frac{f}{l} \sin^2 \alpha$$

and

$$P_1 = P \frac{f}{l} \sin^2 \alpha.$$

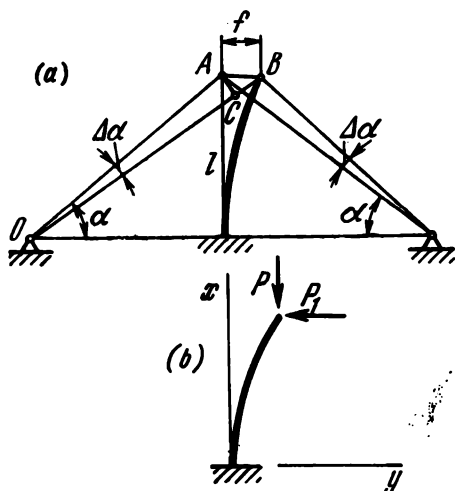


Fig. 354

It remains to determine the critical force for a bar at the free end of which (Fig. 354b) is applied a vertical force  $P$  and a horizontal force  $P_1$

$$EIy'' = P(f - y) - P \frac{f}{l} \sin^2 \alpha \cdot (l - x).$$

Denoting  $P/EI = k^2$ , we obtain

$$y'' + k^2 y = k^2 f - k^2 \frac{f}{l} (l - x) \sin^2 \alpha.$$

Further,

$$y = A \sin kx + B \cos kx + f - \frac{f}{l} (l - x) \sin^2 \alpha.$$

When  $x = 0$ ,  $y = 0$  and  $y' = 0$ ; when  $x = l$ ,  $y = f$ . This leads to the system of equations

$$B + f \cos^2 \alpha = 0, \quad Ak + \frac{f}{l} \sin^2 \alpha = 0,$$

$$A \sin kl + B \cos kl = 0.$$

By equating the determinant to zero, we arrive at the transcendental equation

$$\tan kl = -kl \cot^2 \alpha.$$

From this we determine the value of  $kl$  as a function of  $\alpha$ . Thus, the critical force depends on the angle of inclination of the ropes.

As the angle  $\alpha$  decreases, the critical force for the bar approaches the value

$$P_{cr} = \frac{\pi^2 EI}{4l^2},$$

but then the force  $N$  in the rope tends to infinity.

If  $\alpha = \pi/2$ , then  $kl = \pi$  and

$$P_{cr} = \frac{\pi^2 EI}{l^2}.$$

130. Consider the conditions of equilibrium for a bent element of the ring, of length  $ds$  (Fig. 355).

At the sections of the ring there is a shearing force  $Q$ , a bending moment  $M$ , and a normal force which is represented

as a sum of a subcritical force  $qR$  and a small addition  $N$ . Any specific feature of the behaviour of the external load is accounted for by introducing a normal component  $q_n$  and a tangential component  $q_t$ . In particular, if the ring is loaded by gas or fluid pressure,  $q_n = q_t = 0$ . The new local radius of curvature of the element is denoted by  $R_1$

$$\frac{1}{R_1} = \frac{1}{R} - \kappa, \quad (1)$$

where  $\kappa$  is the change in curvature of the arc of the ring.

We set up the equations of equilibrium for the element

$$Q = \frac{dM}{ds}, \quad \frac{dN}{ds} + q_t + \frac{Q}{R_1} = 0,$$

$$q + q_n + \frac{dQ}{ds} - \frac{N + qR}{R_1} = 0.$$

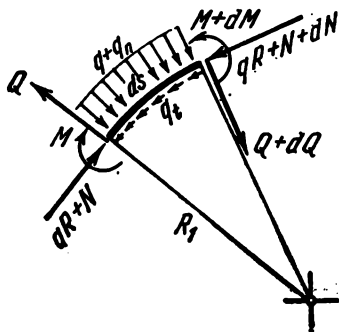


Fig. 355

We eliminate  $1/R_1$  and, noting that  $\kappa$ ,  $Q$ , and  $N$  are small quantities, we retain their first powers only. Then

$$Q = \frac{dM}{ds}, \quad \frac{dN}{ds} + q_t + \frac{Q}{R} = 0, \quad qR\kappa + q_n + \frac{dQ}{ds} - \frac{N}{R} = 0.$$

Since  $M = EI\kappa$ , on eliminating further  $N$  and  $Q$ , we obtain

$$EI \frac{d^3\kappa}{ds^3} + \left( qR + \frac{EI}{R^2} \right) \frac{d\kappa}{ds} + \frac{dq_n}{ds} + \frac{1}{R} q_t = 0. \quad (2)$$

Suppose that the ring is loaded by a pressure which follows up the normal to the surface. Then, as already noted,  $q_n = q_t = 0$  and

$$EI \frac{d^3\kappa}{ds^3} + \left( qR + \frac{EI}{R^2} \right) \frac{d\kappa}{ds} = 0.$$

Assuming  $\kappa = A \sin \frac{ns}{R}$ , we find

$$-EI \frac{n^3}{R^3} + \left( qR + \frac{EI}{R^2} \right) \frac{n}{R} = 0,$$

whence

$$q_{cr} = \frac{(n^2 - 1) EI}{R^3}.$$

The quantity  $q_{cr}$  assumes the smallest non-zero value when  $n = 2$ . As a result, we obtain

$$q_{cr} = \frac{3EI}{R^3}.$$

Let us now consider the other method of producing the load  $q$ . Suppose that the ring is loaded by radial forces produced by means of a large number of rubber cords joined together at the centre (Fig. 124b). In this case the load  $q$  follows up the centre of the ring. As the arc  $ds$  turns, a tangential load component is developed, equal to

$$q_t = q \frac{dw}{ds},$$

where  $w$  is the radial displacement of the points of the ring.

If the cords are sufficiently flexible or if each of them is tensioned independently, the normal component of the external forces does not change during the displacements  $w$ , and hence  $q_n = 0$ .

The change in curvature  $\kappa$  is expressed in terms of  $w$  as follows:

$$\kappa = \frac{d^2w}{ds^2} + \frac{w}{R^2};$$

Eq. (2) then takes the form

$$EI \frac{d^3}{ds^3} \left( \frac{d^2w}{ds^2} + \frac{w}{R^2} \right) + \\ + \left( qR + \frac{EI}{R^2} \right) \frac{d}{ds} \left( \frac{d^2w}{ds^2} + \frac{w}{R^2} \right) + \frac{q}{R} \frac{dw}{ds} = 0. \quad (3)$$

Assuming  $w = A \sin \frac{ns}{R}$ , we obtain

$$q_{cr} = \frac{(n^2 - 1)^2 EI}{(n^2 - 2) R^3}.$$

When  $n = 2$ ,

$$q_{cr} = \frac{9EI}{2R^3},$$

i.e., the critical load is 1.5 times higher than under hydrostatic loading.

If the cords possessing some stiffness are tensioned by a common weight, a redistribution of forces takes place when

the ring is bent. In the region of positive  $w$  the cords are further extended, and in the region of negative  $w$  they are shortened. There is a change in the normal component  $q_n$ . In Eq. (3) we then obtain an additional term  $q_n = Kw$ , where  $K$  is the stiffness factor for the cords. Finally,

$$q_{cr} = \frac{EI}{R^3} \frac{(n^2 - 1)^2 + \frac{KR^4}{EI}}{n^2 - 2}.$$

Increasing the stiffness  $K$  of the cords leads to an increase in the critical load. This is self-evident. The resulting additional forces are so directed that they restore the circular shape of the ring. The lowest critical value  $q_{cr}$  is generally attained not for  $n = 2$ , but for some other integral  $n$  depending on the magnitude of  $K$ .

131. Consider the system in the deflected position of equilibrium (Fig. 356).

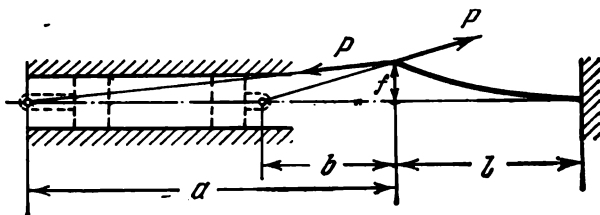


Fig. 356

The length  $a$  of the tie rods is greater than the length  $b$  of the piston rod. Hence, an upward force component is induced, equal to

$$P_1 = P \left( \frac{f}{b} - \frac{f}{a} \right).$$

The deflection  $f$  under the action of this force is

$$f = \frac{P_1 l^3}{3EI}.$$

By eliminating  $P_1$ , we find the value of the critical force

$$P_{cr} = \frac{3EI}{l^3} : \left( \frac{1}{b} - \frac{1}{a} \right).$$

132. The subject of this problem is the same as that of Prob. 131. In the original state the moments are mutually balanced and the bar is unstressed. When the system is deflected, however, the moments behave differently. If the bending occurs in the  $xz$  plane (Fig. 357), the plane of the moment  $M_2$  rotates together with the end section. The plane of the moment  $M_1$  remains unchanged. If the bending takes place in the  $xy$  plane, the plane of  $M_2$  does not change, but the plane of action of the moment  $M_1$  turns.

For simplicity, suppose that the lengths of the ropes, through which the forces  $P$  are transmitted, are sufficiently great. This enables us to assume that the rotation of the moment  $M_1$  in one plane and of  $M_2$  in the other plane is completely coincident with the rotation of the end section. The angles of rotation of this section about the  $y$  and  $z$  axes are denoted by  $\varphi_y$  and  $\varphi_z$ , respectively. The moments at the current section  $A$  about the moving  $y_1$  and  $z_1$  axes are then

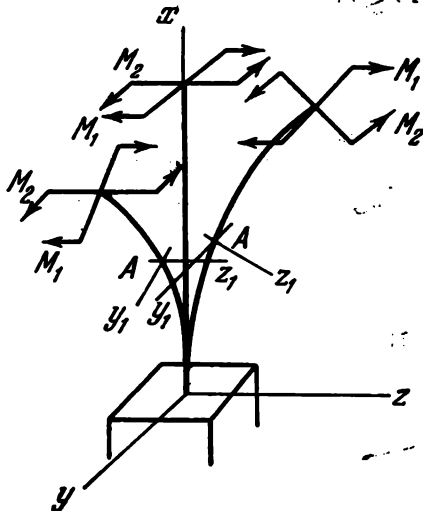


Fig. 357

$$M_{y_1} = M_1 (\varphi_z - y') + M_2 y',$$

$$M_{z_1} = M_1 z' + M_2 (\varphi_y - z').$$

We obtain, finally, two equations

$$\left. \begin{aligned} EI_y z'' &= M_1 (\varphi_z - y') + M_2 y', \\ EI_z y'' &= M_1 z' + M_2 (\varphi_y - z'). \end{aligned} \right\} \quad (1)$$

Since  $I_y = I_z = I$  and  $M_1 = M_2$ , we have

$$EI z'' = M \varphi_z, \quad EI y'' = M \varphi_y,$$

whence

$$\begin{aligned} z &= \frac{M}{EI} \left( \varphi_z \frac{x^2}{2} + A_1 x + B_1 \right), \\ y &= \frac{M}{EI} \left( \varphi_y \frac{x^2}{2} + A_2 x + B_2 \right). \end{aligned}$$

When  $x = 0$ , we have  $z = 0$ ,  $z' = 0$ ,  $y = 0$ ,  $y' = 0$ ; hence  $A_1 = A_2 = 0$ ,  $B_1 = B_2 = 0$ . When  $x = l$ ,  $y' = \varphi_z$  and  $z' = \varphi_y$ ; then

$$\varphi_y = \frac{Ml}{EI} \varphi_z, \quad \varphi_z = \frac{Ml}{EI} \varphi_y.$$

It is obvious that  $\varphi_y$  and  $\varphi_z$  are not zero only if

$$\frac{Ml}{EI} = \pm 1,$$

which gives the value of the critical moment.

133. We revert to Eqs. (1) of the preceding problem. On putting  $M_1 = M$  and  $M_2 = 0$ , we obtain

$$EI_y z'' = M (\varphi_z - y'),$$

$$EI_z y'' = M z'.$$

Hence,

$$y = A \sin \alpha x + B \cos \alpha x + \varphi_z x + C,$$

$$z = \frac{EI_z}{M} (A \alpha \cos \alpha x - B \alpha \sin \alpha x + \varphi_z + D),$$

where

$$\alpha^2 = \frac{M^2}{EI_y EI_z}.$$

When  $x = 0$ , we have  $y = z = 0$  and also  $y' = z' = 0$ . Then

$$B + C = 0, \quad A \alpha + \varphi_z = 0,$$

$$A \alpha + \varphi_z + D = 0, \quad B \alpha^2 = 0,$$

whence

$$B = C = D = 0.$$

When  $x = l$ , the angle  $y' = \varphi_z$ . This gives  $A \cos \alpha l = 0$ . Consequently, the critical state occurs when

$$\alpha l = \frac{\pi}{2}$$

or

$$\frac{Ml}{\sqrt{EI_y EI_z}} = \frac{\pi}{2}.$$

Interchanging  $I_y$  and  $I_z$  does not alter the value of the critical moment. The cases of loading shown in Fig. 127a and b are therefore equivalent.

134. The differential equation of the elastic curve of the bar (Fig. 358) is

$$EIy'' = P(f + R\varphi - y),$$

whence

$$y = A \sin \alpha x + B \cos \alpha x + f + R\varphi,$$

where, as usual,  $\alpha^2 = \frac{P}{EI}$ .

When  $x = 0$ ,  $y = 0$  and  $y' = 0$ ; when  $x = l$ ,  $y = f$  and  $y' = \varphi$ . This gives

$$B + f + R\varphi = 0, \quad A = 0,$$

$$A \sin \alpha l + B \cos \alpha l + R\varphi = 0,$$

$$A\alpha \cos \alpha l - B\alpha \sin \alpha l = \varphi.$$

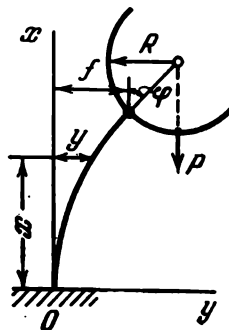


Fig. 358

We set up the determinant of the system of three equations in the unknowns  $B$ ,  $f$ , and  $\varphi$  and equate it to zero. This

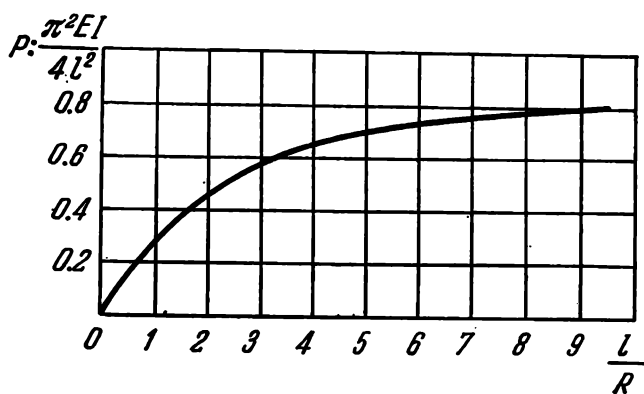


Fig. 359

gives the transcendental equation

$$\frac{l}{R} = \alpha l \tan \alpha l.$$

The relation between the critical force and  $l/R$  is shown in Fig. 359.

135. The differential equation of the elastic curve of the bar (Fig. 360) is as follows:

$$EIy'' = P(f - y) + M. \quad (1)$$

The force  $P$  is obviously equal to the weight of liquid  $P = \gamma\pi R^2 h$ , where  $\gamma$  is the specific weight of liquid.

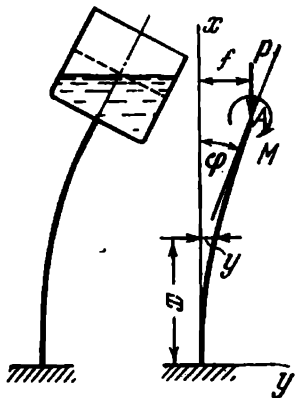


Fig. 360

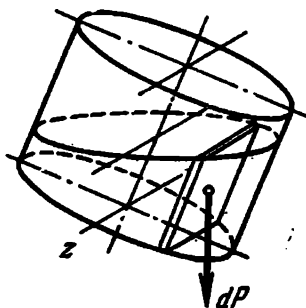


Fig. 361

The moment  $M$  is determined by summing the moments of the elementary forces  $dP$  (Fig. 361) about the  $z$  axis. The angle of rotation  $\varphi$  of the tank is assumed small. On integrating we obtain

$$M = \frac{\gamma\pi R^2}{4} (2h^2 + R^2) \varphi. \quad (2)$$

We solve Eq. (1)

$$y = A \sin \alpha x + B \cos \alpha x + f + \frac{2h^2 + R^2}{4h} \varphi.$$

When  $x=0$ ,  $y=0$  and  $y'=0$ ; when  $x=l$ ,  $y=f$  and  $y'=\varphi$ . These conditions give

$$B + f + \frac{2h^2 + R^2}{4h} \varphi = 0, \quad A = 0,$$

$$A \sin \alpha l + B \cos \alpha l + \frac{2h^2 + R^2}{4h} \varphi = 0,$$

$$A\alpha \cos \alpha l - B\alpha \sin \alpha l = \varphi.$$

From the last two equations we find

$$\frac{\alpha l \tan \alpha l}{4 \frac{h}{l}} \left( 2 \frac{h^2}{l^2} + \frac{R^2}{l^2} \right) = 1.$$

Substituting the value of  $P$ , we obtain

$$\alpha l = \sqrt{\frac{P}{EI}} l = \sqrt{\frac{\gamma \pi R^2 l^3}{EI}} \sqrt{\frac{h}{l}}.$$

The required quantity  $h/l$  is then determined from the transcendental equation

$$\frac{a}{4} \frac{\tan a \sqrt{\frac{h}{l}}}{\sqrt{\frac{h}{l}}} \left( 2 \frac{h^2}{l^2} + b^2 \right) = 1 \quad (3)$$

and depends on two parameters, viz.

$$a = \sqrt{\frac{\gamma \pi R^2 l^3}{EI}} \quad \text{and} \quad b = \frac{R}{l}.$$

In each specific case the level of the liquid at which instability occurs can be found in terms of these parameters.

If the filling of the tank did not possess the properties of fluidity (for example, if the tank were filled with sand), the moment  $M$  would be less than (2), namely

$$M = \gamma \pi R^2 \frac{h^2}{2} \varphi.$$

This would lead to an appreciable increase in the critical load. The difference in critical load is larger the larger the diameter of the tank. The mobility of the filling accounts for the fact that there may also be an instability in the scheme shown in Fig. 362. The critical level of the filling  $h/l$  is determined from the same transcendental equation (3) by replacing the circular by the hyperbolic tangent.

136. The free length of the bar before the application of the force  $P$  is denoted by  $l_0$ . The length of the bar at the

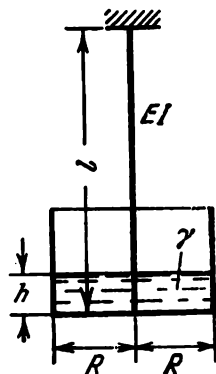


Fig. 362

moment of instability is

$$l = l_0 + \frac{P_{cr}}{2k}. \quad (1)$$

Consider the bar in a displaced position (Fig. 363a). By removing the springs, we obtain a system of forces acting on the strip. This force system is shown in Fig. 363b. The first spring exerts the force  $P/2 - ka\varphi$ , and the second spring  $P/2 + ka\varphi$ , where  $\varphi$  is the angle of rotation of the strip.

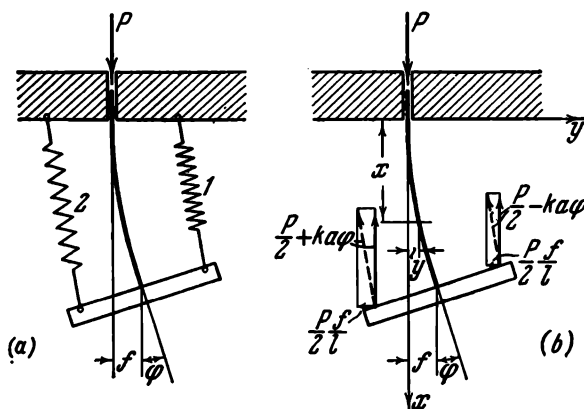


Fig. 363

Each of these forces is resolved into a vertical and a horizontal component. Because of the smallness of the angles the vertical components remain approximately equal to the total values of the forces

$$\frac{P}{2} - ka\varphi \quad \text{and} \quad \frac{P}{2} + ka\varphi.$$

The horizontal components for the first and second springs are, respectively,

$$\frac{f}{l - a\varphi} \left( \frac{P}{2} - ka\varphi \right), \quad \frac{f}{l + a\varphi} \left( \frac{P}{2} + ka\varphi \right),$$

where  $f$  is the displacement of the end of the bar. Retaining only the first powers of the displacements, we obtain

$$\frac{P}{2} \frac{f}{l} \quad \text{and} \quad \frac{P}{2} \frac{f}{l}.$$

We now set up the differential equations of the deflected axis of the bar

$$EIy'' = \left(\frac{P}{2} - ka\varphi\right)(f + a - y) + \left(\frac{P}{2} + ka\varphi\right)(f - a - y) - \\ - \frac{P}{2} \frac{f}{l}(l - x) - \frac{P}{2} \frac{f}{l}(l - x)$$

or

$$y'' + \alpha^2 y = \alpha^2 \frac{f}{l} x - \frac{2ka^2}{EI} \varphi \quad \left(\alpha^2 = \frac{P}{EI}\right),$$

whence

$$y = A \sin \alpha x + B \cos \alpha x + \frac{f}{l} x - \frac{2ka^2}{EI\alpha^2} \varphi.$$

When  $x = 0$ ,  $y = 0$  and  $y' = 0$ ; when  $x = l$ ,  $y = f$  and  $y' = \varphi$ . According to these conditions we obtain

$$B - \frac{2ka^2}{EI\alpha^2} \varphi = 0, \quad A\alpha + \frac{f}{l} = 0,$$

$$A \sin \alpha l + B \cos \alpha l - \frac{2ka^2}{EI\alpha^2} \varphi = 0,$$

$$A\alpha \cos \alpha l - B\alpha \sin \alpha l + \frac{f}{l} - \varphi = 0.$$

By considering  $A$ ,  $B$ ,  $f$ , and  $\varphi$  as unknowns, we equate to zero the determinant of this system

$$\begin{vmatrix} 0 & 1 & 0 & -\frac{2ka^2}{EI\alpha^2} \\ \alpha & 0 & \frac{1}{l} & 0 \\ \sin \alpha l & \cos \alpha l & 0 & -\frac{2ka^2}{EI\alpha^2} \\ \alpha \cos \alpha l & -\alpha \sin \alpha l & \frac{1}{l} & -1 \end{vmatrix} = 0,$$

whence

$$\frac{\alpha l \sin \alpha l}{1 - \cos \alpha l} = -\frac{4ka^2 l}{EI}. \quad (2)$$

The unknown force  $P_{cr}$  enters into both  $\alpha$  and  $l$ . Substitute for  $l$  from (1), i.e.,

$$l = l_0 + \frac{P_{cr}}{2k} = l_0 \left[ 1 + \alpha_0^2 l_0^3 \frac{EI}{2kl_0^3} \right].$$

Equation (2) then becomes

$$\frac{\alpha l_0 \sin [\alpha l_0 (1 + c \alpha^2 l_0^2)]}{1 - \cos [\alpha l_0 (1 + c \alpha^2 l_0^2)]} = - \frac{a^2}{l_0^3} \frac{2}{c}, \quad (3)$$

where

$$c = \frac{EI}{2kl_0^3}. \quad (4)$$

From this equation, with given parameters  $a/l_0$  and  $c$ , we determine  $\alpha l_0$ , and then  $P_{cr}$ .

Figure 364 shows the relation between  $P_{cr}/P_e$  and  $a/l_0$  for several values of  $c$ . With increasing  $a/l_0$  the magnitude of

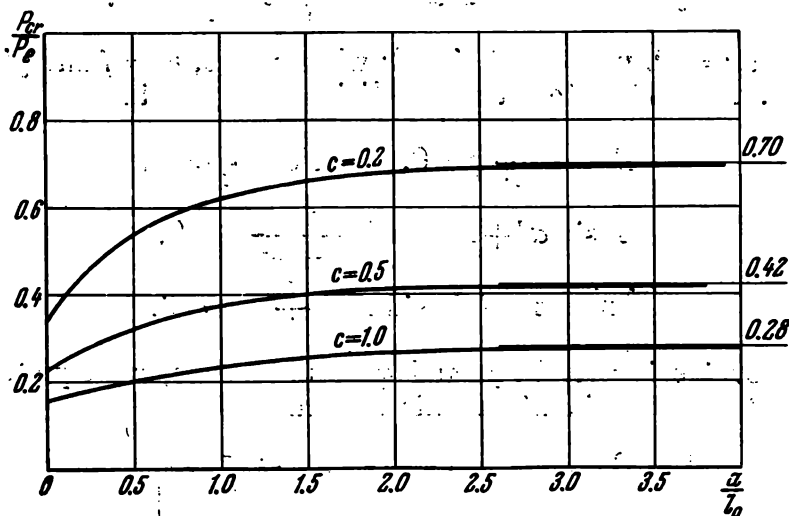


Fig. 364

$P_{cr}$  increases. Also,  $P_{cr}$  increases with decreasing  $c$ , i.e., with increasing spring stiffness  $k$ . When  $k = \infty$ , we have  $c = 0$ . If  $a/l_0 \neq 0$ , we then obtain

$$P_{cr} = \frac{4\pi^2 EI}{l_0^3}$$

i.e.,  $P_{cr}$  is equal to the critical force for a bar with fixed ends. If, however,  $a/l_0 = 0$ , but  $k$  is infinite, as before, we find

$$P_{cr} = \frac{\pi^2 EI}{l_0^3},$$

i.e.,  $P_{cr}$  is equal to the critical force for a bar with hinged ends.

137. The proposed problem involves fundamentally new aspects of stability and cannot be solved by the conventional methods.

Indeed, by reducing the compressive forces shown in Fig. 131c to the bar axis, we obtain the following scheme of loading (Fig. 365). The bar is compressed by the forces  $P$  and is simultaneously bent by two moments  $M = Pe$  in a sense opposite to the rotation of the ends.

The equation of the elastic curve is

$$EIy'' = -Py + Pe$$

or

$$y'' + \alpha^2 y = \alpha^2 e \quad \left( \alpha^2 = \frac{P}{EI} \right),$$

whence

$$y = A \sin \alpha x + B \cos \alpha x + e.$$

When  $x = 0$ , the deflection  $y = 0$ , as for  $x = 2l$ ; consequently,

$$A = e \frac{\cos 2\alpha l - 1}{\sin 2\alpha l}, \quad B = -e,$$

$$y = e \left[ \frac{\cos 2\alpha l - 1}{\sin 2\alpha l} \sin \alpha x - \cos \alpha x + 1 \right].$$

Thus, one obtains quite definite values of deflections which the bar would have if from the very beginning of loading to the bar were applied the moments  $Pe$  that would increase gradually with increased forces  $P$ . The above computations do not catch the critical transition from the straight-line form to the curvilinear form of equilibrium, and we obtain the case of bending induced by axial loading in pure form.

Consider the fundamental principles of stability. An elastic system is said to be stable if for any arbitrarily small (we emphasize arbitrarily small) displacement from the equilibrium position the system, when left to itself, returns to its original state.

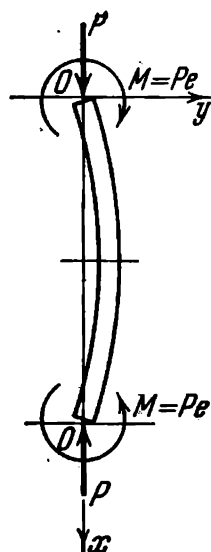


Fig. 365

It remains to be seen, however, whether the elastic system returns into its original position if it is displaced farther out, i.e., if it is given not an arbitrarily small displacement but simply a small but finite displacement larger than a certain preassigned value (even though a very small value). May it happen that the system returns into its original position under arbitrarily small displacements but does not return under certain small displacements larger than a preassigned value?

This may actually happen. The mechanical analogue of the above is provided, for example, by a ball resting on the top of a convexity in a small hollow (Fig. 366). If this ball is given a small displacement, it will return into its original position,

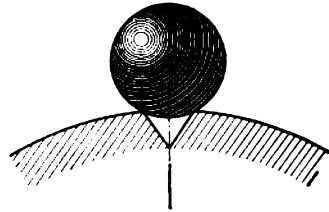


Fig. 366

but if a sufficiently large displacement is imparted, the ball will not return into its original position. If there were no hollow, the position of equilibrium would be simply unstable.

We thus arrive at a new assessment of stability based on imparting to a system not arbitrarily small but small disturbances greater than a preassigned value. This assessment of stability is termed the assessment of stability "in the large". The usual assessment of stability based on imparting to a system arbitrarily small displacements is termed the assessment of stability "in the small".

This terminology is carried over into the stability of elastic systems from the general theory of stability of motion and is at present conventional.

The bar in the example under consideration is stable in the small but not always stable in the large. Indeed, if we impart to the bar a very small displacement from the straight-line form of equilibrium, the restoring moment  $Pe$  will be larger than the disturbing moments  $Py$  (since  $y$  may be made arbitrarily small) and, upon removal of the causes that produced the small displacement, the bar will return to the straight-line form of equilibrium. This happens at any value of  $P$  not exceeding  $4\pi^2 EI/(2l)^2$  when the bar loses stability in the small in the form shown in Fig. 131b.

In actual conditions external disturbances (crookedness of a bar, non-axiality of the application of forces, accidental jerks) always have a finite value and, depending on these conditions, the bar passes into a new form of equilibrium at a larger or smaller force. Hence, the concept of stability and instability in the large is inevitably associated with the absence or presence of the corresponding external disturbances.

Stability in the large is an extension of the classical scheme and a closer approximation to our intuitive everyday concept of stability. This is a complex of the properties of a system and disturbances acting on the system. The analysis of possible forms of equilibrium is therefore only part of the investigation of stability and does not solve the problem completely. This will be seen from the solution of some of the problems considered below.

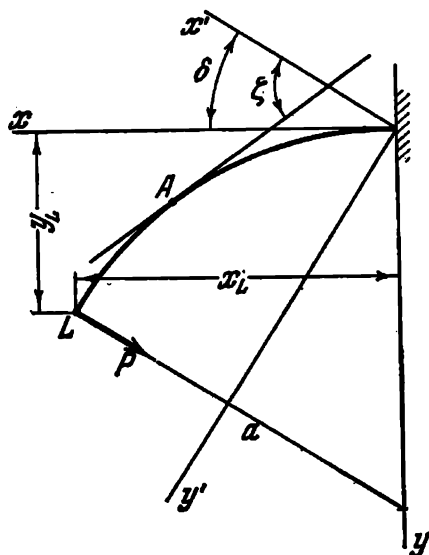


Fig. 367

Revert to the given scheme of a compressed bar and set up the equations of the elastic curve in terms of large displacements. Since these equations will be needed in what follows, we shall derive them here in somewhat more general form than is necessary in the solution of the problem under consideration.\*

Figure 367 shows a part of the bar severely bent by the force  $P$ . We introduce two systems of co-ordinates: a system  $xy$  oriented along the tangent and normal to the elastic curve at the fixed end and a system  $x'y'$  oriented along the force  $P$ .

\* This derivation is taken from the book by E. P. Popov, "Non-linear Problems in the Statics of Thin Bars", Gostekhizdat, Leningrad - Moscow, 1948.

Denote by  $\delta$  the angle between the direction of the force and the  $x$  axis (in our case  $\delta = 0$ );  $\zeta$  is the current angle between the tangent to an arc of the elastic curve and the  $x'$  axis.

The curvature of the rod at an arbitrary point is obviously expressed through the angle  $\zeta$  as follows:

$$\frac{1}{\rho} = \frac{d\zeta}{ds},$$

where  $ds$  is an element of arc length of the rod. The bending moment at the point  $A$  is

$$M_b = P (y'_L - y'),$$

where  $y'_L$  is the co-ordinate of the point  $L$ . It is now obvious that

$$\frac{d\zeta}{ds} = \frac{P}{EI} (y'_L - y').$$

We differentiate this expression with respect to  $s$

$$\frac{d^2\zeta}{ds^2} = -\frac{P}{EI} \frac{dy'}{ds};$$

but

$$\frac{dy'}{ds} = \sin \zeta,$$

hence,

$$\frac{d^2\zeta}{ds^2} = -\frac{P}{EI} \sin \zeta.$$

Denote

$$\frac{P}{EI} = \frac{\beta^2}{l^2}. \quad (1)$$

Then

$$l^2 \frac{d^2\zeta}{ds^2} = -\beta^2 \sin \zeta$$

or

$$l^2 d \left( \frac{d\zeta}{ds} \right) = -2\beta^2 \sin \frac{\zeta}{2} \cos \frac{\zeta}{2} ds.$$

We multiply both sides of equality by  $\frac{d\zeta}{ds}$  and integrate

$$\left( l \frac{d\zeta}{ds} \right)^2 = 4\beta^2 \left( C_1 - \sin^2 \frac{\zeta}{2} \right). \quad (2)$$

The constant  $C_1$  is denoted by  $k^2$  and  $\sin \frac{\zeta}{2}$  by  $k \sin \psi$ , i.e.,

$$\sin \frac{\zeta}{2} = k \sin \psi. \quad (3)$$

Equation (2) then becomes

$$l \frac{d\zeta}{ds} = 2\beta k \cos \psi. \quad (4)$$

But from (3)

$$\frac{d\zeta}{ds} = 2k \frac{\cos \psi}{\sqrt{1 - k^2 \sin^2 \psi}} \frac{d\psi}{ds};$$

hence,

$$l \frac{d\psi}{ds} = \beta \sqrt{1 - k^2 \sin^2 \psi}, \quad \beta \frac{ds}{l} = \frac{d\psi}{\sqrt{1 - k^2 \sin^2 \psi}}.$$

Integrating this expression, we obtain

$$\beta \frac{s}{l} = F(\psi) - F(\psi_0). \quad (5)$$

Here  $F(\psi)$  stands for the elliptic integral of the first kind

$$F(\psi) = \int_0^\psi \frac{d\psi}{\sqrt{1 - k^2 \sin^2 \psi}}.$$

The values of this integral are given by tables in terms of  $k$  and  $\psi$ .

We now determine the equation of the elastic curve  $x'(s)$  and  $y'(s)$

$$dx' = \cos \zeta ds, \quad dy' = \sin \zeta ds$$

or

$$dx' = \left(1 - 2 \sin^2 \frac{\zeta}{2}\right) ds, \quad dy' = 2 \sin \frac{\zeta}{2} \cos \frac{\zeta}{2} ds$$

Substituting

$$\sin \frac{\zeta}{2} = k \sin \psi,$$

we obtain

$$\begin{aligned} \frac{dx'}{l} &= \frac{2}{\beta} \sqrt{1 - k^2 \sin^2 \psi} d\psi - \frac{ds}{l}, \\ \frac{dy'}{l} &= \frac{2}{\beta} k \sin \psi d\psi. \end{aligned}$$

We integrate these expressions from zero to  $s$

$$\left. \begin{aligned} \frac{x'}{l} &= \frac{2}{\beta} [E(\psi) - E(\psi_0)] - \frac{s}{l}, \\ \frac{y'}{l} &= \frac{2}{\beta} k [\cos \psi_0 - \cos \psi], \end{aligned} \right\} \quad (6)$$

where  $E(\psi)$  stands for the elliptic integral of the second kind

$$E(\psi) = \int_0^\psi \sqrt{1 - k^2 \sin^2 \psi} \, d\psi.$$

This function is also given in tables.

By passing to the system of co-ordinates  $xy$ , we obtain

$$\left. \begin{aligned} \frac{x}{l} &= \frac{x'}{l} \cos \delta + \frac{y'}{l} \sin \delta, \\ \frac{y}{l} &= \frac{y'}{l} \cos \delta - \frac{x'}{l} \sin \delta. \end{aligned} \right\} \quad (7)$$

We now proceed to the boundary conditions for the bar under consideration. When  $s = l$ , we have  $M_b = Pe \cos \zeta_L$ . Consequently,

$$\frac{d\zeta}{ds} = - \frac{Pe \cos \zeta_L}{EI}$$

or according to (1)

$$\frac{d\zeta}{ds} l = -\beta^2 \frac{e}{l} \cos \zeta_L.$$

On the basis of expression (4) we have

$$2k \cos \psi_L = -\beta \frac{e}{l} \cos \zeta_L;$$

but since

$$\cos \zeta_L = 1 - 2 \sin^2 \frac{\zeta_L}{2},$$

from (3) we obtain

$$\cos \zeta_L = 1 - 2k^2 \sin^2 \psi_L.$$

Thus, we have the *first* boundary condition in the following final form:

$$\text{when } s = l, \quad 2k \cos \psi_L = -\beta \frac{e}{l} (1 - 2k^2 \cos^2 \psi_L). \quad (8)$$

The *second* boundary condition is as follows:

$$\zeta = 0 \text{ when } s = 0, \text{ or according to (3) } \psi_0 = 0.$$

When  $s = l$ , expression (5) becomes

$$F(\psi_L) = \beta. \quad (9)$$

From (6) we find

$$\frac{x_L}{l} = \frac{x'_L}{l} = \frac{2}{\beta} E(\psi_L) - 1.$$

The approach  $\lambda$  of the ends of the bar is

$$\lambda = 2l - 2x'_L, \quad \frac{\lambda}{l} = 4 \left[ 1 - \frac{1}{\beta} E(\psi_L) \right].$$

The maximum deflection is

$$f = y'_L = \frac{2l}{\beta} k (1 - \cos \psi_L). \quad (10)$$

Let us now plot a curve showing the relation of the force  $P$  to the maximum deflection  $f$  for some given ratio  $e/2l$ . The procedure for computation is as follows. We divide (8) by (9) member by member

$$k \frac{\cos \psi_L}{F(\psi_L)} = -\frac{e}{2l} (1 - 2k^2 \sin^2 \psi_L). \quad (11)$$

For a given  $e/2l$ , assign a value of  $k$  and then from tables choose  $\psi_L$  so as to satisfy Eq. (11). Next, from (9) find  $\beta$  and thereupon

$$\frac{P}{P_e} = \frac{P(2l)^2}{\pi^2 EI} = \frac{4\beta^2}{\pi^2}.$$

From Eq. (10) determine  $f/2l$ . We thus obtain a point of the relation

$$\frac{P}{P_e} = \varphi \left( \frac{f}{2l} \right).$$

Take, for example,  $e/2l = 0.02$  and draw up a table choosing  $k = \sin 5^\circ, \sin 10^\circ, \dots$

$k$	$\psi_L$	$\beta$	$\frac{P}{P_e}$	$\frac{f}{2l}$
0.08716	118°	2.06	1.72	0.0620
0.1736	101°	1.778	1.28	0.118
0.259	97°	1.725	1.21	0.168
0.342	94°	1.694	1.156	0.216
0.707	90°	1.854	1.39	0.381

On the basis of this table we plot the curve shown in Fig. 368. There are two more curves plotted in the same graph. The first curve corresponds to the case  $e = 0$ ; the second

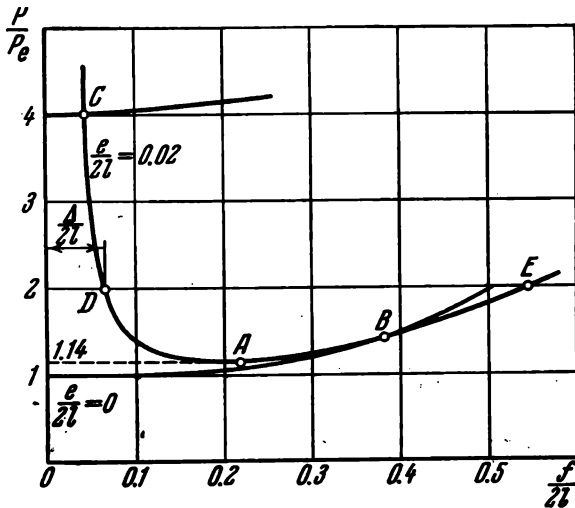


Fig. 368

curve starting at the point  $P/P_e = 4$  corresponds to the bar bent in the form of Fig. 131b.

Let us discuss the result obtained. The curve  $e/2l = 0.02$  falls at small deflections and then, beginning with  $P/P_e = 1.14$ , rises. At the point B it intersects the curve  $e/2l = 0$ . This point is common to all curves, irrespective of  $e/2l$ . Here  $k = 1/\sqrt{2}$  and from Eq. (11) it follows that for every  $e/2l$  we have  $\cos \psi_L = 0$ . This means that the moment

at the end of the bar is zero and the rotation of the end is equal to 90 degrees (Fig. 369).

The curve  $e/2l = 0.02$  does not cross the axis of ordinates. In its left-hand part it asymptotically approaches the straight line  $f/2l \cong 0.04$ . Thus, when  $e/2l \neq 0$  the bar is always stable in the small provided that the instability occurs in the form shown in Fig. 131c. But when the force  $P = 4\pi^2 EI/(2l)^2$ , for every  $e/2l$  the bar buckles in the form of Fig. 131b.

Suppose now that when  $e/2l = 0.02$  the bar is loaded, for example, by the force

$$P = \frac{2\pi^2 EI}{(2l)^2} \quad \left( \frac{P}{P_e} = 2 \right).$$

The bar then retains the straight-line form. Let us try to deflect it slightly from the vertical by assigning some curvature of its axis. If this deflection is small, the bar, when left to itself, will return into its original position.

If, however, the deflection is sufficiently large (larger than  $\Delta/2l$ , Fig. 368), the bar will assume a new curvilinear form of equilibrium corresponding to the point  $E$  (Fig. 368).

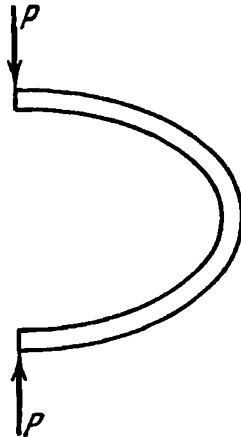


Fig. 369

Depending on the magnitude of the given deflection, the system may return to its original position or may not. But this occurs at a force  $P$  larger than a certain specific value. When  $e/2l = 0.02$ , this happens for both  $P > 1.14 P_e$  (point  $A$  in Fig. 368) and  $P < 4P_e$ , where the instability takes place irrespective of the magnitude of the given deflection. We thus arrive at a new concept of a range of possible critical forces in which there may be a transition to a new position of equilibrium:  $1.14P_e \leq P < 4P_e$ .

The instability occurs in the above range sooner or later depending on the precision with which the bar is made and on how rigorously the axially of the application of the force is fulfilled. But, anyhow, the critical loads in such systems are defined in the above range as probable.

When  $P \geq 4P_e$ , the transition to a new form of equilibrium is inevitable.

138. When solving the problem, it is necessary to consider separately a form of equilibrium (A) (Fig. 370) in which the end of the beam remains pressed against the plane. The transition from the straight-line form to this form of equilibrium takes place, as is known, at a longitudinal force given by

$$P_{cr} \cos \delta = \frac{20.2EI}{l^2}.$$

Let us now consider equilibrium forms of the type (B) (Fig. 370). It is clear that the transition to this form of equilibrium cannot be effected by a small (arbitrarily small) displacement of the system from the initial position. Indeed, by giving the end of the beam some displacement so that the beam does not return to its initial position and assumes the type (B) form, we must select this displacement sufficiently large to make the moment of the force  $P \cos \delta$  deflecting the beam from its initial position larger than the restoring moment of the force  $P \sin \delta$ . In other words, we must give a displacement larger than a certain preassigned value. After that the system, when left to itself, will not return to its initial position.

Let us now see under what conditions equilibrium forms of the type (B) are possible for the beam. In our case the existence of the elastic curve is only possible in the form

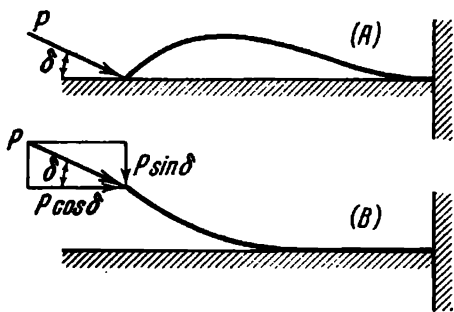


Fig. 370

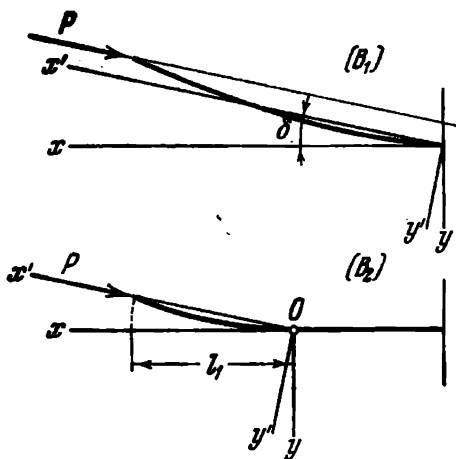


Fig. 371

when all points of the deflected rod are above the horizontal plane. There are two possibilities here: the rod is wholly bent (Fig. 371,  $B_1$ ) and the rod is partly bent ( $B_2$ ).

Consider the first case ( $B_1$ ). At the end of the beam ( $s = l$ ) the curvature is zero ( $d\zeta/ds = 0$ ). From formula (4) of the preceding problem (p. 285) it follows, therefore, that

$$\psi_L = \frac{\pi}{2}.$$

When  $s = 0$ , we have  $\zeta = -\delta$ . From (3) (p. 285) we obtain

$$-\sin \frac{\delta}{2} = k \sin \psi_0 \quad (1)$$

and from (1) and (5) (pp. 284, 285)

$$\beta^2 = \frac{Pl^2}{EI} = \left[ F\left(\frac{\pi}{2}\right) - F(\psi_0) \right]^2. \quad (2)$$

The co-ordinates of the end of the rod in the  $x'y'$  system are, according to (6) (p. 286),

$$\left. \begin{aligned} \frac{x'_L}{l} &= 2 \frac{E\left(\frac{\pi}{2}\right) - E(\psi_0)}{F\left(\frac{\pi}{2}\right) - F(\psi_0)} - 1, \\ \frac{y'_L}{l} &= \frac{2k \cos \psi_0}{F\left(\frac{\pi}{2}\right) - F(\psi_0)}. \end{aligned} \right\} \quad (3)$$

From the first expression of (7) (p. 286) we find the horizontal displacement of the point of application of the force

$$\frac{\lambda}{l} = 1 - \frac{x'_L}{l} \cos \delta - \frac{y'_L}{l} \sin \delta. \quad (4)$$

It is now possible to plot  $Pl^2/EI$  as a function of  $\lambda/l$  for some  $\delta$  ( $10^\circ$ ,  $20^\circ$ ,  $30^\circ$ ) for equilibrium forms ( $B_1$ ). For this, by assigning values of  $k$ , find  $\psi_0$  from (1). From (2) find  $Pl^2/EI$  using tables of elliptic integrals, and from (3) and (4) find the value of  $\lambda/l$ .

Figure 372 shows three curves. In plotting the curves, it is taken into account that for the type ( $B_1$ ) equilibrium

form the force  $P$  passes above the origin and  $\psi_0$  remains greater than  $-\pi/2$ . The dashed curve in Fig. 372 bounds these curves from above. For greater values of  $Pl^2/EI$  the desired relation must be determined according to the type

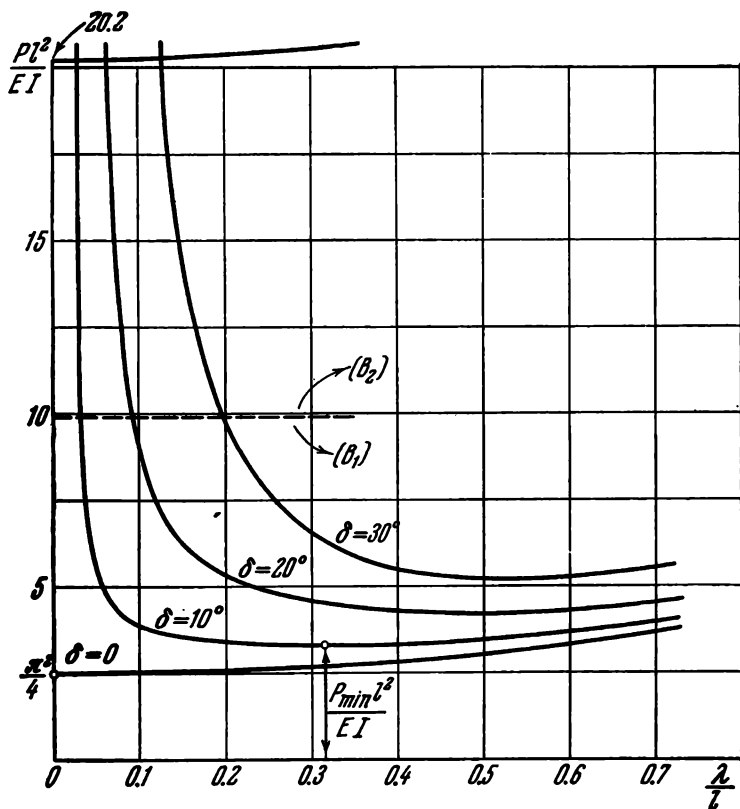


Fig. 372

$(B_2)$  equilibrium form. In this case at the point  $O$  (Fig. 371)  $\psi_0 = -\pi/2$  and instead of (1) we have

$$k = \sin \frac{\delta}{2}. \quad (1')$$

Instead of (2), we obtain

$$\frac{Pl^2}{EI} \frac{l^2}{l^2} = \left[ F\left(\frac{\pi}{2}\right) - F(\psi_0) \right]^2. \quad (2')$$

Instead of (3) and (4), we find

$$\frac{x'_L}{l} \frac{l}{l_1} = 2 \frac{E \left( \frac{\pi}{2} \right) - E(\psi_0)}{F \left( \frac{\pi}{2} \right) - F(\psi_0)} - 1, \quad (3')$$

$$\frac{y_L}{l_1} = 0,$$

$$\frac{\lambda}{l} \frac{l}{l_1} = 1 - \frac{x'_L}{l} \frac{l}{l_1} \cos \delta. \quad (4')$$

Thus, here from (1') we find  $k$ . For some arbitrary  $Pl^2/EI$ , from (2') we find  $l_1/l$ , and from (3') and (4') we find  $\lambda/l$ . The results of calculations are shown by the curves of Fig. 372 situated above the dashed line.

Let us discuss the results obtained. If  $\delta = 0$ , the Euler instability occurs when

$$\frac{Pl^2}{EI} = \frac{\pi^2}{4} \cong 2.46.$$

When  $\delta \neq 0$ , the instability for  $Pl^2/EI < 20.2/\cos \delta$  occurs only in the large. The value of the displacement which must be given to the beam to make it pass into a new position of equilibrium decreases with increasing force  $P$ . At the same time the instability (depending on  $\delta$ ) cannot occur at a force smaller than a certain specific value. Thus, when  $\delta = 10^\circ$ ,

$$\frac{P_{\min} l^2}{EI} \cong 3.25;$$

when  $\delta = 20^\circ$ ,

$$\frac{P_{\min} l^2}{EI} \cong 4.25;$$

when  $\delta = 30^\circ$ ,

$$\frac{P_{\min} l^2}{EI} \cong 5.25.$$

In any case,  $P_{cr}$  is defined as probable in the range

$$P_{\min} < P_{cr} < \frac{20.2EI}{l^2 \cos \delta},$$

with  $P_{\min} = f(\delta)$ .

139. The system is always stable in the small.

Consider the system in a displaced position (Fig. 373). The force compressing the elastic bar is denoted by  $R$ . By equating to zero the sum of the moments of the forces about the point  $O$ , we obtain

$$P \cdot 2l \sin \varphi = R \cdot OA. \quad (1)$$

We next use the well-known rule by which the sum of the projections of the segments of a broken line is equal to the

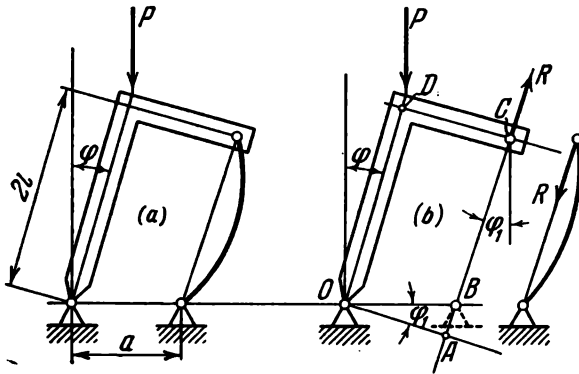


Fig. 373

projection of the closing line, and project the closed quadrilateral  $ODCB$  first on the vertical axis and then on the horizontal axis. We obtain

$$\left. \begin{aligned} 2l \cos \varphi - a \sin \varphi &= BC \cdot \cos \varphi_1, \\ -a + 2l \sin \varphi + a \cos \varphi &= BC \cdot \sin \varphi_1, \end{aligned} \right\} \quad (2)$$

whence we have

$$\tan \varphi_1 = \frac{\sin \varphi - \frac{a}{2l} (1 - \cos \varphi)}{\cos \varphi - \frac{a}{2l} \sin \varphi}.$$

Further we find

$$\begin{aligned} OA = a \cos \varphi_1 &= \frac{a}{\sqrt{1 + \tan^2 \varphi_1}} = \\ &= a \frac{\cos \varphi - \frac{a}{2l} \sin \varphi}{\sqrt{1 - 2 \frac{a}{2l} \sin \varphi + 2 \frac{a^2}{4l^2} (1 - \cos \varphi)}}. \end{aligned}$$

Thus, expression (1) takes the form

$$P = R \frac{a}{2l} \frac{\cot \varphi - \frac{a}{2l}}{\sqrt{1 - 2 \frac{a}{2l} \sin \varphi + 2 \frac{a^2}{4l^2} (1 - \cos \varphi)}}. \quad (3)$$

Obviously, the segment  $BC = 2l - \lambda$ , where  $\lambda$  is the approach of the ends of the elastic bar. By squaring equalities (2) and adding them, we find

$$1 - \frac{\lambda}{2l} = \sqrt{1 - 2 \frac{a}{2l} \sin \varphi + 2 \frac{a^2}{4l^2} (1 - \cos \varphi)}. \quad (4)$$

The force  $R$  appearing in expression (3) depends on  $\lambda$ . The  $(R, \lambda)$  relation is determined from the equations for a slender elastic bar undergoing large displacements (see the solution of Prob. 137). When  $s = 0$ , we have  $d\xi/ds = 0$ , and from Eq. [(4) (p. 285)] it follows that  $\psi_L = \pi/2$ .

When  $s = 0$ , we have  $\xi = 0$ , and from formula (3) (p. 285) we obtain  $\psi_0 = 0$ .

The contraction  $\lambda$  of the bar is  $\lambda = 2l - 2x$ . From (6) (p. 286) we find

$$\frac{\lambda}{2l} = 2 \left[ 1 - \frac{E \left( \frac{\pi}{2} \right)}{\beta} \right].$$

From (5) (p. 285) we obtain

$$\beta = \sqrt{\frac{RI^2}{EI}} = F \left( \frac{\pi}{2} \right).$$

We assign several values of the modulus of the elliptic integrals  $k$  and from tables find  $F(\pi/2)$  and  $E(\pi/2)$ , and then  $\beta$  and  $\lambda/2l$ . We draw up the following table:

arc sin $k$	0	5°	10°	15°	20°	25°	30°
$\beta$	1.571	1.574	1.583	1.598	1.620	1.649	1.686
$\frac{\lambda}{2l}$	0	0.008	0.030	0.068	0.114	0.184	0.262
$\frac{R}{P_e} = \frac{4\beta^2}{\pi^2}$	1	1.004	1.015	1.036	1.062	1.102	1.153

The last line of the table gives the ratio of the force  $R$  compressing the bar to Euler's force  $P_e = \pi^2 EI / (2l)^2$ . The relation

$$\frac{R}{P_e} = f\left(\frac{\lambda}{2l}\right)$$

is shown in the graph of Fig. 374.

We now assign several values of the angle  $\varphi$  and from Eq. (4) determine  $\lambda/2l$ , then from the graph we find  $R/P_e$  and from

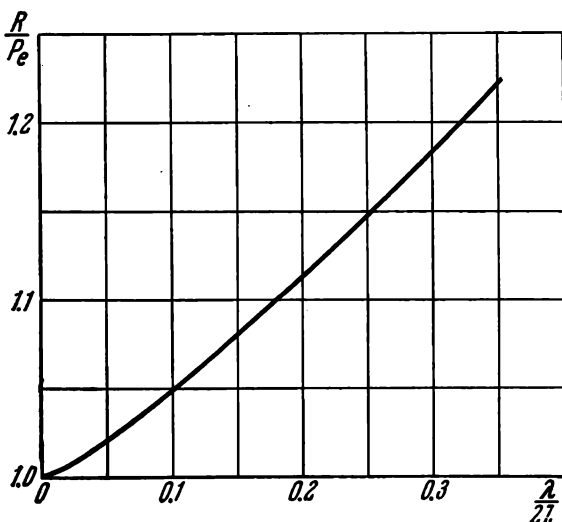


Fig. 374

Eq. (3) the ratio  $P/P_e$ . Thus, we obtain the relation  $P/P_e = f(\varphi)$  shown in the graph of Fig. 375. The meaning of this curve is the same as for the curves of Figs. 368 and 372 which were obtained in the solution of the preceding two problems. In contrast to the cases considered previously, however, here the curve intersects the axis of abscissas. This means that even when the force  $P = 0$  the system may pass into a new position of equilibrium if it is displaced sufficiently far. When  $a/2l = 0.5$ , we have  $\varphi_0 = 63.5^\circ$ , which corresponds to the points  $O$ ,  $B$ , and  $C$  being in the same straight line (Fig. 376).

When the force  $P$  is large, the displacement which must be given to the system in order that it does not return to

its original position is small. If the accuracy of mounting and further external force disturbances are such as to ensure the absence of angles of departure exceeding 5 degrees, according to the graph, it may be said that the limiting

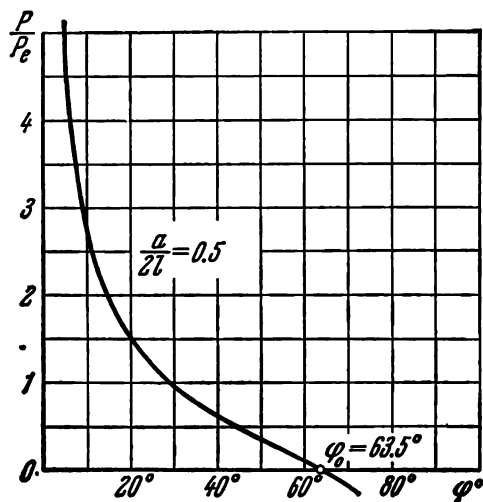


Fig. 375

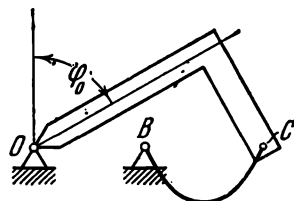


Fig. 376

load  $P$  which the system is capable of sustaining is larger than  $5P_e$ .

In contrast to Probs. 137 and 138 considered previously, the critical force is not bounded from above either. This is a consequence of disregarding the compressibility of the elastic bar. If the compressibility is taken into account, it can easily be ascertained that the system becomes unstable in the small when

$$P = EA \frac{a^2}{4e^2},$$

where  $A$  is the cross-sectional area of the elastic bar.

140. Before losing stability, the ring is subjected to an external uniformly distributed load  $q = P/R$ . In the usual conditions, if  $q$  remains unchanged during the bending of the ring, the instability occurs when

$$q = \frac{3EI}{R^3}.$$

The ring then assumes a shape close to the shape of an ellipse.

In the present problem, however, the ring is always stable in the small. Indeed, if for some reasons the ring begins to bend assuming even though the shape of an ellipse, the distributed load  $q = P/R$  begins to increase where the curvature increases and to decrease where the curvature decreases. At the ends of the major axis of the ellipse  $q$  increases, and at the ends of the minor axis it decreases (Fig. 377). The difference of the loads restores the circular shape of the ring.

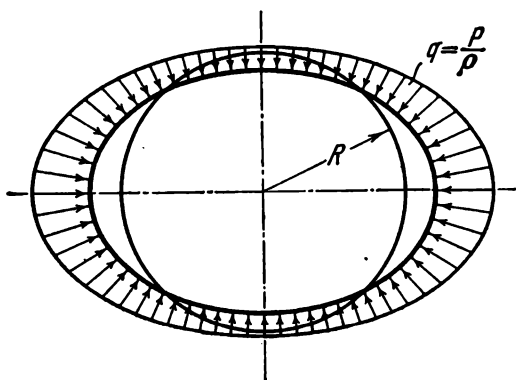


Fig. 377

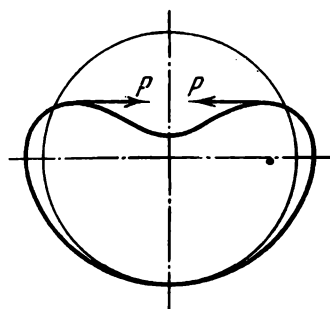


Fig. 378

In order that the circular shape of the ring does not recover, it is obviously necessary to give the ring some sufficiently large curvature such as to make the ring separate off from the string over a certain length. The character of the elastic curve of the ring is then most easily established from a simple test by glueing a ring of paper and tightening it with the usual thin thread.

Figure 378 shows the shape of the buckled ring.

Consider the right-hand half of the ring by cutting it at the point where the string separates off (Fig. 379, point 1). At this section in the ring there is a bending moment  $M_1$  and a normal compressive force  $N$ . The shearing force is obviously zero since otherwise the conditions of equilibrium for the section  $O1$  of the ring would not be fulfilled.

To investigate the conditions of equilibrium for the above shape of the elastic ring we apply the relations developed previously in the solution of Prob. 137. These relations were derived for a straight elastic bar. Here, however, we are dealing with a ring of constant curvature  $1/R$ . But a ring

of constant curvature is obtained from a straight bar by applying a moment  $M = EI/R$  to its ends. Consequently, the problem (and not only the one being considered) of the bending of a flexible rod of constant initial curvature is reduced to the problem of the bending of a straight rod of

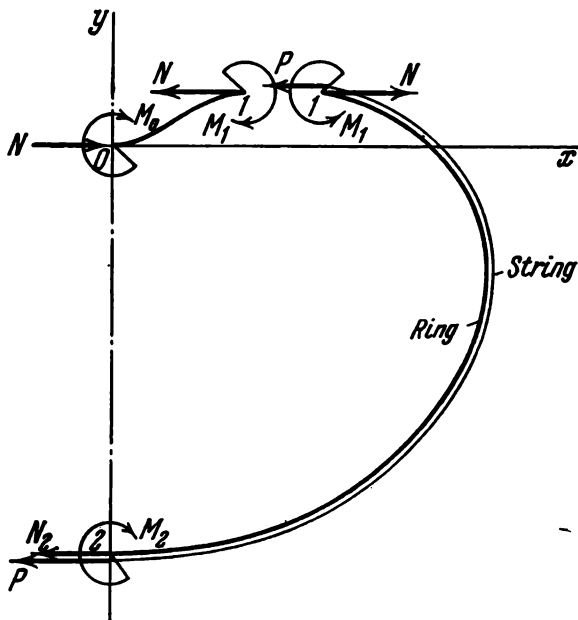


Fig. 379

the same length and rigidity by adding to the given load moments  $M = EI/R$  applied at the ends.

The length of the portion  $O1$  is denoted by  $l_1$ . The arc length  $s$  is measured from  $O$  to 1. Expression (1) (p. 284) for the first portion of the ring takes the form

$$\beta = l_1 \sqrt{\frac{N}{EI}}. \quad (1)$$

When  $s = 0$  and  $s = l_1$ ,  $\zeta_0 = \zeta_1 = 0$ , and according to (3) (p. 285) we obtain

$$\sin \psi_0 = 0, \quad \sin \psi_1 = 0.$$

Since the angle  $\psi$  increases along the arc length  $s$  passing through the value  $\pi/2$  at the point of inflection (see Prob. 137) assuming  $\psi_0 = 0$  we obtain  $\psi_1 = \pi$ .

The curvature of the rod at the point  $1$  is, according to (4) (p. 285),

$$\left(\frac{d\zeta}{ds}\right)_1 = 2 \frac{\beta}{l_1} k_1 \cos \psi_1$$

or

$$\left(\frac{d\zeta}{ds}\right)_1 = -2k_1 \sqrt{\frac{N}{EI}}. \quad (2)$$

Expression (5) on p. 285 for  $s = l_1$  takes the form

$$l_1 \sqrt{\frac{N}{EI}} = F_1(\pi) = 2F_1\left(\frac{\pi}{2}\right), \quad (3)$$

where  $F_1(\pi/2)$  is the complete elliptic integral of the first kind with the modulus  $k_1$ . (For the second portion the modulus is  $k_2$ .) Then

$$F\left(n \frac{\pi}{2}\right) = nF\left(\frac{\pi}{2}\right).$$

The co-ordinates of the point  $1$  are, according to expression (6) (p. 286),

$$x_1 = \frac{2}{\sqrt{\frac{N}{EI}}} 2E_1\left(\frac{\pi}{2}\right) - l_1, \quad (4)$$

$$y_1 = \frac{4k_1}{\sqrt{\frac{N}{EI}}}. \quad (5)$$

We now proceed to the second portion of the ring, namely the portion 1-2. Here the ring is subjected to a distributed load whose magnitude is proportional to the curvature of the ring. It is known that for a uniformly distributed load the problem of large displacements of a bar is solved not in terms of elliptic tabulated integrals but in terms of ultra-elliptic untabulated integrals. In the present case, however, it is much simpler. In view of the fact that the string is absolutely flexible, we may consider the string and ring together as an integral ring with the same rigidity  $EI$  and assume that in the second portion at the point  $1$  the ring is acted on by the compressive force  $N - P$  and the moment  $M_1$ . But for such a load the problem of large displacements is solvable in terms of elliptic integrals.

With this approach to the problem, the load  $q$  acting on the ring externally becomes an internal force acting on both the ring and the string. Incidentally, we may draw a rather general little-known conclusion from the above that for a distributed load proportional to the curvature of a deformed rod the problem of large deflections is solvable in terms of elliptic integrals.

Since there are no points of inflection in the second portion of the ring, and hence  $d\xi/ds$  nowhere vanishes in this portion, the quantity  $C_1$  in expression (2) (p. 284) must be greater than unity. If, as in Prob. 137, we denote  $C_1$  by  $k^2$  and  $\sin \xi/2$  by  $k \sin \psi$ , we come to elliptic integrals with a modulus greater than unity. There are no tables available for such integrals. Expressions (3) to (6) of Prob. 137 must therefore be transformed.

Denote for the second portion

$$\left. \begin{aligned} C_1 &= \frac{1}{k^2}, \\ \sin \frac{\xi}{2} &= \sin \psi. \end{aligned} \right\} \quad (6)$$

Equation (2) (p. 284) then becomes

$$l_2 \frac{d\xi}{ds} = \pm \frac{2\beta}{k_2} \sqrt{1 - k_2^2 \sin^2 \psi},$$

where  $l_2$  is the length of the second portion. Since the curvature is negative in the second portion, we take the minus sign

$$\frac{d\xi}{ds} = -\frac{2}{k_2} \sqrt{\frac{N-P}{EI}} \sqrt{1 - k_2^2 \sin^2 \psi}. \quad (7)$$

Substituting for  $\frac{d\xi}{ds}$  the expression

$$\frac{2 \cos \psi}{\sin \frac{\xi}{2}} \frac{d\psi}{ds}$$

obtained from (6), we find

$$ds = \frac{k_2}{\sqrt{\frac{N-P}{EI}}} \frac{d\psi}{\sqrt{1 - k_2^2 \sin^2 \psi}}, \quad (8)$$

whence

$$s = \frac{k_2}{\sqrt{\frac{N-P}{EI}}} [F_2(\psi) - F_2(\psi_0)]. \quad (9)$$

Further, as in Prob. 137,

$$dx = dx' = \left(1 - 2 \sin^2 \frac{\zeta}{2}\right) ds,$$

$$dy = dy' = 2 \sin \frac{\zeta}{2} \cos \frac{\zeta}{2} ds.$$

Substituting for  $\sin \frac{\zeta}{2}$  from (6) and for  $ds$  from (8), we obtain

$$dx = \frac{2}{k_2 \sqrt{\frac{N-P}{EI}}} \sqrt{1 - k_2^2 \sin^2 \psi} d\psi - \left(\frac{2}{k_2^2} - 1\right) ds,$$

$$dy = \frac{2}{k_2 \sqrt{\frac{N-P}{EI}}} \frac{k_2^2 \sin 2\psi}{2 \sqrt{1 - k_2^2 \sin^2 \psi}} d\psi.$$

Upon integration we find

$$x - x_0 = \frac{2}{k_2 \sqrt{\frac{N-P}{EI}}} [E_2(\psi) - E_2(\psi_0)] - \left(\frac{2}{k_2^2} - 1\right) s, \quad (10)$$

$$y - y_0 = \frac{2}{k_2 \sqrt{\frac{N-P}{EI}}} [\sqrt{1 - k_2^2 \sin^2 \psi_0} - \sqrt{1 - k_2^2 \sin^2 \psi}]. \quad (11)$$

We now consider the boundary conditions for the second portion.

At the point 1, i.e., at the beginning of the second portion,  $\zeta_1 = 0$ , and at the end (point 2)  $\zeta_2 = -180^\circ$ . According to (6)

$$\sin \psi_1 = 0, \quad \sin \psi_2 = -1.$$

Assume  $\psi_1 = 180^\circ$ ,  $\psi_2 = 270^\circ$ .

Since  $F(n\pi/2) = nF(\pi/2)$ , from (9) we obtain for the end of the second portion

$$l_2 = \frac{k_2 F_2\left(\frac{\pi}{2}\right)}{\sqrt{\frac{N-P}{EI}}}. \quad (12)$$

Substituting  $\psi = 180^\circ$  in expression (7), we find the curvature of the ring in the second portion at the point 1

$$\frac{d\epsilon}{ds} = -\frac{2}{k_2} \sqrt{\frac{N-P}{EI}}.$$

The curvature at the point 1 undergoes no discontinuity. We therefore equate the above curvature to that found at the point 1 of the first portion (2), i.e.,

$$k_1 \sqrt{\frac{N}{EI}} = \frac{1}{k_2} \sqrt{\frac{N-P}{EI}}. \quad (13)$$

The co-ordinate  $x$  of the end of the second portion is zero, and the co-ordinate of the origin for the second portion must coincide with the co-ordinate of the end  $x_1$  (4) of the first portion. Hence, from (10) with  $s = l_2$ ,  $x = 0$ , and  $x_0 = x_1$  (4) we obtain

$$-\frac{4}{\sqrt{\frac{N}{EI}}} E_1 \left( \frac{\pi}{2} \right) + l_1 = \frac{2}{k_2 \sqrt{\frac{N-P}{EI}}} E_2 \left( \frac{\pi}{2} \right) - \left( \frac{2}{k_2^2} - 1 \right) l_2. \quad (14)$$

In a similar way we find  $y$ , the distance between the points  $O$  and 2

$$y = \frac{4k_1}{\sqrt{\frac{N}{EI}}} + \frac{2}{k_2 \sqrt{\frac{N-P}{EI}}} (1 - \sqrt{1 - k_2^2}). \quad (15)$$

By eliminating  $\sqrt{N/EI}$  and  $\sqrt{(N-P)/EI}$  from Eqs. (3), (12), (13), and (14), we obtain

$$\begin{aligned} \frac{2}{k_2^2} E_2 \left( \frac{\pi}{2} \right) - \left( \frac{2}{k_2^2} - 1 \right) F_2 \left( \frac{\pi}{2} \right) = \\ = 2k_1 \left[ F_1 \left( \frac{\pi}{2} \right) - 2E_1 \left( \frac{\pi}{2} \right) \right], \end{aligned} \quad (16)$$

$$\frac{l_1}{l_2} = \frac{2k_1 F_1 \left( \frac{\pi}{2} \right)}{F_2 \left( \frac{\pi}{2} \right)}. \quad (17)$$

But the sum of the lengths  $l_1$  and  $l_2$  is equal to half the arc length of the ring

$$l_1 + l_2 = \pi R,$$

whence

$$\frac{l_1}{\pi R} = \frac{\frac{l_1}{l_2}}{1 + \frac{l_1}{l_2}}. \quad (18)$$

From (3) and (13) we find

$$\sqrt{\frac{NR^2}{EI}} = \frac{2F_1 \left( \frac{\pi}{2} \right)}{\pi \frac{l_1}{\pi R}}, \quad (19)$$

$$\frac{PR^2}{EI} = \frac{NR^2}{EI} (1 - k_1^2 k_2^2). \quad (20)$$

Thus, the procedure for calculation is as follows.

Assign  $k_1$  (or a value of the modulus angle  $\alpha_1 = \arcsin k_1$ ) and, using tables of complete elliptic integrals, choose  $k_2$  so as to satisfy Eq. (16). In practice this is most conveniently done by simultaneously plotting the graphs of the right-hand and left-hand sides of the equation against  $k_1$  and  $k_2$ .

From (17), (18) we find  $l_1/\pi R$ , and from (19), (20) the value of the force  $P$  (20). The deflection  $w$  (the decrease in the vertical diameter) corresponding to this force  $P$  is, according to (15),

$$\frac{w}{R} = 2 - \frac{1}{\sqrt{\frac{NR^2}{EI}}} \left[ \frac{2}{k_1 k_2^3} (1 - \sqrt{1 - k_2^2}) - 4k_1 \right]. \quad (21)$$

We thus determine a point of the relation

$$\frac{PR^2}{EI} = f \left( \frac{w}{R} \right).$$

Figure 380 shows the results of the calculations in the form of a curve similar to those obtained in the preceding three problems. The minimum value of the critical force is found to be

$$P_{\min} = 2.1 \frac{EI}{R^2}.$$

This value, however, is lowest only formally, since the displacement  $w/R$  is then equal to 2.65, i.e., the decrease in the diameter of the ring is greater than the diameter itself.

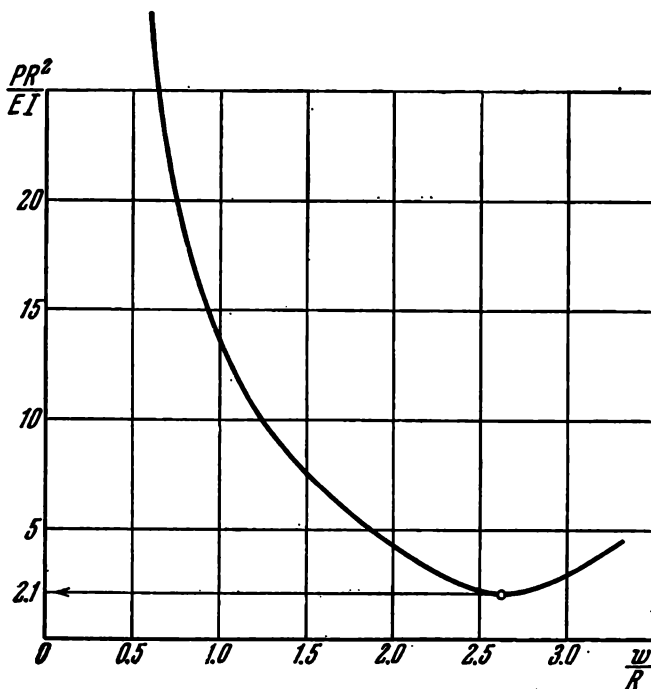


Fig. 380

The contour of the ring assumes the form of the curve shown in Fig. 381.

It is clear that in actual conditions the initial out-of-roundness of the ring is insignificant, i.e.,  $w/R$  remains essentially less than unity. For small values of  $w/R$ , the calculation gives sharply increased values of  $PR^2/EI$  not covered by the curve scale (Fig. 380). In this case the derived formulas can conveniently be transformed taking into account that  $k_1$  and  $k_2$  are small quantities. Note that

$$F_1\left(\frac{\pi}{2}\right) \cong \frac{\pi}{2} \left(1 + \frac{k_1^2}{4} + \dots\right),$$

$$F_2\left(\frac{\pi}{2}\right) \cong \frac{\pi}{2} \left(1 + \frac{k_2^2}{4} + \dots\right).$$

According to (17), (18), (19), and (20)

$$\frac{l_1}{l_2} \cong 2k_1, \quad \frac{l_1}{2\pi} \cong \frac{2k_1}{1+2k_1}, \quad \sqrt{\frac{NR^2}{EI}} \cong \frac{1+2k_1}{2k_1},$$

$$\frac{PR^2}{EI} \cong \frac{1+4k_1}{4k_1^2}. \quad (22)$$

Finally,

$$\frac{w}{R} = 2 - \frac{2k_1}{1+2k_1} \left[ \frac{2}{k_1 k_1^2} \left( 1 - 1 + \frac{k_1^2}{2} \right) - 4k_1 \right],$$

$$\frac{w}{R} \cong 4k_1. \quad (23)$$

Thus, for small  $w/R$ , by eliminating  $k_1$  from (22) and (23), we obtain

$$\frac{PR^2}{EI} \cong 4 \frac{1 + \frac{w}{R}}{\left( \frac{w}{R} \right)^2} \cong \frac{4}{\left( \frac{w}{R} \right)^2}.$$

Returning to the concept of stability in the large developed on p. 282, we see that the problem under consideration has not ultimately received solution. Only the forms of equilibrium are found from the analysis of which it follows that the ring is "very stable". In order to assess the stability of the system, account must be taken of a class of reasonably limited, actually existing disturbances and types of initial imperfections, as crookedness of the ring and inhomogeneity of the material. This kind of analysis has not yet been possible to make in any of the problems.

In this sense the example considered is not an exception.

So far the theory of stability of elastic systems cannot, for example, give any satisfactory solution to extremely impor-

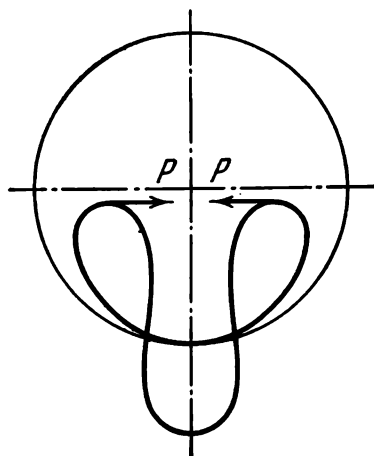


Fig. 381

tant practical problems such as the stability of a spherical shell under external pressure and of a cylindrical shell under axial compression.

141. The problem by its nature is close to the preceding one. Let us first consider the forms of equilibrium of the ring in the case of large displacements.

Suppose that the radius of the ring in a free condition is greater by an amount  $\Delta$  than the radius of the casing.

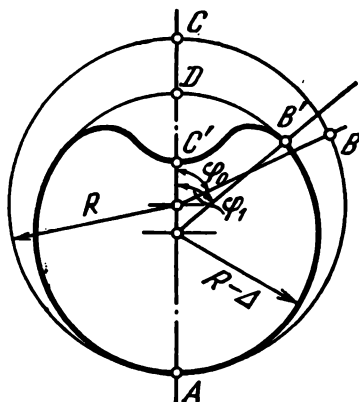


Fig. 382

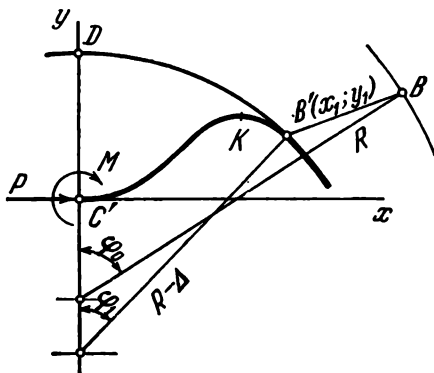


Fig. 383

The arc  $ABC$  (Fig. 382) has the assumed form of equilibrium  $AB'C'$ . The point  $B$  moves to  $B'$ , and  $C$  to  $C'$ . From the condition that the arcs  $AB$  and  $AB'$  are equal we establish a relation between the angles  $\varphi_0$  and  $\varphi_1$

$$\varphi_1 = \pi - \frac{1}{1-e} (\pi - \varphi_0), \quad (1)$$

where  $e$  stands for  $\Delta/R$ .

We now turn to the equations for a flexible bar (see Prob. 137, pp. 284, 285). In the portion  $C'B'$  we have the inflected form. The point  $C'$  is taken as the origin of the arc  $s$ . It will range from zero to the value  $l = R\varphi_0$ . Expression (1) (p. 284) becomes therefore

$$\beta^2 = \frac{PR^2}{EI} \varphi_0^2. \quad (2)$$

At the point  $C'$  the slope of the arc  $\zeta = 0$ . Consequently,  $\sin \psi_0 = 0$ . Assume  $\psi_0 = 0$ . The elliptic angle  $\psi$  will in-

crease along the arc length  $s$ . At the point of inflection (a result which follows from expression (4), p. 285) it is equal to  $\pi/2$ . At the point  $K$  (Fig. 383) it becomes equal to  $\pi$ . Since in the portion  $KB'$  there are no more points of inflection, at the point  $B'$  the angle  $\psi$  remains less than  $3\pi/2$ . Denote its value by  $\psi_1$ . From expression (5) (p. 285), on substituting  $s = l$ , we obtain

$$\beta = F(\psi_1). \quad (3)$$

At the point  $B'$  the curvature of the ring is known. It is equal to the curvature of the casing, i.e.,

$$\frac{d\zeta}{ds} = -\frac{1}{R-\Delta}.$$

Equation (4) (p. 285) gives

$$-\frac{R\varphi_0}{R-\Delta} = 2\beta k \cos \psi_1. \quad (4)$$

Finally, we are given the slope of the curve at the point  $B'$

$$\zeta_{B'} = -\varphi_1.$$

From Eq. (3) (p. 285) we then obtain

$$-\sin\left(\frac{\pi}{2} - \frac{1}{2} \frac{\pi - \varphi_0}{1 - e}\right) = k \sin \psi_1. \quad (5)$$

Equations (6) (p. 286) give the values of the co-ordinates of the point  $B'$  referred to the system of axes  $x, y$  (Fig. 383)

$$\frac{x_1}{R\varphi_0} = \frac{2}{\beta} E(\psi_1) - 1, \quad (6)$$

$$\frac{y_1}{R\varphi_0} = \frac{2k}{\beta} (1 - \cos \psi_1). \quad (7)$$

As seen from Fig. 383,

$$x_1 = (R - \Delta) \sin \varphi_1.$$

We therefore obtain one more equation

$$\frac{1-e}{\varphi_0} \sin \frac{\pi - \varphi_0}{1-e} = \frac{2}{\beta} E(\psi_1) - 1. \quad (8)$$

In Eqs. (3), (4), (5), and (8) the unknowns are: the modulus of the elliptic integrals  $k$ , the elliptic angle  $\psi_1$ , the angle  $\varphi_0$ , and the force  $P$ . They must be determined as a function of  $e = \Delta/R$ . We first eliminate  $\beta$  from Eq. (4) by means of (3)

$$-\frac{\varphi_0}{1-e} = 2k \cos \psi_1 F(\psi_1). \quad (9)$$

Further, from Eqs. (5) and (8) we obtain

$$-\frac{1-e}{\varphi_0} 2k \sin \psi_1 \sqrt{1-k^2 \sin^2 \psi_1} = \frac{2E(\psi_1)}{F(\psi_1)} - 1.$$

We eliminate  $(1-e)/\varphi_0$  by means of Eq. (9). Then

$$\cos \psi_1 [2E(\psi_1) - F(\psi_1)] - \sin \psi_1 \sqrt{1-k^2 \sin^2 \psi_1} = 0. \quad (10)$$

This expression involves only two unknowns,  $k$  and  $\psi_1$ . By using tables of elliptic integrals, it is possible, on the basis of Eq. (10), to draw up the following auxiliary table.

$k$	$\psi_1$	$\sin \psi_1$	$\cos \psi_1$	$F(\psi_1)$	$E(\psi_1)$
0	4.493	-0.9761	-0.2172	4.494	4.494
0.05	4.493	-0.9761	-0.2174	4.497	4.491
0.10	4.493	-0.9760	-0.2178	4.504	4.482
0.15	4.492	-0.9759	-0.2184	4.517	4.469
0.20	4.491	-0.9756	-0.2194	4.536	4.449
0.25	4.490	-0.9753	-0.2207	4.559	4.422
0.30	4.488	-0.9749	-0.2224	4.590	4.391
0.35	4.486	-0.9744	-0.2246	4.626	4.352
0.40	4.482	-0.9738	-0.2274	4.670	4.307
0.45	4.479	-0.9730	-0.2310	4.723	4.255
0.50	4.475	-0.9719	-0.2355	4.784	4.196
0.55	4.469	-0.9704	-0.2414	4.856	4.129
0.60	4.461	-0.9685	-0.2492	4.940	4.052
0.65	4.449	-0.9656	-0.2599	5.038	3.965
0.70	4.433	-0.9613	-0.2757	5.152	3.866
0.75	4.407	-0.9538	-0.3003	5.281	3.750
0.80	4.361	-0.9390	-0.3439	5.421	3.612
0.85	4.259	-0.8989	-0.4382	5.530	3.427
0.90	3.843	-0.6451	-0.7641	5.313	3.000

We further return to Eq. (8) which, upon substitution for  $\beta$ , becomes

$$\frac{1-e}{\varphi_0} \sin \frac{\pi - \varphi_0}{1-e} = 2 \frac{E(\psi_1)}{F(\psi_1)} - 1. \quad (11)$$

By using the table compiled above, we calculate the value of the angle  $\varphi_0$  by Eq. (9) for a given  $e$  and then choose  $k$  so as

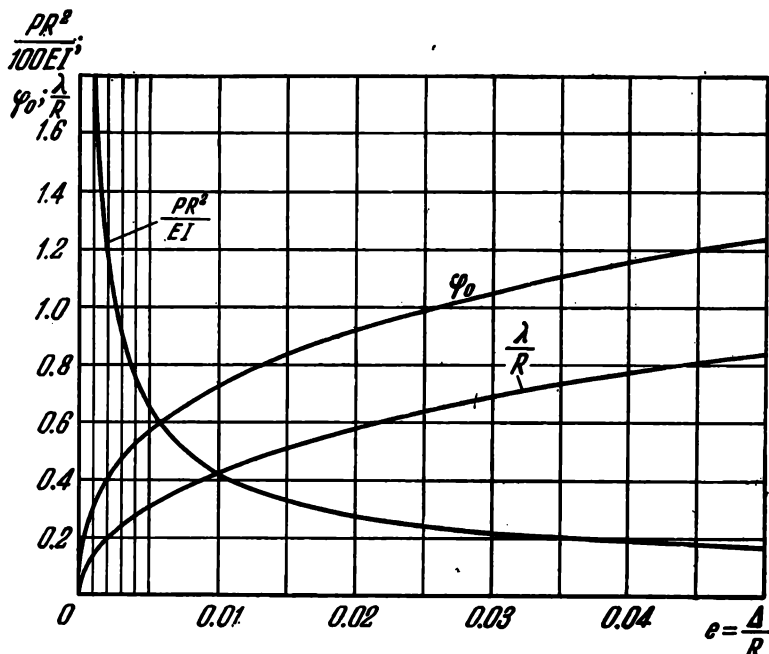


Fig. 384

to satisfy Eq. (11). Finally, from expressions (2) and (3) we find  $PR^2/EI$ .

The value of the deflection  $\lambda$  at the point  $C'$  is determined by the segment  $C'D$  (Fig. 383) and is obviously equal to

$$\lambda = y_1 + (R - \Delta)(1 - \cos \varphi_1)$$

or, according to expressions (1), (3), and (7),

$$\frac{\lambda}{R} = \frac{2k}{F(\psi_1)} (1 - \cos \psi_1) + (1-e) \left( 1 + \cos \frac{\pi - \psi_0}{1-e} \right).$$

The results of the calculations are plotted in Fig. 384. The graph reflects the conditions for the existence of the

form of equilibrium of an incompressible ring placed into a rigid casing.

The incompressibility condition tacitly assumed in the foregoing analysis leaves its mark on the course of the curves obtained. We see that the form of equilibrium of the ring with separation from the casing always exists provided only that the amount  $\Delta$  is different from zero. Actually this is not so, of course. The small difference in the lengths of the ring and the perimeter of the casing is taken up by compression of the ring. The above solution for the forms of equilibrium also holds in the case of a compressible ring. Only by the amount  $\Delta$  must be understood not merely the difference in the radii of the ring and casing, but the same quantity minus the contraction produced by normal forces developed in the ring.

If, for simplicity, we assume that the compressive force is the same for all points of the ring and is equal to  $P$ , we obtain

$$\frac{\Delta_0}{R} = \frac{\Delta}{R} + \frac{P}{EA}$$

or

$$\frac{\Delta_0}{R} = \frac{\Delta}{R} + \frac{PR^2}{EI} K, \quad (12)$$

where

$$K = \frac{I}{R^2 A}. \quad (13)$$

By the amount  $\Delta$  is now understood the difference of the radii compensated for by the separation of the ring from the casing with no change in its length, and by  $\Delta_0$  is meant the true initial difference of the radii.

From expression (12) it is seen that to allow for the compressibility of the ring, each point of the graph in Fig. 384 must be shifted to the right by the amount  $\frac{PR^2}{EI}K$  and the parameters  $PR^2/EI$ ,  $\varphi_0$ , and  $\lambda/R$  must be replotted as a function of  $\Delta_0/R$ . This introduces qualitative changes in the nature of the course of the curves and gives them a new interpretation. The replotting of the curves is shown in Fig. 385. Here are given the quantity  $K$  and the same three curves for  $PR^2/EI$ ,  $\varphi_0$ , and  $\lambda/R$  as in Fig. 384. They are drawn in thin lines. We take an arbitrary point  $a_1$  on the

curve for  $PR^3/EI$ . From the point  $a_1$  to the right we lay off a segment  $KPR^3/EI$  and obtain a point  $b_1$ . Points  $b_2$  and  $b_3$  are determined in a similar way. Then the point  $a_1$  is shifted and accordingly new points  $b_1$ ,  $b_2$ , and  $b_3$  are obtained. In this manner the new curves for  $PR^3/EI$ ,  $\varphi_0$ , and  $\lambda/R$  are

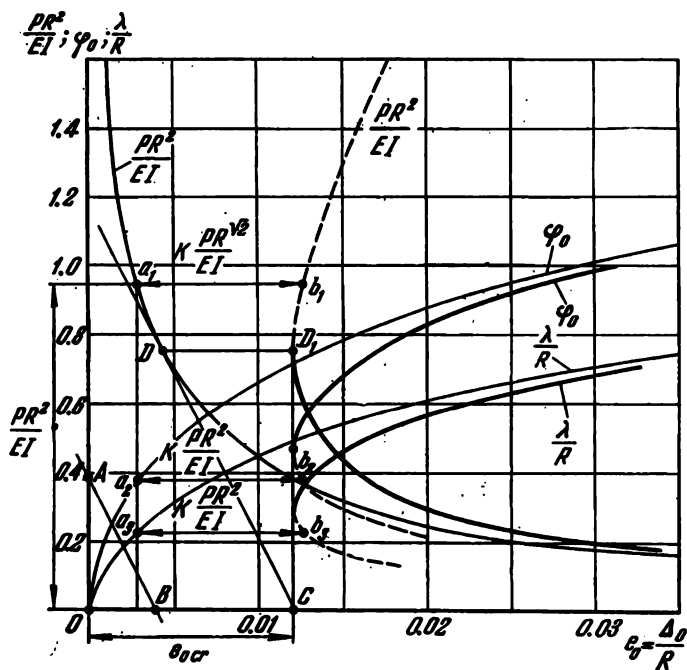


Fig. 385

plotted point by point. Each of these curves has an extremum at the same value  $e_0 = e_0 \text{ cr}$ . The new curves are drawn in heavy lines.

When  $e_0 < e_0 \text{ cr}$ , the compressible ring has no forms of equilibrium with a bent part separated off from the casing. When  $e_0 > e_0 \text{ cr}$ , we have at once two new forms: one stable and the other unstable. The portions of the curves characterizing the stable form are given by solid lines.

It is not at all necessary to plot curves for determining the critical value  $e_0 \text{ cr} = \Delta_0 \text{ cr}/R$ . It can be found in a much easier way. We take an arbitrary point  $A$  on the axis of ordinates and draw a straight line  $AB$  so as to make the

tangent of the angle  $OAB$  equal to  $K$ . We next draw a tangent to the curve for  $PR^2/EI$  parallel to the straight line  $AB$ . We obtain a straight line  $CD$ . The point  $C$  gives just the required value  $e_0$  cr. Indeed, differentiating  $\Delta_0/R$  (12) with respect to  $PR^2/EI$  and equating the derivative to zero, we find

$$\frac{d \frac{\Delta}{R}}{d \frac{PR^2}{EI}} = -K.$$

Thus, the extremum occurs at a value of  $PR^2/EI$  at which the tangent of the angle between the tangent line and the axis of ordinates is equal to  $-K$ . In this way the point  $D$  is determined. The segment  $DD_1$  is equal to  $KPR^2/EI$ . Adding it to  $\Delta/R$  [see (12)], we find the required  $e_0$  cr.

The above construction for a given  $K$  must be performed on the graph of Fig. 384, where the curves are given to scale.

For very small values of  $K$ , i.e., for a relatively thin-walled ring, the determination of  $e_0$  cr from the graph is not possible. Here it is advisable to simplify the foregoing equations by making use of the fact that the modulus of the elliptic integrals  $k$  is small and decreases with the magnitude of  $K$ . Thus, for a small  $k$  we have

$$F(\psi_1) = \int_0^{\psi_1} \frac{d\psi}{\sqrt{1-k^2 \sin^2 \psi}} \cong \int_0^{\psi_1} \left(1 + \frac{1}{2} k^2 \sin^2 \psi\right) d\psi,$$

$$E(\psi_1) = \int_0^{\psi_1} \sqrt{1-k^2 \sin^2 \psi} d\psi \cong \int_0^{\psi_1} \left(1 - \frac{1}{2} k^2 \sin^2 \psi\right) d\psi.$$

Upon integration we obtain

$$F(\psi_1) = \psi_1 + \frac{k^2}{4} (\psi_1 - \sin \psi_1 \cos \psi_1),$$

$$E(\psi_1) = \psi_1 - \frac{k^2}{4} (\psi_1 - \sin \psi_1 \cos \psi_1).$$

The angle  $\psi_1$  differs only slightly from  $3\pi/2$ . Assume  $\psi_1 = 3\pi/2 - \varepsilon$ , where  $\varepsilon$  is a small quantity. Then

$$\sin \psi_1 = -1, \quad \cos \psi_1 = -\varepsilon,$$

$$F(\psi_1) = \frac{3\pi}{2} \left(1 + \frac{k^2}{4}\right), \quad E(\psi_1) = \frac{3\pi}{2} \left(1 - \frac{k^2}{4}\right);$$

from Eq. (10) we now obtain  $\varepsilon = 2/3\pi$ . Equation (9) becomes

$$\varphi_0 = 2k\varepsilon \frac{3\pi}{2} = 2k.$$

In expression (11)  $\sin \frac{\pi - \varphi_0}{1 - e}$  is reduced to

$$\sin \frac{\pi - \varphi_0}{1 - e} = \cos \varphi_0 \sin \pi (1 + e) - \sin \varphi_0 \cos \pi (1 + e)$$

or

$$\sin \frac{\pi - \varphi_0}{1 - e} = -\pi e + \varphi_0 - \frac{\varphi_0^3}{6}.$$

Equation (11) finally gives  $e = \frac{2}{3\pi} k^3$  and hence

$$\varphi_0 = 2 \sqrt[3]{\frac{3\pi}{2} e}.$$

From expressions (2) and (3) we obtain

$$\frac{PR^2}{EI} = \frac{F^2(\psi_1)}{\varphi_0^3},$$

whence

$$e = \frac{9\pi^2}{32} \left( \frac{PR^2}{EI} \right)^{-3/2}.$$

Expression (12) for  $\Delta_0/R$  takes the form

$$\frac{\Delta_0}{R} = \frac{9\pi^2}{32} \left( \frac{PR^2}{EI} \right)^{-3/2} + K \frac{PR^2}{EI};$$

the quantity  $\Delta_0/R$  has a minimum value when

$$\frac{PR^2}{EI} = \left( \frac{27\pi^2}{64K} \right)^{2/5}$$

becoming equal to

$$e_{0 \text{ cr}} = \frac{1}{4} K^{3/5} (9\pi^2)^{2/5} \left[ \left( \frac{3}{2} \right)^{-3/5} + \left( \frac{3}{2} \right)^{2/5} \right]$$

or

$$e_{0 \text{ cr}} \cong 2.9 K^{3/5}.$$

For a ring of rectangular section  $b \times h$

$$K = \frac{h^2}{12R^2},$$

hence

$$e_{0\text{ cr}} = 0.65 \left( \frac{h}{R} \right)^{6/5}. \quad (14)$$

The quantity  $e_0$  may also be interpreted as thermal extension. Then

$$e_{0\text{ cr}} = \alpha t_{\text{cr}} = 0.65 \left( \frac{h}{R} \right)^{6/5}.$$

It is interesting to note that in the problem considered the degree to which the ratio  $h/R$  affects the critical loads is lower than in the usual problem of stability of a ring.

Turning now our attention to the contact pressure between the ring and casing, we obtain

$$q = \frac{\Delta_0}{R} \frac{EA}{R},$$

whence

$$q_{\text{cr}} = 0.65Eb \left( \frac{h}{R} \right)^{11/5}.$$

For the usual loading of a ring by normal or centrally directed forces (see Prob. 130) the critical value of  $q$  is determined by the ratio  $I/R^3$ , i.e., by the ratio  $h/R$  to the third power. Hence, a ring in a rigid "framing" possesses a comparatively high stability.

142.\* It is impossible to give a unique answer to the question posed. Let us consider the process of motion of the bar. The usual stability equation

$$M = EIy'' = -Py$$

is now complicated by introduction of transverse inertial forces of intensity  $q$ , i.e., it becomes

$$EIy^{(IV)} = -Py'' + q.$$

But

$$q = -\frac{\gamma A}{g} \frac{\partial^2 y}{\partial t^2},$$

---

\* This problem was first considered in a similar formulation by M. A. Lavrent'ev and A. Yu. Ishlinskii in the paper *Dynamical Instability Modes of Elastic Systems*, Doklady Akad. Nauk SSSR, 64 (6), 779-782 (1949).

where  $\gamma$  is the specific weight of the bar material and  $A$  is the cross-sectional area. We obtain the differential equation

$$\frac{\gamma A}{g} \frac{\partial^2 y}{\partial t^2} + EI \frac{\partial^4 y}{\partial x^4} + P \frac{\partial^2 y}{\partial x^2} = 0. \quad (1)$$

Assume

$$y = \sum T_m \sin \frac{m\pi x}{l},$$

where  $T_m$  are some functions of the time  $t$ .

Substituting this expression in Eq. (1), we obtain

$$\frac{\gamma A}{g} \frac{d^2 T_m}{dt^2} + \frac{\pi^4 EI}{l^4} m^2 (m^2 - \eta^2) T_m = 0, \quad (2)$$

where

$$\eta^2 = \frac{P}{\frac{\pi^2 EI}{l^2}}.$$

In our case  $\eta^2 = 10$ .

If  $m^2 > \eta^2$ , Eq. (2) is solvable in terms of trigonometric functions, which corresponds to periodic vibrations of the bar.

If  $m^2 < \eta^2$ , Eq. (2) is solvable in terms of exponential functions

$$T_m = A_m e^{k_m t} + B_m e^{-k_m t},$$

where

$$k_m = \sqrt{\frac{\pi^4 EI g}{\gamma A l^4} m^2 (\eta^2 - m^2)}$$

and the quantity  $m$  takes three integral values, 1, 2, 3.

Naturally, we are interested only in terms that increase indefinitely in time. We may therefore write

$$y = A_1 e^{k_1 t} \sin \frac{\pi x}{l} + A_2 e^{k_2 t} \sin \frac{2\pi x}{l} + A_3 e^{k_3 t} \sin \frac{3\pi x}{l}.$$

The exponent  $k_m$  which characterizes the rate of increase of a particular form depends on the value of  $m$ . When  $m = 1, 2, 3$  and  $\eta^2 = 10$ , the quantity  $m^2 (\eta^2 - m^2)$  appearing in the radicand for  $k_m$  takes, respectively, the values 9, 24, and 9. Thus, the rate of increase of deflections for the bending in the form of two half-waves is higher than for

the bending in the form of one or three half-waves. This seems to be the only thing that we can state for certain in connection with the question posed.

The fact is that we know nothing about the quantities  $A_1$ ,  $A_2$ , and  $A_3$  which characterize the initial deflection of the bar. Even if these parameters are treated as statistically equal, the solution obtained for the linear problem says nothing about the behaviour of the bar in the range of large displacements. If we go on in our investigation and try to analyze the behaviour of the bar when the displacements are large, we shall find that the given data are insufficient for the complete solution of the problem.

Indeed, what do we mean by the question: "In what form will the bar bend?". Obviously it is necessary first to agree upon the questions as to where the process of motion ends, what limits the vertical displacement of the upper end of the bar or what is the duration of action of the force. But all these questions would lead us too far off.

143. The proposed problem again involves the fundamental aspects of stability of elastic systems and its solution calls for a new formulation of the stability criterion.

Imagine the bar to be slightly displaced from its original equilibrium position (Fig. 386).

The equation of the elastic curve is

$$EIy'' = P(f - y) - P\varphi(l - x)$$

from which

$$y = A \sin \alpha x + B \cos \alpha x + f - \varphi(l - x),$$

where  $\alpha^2 = \frac{P}{EI}$ .

When  $x = 0$ ,  $y = 0$  and  $y' = 0$ ; when  $x = l$ ,  $y = f$  and  $y' = \varphi$ . To fulfil these conditions we obtain four equations

$$\begin{aligned} B + f - \varphi l &= 0, & A\alpha + \varphi &= 0, \\ A \sin \alpha l + B \cos \alpha l &= 0, & A \cos \alpha l - B \sin \alpha l &= 0. \end{aligned}$$

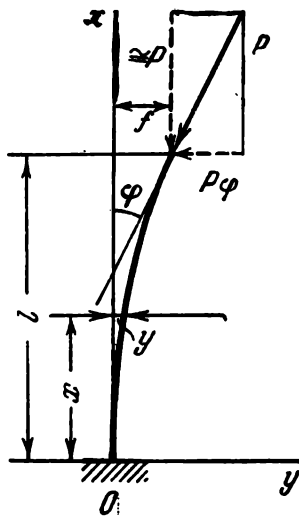


Fig. 386

Considering the last two equations, it is easy to ascertain that irrespective of the choice of  $\alpha l$  the constants  $A$  and  $B$  are equal to zero since the determinant

$$\begin{vmatrix} \sin \alpha l & \cos \alpha l \\ \cos \alpha l & -\sin \alpha l \end{vmatrix}$$

does not vanish. But if  $A = B = 0$ , the only form of equilibrium of the bar is the original straight-line form.

In all the problems considered above we have invariably identified two concepts: "loss of stability" and "existence of other than original forms of equilibrium". In the present case we are therefore confronted with the alternative: either to give up the conventional and deeply rooted identification of the above concepts or to assume that the system maintains stability for all values of the force  $P$ .

The first variant is the correct one. The original form of equilibrium is stable only up to a certain value of the force  $P$ . At a force exceeding this value, which will be termed critical as before, a transition takes place not to a new form of equilibrium, but to a certain form of motion with ever increasing deflection from the original equilibrium position. The stability criterion is the condition for the occurrence of the above form of motion and is called the dynamic stability criterion.

Consider the following mechanical model shown in Fig. 387. Two homogeneous bars of mass  $m_1$  and  $m_2$ , respectively, are connected together by a spring of stiffness  $k$ . The same spring connects the lower bar to a hinged support. The line of action of the force  $P$  is always coincident with the direction of the axis of the upper bar.

The generalized co-ordinates are taken to be the angles of rotation of the bars  $\varphi_1$  and  $\varphi_2$ . The displacements of the centres of mass of the bars are then

$$y_1 = l\varphi_1, \quad y_2 = 2l\varphi_1 + l\varphi_2,$$

where  $2l$  is the length of each bar.

The moments of inertia about the centroidal transverse axes of the bars are, respectively,

$$I_1 = \frac{m_1 l^2}{3} \text{ and } I_2 = \frac{m_2 l^2}{3}.$$

By introducing the forces of interaction in the hinge (Fig. 388), we set up the equations of motion.

For the upper bar

$$\left. \begin{aligned} Y = P, \quad X = P\varphi_2 + m_2 \ddot{y}_2, \\ I_2 \ddot{\varphi}_2 + m_2 \ddot{y}_2 l + k(\varphi_2 - \varphi_1) = 0. \end{aligned} \right\} \quad (1)$$

For the lower bar

$$k\varphi_1 + I_1 \ddot{\varphi}_1 - k(\varphi_2 - \varphi_1) + X2l + m_1 \ddot{y}_1 l - Y2l\varphi_1 = 0. \quad (2)$$

Eliminating  $y_1$ ,  $y_2$ ,  $X$ , and,  $Y$ , and expressing the moments

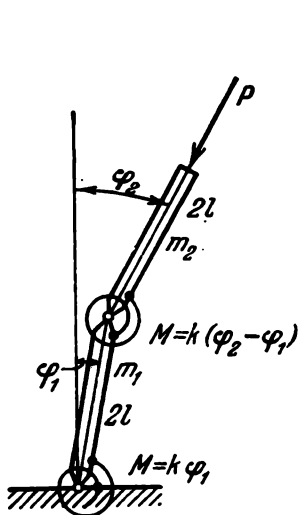


Fig. 387

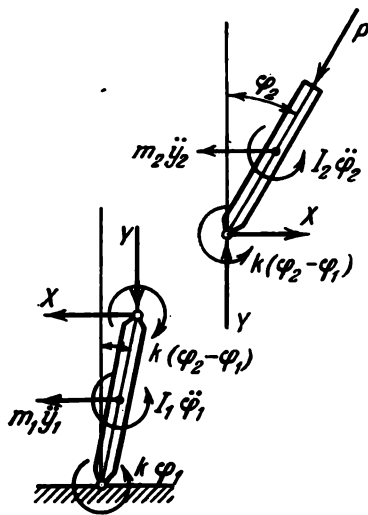


Fig. 388

of inertia in terms of the masses, we obtain two linear differential equations in  $\varphi_1$  and  $\varphi_2$

$$\left. \begin{aligned} \frac{4}{3} m_2 l^2 \ddot{\varphi}_2 + 2m_2 l^2 \ddot{\varphi}_1 + k(\varphi_2 - \varphi_1) = 0, \\ \left( 4m_2 l^2 + \frac{4}{3} m_1 l^2 \right) \ddot{\varphi}_1 + 2m_2 l^2 \ddot{\varphi}_2 + (2k - 2Pl)\varphi_1 + \\ + (2Pl - k)\varphi_2 = 0. \end{aligned} \right\} \quad (3)$$

Assume, as is usually done,

$$\varphi_1 = A_1 e^{\bar{k}t}, \quad \varphi_2 = A_2 e^{\bar{k}t}. \quad (4)$$

Upon substitution we come to two equations in  $A_1$  and  $A_2$

$$\begin{aligned} A_1(2m_2l^2\bar{k}^2 - k) + A_2\left(\frac{4}{3}m_2l^2\bar{k}^2 + k\right) &= 0, \\ A_1\left(4m_2l^2\bar{k}^2 + \frac{4}{3}m_1l^2\bar{k}^2 + 2k - 2Pl\right) + \\ &+ A_2(2m_2l^2\bar{k}^2 + 2Pl - k) = 0. \end{aligned}$$

To determine the conditions for the existence of non-zero solutions, we equate the determinant to zero. This gives a quadratic equation in  $\bar{k}^2$

$$\left(\frac{m_2\bar{k}^2l^2}{k}\right)(3 + 4\mu) + \frac{m_2\bar{k}^2l^2}{k}3\left(8 + \mu - 5\frac{Pl}{k}\right) + \frac{9}{4} = 0, \quad (5)$$

where  $\mu = m_1/m_2$ .

The free term in Eq. (5) is independent of the force  $P$ . Consequently, it is impossible to select  $P$  so as to make  $\bar{k}$  zero, and hence, by reverting to expressions (4), it is seen that the angles  $\varphi_1$  and  $\varphi_2$  cannot be constant. The system has no forms of equilibrium other than the original one. The model under consideration possesses the same property as a fixed bar loaded by a follow-up force.

From Eq. (5) it can readily be verified also that the quantity  $\bar{k}^2$  remains less than zero at any force  $P$ . This means that  $\bar{k}$  has no real values and the conditions for aperiodic motion are non-existent. Assume that

$$\bar{k}l\sqrt{\frac{m_2}{k}} = \varepsilon + i\omega$$

and find the condition under which  $\varepsilon$  may be a positive quantity. This corresponds to the occurrence of a vibratory motion with building-up amplitude.

By separating the real and imaginary parts in Eq. (5), we obtain

$$\begin{aligned} [(\varepsilon^2 - \omega^2)^2 - 4\varepsilon^2\omega^2](3 + 4\mu) + \\ + 3(\varepsilon^2 - \omega^2)\left(8 + \mu - 5\frac{Pl}{k}\right) + \frac{9}{4} &= 0, \\ 4\varepsilon\omega(\varepsilon^2 - \omega^2)(3 + 4\mu) + 6\varepsilon\omega\left(8 + \mu - 5\frac{Pl}{k}\right) &= 0. \end{aligned}$$

We eliminate  $\omega$ . Then

$$\varepsilon^4 4(3 + 4\mu) + \varepsilon^2 6 \left( 8 + \mu - 5 \frac{Pl}{k} \right) + \frac{9}{4} \frac{\left( 8 + \mu - 5 \frac{Pl}{k} \right)^2}{3 + 4\mu} - \frac{9}{4} = 0,$$

whence

$$\varepsilon^2 = \frac{3}{4} \frac{5 \frac{Pl}{k} - 8 - \mu \pm \sqrt{3 + 4\mu}}{3 + 4\mu}.$$

The least value of  $P$  at which  $\varepsilon^2$  (and hence one of the roots  $\varepsilon$ ) assumes a positive value is

$$P_{cr} = \frac{k}{5l} (8 + \mu - \sqrt{3 + 4\mu}).$$

The magnitude of the critical force depends on the mass distribution between the bars. In the case of  $m_1 = m_2$  we have  $\mu = 1$ . Then

$$P_{cr} = \frac{k}{5l} (9 - \sqrt{7}).$$

If the mass of the first bar is small compared with the mass of the second bar,  $\mu = 0$  and

$$P_{cr} = \frac{k}{5l} (8 - \sqrt{3}).$$

As the mass of the upper bar is decreased in comparison with the mass of the lower bar, the quantity  $\mu$  increases indefinitely and so does  $P_{cr}$ . This is clear. If the transverse inertial forces are absent, the upper bar is always on the same straight line with the lower bar.

In systems admitting a stability analysis based on an investigation of equilibrium forms, i.e., in usual systems, the dynamic criterion gives the same results as the static criterion. Consider, for example, the same bar system under conditions of loading by a force maintaining its direction (Fig. 389). In this case, instead of Eqs. (1) we obtain

$$Y = P, \quad X = m_2 \ddot{y}_2, \\ I_2 \ddot{\varphi}_2 + m_2 \ddot{y}_2 l + k(\varphi_2 - \varphi_1) - P 2l \varphi_2 = 0.$$

Equation (2) remains unchanged. In place of Eqs. (3) we have

$$\begin{aligned} \frac{4}{3} m_2 l^2 \ddot{\varphi}_2 + 2m_2 l^2 \ddot{\varphi}_1 + k(\varphi_2 - \varphi_1) - 2Pl\varphi_2 &= 0, \\ \left(4m_2 l^2 + \frac{4}{3} m_1 l^2\right) \ddot{\varphi}_1 + 2m_2 l^2 \ddot{\varphi}_2 + (2k - 2Pl)\varphi_1 - k\varphi_2 &= 0 \end{aligned}$$

and in place of Eq. (5) we obtain

$$\begin{aligned} \left(\frac{m_2 k^2 l^2}{k}\right)^2 (3 + 4\mu) + \frac{m_2 k^2 l^2}{k} 3 \left[8 + \mu - \frac{Pl}{k} (8 + 2\mu)\right] + \\ + \frac{9}{4} \left[1 - \frac{6Pl}{k} + 4 \left(\frac{Pl}{k}\right)^2\right] = 0. \end{aligned} \quad (6)$$

The free term in this equation now depends on the force  $P$  and when

$$P = \frac{k}{4l} (3 \pm \sqrt{5})$$

it becomes zero. Consequently, it is possible to have zero values for  $\bar{k}$  and there is a solution in which  $\varphi_1$  and  $\varphi_2$  (4) are time independent, i.e., there is an equilibrium form when

$$P_{cr} = \frac{k}{4l} (3 - \sqrt{5}).$$

Here the magnitude of the critical force is independent of the mass distribution since the parameter  $\mu$  does not, and cannot, enter into the free term of Eqs. (5) and (6).

We revert to the elastic bar and set up the equation of motion for it. To an element of the bar, of length  $dx$  (Fig. 390), are applied forces and moments at sections and distributed inertial forces of intensity  $\rho A \partial^2 y / \partial t^2$ , where  $\rho$  is the density of the bar material.

By projecting the forces on the normal to the elastic curve, we obtain

$$dQ + P \frac{\partial^2 y}{\partial x^2} dx + \rho A \frac{\partial^2 y}{\partial t^2} dx = 0.$$

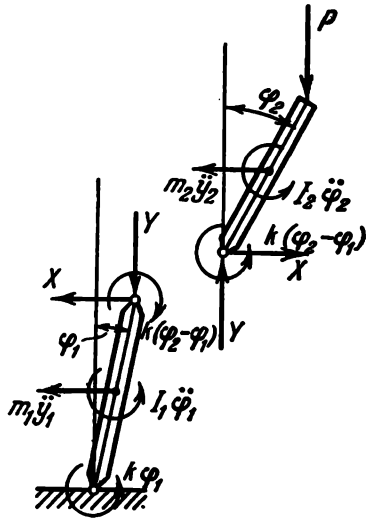


Fig. 389

Since

$$Q = EI \frac{\partial^3 y}{\partial x^3},$$

we have

$$EI \frac{\partial^4 y}{\partial x^4} + P \frac{\partial^2 y}{\partial x^2} + \rho A \frac{\partial^2 y}{\partial t^2} = 0;$$

$\rho A$  is considered to be a constant.

Assume that

$$y = Y e^{i\Omega t},$$

where  $Y$  depends on the co-ordinate  $x$  only. For real values of  $\Omega$  the motion is of the type of harmonic vibrations. If  $\Omega$  is complex

$$\Omega = a \pm bi,$$

then

$$y = Y e^{(\mp b + ia)t} = Y e^{\mp bt} (\cos at + i \sin at). \quad (7)$$

Consequently, the motion takes place with either decreasing or increasing amplitude, depending on the sign of  $b$ .

Substituting for  $y$  in the equation of motion and introducing the non-dimensional parameters

$$\beta^2 = \frac{Pl^2}{EI}, \quad \omega = \Omega l^2 \sqrt{\frac{\rho A}{EI}}, \quad \zeta = \frac{x}{l},$$

we obtain

$$\frac{d^4 Y}{d\zeta^4} + \beta^2 \frac{d^2 Y}{d\zeta^2} - \omega^2 Y = 0. \quad (8)$$

The solution of this equation is

$$Y = C_1 \sin \alpha_1 \zeta + C_2 \cos \alpha_1 \zeta + C_3 \sinh \alpha_2 \zeta + C_4 \cosh \alpha_2 \zeta, \quad (9)$$

where

$$\alpha_1^2 = \frac{\beta^2}{2} + \sqrt{\frac{\beta^2}{4} + \omega^2},$$

$$\alpha_2^2 = -\frac{\beta^2}{2} + \sqrt{\frac{\beta^2}{4} + \omega^2}.$$

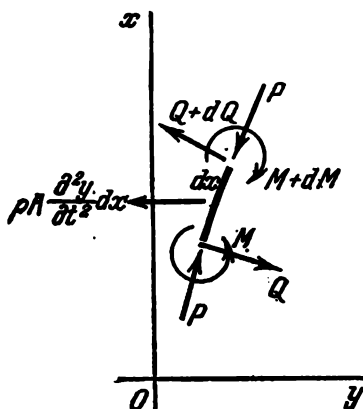


Fig. 390

At the restrained end we have  $Y = 0$  and  $dY/d\zeta = 0$ , irrespective of the loading conditions. Consequently,

$$C_2 + C_4 = 0, \quad \alpha_1 C_1 + \alpha_2 C_3 = 0.$$

At the free end of the bar the bending moment is zero and in the case of a follow-up force the shearing force becomes zero. Hence, when  $x = l$  (or when  $\zeta = 1$ ),

$$\frac{d^2 Y}{d\zeta^2} = 0 \quad \text{and} \quad \frac{d^3 Y}{d\zeta^3} = 0,$$

giving two more equations

$$-C_1 \alpha_1^3 \sin \alpha_1 - C_2 \alpha_1^3 \cos \alpha_1 + C_3 \alpha_2^3 \sinh \alpha_2 + C_4 \alpha_2^3 \cosh \alpha_2 = 0,$$

$$-C_1 \alpha_1^3 \cos \alpha_1 + C_2 \alpha_1^3 \sin \alpha_1 + C_3 \alpha_2^3 \cosh \alpha_2 + C_4 \alpha_2^3 \sinh \alpha_2 = 0.$$

In the case of a force  $P$  keeping its direction unchanged the last condition would be different. Here the shearing force is not zero, but is equal to  $-Py'_{x=l}$ .

We equate to zero the determinant of the four equations obtained above. Then

$$\begin{aligned} & \alpha_1^4 + \alpha_2^4 + \alpha_1 \alpha_2 \times \\ & \times (\alpha_1^2 - \alpha_2^2) \sin \alpha_1 \times \\ & \times \sinh \alpha_2 + 2\alpha_1^2 \alpha_2^2 \cos \alpha_1 \times \\ & \times \cosh \alpha_2 = 0 \end{aligned}$$

or

$$\begin{aligned} & \beta^4 + 2\omega^2 + \beta^2 \omega \sin \alpha_1 \times \\ & \times \sinh \alpha_2 + 2\omega^2 \cos \alpha_1 \times \\ & \times \cosh \alpha_2 = 0. \end{aligned} \quad (10)$$

In the case of a force maintaining its direction, in place of expression (10) we obtain

$$2\omega^2 - \beta^2 \omega \sin \alpha_1 \sinh \alpha_2 + (\beta^4 + 2\omega^2) \cos \alpha_1 \cosh \alpha_2 = 0. \quad (11)$$

Relation (10) enables one to plot the natural frequency  $\omega$  of the bar as a function of the non-dimensional force  $\beta^2$  (Fig. 391). The variation of the frequency for the case of a non-follow-up force is shown dashed in the same graph.

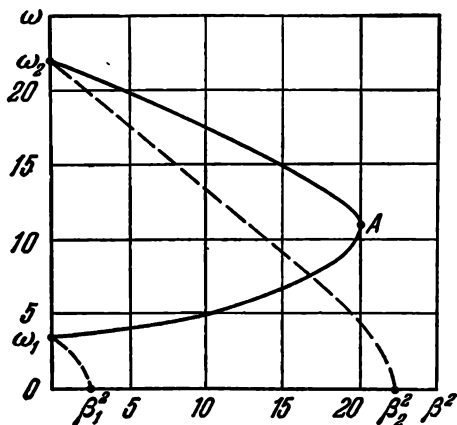


Fig. 391

When  $\beta = 0$ , we have the first  $\omega_1$  and the second  $\omega_2$  natural frequency of a free restrained bar. As the non-follow-up force is increased, these (and higher) frequencies decrease and vanish at a force assuming critical values, i.e.,

$$\text{when } \beta^2 = \beta_1^2 = \frac{\pi^2}{4} \quad \text{or when } P = \frac{\pi^2 EI}{4l^2}$$

and, in general, when

$$P = \frac{n^2 \pi^2 EI}{4l^2} \quad (n = 1, 3, 5, \dots).$$

In the case of a follow-up force the lowest frequency increases with increasing  $P$ , and at the point  $A$  the curves of the first and second tones join up. If the graph is extended to the range of higher frequencies, it can be seen that the same joining up of the curves occurs for the third and fourth frequencies, the fifth and sixth frequencies, etc.

To determine the critical value of the force  $P$  in this case, it is necessary to find the least value of  $P$  at which the multiplicity of roots  $\omega$  in Eq. (10) is obtained. This means that with further increase of  $\beta$  the roots become complex conjugate and there is a root with negative imaginary part, i.e.,  $\Omega = a - bi$ . According to expression (7), this corresponds to the appearance of a mode of vibration with building-up amplitude. From Fig. 391 it is seen that the multiplicity of roots occurs at the point  $A$ .

Carrying out a numerical calculation, we determine

$$\beta^2 = 20.05 \quad (\omega = 11.016);$$

consequently,

$$P_{cr} = 20.05 \frac{EI}{l^2}.$$

The result obtained is true only for a uniform mass distribution along the length of the bar. For any other mass distribution the critical force will be different. It is very important to note this in view of the fact that sometimes attempts are made to determine the critical force in such problems by means of various tricks without recourse to the laws of dynamics, which predetermines the neglect of mass distribution and the basic incorrectness of the solution.

144. The case of loading (a) has become known in the literature as the Reut problem.\*

The bar has no forms of equilibrium other than the original straight-line form. Indeed,

$$EIy'' = -Py$$

(Fig. 392); further,

$$y = A \sin \alpha x + B \cos \alpha x;$$

when  $x = 0$ ,  $y = 0$  and  $y' = 0$ ; consequently,

$$B = 0 \text{ and } A = 0.$$

We proceed to the analysis of modes of motion. Suppose that the mass of the flat disk at the end of the bar is small. The function  $Y$  [formula (9)] found in the solution of the preceding problem holds good. The first two boundary conditions also remain true:

$$\text{when } \zeta = 0, \quad Y = 0 \text{ and } \frac{dY}{d\zeta} = 0,$$

i.e.,

$$C_2 + C_4 = 0, \quad \alpha_1 C_1 + \alpha_2 C_2 = 0.$$

When  $x = l$  ( $\zeta = 1$ ), we have

$$EIy'' = -Py, \quad EIy''' = -Py'$$

or

$$Y'' + \beta^2 Y = 0, \quad Y''' + \beta^2 Y' = 0.$$

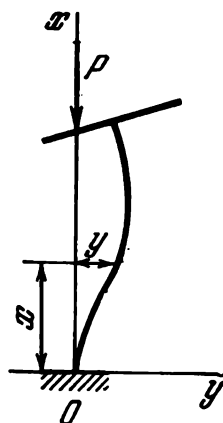


Fig. 392

Turning now to solution (9) of the preceding problem, we obtain

$$\begin{aligned} C_1(-\alpha_1^2 + \beta^2) \sin \alpha_1 + C_2(-\alpha_1^2 + \beta^2) \cos \alpha_1 + \\ + C_3(\alpha_2^2 + \beta^2) \sinh \alpha_2 + C_4(\alpha_2^2 + \beta^2) \cosh \alpha_2 = 0, \\ C_1(-\alpha_1^3 + \beta^2 \alpha_1) \cos \alpha_1 + C_2(\alpha_1^3 - \beta^2 \alpha_1) \sin \alpha_1 + \\ + C_3(\alpha_2^3 + \beta^2 \alpha_2) \cosh \alpha_2 + C_4(\alpha_2^3 + \beta^2 \alpha_2) \sinh \alpha_2 = 0. \end{aligned}$$

\* Reut V. I., *On the Theory of Elastic Stability*, Trudy Odessk. Inst. Inzh. Grazhd. i Komm. Stroït., Vyp. 1, 115-190 (1939).

By equating to zero the determinant of the system, we arrive at the transcendental equation

$$\beta^4 + 2\omega^2 + \beta^2\omega \sin \alpha_1 \sinh \alpha_2 + 2\omega^2 \cos \alpha_1 \cosh \alpha_2 = 0$$

which is identical with Eq. (10). Thus, the critical force is the same as in the preceding problem

$$P_{cr} = \frac{20.05EI}{l^2}.$$

The coincidence of the results could have been guessed from the start. The forces at the ends of the bar are identical in

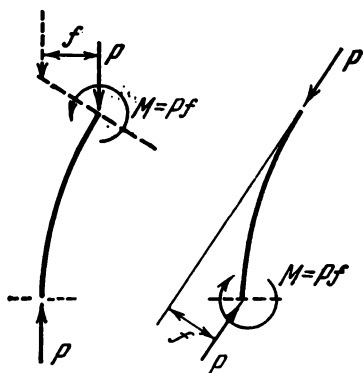


Fig. 393

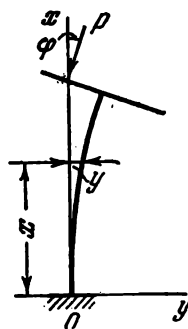


Fig. 394

both cases. The only difference is in the reference system for  $y$  and  $x$  (Fig. 393).

In the case of loading (b) (Fig. 394) the problem is solved on the basis of the usual analysis of equilibrium forms.

We have the equation

$$EIy'' = -Py - P\varphi(l - x)$$

or

$$y'' + \alpha^2 y = -\alpha^2 \varphi(l - x) \quad \left( \alpha^2 = \frac{P}{EI} \right)$$

from which

$$y = A \sin \alpha x + B \cos \alpha x - \varphi(l - x).$$

When  $x = 0$ ,  $y = 0$  and  $y' = 0$ ; when  $x = l$ ,  $y' = \varphi$ . We then obtain the following three equations:

$$B - \varphi l = 0, \quad A\alpha + \varphi = 0, \quad A \cos \alpha l - B \sin \alpha l = 0.$$

By equating to zero the determinant of this system, we obtain

$$\tan \alpha l = -\alpha l.$$

The least non-zero root of this equation is

$$\alpha l = 2.029,$$

whence

$$P_{cr} = \frac{4.115EI}{l^2}.$$

145. The system is analogous to that considered in Prob. 143. To analyze the stability we must set up the equations of motion.

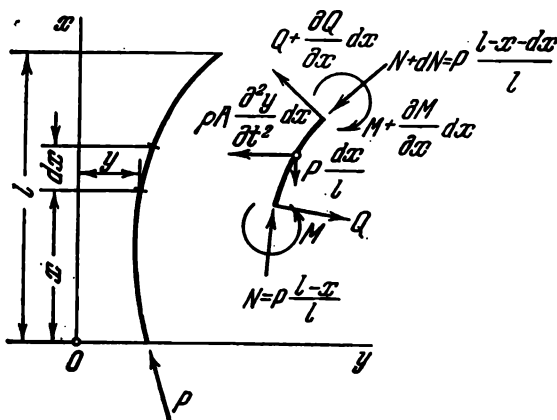


Fig. 395

Consider an element of length  $dx$  (Fig. 395). By equating to zero the sum of the projections of the forces on the  $y$  axis, we obtain

$$\begin{aligned} \frac{\partial Q}{\partial x} dx + \rho A \frac{\partial^2 y}{\partial t^2} dx + \\ + P \frac{l-x-dx}{l} \left( \frac{\partial y}{\partial x} + \frac{\partial^2 y}{\partial x^2} dx \right) - P \frac{l-x}{l} \frac{\partial y}{\partial x} = 0 \end{aligned}$$

or

$$\frac{\partial Q}{\partial x} + \rho A \frac{\partial^2 y}{\partial t^2} + \frac{\partial}{\partial x} \left[ P \frac{l-x}{l} \frac{\partial y}{\partial x} \right] = 0.$$

But since

$$\frac{\partial Q}{\partial x} = EI \frac{\partial^4 y}{\partial x^4},$$

we have

$$EI \frac{\partial^4 y}{\partial x^4} + \frac{\partial}{\partial x} \left[ P \frac{l-x}{l} \frac{\partial y}{\partial x} \right] + \rho A \frac{\partial^2 y}{\partial t^2} = 0. \quad (1)$$

Here  $\rho$  is, as usual, the density of the material and  $A$  is the cross-sectional area. These quantities (as well as  $EI$ ) are independent of  $x$ .

Equation (1) has a structure that predetermines the application of computers. True, for a homogeneous bar it is hoped that the solution of the equation may be reduced to tabulated Bessel functions or related functions. But even in this case the problem is most quickly solved by using electronic digital computers. Assume

$$y = Y e^{i\Omega t}$$

and transform to a non-dimensional form

$$\frac{d^4 Y}{d\zeta^4} + \beta^2 \frac{d}{d\zeta} \left[ (1-\zeta) \frac{dY}{d\zeta} \right] - \omega^2 Y = 0,$$

where

$$\beta^2 = \frac{Pl^2}{EI}, \quad \omega^2 = \frac{\rho Al^4}{EI} \Omega^2, \quad \zeta = \frac{x}{l}.$$

The boundary conditions are:

$$\begin{aligned} \text{when } \zeta = 0, \quad & \frac{d^2 Y}{d\zeta^2} = 0, \quad \frac{d^3 Y}{d\zeta^3} = 0, \\ \text{when } \zeta = 1, \quad & \frac{d^2 Y}{d\zeta^2} = 0, \quad \frac{d^3 Y}{d\zeta^3} = 0. \end{aligned}$$

The solution is sought in the form of a series

$$Y = \sum_{n=0, 1, 2, \dots} A_n \zeta^n.$$

According to the conditions at the ends,  $A_2 = A_3 = 0$ ,

$$\Sigma A_n n (n-1) = 0, \quad \Sigma A_n n (n-1) (n-2) = 0. \quad (2)$$

For the determination of the terms of the series we have the following recurrence formula:

$$\begin{aligned} A_n = & \frac{1}{n(n-1)(n-2)(n-3)} \times \\ & \times \{ \omega^2 A_{n-4} + \beta^2 [A_{n-3}(n-3)^2 - A_{n-2}(n-2)(n-3)] \}. \end{aligned}$$

The constants  $A_0$  and  $A_1$  remain undetermined. They must be selected so as to fulfil the last two boundary conditions. Since  $A_0$  and  $A_1$  enter linearly into expressions (2), we may write

$$\sum A_n n(n-1) = K_0 A_0 + K_1 A_1 = 0,$$

$$\sum A_n n(n-1)(n-2) = L_0 A_0 + L_1 A_1 = 0.$$

The condition for the existence of non-zero solutions is obviously as follows:

$$K_0 L_1 - K_1 L_0 = D = 0. \quad (3)$$

The procedure for calculation.

Assign  $\beta$  and  $\omega$ .

Assume  $A_0 = 1$  and  $A_1 = 0$  and determine the terms of the series by the recurrence formula. In the problem under

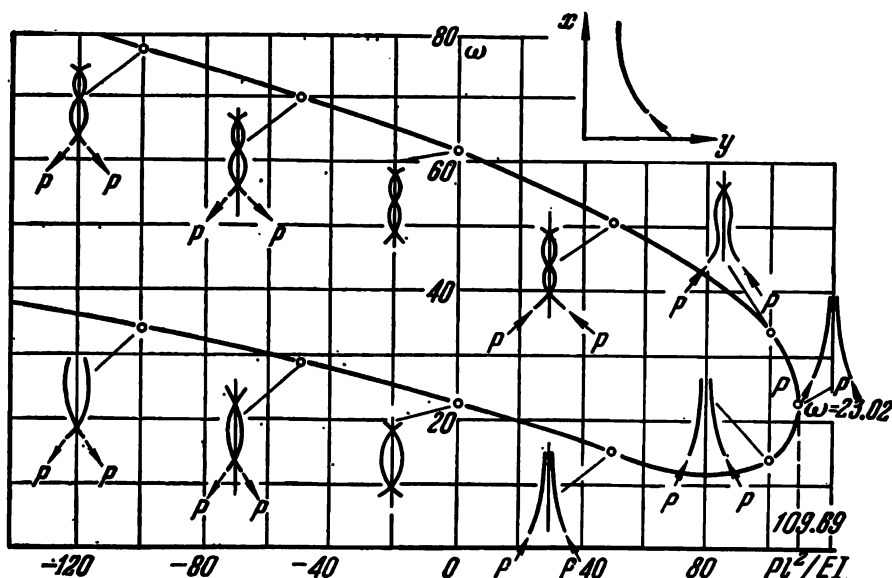


Fig. 396

consideration it is sufficient to take 20 or 30 of them. Next calculate  $\sum A_n n(n-1) = K_0$  and  $\sum A_n n(n-1)(n-2) = L_0$ .

Assuming  $A_0 = 0$  and  $A_1 = 1$ , repeat the calculation; the sums so found are then equal, respectively, to  $K_1$  and  $L_1$ .

Further the quantity  $D$  (3) is calculated. Change  $\omega$  and again calculate  $D$ . Compare it with the preceding value. If the sign of  $D$  has not changed, we proceed further; if it has changed, this means that the value of the frequency for the given force has been passed. By interpolation  $\omega$  is determined. As a result, the graph of  $\omega$  against  $\beta^2$  is plotted as shown in Fig. 396.

As in Prob. 143, at the critical force  $P$  there is coincidence of the frequencies of the first and second tones

$$\beta_{cr}^2 = 109.69 \quad ..(\omega = 23.02).$$

The critical force is

$$P_{cr} = \frac{109.69EI}{l^2}.$$

Figure 396 shows modes of vibration of the bar for a series of values of  $P$ , consideration being given not only to a compressive force  $P$ , but also to a tensile force. It is interesting that the node points become imaginary for some values of  $P$ .

146. Here we obviously have a restatement of Prob. 143 but with other boundary conditions. Expression (9) of Prob. 143 holds and the boundary conditions change to

$$\begin{aligned} \text{when } \zeta = 0, \quad & \frac{d^2 Y}{d\zeta^2} = 0 \quad \text{and} \quad \frac{d^3 Y}{d\zeta^3} = 0, \\ \text{when } \zeta = 1, \quad & \frac{d^2 Y}{d\zeta^2} = 0 \quad \text{and} \quad \frac{d^3 Y}{d\zeta^3} = 0. \end{aligned} \quad (1)$$

We further obtain four equations

$$\begin{aligned} -\alpha_1^3 C_2 + \alpha_2^3 C_4 &= 0, \\ -\alpha_1^3 C_1 + \alpha_2^3 C_3 &= 0, \\ -\alpha_1^3 C_1 \sin \alpha_1 - \alpha_1^3 C_2 \cos \alpha_1 + \alpha_2^3 C_3 \sinh \alpha_2 + \alpha_2^3 C_4 \cosh \alpha_2 &= 0, \\ -\alpha_1^3 C_1 \cos \alpha_1 + \alpha_1^3 C_2 \sin \alpha_1 + \alpha_2^3 C_3 \cosh \alpha_2 + \alpha_2^3 C_4 \sinh \alpha_2 &= 0. \end{aligned}$$

By equating the determinant to zero, we obtain a transcendental equation

$$\omega (\cos \alpha_1 \cosh \alpha_2 - 1) + \beta^2 \sin \alpha_1 \sinh \alpha_2 = 0 \quad (2)$$

which is subjected to analysis,

The question of the behaviour of the bar is solved according to the nature of the function  $\omega = f(\beta)$ . If for some values of the non-dimensional force  $\beta^2$  the frequency  $\omega$  vanishes, the bar has forms of equilibrium other than the straight-line one. If there are no zero points for  $\omega$ , it is necessary to determine the conditions for the multiplicity of frequencies, this corresponding to the conditions for the occurrence of a motion with building-up amplitude.

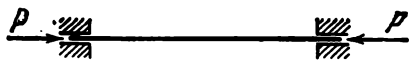


Fig. 397

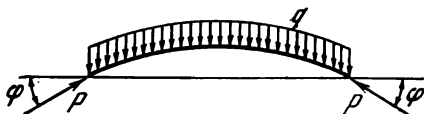


Fig. 398

Another solution suggested by L. I. Balabukh looks very effective. We turn to Eq. (8) of Prob. 143. By differentiating it twice with respect to  $\zeta$  and denoting  $d^2Y/d\zeta^2 = Y_0$ , we obtain the same equation

$$\frac{d^4Y_0}{d\zeta^4} + \beta^2 \frac{d^2Y_0}{d\zeta^2} - \omega^2 Y_0 = 0,$$

but the boundary conditions are now different:

$$\begin{aligned} \text{when } \zeta = 0, \quad Y_0 = 0 \quad \text{and} \quad \frac{dY_0}{d\zeta} = 0, \\ \text{when } \zeta = 1, \quad Y_0 = 0 \quad \text{and} \quad \frac{dY_0}{d\zeta} = 0. \end{aligned} \tag{3}$$

Consequently, the solution is the same as for a compressed bar fixed at its ends (Fig. 397). But here it is known that the bar has no vibrational instability modes. A new form of equilibrium occurs at  $P_{cr} = 4\pi^2 EI/l^2$ .

This can also be verified by analysis of Eq. (2) which, incidentally, remains the same for both the boundary conditions (1) and conditions (3).

It is clear that the form of equilibrium for the bar shown in Fig. 397 is relative, in the sense that it must be considered in a body axes system which moves with acceleration in space together with the bar (Fig. 398). Here two components  $P\varphi$  are balanced by D'Alembert's inertial forces  $q = 2P\varphi/\rho Al^2$ .

It is apparent that the above operation of double differentiation of the equation leads to the foregoing conclusions only for the case of a homogeneous bar. For a non-uniform mass distribution or for a variable rigidity the result will be different.

As an analogue we may consider two rigid bars connected together by a spring of stiffness  $k$  (Fig. 399). When the angle of rotation  $\varphi$  is brought about, the system moves with acceleration. By introducing balanced inertial forces at the centre of mass, we obtain a stability condition in the form

$$2k\varphi = P\varphi a$$

or

$$P_{cr} = \frac{2k}{a},$$

where  $a$  is the distance from the hinge to the centre of mass.

If the loading were produced by forces  $P$  maintaining their direction (Fig. 400), the mass distribution would naturally be of no importance. In this case

$$P_{cr} = \frac{2k}{l},$$

where  $l$  is the length of one bar.

147. The stated problem, in spite of its apparent simplicity, involves difficulties of the same nature as we encountered in the preceding problems.

Let us try to find conditions for the existence of equilibrium forms different from the original one. To do this, we imagine the beam to buckle and go out of the plane of initial bending (Fig. 401). Denote the lateral displacement of the axis of the rod by  $y$ , and the angle of rotation of the section about the  $x$  axis by  $\varphi$ . The positive directions for  $y$  and  $\varphi$  are chosen as shown in the drawing.

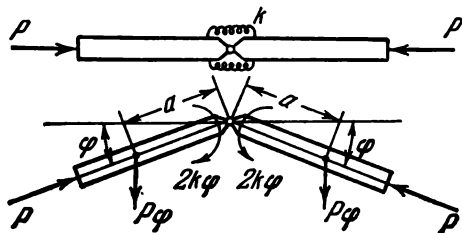


Fig. 399

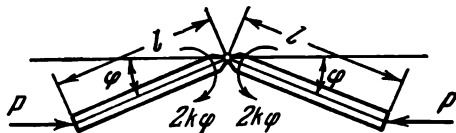


Fig. 400

In a displaced position a bending moment occurs at the sections of the rod in the plane of minimum rigidity. This moment is equal to  $M\varphi$  and tends to increase the curvature of the rod. The twisting moment occurring at the section of the deflected rod is equal to  $My'$  and is directed so as to decrease the angle  $\varphi$ . Consequently,

$$M_b = + M\varphi, \quad M_t = -My'.$$

On the other hand,

$$M_b = EIy'', \quad M_t = GI_*\varphi',$$

where

$$I = \frac{bh^3}{12}, \quad I_* = \frac{bh^3}{3}.$$

We now obtain the equations

$$EIy'' = M\varphi, \quad GI_*\varphi' = -My'. \quad (1)$$

Their solution is as follows:

$$\begin{aligned} \varphi &= A \sin \alpha x + B \cos \alpha x, \\ y &= -\frac{GI_*}{M} (A \sin \alpha x + B \cos \alpha x) + C, \end{aligned}$$

where

$$\alpha^2 = \frac{M^2}{EIGI_*}.$$

$A$ ,  $B$ , and  $C$  are arbitrary constants which are determined from the following conditions: when  $x = 0$ , we have  $\varphi = 0$ ,  $y = 0$ ,  $y' = 0$ . We then obtain

$$\begin{aligned} B &= 0, \\ -\frac{GI_*}{M} B + C &= 0, \\ A &= 0. \end{aligned}$$

Since  $A = B = C = 0$ , it follows that for any finite values of the moment  $M$  there exist no equilibrium forms different from the plane mode of bending. It remains to investigate the modes of motion and try to find conditions under which the bar may have a motion with a deflection increasing in time.

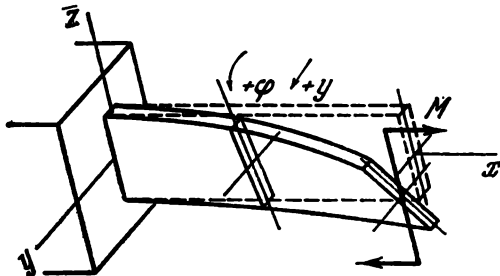


Fig. 401

Before proceeding to this analysis, we note that in the case of a moment following up the end section (Fig. 402) the bar has no forms of equilibrium other than the original form of plane bending. It is only in the case of a "semifollow-up" moment such as shown in Fig. 402 by a dashed line that a new form of equilibrium may exist when

$$M = \frac{\pi}{2l} \sqrt{EIGI_*}.$$

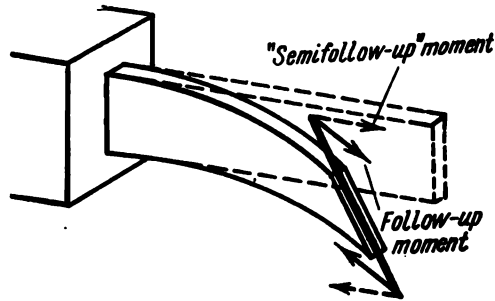


Fig. 402

A "semifollow-up" moment may be realized by means of two weights (Fig. 403). It is interesting to note that the possibility of realizing given forces or moments by means of gravity forces in all known cases is so far an invariable guarantee that the stability of a system may be investigated by finding neighbouring forms of equilibrium. As yet, there

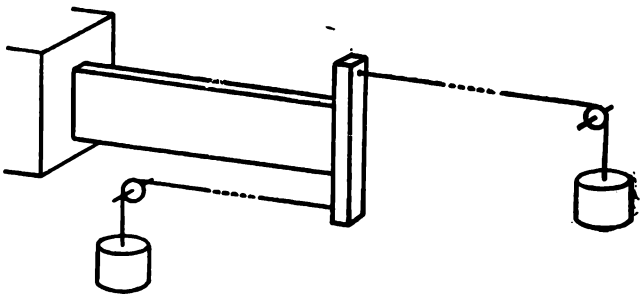


Fig. 403

has been no necessity of finding modes of motion under loadings produced by gravity forces.

Let us set up the equations of motion of the bar. For this purpose, it is necessary to introduce into consideration a distributed inertial load

$$q_i = -\rho A \frac{\partial^2 y}{\partial t^2}$$

and a distributed inertial moment associated with the rotation of the masses about the bar axis

$$m_i = \rho I_p \frac{\partial^2 \varphi}{\partial t^2},$$

where  $\rho$  is the density of the material and  $I_p$  is the polar moment of inertia of the section.

As is known,

$$q = \frac{\partial^2 M_b}{\partial x^2}, \quad m = \frac{\partial M_t}{\partial x};$$

hence, differentiating the first of Eqs. (1) with respect to  $x$  twice and the second equation once, and adding to the right-hand sides, respectively,  $q_i$  and  $m_i$ , we obtain

$$\left. \begin{aligned} EI \frac{\partial^4 y}{\partial x^4} &= M \frac{\partial^2 \varphi}{\partial x^2} - \rho A \frac{\partial^2 y}{\partial t^2}, \\ GI_* \frac{\partial^2 \varphi}{\partial x^2} &= -M \frac{\partial^2 y}{\partial x^2} + \rho I_p \frac{\partial^2 \varphi}{\partial t^2}. \end{aligned} \right\} \quad (2)$$

Assume

$$y = Y l e^{i\omega \sqrt{\frac{EI}{\rho A l^4}} t}, \quad \varphi = \Phi \sqrt{\frac{EI}{GI_*}} e^{i\omega \sqrt{\frac{EI}{\rho A l^4}} t},$$

where  $Y$  and  $\Phi$  are non-dimensional quantities depending on the non-dimensional co-ordinate  $\xi = x/l$ ,  $\omega$  is the non-dimensional frequency.

Equations (2) become

$$\left. \begin{aligned} \frac{\partial^4 Y}{\partial \xi^4} - M_0 \frac{\partial^2 \Phi}{\partial \xi^2} - \omega^2 Y &= 0, \\ \frac{\partial^2 \Phi}{\partial \xi^2} + M_0 \frac{\partial^2 Y}{\partial \xi^2} + k^2 \omega^2 \Phi &= 0, \end{aligned} \right\} \quad (3)$$

where  $M_0$  is a non-dimensional moment and  $k$  is a geometrical characteristic given by

$$M_0 = \frac{M l}{\sqrt{EI GI_*}}, \quad k^2 = \frac{EI}{GI_*} \frac{I_p}{A l^2}. \quad (4)$$

The investigation of system (3) by the techniques of functional analysis leads to very cumbersome transformations.

Hence, here it is most convenient to resort to a computer. We represent the functions  $Y$  and  $\Phi$  in the form of power series

$$Y = \sum_{n=0, 1, 2, \dots} A_n \zeta^n, \quad \Phi = \sum_{n=0, 1, 2, \dots} B_n \zeta^n.$$

Substituting for  $Y$  and  $\Phi$  in Eqs. (3), we come to the recurrence formulas

$$A_n = \frac{1}{n(n-1)(n-2)(n-3)} [\omega^2 A_{n-4} + M_0 B_{n-2} (n-2)(n-3)], \quad (5)$$

$$B_{n-2} = -M_0 A_{n-2} - \frac{k^2 \omega^2}{(n-2)(n-3)} B_{n-4}.$$

In calculations we may limit the series to 20 or 30 terms.

At the fixed end where  $x = 0$  ( $\zeta = 0$ ) we have  $y = 0$ ,  $\partial y / \partial x = 0$  and  $\varphi = 0$ ; consequently,  $A_0 = A_1 = B_0 = 0$ .

At the end of the bar ( $\zeta = 1$ ) we have

$$EI \frac{\partial^2 y}{\partial x^2} = M\varphi, \quad GI_* \frac{\partial \varphi}{\partial x} = -M \frac{\partial y}{\partial x},$$

$$EI \frac{\partial^3 y}{\partial x^3} = M \frac{\partial \varphi}{\partial x}.$$

The last boundary condition expresses zero shearing force at the end of the bar. Indeed, the shearing force is determi-

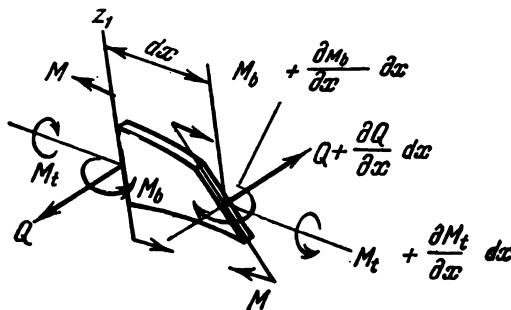


Fig. 404

ned from the conditions of equilibrium of an element (Fig. 404). By equating to zero the sum of the moments of the forces about the  $z_1$  axis, we find

$$Q = \frac{\partial M_b}{\partial x} - M \frac{\partial \varphi}{\partial x}$$

or

$$Q = EI \frac{\partial^3 y}{\partial x^3} - M \frac{\partial \varphi}{\partial x}.$$

By transforming to the non-dimensional parameters, we obtain

$$\begin{aligned} \frac{d^2 Y}{d\zeta^2} - M_0 \Phi &= 0, & \frac{d\Phi}{d\zeta} + M_0 \frac{dY}{d\zeta} &= 0, \\ \frac{d^3 Y}{d\zeta^3} - M_0 \frac{d\Phi}{d\zeta} &= 0 \end{aligned}$$

or, setting  $\zeta = 1$ ,

$$\left. \begin{aligned} \sum A_n n(n-1) - M_0 \sum B_n &= 0, \\ \sum B_n n + M_0 \sum A_n n &= 0, \\ \sum A_n n(n-1)(n-2) - M_0 \sum B_n n &= 0. \end{aligned} \right\} \quad (6)$$

In calculating the coefficients  $A_n$  and  $B_n$  the first three of them,  $A_2$ ,  $A_3$ , and  $B_1$ , remain undetermined. They must be selected so as to fulfil conditions (6). But Eqs. (6) are homogeneous in the constants  $A_2$ ,  $A_3$ , and  $B_1$ . They may therefore be written as

$$\begin{aligned} a_{11}A_2 + a_{12}A_3 + a_{13}B_1 &= 0, \\ a_{21}A_2 + a_{22}A_3 + a_{23}B_1 &= 0, \\ a_{31}A_2 + a_{32}A_3 + a_{33}B_1 &= 0. \end{aligned}$$

In order to obtain a non-zero solution, it is necessary to fulfil the condition

$$D = \begin{vmatrix} a_{11} & a_{12} & a_{13} \\ a_{21} & a_{22} & a_{23} \\ a_{31} & a_{32} & a_{33} \end{vmatrix} = 0.$$

The procedure for calculation is now as follows.

Assign the parameter

$$k^2 = \frac{EI}{GI_*} \frac{I_P}{Al^2} = \frac{1+\mu}{24} \frac{b^2}{l^2}.$$

Fix  $M_0$  and  $\omega$ .

Assume further  $A_2 = 1$ ,  $A_3 = B_1 = 0$  and calculate the coefficients  $A_n$  and  $B_n$  by the recurrence formulas (5) and then the left-hand sides of Eqs. (6). They are equal, respectively, to  $a_{11}$ ,  $a_{21}$ , and  $a_{31}$ . Assume next  $A_2 = 0$ ,  $A_3 = 1$ ,  $B_1 = 0$ . The left-hand sides of Eqs. (6) then give the values of  $a_{12}$ ,  $a_{22}$ , and  $a_{32}$ . Finally, assuming  $A_2 = A_3 = 0$  and  $B_1 = 1$ , we find  $a_{13}$ ,  $a_{23}$ , and  $a_{33}$ . By calculating the determinant, we ascertain that it is not, in general, zero. Then, by changing the value of  $\omega$ , we achieve  $D = 0$ . In this way the natural frequencies are determined for a given moment  $M_0$ .

By varying  $M_0$ , we follow the behaviour of the frequencies and, just as was done in the preceding examples, determine the conditions for their multiplicity.

When  $M_0 = 0$ , we have the frequencies of natural vibrations,  $\omega_b$  (bending) and  $\omega_t$  (torsional). As  $M_0$  increases, the frequencies come closer and closer together, and at the critical value of the moment  $M_0$  the frequencies become multiple (points A in Fig. 405).

Figure 406 shows the relation between  $M_{0\text{ cr}}$  and the parameter  $k$ . When  $k = 0.445$ ,  $M_{0\text{ cr}}$  becomes zero. This occurs when the frequency  $\omega_b$  of the first bending-vibration mode coincides with the frequency  $\omega_t$  of the first torsional-vibration mode.

It may be noted that the first lowest frequency always coincides with the second, irrespective of whether it is interpreted by us as bending or torsional. For example, when  $k = 0.05$ , the first torsional frequency is  $\omega_{1t} = 31.4$ , while

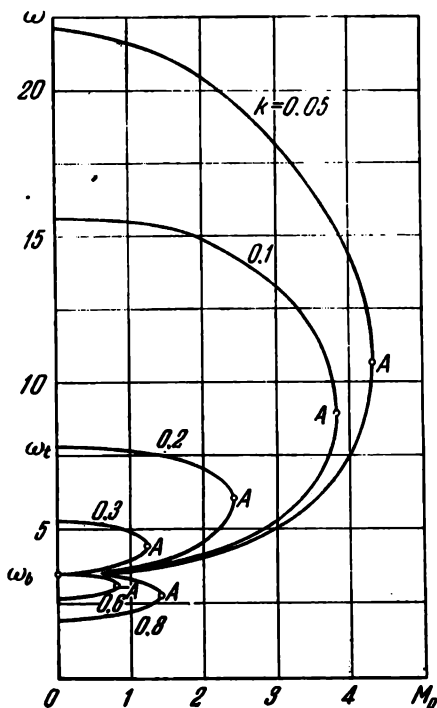


Fig. 405

the bending frequencies are  $\omega_{1b} = 3.5$  and  $\omega_{2b} = 22$ . As the moment increases, the bending frequencies are brought into coincidence. If the parameter  $k$  is increased, the first torsional frequency falls and, when it becomes lower than the

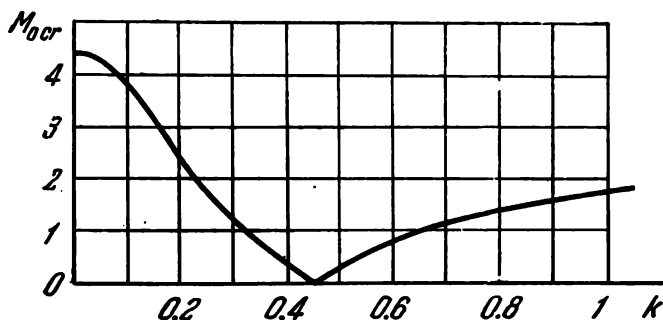


Fig. 406

second bending frequency, the first bending frequency coincides with it as  $M_0$  increases. This is also seen from the curves shown in Fig. 405.

In the case of a follow-up moment, i.e., a moment turning together with the end plane, the boundary conditions are different, and instead of (6) we have

$$\left. \begin{aligned} \sum A_n n(n-1) &= 0, \\ \sum B_n n &= 0, \\ \sum A_n n(n-1)(n-2) &= 0. \end{aligned} \right\} \quad (7)$$

The critical values of the moment for conditions (7) are the same as for conditions (6). This coincidence of the results is not fortuitous. It follows from the mutual inversion of the loading conditions for the bar at the left and right ends, as was the case for the systems considered in Probs. 143 and 144.

148. The problem has come into the literature as E. L. Nikolai's problem. It is the solution of this problem that first revealed in 1927 the existence of systems the analysis of whose stability cannot be made by determination of Euler equilibrium forms. Indeed, in the simplest case when

the rigidities of the bar in two principal planes are equal we have the following equations of equilibrium:

$$\left. \begin{aligned} EIy'' &= -Py + Mz', \\ EIz'' &= -Pz - My'. \end{aligned} \right\} \quad (1)$$

They are obtained from Eqs. (1) of Prob. 113 (see p. 251) by reversing the sign of  $P$ .

The solution of the equations remains the same

$$y = A \cos \alpha_1 x + B \sin \alpha_1 x + C \cos \alpha_2 x + D \sin \alpha_2 x,$$

$$z = A \sin \alpha_1 x - B \cos \alpha_1 x + C \sin \alpha_2 x - D \cos \alpha_2 x,$$

where  $\alpha_1$  and  $\alpha_2$  are the roots of the quadratic equation

$$\alpha^2 + \frac{M}{EI} \alpha - \frac{P}{EI} = 0. \quad (2)$$

In setting up Eq. (1) it was assumed that the displacements  $y$  and  $z$  were measured from the line of action of the force  $P$ . By placing the origin of  $x$ ,  $y$ , and  $z$  at the point of application of the force  $P$  (Fig. 407), we therefore arrive at the boundary conditions: when  $x = 0$ ,  $y = z = 0$ ; when  $x = l$ ,  $y' = z' = 0$ .

This gives

$$\begin{aligned} A + C &= 0, & B + D &= 0, \\ -A\alpha_1 \sin \alpha_1 l + B\alpha_1 \cos \alpha_1 l - C\alpha_2 \sin \alpha_2 l + D\alpha_2 \cos \alpha_2 l &= 0, \\ A\alpha_1 \cos \alpha_1 l + B\alpha_1 \sin \alpha_1 l + C\alpha_2 \cos \alpha_2 l + D\alpha_2 \sin \alpha_2 l &= 0. \end{aligned}$$

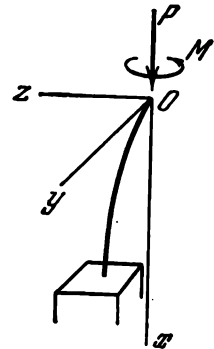


Fig. 407

By equating to zero the determinant of this system of equations, we obtain

$$\alpha_1^2 + \alpha_2^2 = 2\alpha_1\alpha_2 \cos(\alpha_1 - \alpha_2) l. \quad (3)$$

But according to Eq. (2)

$$\alpha_1\alpha_2 = -\frac{P}{EI}, \quad \alpha_1^2 + \alpha_2^2 = \left(\frac{M}{EI}\right)^2 + \frac{2P}{EI},$$

$$\alpha_1 - \alpha_2 = 2 \sqrt{\left(\frac{M}{2EI}\right)^2 + \frac{P}{EI}};$$

Eq. (3) becomes therefore

$$\cos \sqrt{\left(\frac{Ml}{EI}\right)^2 + \frac{4Pl^2}{EI}} = -\left(1 + \frac{M^2}{2PEI}\right).$$

For values of the moment  $M$  different from zero, this equation cannot be satisfied since the right-hand side is greater than unity in absolute value. Only in the case of  $M = 0$

$$\cos \sqrt{\frac{4Pl^2}{EI}} = -1$$

and we then obtain the usual value for the critical force

$$P_{cr} = \frac{\pi^2 EI}{4l^2}.$$

Thus, for an arbitrarily small non-zero value of  $M$  and an arbitrarily large force  $P$ , the bar has no forms of equilibrium other than the straight-line one. Exactly the same result is obtained in the case when the plane of the moment  $M$  turns together with the end section during the bending of the bar. In the case of a "semifollow-up" moment produced by two weights the system, as we have already seen in the solution of Prob. 133, has forms of equilibrium different from the original one. Thus, an analogy may be drawn here with the behaviour of the system considered in the preceding problem. There, however, we had a single external force factor, viz. a moment  $M$ . In the present problem we have two force factors, viz. a force  $P$  and a moment  $M$ . If only a force  $P$  is applied, a transition to a new form of equilibrium takes place as the force increases. For a moment (with the exception of a "semifollow-up" moment), however, a transition to new modes of motion is typical. It is therefore interesting to trace the behaviour of a system in the range of combined action of the two factors and to determine where a mode of motion occurs first and where a form of equilibrium.

Differentiating expressions (1) twice with respect to  $x$  and adding terms corresponding to inertial forces, we obtain

$$\left. \begin{aligned} EI_1 \frac{\partial^4 y}{\partial x^4} - M \frac{\partial^3 z}{\partial x^3} + P \frac{\partial^2 y}{\partial x^2} + \rho A \frac{\partial^2 y}{\partial t^2} &= 0, \\ EI_2 \frac{\partial^4 z}{\partial x^4} + M \frac{\partial^3 y}{\partial x^3} + P \frac{\partial^2 z}{\partial x^2} + \rho A \frac{\partial^2 z}{\partial t^2} &= 0. \end{aligned} \right\} \quad (4)$$

As will be seen later, the behaviour of the system depends greatly on the ratio of the flexural rigidities in the principal planes. Hence, instead of one rigidity  $EI$ , two rigidities,  $EI_1$  and  $EI_2$ , are introduced into Eqs. (4).

It is now more convenient to place the origin at the fixed end (Fig. 408). Whatever the loading conditions, when  $x = 0$  we have  $y = z = 0$  and  $\partial y / \partial x = \partial z / \partial x = 0$ .

The expressions for the shearing forces  $Q_x$  and  $Q_y$  for the bent bar are complicated by introducing a term containing the torque, i.e.,

$$Q_y = \frac{\partial M_{z_1}}{\partial x} - M \frac{\partial^2 z}{\partial x^2},$$

$$Q_z = \frac{\partial M_{y_1}}{\partial x} + M \frac{\partial^2 y}{\partial x^2},$$

where  $M_{z_1}$  and  $M_{y_1}$  are the bending moments with respect to the moving axes  $y_1, z_1$ . The necessary relations are easily obtained by equating to zero the sums of the moments of the forces, acting on the element  $dx$ , with respect to the  $y_1$  and  $z_1$  axes (see Fig. 409 which shows the projections of this element on the  $xy$  and  $xz$  planes). At the end of the bar

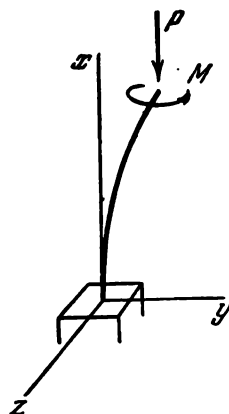


Fig. 408

$$Q_y = -P \frac{\partial y}{\partial x}, \quad Q_z = -P \frac{\partial z}{\partial x};$$

hence, when  $x = l$ , regardless of the behaviour of the moment  $M$ , we have two boundary conditions

$$\left. \begin{aligned} \left| EI_1 \frac{\partial^3 y}{\partial x^3} + P \frac{\partial y}{\partial x} - M \frac{\partial^2 z}{\partial x^2} \right|_{x=l} &= 0, \\ \left| EI_2 \frac{\partial^3 z}{\partial x^3} + P \frac{\partial z}{\partial x} + M \frac{\partial^2 y}{\partial x^2} \right|_{x=l} &= 0. \end{aligned} \right\} \quad (5)$$

If the plane of action of the moment  $M$  turns together with the end section during the bending of the bar, then, obviously, when  $x = l$ ,  $M_{y_1} = M_{z_1} = 0$  and we have two more conditions

$$\left| \frac{\partial^2 y}{\partial x^2} \right|_{x=l} = 0, \quad \left| \frac{\partial^2 z}{\partial x^2} \right|_{x=l} = 0. \quad (6)$$

If the plane of action of the moment  $M$  does not turn during the bending of the bar, then, when  $x = l$ , we have  $M_{y_1} = M \partial z / \partial x$  and  $M_{z_1} = -M \partial y / \partial x$ , giving

$$\left. \begin{aligned} EI_1 \frac{\partial^2 y}{\partial x^2} - M \frac{\partial z}{\partial x} \Big|_{x=l} &= 0, \\ EI_2 \frac{\partial^2 z}{\partial x^2} + M \frac{\partial y}{\partial x} \Big|_{x=l} &= 0. \end{aligned} \right\} \quad (7)$$

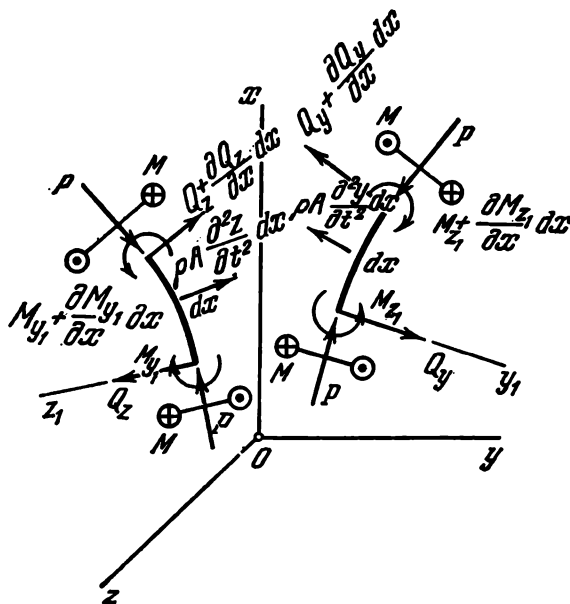


Fig. 409

Finally, in the case of a "semifollow-up" moment we obtain

$$\left. \begin{aligned} EI_1 \frac{\partial^2 y}{\partial x^2} - M \frac{\partial z}{\partial x} \Big|_{x=l} &= 0, \\ \frac{\partial^2 z}{\partial x^2} \Big|_{x=l} &= 0. \end{aligned} \right\} \quad (8)$$

We transform to non-dimensional parameters. For this purpose we assume that

$$y = Y e^{i\omega A_* t}, \quad z = \sqrt{\frac{EI_2}{EI_1}} Z e^{i\omega A_* t},$$

where  $Y$  and  $Z$  are non-dimensional unknown functions depending on  $x$  only,  $\omega$  is the non-dimensional frequency, and

$$A_* = \sqrt{\frac{EI_1}{\rho A l^4}}.$$

As an independent variable we take  $\zeta = x/l$  in place of  $x$ . After substituting for  $x$ ,  $y$ , and  $z$  in Eqs. (4) we obtain a system of ordinary differential equations

$$\left. \begin{aligned} \frac{d^4 Y}{d\zeta^4} - M_0 \frac{d^3 Z}{d\zeta^3} + \beta^2 \frac{d^2 Y}{d\zeta^2} - \omega^2 Y &= 0, \\ \frac{d^4 Z}{d\zeta^4} + M_0 \frac{d^3 Y}{d\zeta^3} + \frac{\beta^2}{k^2} \frac{d^2 Z}{d\zeta^2} - \frac{\omega^2}{k^2} Z &= 0, \end{aligned} \right\} \quad (9)$$

where  $M_0$  and  $\beta^2$  are the non-dimensional moment and force, respectively,

$$M_0 = \frac{Ml}{\sqrt{EI_1 EI_2}}, \quad \beta^2 = \frac{Pl^2}{EI_1}.$$

The quantity  $k$  characterizes the ratio of the rigidities

$$k = \sqrt{\frac{EI_2}{EI_1}}.$$

It is assumed that  $EI_1$  is the minimum rigidity; hence,  $k \geq 1$ .

By using the non-dimensional parameters, we also transform the boundary conditions.

$$\text{When } \zeta = 0, \text{ we have } Y = Z = 0, \quad \frac{dY}{d\zeta} = \frac{dZ}{d\zeta} = 0.$$

For the end of the bar, i.e., when  $\zeta = 1$ , in the case of loading by a moment whose plane turns together with the end section we obtain

$$\left\{ \begin{aligned} \left| \frac{d^3 Y}{d\zeta^3} + \beta^2 \frac{dY}{d\zeta} - M_0 \frac{d^2 Z}{d\zeta^2} \right|_{\zeta=1} &= 0, \\ \left| \frac{d^3 Z}{d\zeta^3} + \frac{\beta^2}{k^2} \frac{dZ}{d\zeta} + M_0 \frac{d^2 Y}{d\zeta^2} \right|_{\zeta=1} &= 0, \end{aligned} \right\} \quad (10)$$

$$\left| \frac{d^2 Y}{d\zeta^2} \right|_{\zeta=1} = 0, \quad \left| \frac{d^2 Z}{d\zeta^2} \right|_{\zeta=1} = 0. \quad (11)$$

If the plane of action of a moment does not turn, the first two conditions hold and the last two become

$$\left| \frac{d^2 Y}{d\zeta^2} - M_0 \frac{dZ}{d\zeta} \right|_{\zeta=1} = 0, \quad \left| \frac{d^2 Z}{d\zeta^2} + M_0 \frac{dY}{d\zeta} \right|_{\zeta=1} = 0. \quad (12)$$

In the case of a "semifollow-up" moment conditions (10) again hold good and in place of expressions (11) we obtain

$$\left| \frac{d^2 Y}{d\zeta^2} - M_0 \frac{dZ}{d\zeta} \right|_{\zeta=1} = 0, \quad \left| \frac{d^2 Z}{d\zeta^2} \right|_{\zeta=1} = 0. \quad (13)$$

To solve the problem, the only advisable thing is to apply computerized analysis. The algorithm has already been worked out in the solution of the preceding problems.

Assume that

$$Y = \sum A_n \zeta^n, \quad Z = \sum B_n \zeta^n$$

and substitute for  $Y$  and  $Z$  in Eqs. (9), whereupon we obtain the following recurrence formulas:

$$\left. \begin{aligned} A_n &= \frac{1}{n(n-1)(n-2)(n-3)} [M_0 B_{n-1}(n-1)(n-2) \times \\ &\quad \times (n-3) - \beta^2 A_{n-2}(n-2)(n-3) + \omega^2 A_{n-4}], \\ B_n &= \frac{1}{n(n-1)(n-2)(n-3)} \left[ -M_0 A_{n-1}(n-1) \times \right. \\ &\quad \times (n-2)(n-3) - \frac{\beta^2}{k^2} B_{n-2}(n-2)(n-3) + \frac{\omega^2}{k^2} B_{n-4} \left. \right]. \end{aligned} \right\} \quad (14)$$

Since at the fixed end  $Y = Z = 0$ ,  $\frac{dY}{d\zeta} = \frac{dZ}{d\zeta} = 0$ , obviously,

$$A_0 = A_1 = B_0 = B_1 = 0.$$

The other four coefficients,  $A_2$ ,  $A_3$ ,  $B_2$ , and  $B_3$ , must be chosen so as to fulfil the boundary conditions at the end of the bar, i.e., when  $\zeta = 1$ . With this aim in view, we turn our attention to expressions (10) and also to expressions (11), (12), or (13) depending on the loading conditions.

Since the coefficients  $A_2$ ,  $A_3$ ,  $B_2$ , and  $B_3$  enter linearly into all the above-enumerated expressions, the four equations

in these coefficients may be written as

$$\left. \begin{aligned} a_{11}A_2 + a_{12}A_3 + a_{13}B_2 + a_{14}B_3 &= 0, \\ a_{21}A_2 + a_{22}A_3 + a_{23}B_2 + a_{24}B_3 &= 0, \\ a_{31}A_2 + a_{32}A_3 + a_{33}B_2 + a_{34}B_3 &= 0, \\ a_{41}A_2 + a_{42}A_3 + a_{43}B_2 + a_{44}B_3 &= 0. \end{aligned} \right\} \quad (15)$$

The first two equations are obtained from expressions (10), and the other two from (11), (12), or (13) depending on the particular moment  $M$  by which the bar is loaded.

If for preassigned values of the parameters  $M_0$ ,  $\beta$ ,  $k$ , and  $\omega$  we assume  $A_2 = 1$  and  $A_3 = B_2 = B_3 = 0$ , then by the recurrence formulas (14) we can find  $A_4$ ,  $B_4$ ,  $A_5$ ,  $B_5$ , . . . . Next, by summation to a certain  $n$ , for example to  $n = 30$ , we find the values of the derivatives of the functions  $Y$  and  $Z$  when  $\zeta = 1$ , i.e.,

$$\left| \frac{dY}{d\zeta} \right|_{\zeta=1} = \sum A_n n, \quad \left| \frac{dZ}{d\zeta} \right|_{\zeta=1} = \sum B_n n, \\ \left| \frac{d^2Y}{d\zeta^2} \right|_{\zeta=1} = \sum A_n n(n-1), \quad \dots$$

The above sums are substituted in expressions (10) and (11), (12), or (13). Accordingly, we obtain the coefficients  $a_{11}$ ,  $a_{21}$ ,  $a_{31}$ , and  $a_{41}$  of system (15). If all computations are repeated on the assumption that  $A_2 = 1$  and  $A_3 = B_2 = B_3 = 0$ , we obviously find the coefficients  $a_{12}$ ,  $a_{22}$ ,  $a_{32}$ , and  $a_{42}$ . It must further be taken that  $B_2 = 1$  and, finally,  $B_3 = 1$ . As a result of the fourfold repetition of the cycle we find all the coefficients of system (15).

The condition for the existence of non-zero solutions for  $Y$  and  $Z$  is that the corresponding determinant be zero, i.e.,

$$\begin{vmatrix} a_{11} & a_{12} & a_{13} & a_{14} \\ a_{21} & a_{22} & a_{23} & a_{24} \\ a_{31} & a_{32} & a_{33} & a_{34} \\ a_{41} & a_{42} & a_{43} & a_{44} \end{vmatrix} = D = 0. \quad (16)$$

Thus, the stability analysis is reduced to the determination of such relations among  $M_0$ ,  $\beta$ ,  $\omega$ , and  $k$  for which condition (16) is fulfilled. In practice, it is necessary first

of all to fix the parameter  $k$ , then  $\beta$  and finally  $M_0$ . By giving  $\omega$  various values, we select the one for which the determinant  $D$  vanishes. Then  $M_0$  is changed and  $\omega$  is again selected. In this way the relation between  $\omega$  and  $M_0$  is determined for fixed  $\beta$  and  $k$ . Figure 410 shows this relation for  $k = 2$ .

Obviously, there is no need to plot all graphs or to put a host of data into printing. It is not difficult to introduce

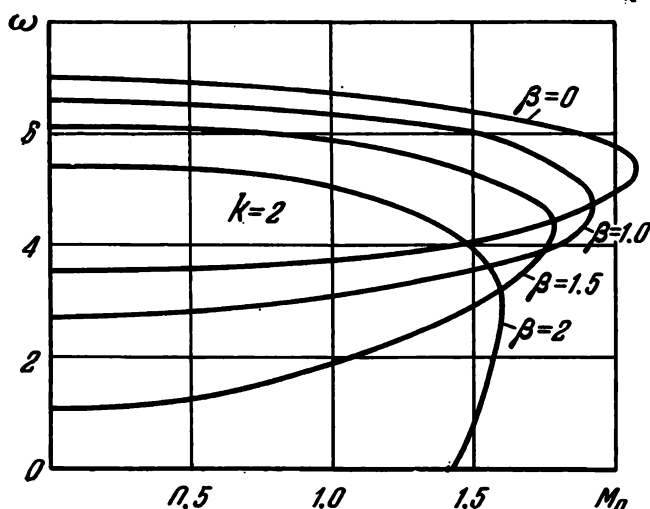


Fig. 410

into the program logic indices from which one can judge the behaviour of the frequency as a function of  $M_0$  and  $\beta$ . If the frequency vanishes, this means that a new form of equilibrium is found. If the frequencies of the first two forms coincide, it follows that a mode of motion is found. Naturally, the ratio of the rigidities  $k^2$  must remain unchanged in this search.

The results of searching for the critical values of the parameters  $\beta$  and  $M_0$  are represented in Fig. 411. For the boundary conditions (11) and (12) they are found to be exactly the same. In other words, the difference between loading by a follow-up and a non-follow-up moment is not detected. For each fixed  $k = \sqrt{EI_2/EI_1}$ , the stability region (Fig. 411) is bounded by the curvilinear quadrilateral  $OABC$ . The

point  $A$  is common to all curves. Here  $\beta = \frac{\pi}{2} = \sqrt{Pl^2/EI_1}$ , which corresponds to the value of the critical force

$$P_{cr} = \frac{\pi^2 EI_1}{4l^2}.$$

The curves  $AB$  give the conditions for the passage to a new form of equilibrium and correspond to bending in the plane of minimum rigidity ( $EI_1$ ). It is interesting that as the moment increases, so does the critical force. This happens because the applied moment causes the bar to deflect from the plane of minimum rigidity during bending.

The upper part of the curves  $ABD$  shown in Fig. 411 corresponds to a form of equilibrium associated with bending in the plane of maximum rigidity. The value of the parameter  $\beta$  at the points  $D$  is greater by a factor of  $k$  than at the point  $A$ .

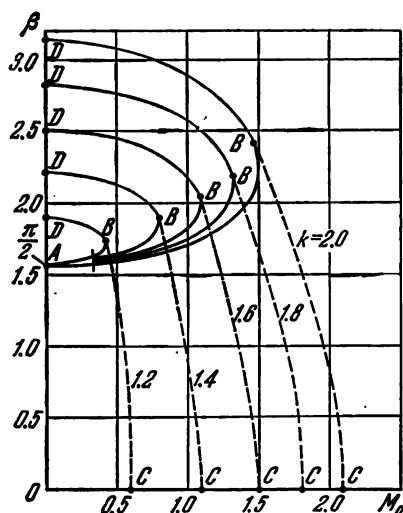


Fig. 411

On the right side the stability region is bounded by the condition for transition to a vibratory mode of motion. The transition boundaries are marked in Fig. 411 by dashed lines  $BC$ .

As  $k \rightarrow 1$ , the stability region contracts into a line segment  $OA$ . The point  $D$  coincides with  $A$ , and  $C$  with  $O$ .

As might be expected, for a "semifollow-up" moment the modes of motion with building-up amplitude are not found. For certain values of  $M$  and  $P$ , only new forms of equilibrium occur ( $\omega = 0$ ).

Here the determination of critical states could be performed analytically, but it is not advisable to do this when a worked-out program is available; it is more convenient to

shift the calculations at once on to a computer by the already developed algorithm.

The curves bounding the stability region are represented in Fig. 412 and are self-evident.

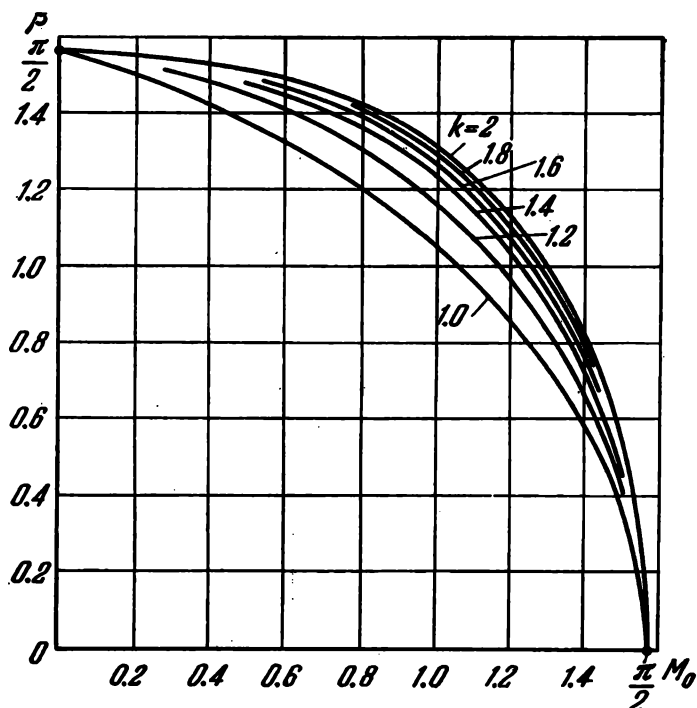


Fig. 412

149. We revert to the solution of Prob. 119. It can easily be verified that the pipe fixed at one end has no forms of equilibrium different from the original straight-line form. Indeed, from the solution of Prob. 119 we use

$$y = A \sin \alpha x + B \cos \alpha x + Cx + D$$

but for other boundary conditions, namely: when  $x = 0$ ,  $y = 0$  and  $y' = 0$ ; when  $x = l$ ,  $y'' = 0$  and  $y''' = 0$ . Hence,

$$B + D = 0, \quad A\alpha + C = 0,$$

$$A \sin \alpha l + B \cos \alpha l = 0,$$

$$A \cos \alpha l - B \sin \alpha l = 0.$$

From the last two expressions it follows that the non-zero solutions for  $A$  and  $B$  exist if

$$\sin^2 \alpha l + \cos^2 \alpha l = 0,$$

which is impossible. Consequently,  $A = B = C = D = 0$  and the bar has no forms of equilibrium other than the original straight-line form.

It is necessary now to turn to searching for modes of motion. Incidentally, we note that the existence of these modes is easily revealed if the air from a compressor is delivered under sufficient pressure through a flexible rubber hose. Exactly the same vibratory motion can be observed when water is delivered through a hose lying, for example, on a wet slippery ice during flooding a skating-rink.

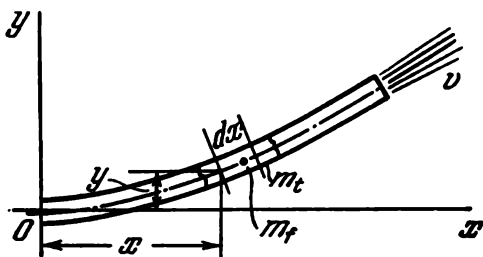


Fig. 413

Let the mass of the tube per unit length be  $m_t$ , and the fluid mass also calculated per unit length  $m_f$ . Over a section  $dx$  (Fig. 413) we have, respectively, the masses  $m_t dx$  and  $m_f dx$ . When the pipeline moves laterally, an inertial force is developed over the section  $dx$  equal to

$$-\frac{\partial^2 y}{\partial t^2} (m_t + m_f) dx.$$

In view of the fact that the particle flux rotates with an angular velocity  $\partial^2 y / \partial x \partial t$  a Coriolis acceleration is developed. The corresponding inertial force is

$$-2 \frac{\partial^2 y}{\partial x \partial t} v^2 m_f dx.$$

We write an expression, with the same sign, for a force associated with the curvature of the flux (or with the normal acceleration)

$$-\frac{\partial^2 y}{\partial x^2} v^2 m_f dx.$$

The sum of these forces divided by  $dx$  gives the intensity of transverse "external" load. Consequently,

$$EI \frac{\partial^4 y}{\partial x^4} = -\frac{\partial^2 y}{\partial t^2} (m_t + m_f) - 2 \frac{\partial^2 y}{\partial x \partial t} v m_f - \frac{\partial^2 y}{\partial x^2} v^2 m_f.$$

We transform at once to a non-dimensional form. Assume that

$$y = Y l e^{(\varepsilon + i\omega)At}, \quad A = \sqrt{\frac{EI}{(m_t + m_f) l^4}}, \quad x = l\zeta. \quad (1)$$

We then obtain

$$\frac{d^4 Y}{d\zeta^4} + \beta^2 \frac{d^2 Y}{d\zeta^2} + 2\beta\kappa(\varepsilon + i\omega) \frac{dY}{d\zeta} + (\varepsilon + i\omega)^2 Y = 0, \quad (2)$$

where

$$\beta = v \sqrt{\frac{m_f l^2}{EI}}, \quad \kappa = \sqrt{\frac{m_f}{m_t + m_f}}. \quad (3)$$

The first parameter characterizes the rate of fluid flow through the pipeline, the second parameter gives the relation between the fluid mass and the mass of the tube.

At the fixed end ( $\zeta = 0$ ) of the bar  $Y = 0$  and  $dY/d\zeta = 0$ . At the free end ( $\zeta = 1$ ) we have

$$\frac{d^2 Y}{d\zeta^2} = 0 \quad \text{and} \quad \frac{d^3 Y}{d\zeta^3} = 0.$$

The problem is now reduced to the determination of the ranges of the parameters  $\beta$  and  $\kappa$  for which the real part  $\varepsilon$  of the exponent  $\varepsilon + i\omega$  (1) takes positive values.

With a view to shifting the search operation on to an electronic digital computer, we assume

$$Y = \sum C_n \zeta^n.$$

From the first two boundary conditions it follows that  $C_0 = C_1 = 0$ . The other two conditions take the form

$$\sum C_n n(n-1) = 0, \quad \sum C_n n(n-1)(n-2) = 0. \quad (4)$$

Assuming the coefficients  $C_2$  and  $C_3$  undetermined, we write Eqs. (4) as follows:

$$\left. \begin{aligned} aC_2 + bC_3 &= 0, \\ cC_2 + dC_3 &= 0. \end{aligned} \right\} \quad (5)$$

The condition for the existence of non-zero solutions is obviously given by

$$\begin{vmatrix} a & b \\ c & d \end{vmatrix} = ad - bc = 0. \quad (6)$$

We now change from the complex form of writing the equations to the real form. Assume that

$$Y = Y_1 + iY_2$$

and accordingly

$$C_n = A_n + iB_n, \quad Y_1 = \sum A_n \zeta^n, \quad Y_2 = \sum B_n \zeta^n.$$

Substituting for  $Y$  in Eq. (2) and dividing it into a real and an imaginary part, we obtain recurrence formulas for determining  $A_n$  and  $B_n$

$$\left. \begin{aligned} A_n &= \frac{1}{n(n-1)(n-2)(n-3)} \{ -\beta^2 A_{n-2}(n-2)(n-3) - \\ &\quad - 2\beta\kappa\epsilon A_{n-3}(n-3) + (\omega^2 - \epsilon^2) A_{n-4} + \\ &\quad + 2\beta\kappa\omega B_{n-3}(n-3) + 2\omega\epsilon B_{n-4} \}, \\ B_n &= \frac{1}{n(n-1)(n-2)(n-3)} \{ -\beta^2 B_{n-2}(n-2)(n-3) - \\ &\quad - 2\beta\kappa\epsilon B_{n-3}(n-3) + (\omega^2 - \epsilon^2) B_{n-4} - \\ &\quad - 2\beta\kappa\omega A_{n-3}(n-3) - 2\omega\epsilon A_{n-4} \}. \end{aligned} \right\} \quad (7)$$

Equation (6) is also divided into a real and an imaginary part assuming

$a = a_1 + ia_2$ ,  $b = b_1 + ib_2$ ,  $c = c_1 + ic_2$ ,  $d = d_1 + id_2$ . We then obtain two equations

$$\left. \begin{aligned} D_1 &= a_1 d_1 - a_2 d_2 - b_1 c_1 + b_2 c_2 = 0, \\ D_2 &= a_1 d_2 - a_2 d_1 - b_1 c_2 - b_2 c_1 = 0. \end{aligned} \right\} \quad (8)$$

If we set  $C_2 = 1$  ( $A_2 = 1$ ,  $B_2 = 0$ ) and  $C_3 = 0$  ( $A_3 = B_3 = 0$ ), then from a comparison of expressions (4) and (5) it is seen that the first sum of (4) is equal to  $a$  and the second sum is equal to  $c$ . Consequently, when  $A_2 = 1$  and  $B_2 = A_3 = B_3 = 0$  we have

$$\begin{aligned} a_1 &= \sum A_n n(n-1), & a_2 &= \sum B_n n(n-1), \\ c_1 &= \sum A_n n(n-1)(n-2), & c_2 &= \sum B_n n(n-1)(n-2). \end{aligned}$$

Assuming that  $C_2 = 0$  and  $C_3 = 1$ , i.e., setting  $A_2 = B_2 = B_3 = 0$ ,  $A_3 = 1$ , and calculating the coefficients  $A_n$  and  $B_n$  by the recurrence formulas (7), we obtain

$$\begin{aligned} b_1 &= \sum A_n n(n-1), & b_2 &= \sum B_n n(n-1), \\ d_1 &= \sum A_n n(n-1)(n-2), & d_2 &= \sum B_n n(n-1)(n-2). \end{aligned}$$

In this way the quantities involved in Eqs. (8) are calculated.

This, in fact, determines the procedure for calculation on a computer.

It is necessary first to compile a subprogram for computing the quantities  $D_1$  and  $D_2$  (8) with fixed parameters  $\kappa$ ,  $\beta$ ,  $\omega$ , and  $\varepsilon$ . The power series converge rapidly, and the quantities  $A_n$  and  $B_n$  with  $n > 30$  have, as a rule, values less than the machine zero.

Next, for fixed  $\kappa$  and  $\beta$  we determine  $\varepsilon$  and  $\omega$  so as to satisfy system (8). The search is realized by means of the simplest linear interpolation. By assigning three points on the  $\varepsilon$ ,  $\omega$  plane, we determine three values of  $D_1$  and  $D_2$  (8) corresponding to these points. By using the three values of  $D_1$  and  $D_2$ , we construct two planes in space

$$D_1 = D_1(\varepsilon; \omega) \text{ and } D_2 = D_2(\varepsilon; \omega).$$

Their line of intersection crosses the  $\varepsilon$ ,  $\omega$  plane at a point whose co-ordinates correspond to the roots of system (8). Further the subsequent improvement is made until the given accuracy condition is fulfilled. If the calculations are carried out with varying parameter  $\beta$ , it is possible to see how the frequency  $\omega$  and the damping parameter  $\varepsilon$  vary as a function of the rate of flow for a given  $\kappa$ , i.e., for a given relation between the flow and bar masses.

Figure 414 shows several such curves. It is characteristic that in the problem under consideration there is no coincidence of the frequencies which we have encountered previously. This is due to the fact that the rate of flow is not only an exciting factor, but simultaneously a damping factor giving rise to Coriolis forces. Even at a very small rate  $v$  there is a certain amount of damping, and the roots of the characteristic equation are not imaginary, but complex.

As the rate of flow increases, the first frequency  $\omega$  (for small values of  $\kappa$ ) increases, then begins to decrease and

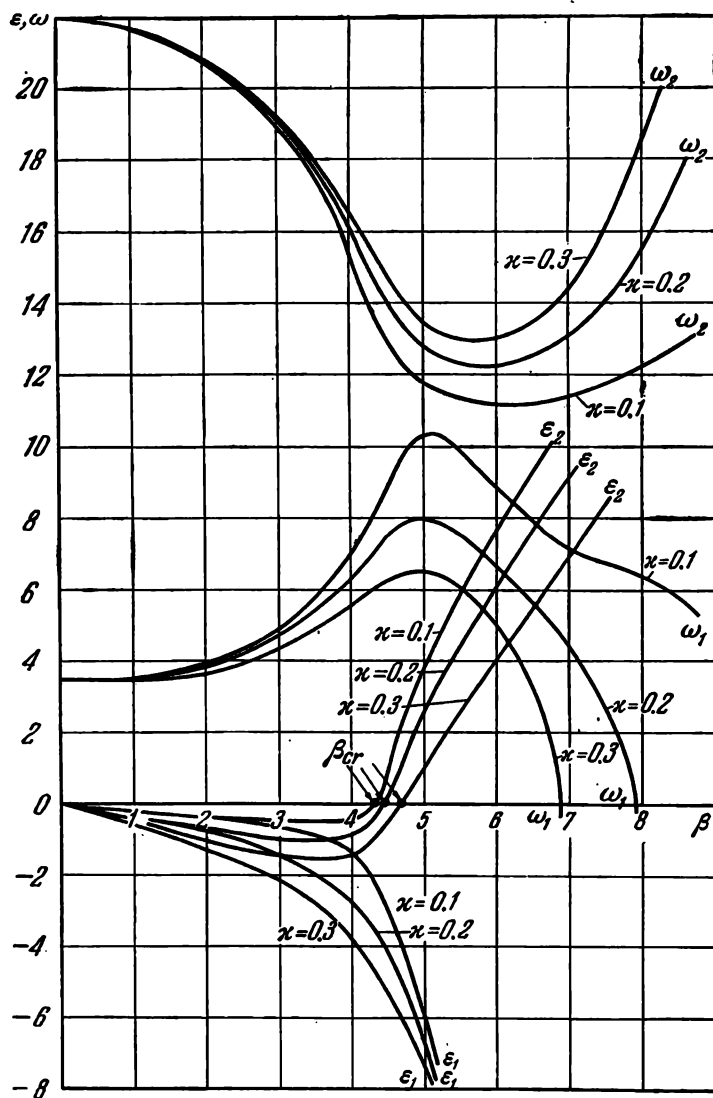


Fig. 414

vanishes, but  $\epsilon$  remains negative in all cases. This means that no building-up deviations in the form of the first tone occur, but there is either vibratory or aperiodic damping.

The first transition of  $\varepsilon$  into a positive region occurs at frequencies corresponding to the second tone. The relevant curves in the graph (Fig. 414) are indexed ( $\varepsilon_2$ ,  $\omega_2$ ).

The relation of the frequency  $\omega$  and of the critical rate of flow  $\beta$  to the parameter

$$\kappa = \sqrt{\frac{m_f}{m_t + m_f}}$$

has a quaint appearance (Fig. 415). When  $\kappa < 0.545$ , vibrations of the second tone are excited. At larger values of  $\kappa$ ,

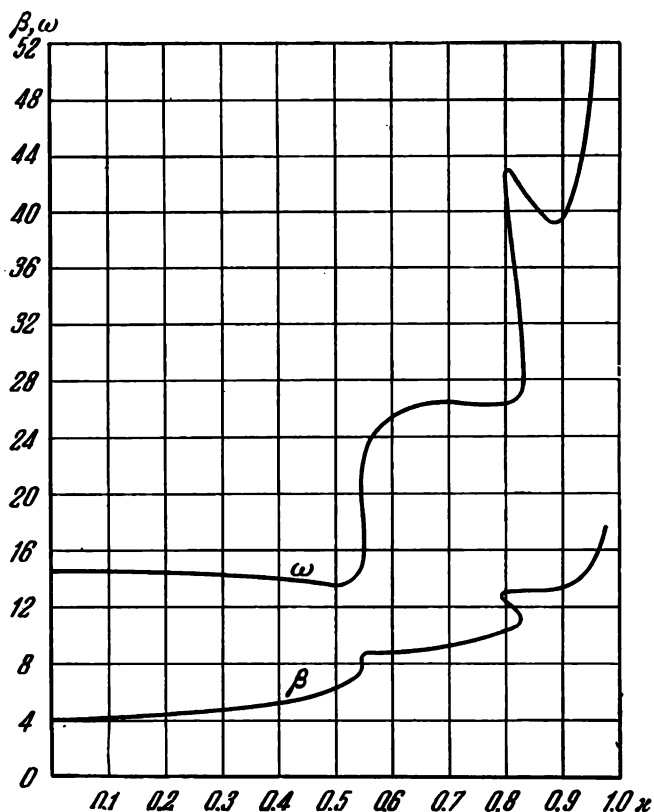


Fig. 415

vibrations of the third tone are set up, which is reflected by an abrupt increase of the frequency. Then, for a larger relative fluid mass the vibrations occur in the fourth tone and the frequencies grow. In the limiting case when the tube

mass is small compared with the fluid mass, the frequency and the critical rate increase indefinitely. If the mass of the bar is zero, the system is stable at any rate of flow.

150. Assume that the cross sections of the strip do not warp. The axial extensions can then be represented as a linear function of  $y$  (Fig. 416.)

$$\varepsilon_x = \varepsilon_0 + \kappa y,$$

where  $\kappa$  is the change in curvature of the strip in the  $xy$  plane. The axial stress is obviously given by

$$\sigma_x = E (\varepsilon_0 + \kappa y - \alpha t),$$

where  $\alpha t$  is the temperature extension.

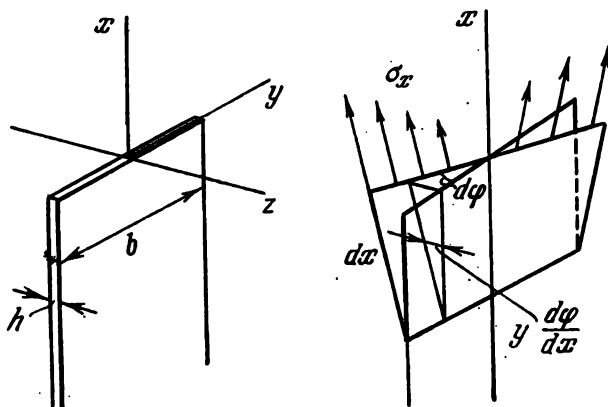


Fig. 416

Since the normal force at the section and the bending moment  $M_z$  are zero, we have

$$\int_A \sigma_x dA = 0, \quad \int_A \sigma_x y dA = 0,$$

whence

$$\varepsilon_0 = \frac{1}{b} \int_{-b/2}^{+b/2} \alpha t dy, \quad \kappa = \frac{12}{b^3} \int_{-b/2}^{+b/2} \alpha t y dy.$$

When twisting occurs, the stresses  $\sigma_x$  form a moment about the  $x$  axis (Fig. 416), equal to

$$M_x = \int_A \frac{y}{dx} \frac{d\varphi}{dx} \sigma_x y dA$$

or

$$M_x = \frac{d\varphi}{dx} \int_A \sigma_x y^2 dA.$$

Moreover, during twisting the strip develops a moment of the shearing stresses equal, as is known, to

$$M_\tau = \frac{1}{3} b h^3 G \frac{d\varphi}{dx}.$$

The sum of these moments is zero; hence,

$$\frac{1}{3} b h^3 G + \int_A \sigma_x y^2 dA = 0.$$

Substituting for  $\sigma_x$ , we find

$$- \int_{-b/2}^{+b/2} (\epsilon_0 + \kappa y - \alpha t) y^2 dy = \frac{b h^2}{6(1+\mu)},$$

where  $\mu$  is Poisson's ratio. By eliminating  $\epsilon_0$ , we obtain

$$\int_{-b/2}^{+b/2} \alpha t \left( y^2 - \frac{b^2}{12} \right) dy = \frac{b h^2}{6(1+\mu)}. \quad (1)$$

This is the condition for transition to a new form of equilibrium.

Note that if the temperature extensions are distributed along the  $y$  axis according to a linear law, i.e., if

$$\alpha t = A + B y,$$

the left-hand side of expression (1) vanishes for all values of  $A$  and  $B$ . Consequently, if the temperature is linearly distributed, no new form of equilibrium exists.

Assume that the temperature extensions in the left half of the strip are distributed according to a quadratic law

$$\alpha t = \frac{4\alpha t_1}{b^2} y^2$$

(Fig. 417). Expression (1) then becomes

$$\int_{-b/2}^0 \frac{4\alpha t_1}{b^2} y^2 \left( y^2 - \frac{b^2}{12} \right) dy = \frac{bh^2}{6(1+\mu)}$$

or

$$\alpha t_1 \text{ cr} = \frac{15}{1+\mu} \frac{h^2}{b^2}.$$

Note that the smaller is the relative thickness of the sheet, the lower is the temperature at which instability (warping) occurs.

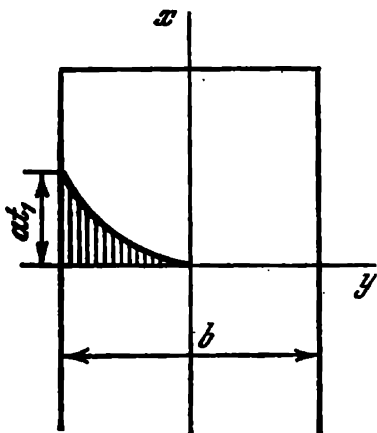


Fig. 417

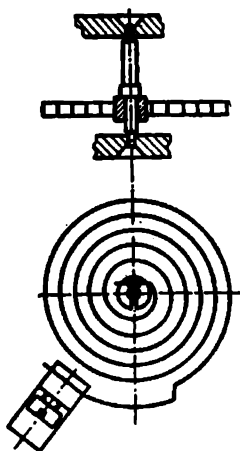


Fig. 418

151. In this case the beam may also buckle out of its plane, but this occurs at large displacements in the severely bent beam, which excludes the application of the ordinary theory of stability of plane form of bending.

When referring to lateral buckling of a strip with narrow rectangular section, the word "narrow" is added not to show that otherwise there will be no buckling, as may seem at first sight, but to emphasize that the beam hardly deflects in the plane of bending at the moment of buckling.

A graphic example of the fact that a strip in the plane of minimum rigidity may buckle out of its plane is the so-called entanglement of a hairspring in instruments.

By a hairspring is meant the well-known flat spiral spring which is mounted on the balance axle of pocket and wrist watches (Fig. 418). A hairspring is also mounted on the

pointer axle in most measuring instruments, such as manometers, barometers, aircraft speed indicators, altimeters, voltmeters, ammeters, etc.

The band of a hairspring mounted in an instrument bends in the plane of minimum rigidity. At a certain angle of rotation of the axle which is commonly termed the angle of entanglement, the hairspring buckles out of its plane, i.e., becomes entangled. The operating angle of rotation is therefore always set below the angle of entanglement.

152. The proposed problem gives a sufficiently wide scope for investigations. On the one hand, the analysis may be restricted to stability against axially symmetric overturning. This solution presents no difficulties. On the other hand, it is of interest to consider the existence of unsymmetrical forms of equilibrium and to establish the conditions under which the ring bends out of the plane of curvature with twisting. Here it is necessary first to derive equilibrium equations of somewhat more general form than those used in the investigation of stability of plane form of bending.

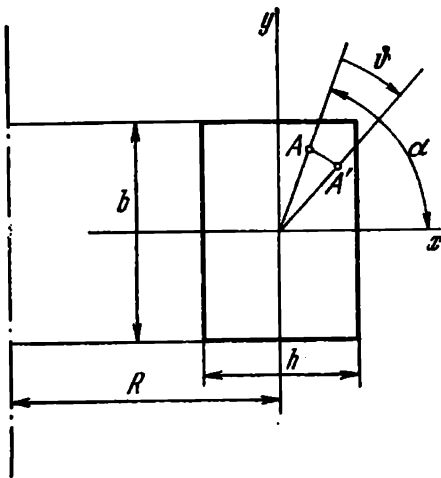


Fig. 419

To begin with we consider the stability of the ring against axially symmetric overturning.

At the point  $A$  with co-ordinates  $x, y$  (Fig. 419) there is an initial circumferential strain  $\varepsilon = 2x/R$  resulting from the prior operation of turning the ring inside out. We give the ring a small axially symmetric angular displacement  $\vartheta$ . The point  $A$  assumes a position  $A'$  and an additional extension is produced which is equal to the ratio of the projection of the segment  $AA'$  on the  $x$  axis to the radius  $R$

$$\Delta\varepsilon = \frac{OA}{R} [\cos(\alpha - \vartheta) - \cos\alpha].$$

Since the angle  $\vartheta$  is small, we replace  $\sin \vartheta$  by  $\vartheta$  and  $\cos \vartheta$  by  $1 - \frac{\vartheta^2}{2}$ ; then

$$\varepsilon + \Delta\varepsilon = \frac{2x}{R} + \frac{1}{R} \left( y\vartheta - x \frac{\vartheta^2}{2} \right).$$

The elastic strain energy is

$$U = \frac{1}{2} E \int \int_A (\varepsilon + \Delta\varepsilon)^2 dA ds,$$

where the integration is carried out over the circular arc  $s$  and the cross-sectional area  $A$ .

Since the deformations are axially symmetric,  $\varepsilon + \Delta\varepsilon$  is independent of  $s$  and we have

$$U = \frac{\pi E}{R} \int_A \left( 2x - x \frac{\vartheta^2}{2} + y\vartheta \right)^2 dA$$

or

$$U = \frac{\pi E}{R} \left[ \left( 2 - \frac{\vartheta^2}{2} \right)^2 I_y + I_x \vartheta^2 \right],$$

where  $I_x$  and  $I_y$  are the moments of inertia of the section with respect to the principal  $x$  and  $y$  axes.

The derivative of  $U$  with respect to  $\vartheta$  is expressed as

$$\frac{\partial U}{\partial \vartheta} = \frac{\pi E}{R} \left[ -2 \left( 2 - \frac{\vartheta^2}{2} \right) \vartheta I_y + 2I_x \vartheta \right].$$

This derivative vanishes when  $\vartheta = 0$ . Consequently, the ring turned inside out is in a position of equilibrium. To examine whether this position of equilibrium is stable or unstable, we take the second derivative

$$\frac{\partial^2 U}{\partial \vartheta^2} \Big|_{\vartheta=0} = \frac{\pi E}{R} (-4I_y + 2I_x).$$

When  $\frac{\partial^2 U}{\partial \vartheta^2} \Big|_{\vartheta=0} > 0$ , the position of equilibrium is stable; when  $\frac{\partial^2 U}{\partial \vartheta^2} \Big|_{\vartheta=0} < 0$ , it is unstable. Consequently, the condition for the stability of the ring turned inside out for

axially symmetric disturbances is as follows:

$$I_x > 2I_y$$

or

$$b > h\sqrt{2}.$$

We now proceed to a more complete investigation of the question.

We set up the equations of equilibrium for a rod bent in the principal plane in the presence of small disturbances associated with twisting and bending in the second plane. Let us do this in a somewhat more general form than required for the present problem with a view to using the resulting equations in what follows.

Thus, suppose we have an element of the rod of small curvature, of length  $ds$  (Fig. 420). At the cross sections there are six force factors. On the invisible face there

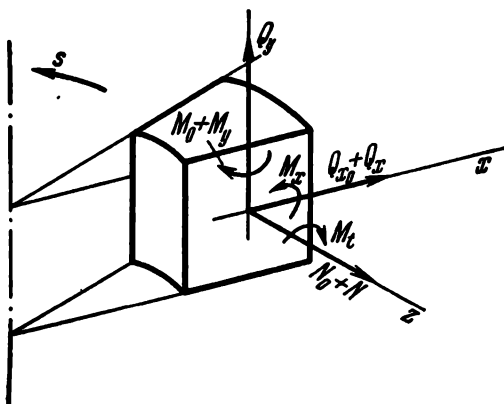


Fig. 420

are mutual force factors having the corresponding increments. For simplicity, they are not shown in the drawing.

In a subcritical state the only non-vanishing force factors are those lying in the plane of curvature, viz.  $M_0$ ,  $Q_{x0}$ , and  $N_0$ . After the rod is further bent and twisted, there occur additional force factors, viz.  $Q_x$ ,  $Q_y$ ,  $N$ ,  $M_x$ ,  $M_y$ , and  $M_z$ , whose magnitude is assumed to be small.

Denoting by  $p$  and  $q$  the small changes in curvature in the  $yz$  and  $xz$  planes, and by  $r$  the twist, we set up linear equations of equilibrium for the deformed element. The principle of linearization is common. The force factors of the subcritical state are introduced into the equations of equilibrium with account taken of the change in shape of the element, and the small additional force factors are introduced without regard to the change in shape, i.e., based on the shape for the subcritical state.

To make this procedure more clear, the first equation of equilibrium will be derived in detail. We equate to zero the sum of the projections of all forces on the  $x$  axis

$$Q_{x_0} + Q_x - (Q_{x_0} + Q_x + dQ_{x_0} + dQ_x) - \\ - (N_0 + N + dN_0 + dN) \left( \frac{1}{R} + q \right) ds - (Q_y + dQ_y) r ds = 0.$$

Rejecting small quantities of higher order and the products of  $Q_x$  by  $q$  and  $Q_y$  by  $r$ , we obtain

$$-Q'_{x_0} - Q'_x - \frac{N_0}{R} + N_0 q + \frac{N}{R} = 0.$$

In the subcritical state  $Q_x = N = 0$ ,  $q = 0$ , and hence

$$Q'_{x_0} + \frac{N_0}{R} = 0. \quad (\text{A})$$

We add the first equation to the second. Then

$$Q'_x + N_0 q + \frac{N}{R} = 0.$$

Similarly, by equating to zero the sums of the projections of the forces on the  $y$  and  $z$  axes and the sums of the moments about the three axes, we obtain five more equations. We write them out as follows:

$$Q'_x + N_0 q + \frac{N}{R} = 0, \quad (1)$$

$$Q'_y + rQ_{x_0} - pN_0 = 0, \quad (2)$$

$$N' - Q_{x_0}q - \frac{Q_x}{R} = 0, \quad (3)$$

$$M'_x + \frac{M_t}{R} - Q_y - M_0 r = 0, \quad (4)$$

$$M'_y + Q_x = 0, \quad (5)$$

$$M'_i - \frac{M_x}{R} + M_0 p = 0. \quad (6)$$

In addition to the equation (A) we obtain two more equations of equilibrium for the subcritical state, i.e., there are

altogether three equations

$$Q'_{x_0} + \frac{N_0}{R} = 0, \quad (7)$$

$$N'_0 - \frac{Q_{x_0}}{R} = 0, \quad (8)$$

$$M'_0 + Q_x = 0. \quad (9)$$

In all the above equations, by  $1/R$  is meant the curvature of the rod in the subcritical state, related to the magnitude of the moment  $M_0$ .

The changes in curvature  $p$  and  $q$  and the twist  $r$  are proportional to the moments  $M_x$ ,  $M_y$ , and  $M_t$ :

$$M_x = EI_x p,$$

$$M_y = EI_y q,$$

$$M_t = GI_t r.$$

We now proceed from the general equations to the problem under consideration. For the ring turned inside out Eqs. (1) through (6) are simplified by the fact that  $N_0 = Q_{x_0} = 0$  and  $M_0$ ,  $1/R$  are constants. Hence,

$$Q'_x + \frac{N}{R} = 0, \quad (10)$$

$$Q'_y = 0, \quad (11)$$

$$N' - \frac{Q_x}{R} = 0, \quad (12)$$

$$M'_x + \frac{M_t}{R} - Q_y - M_0 r = 0, \quad (13)$$

$$M'_y + Q_x = 0, \quad (14)$$

$$M'_t - \frac{M_x}{R} + M_0 p = 0. \quad (15)$$

We differentiate expression (13) with respect to  $s$  noting that  $Q'_y = 0$ . As a result, we obtain

$$M''_x + \frac{1}{R} M'_t - M_0 r' = 0$$

or

$$EI_x p'' + \left( \frac{1}{R} GI_t - M_0 \right) r' = 0.$$

Equation (15) becomes

$$GI_t r' = \left( \frac{1}{R} EI_x - M_0 \right) p. \quad (16)$$

We eliminate  $r$

$$p'' + \frac{k^2}{R^2} p = 0,$$

where

$$k^2 = \frac{R^2}{EI_x GI_t} \left( \frac{1}{R} GI_t - M_0 \right) \left( \frac{1}{R} EI_x - M_0 \right). \quad (17)$$

We thus obtain

$$p = A \sin \frac{ks}{R} + B \cos \frac{ks}{R},$$

$$r = \frac{1}{GI_t} \left( \frac{1}{R} EI_x - M_0 \right) \frac{R}{k} \left( -A \cos \frac{ks}{R} + B \sin \frac{ks}{R} \right) + C.$$

Since the ring is closed, the functions  $p$  and  $r$  must possess periodicity, i.e., when  $s$  is changed by  $2\pi R$  they must regain their former values. Consequently,  $k$  must be integral.

For the ring turned inside out

$$M_0 = \frac{2}{R} EI_y$$

and from expression (17) we obtain

$$n^2 = \left( 1 - 2 \frac{EI_y}{GI_t} \right) \left( 1 - 2 \frac{EI_y}{EI_x} \right), \quad (18)$$

where  $n$  is any integer.

If  $EI_x = 2EI_y$ , then  $n = 0$  and we come to the case of the axially symmetric overturning of the ring. We now assume that  $EI_x > 2EI_y$ . The second factor on the right-hand side of expression (18) is then positive. We determine the sign of the first factor

$$1 - 2 \frac{EI_y}{GI_t} = 1 - 2 \frac{2E \frac{bh^3}{12}}{\frac{E}{2(1+\mu)} \beta bh^3} = 1 - \frac{1+\mu}{3\beta}.$$

The torsional rigidity factor  $\beta$  for a rod of rectangular section is less than 0.333. Consequently, the above expression is negative, and hence  $n^2 < 0$ .

Thus, if  $EI_x > 2EI_y$ , or alternatively if  $b > h\sqrt{2}$ , then  $n^2 < 0$  and there are no unsymmetrical forms of equilibrium. Hence, the condition for the stability of a ring turned inside out

$$b > h\sqrt{2}$$

is valid for both symmetrical and unsymmetrical modes of instability.\*

153. The solution is completely covered by the equations derived for the preceding problem.

If heat is supplied through the inner surface, then  $t_1 > t_2$  and the ring develops a constant moment

$$M_0 = EI_y \alpha \frac{t_1 - t_2}{h},$$

where  $\alpha$  is the coefficient of thermal expansion.

The quantity  $k^2$  (17) must be integral

$$n^2 = \frac{R^2}{EI_x GI_t} \left( \frac{GI_t}{R} - M_0 \right) \left( \frac{EI_x}{R} - M_0 \right),$$

whence

$$M_0 = \frac{1}{2R} [EI_x + GI_t \pm \sqrt{(EI_x + GI_t)^2 + 4EI_x GI_t (n^2 - 1)}].$$

The least positive value of the moment  $M_0$  is when  $n = 0$

$$M_{0cr} = \frac{EI_x}{R}.$$

(The case of  $n = 0$  and  $M_0 = \frac{GI_t}{R}$  does not satisfy the continuity condition for displacements.)

If heat is supplied through the outer surface and  $t_2 > t_1$ , then we must seek the numerically least negative value for  $M_0$ . This occurs when  $n = 2$

$$|M_{0cr}| = \frac{1}{2R} [\sqrt{EI_x + GI_t)^2 + 12EI_x GI_t} - EI_x - GI_t].$$

---

\* Problems similar to that considered here and related to the overturning of a ring under distributed and concentrated moments are considered in great detail in the fundamental monograph by C. B. Biezeno and R. Grammel, "Technische Dynamik", Bd. 1, Springer-Verlag, Berlin, 1939.

Thus, under internal heating the instability occurs in symmetrical form, and under external heating, in unsymmetrical form with twisting.

154. The answer to the question posed is again given by the equations derived in the solution of Prob. 152.

Since  $1/R = 0$ , Eqs. (14), (13), and (15) become

$$\begin{aligned} Q'_y &= 0, \\ M'_x - Q_y - M_0 r &= 0, \\ M'_t + M_0 p &= 0, \end{aligned}$$

where the position of the axes corresponds to Fig. 421.

Substituting  $M_x = EI_x p$  and  $M_t = GI_t r$  and eliminating  $r$ , we find

$$p'' + \frac{M_0^2}{GI_t EI_x} p = 0.$$

But  $M_0 = EI_y/R$ , where by  $R$  is now meant the initial radius of the uncut ring and not the radius of curvature in the subcritical state.

Denote

$$\frac{(EI_y)^2}{GI_t EI_x} = k^2.$$

Then

$$p = A \sin \frac{ks}{R} + B \cos \frac{ks}{R}.$$

The angle of rotation of the section about the  $x$  axis is determined by integrating  $p$  with respect to  $s$

$$\vartheta_x = A \frac{R}{k} \left( 1 - \cos \frac{ks}{R} \right) + B \frac{R}{k} \sin \frac{ks}{R}.$$

Here the arbitrary integration constant has already been chosen so that when  $s = 0$  the angle  $\vartheta_x$  vanishes.

In order to obtain the transverse displacement along the  $y$  axis, the last expression must be integrated once more with respect to  $s$

$$y = A \frac{R}{k} \left( s - \frac{R}{k} \sin \frac{ks}{R} \right) + B \frac{R^2}{k^2} \left( 1 - \cos \frac{ks}{R} \right).$$

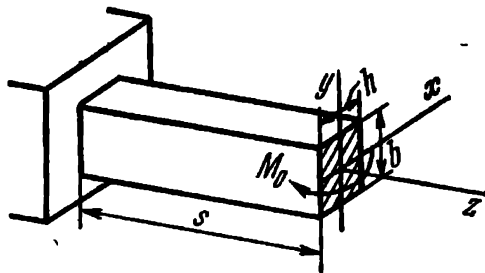


Fig. 421

Here again, the integration constant is chosen so as to make the displacement zero at the origin. Since, when  $s = 2\pi R$  the quantities  $\vartheta_x$  and  $y$  vanish, we obtain two equations

$$\begin{aligned} A(1 - \cos 2\pi k) + B \sin 2\pi k &= 0, \\ A\left(2\pi R - \frac{R}{k} \sin 2\pi k\right) + B \frac{R}{k}(1 - \cos 2\pi k) &= 0. \end{aligned}$$

We equate the determinant to zero and find the smallest root  $2\pi k = 2\pi$ . Consequently,  $k = 1$  and then

$$\frac{EI_y}{\sqrt{GI_t EI_x}} = 1.$$

But

$$EI_x = E \frac{b^3 h}{12}, \quad EI_y = E \frac{bh^3}{12}, \quad GI_t = \frac{E}{2(1+\mu)} \beta h^3 b$$

from which it follows that

$$\frac{b^2}{h^2} = \frac{1+\mu}{6\beta}. \quad (\text{A})$$

Assume  $\mu = 0.3$ . As regards the torsional rigidity factor  $\beta$ , it depends in some complicated way on the ratio  $b/h$ .

The tabular data on the factor  $\beta$  presented in courses in strength of materials are insufficient to solve this transcendental equation. We therefore use the relation\*

$$\beta = \frac{1}{3} \left[ 1 - \frac{192}{\pi^6} \frac{h}{b} \sum_{i=1,3,\dots} \frac{1}{i^6} \tanh \frac{i\pi b}{2h} \right].$$

After several numerical trials we find the solution of the equation (A)

$$\frac{b}{h} = 1.16.$$

The straight-line form of equilibrium is stable when

$$b > 1.16h.$$

---

\* See Arutyunyan N. Kh., Abramyan B. L., "Torsion of Elastic Bodies", Fizmatgiz, Moscow, 1963.

155. The probability of buckling of the bar in one way or another is determined by its initial deflection, random inhomogeneities in the material and departures of the line of action of the force  $P$  from the axis of the bar. The extent to which accidental factors may have influence depends on the rigidity of the bar. Obviously, bending is most likely to occur in the plane of minimum rigidity, i.e., in the present case about the  $z$  axis (Fig. 422). It remains to check whether the flexural rigidity varies with the sense of the moment. If the rigidity remains unchanged, buckling of the bar to the right or to the left is equiprobable. If the rigidity turns out to be different, the bar is most likely to bend in the direction of least rigidity.

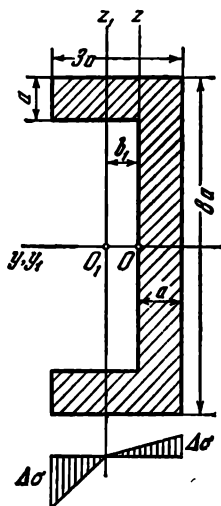


Fig. 422

Suppose the compression stress-strain diagram of the material is given (Fig. 423). The stress  $\sigma$  occurring at cross sections of the bar exceeds, according to the condition of the problem, the yield stress (point  $A$  in the diagram).

When the bar bends, the layers located on the concave side are additionally loaded and the stresses increase as a function of  $\varepsilon$  along the straight line 1. On the convex side unloading takes place and the relation between  $\sigma$  and  $\varepsilon$  is represented by the straight line 2. The slope of the straight line 1 is denoted by  $D$ , and the slope of the straight line 2 by  $E$ , where  $E$  is the modulus of elasticity. As a result, the additional bending stress diagram assumes the form of a broken line (Fig. 422). The position of the neutral line  $z_1$  is de-

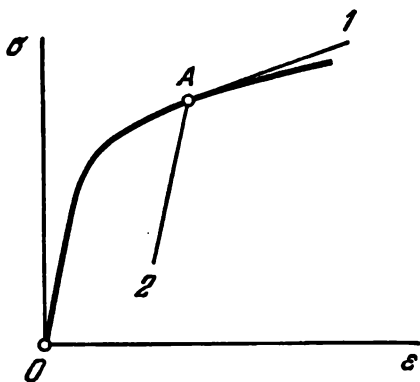


Fig. 423

ditional bending stress diagram assumes the form of a broken line (Fig. 422). The position of the neutral line  $z_1$  is de-

terminated from the condition that

$$\int_A \Delta \sigma dA = 0 \quad (1)$$

since the normal force at the section does not change and is always equal to  $P$ .

If the bar buckles to the left, the  $z_1$  axis is also displaced from the centroidal  $z$  axis to the left. If the bar buckles to the right, the neutral axis moves to the right.

Consider the first case. The  $z_1$  axis is shifted to the left. On the convex side of the bar

$$\Delta \sigma = E \frac{y_1}{\rho} \quad (y_1 \geq 0)$$

and on the concave side

$$\Delta \sigma = D \frac{y_1}{\rho} \quad (y_1 \leq 0).$$

According to expression (1) we have

$$E \int_{\text{left}} y_1 dA = D \int_{\text{right}} y_1 dA,$$

where the first integral extends over the region to the left of the  $z_1$  axis, and the second integral to the right of the  $z_1$  axis (Fig. 422). By taking the static moments of these regions with respect to the  $z_1$  axis, we find

$$b_1 = \frac{2a}{1-d} (1 + 2d - \sqrt{6d + 3d^2}),$$

where  $d = D/E$ .

When the bar buckles to the right, the  $z_1$  axis is displaced to the right by the amount

$$b_2 = \frac{a}{2(1-d)} (2 + d - \sqrt{12d - 3d^2}).$$

We now determine the moment of the stresses  $\Delta \sigma$  about the transverse axis  $z_1$ . Note that the axis may be taken arbitrarily in view of the fact that the normal force due to the stresses  $\Delta \sigma$ , with  $b_1$  and  $b_2$  found above, is zero.

When the bar buckles to the left

$$M_1 = \frac{1}{\rho_1} \left[ E \int_{\text{left}} y_1^2 dA + D \int_{\text{right}} y_1^2 dA \right].$$

This expression may be written as

$$M_1 = \frac{EI_1}{\rho_1},$$

where

$$I_1 = \frac{2}{3} a (2a - b_1)^3 + \frac{d}{3} [8a (a + b_1)^3 - 6ab_1^3].$$

By eliminating  $b_1$ , we obtain

$$I_1 = \frac{8a^4d}{(1-d)^2} [7 + 22d + 7d^2 - 4(2+d)\sqrt{6d+3d^2}].$$

When the bar buckles to the right, we obtain in a similar way

$$I_2 = \frac{2a^4d}{(1-d)^2} [10 - 2d + d^2 - (4-d)\sqrt{12d-3d^2}].$$

In the range of  $d$  from zero to unity we obtain

$$I_2 \leq I_1.$$

Consequently, the probability that the bar deflects to the right is greater than to the left. During buckling the bar is most likely to bend so that the open side of the section is situated on the concave side of the rod.

156. Instability is possible for tension springs wound with winding tension.

In this kind of springs the coils are closely adjusted to one another.

As the tensile force increases,

the contact pressure between the coils decreases. The extension of the spring is produced only by a force larger than the prestressing force  $P_0$  (Fig. 424).

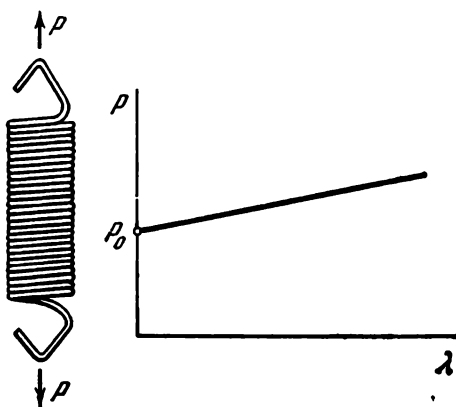


Fig. 424

The instability occurs with distortion and bending of the coils (Fig. 425). It turns out that each coil is not "waiting" for the moment when it can separate off from the adjacent coil but slips on the contact surface and bends in its plane.

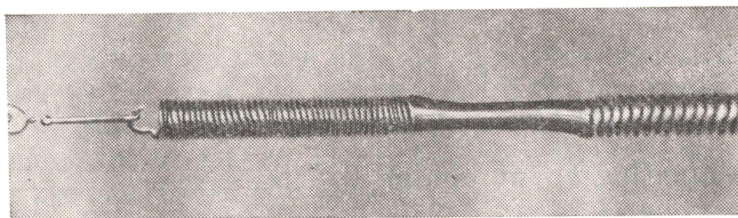


Fig. 425

The work done by the force  $P$  during the resulting axial displacement is transformed into the strain energy of the coils due to bending.

The schematic diagram for determining the critical forces is shown in Fig. 426. According to formula (3) (see the solution of Prob. 54, p. 151)

$$\Delta\phi = \frac{Q}{C_{sh}}.$$

But  $Q = P\Delta\phi$ . By eliminating  $Q$ , we obtain

$$P_{cr} = C_{sh}.$$

From formula (4) of the same problem we find

$$P_{cr} = \frac{Ed^4l}{8D^3n}.$$

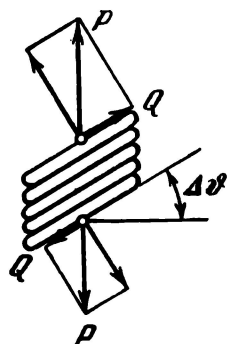


Fig. 426

Since in the present case  $l/n = d$ , we have

$$P_{cr} = \frac{Ed^5}{8D^3}.$$

**157.** Consider the system in a displaced position from the vertical.

The equations of equilibrium for the joint (Fig. 427a) are as follows:

$$\left. \begin{aligned} P &= N_1 \sin \alpha_1 + N_2 \sin \alpha_2, \\ N_1 \cos \alpha_1 &= N_2 \cos \alpha_2. \end{aligned} \right\} \quad (1)$$

From the triangle  $ABC$  (Fig. 427b) we have

$$\left. \begin{aligned} (l - \Delta l_1) \cos \alpha_1 + (l - \Delta l_2) \cos \alpha_2 &= 2l \cos \alpha_0, \\ (l - \Delta l_1) \sin \alpha_1 &= (l - \Delta l_2) \sin \alpha_2. \end{aligned} \right\} \quad (2)$$

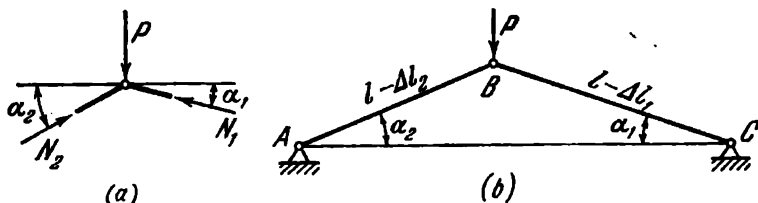


Fig. 427

Let us consider small displacements from the vertical and large displacements along the vertical. Denote

$$\alpha_2 = \alpha + \beta, \quad \alpha_1 = \alpha - \beta,$$

where the angle  $\alpha$  characterizes the displacement of the joint downward, and the small angle  $\beta$  defines the displacement along the horizontal. Similarly,

$$N_1 = N - \Delta N, \quad N_2 = N + \Delta N.$$

Denote by  $k$  the compression stiffness of the bars

$$\Delta l_1 = \frac{N - \Delta N}{k}, \quad \Delta l_2 = \frac{N + \Delta N}{k}.$$

We further substitute for  $\alpha_1$ ,  $\alpha_2$ ,  $N_1$ ,  $N_2$ ,  $\Delta l_1$ , and  $\Delta l_2$  in Eqs. (1) and (2) and linearize them neglecting small products  $\beta \Delta N$ . We retain only the first powers of these quanti-

ties. As a result, instead of (1) and (2) we obtain

$$\begin{aligned} P &= 2N \sin \alpha, \\ N\beta \sin \alpha - \Delta N \cos \alpha &= 0, \\ \left(l - \frac{N}{k}\right) \cos \alpha &= l \cos \alpha_0, \\ \left(l - \frac{N}{k}\right) \beta \cos \alpha - \frac{\Delta N}{k} \sin \alpha &= 0. \end{aligned}$$

The first and third of these equations enable one to determine the angle  $\alpha$  as a function of the force  $P$  for the symmetrical form of equilibrium

$$\frac{P}{2kl} = \sin \alpha \left(1 - \frac{\cos \alpha_0}{\cos \alpha}\right). \quad (3)$$

The second and fourth equations are homogeneous in the unknowns  $\beta$  and  $\Delta N$  which characterize the lateral displacement. We equate to zero the determinant of this system

$$\begin{vmatrix} N \sin \alpha & -\cos \alpha \\ \left(l - \frac{N}{k}\right) \cos \alpha & -\frac{1}{k} \sin \alpha \end{vmatrix} = 0,$$

whence

$$\frac{N}{k} - l \cos^2 \alpha = 0.$$

By replacing  $N$  by  $P$ , we obtain

$$\frac{P}{2kl} - \sin \alpha \cos^2 \alpha = 0$$

or, according to expression (3),

$$\cos \alpha_0 = \cos \alpha - \cos^3 \alpha.$$

Figure 428 shows the graph of  $\cos \alpha$  plotted against  $\cos \alpha_0$ . This graph should be understood as follows. The angle  $\alpha_0$  is given. The system is not loaded. Then  $\alpha = \alpha_0$  (point  $A$  in Fig. 428). As the system is loaded, the angle  $\alpha$  decreases and  $\cos \alpha$  increases. The point  $B$  characterizes the transition to an unsymmetrical form. The value of the corresponding force  $P$  can be determined from expression (3). When the angle  $\alpha$  has sufficiently decreased, the symmetrical form

of equilibrium again becomes stable (point  $C$  in the graph). The occurrence of unsymmetrical forms is possible only when  $\cos \alpha_0 < 2\sqrt{3}/9$  or when  $\alpha_0 > 67^\circ 25'$ .

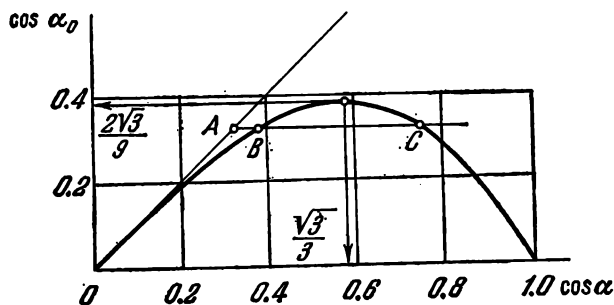


Fig. 428

The behaviour of the system in the postcritical condition can be investigated by rejecting the assumption that the angle  $\beta$  is small. Here, however, it is more convenient to solve the problem by the energy method. By introducing

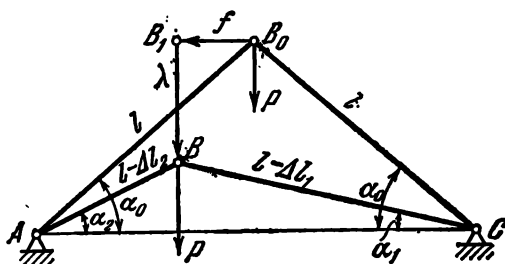


Fig. 429

into consideration the displacements  $\lambda$  and  $f$  (Fig. 429), from the quadrangles  $CBB_1B_0$  and  $ABB_1B_0$  it is easy to obtain the following relations:

$$l \cos \alpha_0 + f = (l - \Delta l_1) \cos \alpha_1,$$

$$l \sin \alpha_0 - \lambda = (l - \Delta l_1) \sin \alpha_1,$$

$$l \cos \alpha_0 - f = (l - \Delta l_2) \cos \alpha_2,$$

$$l \sin \alpha_0 - \lambda = (l - \Delta l_2) \sin \alpha_2.$$

By eliminating  $\alpha_1$  and  $\alpha_2$ , we obtain

$$\Delta l_1 = l - \sqrt{(l \sin \alpha_0 - \lambda)^2 + (l \cos \alpha_0 + f)^2},$$

$$\Delta l_2 = l - \sqrt{(l \sin \alpha_0 - \lambda)^2 + (l \cos \alpha_0 - f)^2}.$$

The total potential energy of the system is

$$U = \frac{1}{2} k (\Delta l_1)^2 + \frac{1}{2} k (\Delta l_2)^2 - P\lambda.$$

The first derivatives of  $U$  with respect to  $\lambda$  and  $f$  in the equilibrium position are zero, and the sign of the second derivatives determines whether the equilibrium form is stable or unstable.

We leave it as an exercise for the reader to make this analysis.

158. Imagine that the balls  $BB$  have rotated through a small angle  $\varphi$  about the axis  $OA$  (Fig. 430). The inertial forces of the balls  $m\omega^2 l$  are no longer parallel to the axis  $OA$  and give a couple with the moment

$$M = m\omega^2 l a 2a$$

twisting the bar  $OA$ . But since  $\alpha = \varphi a/l$ , we have

$$M = 2m\omega^2 a^3 \varphi.$$

On the other hand, for the twisted bar

$$M = \frac{GI_p}{l} \varphi,$$

where  $GI_p$  is the rigidity of the bar; thus,

$$\omega = \sqrt{\frac{GI_p}{2mla^2}}.$$

This is the critical angular velocity for the given system. At a velocity higher than the above value the bar  $OA$  becomes twisted.

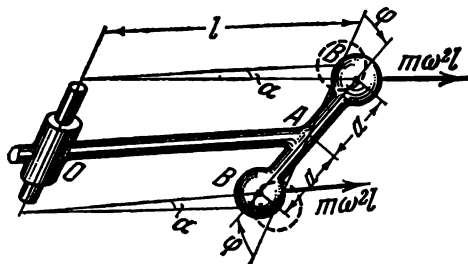


Fig. 430

159. Imagine that a certain section distant  $\zeta$  from the axis has rotated through an angle  $\varphi$  as a result of the twisting of the bar (Fig. 431). Isolate an element  $d\zeta dy h$  from the bar at a distance  $y$  from the axis of the bar. As the sec-

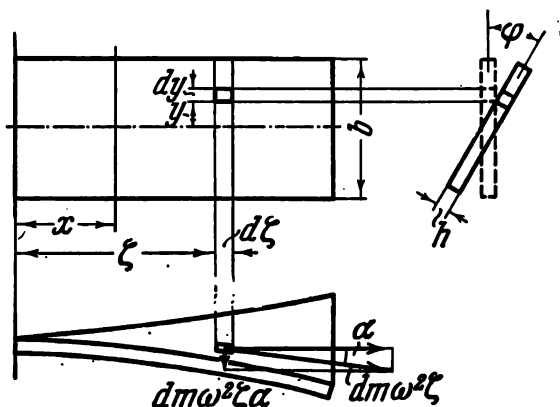


Fig. 431

tion rotates through the angle  $\varphi$ , the elementary inertial force  $dm\omega^2\zeta$  gives a transverse component  $dm\omega^2\zeta\alpha$ .

The elementary twisting moment of this force is

$$dM = dm\omega^2\zeta\alpha y.$$

But

$$dm = \frac{\gamma}{g} h d\zeta dy, \quad \alpha = \varphi \frac{y}{\zeta},$$

where  $\gamma$  is the specific weight of the bar material. The twisting moment at the section  $x$  is then determined as

$$M = \int_{-b/2}^{+b/2} \int_0^l \frac{\gamma}{g} h \omega^2 \varphi y^2 dy d\zeta = \frac{\gamma}{g} \frac{b^3 h}{12} \omega^2 \int_0^l \varphi d\zeta.$$

The normal force at the same section is determined by integrating the expression

$$\omega^2\zeta dm = \frac{\gamma}{g} \omega^2 h \zeta d\zeta dy,$$

giving

$$N = \int_{-b/2}^{+b/2} \int_x^l \frac{\gamma}{g} \omega^2 h \zeta d\zeta dy = \frac{\gamma}{g} \frac{\omega^2 b h}{2} (l^2 - x^2).$$

From the conditions of twisting of the bar we have

$$\frac{d\varphi}{dx} = \frac{M_t}{C},$$

where  $C$  is the torsional rigidity. The latter depends on the force  $N$  in the present case (see Prob. 29)

$$C = \frac{1}{3} b h^3 G + \frac{N b^2}{12},$$

$$C = \frac{1}{3} b h^3 G + \frac{\gamma}{g} \frac{b^3 h}{24} \omega^2 (l^2 - x^2).$$

In the preceding example the bars  $OA$  were circular and their rigidity was independent of the tensile force. We now obtain

$$\frac{d\varphi}{dx} C = \frac{\gamma}{g} \frac{b^3 h}{12} \omega^2 \int_x^l \varphi d\xi.$$

We differentiate both sides of this equation with respect to  $x$

$$\frac{d}{dx} \left( C \frac{d\varphi}{dx} \right) = - \frac{\gamma}{g} \frac{b^3 h}{12} \omega^2 \varphi.$$

But from the expression for  $C$  it follows that

$$- \frac{\gamma}{g} \frac{b^3 h}{12} \omega^2 = \frac{1}{x} \frac{dC}{dx};$$

hence

$$x \frac{d}{dx} \left( C \frac{d\varphi}{dx} \right) = \frac{dC}{dx} \varphi.$$

Whatever the form of the function  $C$ , the solution of this equation is

$$\varphi = x \left[ A \int \frac{dx}{x^2 C} + B \right],$$

where  $A$  and  $B$  are arbitrary constants.

Take the integral

$$\begin{aligned} \int \frac{dx}{x^2 C} &= \int \frac{dx}{\left[ \frac{1}{3} b h^3 G + \frac{\gamma}{g} \frac{b^3 h}{24} \omega^2 (l^2 - x^2) \right] x^2} = \\ &= \frac{1}{p} \left[ -\frac{1}{x} + \frac{k}{2} \ln \frac{1+kx}{1-kx} \right], \end{aligned}$$

where the following notation has been used

$$p = \frac{1}{3} b h^3 G + \frac{\gamma}{g} \frac{b^3 h}{24} \omega^2 l^2,$$

$$k^2 = \frac{1}{p} \frac{\gamma}{g} \frac{b^3 h}{24} \omega^2.$$

Thus,

$$\varphi = \frac{A}{p} \left( -1 + \frac{k}{2} x \ln \frac{1+kx}{1-kx} \right) + Bx.$$

When  $x = 0$ ,  $\varphi = 0$ , whence  $A = 0$ . Further, when  $x = l$ , we have  $M_t = 0$  ( $d\varphi/dx = 0$ ) and then  $B = 0$ .

Consequently, at any angular velocity  $\omega$  the bar remains straight.\* If the torsional rigidity were independent of the normal force, it would be possible to indicate the critical angular velocity for the bar.

160. A thin homogeneous disk rotating about an axis perpendicular to its plane can lose stability. But for disks of

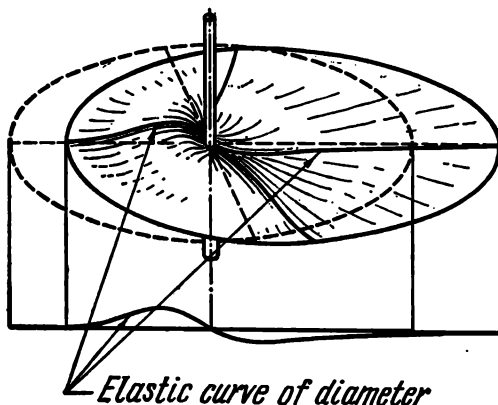


Fig. 432

usual thickness the critical velocity  $\omega_{cr}$  lies above that at which fracture occurs. By considering a very thin metal or, better still, rubber disk, one can experimentally obtain the instability mode shown in Fig. 432.

---

\* When the author was preparing the first edition of this book L. I. Balabukh showed that a prismatic bar of any shape of cross section has no critical angular velocity.

The occurrence of this form of equilibrium can be given the following explanation. Assume that the disk is perfectly balanced and suppose that some external cause has produced a certain deformation of the disk in its plane so that the balance of the disk is disturbed. If the centre of gravity of the disk has shifted to the right, as shown in Fig. 432, then compressive radial stresses are developed near the fixed axis on the left side. Hence, at a sufficiently high angular velocity the disk may buckle in this zone, with the result that

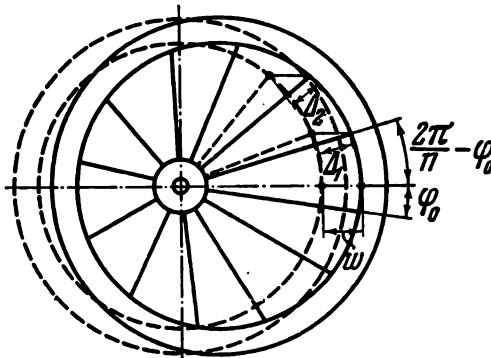


Fig. 433

the disbalance is still further increased. If the disk does not fracture, its shape after buckling will be such as shown in Fig. 432.

161. Determine the force  $P$  that must be applied to the ring in order to displace it from the axis by a small amount  $w$  (Fig. 433). Obviously,

$$P = \sum_1^n N_i \cos \left( i \frac{2\pi}{n} - \varphi_0 \right),$$

where  $i$  is the spoke number and  $N_i$  is the normal force induced at its sections.

If the elongation of the  $i$ th spoke is denoted by  $\Delta_i$ , then

$$N_i = \frac{EA\Delta_i}{l}.$$

But

$$\Delta_i = w \cos \left( i \frac{2\pi}{n} - \varphi_0 \right);$$

we obtain therefore

$$P = w \frac{EA}{l} \sum_1^n \cos^2 \left( i \frac{2\pi}{n} - \varphi_0 \right).$$

It may be shown that

$$\sum_1^n \cos^2 \left( i \frac{2\pi}{n} - \varphi_0 \right) = \frac{n}{2}$$

and then

$$P = w \frac{EA n}{2l}.$$

The critical number of revolutions is determined from the condition

$$P = m \omega_{cr}^2 w = w \frac{EA n}{2l}$$

from which we have

$$\omega_{cr} = \sqrt{\frac{EA n}{2ml}}.$$

**162.** At a certain pressure (in the range of marked extensions) the spherical form of equilibrium becomes unstable.

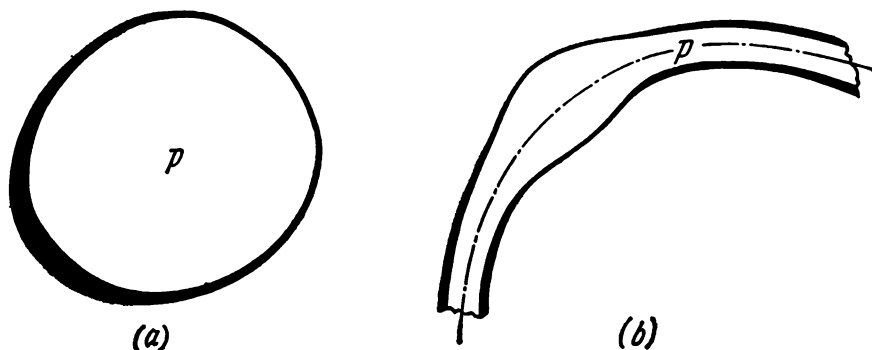


Fig. 434

If for some reason or other a local thinning is produced in the wall, it continues to develop. The wall thickness becomes non-uniform and the sphere slightly elongates (Fig. 434a). This phenomenon is similar to the necking process in a ten-

sion specimen. It may be observed when inflating a volleyball bladder. A similar phenomenon is also observed when inflating a bicycle inner tube (Fig. 434*b*).

163. If some external cause produces necking in a specimen, the latter, if subjected to a small tensile force, recovers its cylindrical shape after the cause initiating this necking is removed. Thus, up to a certain specific value of the tensile force the cylindrical shape of the specimen is stable.

At a sufficiently large tensile force the slightest necking results in an increase of the stresses in the zone of necking of such an amount that, upon the removal of the cause producing this necking, the bar cannot recover its cylindrical shape. The reduction of area progresses and a neck forms in the specimen. The cylindrical form of equilibrium is unstable.

## V. Miscellaneous Questions and Problems

164. The maximum ultimate tensile strength is found in some types of special steel used for making pressure vessels; it reaches

$$\sigma_{u.t} = 245 \text{ kgf/mm}^2.$$

Still higher indices are provided by a thin cold-drawn steel or tungsten wire. For the former, the ultimate tensile strength is close to  $350 \text{ kgf/mm}^2$ , and for the latter,  $420 \text{ kgf/mm}^2$ . The ultimate compressive strength for carbon steel reaches  $450 \text{ kgf/mm}^2$ , and for tungsten,  $500 \text{ kgf/mm}^2$ .

The special metal carboloy (tungsten carbide cemented by cobalt) used in high-pressure technique gives, according to published data,  $\sigma_{u.c} = 650 \text{ to } 670 \text{ kgf/mm}^2$ . This material is, however, weaker in tension than steel.

A very high ultimate strength is furnished by artificially grown filamentary crystals of metals and jewels to which a significant part is assigned in engineering of the near future. The reader should, however, be warned against identifying the concepts of "strength of a specimen" and "strength of structures".

The strength of a specimen in testing conditions is actually determined by the value of the ultimate strength. As regards the strength of a part made from the same material, it is determined in operating conditions not only by the ultimate strength but also by other indices among which the most important characteristics are the ultimate elongation and some other characteristics that are not uniquely determinable, such as local stress sensitivity, resilience, etc. Hence, a part made of a material with higher ultimate strength is quite often not so strong in operating conditions as the same part but made of another material with lower ultimate strength.

The ultimate strength of some steels may be raised to  $280 \text{ or } 300 \text{ kgf/mm}^2$  by the methods of heat treatment in

combination, for example, with intermediate cold working. The significance of the result achieved, however, cannot be estimated from this index alone.

165. Wood in tension parallel to the grain. For example, for dry white wood the ultimate compressive strength is  $\sigma_{u.c} = 5.50 \text{ kgf/mm}^2$ , and the ultimate tensile strength is  $\sigma_{u.t} = 7.20 \text{ kgf/mm}^2$ ; for beech

$$\sigma_{u.c} \cong 6.70 \text{ kgf/mm}^2, \quad \sigma_{u.t} \cong 8.20 \text{ kgf/mm}^2.$$

The above property of wood is a consequence of its anisotropy. In wood, hard layers alternate with soft ones. Under longitudinal compression, most of the load is carried by the hard layers. At sufficiently large forces local buckling starts to occur in these layers, which leads to rapid fracture of the specimen. The same property is found in textolite.

166. It is widely known that the elastic modulus of steel is  $2 \times 10^4 \text{ kgf/mm}^2$ , but few people know in what materials the elastic modulus is higher than this value. In the order of increasing elastic modulus the following data may be given for metals:

	kgf/mm <sup>2</sup>
Cobalt and nickel	21,100
Rhodium	29,800
Beryllium	29,900
Tungsten and molybdenum	35,200
Carboloy	70,000

167. For some types of rubber the elastic modulus is 0.04 to 0.05 kgf/mm<sup>2</sup>. Among metals, the lowest elastic modulus is observed in lead ( $E = 1830 \text{ kgf/mm}^2$ ) and in calcium ( $E = 2110 \text{ kgf/mm}^2$ ).

168. The answer to this question depends on how large deformations are involved. It is customary to assume that rubber does not obey Hooke's law. The fact that large strains of the order of 100 per cent and higher are implied is, however, passed over in silence.

At strains not exceeding 10 or 20 per cent all types of rubber may, as a rule, be assumed to obey Hooke's law, with an accuracy quite sufficient for practical purposes. No other material gives so large deformations within the proportional limit.

169. We are accustomed to assuming that in simple tension the ratio of the lateral strain to the longitudinal strain, known as Poisson's ratio, must be less than 0.5. This condition, however, is valid only for an isotropic material and there is no reason to suppose that it must be fulfilled for anisotropic materials, and in particular for wood.

Thus, if there is no reason to doubt the accuracy of measurements and the correctness of the experimental procedure, the ratio 0.6 obtained for wood may be accepted without reservation.

170. Because the elongation of a rope in tension is due not only to the elongations of the cords but also to their partial bending and twisting. The reduced modulus of elasticity of the rope in tension does not remain constant, i.e., the tensile test diagram of the rope is not linear even at elastic strains in the cords. In the first stage of the extension the cords tighten up and the clearances between them gradually decrease. In a further extension the effect of local deformations occurring in the zones of contact between the cords becomes more and more pronounced.

171. The fibres constituting a thread are shorter than the thread itself. The strength of the thread therefore depends not only on the strength of the fibres themselves, but also on their mutual cohesion. The latter is determined by frictional forces acting between the fibres. In a twisted thread each fibre is wound round and constricted by the adjacent fibres, and the cohesive forces of the fibres are much larger than for an untwisted thread.

The magnitudes of the cohesive forces depend greatly on the fibre length. That is why, for example, long-stapled cotton is rated higher than short-stapled cotton.

It is of interest that threads twisted from man-made fibres are less strong in tension than untwisted threads. A man-made fibre has a large length equal to the length of the thread. The fibres, therefore, no longer need mutual cohesion, and the presence of twisting produces, in this case, only additional stresses which lead to more rapid rupture.

Nevertheless the threads of man-made fibres are twisted or interlaced. This is necessary in practice in order to prevent the threads from separating into fibres and from tearing by single fibres.

172. The student confused the concepts of strength and stiffness.

When one speaks of a high-quality material, its strength indices are meant. An alloy steel has higher strength indices, but its modulus of elasticity  $E$  is approximately the same as for all other grades of steel, i.e., about  $2 \times 10^4$  kgf/mm<sup>2</sup>. Hence, the replacement of the simple steel by an alloy steel gives nothing in this case.

173. According to the condition of the problem, the displacements in the beam are proportional to the applied load.

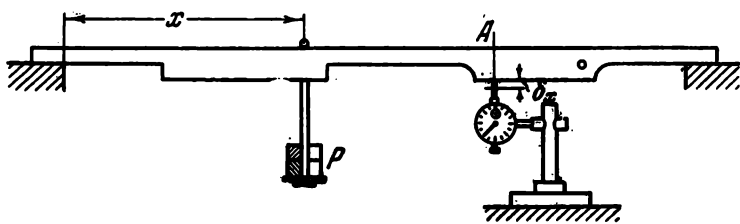


Fig. 435

Consequently, the reciprocity law for displacements is applicable to the system under consideration.

The displacement at the  $x$ th section can be determined by mounting an indicator under the point  $A$  and by loading the beam at the  $x$ th section (Fig. 435). By moving the weight, we measure  $\delta_x$  at the point  $A$  for different values of  $x$ . The relation  $\delta_x = f(x)$  thus obtained represents the elastic curve of the beam.

If the weight  $P$  is so great that its movement presents difficulty, it can be reduced and then, according to the prescribed condition, the elastic curve for the given value of the force  $P$  is obtained by a proportional increase of the measured deflections.

174. Consider two states of any elastic body (not necessarily a cylinder) resting on a rigid plane.

The first state: the body is under the action of its own weight. The second state: the body is subjected to a pressure  $p$  uniformly distributed over its surface. By the reciprocity theorem, the work done by the first force system during the displacements caused by the second system is equal to the

work done by the second force system during the displacements of the first system.

For the first of the above states of the elastic body, the work done by the gravity forces during the displacements caused by the pressure is

$$\int_V \gamma dV w_p,$$

where  $\gamma$  is the specific weight,  $\gamma dV$  is the weight of an element of volume,  $w_p$  is the vertical displacement of some point of the elastic body subjected to a uniform pressure  $p$ . This displacement is naturally measured with respect to the rigid plane. But the elastic extensions at all points of the body under uniform pressure are constant and equal to

$$\varepsilon = -\frac{p}{E}(1-2\mu).$$

Consequently, the vertical displacement  $w_p$  is proportional to the distance from the rigid plane. Then

$$\int_V \gamma w_p dV = \gamma \int_V w_p dV = \gamma V w_p^*,$$

where  $w_p^*$  is the displacement of the centre of gravity of the elastic body.

If the centre of gravity of the elastic body is at a distance  $H$  from the base, then

$$w_p^* = H \frac{p}{E} (1-2\mu).$$

Thus,

$$\int_V \gamma w_p dV = \gamma V \frac{Hp}{E} (1-2\mu).$$

On the other hand, by the reciprocity theorem, this quantity is equal to the work done by the pressure  $p$  in the unknown change of volume  $\Delta V$  produced by the gravity forces, i.e.,

$$\gamma V \frac{Hp}{E} (1-2\mu) = p\Delta V$$

from which we obtain

$$\Delta V = \gamma V H \frac{1-2\mu}{E}.$$

If the body is turned so that its centre of gravity is at a different height,  $\Delta V$  is correspondingly changed.

The solution obtained is naturally valid for any body irrespective of its shape. For the given cylinder, as one passes from position *I* to position *II* (Fig. 156) the volume is obviously increased by

$$P \left( \frac{H}{2} - R \right) \frac{1-2\mu}{E}.$$

175. The problem is solved in exactly the same way as the preceding one

$$p \Delta V_P = P \Delta (AB)_p,$$

where  $\Delta V_P$  is the unknown change of volume produced by the forces  $P$ , and  $\Delta (AB)_p$  is the change in distance between the points  $A$  and  $B$  produced by the pressure  $p$ . Obviously,

$$\Delta (AB)_p = -p \frac{1-2\mu}{E} (AB),$$

where  $AB$  is the distance between the points of application of the forces. Consequently, the required volume change is

$$\Delta V_P = -P (AB) \frac{1-2\mu}{E}.$$

176. The explanation is erroneous. According to the quoted reasoning, the tube, regardless of the shape of the cross section, must always reduce its curvature, i.e., straighten out, under internal pressure. Experiment, however, shows that a tube of circular section does not respond to internal pressure at all, and a tube having a section with interchanged positions of the major and minor axes does not reduce, but increase its curvature under internal pressure.

The author of the above-cited explanation did not take into account that, in addition to the forces  $P_1$  and  $P_2$  acting on the surfaces  $S_1$  and  $S_2$ , there is a force acting on the bottom of the tube. This force gives a moment exactly equal to the difference of the moments of the forces  $P_1$  and  $P_2$ , so that the bending moment at any section of the tube is

zero. There is no need to calculate the magnitudes of these forces for verification of the above. The surface of the tube to the right of an arbitrarily taken section  $A - A$  (Fig. 436) is a closed surface and the pressure gives, at this section,

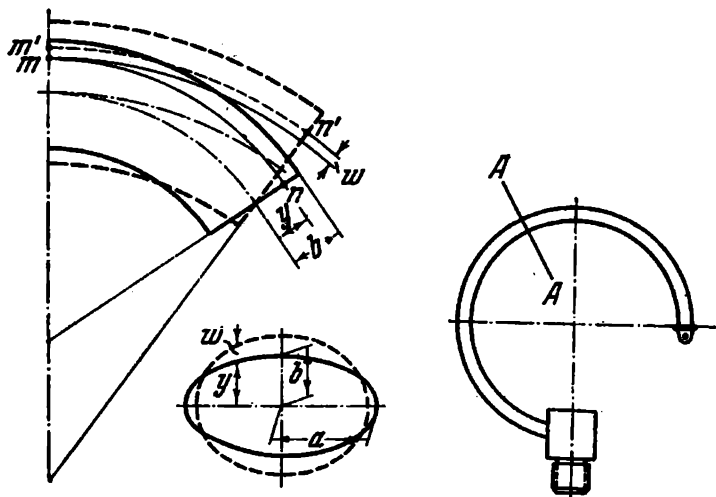


Fig. 436

only a normal force equal to the product of the pressure and the clear area.

Whatever the shape of the tube, the pressure forces give no bending moment at all. The necessary condition for the operation of the tube is the deformation of the contour of the cross section. No matter what the non-circular shape of the tube section may be, the contour of this section tends to assume the shape of a circle under internal excessive pressure. The minor axis of the section then slightly increases and the major axis decreases; the whole contour assumes a shape such as shown dashed in Fig. 436. Each longitudinal fibre of the tube then undergoes a displacement in a direction parallel to the minor axis of the section. In Fig. 436 this displacement for the fibre  $mn$  is denoted by  $w$ .

When the fibre  $mn$  is displaced by the amount  $w$ , it passes into an arc of larger radius and develops tensile stresses. The fibres lying below the neutral axis develop compressive stresses. The tube then straightens out,

In the light of the above it becomes clear why a tube of circular section does not respond to internal pressure. In this case the contour of the section is only extended and  $w$  is negligible. Hence, the change in curvature of a tube of circular section is very small and is not detected in the usual experimental procedure.

If the major axis of the section is situated in the plane of symmetry of a tube, the quantity  $w$  is of opposite sign and the curvature of the tube does not decrease but increases under internal pressure.

177. In the general case  $f_1/f_2 \neq E_{2t}/E_{1t}$  for plywood since the flexural rigidity of plywood depends not only on the

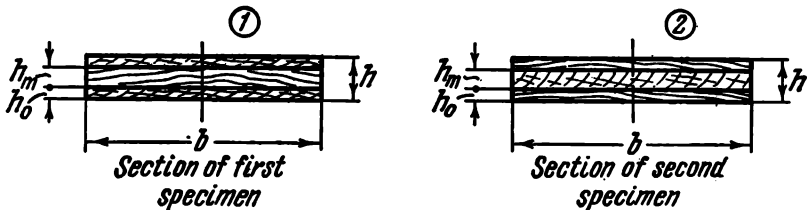


Fig. 437

thickness and orientation of the plies but also on their distance from the middle plane.

As a simple example we consider three-ply plywood (Fig. 437). Denote the thickness of the outer plies by  $h_o$ , the thickness of the middle ply by  $h_m$ . The moduli of elasticity of the wood perpendicular and parallel to the grain are, respectively,  $E'$  and  $E''$ .

We now calculate  $E_{1t}$  and  $E_{2t}$ . For the first specimen subjected to a tensile force  $P$  we have

$$\begin{aligned}\sigma'bh_m + 2\sigma''bh_o &= P, \\ \varepsilon(E'bh_m + 2E''bh_o) &= P.\end{aligned}$$

But since  $\varepsilon E_{1t} = P/bh$ , the modulus of the first strip is

$$E_{1t} = \frac{E'h_m + 2E''h_o}{h}. \quad (1)$$

By interchanging  $E'$  and  $E''$  we find the modulus of the second strip

$$E_{2t} = \frac{E''h_m + 2E'h_o}{h}. \quad (2)$$

Let us now find the reduced moduli of elasticity in bending,  $E_{1b}$  and  $E_{2b}$ . For the first specimen subjected to bending by a moment  $M$  we have

$$2b \int_0^{h_m/2} \sigma' z \, dz + 2b \int_{h_m/2}^{h_m/2+h_o} \sigma'' z \, dz = M,$$

where  $z$  is the current distance from the neutral axis,

$$\sigma' = E' \frac{z}{\rho}, \quad \sigma'' = E'' \frac{z}{\rho}.$$

Hence,

$$2b \frac{E'}{\rho} \int_0^{h_m/2} z^2 \, dz + 2b \frac{E''}{\rho} \int_{h_m/2}^{h_m/2+h_o} z^2 \, dz = M$$

or upon integration

$$\frac{2}{3} \frac{b}{\rho} \left\{ E' \frac{h_m^3}{8} + E'' \left[ \left( \frac{h_m}{2} + h_o \right)^3 - \left( \frac{h_m}{2} \right)^3 \right] \right\} = M.$$

But, as is known,

$$E_{1b} \frac{bh^3}{12} \frac{1}{\rho} = M,$$

whence

$$E_{1b} = (E' - E'') \left( \frac{h_m}{h} \right)^3 + E''. \quad (3)$$

By interchanging  $E'$  and  $E''$  we find

$$E_{2b} = (E'' - E') \left( \frac{h_m}{h} \right)^3 + E'. \quad (4)$$

From expressions (1), (2), (3), and (4) it is seen that in the general case

$$\frac{E_{1t}}{E_{2t}} \neq \frac{E_{1b}}{E_{2b}}.$$

For example, if we take  $h_m = h/2$  and  $h_o = h/4$ , then

$$\frac{E_{1t}}{E_{2t}} = 1, \quad \frac{E_{1b}}{E_{2b}} = \frac{E' + 7E''}{7E' + E''}.$$

178. All calculations in the proposed problem are made correctly and there is no mistake as such. The result obtained

is a consequence of the fact that at the basis of the solution is the assumption of zero shearing forces and bending moments at the sections of the shell.

If these force factors are taken into account, the calculated displacements will have a finite value. The correct solution can also be obtained by the membrane theory if allowances are made for a change in internal forces due to a change in the shape of the shell during loading.

To sum up, it may be said that in determining the stresses the neglect of the flexural rigidity introduces no serious error in the solution of the problem. In assessing the displacements, however, such a neglect is not always permissible.

179. Consider one section of the shaped cylinder (Fig. 438). Let  $p$  be an internal pressure and  $[\sigma]$  the allowable stress.

The thickness of the cylindrical portion of the section is determined from the allowable stress as follows:

$$\delta = \frac{pr}{[\sigma]}.$$

The supporting inner web is in tension and is subjected to forces exerted by two adjacent circular cylinders. The force per unit height of the cylinder is  $pr$ . The tensile force in the web is

$$2pr \sin(\beta - \alpha).$$

The allowable stress for the web is assumed to be the same as for the circular cylinder. The web thickness is therefore

$$h = \frac{2pr \sin(\beta - \alpha)}{[\sigma]}.$$

We now find the structural weight per unit length of the shaped cylinder

$$P = \gamma n (2\beta r \delta + ah),$$

where  $\gamma$  is the specific weight of the material and  $n$  is the number of sections.

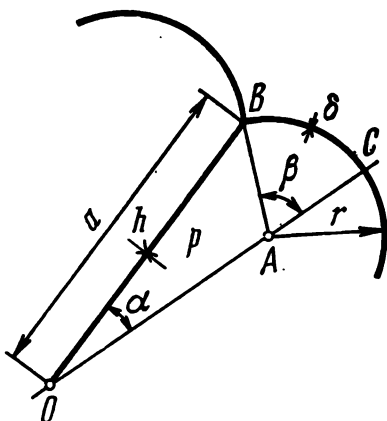


Fig. 438

On substituting for  $\delta$  and  $h$  we obtain

$$P = 2\gamma n \frac{Pr}{[\sigma]} [\beta r + a \sin(\beta - \alpha)]. \quad (1)$$

Let us find the internal volume per unit height.

The volume of the sector  $ABC$  is  $\frac{1}{2} \beta r^2$  and for the triangle  $OAB$  we have  $\frac{1}{2} ar \sin(\beta - \alpha)$ ; hence

$$V = 2n \left[ \frac{1}{2} \beta r^2 + \frac{1}{2} ar \sin(\beta - \alpha) \right]$$

or

$$V = nr [\beta r + a \sin(\beta - \alpha)].$$

Reverting to expression (1) we obtain

$$P = 2 \frac{\gamma P}{[\sigma]} V.$$

This means that for a given volume of compressed gas the weight of the structure cannot be changed by varying the quantities  $\alpha$ ,  $\beta$ ,  $a$ , and  $n$ . An ordinary smooth cylinder with the same internal volume has the same weight but is easier in fabrication. Thus, the proposed structure does not justify the hopes set on it.

180. In the question posed the manner in which the load  $P$  is applied to the spring is not specified. Gradually or suddenly? If the load is applied gradually, by small portions, so that at any moment of loading the system is in equilibrium, then expression (1) is wrong. The energy of position lost by the weight is not  $P^2/k$  but  $P^2/2k$  and the energy balance comes right.

If, however, the load is applied suddenly, then during compression the weight also possesses a kinetic energy equal to the difference of energies (1) and (2). Subsequently the weight performs a vibratory motion about the equilibrium position until its kinetic energy is dissipated.

181. At best, the following answer to the question posed is usually to be heard.

The angle of rotation of a coil in the axial plane is determined by the twisting of a portion of the spring over the



The angle of rotation of section (2) in the axial plane is obviously given by

$$d\psi = d\varphi - \vartheta \frac{ds}{R};$$

but it is known that

$$\vartheta = PR^2/GI_p$$

and since  $M_t = PR$  we obviously have  $d\psi = 0$ .

182. We consider the spring as a three-dimensional rod. At each section of a coil of the stretched spring there is a twisting moment  $M_t = PR \cos \alpha$  and a bending moment  $M_b = PR \sin \alpha$  (Fig. 440).

We first determine the increase in height of the spring  $\Delta H$

$$\Delta H = \int_l \frac{M_b M_{1b} ds}{EI} + \int_l \frac{M_t M_{1t} ds}{GI_p},$$

where  $M_{1b}$  and  $M_{1t}$  are the bending and twisting moments due to unit forces applied instead of the forces  $P$ , which are, respectively, equal to  $M_{1b} = R \sin \alpha$ ,  $M_{1t} = R \cos \alpha$ ; consequently,

$$\Delta H = \frac{PR^2 l}{EI} \sin^2 \alpha + \frac{PR^2 l}{GI_p} \cos^2 \alpha, \quad (1)$$

where  $l$  is the length of the coils of the spring.

Let us find the angle through which the upper end of the spring turns relative to the lower end in the horizontal plane. We apply unit moments to the ends of the spring (Fig. 441a). We then have

$$\begin{aligned} M_{1b} &= -\cos \alpha, & M_{1t} &= \sin \alpha; \\ \Delta \varphi &= \int_l \frac{M_b M_{1b} ds}{EI} + \int_l \frac{M_t M_{1t} ds}{GI_p}; \\ \Delta \varphi &= P R l \left( \frac{1}{GI_p} - \frac{1}{EI} \right) \sin \alpha \cos \alpha. \end{aligned} \quad (2)$$

Consider the unwrapped spring (Fig. 441b). Obviously,

$$R^2 \varphi^2 + H^2 = l^2,$$

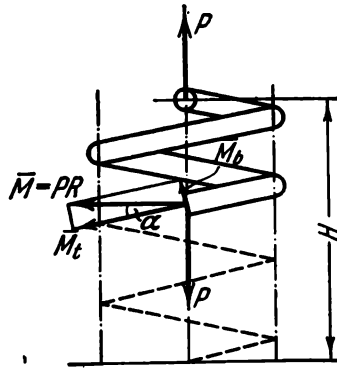


Fig. 440

Since  $l$  remains constant,

$$2R\varphi^2\Delta R + R^22\varphi\Delta\varphi + 2H\Delta H = 0,$$

where the symbol  $\Delta$  represents an increment of the corresponding parameter. From this expression we obtain

$$\Delta R = -\frac{R}{\varphi}\Delta\varphi - \frac{H}{R\varphi^2}\Delta H.$$

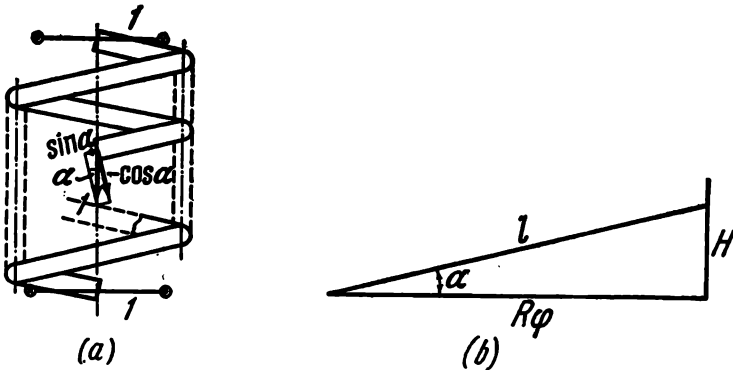


Fig. 441

Substituting for  $\Delta\varphi$  and  $\Delta H$  gives

$$\Delta R = -\frac{PR^2l}{\varphi} \left( \frac{1}{GI_p} - \frac{1}{EI} \right) \sin \alpha \cos \alpha - \frac{PHRl}{\varphi^2} \left( \frac{\sin^2 \alpha}{EI} - \frac{\cos^2 \alpha}{GI_p} \right). \quad (3)$$

From the triangle of Fig. 441b it follows that

$$l = \frac{\varphi R}{\cos \alpha} \quad \text{and} \quad H = \varphi R \tan \alpha.$$

Besides,

$$\varphi = 2\pi n, \quad \Delta\varphi = 2\pi\Delta n,$$

where  $n$  is the number of coils. Eliminating  $l$ ,  $H$ , and  $\varphi$  from expressions (1), (2), and (3) gives

$$\Delta H = \frac{PR^3n2\pi}{\cos \alpha} \left( \frac{\sin^2 \alpha}{EI} + \frac{\cos^2 \alpha}{GI_p} \right),$$

$$\Delta n = PR^2n \left( \frac{1}{GI_p} - \frac{1}{EI} \right) \sin \alpha,$$

$$\Delta R = -\frac{2PR^3 \sin \alpha}{GI_p} + \frac{PR^3}{EI} \sin \alpha (1 - \tan^2 \alpha).$$

If the spring is made from a round wire of diameter  $d$ , then

$$GI_p = G \frac{\pi d^4}{32},$$

$$EI = G(1 + \mu) \frac{\pi d^4}{32}$$

and we obtain

$$\Delta H = + \frac{64PR^3n}{Gd^4} \frac{1 + \mu \cos^2 \alpha}{(1 + \mu) \cos \alpha},$$

$$\Delta n = + \frac{32PR^2n}{G\pi d^4} \frac{\mu \sin \alpha}{1 + \mu},$$

$$\Delta R = - \frac{32PR^3}{G\pi d^4} \frac{\sin \alpha}{1 + \mu} \frac{1 + 2\mu \cos^2 \alpha}{\cos^2 \alpha}.$$

The signs in front of the right-hand members of the above expressions indicate that during the extension of the spring its length increases ( $\Delta H > 0$ ), the number of coils increases ( $\Delta n > 0$ ), and the radius decreases ( $\Delta R < 0$ ). If the angle  $\alpha$  is small, we find

$$\Delta H = \frac{64PR^3n}{Gd^4},$$

$$\Delta n = \frac{32PR^2n}{G\pi d^4} \frac{\mu \alpha}{1 + \mu},$$

$$\Delta R = - \frac{32PR^3}{G\pi d^4} \frac{1 + 2\mu}{1 + \mu} \alpha.$$

183. For this purpose, the shaped spring must be precompressed, for example, by means of another spring (Fig. 442). When such a system is loaded, the number of operating coils increases.

184. The system is not in equilibrium in the position shown. If we try to determine the magnitude of the reaction at the lower support without regard to deformations of the system, we obtain a result having no practical meaning

$$R = \pm \infty.$$

Indeed, by equating to zero the sum of the moments of all forces about the upper hinge (Fig. 443), we obtain

$$R \cdot 0 + Pa = 0$$

from which we find the above value of the reaction  $R$ .

The determination of the reaction therefore requires the consideration of the horizontal displacement of the lower roller. Suppose that the equilibrium of the system is estab-

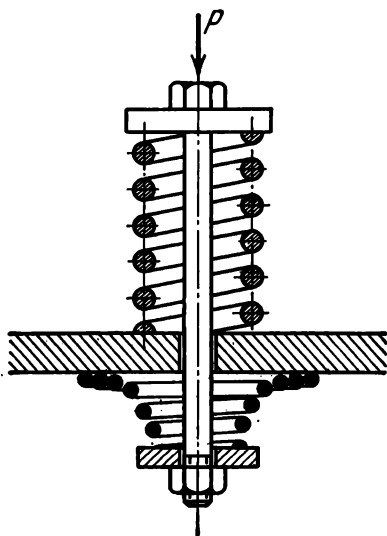


Fig. 442;

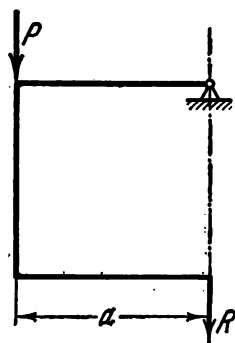


Fig. 443

lished when the angular displacement of the lower support is  $\varphi$  (Fig. 444).

From the conditions of equilibrium we obviously have  $P = R\varphi$ . As a result of the deformation of the frame the segment  $AB$  increases by

$$a(1 - \cos \varphi) \cong \frac{a\varphi^2}{2}.$$

On the other hand, the same quantity can be determined by multiplying the given force diagrams by the unit force diagrams (Fig. 445). We thus obtain

$$\frac{Ra^3}{EI} \frac{5}{3} \left(1 + \frac{\varphi}{2}\right) = \frac{a\varphi^2}{2}.$$

Since the displacements of the frame are small, the quantity  $\varphi/2$  in the parentheses may be neglected in comparison with unity. Further, substituting  $P/R$  for  $\varphi$  into the right

side of the equation, we obtain

$$R = \sqrt[3]{\frac{3P^2 EI}{10a^2}}.$$

185. For a system such as shown in Fig. 169, new forms of equilibrium occur when the displacements are large.

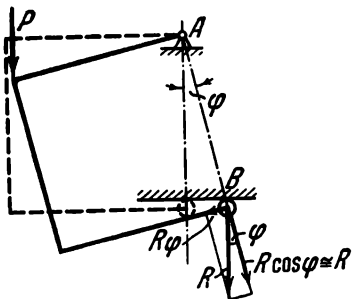


Fig. 444

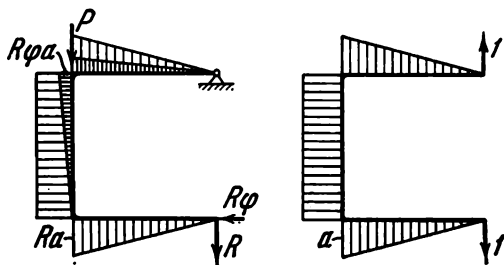


Fig. 445

In particular, if the stresses in the beam do not exceed the proportional limit, then, when  $P > 3.2 EI/l^2$ , the beam has, in addition to the basic initial form, two more forms (2 and 3) (Fig. 446). Form 2 is stable and 3 is unstable. When  $P > 7.1 EI/l^2$ , there may be unstable forms of equilibrium 4 and 5 (Fig. 446), etc.

As the force  $P$  is gradually increased, form 1, naturally, cannot pass into form 2 or any other form.

If, however, the rod is first thrown to the left and then loaded by a force larger than  $3.2 EI/l^2$ , the rod assumes the equilibrium form 2.

186. Let us take two arbitrarily oriented systems of coordinates: a system  $X, Y, Z$  with origin at the point  $A$ , and a system  $x, y, z$  with origin at the point  $B$  (Fig. 447).

The components of the force  $P$  along the axes  $X, Y, Z$  are denoted by  $P_x, P_y, P_z$  with

$$P_x = Pl, \quad P_y = Pm, \quad P_z = Pn,$$

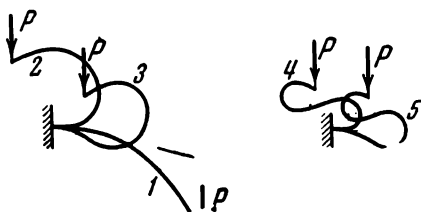


Fig. 446

where  $l, m, n$  are the direction cosines of the force  $P$  in the co-ordinate system  $X, Y, Z$ .

The displacements of the point  $B$  along the axes  $x, y, z$  are denoted by  $x, y, z$ . These displacements are related to the force components by linear equations

$$\left. \begin{aligned} P_x = Pl &= c_{xx}x + c_{xy}y + c_{xz}z, \\ P_y = Pm &= c_{yx}x + c_{yy}y + c_{yz}z, \\ P_z = Pn &= c_{zx}x + c_{zy}y + c_{zz}z, \end{aligned} \right\} \quad (1)$$

where  $c_{xx}, c_{xy}, \dots$  are some constant factors having the nature of stiffness. For example,  $c_{xy}$  is the force that must

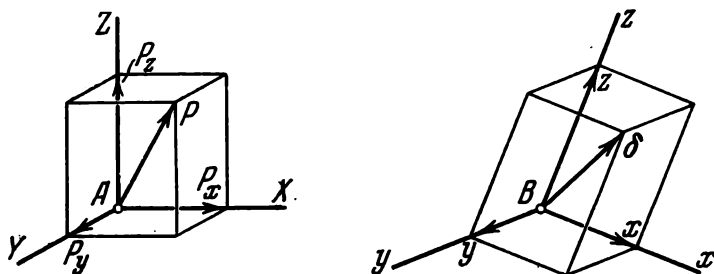


Fig. 447

be applied at the point  $A$  in the  $x$  direction in order to obtain a unit displacement at the point  $B$  in the  $y$  direction.

By squaring both sides of each of equalities (1) and adding them up, we obtain

$$\begin{aligned} P^2 &= (c_{xx}^2 + c_{yx}^2 + c_{zx}^2) x^2 + (c_{xy}^2 + c_{yy}^2 + c_{zy}^2) y^2 + \\ &\quad + (c_{xz}^2 + c_{yz}^2 + c_{zz}^2) z^2 + 2(c_{xx}c_{xy} + c_{yx}c_{yy} + c_{zx}c_{zy}) xy + \\ &\quad + 2(c_{xx}c_{xz} + c_{yx}c_{yz} + c_{zx}c_{zz}) xz + 2(c_{xy}c_{xz} + c_{yy}c_{yz} + c_{zy}c_{zz}) yz. \end{aligned}$$

Thus, we see that the displacement vector at the point  $B$  describes a second-degree surface centred at the same point. This may be a hyperboloid of one sheet or a hyperboloid of two sheets, or an ellipsoid. According to the physical significance of the problem, the surface must not have points at infinity; consequently, this is an ellipsoid or a surface into which an ellipsoid may degenerate.

It is clear that the foregoing is not yet a full proof, but is mere guess-work. A rigorous proof which is not presented here because of unwieldy computations consists in the following. By rotation of the co-ordinate systems  $X, Y, Z$  and  $x, y, z$  Eqs. (1) are transformed so as to make the six coefficients,  $c_{xy}$ ,  $c_{yx}$ ,  $c_{xz}$ ,  $c_{zx}$ ,  $c_{yz}$ , and  $c_{zy}$ , zero. To do this requires a suitable selection of three angles of rotation for one co-ordinate system and three angles of rotation for the other. Then

$$Pl = c_{xx}x, \quad Pm = c_{yy}y, \quad Pn = c_{zz}z$$

from which, by eliminating  $l, m, n$ , we obtain the equation of an ellipsoid

$$\frac{x^2}{\left(\frac{P}{c_{xx}}\right)^2} + \frac{y^2}{\left(\frac{P}{c_{yy}}\right)^2} + \frac{z^2}{\left(\frac{P}{c_{zz}}\right)^2} = 1.$$

187. When the section of the ring is rotated in the axial plane through an angle  $\varphi$ , a circumferential extension

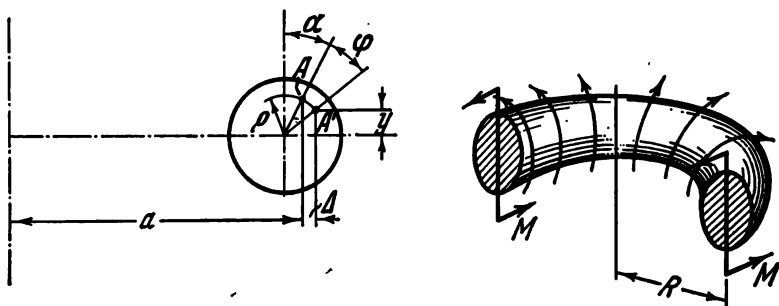


Fig. 448

$\varepsilon = \Delta/a$  is produced at a point  $A$  with co-ordinates  $\rho, \alpha$  (Fig. 448). But from the data of the figure

$$\Delta = \rho [\sin (\alpha + \varphi) - \sin \alpha], \quad a = R + \rho \sin \varphi.$$

Since  $\rho$  is much less than  $R$ ,  $a \cong R$ . We have therefore

$$\varepsilon = \frac{\rho}{R} [\sin (\alpha + \varphi) - \sin \alpha],$$

$$\sigma = E \frac{\rho}{R} [\sin (\alpha + \varphi) - \sin \alpha]. \quad (1)$$

The stresses  $\sigma$  give, at the section of the ring, a bending moment about the horizontal diameter equal to

$$M = \int_A \sigma y dA,$$

where  $dA$  and  $y$  are, respectively,

$$dA = \rho d\alpha d\rho, \quad y = \rho \cos(\alpha + \varphi).$$

We then obtain

$$M = \frac{E}{R} \int_0^r \int_0^{2\pi} \rho^3 [\sin(\alpha + \varphi) - \sin \alpha] \cos(\alpha + \varphi) d\rho d\alpha \quad (2)$$

or

$$M = \frac{Er^4}{4R} \pi \sin \varphi.$$

On the other hand, from the conditions of equilibrium for one half of the ring (Fig. 448) it follows that  $M = mR$ . Consequently,

$$\sin \varphi = \frac{4mR^2}{E\pi r^4}.$$

When  $0 \leq \varphi \leq \pi/2$ , the moment  $m$  increases and attains a maximum value at  $\varphi = \pi/2$

$$m_{\max} = \frac{E\pi r^4}{4R^2}.$$

A further increase of the angle  $\varphi$  requires a smaller moment. When  $\varphi = \pi$ , i.e., when the ring is "turned inside out",  $m = 0$ . The ring is then in a state of unstable equilibrium and, if slightly displaced, returns into its original position.

When  $\varphi > \pi$ , the moment  $m < 0$ . This means that to maintain the ring in a given position it is necessary in this case to apply a moment of opposite sign.

The value of  $m_{\max}$  obtained above may be regarded as the critical value of the moment at which, as is said, "overturning" of the ring occurs.

188. Expression (1) obtained for the stresses  $\sigma$  in the preceding problem

$$\sigma = E \frac{\rho}{R} [\sin(\alpha + \varphi) - \sin \alpha]$$

is changed by introducing an additional term

$$\frac{Ex}{\rho} = E \frac{\rho \sin \alpha}{R}$$

which reflects the prior bending stress. We now have

$$\sigma = \frac{E\rho}{R} \sin(\alpha + \varphi).$$

Instead of expression (2) we obtain

$$M = \frac{E}{R} \int_0^r \int_0^{2\pi} \rho^3 \sin(\alpha + \varphi) \cos(\alpha + \varphi) d\rho d\varphi = 0.$$

This means that a ring having the above-mentioned prestresses turns inside out in the axial plane without applying external forces. Such a ring is a kind of elastic mechanism. The reader can verify the above in experiment without much difficulty.

There are suggestions to use the foregoing effect for measuring the so-called internal friction developed in materials during deformation.

189. The stated problem can be solved within the framework of static approach.

Without considering the dynamic effect due to non-uniform rotation of the cable, we determine the law of variation of the balancing moment at exit when the moment at entry is unchanged. Denote the curvature of the cable by  $1/\rho$  and, neglecting frictional forces, set up the equation of equilibrium for an element of the cable of length  $ds$  (Fig. 449). The reactions exerted by the covering on the element are normal to the surface of the cable and give no moment about the  $x$  axis. By equating to zero the sum of the moments about the  $x$  axis, we therefore obtain

$$\frac{dM_x}{ds} = \frac{M_y}{\rho}. \quad (1)$$

Consequently, in the absence of frictional forces the moment  $M_x$  varies along the axis in so far as there is a moment

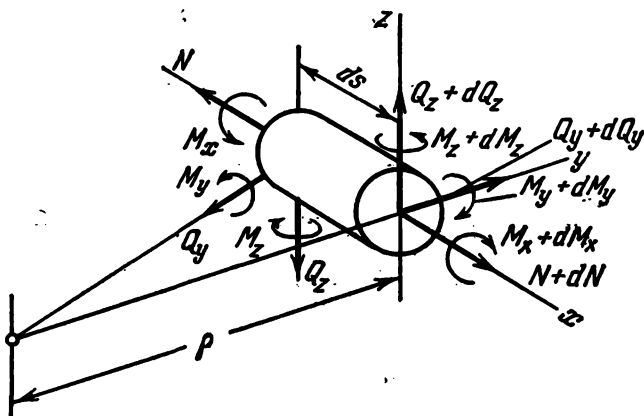


Fig. 449

$M_y$ , i.e., a bending moment in the plane perpendicular to the plane of curvature of the cable.

Consider a point  $A$  with polar co-ordinates  $r$  and  $\psi$  in the section of the cable (Fig. 450). The normal stress at this point may be represented as the sum of two terms. The first term is the stress which is produced in the cable when it is bent in the form of the covering, i.e.,

$$\sigma' = Er \sin \psi \left( \frac{1}{\rho} - \frac{1}{\rho_0} \right),$$

where  $1/\rho_0$  is the curvature of the cable which it had before placed into the covering.

The second term represents the stress which occurs at the point  $A$  after the cable has rotated in the covering through an angle  $\varphi$ .

We first find the displacement of the point  $A$  along the  $y$  axis (Fig. 450)

$$r \sin (\psi + \varphi) - r \sin \psi.$$

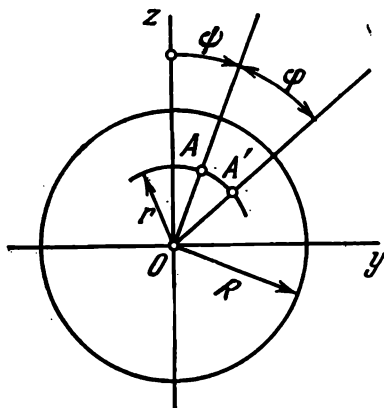


Fig. 450

The unit elongation along the  $x$  axis is

$$\frac{r}{\rho} [\sin (\psi + \varphi) - \sin \psi]$$

and the stress is given by

$$\sigma' = E \frac{r}{\rho} [\sin (\psi + \varphi) - \sin \psi].$$

The total stress is

$$\sigma_x = \sigma' + \sigma'' = Er \left[ \frac{1}{\rho} \sin (\psi + \varphi) - \frac{1}{\rho_0} \sin \psi \right].$$

We now find the bending moment  $M_y$

$$M_y = \int_A \sigma z dA$$

or

$$M_y = \int_0^R \int_0^{2\pi} Er \left[ \frac{1}{\rho} \sin (\psi + \varphi) - \frac{1}{\rho_0} \sin \psi \right] r \cos (\psi + \varphi) r d\psi dr,$$

whence

$$M_y = \frac{EI}{\rho_0} \sin \varphi$$

Equation (1) becomes

$$\frac{dM_x}{ds} = \frac{EI}{\rho\rho_0} \sin \varphi.$$

We integrate this expression with respect to  $s$  assuming that all sections have rotated through the same angle  $\varphi$

$$M_x = EI \sin \varphi \int_0^s \frac{ds}{\rho\rho_0} + C.$$

If a moment  $M_1$  is applied at one end of the cable (at  $s=0$ ), the balancing moment  $M_2$  at  $s=l$  is the following:

$$M_2 = M_1 + EI \sin \varphi \int_0^l \frac{ds}{\rho\rho_0}.$$

Thus, we see that the balancing moment at the end of the cable incorporates an additional term which varies in pro-

portion to the sine of the angle of rotation of the cable. If, however, the moments  $M_1$  and  $M_2$  are made equal, then during rotation of the cable the equilibrium conditions will not be fulfilled and the rotation at exit will not be uniform.

The moment  $M_2$  will be independent of the angle  $\varphi$  if

$$\int_0^l \frac{ds}{\rho \rho_0} = 0.$$

The sufficient condition for the normal operation of the speedometer cable is that  $1/\rho_0 = 0$ , i.e., it is sufficient that the cable be straight before being placed into the covering.

190. The fundamental frequency of a string is determined, as is known, by the formula

$$v = \frac{1}{2} \sqrt{\frac{T}{ml}},$$

where  $T$  is the tension in the string,  $m$  is its mass, and  $l$  its length.

In the first case of fixing, as the tension increases, the mass of the vibrating string varies while the length  $l_0$  is unchanged; this mass is obviously equal to

$$m_0 \frac{l_0}{l_0 + \Delta l},$$

where  $m_0$  is the mass of the taut string having the length  $l_0$ . We thus obtain

$$v_1 = \frac{1}{2} \sqrt{\frac{T}{m_0 l_0^3} (l_0 + \Delta l)} = \frac{1}{2} \frac{\sqrt{T \left(1 + \frac{\Delta l}{l_0}\right)}}{\sqrt{m_0 l_0}},$$

$$2v_1 \sqrt{m_0 l_0} = \sqrt{T \left(1 + \frac{\Delta l}{l_0}\right)}.$$

In the second case we find

$$v_2 = \frac{1}{2} \sqrt{\frac{T}{m_0 (l_0 + \Delta l)}},$$

$$2v_2 \sqrt{m_0 l_0} = \sqrt{\frac{T}{1 + \frac{\Delta l}{l_0}}}.$$

In both cases  $\Delta l/l_0$  is given as a function of the tension (Fig. 175); hence, the relation of  $\nu_1$  and  $\nu_2$  to  $T$  is easily determined. Figure 451 shows the required relation.

Thus, we see that for the first mode of tightening the frequency of vibration of the string increases with the ten-

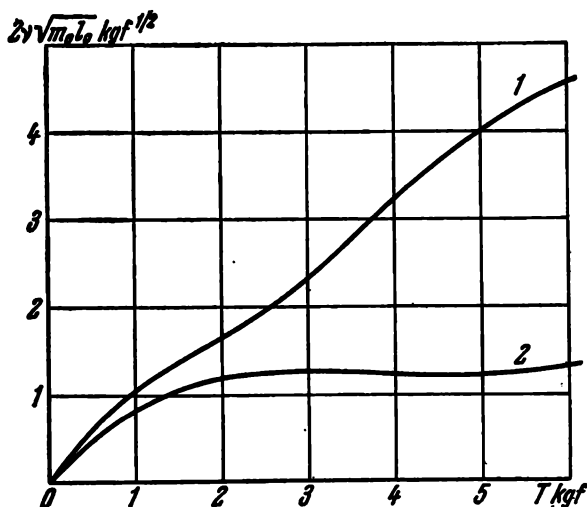


Fig. 451

sion. In the second case the frequency may decrease with increasing force. In experiment this phenomenon is well observed. It should only be remembered that not all rubbers have tensile test diagrams of the type considered.

191. The problem involves no difficulties in principle. It is natural that the beam formed by the procedure described will vibrate about the equilibrium position as a usual fixed-ended beam and the displacement  $h$  has no effect on the frequency.

We write the equation of motion of the elastic beam (Fig. 452)

$$EI y^{(IV)} = -\frac{q}{g} \frac{\partial^2 y}{\partial t^2},$$

where  $y$  is the displacement measured from the equilibrium position.

Assuming  $y = Y \sin \omega t$ , we obtain

$$Y^{(IV)} - a^4 Y = 0 \quad \left( a^4 = \frac{q\omega^2}{gEI} \right),$$

whence

$$Y = A \sin ax + B \cos ax + C \sinh ax + D \cosh ax.$$

This function must satisfy the following boundary conditions: when  $x = 0$ ,  $Y = 0$  and  $Y' = 0$ ; when  $x = l$ ,  $Y = 0$  and  $Y' = 0$ .

By equating to zero the determinant of the resulting homogeneous system of equations, we arrive at the following transcendental equation:

$$\cos al \cosh al = 1.$$

From this  $al = 4.73$  or

$$\omega = 4.732 \sqrt{\frac{gEI}{ql^4}}.$$

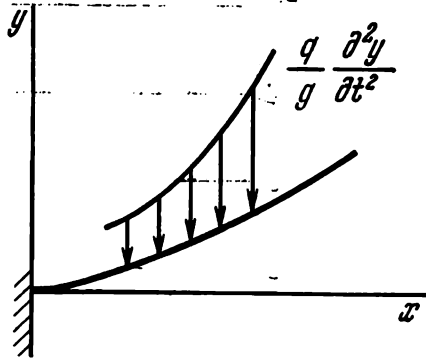


Fig. 452

To this point the solution has followed the normal path. But in the presented problem the length  $l$  itself depends on  $q$ .

The shape of the elastic curve in the original position of equilibrium represents a fourth-order curve

$$y_0 = \frac{q}{EI} \left( \frac{x^4}{24} + C_3 x^3 + C_2 x^2 + C_1 x + C_0 \right).$$

Since when  $x = 0$   $y_0$  and  $y'_0$  vanish,  $C_0 = C_1 = 0$ . When  $x = l$ , we have  $y'_0 = 0$  and  $y''_0 = 0$ . This gives

$$y_0 = \frac{q}{EI} \left( \frac{x^4}{24} - \frac{lx^3}{9} + \frac{l^2 x^2}{12} \right).$$

But when  $x = l$ , the displacement is equal to  $h$ . From this the length  $l$  is determined as

$$l^4 = \frac{72EIh}{q}.$$

We now return to the expression for the frequency from which we eliminate  $l^4$

$$\omega = \frac{4.732}{\sqrt{72}} \sqrt{\frac{g}{h}} = 2.63 \sqrt{\frac{g}{h}}.$$

The fundamental frequency of the beam thus formed is found to be independent of either the mass of the beam or its rigidity, and is determined by the quantity  $h$  alone.

It is interesting, isn't it? At any rate, it seems interesting to many people.

Paraphrasing Gardner's sophism about interesting numbers,\* it may be said that there are no uninteresting problems, for otherwise all known problems could be divided into two classes, interesting and uninteresting problems. But among uninteresting problems, we could find at least one, the most uninteresting, problem and this would induce us to show interest in it and carry it over into the class of interesting problems. Proceeding in this way, we should come to the conclusion that there are no uninteresting problems among those known to us.

192. Suppose that the cylinder turned inside out has the former shape, i.e., the shape of a cylinder of radius  $R$ ,

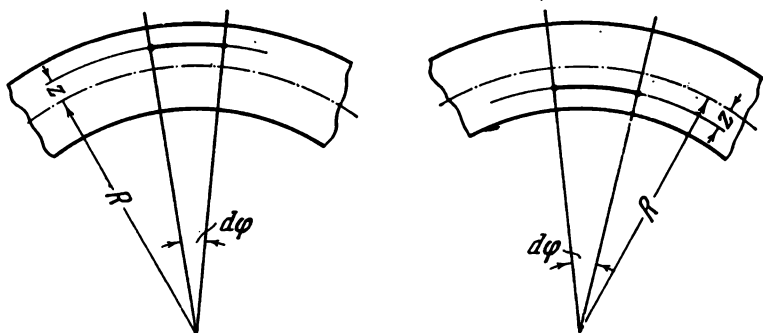


Fig. 453

and determine the stresses developed in it under this condition.

The tensile strain in the circumferential direction for layers distant  $z$  from the middle surface (Fig. 453) is determined by changing the curvature of the cylinder from  $1/R$  to  $-1/R$ . If the length of this fibre in the element  $d\phi$  before deformation (Fig. 453) was

$$(R + z) d\phi,$$

\* Gardner M., "Mathematical Puzzles and Diversions", Penguin Books, 1965.

for the turned-out cylinder it is equal to

$$(R - z) d\varphi.$$

The tensile strain in the circumferential direction is

$$\varepsilon_t = \frac{(R-z) d\varphi - (R+z) d\varphi}{(R+z) d\varphi} \cong -z \frac{2}{R}.$$

The tensile strain  $\varepsilon_x$  in the axial direction is zero. Consequently, we obtain

$$\sigma_t = \frac{E}{1-\mu^2} (\varepsilon_t + \mu \varepsilon_x) = -\frac{zE}{1-\mu^2} \frac{2}{R},$$

$$\sigma_x = \frac{E}{1-\mu^2} (\varepsilon_x + \mu \varepsilon_t) = -\mu \frac{zE}{1-\mu^2} \frac{2}{R}.$$

Thus, we come to the conclusion that in order for the turned-out cylinder to maintain its cylindrical shape, the stresses  $\sigma_x$  shown in Fig. 454 must be applied at its ends.

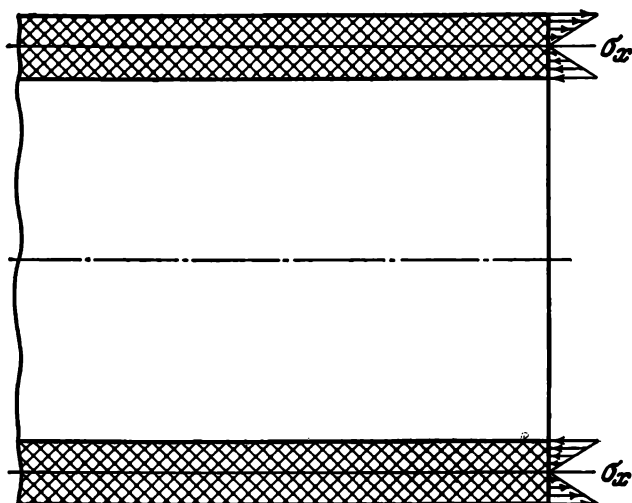


Fig. 454

Obviously, the actual shape of the turned-out cylinder is the same as the cylinder would take if it were loaded at the ends by the opposite system of forces (Fig. 455). The mo-

ment  $M$  to which the stresses  $\sigma_x$  reduce over a unit arc length of the contour is

$$M = \int_{-h/2}^{+h/2} \sigma_x z \, dz = \mu \cdot \frac{Eh^3}{12(1-\mu^2)} \frac{2}{R}.$$

We isolate a strip of unit width from the cylinder by two axial sections (Fig. 456). This strip may be regarded as a beam on an elastic foundation since the radial component

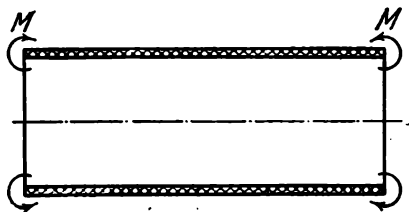


Fig. 455

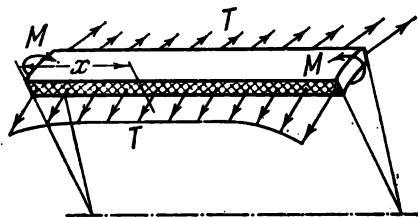


Fig. 456

of the forces  $T$  exerted on this strip by the adjacent parts of the shell is proportional to the deflection  $w$  of the strip.

The force  $T$  per unit length is

$$T = \frac{w}{R} Eh$$

and its radial component is given by

$$q = -\frac{T}{R} = -\frac{w}{R^2} Eh.$$

The minus sign for  $q$  is taken because this load is directed oppositely to the deflection. But

$$\frac{EI}{1-\mu^2} w^{(IV)} = q = -\frac{w}{R^2} Eh,$$

where

$$\frac{EI}{1-\mu^2} = \frac{Eh^3}{12(1-\mu^2)}$$

is the stiffness of the strip in constrained bending. We then have

$$w^{(IV)} + 4k^4 w = 0, \quad 4k^4 = \frac{12(1-\mu^2)}{R^2 h^3}.$$

By solving this equation, we obtain

$$w = e^{-kx}(A \sin kx + B \cos kx) + e^{+kx}(C \sin kx + D \cos kx).$$

Since the cylinder is sufficiently long, we restrict our attention to displacements in the zone of one contour. By

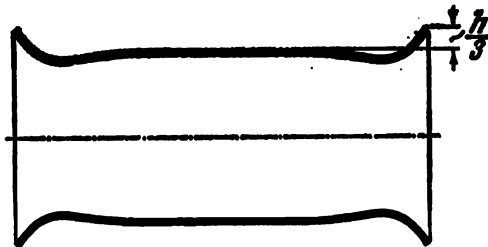


Fig. 457

rejecting the increasing part of the solution, i.e., assuming  $C = D = 0$ , we obtain

$$w = e^{-kx}(A \sin kx + B \cos kx).$$

The constants  $A$  and  $B$  are determined from the following conditions: when  $x = 0$ ,

$$M_b = \frac{EI}{1-\mu^2} w'' = M;$$

when  $x = 0$ ,

$$Q = M'_b = 0 \quad (w''' = 0)$$

or

$$-\frac{Eh^3}{12(1-\mu^2)} 2k^2 A = \mu \frac{Eh^3}{12(1-\mu^2)} \frac{2}{R}, \quad A + B = 0,$$

whence

$$A = -B = -\frac{\mu}{k^2 R},$$

$$w = \frac{\mu}{k^2 R} e^{-kx} (\cos kx - \sin kx), \quad w_{\max} = w|_{x=0} = \frac{\mu}{k^2 R}.$$

But since

$$k^2 = \frac{\sqrt{3(1-\mu^2)}}{Rh},$$

we have

$$w_{\max} = \frac{\mu h}{\sqrt{3(1-\mu^2)}}.$$

When  $\mu = 1/2$ ,

$$w_{\max} = h/3.$$

The shape of the turned-out cylinder is shown (exaggerated) in Fig. 457.

193. We find the roots of the characteristic equation

$$\alpha^4 - \frac{h\sigma_x}{D} \alpha^2 + 4k^4 = 0.$$

That is,

$$\alpha^2 = \frac{h\sigma_x}{2D} \pm \sqrt{\left(\frac{h\sigma_x}{2D}\right)^2 - 4k^4}.$$

Neglecting the term indicated in the condition of the problem is permissible if

$$\frac{h\sigma_x}{2D} \ll 2k^2,$$

which leads, upon substitution of the values of  $D$  and  $k$ , to the condition

$$\sigma_x \ll \frac{E}{\sqrt{3(1-\mu^2)}} \frac{h}{R}.$$

It can easily be established that in many practical problems this condition is not always fulfilled. In the analysis of edge effect this circumstance must therefore be kept in mind.

In the case of very small thickness i.e., for shells with vanishingly small flexural rigidity (soft shells), the edge effect can be investigated only if the term containing the second derivative of  $w$  is taken into account. Here, in Eq. (1) (see the condition of the problem) a limiting process is possible. By multiplying all terms of the equation by  $D$  and setting it equal to zero, we obtain

$$w'' - \beta^2 w = -\frac{p}{h\sigma_x} + \frac{\mu}{R},$$

where  $\beta^2 = \frac{E}{R^2 \sigma_x}.$

From this

$$w = Ae^{-\beta x} + Be^{+\beta x} + \frac{1}{\beta^2} \left( \frac{p}{h\sigma_x} - \frac{\mu}{R} \right),$$

By rejecting the increasing part of  $w$  and choosing  $A$  so as to make  $w$  vanish when  $x = 0$ , we obtain

$$w = R \left( \frac{pR}{Eh} - \mu \frac{\sigma_x}{E} \right) (1 - e^{-\beta x}).$$

The rate of damping is determined by  $\beta$ .

194. From the conditions of equilibrium we have

$$m\omega^2 (l + u) = P = f(u).$$

We solve this equation for  $u$  graphically (Fig. 458). The roots of the equation are determined by the co-ordinates of the points of intersection of the straight lines  $m\omega^2 (l + u)$  and the curve  $P = f(u)$ . By drawing several rays, we plot  $m\omega^2 l$  as a function of  $u$  (Fig. 458).

When  $m\omega^2 l = 1.0$ , the ball abruptly changes its position moving from the point characterized by the displacement  $u = 1.8$  to a point  $u = 7$ . The reverse jump occurs when  $m\omega^2 l = 0.8$ .

The direct jump may also occur, of course, when  $m\omega^2 l$  is less than 1.0 (but greater than 0.8) if only the ball is given a sufficiently large disturbance.

195. The height of the point  $O$  of the deformed system above the horizontal plane is  $H - w$ . The angle of inclination of the bars to the horizon is then

$$\alpha = \frac{H - w}{l}.$$

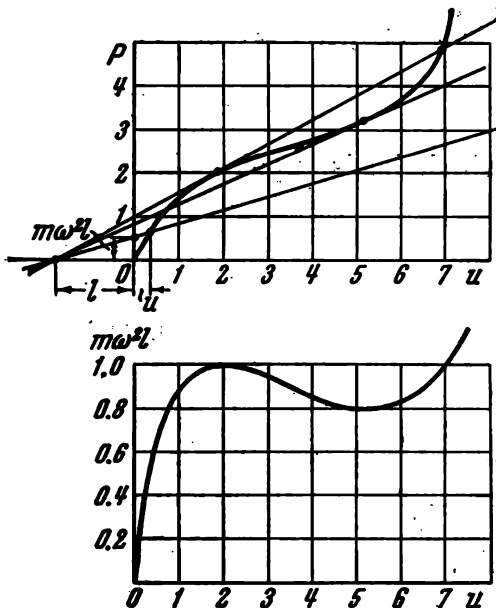


Fig. 458

If the compressive force in the bars is denoted by  $N$ , from the conditions of equilibrium we obviously obtain

$$P = 3N\alpha = 3N \frac{H-w}{l}.$$

On the other hand, the force  $N$  is determined by the amount of contraction of each bar

$$N = \frac{EA\Delta l}{l}.$$

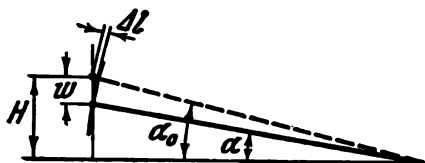


Fig. 459

From purely geometrical considerations (Fig. 459),  $\Delta l$  is expressed in terms of  $w$  as

$$\Delta l = l - l \frac{\cos \alpha_0}{\cos \alpha}.$$

Because of the smallness of the angles  $\alpha_0$  and  $\alpha$  we have

$$\Delta l \cong l \left[ 1 - \frac{1 - \frac{\alpha_0^2}{2}}{1 - \frac{\alpha^2}{2}} \right] = \frac{l}{2} (\alpha_0^2 - \alpha^2).$$

Substituting for  $\alpha_0$  and  $\alpha$ , we obtain

$$\Delta l = \frac{w}{l} \left( H - \frac{w}{2} \right).$$

The force  $N$  is then

$$N = \frac{EA}{l^2} w \left( H - \frac{w}{2} \right).$$

The force  $P$  has the following expression:

$$P = \frac{3EA}{l^3} w (H - w) \left( H - \frac{w}{2} \right).$$

The relation obtained may be rewritten in non-dimensional form

$$\frac{Pl^3}{3EAH^3} = \frac{w}{H} \left(1 - \frac{w}{H}\right) \left(1 - \frac{1}{2} \frac{w}{H}\right)$$

and represented as a curve (Fig. 460). This curve has two extreme points, *A* and *B*. In the first portion *OA* the load and deflection increase simultaneously. When the force *P*

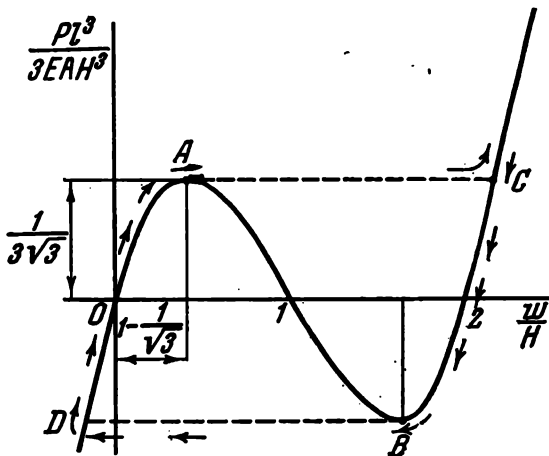


Fig. 460

attains a value corresponding to the first extremum, the deflection changes abruptly (*AC*, as is shown by arrows). With further increase in the load the displacement *w* continues to increase. If the system is now unloaded, the bars remain in a free condition with  $w/H = 2$ , i.e., the joint of the bars is by the amount *H* below the fixed horizontal plane. By applying a load of opposite sign, it is possible to produce the reverse snapping of the system, *BD*, and return it into its initial position.

The portion *AB* of the curve corresponds to unstable forms of equilibrium.

Thus, for values of the force *P* lying between the two extrema (Fig. 460)

$$-\frac{1}{\sqrt{3}} \frac{EAH^3}{l^3} < P < +\frac{1}{\sqrt{3}} \frac{EAH^3}{l^3}$$

the system has three forms of equilibrium: two stable forms and one unstable (intermediate) form.

In particular, when  $P = 0$  this unstable form corresponds to the position of the bars in the horizontal plane ( $w/H = 1$ ). If the bar system is slightly displaced from this position, it assumes either the upper or the lower position.

196. Suppose that the rectangular cross section does not deform but rotates as a result of the force action through an angle  $\varphi$  about a point  $O$  distant  $c$  from the axis of rotation (Fig. 461).

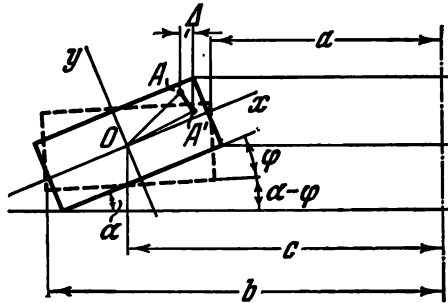


Fig. 461

Consider a point  $A$  in the section of the spring with co-ordinates  $x$  and  $y$ . After the section has rotated, this point assumes the position  $A'$  and comes nearer to the axis of symmetry by

$$\Delta = [x \cos (\alpha - \varphi) - y \sin (\alpha - \varphi)] - [x \cos \alpha - y \sin \alpha].$$

Since the angles  $\alpha$  and  $\varphi$  are small, we may write

$$\cos \alpha \cong 1 - \frac{1}{2} \alpha^2, \quad \sin \alpha \cong \alpha;$$

$$\cos (\alpha - \varphi) \cong 1 - \frac{1}{2} (\alpha - \varphi)^2, \quad \sin (\alpha - \varphi) \cong (\alpha - \varphi),$$

giving

$$\Delta = x\varphi \left( \alpha - \frac{\varphi}{2} \right) + y\varphi.$$

The circumferential tensile strain corresponding to the displacement  $\Delta$  is

$$\varepsilon_t = \frac{\Delta}{c - x \cos \alpha + y \sin \alpha} \cong \frac{\Delta}{c - x},$$

$$\varepsilon_t = \frac{x\varphi \left( \alpha - \frac{\varphi}{2} \right) + y\varphi}{c - x}.$$

The stress  $\sigma_t$  is equal to  $E\varepsilon_t$ .

We now determine the normal force at the axial section of the spring

$$N = \int_{c-b}^{c-a} \int_{-h/2}^{+h/2} \sigma_t dx dy.$$

Substituting the expression for  $\sigma_t$  obtained above, we have

$$\begin{aligned} N &= E \int_{c-b}^{c-a} \int_{-h/2}^{+h/2} \frac{x\varphi \left( \alpha - \frac{\varphi}{2} \right) + y\varphi}{c-x} dx dy = \\ &= Eh\varphi \left( \alpha - \frac{\varphi}{2} \right) \left( a - b + c \ln \frac{b}{a} \right). \end{aligned}$$

But, by considering the conditions of equilibrium for one

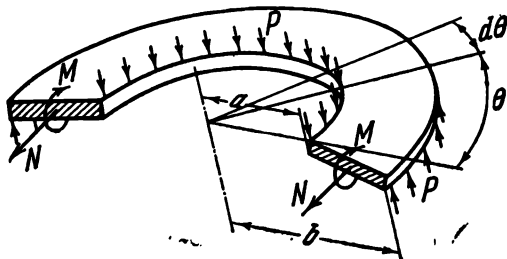


Fig. 462

half of the ring (Fig. 462), we ascertain that  $N = 0$ . From this condition we find

$$c = \frac{b-a}{\ln \frac{b}{a}}.$$

We now find the moment  $M$

$$\begin{aligned} M &= \int_{c-b}^{c-a} \int_{-h/2}^{+h/2} \sigma_t [x \sin(\alpha - \varphi) + y \cos(\alpha - \varphi)] dx dy, \\ M &= E \int_{c-b}^{c-a} \int_{-h/2}^{+h/2} \frac{x\varphi \left( \alpha - \frac{\varphi}{2} \right) + y\varphi}{c-x} [x(\alpha - \varphi) + y] dx dy, \\ M &= Eh \left[ \varphi \left( \alpha - \frac{\varphi}{2} \right) (\alpha - \varphi) \left( \frac{b^2}{2} - \frac{a^2}{2} + 2ca - 2cb + \right. \right. \\ &\quad \left. \left. + c^2 \ln \frac{b}{a} \right) + \frac{h^2}{12} \varphi \ln \frac{b}{a} \right]. \end{aligned}$$

On the other hand, from the conditions of equilibrium for the semi-ring (Fig. 462) it follows that

$$2M = \int_0^\pi \frac{P}{2\pi b} b^2 \sin \theta d\theta - \int_0^\pi \frac{P}{2\pi a} a^2 \sin \theta d\theta, \quad M = \frac{P}{2\pi} (b-a).$$

We thus obtain

$$\begin{aligned} \frac{P}{2\pi} (b-a) = Eh\varphi \left[ \left( \alpha - \frac{\varphi}{2} \right) (\alpha - \varphi) \left( \frac{b^2}{2} - \frac{a^2}{2} + \right. \right. \\ \left. \left. + 2ca - 2bc + c^2 \ln \frac{b}{a} \right) + \frac{h^2}{12} \ln \frac{b}{a} \right]. \end{aligned}$$

By eliminating  $c$  from this and substituting  $H/(b-a)$  and  $w/(b-a)$  for  $\alpha$  and  $\varphi$ , respectively, where  $w$  is the deflection of the spring, we find

$$P = \frac{2\pi Eh}{(b-a)^2} w \left[ \left( H - \frac{w}{2} \right) (H - w) \left( \frac{1}{2} \frac{b+a}{b-a} - \frac{1}{\ln \frac{b}{a}} \right) + \frac{h^2}{12} \ln \frac{b}{a} \right].$$

By a direct numerical verification it may be established that when  $1 < b/a < 4$  the following relation is valid:

$$\frac{1}{2} \frac{b+a}{b-a} - \frac{1}{\ln \frac{b}{a}} \cong \frac{1}{12} \ln \frac{b}{a}.$$

Hence,

$$P = \frac{\pi Eh}{6(b-a)^2} w \ln \frac{b}{a} \left[ \left( H - \frac{w}{2} \right) (H - w) + h^2 \right].$$

The above relation between the force  $P$  and the deflection of the spring  $w$  is non-linear and may have different character depending on the ratio  $H/h$ .

Figure 463 shows curves representing the relation between

$$P_0 = P \frac{6(b-a)^2}{\pi Eh^4 \ln \frac{b}{a}}$$

and  $w/h$  for different  $H/h$ , i.e.,

$$P_0 = \frac{w}{h} \left[ \left( \frac{H}{h} - \frac{1}{2} \frac{w}{h} \right) \left( \frac{H}{h} - \frac{w}{h} \right) + 1 \right].$$

Let us see how the form of the spring characteristic  $P_0 = f(w/h)$  varies with  $H/h$ . The curve corresponding to  $H/h = 0$  represents a characteristic of a flat disk spring. Increasing the height  $H$  causes, in the first instance, an increase in the initial stiffness of the spring and then the violation of the monotony of the curve behaviour. When

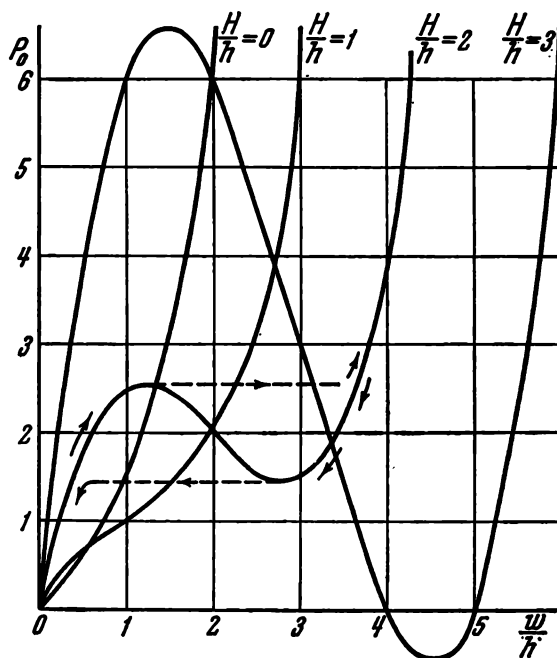


Fig. 463

$\overline{H/h} = \sqrt{2}$  (this can easily be deduced from analysis of the expression obtained), on the spring characteristic there appears a portion with a negative derivative situated between two extreme points. This portion may be termed a portion of negative stiffness since the deflection increases in this case with reduction in the load. Such an operation of the spring is unstable, and the forces corresponding to the extreme points are critical for the given spring. Once the force reaches the first extremum, the spring, passing the unstable portion, abruptly changes its deflection. Further operation proceeds over the right-hand stable increasing part of the characteristic. The unloading of the spring

produces an opposite sudden change of the deflection corresponding to the second critical force.

A further increase in the height of the spring  $H$  gives, as seen from Fig. 463, a still greater bend of the characteristic, and for values  $H/h > 2\sqrt{2}$  the latter begins to cross the axis of abscissas. Consequently, when the force  $P = 0$  the spring has three forms of equilibrium of which two forms are stable and one (intermediate) form is unstable. After snapping and unloading such a spring does not return into its initial position and preserves an elastic permanent deflection corresponding to the point of intersection of the curve with the axis of abscissas.

Compare the solutions of this problem and Prob. 195.

197. Consider the condition of equilibrium for the tube in a displaced position (Fig. 464). If  $H$  denotes the distance from the upper edge of the piston to the hinge at the beginning of loading, then obviously

$$P \left( H - \frac{P \cos \varphi}{k_1} \right) \sin \varphi = k \varphi \quad (1)$$

from which we obtain

$$\frac{P}{Hk_1} = \frac{1}{2 \cos \varphi} \left[ 1 \pm \sqrt{1 - \frac{4k}{k_1 H^2} \varphi \cot \varphi} \right].$$

Denote

$$\frac{P}{Hk_1} = p, \quad \frac{4k}{k_1 H^2} = \lambda. \quad (2)$$

We then have

$$p = \frac{1}{2 \cos \varphi} [1 \pm \sqrt{1 - \lambda \varphi \cot \varphi}].$$

The  $p - \varphi$  relation is different in character for different  $\lambda$ . Figure 465 shows this relation for the values  $\lambda = 0.5, 1.0$  and  $1.2$  when  $0 \leq \varphi < \pi$ . The curves obtained

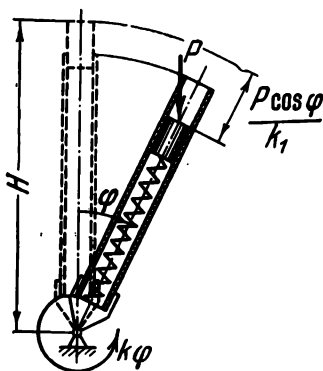


Fig. 464

correspond to equilibrium forms for the system in a displaced position from the vertical. Besides, there exists an equilibrium form for the vertically placed bar [Eq. (1)

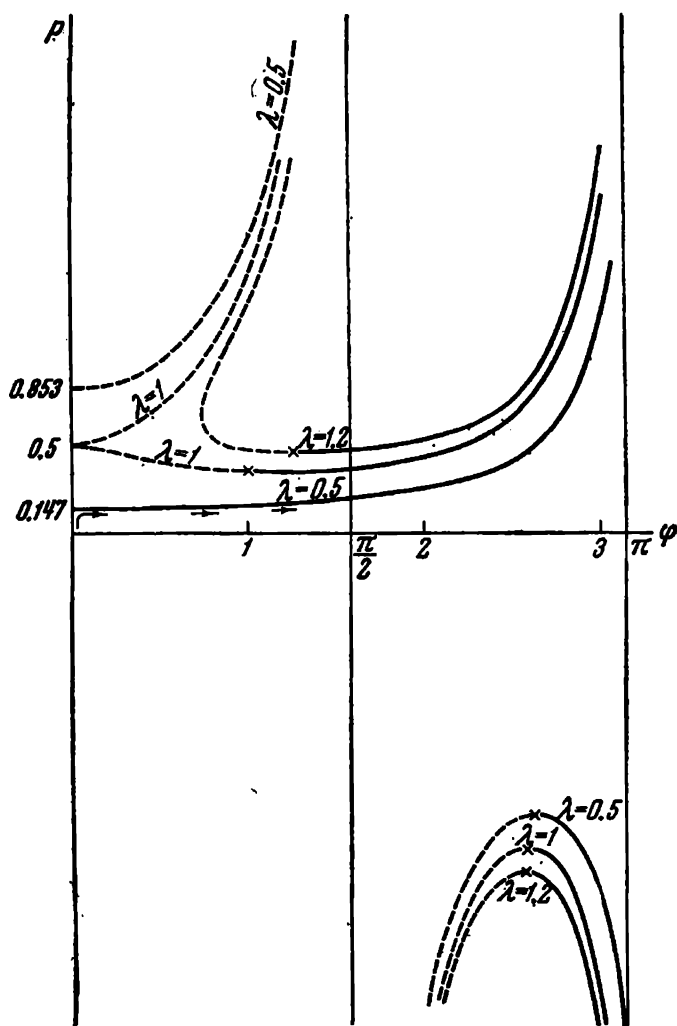


Fig. 465

is always satisfied for  $\varphi = 0$ ). In Fig. 465 this form of equilibrium is represented by points lying on the axis of ordinates. For  $\lambda = 0.5$  and, in general, for all values  $0 < \lambda < 1$ , the curves  $p = p(\varphi)$  intersect the axis of ordinates in two

points the lower of which corresponds to the first critical value of the parameter  $p$ . For  $\lambda = 0.5$ ,  $p_{cr} = 0.147$ . In general,

$$P_{cr} = \frac{1}{2}(1 - \sqrt{1 - \lambda})$$

or

$$P_{cr} = \frac{Hk_1}{2} \left[ 1 - \sqrt{1 - \frac{4k}{k_1 H^2}} \right].$$

The question now arises as to the stability of these forms of equilibrium. The criterion for a stable equilibrium position is a minimum of the total potential energy

$$U = \frac{k\varphi^2}{2} + \frac{k_1 \Delta^2}{2} + P(H - \Delta) \cos \varphi.$$

The first two terms of this expression represent the strain energy, and the last term expresses the change in the potential of the external force  $P$ . Since  $\Delta = (P \cos \varphi)/k_1$ , we obtain

$$U = \frac{k\varphi^2}{2} + PH \cos \varphi - \frac{P^2 \cos^2 \varphi}{2k_1}.$$

The condition  $dU/d\varphi = 0$  is an equilibrium condition (condition for an extremum of the energy) and leads us, as might be expected, to Eq. (1) obtained previously. The condition for a minimum of the energy is written as

$$\frac{d^2 U}{d\varphi^2} > 0$$

or

$$k - PH \cos \varphi + \frac{P^2}{k_1} \cos 2\varphi > 0.$$

According to notation (2) we have

$$\frac{\lambda}{4} - p \cos \varphi + p^2 \cos 2\varphi > 0.$$

By examining the curves obtained, we note that the stability condition is fulfilled for some portions of these curves, and is not fulfilled for others. In Fig. 465 the portions corresponding to unstable equilibrium are shown by dashed

lines. For the axis of ordinates the stability condition is written in the form

$$\frac{\lambda}{4} - p + p^2 > 0$$

from which we obtain

$$p < \frac{1}{2}(1 - \sqrt{1 - \lambda}) \text{ and } p > \frac{1}{2}(1 + \sqrt{1 - \lambda}).$$

For  $\lambda = 0.5$ , for example, the vertical position of the tube is unstable when

$$0.853 > p > 0.147.$$

In Fig. 465 the arrows show the increase of the angle  $\varphi$  as a function of the force  $P$  in the case of  $\lambda = 0.5$ . At first the angle  $\varphi$  remains equal to zero. When  $p = 0.147$ , the tube deflects from the vertical and subsequently, as the force  $P$  increases, the angle  $\varphi$  asymptotically approaches the value  $\varphi = \pi$ . When  $\varphi > \pi/2$ , the piston is pulled out of the tube by the force  $P$ . In an actual system the displacement of the piston, along with the increase of the force  $P$ , is limited by the length of the tube.

The curves thus plotted show that the angle  $\varphi$  may also asymptotically approach the value  $\pi/2$ , for example, for the case  $\lambda = 0.5$  when  $p > 0.853$ . This means that at a sufficiently large force the deflection of the spring inserted into the tube increases so sharply and at the same time the arm of the force  $P$  decreases so rapidly that the latter is unable to throw the tube below the horizontal. In the limit, when  $\varphi = \pi/2$ , the deflection of the spring  $(P \cos \varphi)/k_1$  is, as can easily be established,  $H$ . These forms of equilibrium are, however, unstable.

When  $\lambda > 1$ , i.e., when the stiffness of the spiral spring is sufficiently large, or when the height or the stiffness of the second spring  $k_1$  is sufficiently small, the vertical position of the tube remains always stable for all values of the force  $P$ , though there exist equilibrium forms for the tube in a displaced position. In order for the tube to assume this form of equilibrium, it must be given a large lateral displacement by means of an external force.

Figure 465 also represents branches of the curves  $p = p(\varphi)$  for negative values of  $p$ . These curves show that

when  $\pi/2 \leq \varphi < \pi$  the tube may be in equilibrium under a force of opposite sign. This mode of equilibrium can easily be visualized if it is remembered that theoretically the piston can move in the tube by amounts greater than  $H$ . When  $\Delta > H$ , the force  $P$ , having an opposite sign, maintains the tube in the indicated position of equilibrium.

We have thus considered equilibrium forms when  $0 \leq \leq \varphi < \pi$ . This, however, does not exhaust all the variety of possible forms. The analysis of this question could be continued by broadening the range of the angle  $\varphi$  beyond  $\pi$  to the right and beyond zero to the left.

The example considered is an example of the simplest non-linearity where it is possible, without much difficulty, to obtain a complete solution and to show, in a vivid way, its multiple-valuedness. In the general case, however, the solution of non-linear problems is one of the most complex and topical questions of modern mathematics and mechanics.

198. The problem is a typical large-displacement problem for an elastic rod.

We turn to the solution of Prob. 137. The elastic beam shown in Fig. 367 (p. 283) may be likened to one half of a bow arch.

When  $s = l$ , expression (5) (p. 285) becomes

$$\beta = F(\psi_L) - F(\psi_0). \quad (1')$$

When  $s = l$ , the curvature of the rod is zero ( $d\zeta/ds = 0$ ). Hence, from (4) (p. 285) it follows that

$$k \cos \psi_L = 0 \quad \left( \psi_L = \frac{\pi}{2} \right). \quad (2')$$

When  $s = 0$ ,  $\zeta = \delta$ . From this condition and from expression (3) (p. 285) we obtain

$$\sin \frac{\delta}{2} = k' \sin \psi_0. \quad (3')$$

Let us consider the first stage of bending the rod, viz. tying up the string (Fig. 466). In this case, as seen from Fig. 367,  $\delta = 0$ . Hence, from (3') it follows that  $\psi_0 = 0$ . For the same case we have

$$x_L = a, \quad y_L = h.$$

Expressions (5) and (7) (pp. 285 and 286) give

$$\beta = l \sqrt{\frac{P_1}{EI}} = F\left(\frac{\pi}{2}\right),$$

$$\frac{a}{l} = \frac{2}{\beta} E\left(\frac{\pi}{2}\right) - 1, \quad \frac{h}{l} = \frac{2k}{\beta}.$$

By assigning several values of  $k$  and using tables of elliptic integrals, we find  $\beta$ ,  $a/l$ , and  $h/l$  from the last equations. The results are summarized in the following table:

arc sin $k$	0	5°	10°	15°
$\beta$	1.571	1.574	1.583	1.598
$\frac{a}{l}$	1	0.990	0.967	0.931
$\frac{h}{l}$	0	0.111	0.219	0.324

By interpolation of the results obtained we find, for the given  $h/l = 0.3$ , the following values:

$$\beta = l \sqrt{\frac{P_1}{EI}} = 1.59, \quad \frac{a}{l} = 0.945.$$

We thus obtain the force  $P_1$  in the taut string and the length  $a$  of the string which remains unchanged during further deformation of the system.

Let us now consider the second stage of bending the rod. Here the quantity  $\psi_0$  is different from zero and remains unknown. The determination of this quantity will be performed as follows. Assign  $k$  and  $\psi_0$ .

From expression (3') we find  $\delta$  according to the condition

$$k \sin \psi_0 = \sin \frac{\delta}{2}.$$

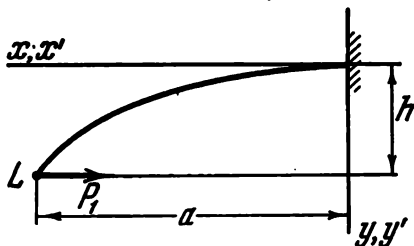


Fig. 466

Then, from (1') we determine

$$\beta = F\left(\frac{\pi}{2}\right) - F(\psi_0).$$

Expressions (6) (p. 286) give

$$\frac{x'_L}{l} = \frac{2}{\beta} \left[ E\left(\frac{\pi}{2}\right) - E(\psi_0) \right] - 1,$$

$$\frac{y'_L}{l} = \frac{2}{\beta} k \cos \psi_0,$$

and from expressions (7) (p. 286) we find

$$\frac{x_L}{l} = \frac{x'_L}{l} \cos \delta + \frac{y'_L}{l} \sin \delta,$$

$$\frac{y_L}{l} = \frac{y'_L}{l} \cos \delta - \frac{x'_L}{l} \sin \delta.$$

Finally, we determine the length  $a$  of the string (Fig. 467)

$$a = \frac{x_L}{\cos \delta},$$

whence

$$\frac{a}{l} = \frac{\frac{x_L}{l}}{\cos \delta}.$$

This ratio must be equal to 0.945. For a constant  $k$  we assign several values of  $\psi$  and repeat the calculations until  $a/l$  is equal to 0.945. Such a selection is made for several values of  $k$ . The results are tabulated as follows:

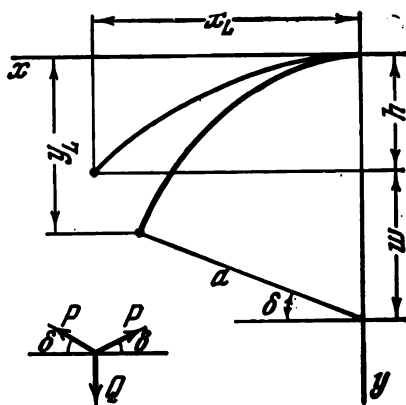


Fig. 467

arc sin $k$	15°	20°	25°	30°	35°
$\psi_0$	6°	15°	20°	21°	23°
$\frac{x}{l}$	0.943	0.932	0.906	0.883	0.850
$\frac{y}{l}$	0.294	0.325	0.366	0.425	0.472
$\beta$	1.493	1.358	1.299	1.317	1.326

We next calculate the displacement  $w$  (Fig. 467)

$$\frac{w}{l} = \frac{a}{l} \sin \delta + \frac{y_L}{l} - \frac{h}{l}$$

and the force  $Q$  (Fig. 467)

$$Q = 2P \sin \delta,$$

$$\frac{Ql^2}{EI} = 2\beta^2 \sin \delta.$$

For the same values of  $k$  and  $\psi_0$  we obtain

$\frac{[w]}{l}$	$\frac{Ql^2}{EI}$
0.045	0.24
0.192	0.651
0.337	0.967
0.459	0.22
0.585	1.54

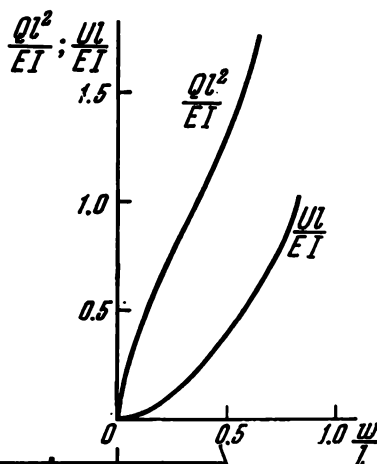


Figure 468 shows the graph of  $Ql^2/EI$  against  $w/l$ . The area bounded by this curve on the interval from 0 to  $w/l$  gives the expression for the elastic energy imparted to the arrow upon release. Figure 468 also shows the integral curve for the energy  $U$ . This curve is obtained by a simple computation of the area under the first graph.

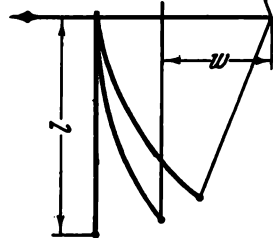


Fig. 468

We now proceed to a numerical calculation. For the given  $w/l = 0.6$  we read from the curve

$$\frac{Ul}{EI} = 0.53,$$

$$U = 0.53 \frac{EI}{l} = 0.53 \frac{10^6 \pi 2^4}{64 \times 60} = 695 \text{ kgf-cm.}$$

This energy is equated to the kinetic energy of the arrow

$$U = \frac{mv^2}{2}, \quad v = \sqrt{\frac{2U}{m}},$$

$$v = \sqrt{\frac{2 \times 695 \times 981}{0.040}} = 5800 \text{ cm/sec} = 58 \text{ m/sec.}$$

Actually the velocity  $v$  is somewhat less since part of the energy is expended in imparting the kinetic energy to the string and the bow arch. The force  $Q$  that must be applied to the bow in order to give the arrow the calculated velocity is also determined from the graph of Fig. 468

$$\frac{Ql^2}{EI} \Big|_{w=0.6} = 1.6, \quad Q = 1.6 \frac{10^5 \pi 2^4}{64 \times 60^2} = 35 \text{ kgf.}$$

# Literature

1. Andreeva, L. E. *Elastic Elements of Instruments*, Mashgiz, Moscow, 1962 (in Russian).
2. Biderman, V. L., Boyarshinov, S. V. *Design of a Spring-type Ratchet*, in "Transactions of the Department of Strength of Materials at the Bauman Higher Technical School in Moscow", Izd. MVTU, Moscow, 1947, (in Russian).
3. Bolotin, V. V. "Non-conservative Problems of the Theory of Elastic Stability", Fizmatgiz, Moscow, 1961 (in Russian). Transl.— Pergamon Press, London, 1963.
4. Dinnik, A. N. "Buckling. Theory and Applications", Gos. Objed. Nauchno-tekh. Izd., Moscow-Leningrad, 1939 (in Russian).
5. Filonenko-Borodich, M. M. "Course in Strength of Materials", Part I, Fizmatgiz, Moscow, 1961 (in Russian).
6. Filonenko-Borodich, M. M. "Course in Strength of Materials", Part II, Gostekhizdat, Moscow, 1956 (in Russian).
7. Korobov, A. P. *Design of Wheels with a Large Number of Spokes*, Izv. Novochoerkassk. Industr. Inst., Stroit. Chast, 4(18) (1935-1936) (in Russian).
8. Love, A. E. H. "A Treatise on the Mathematical Theory of Elasticity", 4th ed., Cambridge Univ. Press, 1927.
9. Mukhin, O. N. *A Dynamic Criterion for the Stability of a Pipeline with Flowing Liquid*, Izv. Akad. Nauk SSSR. Mekh., No. 3 (1965) (in Russian).
10. Panovko, Ya. G., Gubanov, I. I. "Stability and Oscillations of Elastic Systems: Paradoxes, Fallacies, and New Concepts", Nauka, Moscow, 1964 (in Russian). Transl.— Consultants Bureau, New York, 1965.
11. Popov, E. P. "Non-linear Problems in the Statics of Thin Bars", Gostekhizdat, Leningrad-Moscow, 1948 (in Russian).
12. Rzhantsyn, A. R. "Plastic Analysis of Structures", Stroivoenmorizdat, Moscow, 1949 (in Russian).
13. Rzhantsyn, A. R. "Some Problems in the Mechanics of Systems Deforming in Time", Gostekhizdat, Moscow-Leningrad, 1949 (in Russian).
14. Yasinskii, F. S. "Selected Works on the Stability of Compression Members", Fizmatgiz, Moscow, 1962 (in Russian).
15. Ziegler, H. *On the Concept of Elastic Stability*, in "Advances in Applied Mechanics", Vol. 4, Acad. Press, New York, 1956.

## TO THE READER

Mir Publishers would be grateful for your comments on the content, translation and design of this book. We would also be pleased to receive any other suggestions you may wish to make.

Our address is:

USSR, 129820, Moscow, I-110, GSP

Pervy Rizhsky Pereulok, 2

MIR PUBLISHERS

*Printed in the Union of Soviet Socialist Republics*



Prof. Vsevolod Feodosyev, D.Sc., is a leading Soviet researcher in the field of the theory of elasticity and problems of the strength of mechanical elements, and is a laureate of the Lenin Prize.

Prof. Feodosyev's published works include "Methods of Strength Analysis in Mechanical Engineering", "Elastic Elements in Instrument-Making", and "Strength of Heat-Stressed Units in Rocket Engines".

In addition to his extensive research work, Prof. Feodosyev is actively engaged in teaching, holding a chair at the Bauman Higher Technical School in Moscow, one of the oldest higher educational institutions in the USSR.

